BUDKER INSTITUTE OF NUCLEAR PHYSICS
of Siberian Branch of Russian Academy of Sciences

ANNUAL REPORT
2014

NOVOSIBIRSK 2015

Contents

INTRODUCTION

In May 1958, the USSR Council of Ministers declared creation of the Institute of Nuclear Physics of the Siberian Branch of the USSR Academy of Sciences. The new institute was created on the basis of the Laboratory of new acceleration methods, headed by G.I. Budker, of the Nuclear Energy Institute, directed by I.V. Kurchatov. Since 1977, the Institute of Nuclear Physics was directed by academy member A.N. Skrinsky.

Currently, BINP SB RAS with over 2,800 employees is the largest academic institute of Russia. The Institute research staff of 413 members includes 9 members and corresponding members of the Russian Academy of Sciences, 62 Doctors of Sciences and 168 Candidates of Sciences. BINP has a large experimental production department (about 1,000 employees) with high-level engineering and technology equipment.

The Institute is doing much for training of scientific and technical personnel of high qualification. BINP is a base institution for seven subdepartments of the Physics Department of the Novosibirsk State University (NSU) and the Physicotechnical Department of the Novosibirsk State Technical University (NSTU) (in total about 200 students). Over 60 post-graduate students are pursuing post-graduate studies at BINP, the NSU and the NSTU.

BINP is one of the world's leading centers in a number of areas of high energy physics, accelerator physics, plasma physics and controlled fusion physics. The Institute conducts large-scale elementary particle physics experiments on electron-positron colliders and a unique complex of open plasma traps and develops up-to-date accelerators, high-power sources of synchrotron radiation and free electron lasers. In most of these areas, the Institute is the only research institution in Russia.

Below are listed the main BINP achievements in science and technology.

In the field of elementary particle physics and nuclear physics:
- pioneering works on the development of the colliding beam technique, which is now the leading one in the high energy physics:
  o first experiments on the electron-electron interaction (simultaneously with the Princeton/Stanford works) (1965),
  o world's first experiments on the electron-positron interaction (1967),
  o world's first observation of double bremsstrahlung (1967),
  o pioneering works in the two-photon physics;
- research on the characteristics of vector mesons on the installations with colliding electron-positron beams VEPP-2, VEPP-2M and VEPP-4 (since 1967);
- discovery of the phenomenon of multiple production of hadrons in electron-positron annihilation;
- precision measurement of the contribution of hadronic polarization of vacuum to the value of muon anomalous magnetic moment for one of the most sensitive tests of the Standard Model, which is conducted in cooperation with the Brookhaven National Laboratory (1984 - 2005);
- development of the resonance depolarization method for precision measurement of the masses of elementary particles and achievement of record accuracy in measurements of the masses of K, rho, omega, phi and psi mesons and upsilon mesons (1975 - 2004);
- discovery of parity violation effects in atomic transitions and confirmation to the unified theory of electroweak interactions (1978);
- development of experiments on hyperfine internal targets on storage rings (since 1967) and investigation into the electromagnetic structure of deuteron in polarization experiments (since 1984);
- development of a technique for production of intense fluxes of labeled high-energy gamma quanta through the use of inverse Compton scattering (1980 - 1982); experimental observation of photon splitting in the Coulomb field of nucleus (1997);
- development of new methods for detection of high-energy charged and neutral particles and creation of unique detectors for installations with colliding beams (OLYA, CMD-1, MD-1, CMD-2, CMD-3, ND, SND, and KEDR);
- development of X-ray detectors for medical applications and creation of a low-dose digital radiographic installation on their basis, with an ultra-low level of patient exposure, and the X-ray system "Sibscan" for inspection of people (since 1981).

In the field of theoretical physics:
- development of the resonance theory of dynamical chaos and pseudochaos in the classical and quantum mechanics (since 1959);
- the first-time computation of charge renormalization in the Yang-Mills theory (1969);
- development of the method of the QCD sum rules (1979 - 1984);
- prediction of large enhancement of parity violation effects in neutron resonances in heavy nuclei (1980 - 1985);
- development of the theory of hard exclusive reactions in the QCD (1977 - 1984);
- development of an operator approach to quantum electrodynamics in external fields (1974);
- development of quantum electrodynamics in periodic structures, including a laser wave (1972 - 1997);
- development of the theory of radiation effects in passage of high-energy charged particles and photons through orientated single crystals (since 1978);
- derivation of evolution equation in the QCD for energy distribution of partons (the BFKL equation) (1975 - 1997);
- prediction of the coherence effect in the emission of gluons in the QCD and investigation into its influence on hadron distribution (1981 - 1982).

In the field of accelerator physics and technology:

- successful long-term experience in the creation of storage rings and installations with colliding beams;
- invention, development and experimental verification of the "electron cooling" method for heavy-particle beams, which is currently used at laboratories around the world; delivery of efficient "coolers" to heavy-ion accelerator complexes in Germany, China and at CERN (1965 - 2005);
- invention and development of new types of high-power RF generators (gyrocon, relativistic klystron and Magnicon) (since 1967);
- suggestion of a technique of linear electron-positron colliding beams for production of super-high energies (1968) and presentation of a physically self-consistent project (1978);
- development of components of intense-field pulsed magnetic optics (X lenses and lithium lenses), which are currently used at different laboratories (since 1962);
- invention and experimental verification of the method of charge-exchange injection, which is currently applied at all the major proton accelerators (1960 - 1964);
- theoretical and experimental investigation into the generation of polarized beams and spin dynamics in accelerators and colliders and conceptual designing and creation of highly efficient spin rotators and "Siberian snakes" for a number of accelerator complexes, (1966 - 1995);
- theoretical and experimental research on the stochastic instability and "collision effects", which impose limitations on the luminosity of colliding-beam installations (since 1966);
- development of the physical concept of a new generation of electron-positron colliders of very high luminosity, so-called electron-positron factories (since 1987);
- suggestion and development of a method of ionization cooling of muons for creation of muon colliders and neutrino factories (since 1969);
- development and creation of high-power low-energy electron accelerators for a variety of technological applications, including environment protection (accelerators ELV-12 with a power of 500 kW and an energy of 1 MeV and ILU-10 with a power of up to 50 kW and an energy of 5 MeV) (since 1963);
- suggestion and implementation of a scheme of energy recovery linac for high-gain free electron lasers (1979 - 2003).

In the field of plasma physics and nuclear fusion:

- invention (1954) and creation (1959) of the "classical" open magnetic trap (magnetic bottle) for hot plasma confinement;
- invention and development of new schemes of open traps (multiple-mirror, rotating-plasma, ambipolar, and gas-dynamical ones); experimental realization of multiple-mirror confinement of plasma with sub-fusion parameters in the trap GOL-3; experimental implementation of MHD instability stabilization in an axially symmetric gas-dynamic trap (on the installation GDT) (since 1971);
- discovery of collisionless shock waves in plasma (1961);
- development of a technique of plasma heating with relativistic electron beams (since 1971);
- development of high-intensity surface-plasma sources of negative ions, now widespread in the world (1969 - 1981);
- suggestion and development of a concept of a high-power open-trap fusion source of neutrons for materials science (since 1987).
- theoretical prediction of the Langmuir collapse (1972) and experimental discovery of strong Langmuir turbulence and collapse of Langmuir waves in a magnetic field (1989 - 1997);
- creation of a series of unique high-power precision sources of hydrogen atoms for high-temperature plasma investigation for a number of large installations (since 1997).

In the field of synchrotron radiation and free electron lasers:

- application of synchrotron radiation of the BINP storage rings to science and technology and establishment of the international Siberian Synchrotron Radiation Center based on VEPP-2M, VEPP-3 and VEPP-4 storage rings (since 1973);
- theoretical and experimental research on particle emission in periodic structures (undulators, wigglers, and crystals) (since 1972);
- development and creation of specialized sources of synchrotron radiation (since 1983);
- development and creation of one- and two-coordinate detectors for experiments with synchrotron radiation (since 1975);
- invention and development of the optical klystron (1977) and generation of coherent radiation in the infrared to the ultraviolet spectrum (since 1980);
- development and creation of a high-power free electron laser (for photochemical research and technological applications, as well as for energy transfer from the Earth to a satellite) on the basis of the most promising scheme, which uses a recuperator microtron; generation of high-power (400 W) laser radiation in the terahertz range (since 1987);
- creation of a series of intense-field superconducting magnetic devices for SR sources and electron storage rings (wigglers and bending magnets with fields of up to 10 T and solenoids with fields of up to 13 T) (since 1996).

Applied works performed by BINP SB RAS rely entirely on the results of the basic research performed by the Institute and are focused on the following main areas:

- industrial high-power electron accelerators for modification of polymers, treatment of industrial and domestic waste, production of nanopowders of pure metals, silica, and oxides, carbides and nitrides of metals, radiation processing of food, sterilization of medical equipment, disposable instruments and garments and other technological applications;
- low-dose scanning-type digital radiographic installations with ultra-low patient exposure, for medical and security systems;
- development of nuclear medicine facilities for proton-, ion- and boron-neutron-capture therapy of malignant tumors;
- electron beam welders;
- radiographic equipment for defense research.

During the past 25 years, BINP has financed its basic and applied research from assets received from contract works. The cost of high-tech products developed, manufactured and supplied annually by BINP to customers in Europe, Asia, and North and South Americas (over 20 countries), as well as in Russia, makes hundreds of millions rubles. The so earned money was used for the completion and commissioning of the accelerator complex VEPP-4M with the unique detector KEDR and designing and construction of large unique installations (the electron-positron collider VEPP-2000, the free electron laser and a new injection system for the existing and future BINP facilities). Throughout the post-Soviet period, these funds have maintained the continuous work of the BINP facilities and related infrastructure.

BINP excels in long-term international cooperation with most major foreign and international research centers. A striking example is the BINP participation in the largest international project – creation of the Large Hadron Collider at the European Organization for Nuclear Research (Geneva). Within the framework of this cooperation, BINP has developed, manufactured and delivered to CERN unique hi-tech equipment for an amount of over 100 million Swiss francs.

BINP has played a key role in several major Russian projects, including the following: the Center for Synchrotron Radiation at the Research Center 'Kurchatov Institute', the accelerator complex at JINR in Dubna, and radiographic equipment for defense research at VNIITF in Snezhinsk.

In 2014, the state task to the Institute included 26 'baseline' projects within 8 programs in two areas of the Program for Basic Research by the State Academies of Sciences for 2013-2020, as well as 19 projects under the programs of the Presidium of the Russian Academy of Sciences and the Division of Physical Sciences of the Russian Academy of Sciences. The Institute is executing 3 agreements under the Federal Target Program 'Research and development in priority directions of the science-and-technology complex of Russia for 2014– 2020; four projects are supported by the Russian Science Foundation.

Every year, members of the Institute make about 200 reports at international and Russian conferences, publish about 500 articles in leading Russian and foreign scientific journals and issue monographs and educational aids. According to data published in the review 'Bibliometric indicators of the Russian Science and Russian Academy of Sciences" (RAS Bulletin, June 2009, Volume 79, № 6), the number of references to papers by BINP members that are accounted in the authoritative international database ESI was 28,267 in 1997-2007. In accordance with the survey data, this is a maximum value among all the institutions of the Russian Academy of Sciences. Four members of the Institute are winners of the Elsevier special premium as the most cited authors in the post-Soviet area in the field of natural sciences.

Below are listed works the BINP Scientific Council recognized as the best in 2014.

In the field of **nuclear physics, elementary particle physics and physics of basic interactions:**

1) For the first time near the reaction threshold, the cross section of production of neutron-antineutron pairs in electron-positron annihilation was measured. The experiment was performed at the collider VEPP-2000 with the detector SND;

2) The rate of $J/\psi \to \gamma \eta_c$ decay was measured with high precision, which enabled elimination of the contradiction between experimental data and theoretical predictions. The experiment was performed at the electron-positron collider VEPP-4M with the detector KEDR.

3) The most stringent limit on the probability of decay of the $\eta'(958)$ meson into an electron-positron pair was determined. The experiment was performed at the electron-positron collider VEPP 2000 with detector CMD-3.

4) The τ lepton mass was measured with the world's best precision in a joint experiment with the detector BES-III at the electron-positron collider BEPC-II (Beijing, China).

5) For the first time, the asymmetry of the cross sections of elastic scattering of positrons and electrons on protons was measured, which enabled determination of the contribution of two-photon exchange in the reaction.

6) The charge asymmetry in photoproduction processes at high energy of muon-antimuon pairs in a heavy atom field was predicted and calculated for the first time.

In the field of **plasma physics:**

1) With additional microwave heating of plasma at the GDT facility, an electron temperature of 900 eV was attained, which is a record value for quasi-stationary magnetic traps of open type.

2) An analytical solution to the three-dimensional Pierce problem was obtained for the first time.

3) Calculations of tungsten resistance to mechanical destruction in pulsed heat loads were done <u>for the first time</u> with due account of development of plastic deformation.

4) <u>For the first time</u>, a high-current surface-plasma source of negative ions with active control of the temperature of the grid system and distributed supply of cesium on the surface of large area emitter was created. An H-ion beam was generated with a current of about 1 A and energy of 86 keV in pulses of up to 8 seconds.

5) A <u>new</u> method of longitudinal confinement of plasma in linear open traps was created. It is based on active control of plasma flow via its rotation in a spirally-corrugated magnetic field.

In the field of **the physics and technology of charged particle accelerators, SR sources and FELs:**

1) <u>Unique</u> accelerating wide-band RF stations on the basis of new amorphous magnetic materials were designed, manufactured and delivered to JINR (Dubna) for the booster of the collider NIKA.

2) A <u>new</u> source of electrons with large average current on the basis of RF resonator with a grid-controlled hot cathode for the specialized accelerator at VNIIEF (Sarov) was designed, manufactured and successfully tested.

3) A first commercial electron accelerator ILU-14 with a unique set of parameters (beam energy of up to 10 MeV and beam power of up to 100 kW) was commissioned at Burnazyan Federal Medical Biophysical Center of the FMBA of Russia for development of new radiation technologies.

4) A <u>new</u> system for suppression of secondary processes in an accelerating tube was developed and successfully implemented. It enabled <u>one-order</u> reduction in the time required for attaining the design parameters at the electron accelerator ELV.

5) A <u>unique</u> method of separation of pure radiocarbon beam was developed. As a result, statistical accuracy of concentration measurement better than 1% was attained at the accelerator mass spectrometer at the shared–equipment SB RAS Center "Geochronology of Cenozoic".

6) A <u>unique</u> magnetic equipment for the ion synchrotron for cancer therapy MEDAUSTRON (Austria) was designed and manufactured. A therapeutic beam with design parameters will be generated soon.

7) <u>For the first time</u>, a scale effect was revealed in the research on the dynamics of formation of detonation diamonds using hard SR (LIH SB RAS, ISSCM SB RAS, BINP SB RAS, and VNIITF).

8) An ellipsometer using frequency-tunable terahertz radiation of free electron laser was tested and upgraded (BINP SB RAS, ISP SB RAS, Institute of Internal Medicine SB RAMS, and Institute of Molecular Biology and Biophysics of the Academy of Medical Sciences).

By decree 402 from June 4, 2014, the President of the Russian Federation awarded the Order of Friendship to RAS member Gennady Kulipanov.

Aleksandr Yurevich Vlasov and Leonid Vasilievich Kardapoltsev became winners of the Novosibirsk mayor's office contest for grants to young scientists and specialists in the field of innovation activity in 2014.

The three Thesis Boards of the Institute, which are entitled to accept Doctor of Sciences (Candidate of Sciences) theses, continued their work in 2014. 5 meetings of the Boards took place, at which 2 Doctor of Sciences theses and 3 Candidate of Sciences theses were defended.

Over 50 tours of the BINP facilities were conducted for school pupils, students, school and university teachers, members of other organizations and guests of the Institute, in total about 2,000 people. Lectures were delivered at Novosibirsk schools.

1
PARTICLE PHYSICS

1.1. CMD-3 DETECTOR

Fig. 1.1.1 shows a photo of the CMD-3 detector in the experimental hall of VEPP-2000.

Fig. 1.1.1. CMD-3 detector in experiment hall of VEPP-2000.

In 2014 the CMD-3 detector systems were upgraded and prepared for work on the renovated VEPP-2000 complex with increased luminosity.

The wires of the drift chamber were checked. Breakdowns and short circuits revealed were fixed. Currently, 99.2% of the wires are in working condition. A system of control and registration of breakdowns was designed, fabricated and installed on the detector. The system will significantly improve the reliability of the chamber. The composition of the gas mixture was also thoroughly selected.

The Z chamber of the detector was renovated in 2014. The chamber was designed in 1988 - 1991 and reliably worked in 1991 - 2000 with the CMD-2 detector and in 2010 - 2013 with the CMD-3 detector. Comparison of the new electronics of the Z chamber with the KLYUKVA standard electronics, which was used in the chamber until 2013, demonstrated that the new electronics 1.5 times improved the coordinate resolution.

The CMD-3 detector has a unique electro-magnetic calorimeter, the cylindrical part of which consists of a liquid-xenon calorimeter and a CsI crystal calorimeter. The end part of the calorimeter is made on the basis of crystals of bismuth orthogermanate ($Bi_4Ge_3O_{12}$). The thickness of the calorimeter both in the end and in the cylindrical part is about 13 radiation lengths. In 2014, a procedure was developed for joint calibration of all parts of the calorimeter. Much was done for creation of algorithms for linking of clusters in different parts of the calorimeter in a single cluster. Corrections for photon energies measured in the calorimeter were identified.

During testing of the calorimeter in 2014, non-linear effects in the calorimeter electronics were revealed, which showed up differently in different components of the system. It was decided to upgrade the calorimeter electronics to eliminate these non-linearities.

New time-of-flight counters were installed on the CMD-3 detector. This system, which was created in collaboration with scientists from the Institute of Theoretical and Experimental Physics (Moscow), is made on scintillator plates that collect light using silicon photomultipliers. The time resolution obtained with the prototype system is 0.8 ns, as shown in Fig.1.1.2.
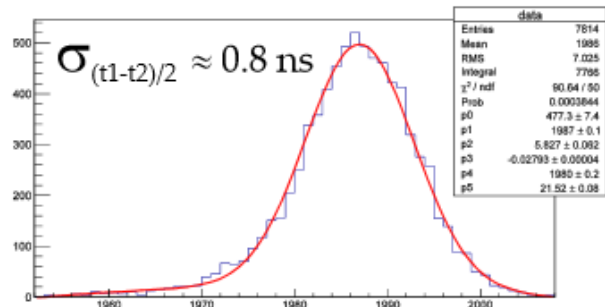
Fig.1.1.2. Distribution by difference in time of signal arrival at opposite ends of time-of-flight counter.

The new system is more reliable and has more channels. The electronics for it is being produced now.

In 2014, the electronics of the data acquisition system of the CMD-3 detector were completely replaced with a new in-house system. The standard developed uses up-to-date architecture and circuit design; data exchange is performed on the basis of simple and quick data transfer protocol. As a result, the dead time of the data acquisition system was reduced to about 50 μs, which corresponds to the requirements of operation at a VEPP-2000 luminosity of 10^{32} cm^{-2}s^{-1}. The electronics of the liquid-xenon calorimeter of the CMD-3 detector will be replaced in 2015.

The system for offline processing of data from the CMD-3 detector was optimized in 2014. As a result, the number of simultaneously processed runs was doubled (up to 732). That enabled complete processing of all data collected with the detector (37 TB in disks) within two days. In 2014, the analysis of earlier acquired data took about one million CPU hours.

The data collected with the detector in 2011-2013 were under intense analysis in 2014. The development and optimization of the procedure for determination of integrated luminosity made great progress. The integrated luminosity values obtained from events of electron-positron scattering and from $e^+e^- \to \gamma\gamma$ events coincide with an accuracy of fractions of percent, as shown in Fig. 1.1.3. This demonstrates the high systematic accuracy of the determination of the quantity that is critical for precision measurements.
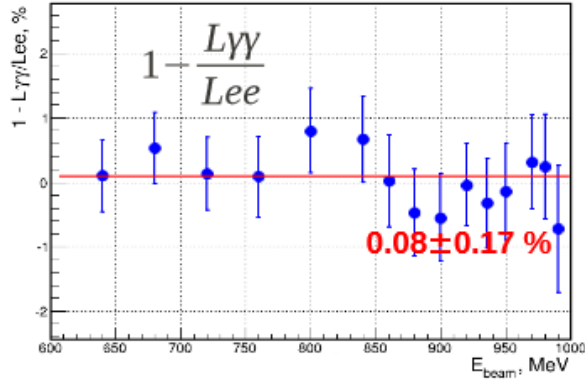
Fig.1.1.3. Comparison of integrated luminosities determined at energy points of season 2012 from events of e+e- scattering and $e^+e^- \rightarrow \gamma\gamma$ events.

In addition, a search for direct production of the η' meson was performed, based on data collected in 2013 with the CMD-3 detector at an energy of 958 MeV in the center of mass system. This process goes as a result of annihilation of two photons, and if both the photons are real, the theory predicts the process probability to be about BF($\eta' \rightarrow e^+e^-$) = 3.7x10^{-11}. However, if at least one of the photons is virtual or if the dynamics of the production process is more complicated, this probability can be several orders of magnitude higher.

As a result of this analysis, no one event of direct production of the η' 'meson was found and the upper limit of B($\eta' \rightarrow e^+e^-$) < 1.2x10^{-8} was set at a 90% confidence level. This value is 20 times less than the same result obtained earlier with the ND detector.

Investigation into the $e^+e^- \rightarrow \phi(1020)\eta$ process was started, when the $\phi(1020)$ decays into a pair of charged kaons, and the η mezon is searched for in the mass spectrum of recoil to K^+K^-. Fig. 1.1.4 shows a preliminary section of the process obtained on CMD-3 detector (points without horizontal errors) in comparison with the results of the BaBar experiment.
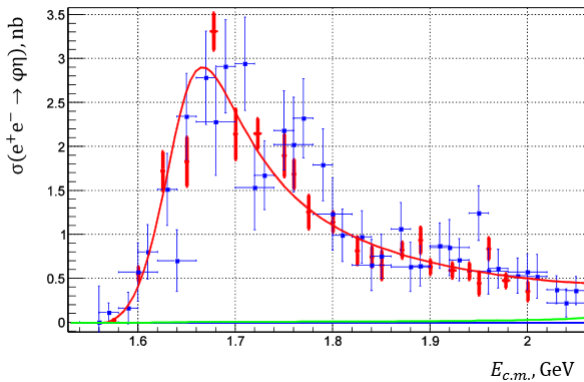
Fig. 1.1.4. $e^+e^- \rightarrow \phi(1020)\eta$ preliminary section as obtained on CMD-3 detector (points without horizontal errors) in comparison with results of BaBar experiment.

1.2. THE SND DETECTOR

1.2.1. The main developments in 2014.

In 2014 the reconstruction of the VEPP-2000 complex was continued which, according to the plans will lead to an increase in luminosity of about 40 times. At the SND detector the modernization process is ongoing whose main objective is to secure an ability of the modernized detector to record and process the experimental data under the expected increase of the collider luminosity. During the year, analysis of the experimental data collected in the 2010-2013 period was continued.

1.2.2. Detector status.

Work is being completed on the production of the second copy of the SND tracking system (TS) (Fig.1.2.1), which is expected to decrease the mutual interference between the cathode strips and, therefore, improve the rate capacity of the system. Pinout of the high voltage crosses at the ends of the chamber is finished, flange-mounted intermediate boards to pick-up signals from the anode wires and from the cathode strips are installed. Cables for connecting the tracking system to the SND front-end electronics were manufactured.
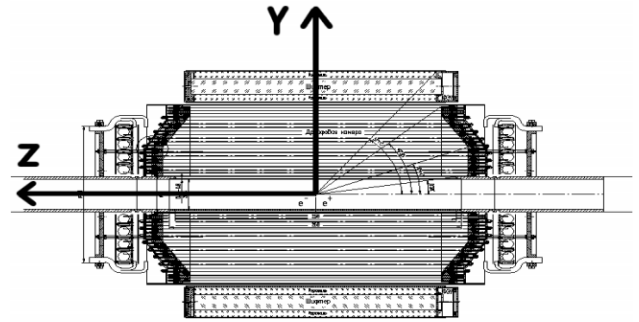
Fig. 1.2.1. SND Tracking system.

The main part of the SND detector is a calorimeter consisting of 1640 scintillation counters, based on NaI(Tl) crystals. The significant problem of the calorimeter operation is a failure of charge-sensitive preamplifiers and phototriodes with a rate of about 8 channels per year (0.5%/year). Repair is required in every 2-3 years. To improve maintainability of the calorimeter channels, new electronics was developed. In 2014, the replacement of

the electronics was completed and tests of the calorimeter by cosmic rays were conducted.

To increase the rate capacity of the SND data acquisition system (DAS) it is necessary to decrease the dead time of electronics and increase the bandwidth of DAS. Dead time of SND electronics is conditioned by special implementation of signal digitizing boards in the KLUKVA standard. The main contribution to the dead time comes from the calorimeter digitizing boards (40 μs) and from the read-out of the digitized data via KLUKVA bus (about 75 μs). In previous experiments, the total dead time of SND electronics was 122 μs, which corresponds to the dead time up to 10% at loadings up to 1 kHz.

Gradual transition from the readout of the electronic boards via KLUKVA bus to their readout via Ethenet is planned. KLUKVA will be used just as a carcass construction. The first step in this direction was a development of new electronic boards for TS cathode strips. The new board for cathode strips contains 24 channels of 12-bit flash ADC. The readout takes place via TCP/IP protocol. The maximum readout speed is about 40 Mb/s. This will reduce the dead time of electronics up to 90 μs and increase the loading capacity of electronics by about 2 times.

To increase loading capacity of the SND DAQ system, work is conducted to organize a network with sufficient bandwidth to read fragments of events via new network interfaces of digitizing electronics. The network power is gradually increasing as more and more electronics are being integrated in the network. At the first stage a network was organized to read the new drift chamber strips cards separately from the rest of the electronics. Moreover, the power of corresponding computer subsystem is increasing.

In 2014 a new farm was assembled from 8 servers of the type HP ProLiant DL380e Gen8: motherboard Supermicro X9DRD-iF with two 6-core processors Intel Xeon CPU E5-2620 with hyperthreading (12 thread/ processor). The farm configuration is controlled via the centralized control system Puppet. On the farm it is planned to combine data readout and event building with software algorithms for event selection.

1.2.3. Software Status

A prototype of the readout program incorporating new electronics modules was developed. At present, the prototype is being tested and works for its integration into the DAQ system is carried out. Major changes in the software (SW) is associated with the necessity to read date from the new electronics modules and to build events from heterogeneous sources (KLUKVA and new electronic boards). In the future plans there are a deep parallelization of the readout program and a gradual migration of some components of the trigger from the hardware electronics into software.

Major changes in the software of the data processing system are the following: a new track extraction algorithm was incorporated (histograming method for pairs of points) with more accurate calibration used; MC simulation became more realistic. New calibration methods were developed to determine absolute position and orientation of the calorimeter and the position of the interaction point with regard to the tracking system. With the help of the proportional chamber, absolute calibration of the drift chamber was performed. A set of new calibrations were developed for Cerenkov counters (ChC). Accumulated experimental events (seasons 2010, 2011, 2012, 2013) were reprocessed with the use of the new software and calibration.

A new MC simulation was performed by taking into account the calibrated calorimeter and interaction point positions and the developed calibrations of ChC. The realistic (calibrated) refractive indices in ChC are used. Particles energy depositions in the calorimeter are adjusted, as well as the amplitudes in the proportional chamber, the effect of the amplitude saturation in the drift chamber is taken into account, thresholds of the muon system are more accurately specified. Primary generators were developed to simulate a birth of particles at rest to study η and η' production.

1.2.4. SND data analysis.

Analysis of the process $e^+e^- \to \pi^+\pi^-\pi^0$ is completed and the corresponding article is submitted to ZhETP. On Fig.1.2.2 the measured cross section of the process is shown together with the data from previous experiments: SND at VEPP-2M and BABAR. The results on the cross section are consistent with the measurements of SND at VEPP-2M and with the BABAR experimental data. Today it is the most accurate measurement of this cross section. Two maxima in the cross section correspond to resonances ω(1450) and ω(1680). Their contributions interfere with the contributions from ω(782) and Φ(1020) mesons and among themselves. $e^+e^- \to \pi^+\pi^-\pi^0$ is the only reaction in which the ω(1450) resonance is seen. Above 1.8 GeV contributions of the known resonances is not enough to describe the measured cross section.
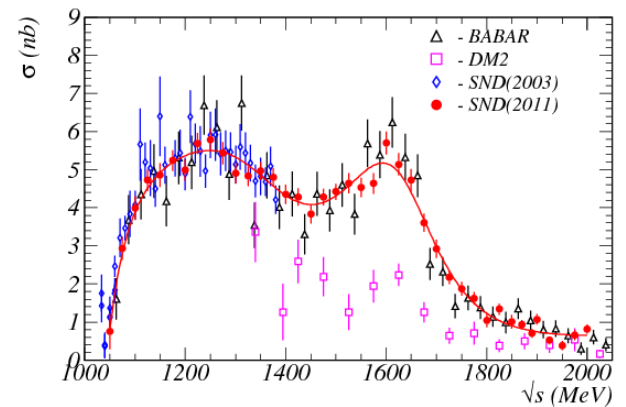
Fig. 1.2.2. Cross section of the process $e^+e^- \to \pi^+\pi^-\pi^0$.

An article was prepared based on the analysis of the process $e^+e^- \to \pi^+\pi^-\eta$ and it was submitted to the journal Phys. Rev. D (arXiv:1412.1971). It is usually assumed that the reaction is dominated by an intermediate state $\rho^0(770)\eta$. Fig. 1.2.3. shows the experimental (points with errors) and simulated (the histogram) in the hypothesis of the $\rho^0(770)\eta$ intermediate state distributions over the two-pions invariant mass. It is evident that there is a contribution from an another mechanism, supposedly from $\rho^0(1450)\eta$, in this reaction.
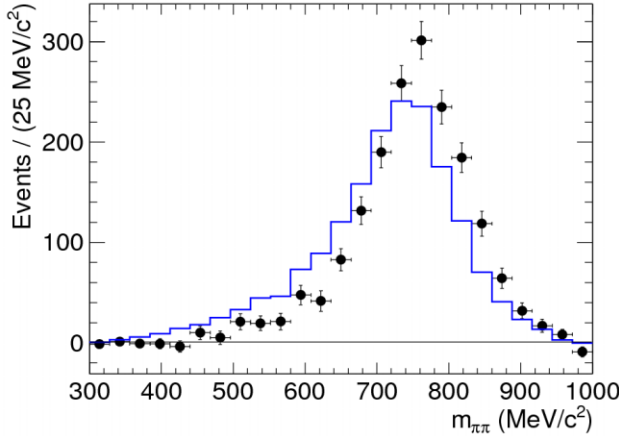
Fig. 1.2.3. The distribution over the invariant mass of two pions.

The cross section of the process $e^+e^- \to \pi^+\pi^-\eta$ is shown in Fig. 1.2.4. The measured cross section is consistent with the experimental data from BABAR, but has better accuracy. The cross section is dominated by the contribution of the $\rho(1450)$ resonance. Contribution from the $\rho(1700)$ resonance is small.
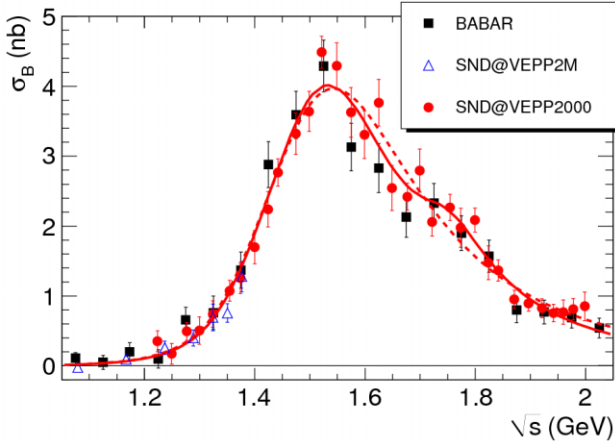
Fig. 1.2.4. Cross section of the process $e^+e^- \to \pi^+\pi^-\eta$.

When approximating the cross section the following result was obtained:

$$B(\rho' \to e^+e^-)B(\rho' \to \pi^+\pi^-\eta) = (4.3 \pm 1.1)\times10^{-7}.$$

From a comparison with other decay channels of the $\rho(1450)$ resonance it was obtained that

$$B(\rho' \to \omega\pi) : B(\rho' \to \pi^+\pi^-\eta) : B(\rho' \to \pi^+\pi^-) =$$

$$(12.3 \pm 3.1) : 1 : (1.3 \pm 0.4).$$

The predictions for these ratios in different models vary in the following ranges: (7 - 8): 1: (4 - 10). It can be seen that there is a poor agreement between the theory and experiment for the decay $\rho' \to \pi^+\pi^-$. According to the conserved vector current hypothesis (CVC), the same hadronic current is involved in the decay $\tau \to \eta\,\pi^-\pi^0\,\nu_\tau$ and in the reaction $e^+e^- \to \pi^+\pi^-\eta$. The decay probability

$$B_{CVC}(\tau \to \eta\,\pi^-\,\pi^0\,\nu_\tau) = (0.156\pm 0.011)\%$$

calculated within this hypothesis using the results of the SND experiment agrees well with the measured value

$$B_{exp}(\tau \to \eta\,\pi^-\,\pi^0\,\nu_\tau) = (0.139 \pm 0.010)\%.$$

Preliminary results were obtained in the study of the process $e^+e^- \to K^+K^-$. Events were selected using the Cherenkov counter. Fig. 1.2.5 shows the spectrum of the energy deposition in the calorimeter for events with two collinear tracks provided that one of the particles have not triggered the Cherenkov counter. Process $e^+e^- \to e^+e^-$ is suppressed by this condition 300 times.
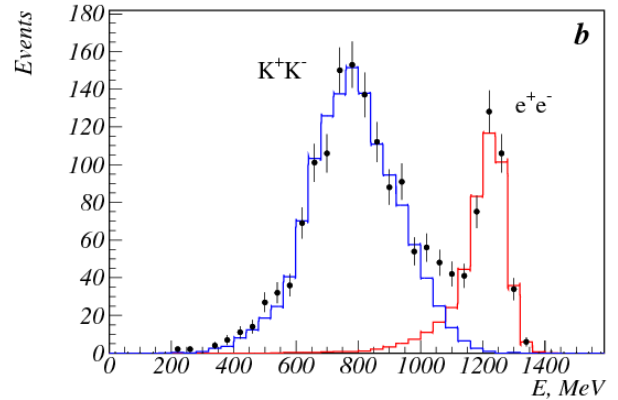
Fig. 1.2.5. The spectrum of the energy deposition in the calorimeter for events with two collinear tracks provided that one of the particles have not triggered the Cherenkov counter.

Fig. 1.2.6 shows the preliminary results of measurements of the total cross section of the process $e^+e^- \to K^+K^-$.
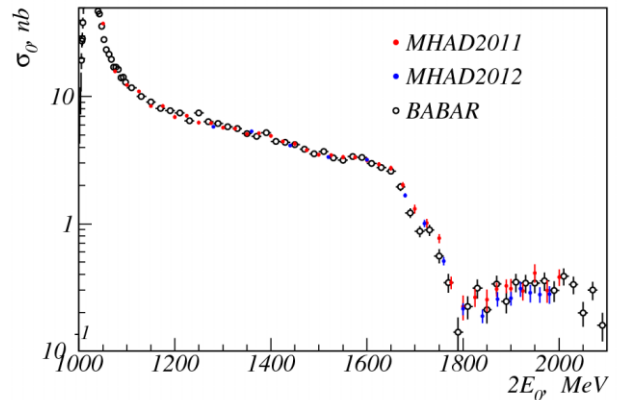
Fig. 1.2.6. Cross section of the process $e^+e^- \to K^+K^-$.

Our results are consistent with the BABAR experimental data and have a comparable accuracy. The measured cross section has a complex structure.

Fig. 1.2.7 shows the preliminary results of the cross section measurements for the process $e^+e^- \to$ p anti-p based on the 2011 and 2012 scans.
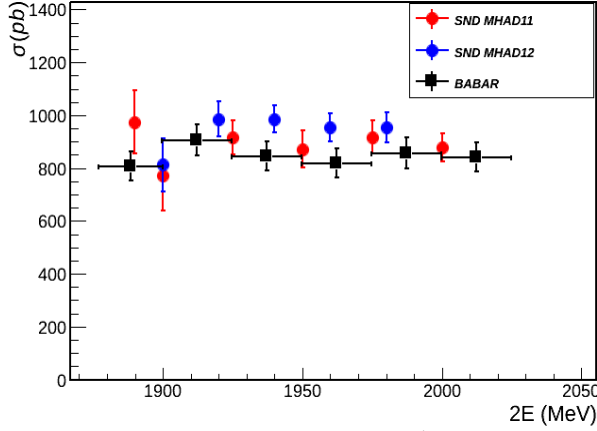
Fig. 1.2.7. Cross section of the process $e^+e^- \to$ p anti-p.

The cross section is almost constant near the threshold, even though it was natural to expect its falling as $\beta = (1-4m_p^2/s)^{1/2}$. Fig. 1.2.8 shows the measured angular distribution of protons. When approximating the distribution, the following form factors ratio was obtained $|G_E/G_M|=1,64\pm0,26$. We confirm the BABAR result that the $|G_E/G_M|$ ratio near the threshold is significantly different from unity. This result is unexpected since at the threshold $G_E = G_M$.
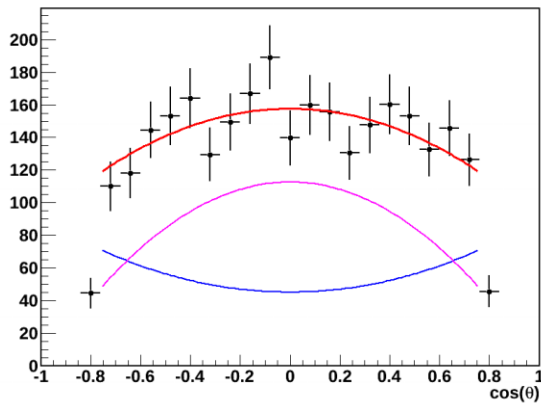
Fig. 1.2.8. Polar angle dependence of the $e^+e^- \to$ p anti-p process cross section.

Results on the process $e^+e^- \to$ n anti-n obtained in 2014 were published as a scientific article (Phys. Rev. D 90, 112007). Fig. 2.1.9 shows the measured cross section. It can be seen that the $e^+e^- \to$ n anti-n cross section is constant and up to the errors coincides with the proton cross section, which is in contradiction with the naive quark model prediction based on the quark charge values: $\sigma_p/\sigma_n = 4$.

From the equality of the neutron and proton cross sections it follows that the processes $e^+e^- \to$ N anti-N are dominated either by isoscalar (I = 0), or by isovector (I = 1) amplitudes. Possible reasons for such a behavior of the cross section can be either subthreshold resonance or the final state interactions. Fig. 1.2.10. shows the measured form factors of n anti-n (SND) and p anti-p (BABAR). It is evident that the neutron and proton form factors are equal near the threshold.
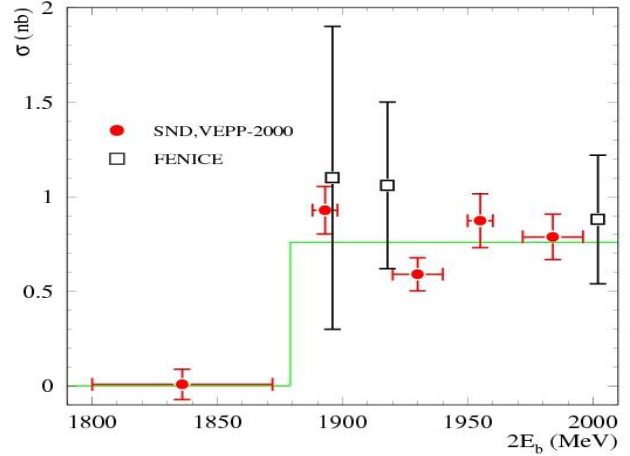
Fig. 1.2.9. Cross section of the process $e^+e^- \to$ n anti-n.

The problem of equality of the neutron and proton cross sections was investigated in the article V. F.Dmitriev, A.I.Milstein, S.G.Salnikov Phys.Atom.Nucl. 77 (2014) 1173. It was shown that the N anti-N potential provides an attraction when I = 0 and repulsion when I = 1, and the predicted energy behavior of the $e^+e^- \to$ p anti-p cross section reproduces the shape of the experimental cross section from the threshold up to 2E=2.2 GeV.

In the article A.E. Obrazovsky, S.I. Serednyakov JETP Lett. 99 (2014) 363 the energy dependance of the cross section of the isovector processes $e^+e^- \to 3(\pi^+\pi^-) + 2(\pi^+\pi^-\pi^0)$ was studied. It was shown that in the total cross section $e^+e^- \to hadrons$ emergence of the process $e^+e^- \to$ N anti-N fully compensates a negative discontinuity in the cross section of the processes $e^+e^- \to 3(\pi^+\pi^-) + 2(\pi^+\pi^-\pi^0)$ (Fig.1.2.11). No other discontinuities of comparable magnitude are observed near the N anti-N threshold in cross sections of other processes.
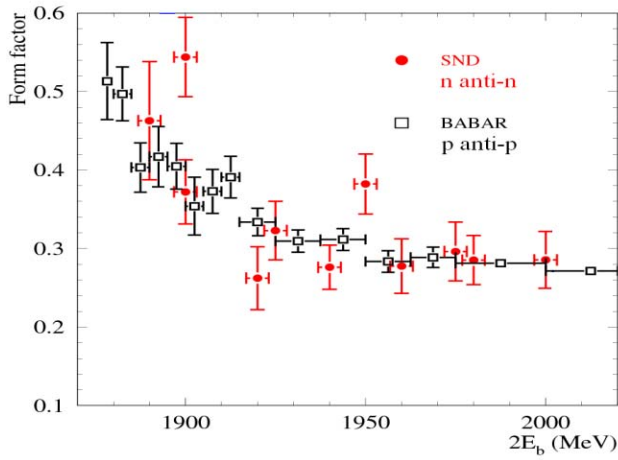
Fig. 1.2.10. The measured form factors of n anti-n (SND) and p anti-p (BABAR).
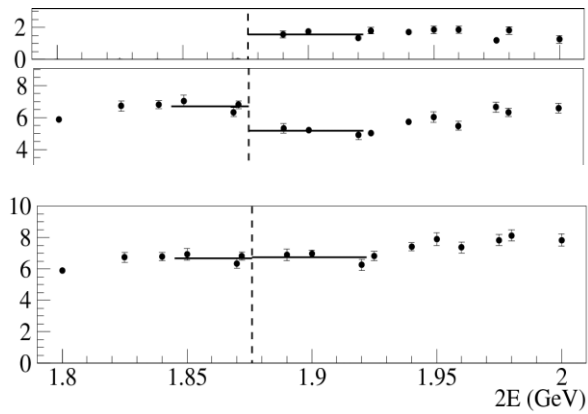
Fig. 1.2.11. The top graph shows the sum of p anti-p and n anti-n cross sections, the middle graph is the 6π cross section and the bottom graph is the sum of the cross sections p anti-p, n anti-n and 6π. Cross sections are given in nb.

18

1.3. DETECTOR KEDR

The KEDR detector is a universal magnetic detector working on the e^+e^- collider VEPP-4M in the energy range from 2 to 11 GeV in the center of mass system. The detector includes a system for detection of scattered electrons for study of the $\gamma\gamma$ physics and a luminosity monitor. Parameters of the detector are similar to those of the world's best detectors operating in this energy range.

A pilot run was started in May 2014. The purpose of the experiment is measurement of R in the CMS in the beam energy range of 3.08-3.72 GeV. This energy range was already scanned in 2011; the preliminary results of the measurements of R will be reported below. Additional statistics with the upgraded detector will lower the level of systematic errors.

It was planned to collect integrated luminosity at 7 energy points with an increment of 50 MeV. To account for radiative corrections by subtraction of the resonance contribution, it is necessary to perform scanning of J/ψ and $\psi(2S)$ at 5 points each. In 2014, an integrated luminosity of about 1.3 pb^{-1} was collected at 6 points. Collection of statistics to measure R will be continued in 2015.

Research on decays of J/ψ to two charged hadrons and a photon was started. Although the $J/\psi \rightarrow \pi^+\pi^-\gamma$ and $J/\psi \rightarrow K^+K^-\gamma$ processes have been observed in a number of experiments with considerable statistics, their inclusive branchings were not measured; only the contributions from different resonances to them were registered. The KEDR detector enables first measurements of the inclusive branchings of $J/\psi \rightarrow \pi^+\pi^-\gamma$ and $J/\psi \rightarrow K^+K^-\gamma$ and significant improvement in the accuracy of measurement of $J/\psi \rightarrow p\bar{p}\gamma$. The separation will be performed with a system of aerogel Cherenkov counters. The system was installed in the detector in 2013. Statistics of about 100 nb^{-1} were collected, and thus the treatment of these processes can be started.

1.3.1. Results of work of KEDR detector on collider VEPP-4M in 2014

The statistics collected on the collider VEPP-4M in the KEDR experiment were under processing in 2014. Below are summarized the main results.

– The result of direct measurement of $\Gamma_{ee}\Gamma_{\mu\mu}/\Gamma\, of\, \psi(2S)$ meson was published.

– Research on the $J/\psi \rightarrow \gamma\eta_c$ process was completed.

– A preliminary measurement of R by data of year 2011 was carried out.

– Research on the $J/\psi \rightarrow \pi^+\pi^-\gamma$ and $J/\psi \rightarrow K^+K^-\gamma$ decays was started.

Below is given a description of these works in more detail.

1.3.2. Measuring $\Gamma_{ee}\Gamma_{\mu\mu}/\Gamma$ of $\psi(2S)$ meson

A direct measurement of the product of the leptonic width by the probability of $\psi(2S)$ meson decay to a pair of muons was carried out, and the following result was obtained:

$\Gamma_{ee}\Gamma_{\mu\mu}/\Gamma = (19.4 \pm 0.4 \pm 1.1)$ eV.
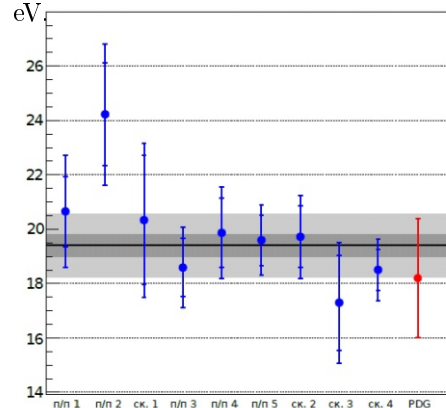
Fig. 1.3.1. Comparison of $\Gamma_{ee}\Gamma_{\mu\mu}/\Gamma$ obtained in different experiments. The position of the band and its width are in agreement with the worldwide average value and uncertainty of the $\Gamma_{ee}\Gamma_{\mu\mu}/\Gamma$ by PDG data.

The accuracy of the result (Fig.1.3.1) is about two times better than the worldwide average one, which is calculated as the product of $\Gamma_{e^+e^-}$ and $B_{\mu\mu}$.

1.3.3. Measurement of probability of $J/\psi \rightarrow \gamma\eta_c$ decay and parameters of η_c meson on KEDR detector.

The radiative magnetic dipole transition $J/\psi \rightarrow \gamma\eta_c$ noticeably shows up among the known radiative transitions between the levels of charmonium. On the one hand, the probability of its decay can be easily calculated using potential models. In the nonrelativistic approximation, this probability is independent on the potential model, since the transition matrix element is determined by the overlap of the wave functions of the initial and final states, which are the same for this transition between the 1S levels in charmonium, and therefore the transition matrix element is equal to unity. From calculation without including the relativistic corrections, the relative probability of the decay is estimated as $B(J/\psi \rightarrow \gamma\eta_c) = 3.05\%$. It can be assumed that relativistic corrections to this value, as well as to electric dipole transitions in charmonium, will be of the order of $(v/c)^2 \approx 20 - 30\%$, where v is the

characteristic velocity of the c quark in charmonium, and c is the velocity of light. Numerous calculations with due account of the relativistic corrections confirm this. On the other hand, experimental values for this probability are markedly different from predictions. In 1986, the Crystal Ball group performed a measurement in the inclusive spectrum of photons and obtained a value of $B(J/\psi \to \gamma\eta_c) = (1.27 \pm 0.36)\%$. In 2009, the CLEO group measured the probability of this transition by analysis of the spectra of photons for several exclusive channels of decay of η_c. The resulting value $B(J/\psi \to \gamma\eta_c) = (1.98 \pm 0.09 \pm 0.30)\%$ is closer to the theoretical predictions, but still is in poor agreement with the latest, most accurate calculations by the lattice QCD techniques, which give the value $B(J/\psi \to \gamma\eta_c) = (2.84 \pm 0.12)\%$. Thus, for a given decay there is an evident discrepancy in the theoretical predictions and experimental data, whereas for other radiative transitions in charmonium the theory and experiment are in good agreement.

In 2013-2014, the KEDR detector of accelerator complex VEPP-4M was used for a new measurement of the probability of this decay, as well as mass and width of the η_c- meson. The measurement was performed using the statistics gathered in 2007-2009. The luminosity integral accumulated was $1.5\ pb^{-1}$ in the peak of the J/ψ meson, which corresponds to approximately $6 \cdot 10^6$ produced J/ψ.
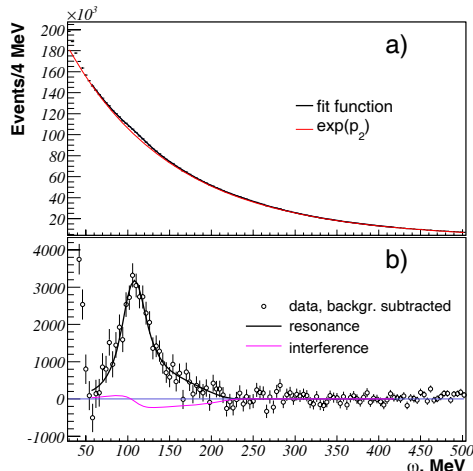
Fig. 1.3.2. Top: inclusive spectrum of photons in the decay $J/\psi \to \gamma\eta_c$. Bottom: spectrum after subtraction of the substrate.

The data analysis was performed in the inclusive spectrum of photons with due account of the asymmetry of the photon line and interference with non-resonant substrate. Fig. 1.3.2. shows the inclusive photon spectrum and its fit with the sum of the signal and the substrate. The signal is of the shape of $d\Gamma/d\omega \sim \omega^3 f(\omega) BW(\omega)$, where ω is the photon energy; $BW(\omega)$ is the Breit-Wigner function; $f(\omega)$ is the correction function, which is approximately equal

to unity near the resonance. Due to the factor ω^3 and since the η_c meson is rather wide (the ratio of the width to the transition energy is $\Gamma/\omega_0 \sim 30$ MeV/114 MeV $\sim 1/4$), the line shape in this decay is markedly different from the Breit-Wigner one. In addition, there is a noticeable spectrum «tail» at high photon energies, which leads to a large model uncertainty in the measurement of the decay branching. Therefore, it is more convenient to measure another quantity that characterizes the transition rate and has a small model error, i.e. the partial width of the decay in the narrow resonance limit. It is determined mainly by the height of the resonance and weakly depends on the «tail» of the spectrum.

The data analysis yielded the following values for the mass and width of η_c meson:

$$M_{\eta_c} = \left(2983.5 \pm 1.4^{+1.6}_{-3.6}\right) \text{MeV}/c^2,$$

$$\Gamma_{\eta_c} = \left(27.2 \pm 3.1^{+5.4}_{-2.6}\right) \text{MeV}.$$
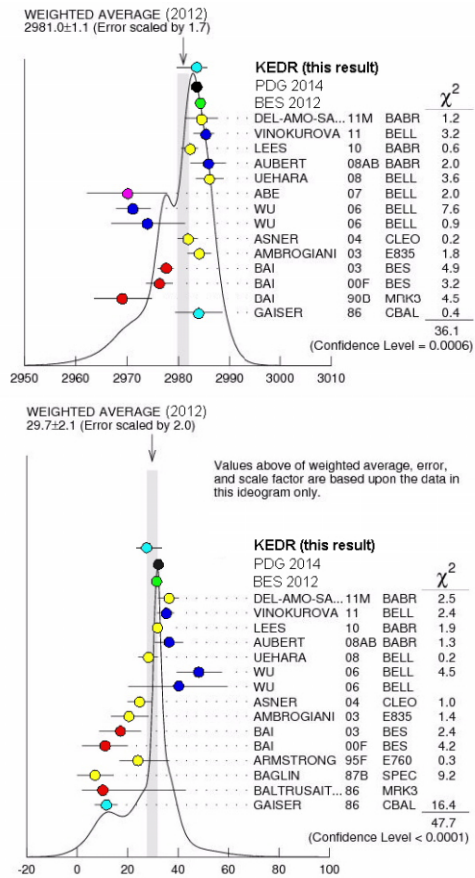
Fig. 1.3.3. Comparison of results of KEDR detector measurements of mass (top) and width (bottom) of η_c meson with results of other experiments.

Within the measurement error, these values are consistent with worldwide average values. Fig. 1.3.3. shows these results in comparison with those obtained by other groups in decays of J/ψ mesons and B

mesons and $\gamma\gamma$ and $p\bar{p}$ collisions. The MARK3 and BES groups also performed measurements in decays of J/ψ, but the resonance in the spectrum was fitted with just the Breit-Wigner curve, without including the factor ω^3. As a result, the weight values obtained were underestimated by about 4-5 MeV. In the experiment by the Crystal Ball group, the above factor was taken into account, and the mass value obtained agrees well with the latest most accurate measurements.

For the partial width of the decay $J/\psi \to \gamma\eta_c$ in the narrow resonance limit, the following value was obtained:

$$\Gamma^0_{\eta_c} = 2.98 \pm 0.18^{+0.15}_{-0.33} \text{ keV}.$$
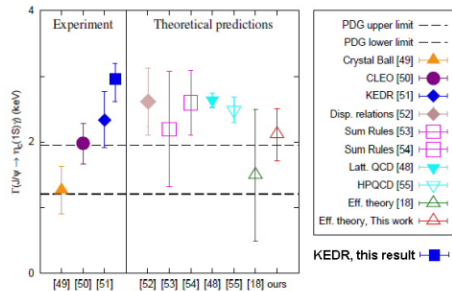
Fig. 1.3.4. Partial decay width $J/\psi \to \gamma\eta_c$ in narrow resonance limit.

Fig. 1.3.4. shows this result in comparison with the results of previous measurements by Crystal Ball, CLEO, and KEDR (2010), as well as with theoretical calculations. Our result lies significantly higher than previous measurements by Crystal Ball and CLEO, but is in good agreement with recent calculations based on lattice QCD.

1.3.4 Measurement of R at KEDR

The quantity R is defined as the ratio of the total hadronic cross section in electron-positron annihilation to the theoretical cross section of $\mu\mu$ production. R measurements are critical for determination of the anomalous magnetic moment of the muon $(g-2)_\mu$ and the value of the running constant of fine structure.

It should be noted that systematic errors dominate in all experiments on measurement of R in the energy region between J/ψ and $\psi(2S)$. Thus this is a good motivation for new experiments on the precise measurement of R in this energy range.

In 2011 the region of the J/ψ and $\psi(2S)$ resonances was scanned in the KEDR experiment with an integrated luminosity of about 1.4 pb^{-1}.

Analysis was performed with subtraction of the «tails» of the J/ψ and $\psi(2S)$ resonances from the cross section. The vacuum polarization was calculated without the contribution of these resonances. Such background physical processes as $\mu\mu$ and $\tau\tau$
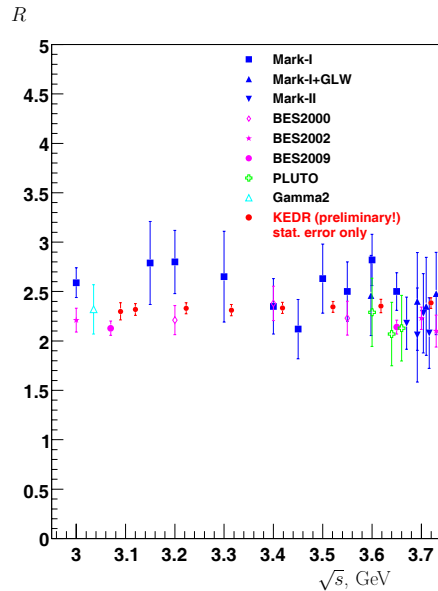
Fig. 1.3.5. Summary of R values at energies 3.1-3.7 GeV and preliminary KEDR results

production and two-photon production of hadrons were taken into account.

$$R = \frac{\sigma_{obs}(s) - \sum \epsilon^{tail}_\psi(s)\sigma^{tail}_\psi(s) - \sum \epsilon^i_{bg}(s)\sigma^i_{bg}(s)}{\epsilon(s)(1 + \delta(s))\sigma^0_{\mu\mu}} \quad (1)$$

where $\sigma_{obs}(s) = \frac{N_{mh} - N_{res.bg.}}{\int \mathcal{L}dt}$; N_{mh} represents all events that passed the multi-hadron selection criteria; $N_{res.bg.}$ is the residual machine background; $\epsilon(s)$ is the hadron efficiency. The code for multihadronic generation was kindly provided by the BES collaboration.

$\sum \epsilon^{tail}_\psi(s)\sigma^{tail}_\psi(s)$ is the contribution from the J/ψ and $\psi(2S)$ resonances; $\sum \epsilon^i_{bg}(s)\sigma^i_{bg}(s)$ is the contribution from physical processes $e^+e^- \to l^+l^-$ and $\gamma\gamma$.

$$1 + \delta(s) = \int dx \frac{\mathcal{F}(s,x)}{\left|1 - \Pi_0(s(1-x))\right|^2} \frac{R(s(1-x))\epsilon(s(1-x))}{R(s)\epsilon(s)},$$
$$(2)$$

where $\mathcal{F}(s,x)$ is the probability of loss of the x component in the invariant s during emission in the initial state. The vacuum polarization Π_0 does not include the J/ψ and $\psi(2S)$ resonances.

Our preliminary results presented in Fig. 1.3.5. The major sources of the systematic uncertainty are listed in Table 1.3.1.

The following sources of systematic uncertainty have been considered for the R measurement at each energy point: luminosity, radiative corrections, primary modeling of multi-hadron events, detector response, and residual background from the accelerator.

Table1.3.1. Main systematic uncertainties in R value.

Source	Error,%
Luminosity measurement	1.0-2.0
Simulation	3.0-3.5
Radiative correction calculation	1.0
Detector response	1.0
Accelerator residual background	1.0
Sum in quadrature	3.6-4.4

A preliminary result of R measurements in the energy range of 3.1-3.7 GeV was presented. To improve R precision we plan to take additional data at the $J/\psi - \psi(2S)$ energy during 2014.

Conclusion

1.4. CRYOGENIC AVALANCHE DETECTORS

Earlier, the direction of cryogenic avalanche detectors (CRAD) was described in BINP reports within the subsection of microstructured gas detectors. In 2014, this topic was separated in a section. The following work was being done in 2014:

1) development of two-phase cryogenic avalanche detectors (CRADs) based on thick GEMs (THGEMs) for low-background experiments on search for dark matter and detection of coherent scattering of neutrinos on nuclei;

2) measurement of the ionization yield of recoil nuclei in liquid Ar using a two-phase CRAD and a neutron generator for solving the task of energy calibration of dark matter detectors;

3) participation in the international collaboration RD51 (CERN) on the development of microstructured gas detectors.

The main groundwork in the area of CRADs was done at the Joint Laboratory for Cosmology and Elementary particles at the Physics Department of the Novosibirsk State University and BINP. The Laboratory was created in 2011-2014 under the NSU Megagrant. The key target of experiments performed by the Laboratory is development of new methods for detection of recoil nuclei for experiments on search for dark matter and detection of coherent scattering of neutrinos on nuclei via development of two-phase liquid-Ar CRADs of ultimate sensitivity. The equipment of the laboratory is placed at BINP. In 2014, the cryogenic vacuum systems of the dark matter detector under development were equipped with all components; the systems for charge and optical reading of signals and reading electronics were partially equipped.

Fig. 1.4.1 shows a schematic diagram of two-phase CRAD in Ar for search for dark matter and coherent scattering of neutrinos. The ultimate goal of this project is to develop new methods of dark matter registration using two-phase GEM-based CRADs of ultimate sensitivity in Ar and Xe. The method is based on amplification of extremely weak signals from recoil nuclei originating in the cryogenic fluid from the scattering of dark matter particles. The signals are amplified in the gas phase using electron multiplier based on multi-stage GEMs. The uniqueness of the two-phase CRAD is its ability to operate in the mode of counting of single primary-ionization electrons, which means very small energy released in the liquid (less than 1 keV), and with a sufficiently high spatial resolution (less than 1 cm) and very low noise. The ultimate sensitivity of the detector is attained due to an

original idea of using a combined multiplier consisting of THGEM and Geiger avalanche photodiodes (G-APDs), which perform optical reading from the THGEM in the near infrared (IR) spectral region. Such a detector would have sensitivity that significantly (several times) exceeds that of the available detectors for dark matter due to its ability to work in the single-electron counting mode with improved (less than 1 cm) spatial resolution

For this project, two unique installations are to be created: 2 two-phase CRADs with the cryogenic chamber volume of 9 l and 160 liters, respectively. The first installation will be engaged in measurements for obtaining planned results on the two-phase CRAD with combined multiplier (GEM/G-APD matrix) and on the two-phase CRAD response to neutron scattering for measurement of the ionization yield of recoil nuclei. As concerns the second installation, its basic elements will be refined with a view of creation of a practical two-phase CRAD.

Besides that, the plasma Laboratory staff of BINP was engaged in the designing and creation of 2.45 MeV neutron DD generator. In particular, Fig. 1.4.2 shows the experimental setup with the two-phase CRAD with the cryogenic chamber volume of 9 l and the neutron generator.
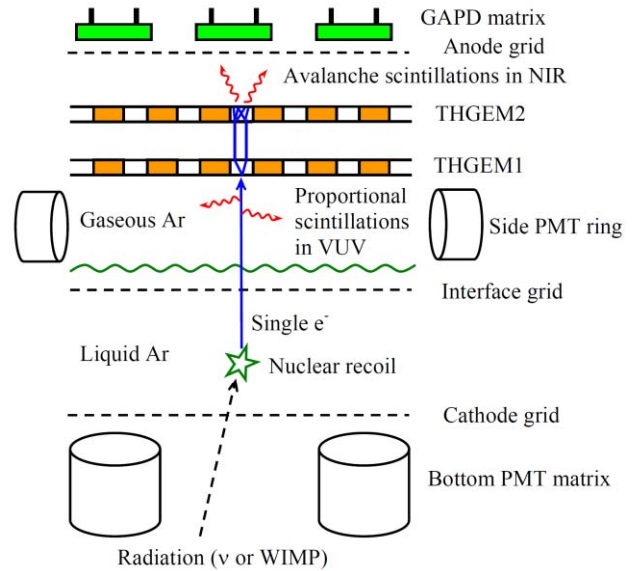
Fig. 1.4.1. Schematic diagram of two-phase Ar CRAD with combined multiplier (THGEM/G-APD matrix).
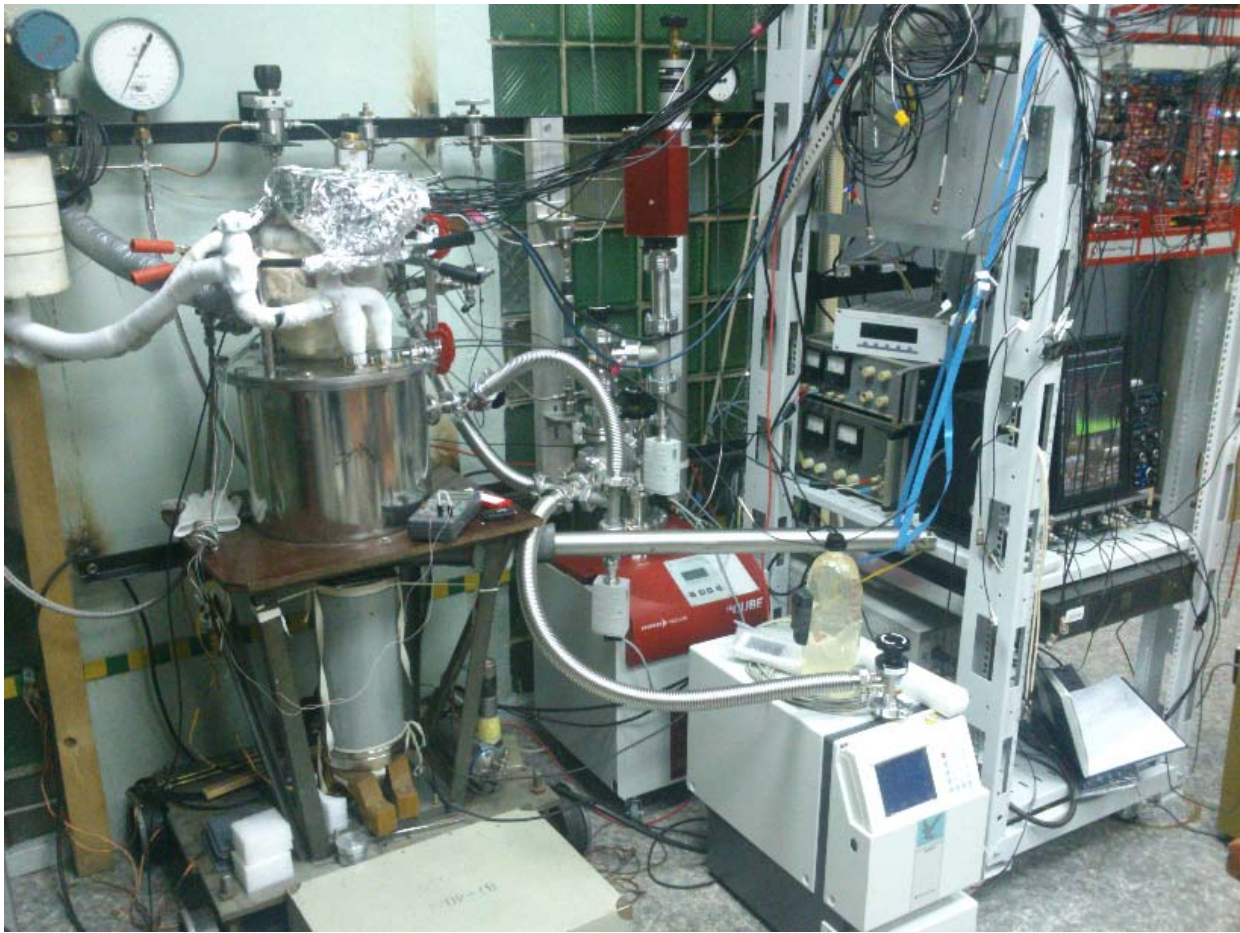
Fig. 1.4.2. Appearance of experimental setup with two-phase CRAD with 9 l cryogenic chamber volume and neutron generator (long tube under two-phase CRAD).
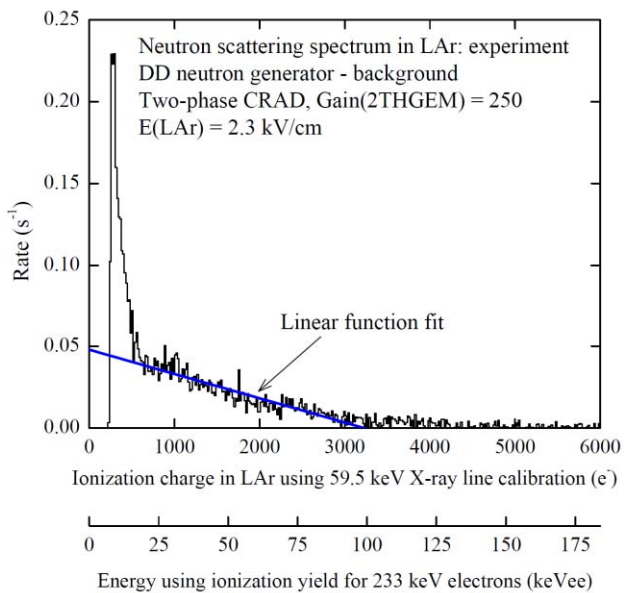
Fig. 1.4.3. Distribution of count rate of signals from recoil nuclei in liquid Ar from 2.45 MeV neutron scattering over ionization charge with field of 2.3 kV/cm.

The main scientific result of 2014 was the measurement of the ionization yield of recoil nuclei in liquid Ar, for the first time in the energy range of 80-230 keV. It should be noted that this is also the first example of using the technique of two-phase GEM-based CRADs in the search for dark matter. The measurements of the ionization yield are necessary for solution of the problem of energy calibration of dark matter detectors.

Fig. 1.4.3 shows the distribution of the count rate of signals from recoil nuclei induced by neutron scattering over the ionization charge of electrons that escaped recombination in the liquid Ar. This experimental spectrum should be compared with that of Fig. 1.4.4 in the theoretical recoil nucleus energy. Dividing one by the other in the characteristic points of the spectrum, namely, at the end of the spectrum at an energy of 233 keV and at the kinking of the spectrum at an energy of 80 keV, one can get the desired ionization yield for recoil nuclei.

The ionization yield results are shown in Fig. 1.4.5 in comparison with the data of the LLNL group (USA) obtained at a lower energy. It can be seen that the results are in reasonable agreement. Furthermore, one can see that the ionization yield is quite high - about 6-9 e-/keV.
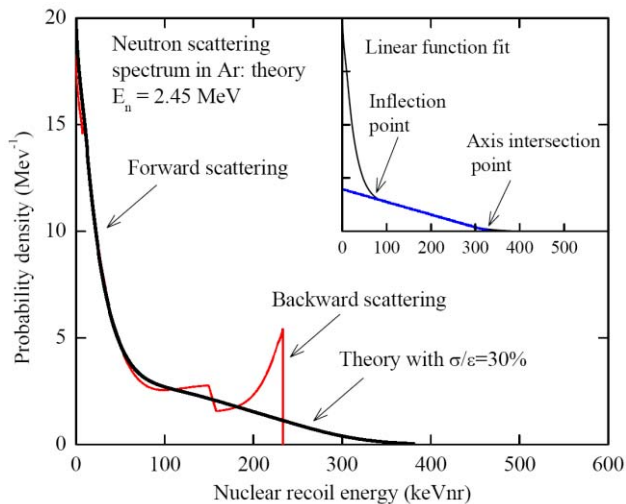
Fig. 1.4.4. Theoretical spectrum of recoil nucleus energy in liquid Ar from 2.45 MeV neutron scattering, the amplitude resolution of two-phase CRAD (30%) taken into account.
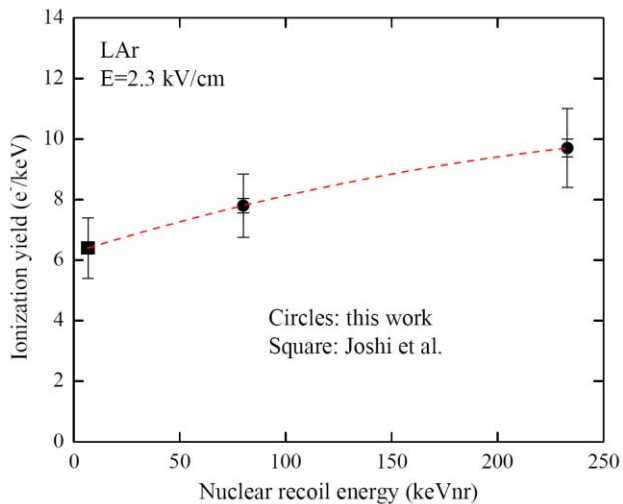
Fig. 1.4.5. Ionization yield for recoil nuclei in liquid Ar vs. energy measured at BINP and LLNL (USA).

BINP participates in the international collaboration RD51 at CERN for the development of microstructure gas detectors,. The collaboration was formed in 2008. In 2014, the BINP group continued its participation in this collaboration.

1.5. LHCB EXPERIMENT

1.5.1. Data analysis: measurement of angle γ in Unitary Triangle.

The angle γ in the Unitary Triangle is one of the parameters of the Standard Model of electroweak interactions, which potentially can be measured with great accu-

racy due to the virtual absence of theoretical uncertainties in the measurement. Together with other measurements of parameters of the Unitary Triangle, this will enable conduction of search for manifestations of effects of new physics beyond the Standard Model.

The amount of data collected in the LHCb experiment by 2013 is about 3 fb^{-1}. The respective number of reconstructed decays of B mesons is already much higher than the statistics acquired at the electron-positron B factories (at least, in final states containing no π^0 or photons). In addition, there are available numerous decays of Bs and B baryons, which are not produced in the electron-positron machines at all or are produced in small amounts. This allows attaining sensitivity to CP violation parameters significantly better than that achieved at the B factories.

Below is given an overview of the physical results relating to the measurement of the angle γ obtained by the LHCb collaboration with participation of the BINP group in 2014.

BINP staff has considerable experience in analyses directly related to the measurement of the angle γ in decays of the B → DK type and those connected with the study of other decays of B mesons into states with open charm. These studies were initiated in the Belle experiment at the electron-positron factory KEKB in Japan and are now continued at LHCb. In addition, the BINP members published a few phenomenological works on the subject, which offer new approaches of precision measurements of the angle γ and investigation into systematic fine effects. In 2013-2014, BINP member A. Poluektov was the coordinator of the working group of the LHCb experiment on the study of the B decays into states with open charm (Beauty to Open Charm Working Group), which is one of the eight physics working groups of the experiment.

Earlier, in 2011 and 2012, the LHCb experiment yielded a few results relating to the angle γ measurement. Those include analysis of the decay B → DK, where D is reconstructed in the two-particle state D → Kπ, KK or ππ (the so-called GLW and ADS methods of γ measurement). In these decays, for the first time a charge asymmetry in the decay probability was reliably observed (CP violation), which allowed reliable ascertainment of the fact that γ is not zero and setting limits to its value. In 2014, the LHCb collaboration completed and published analysis of the B → DK decay with the D meson reconstructed in the final states $K_S\pi\pi$ and K_SKK by a method first proposed by the BINP group. This analysis, which was done with all the available LHCb statistics, gave γ = $(62^{+15}_{-14})°$. This is the most precise individual measurement so far. Besides that, the first measurement of charge asymmetry in the decay B → DK with D decaying into final state $K_SK\pi$ was published.

Different approaches to the measurement of the angle γ complement each other. In addition to γ, two other unknown parameters measured: the amplitude ratio r_B and the strong phase δ_B. Due to the fact that correlations between these parameters are different in each approach, a combination of several measurements can give γ measurement accuracy better than in simply averaging of the

values. The combined measurement of the angle γ was published in 2014. In this combination, six independent analyses of decays sensitive to the angle γ were used, including the aforementioned two measurements in 2014. For the first time, the γ measurement accuracy achieved in one experiment turned out to be better than 10°: $\gamma = (73^{+9}_{-10})°$. The results of the combined measurement were published in a CERN pre-print and were presented at the working meeting CKM2014.

In addition to the above decays, the LHCb experiment investigates a number of other processes that may manifest CP violation and potentially can be sensitive to the angle γ. Although the current set of data may be insufficient for reliable measurement of the CP violation in these processes, they can be used later on, after the maintenance works on the LHC, as well as after the upgrade to the LHCb detector in 2018. Combining a large number of independent measurements makes it possible to get better γ measurement accuracy and to more reliably control the systematic errors. Study of such processes with the current set of data makes it possible to refine the procedures of event selection and to more accurately predict the future accuracy of the γ measurement. In addition, many of these processes are interesting in themselves, as intermediate resonance states of hadrons can be investigated, new states can be search for, and the theoretical predictions of the quark model can be verified.

For instance, the angle γ can be measured in a study of the decay of Λ_b^0 into DpK. The BINP group suggested this method to observe the CP violation. This analysis, using the statistics of 2011 (1 fb^{-1}), was completed in 2013. An article describing the analysis and its results was published in 2014 in *Phys. Rev. D*. The results of the analysis includes the first-time observation of the decay $\Lambda_b^0 \rightarrow$ DpK and measurement of its probability, as well as the first-time observation of the decay $\Lambda_b^0 \rightarrow \Lambda_c^+ K^-$ and measurement of its probability.

Three-particle decays of B mesons with the D meson in the final state are also of interest for future measurements of γ. In this case, the angle γ value is obtained from comparison of the phase differences of separate two-particle components of the decay amplitudes. A first step in this direction is the study of the amplitude of the decay $B^0 \rightarrow$ DKpi and the decay $B^s \rightarrow$ DKpi, which is similar, but has a higher probability. In 2014, we conducted and published a measurement of the amplitude of the decay $B_s \rightarrow$ DKpi. This decay is a background process for the decay $B^0 \rightarrow$ DKpi, which is of interest to us. Besides that, the decay $B_s \rightarrow$ DKpi provides means to study the excited states of the D_s meson that decay into the D meson and the kaon. In that analysis, it was found that the excited state of the D_s meson with a mass of about 2.86 GeV, which was observed earlier in other experiments, is the interference of two states with spins of 1 and 3. This is a first observation of a spin-3 particle containing a heavy quark, and a first observation of a spin-3 state in decay of the B meson.

1.5.2. Maintenance of simulation on HLT cluster and web application for visualization of background simulation results.

While LS1 is under shutdown, the released resources of the online HLT cluster are used for simulation by the radiation safety group. The simulation yields a large amount of files to process, which is done using a two-stage system. At the first level, the primary results of the simulation are processed; at the second stage, the results of averaging at the first level are handled.

It became necessary to separately calculate the standard error of the mean to assess the adequacy of the result. To this end, the system of processing of results was redesigned and generation of additional files was implemented with absolute and relative (percentage) error in the mean.

For visualization of simulation results a web application cern.ch/lhcbrad was developed and put into operation (access only for the LHCb personnel). Next, the groups involved in the modeling of the radiation backgrounds needed optimization of publication of the results, which was done manually. This process was automated after development of a set of scripts in Python to perform heuristic analysis of results and generate a manifest file to use in the web visualization system.

1.5.3. Porting of hadron calorimeter (HCal) calibration utility from windows platform to linux platform.

The Hadron Calorimeter periodically needs calibration without beam. The calorimeter is arranged in such a way that a tube with water goes through all the cells of the calorimeter; a capsule with radioactive Cesium source is introduced in the tube and a pump runs the capsule through the calorimeter. As the capsule is moving through the calorimeter cells, data are read and coefficients required for analysis and operation are calculated on their basis. The control of the motion of the capsule and acquisition of sensor data are performed by special equipment, connected with the computer via CAN and SPECS buses.

There was a calibration software utility, which was written under the Microsoft Windows operating system in 2003. In the course of the all-round conversion to the new version of MS Windows, it became clear that there are no SPECS drivers for the new versions of Windows OS. However, it turned out that the required drivers for CAN-bus and SPECS had been written under Scientific Linux OS. Therefore, it was decided to port the existing maintenance software to Linux.

The code of the special server application written for Windows OS in Visual Studio 2003 was thoroughly researched, refactored and ported to Scientific Linux 6.5. The process was complicated because of the simultaneous transition to the 64-bit platform, because the driver SPECS cannot work in a mixed 32-on-64 mode. In the course of tests, bugs in the program logic that did not

show up on Win32 because of significant differences in synchronization primitives in the Linux and Windows were identified and fixed.

The resulting native server application for the Linux operating system is controlled via the SCADA system, used in CERN WINCC (formerly known as PVSS). Test calibration runs performed on the new system demonstrated correct operation and preservation of backwards compatibility of data formats, which was a prerequisite in the specification.

1.6. PARTICIPATION IN THE ATLAS EXPERIMENT AT THE LARGE HADRON COLLIDER (LHC)

During 2010-12 the ATLAS and other LHC detectors were collecting statistics at a record energy of colliding protons of 7 (in 2010-11) and 8 (in 2012) tera-electron-volt (TeV) in the center of mass system. About 0.04, 4.7 and 20.7 inverse femtobarn have been accumulated, respectively.

The most important result is the reliable observation of a signal from a new particle with properties similar to those expected for the Higgs boson. The Nobel Prize in Physics 2013 was awarded to P. Higgs and F. Englert «for the theoretical discovery of a mechanism that contributes to our understanding of the origin of mass of subatomic particles, and which recently was confirmed through the discovery of the predicted fundamental particle, by the ATLAS and CMS experiments at CERN's Large Hadron Collider».

In the begin of 2013, the Large Hadron Collider and detectors were interrupted for two-year shutdown to prepare for the work at the LHC design parameters − energy of colliding protons of 13-14 TeV in the center of mass system and luminosity of 10^{34} cm^{-2}s^{-1}. For the ATLAS detector the following actions were performed:

- Repair and replacement of broken elements of the detector and electronics
- Installation of new detector elements, in particular, of the additional layer of the inner detector for detection of particles, containing b-quark
- Improving efficiency and speeding-up the triggering and reconstruction algorithms
- Preparation of entire computing infrastructure (both hardware and software parts) for handling substantially larger amount of data

Also the work on analysis of the data taken in 2011-12 was activated, aiming to publication of the results. The most important task is detailed study of the properties of recently discovered higgs-like particle (the spin, parity, decay branching ratios, and coupling constants). The BINP group participated in the analysis of the Higgs boson decay into four leptons (electrons/positrons or muons). Thanks to improved accuracy of the calibration of electrons energies and muons momenta, the systematic uncertainty on the Higgs boson mass was reduced. The new

value of the Higgs boson mass, determined from the decay to four leptons, is (124.51 ± 0.52) GeV, and combined with the results for the decay to two photons is (125.36 ± 0.41) GeV.

Also the important result was obtained for one more decay channel of the Higgs boson to the Standard Model vector bosons. The signal significance for the H→WW* channel is 6.1 standard deviations (σ), while expected significance, obtained from Monte-Carlo simulations in the Standard Model, is 5.8 σ, that means the reliable observation. For the first time, the experimental evidence that the recently discovered Higgs boson decays also to fermions, was obtained. The signal significance of the Higgs boson decay to two tau-leptons is 4.5 σ, while expected in the Standard Model significance is 3.5 σ. In Fig. 1.6.1 the "signal strength" (the ratio of measured cross-section to computed in the Standard Model) is presented for five Higgs boson decay channels. At the present level of experimental errors the results are in a good agreement with the Standard Model predictions. The analysis of angular distributions in various decay channels of the Higgs boson also shows that the data are compatible with the Standard Model spin-parity $J^P = 0^+$ quantum numbers, whereas all alternative hypotheses studied ($J^P = 0^-$, 1^+, 1^-, 2^+ models) are excluded at confidence levels above 97.8%.
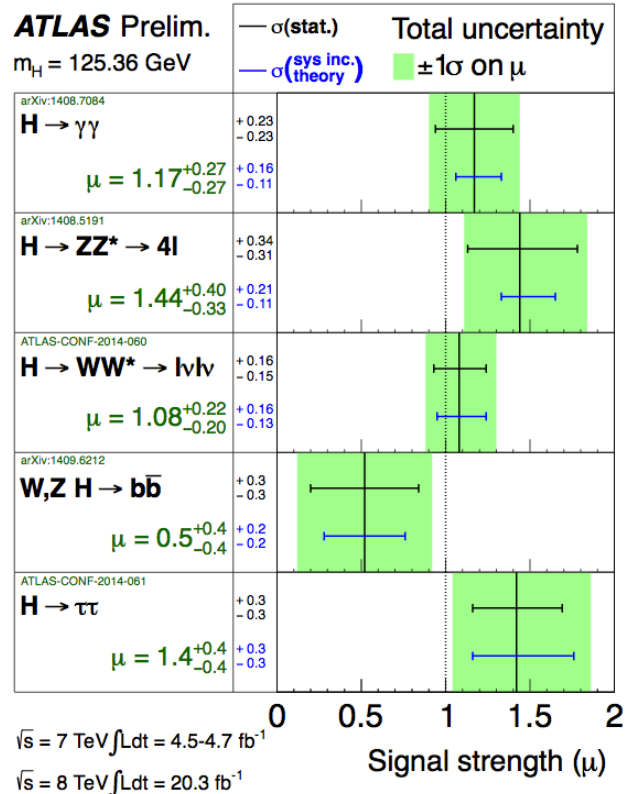
Fig. 1.6.1. The "signal strength" (the ratio of measured cross-section to computed in the Standard Model) for five Higgs boson decay channels. The statistical error is shown in black, the systematical error in blue, the total error is shown as a green band.

The search for new physics goes beyond the Higgs bosons. In particular, BINP physicists continued to search for heavy neutrinos in the channel with leptons and hadronic jets in the final state. Two theoretic models were examined – the Left-Right Symmetric Model, in which the neutrino is generated through the hypothetic right-handed vector boson W_R, and the model with the virtual W boson of the Standard Model. The world's best upper limits have been obtained for the masses (up to the level of 2 TeV), production cross sections and coupling constants of heavy neutrinos. However, further significant improvement is possible only with an increase in the energy of colliding protons in the LHC, which is, as mentioned above, planned after the resuming the data taking in summer 2015.

After the start of the data taking in 2010, the ATLAS collaboration with participation of BINP authors published 379 papers based on the collision data, including 96 papers in 2014.

Since 2015, in addition to the increase of the energy of colliding protons almost by a factor of two, the increase of the luminosity is planned, which will lead to growth of the rates in the detector's systems. This will strengthen the demands on the performance and the speed of the algorithms used for trigger, signal digitization, data quality control etc. The BINP physicists participate in the work on corresponding adaptation of the software for the liquid argon calorimeters. The BINP group also works on the calorimeter calibration and on improving the simulation and the reconstruction of electrons and photons. For example, the full GEANT 4 simulation in the liquid argon electromagnetic calorimeters was speed-up by 25-30 %.

In addition, the work on the support and development of the computer infrastructure and software is going on. The BINP GRID cluster is upgraded. The volume of the data storage system based on disk arrays is increased, the capacity reached 96 TB. The pilot storage system based on distributed file system ceph is deployed. The storage for back-up copies with the capacity of 4 TB is set up. The configuration management system Puppet is deployed, it enables the control of configuration for all 30 servers and 64 computing elements, fast recovery in case of failures and quick installation of new equipment.

Since 2007, BINP specialists have continuously participated in the activities of the Trigger and Data Acquisition System administration group, which deals with the maintenance and development of the hardware and software for the High Level Trigger (HLT), Event Builder and other parts of the Data Acquisition System. The equipment includes about 2,300 network booted servers (in total, about 17,000 CPU cores), 50 servers supporting the ATLAS control room, and many other units of the IT infrastructure of the experiment.

In the middle of 2013 at CERN the transition has started from custom server configuration management system CDB+Quattor to new, widely used in the industry, Foreman+Puppet. At the same time the change of the virtualization platform has been initiated from the Microsoft Hypervisor to OpenStack based on the Linux KVM (so called Agile Infrastructure). By the end of 2014 these tasks were fully completed – all important services have been switched to the new infrastructure. During the transition period, several techniques have been – balancing of the workload at the level of DNS, adaptation of the client software, backward compatibility at the server side. Also during a scheduled shutdown, significant part of the computing resources of the DAQ system was used for the simulation of events in the ATLAS detector. To make it possible, a special system configuration was deployed with participation of the BINP group.

Of great importance is the work on the support and administration of the ATLAS central computers (~300 units), located in the CERN main computer building. These computers ensure uninterrupted operation of critical services: numerous components of the ATLAS distributed computing system, data bases, electronic logbook of the detector, data quality monitor, event display etc. In 2014, the work was primarily connected with the transition to new configuration and virtualization systems. Also some vulnerabilities in the system software have been spotted and eliminated.

Since 2008, BINP specialists have made a significant contribution to the creation and development of important services and applets to manage the ATLAS Distributed Computing system (ATLAS GRID). The ATLAS GRID Information System (AGIS) has become the basic source of the information on the topology of the ATLAS computing resources and on available software releases. It is integrated with other key components of the distributed computing system: central data replication and data storage system (DDM, ATLAS Distributed Data Management System), a system for distributed analysis and job submission (PanDA, ATLAS Production and Distributed Analysis), monitoring services.

It is planned that the LHC luminosity will increase from present level of $7 \cdot 10^{33}$ cm^{-2}s^{-1} to $2 \cdot 10^{34}$ cm^{-2}s^{-1} in 2019 and to $5 \cdot 10^{34}$ cm^{-2}s^{-1} in 2024. Accordingly, the work is activated on the preparation of the detector upgrade in future years. The so called "the Phaze 1 upgrade" is scheduled to 2018-19 and will mostly concern the trigger electronics. The BINP group participates in developments of the back-end (digital) part of the liquid argon calorimeter electronics (programming of FPGA microchips). The BINP team also takes part in the experiment on the study of operation of the ATLAS liquid argon calorimeters at high rates. In April 2012 and March 2013, two last (in a series) regular data acquisition sessions were carried out at the U-70 accelerator in Protvino with new front-end electronics, much better adapted for the high-rate environment. Another important improvement in these runs was better control of parameters of the 50 GeV proton beam. Data analysis and comparison with simulation is ongoing.

1.7. BABAR EXPERIMENT

Experiments with the BABAR detector were carried out on the e+e- collider PEP-II at SLAC (USA) from 1999 to 2008. Now the data collected in the experiment are being processed. The BABAR collaboration includes about 300 physicists, with 10 BINP members among them. The latter are involved in the analysis of data on the measurement of the CKM matrix element V_{ub}, measurement of the cross sections of e+e- annihilation into hadrons using the radiative return method and study of two-photon processes with registration of scattered electrons. In 2014, the collaboration published 12 articles.

In the BABAR experiment in the energy range from the threshold up to 2.2 GeV, the BINP physicists measured the cross section of the $e^+e^- \to K_L K_S$ process. Except for a narrow range near the φ meson resonance, this is the most precise measurement of the cross section so far. A complex energy behaviour of the cross section was confirmed, including the sharp drop by a few orders with a resonance-like increase of about 1.7 GeV, which is interpreted as the φ(1680) (Fig. 1.7.1). This behaviour contrasts sharply with the behaviour of the annihilation cross section in a pair of charged kaons, which means strong destructive interference of the iso-vector and iso-scalar components in the production amplitude, which is not described so far in terms of the existing theoretical models.

The cross sections for the $e^+e^- \to K_S K_L \pi^+\pi^-$ and $K_S K_S \pi^+\pi^-$ reactions (Fig. 1.7.2) were measured for the first time, which makes it possible to lower the uncertainty in the calculation of the hadron contribution to the anomalous magnetic moment of the muon.

Currently, the BINP physicists are performing analysis of the higher-accuracy measurement of the parameter V_{ub}. Works on the cross-section measurements by the radiative return method are going on.
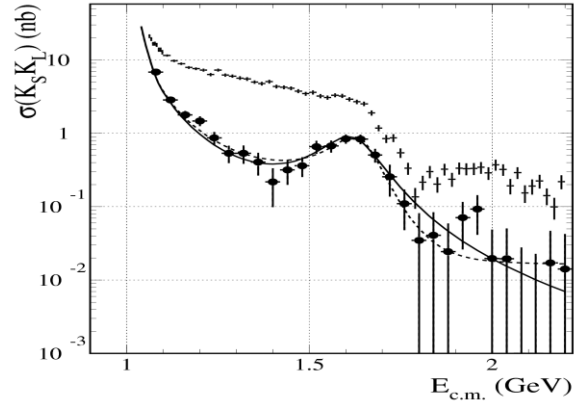
Fig. 1.7.1 Energy behaviour of cross section.
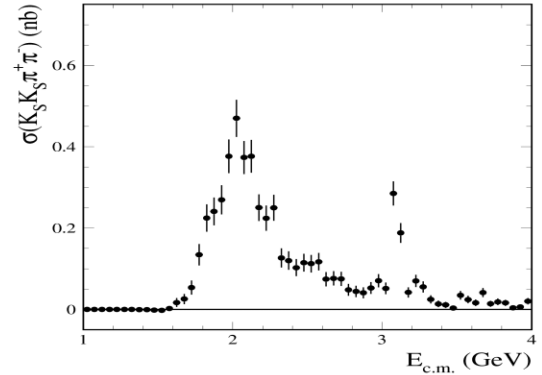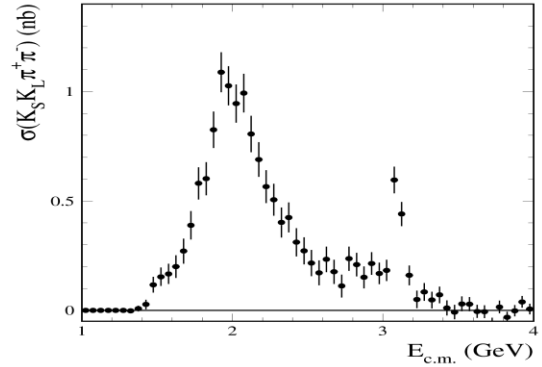
Fig. 1.7.2. Cross section of $e^+e^- \to K_S K_L \pi^+\pi^-$ and $K_S K_S \pi^+\pi^-$ reactions.
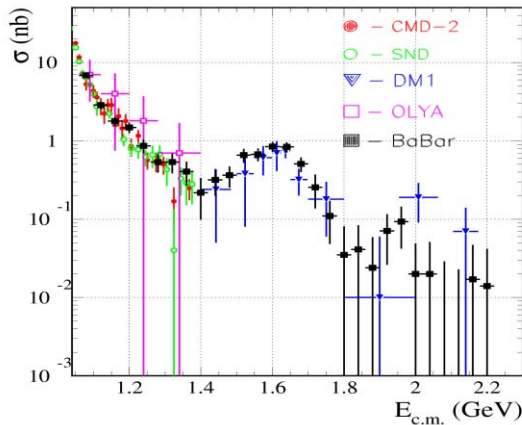
1.8. BELLE EXPERIMENT

1.8.1. Main results.

The main focus of the BINP group activity is cooperation in the field of particle physics with the High-Energy Accelerator Laboratory (KEK), Tsukuba, Japan, which is one of the largest and fastest-growing laboratories in the world in the field of high energy physics. In recent years, KEK management has actively expanded the international cooperation to make KEK an international high energy physics center. Research on CP violation in B meson decays with the Belle detector on the electron-positron storage ring with a very high

luminosity (the so-called B-factory) is now one of the main experiments in elementary particle physics in Japan.

The BINP members made a great contribution to the creation of the electromagnetic calorimeter of the Belle detector, including the designing and the manufacture of the elements of the world's largest calorimeter based on single crystals of cesium iodide, its assembly and commissioning.

In 2010, the Belle detector was stopped for upgrade. The currently collected integrated luminosity exceeds 10^3 inverse femtobarn. Now these experimental data are being processed and the detector and accelerator are being upgraded for the purpose of increasing the luminosity of the installation and preparation of experiments that will improve the accuracy of measurement of parameters of CP violation and may enable observation of manifestation of physical phenomena beyond the Standard Model.

The BINP members take an active part in the works on the upgrade to the detector and processing of experimental data collected.

Below are presented the main results of the work in 2014.

- Search for decays of B mesons to final states with the η_c meson was performed. Based on the analysis of these decays, the upper limits on the product of relative probabilities of production and decay of particles that are bound states of D(*) mesons were set.
- Y(5S) $\rightarrow$ Y(1,2S)h decays were detected for the first time; their relative decay probabilities were measured
- A Dalitz analysis of the $B^0 \rightarrow D^*\omega\pi$ decay was performed. Dynamic efficiency interaction parameters and interference phase that describe the decay features were measured; the resonance structure of the $D^*\pi$ and $\omega\pi$ hadronic systems was investigated.
- Final results were obtained on the measurement of the relative probabilities of τ lepton decays with the K^0_S meson in the final state.
- Research on the Michel parameters in leptonic decays of the τ lepton is going on.
- Research on decays of the τ lepton to final states with three pseudoscalar mesons and the neutrino was started.
- Measurement of the relative probability of semileptonic decays $\Lambda_c^+ \rightarrow \Lambda l^+ \nu$ is going on.
- The quantum numbers of the two earlier detected charged bottomium-like states $Z_b(10610)$ and $Z_b(10650)$ were determined.
- 324 shaper digitizers for the cylindrical calorimeter of the Belle II detector were produced and delivered to KEK.
- All the crates of the cylindrical part of the calorimeter were installed on the detector, equipped with the modules of the shaper digitizers and collectors, and connected to the counters of the cylindrical calorimeter.
- The software and projects for programmable logics were developed; they allow one to load arrays of coefficients to the modules of the shapers and collectors and then read and transmit data to the data acquisition system of the detector.
- First data containing events of registration of cosmic particles with the calorimeter were collected
- A final check of the end version of the shapers digitizers was performed and an order for mass production of the modules was placed.
- An upgrade to the front end calorimeter was carried out.
- A calorimeter calibration procedure was implemented, which allows measurement of calibration constants required for reconstruction of the energy and time of clusters in the simulation.

The group also took part in the study of mixing processes in neutral *D* mesons, as well as decays of charmed baryons and *B* mesons.

1.8.2. Data analysis.

Search for decays of B mesons to final states with η_c meson

The exotic state X(3872) was first found out by the Belle collaboration in 2002, in exclusive decays $B^+ \rightarrow K^+\pi^+\pi^- J/\psi$. The mass of this state is close to the threshold of $M(D^0) + M(\overline{D}^{*0})$, which gave rise to a hypothesis that the X(3872) may be a $D^0\overline{D}^{*0}$ molecule. Thus, it was supposed that there might be other similar particles that are also bound states of $D^{(*)}$ mesons. If these states exist, their quantum numbers differ from that of the X(3872), and thus they can be found in decays with participation of the η_c meson. If molecule states of the $D^0\overline{D}^0$ and D^{*0} types are possible, such particles have mass other than 3872 MeV. They were designated as the X(3730) and X(4014), respectively. In decays of charged B mesons, the BINP group searched for decay of exotic states similar to the X(3872) to various modes with the η_c: $\eta_c\pi^+\pi^-$, $\eta_c\omega$, $\eta_c\eta$, and $\eta_c\pi^0$. No statistically significant signal was detected in any studied channel of the X decay, and thus the upper limits on the corresponding products of the relative probabilities of X production and decay were set.

In addition to the search for the exotic states, decays of B mesons to the above final states but without intermediate resonances were searched. So, the upper limits for the relative probabilities of the $B^\pm \rightarrow K^\pm \eta_c \pi^+\pi^-$, $B^\pm \rightarrow K^\pm \eta_c \omega$, $B^\pm \rightarrow K^\pm \eta_c \eta$ and $B^\pm \rightarrow K^\pm \eta_c \pi^0$ decays were set. The results of this work will be published in a peer-reviewed journal next year.

Research on Y(5S)$\rightarrow$Y(1,2S)η decays

Measurement of the width of transitions between bottomium through the η meson will test the predictions of the theoretical models. The QCD multipole expansion model predicts noticeable suppression of these transitions as compared with $\pi^+\pi^-$. However, the measured transition widths are not consistent with this hypothesis:

- $\Gamma(Y(2S)\rightarrow Y(1S)\eta)$ is twice less than expected;
- $\Gamma(Y(4S)\rightarrow Y(1S)\eta)$ is two orders higher than predicted.

For this discrepancy to be resolved, new information is required. The BINP members searched for such transitions using the unique statistics collected with the Belle detector at the Y(5S) resonance. The Y(5S)→Y(1,2S)η decays were found for the first time; their relative probabilities were measured. The results were presented at the ICHEP International Conference. An article to *Phys. Rev. D* is being prepared now.

Research on $B^0 \to D^* \omega \pi$ decay

Hadronic decays of B mesons are of interest for the study of dynamic effects in a system of final particles including the D meson (or its excitations, D^*- or D^{**} states). Research on the properties of the excited states of D mesons will help to reduce the uncertainties in the measurements of semileptonic decays and thus in determining the matrix elements |Vcb| and |Vub|. In addition, research on the properties of D** -states is useful for study of the background in the $B \to D^* \tau \nu$ decay, which is sensitive to search for charged Higgs bosons.

In the spectator mechanism of decay of B mesons, the quark pair bound with the virtual W boson is hadronized to the meson or a system of light mesons. Hadronic weak currents describing production of such mesons are divided into currents of the first kind, which dominate in the nature, and currents of the second kind, which are suppressed ones. Research on the first-kind currents and search for the second-kind currents is a basic problem. In the $D^* \omega \pi$ system, the second-kind currents are caused by contributions from the b1(1235) resonance.

A Dalitz analysis of the $B^0 \to D^* \omega \pi$ decay was performed. The effective dynamic parameters of the interaction and interference phases describing the decay features were measured; the resonance structure of the hadronic systems $D^* \pi$ and $\omega \pi$ was investigated for separation of the relative contributions of different D** states and light hadrons that decay into the $\omega \pi$ final state and are described with first and second kind currents. It was found that the main contribution to the final state is given by decays and ρ-like mesons: ρ(770) beyond the mass surface and ρ(1450). The contribution to the $b_1(1235)$ was found to be insignificant, and the upper limit of the probability of its production was set. In the system of D** states, the main contribution is given by the broad $D_1(2430)$ state.

Results of the experimental data fit in two different kinematic regions are shown in Fig. 1.8.1. The work is ready for publication and currently is being discussed within the collaboration.
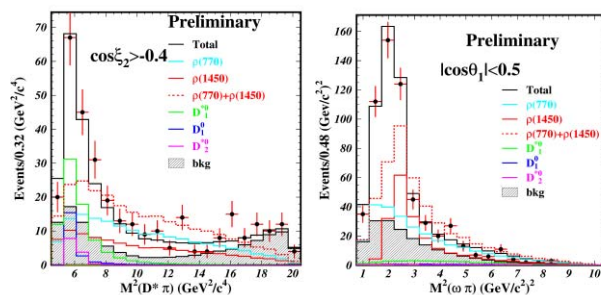
Fig. 1.8. 1. Fit of distribution of squared invariant masses of D*π pair in area of saturation of D** states and of ωπ pair in area of saturation of ρ(770) and ρ (1450).

Research on τ lepton physics

Final results were obtained on the measurement of the relative probabilities of τ lepton decays with the K^0_S meson in the final state. This analysis was done using statistics corresponding to an integrated luminosity of 669 fb[-1] or 616×10^6 pairs of τ leptons produced. In particular, final values were obtained for the relative probabilities of the inclusive decay $\tau^- \to K^0_S X^- \nu_\tau$ and six exclusive decay channels: $\tau^- \to K^0_S \pi^- \nu_\tau$, $\tau^- \to K^0_S K^- \nu_\tau$, $\tau^- \to \pi^0 K^0_S \pi^- \nu_\tau$, $\tau^- \to \pi^0 K^0_S K^- \nu_\tau$, $\tau^- \to K^0_S K^0_S \pi^- \nu_\tau$, and $\tau^- \to K^0_S K^0_S \pi^- \pi^0 \nu_\tau$ (see Fig. 1.8.2). For the latter channel, the mass spectra of the final hadronic states $K^0_S K^0_S \pi^0$ and $K^0_S \pi^-$ were found. In the first case, one can clearly see an intermediate structure corresponding to the production of the $f_1(1285)$ with a significance over 5 standard deviations, and in the second case one can see the $K^{*-}(892)$ meson. The results were published in *Phys. Rev. D.*

Investigation into the Michel parameters in leptonic decays of the τ lepton goes on. This analysis was performed using statistics corresponding to an integrated luminosity of 485 fb[-1] or 446×10^6 pairs of produced τ leptons. The Michel parameters are derived by the unbinned maximum likelihood method in a complete nine-dimensional phase space. Work on systematic errors is going on. Preliminary results were presented at a meeting on τ lepton physics in Aachen in September 2014.

Decays of the τ lepton into final states with three pseudoscalar mesons and the neutrino – $\pi^+\pi^-\pi^-\nu_\tau$, $\pi^+\pi^-K^-\nu_\tau$, $K^+K^-\pi^-\nu_\tau$, and $K^+K^-K^-\nu_\tau$ – were studied in the Belle and BaBar experiments. The probabilities obtained for decay channels with one and three kaons are not consistent with each other, which necessitates independent measurement of decay probability in these channels. For today, the collected luminosity integral increased by half as compared with the amount of data used in the previous analyzes. This holds out a hope of obtaining more accurate results and solution to the problem of coherence of τ lepton decay probabilities. All the currently available experimental statistics have been processed. The influence of the trigger efficiency and the background conditions on the measured probabilities is being studied. Preliminary results are anticipated next year.

Measurement of relative probability of semileptonic decays $\Lambda_c^+ \to \Lambda l^+ \nu$

The widths of semileptonic decays are important quantities for physics of quarks. Semileptonic decays occur only through external emission of the W boson and are free from the effects of mixing with the internal emission of the W boson. Measurement of the width of the $\Lambda_c^+ \to \Lambda l^+ \nu$ decay along with other semileptonic decays may be helpful in determination of the general parameters (form factors) for the theory of weak annihilations. The semileptonic decays of Λ_c^+ have been experimentally measured with high uncertainty so far.

A model-independent technique is applied, which was developed for measuring the absolute value of the relative probability of the $\Lambda_c^+ \to p K^- \pi^+$ decay. The ratio of the number of events with the reconstructed recoil neutrino to the number of events with the reconstructed recoil Λ_c^+ baryon gives us the desired relative probability of the decay. Preliminary results show a significant improvement in the accuracy of the probability of the decay $\Lambda_c^+ \to \Lambda l^+ \nu$. The final results will be available next year.

Investigation into bottomium exotic states

In 2014, the BINP group within the Belle collaboration completed analysis of data on $e+e-$ annihilation to $Y(nS)\pi^+\pi^-$ (n=1,2,3) final states. The most important finding was the determination of the quantum numbers of the two earlier-detected bottomium-like charged states $Z_b(10610)$ and $Z_b(10650)$. To this end, we expanded the earlier developed technique of amplitude analysis into four-particle final states, i.e. the subsequent decay $Y(nS)\to\mu^+\mu^-$ was taken into account. The investigation into the distribution of signal events in the six-dimensional phase space resulted in the determination of the spin and parity of both the Z_b states. $J^P = 1^+$ is a combination that describes the experimental data in the best way. Other possible combinations were precluded with reliability. The results are shown in Table 1.8.1. Based on the study, an article was prepared, which is under review now.

With decays of the form $Z_b \to Y(nS)\pi^\pm$ and $Z_b \to h_b(mP)\pi^\pm$ there can be no combinations $J^P = 0^\pm$, and Z_b cannot be classified as two-quark systems. Therefore, the minimum set consists of four quarks. The internal quark structure of these states and possible ways of its experimental study are a subject of intense debate among theorists. The BINP members and their Russian and foreign colleagues suggested considering the new states as a weakly coupled system of the B and B^* mesons in the case of the $Z_b(10610)$ state and a system of the B^*B^* mesons in the case of the $Z_b(10650)$ state.

The model proposed leads to a conclusion that the dominant decay channels for the $Z_b(10610)$ and $Z_b(10650)$ will be decays into the BB^* and B^*B^*, respectively. The large amount of data collected in the Belle experiment enables separation of the three-particle processes $Y(5S) \to BB^*\pi$ and $B^*B^*\pi$ and a first-time analysis of the dynamics of these transitions.
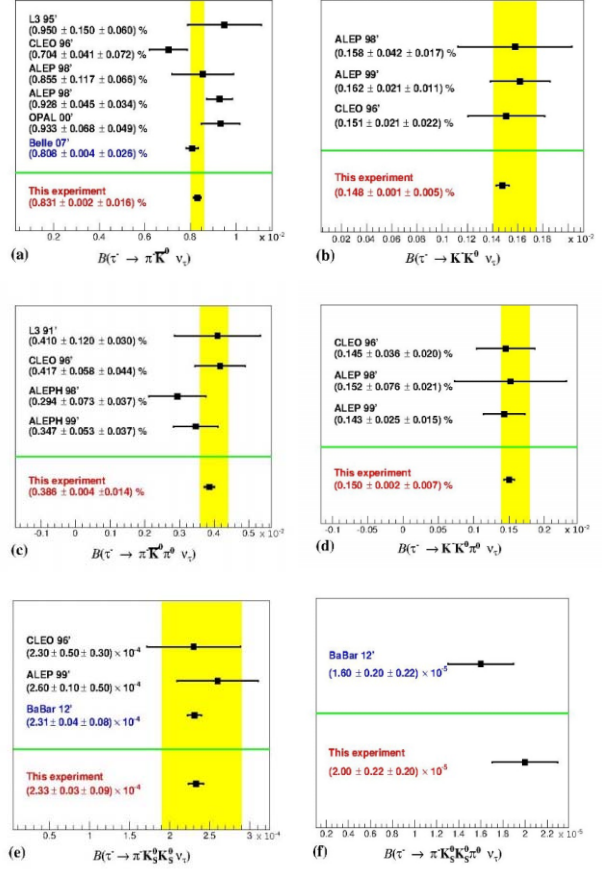
Fig. 1.8.2. Comparison of results of measurement of relative probabilities of decays (a) $\tau^- \to K^0_S\pi^-\nu_\tau$, (b) $\tau^- \to K^0_S K^-\nu_\tau$, (c) $\tau^- \to \pi^0 K^0_S\pi^-\nu_\tau$, (d) $\tau^- \to \pi^0 K^0_S K^-\nu_\tau$, (e) $\tau^- \to K^0_S K^0_S\pi^-\nu_\tau$, and (f) $\tau^- \to K^0_S K^0_S\pi^-\pi^0\nu_\tau$.

Table 1.8.1. Results of approximation of data on $e^+e^- \to Y(2S)\pi^+\pi^-$ $(Y(3S)\pi^+\pi^-)$ in different hypotheses on combinations of quantum numbers J^P for Z_b states; values of likelihood function for model $J^P = 1^+$.

$Z_b(10650)$ / $Z_b(10610)$	1^+	1^-	2^+	2^-
1^+	0 (0)	60 (33)	42 (33)	77 (63)
1^-	226 (47)	264 (73)	224 (68)	277 (106)
2^+	205 (33)	235 (104)	207 (87)	223 (128)
2^-	289 (99)	319 (111)	321 (110)	304 (125)

Shows the invariant mass distributions of the $B B^*$ and B^*B^* systems and results of approximation with different models. The preliminary results are consistent with the hypothesis that the three-particle processes $e^+e^- \to BB^*\pi$ and $e^+e^- \to B^*B^*\pi$ occur mainly through intermediate production of Z_b states. The results were presented at international conferences.

1.8.3. Upgrade to detector.

Currently, they work intensely on the upgrade to the detector (Belle II) and the collider to increase the luminosity of the installation up to 8×10^{35} cm^{-2}s^{-1}. The new experiment will enable measurement of all the angles of the unitarity triangle with an accuracy of a few per cent and possibly going beyond the Standard Model. In addition to studying the mechanism of CP violation, the large set of data obtained in this experiment will give new results on the physics of decays of the B and D mesons and the τ lepton.

The increase in luminosity and background load on the collider imposes new requirements to the systems of the detector. The calorimeter also needs upgrade. The BINP group is involved in the methodological works to modernize the calorimetry system of the detector.

In the cylindrical part of the calorimeter, the electronics will be replaced with new equipment, which will provide continuous digitization of signals from the counters and subsequent adjustment of data with a response of a known form. Such a procedure will enable determination of the energy and time of arrival of signal. With the time information the rate of occurrence of false clusters can be reduced a few times.

For the end part, where the background conditions are most severe, at the first stage the electronics will be upgraded and then the scintillation CsI(Tl) crystals will be replaced with crystals of pure CsI with smaller decay times. This will 30 times improve the time resolution of the counters and, with signal shape fitting, ensure reduction of the background by a factor of over 150.

The electronics of the calorimeter are shown in Fig. 1.8.4. A signal from the preamplifier arrives at the module of the shaper digitizers, where it is shaped and continuously digitized. Once a trigger signal arrives, the digitized data are fitted with a signal of a known shape and the signal amplitude and time are determined. The collector module reads the latter information, which is then transferred to the data collection system of the detector. The module of the shaper digitizers receives signals from 16 counters. In addition, a shaper digitizer generates a fast sum signal of the 16 channels, which is used for forming of a neutral trigger. The electronics of the calorimeter include 52 9U VME crates, each comprising 8 to 12 modules of shaper digitizers, a collector module and a trigger module (FAM).

112 modules of shaper digitizers were manufactured in 2013. The remaining 324 modules for the cylindrical calorimeter were manufactured and delivered to KEK in 2014. Before mounting in the detector, all the modules were tested on a special stand. Fig. 1.8.5 shows distribution by the measured parameters of the shapers.
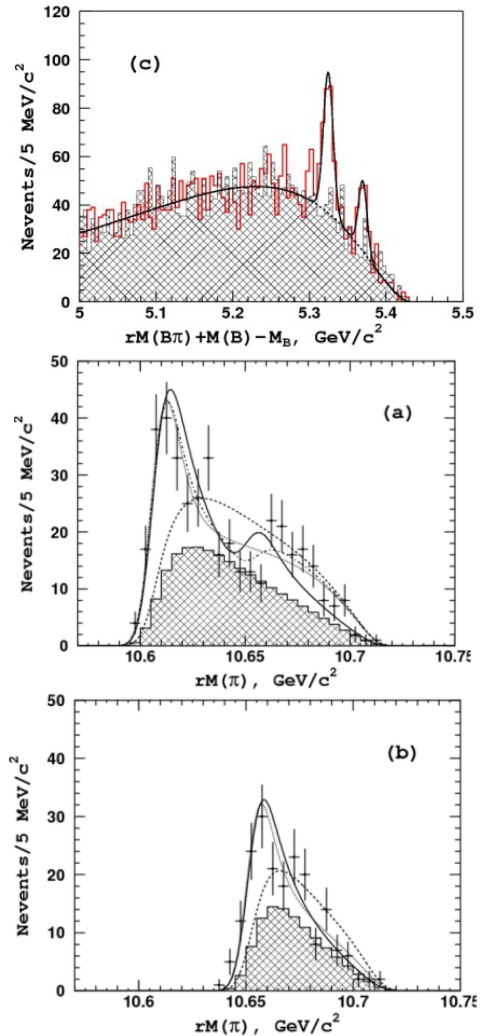
Fig. 1.8.3. Distributions by mass of recoil to $B\pi$ system (left), invariant mass of BB^* system (center) and B^*B^* system (right) for events $Y(5S)\rightarrow BB^*\pi$ and $Y(5S)\rightarrow B^*B^*\pi$, respectively. Points: experimental data; lines: approximation results; shaded histogram: expected level of background events.
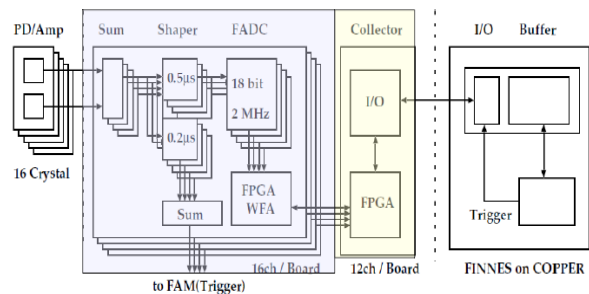
Fig. 1.8.4. Diagram of electronics of Belle II.

All the crates of the cylindrical portion of the calorimeter were installed on the detector, equipped with the modules of the shaper digitizers and collectors, and connected

to the counters of the cylindrical calorimeter. After connection of each crate, the counters were subjected to a test using a temporal data acquisition system. The testing covered the electronics noise, the calibration signal position and location of the peak of space minimum-ionization particles. All the channels turned out to be workable. Fig. 1.8.6 shows the spectrum of energy release by cosmic particles in the counter of the cylindrical calorimeter. Data from several modules were used for reconstruction of the tracks of cosmic particles in the calorimeter and validation of the connection of the counters. This procedure allowed us to correct all mistakes made during the connection of the counters.

After the check all the collectors were connected via an optical cable to the receiving boards of the data acquisition system in the detector control room, as well as to the systems of trigger synchronization and distribution. Software and projects were developed for programmable logic integrated circuits, which enable downloading of arrays of coefficients to the modules of the shapers and collector and then reading and transmission of data to the data acquisition system of the detector. First data, containing events of registration of cosmic particles, were collected in the autumn. Fig.1.8.7 shows an example of event detected by the calorimeter.

The Belle II experiment is expected to show a much larger flow of neutrons from the interaction of lost beam electrons with the material of the accelerator and the detector. The dark current of semiconductor photodetectors increases in proportion to the integrated neutron flux through the photodetector. The power supply filter of the photodetector of the rear end calorimeter was under upgrade in March 2013. The front end calorimeter was upgraded in February-March 2014. The upgrade consisted in replacement of the power supply filter resistors with resistors of smaller rating for the photodetectors to be operable after exposure to neutron flux. The following was to be done: disassembling of the calorimeter, demounting of the preamps, replacement of resistors in them, check-up of their performance, installation of the preamps on the crystals, closing of the calorimeter and final check on cosmic particles. The stages of disassembly of a sector (1/16) of the calorimeter are shown in Fig. 1.8.8. This work was done by a team of five people and took about two months. As a result, all the filters were upgraded, and all the 1152 channels were found to be operable.

The data collected in the calorimeter require software, including a simulator of the calorimeter. During the calibration procedure, a calorimeter calibration procedure was implemented. The procedure allows measurement of calibration constants required for the reconstruction of the time and energy of clusters in the simulation. In future, this program will determine parameters for the experimental data. During this work, the BINP members also mastered the software of the Belle II calorimeter.
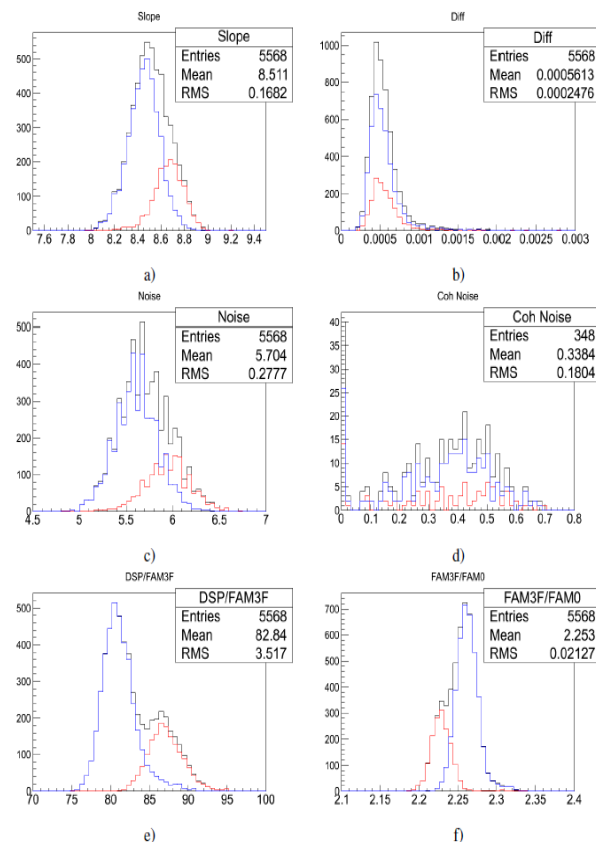
Fig. 1.8.5. Distributions by parameters of shaper digitizers as measured on the stand: conversion factor (a), non-linearity (b), noise (c), coherent noise (d), ratio of signals in main and fast channels (e), ratio of maximum and minimum attenuation signals in fast channel (f).

The shaper digitizer version for the end calorimeter is slightly different from the module of the cylindrical part. The final check of the end-part version was done in the spring of 2014, and an order for mass production of the modules was placed.
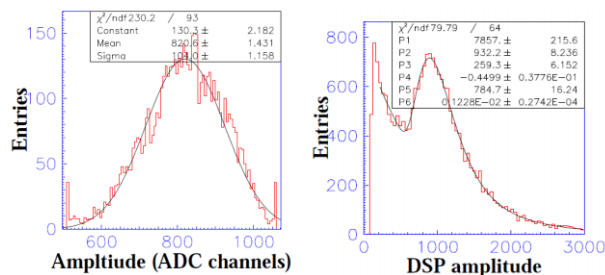
Fig.1.8.6. Spectrum of amplitudes of minimum-ionization particles and position of peak of cosmic particles for all cylindrical counters.
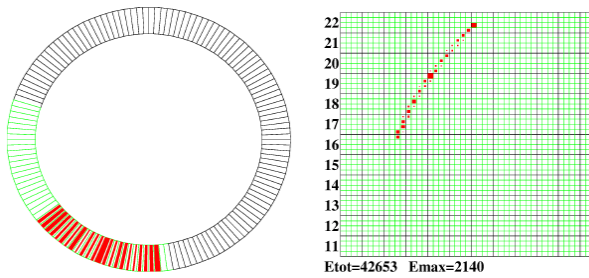
Fig. 1.8.7. Example of cosmic event recorded in cylindrical calorimeter.

140 modules of shaper digitizers for the end calorimeter will be received and tested in 2015. It is necessary to inspect the counters of the end calorimeter. It is also necessary to complete the development of the procedure and to create software for the amplitude and time calibration of the calorimeter, and then to perform calibration of the channels of the cylindrical calorimeter. It is also planned to install the electronics of the end calorimeter in the detector. In addition, it is planned to complete the development and begin the fabrication of the unit of luminance measurement by data from the calorimeter.

1.8.4. Computer calculations for Belle II.

Present-day experiments require distributed computing systems for simulation and data processing and analysis. The Belle II experiment is now at the preparatory stage. At the same time, the development and testing of a distributed computing system for this unique experiment goes on. The computing means of Novosibirsk were included in this system for the first time. With the help of DIRAC (Distributed Infrastructure with Remote Agent Control), the high-performance clusters of BINP, the Novosibirsk State University (NSU) and the Novosibirsk Supercomputer Center (NSC) were connected. That allowed the BINP group to take part in the simulation of the Belle II detector, as well as to debug and optimize our computer system. The Novosibirsk contribution amounted to about 5%, which meets the requirements of the Belle II collaboration. The results were reported at the international conference ACAT.

Fig. 1.8.8. Stages of disassembly of sector of calorimeter and replacement of resistors.

2

ELECTRO- AND PHOTONUCLEAR PHYSICS

2. EXPERIMENTS WITH INTERNAL TARGETS

I. Accounting for two-photon exchange (TPE) contribution to the elastic scattering of electrons on the proton will probably explain the contradiction in the results of measurement of the electromagnetic form factors of the proton in a variety of experimental techniques. To date, three experiments were already conducted in the world on determination of the TPE contribution to the process. Those are experiments by the collaborations OLYMPUS (DESY, Germany) and CLAS (TJNAF, USA) and the BINP experiment on VEPP-3 storage ring. In all the three cases, the TPE contribution was determined from measurements of the quantity R, which is the ratio of the cross sections of elastic scattering of electron/positron by the proton. At BINP, the data were collected at two electron/positron beam energies, of 1.6 GeV and 1.0 GeV. The data acquisition was completed in 2012. In 2014 we analyzed the experimental data. The investigation included making various corrections, as well as an analysis of systematic errors. The presence of two almost identical registration systems located on opposite sides of beam suppressed changes in their total counts caused by small beam displacements in the storage ring. Negligible magnetic fields in the vicinity of the particle detector eliminated the problem of equality of acceptance of the particle detectors in case of scattering of electrons/positrons (this is a big problem for OLYMPUS and CLAS). The allowance for the contribution of radiative corrections was an important step in the analysis: it accounts for a significant part of the deviation of the measured value from unity. The work on the calculation of radiative corrections was completed; the results were published in *Journal of Physics G: Nuclear and Particle Physics*. Fig. 2.1. presents the measurement results vs. ε (virtual photon polarization). Measurements with highest ε were used for normalization at both the energies. The normalization value was set equal to 1. The figure also shows results of previous experiments, with much larger errors. The lines show some theoretical predictions for R. It should be noted that calculations by P.G. Blunden. et al. and D. Borisyuk and A. Kobushkin practically coincide. The experimental data points obtained in this work lie approximately midway between this pair of curves and the curve from a work by J.C. Bernauer et al. A recent study found the parameterizations of the form factors of the proton, the Coulomb corrections and TPE contribution. The parameterizations describe well a large set of experimental data, including results of both unpolarized measurements (data of differential cross sections were used) and polarized measurements (the measured ratios of the form factors were used). That is, this approach removes the above-mentioned contradiction between the proton form factor results obtained by the Rosenbluth method and by the polarization transfer method. Calculations by P. G. Blunden et al. also show

the TPE contribution to eliminate this contradiction. The results of the experiment were published in Arxiv and accepted for publication in *Physical Review Letters*.

II. Coherent photoproduction of the neutral pion on the deuteron is an essential process in nuclear physics, providing valuable information about the deuteron structure and pion-nucleon and nucleon-nucleon interactions. The presence of only two particles in the final state simplifies the calculations and allows one to make more definite predictions on their interactions and intermediate states of the proton-neutron pair.

Although theoretical studies of the reaction have been carried out for a long time (since the 70s), detailed experimental data on the differential cross sections appeared relatively recently. As for polarization observables in this reaction, there are only a few measurements of the sigma asymmetry. There were no measurements of the tensor analyzing powers of the reaction until our data were derived from the statistical data of the experiment on the photo-disintegration of the deuteron (Nikolenko D.M. et al. *JETP Letters* 89, 518 (2009)). The accuracy of those measurements was low. In May-July 2013, data on the coherent production of the neutral pion on a tensor-polarized deuteron target were collected. The integrated charge that crossed the target during the data collection was 154 kCoulomb. The average value of the tensor polarization of the target was $37.3 \pm 1.1\%$. It is expected that the accuracy of the tensor analyzing power of the T_{20} reaction will be improved several times and data on the differential cross sections will be obtained. Some data collected were processed in 2014. Fig. 2.2 presents some preliminary results of the experiment to measure the tensor analyzing power of the T_{20} reaction. As can be seen, a discrepancy between our data and the theoretical prediction at high photon energies is beginning to show.

Theoretical predictions: solid curves (calculation by A. Fix, private communication) and dashed lines (calculation by S. Kamalov et al.).

III. Another check of the photon tagging system (PTS) was carried out in 2014. A computer modeling identified the following main factors influencing the angular and energy resolution of the PTS: the accuracy of determination of the coordinate of the electron emission point, multiple scattering of electrons on the vacuum chamber wall, and the accuracy of determination of the coordinates of the electron track. For the purpose of suppression of bremsstrahlung backgrounds by the anticoincidence method, the PTS has a scintillation 28-period sandwich detector to register bremsstrahlung gamma quanta and a 4-period scintillation sandwich detector in the electron detection arm. Accurate measurement of the coordinates of electron tracks is performed with stage gas electron multipliers (GEMs) with resolution better than 100 microns.

The PTS was tested on the bremsstrahlung (these sandwiches set at small angles were detecting coincidence of a bremsstrahlung photon and a scattered electron). PTS test results are presented in Fig. 2.3, which shows the

coordinate dependence of energy release in the sandwiches in 2 GEMs with 600 MeV electrons in VEPP-3. As can be seen, the experimental dependences of energy release in the sandwiches are in good agreement with the simulation results.
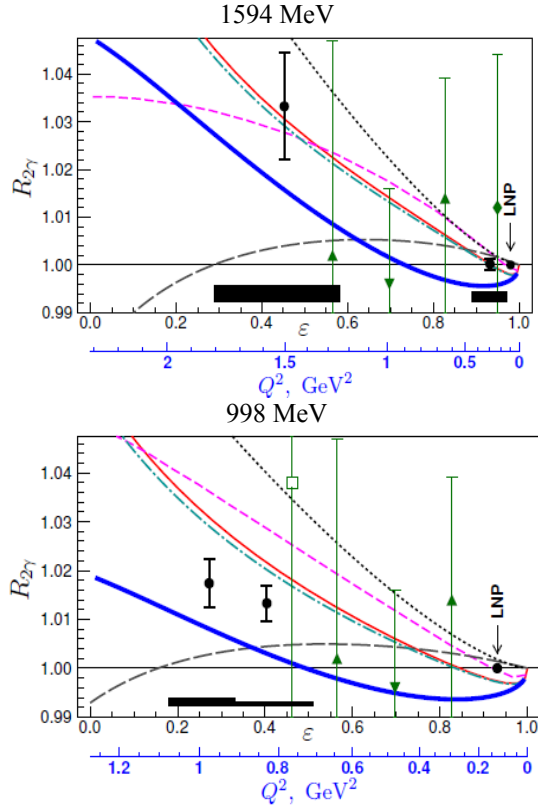
Fig. 2.1. Experiment results: $R_{2\gamma}$ ratio vs. ε and Q^2. Black circles: data from this experiment.

The accelerator time provided (about one week of work with beam) was not enough for joint data acquisition by the PTS and the secondary particle detector for comprehensive test of the PTS.

IV. Works on the creation of a prototype of source of polarized molecules of hydrogen isotopes continued. All components of the experimental setup were fabricated, and part of the installation was mounted. The source of molecules was fully assembled and checked for leaks. The chamber for measurement of intensity of polarized molecules is under assembly.

The experiments with internal targets were carried out in collaboration with physicists from Tomsk, NIKHEF (Netherlands), and ANL (USA).

The works at the installation Deuteron in 2014 resulted in publication of 11 articles and 4 reports delivered at international conferences
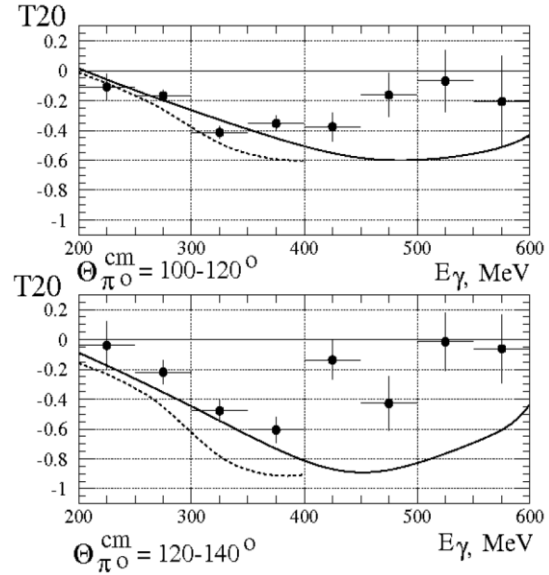
Fig. 2.2. Preliminary results on tensor analyzing power of T_{20} reaction of coherent photoproduction of neutral pion on deuteron vs. gamma quantum energy. Top graph: for pion emission angles of 100 to 120 degrees in center of mass system. Bottom graph: for pion emission angles of 120 to 140 degrees.
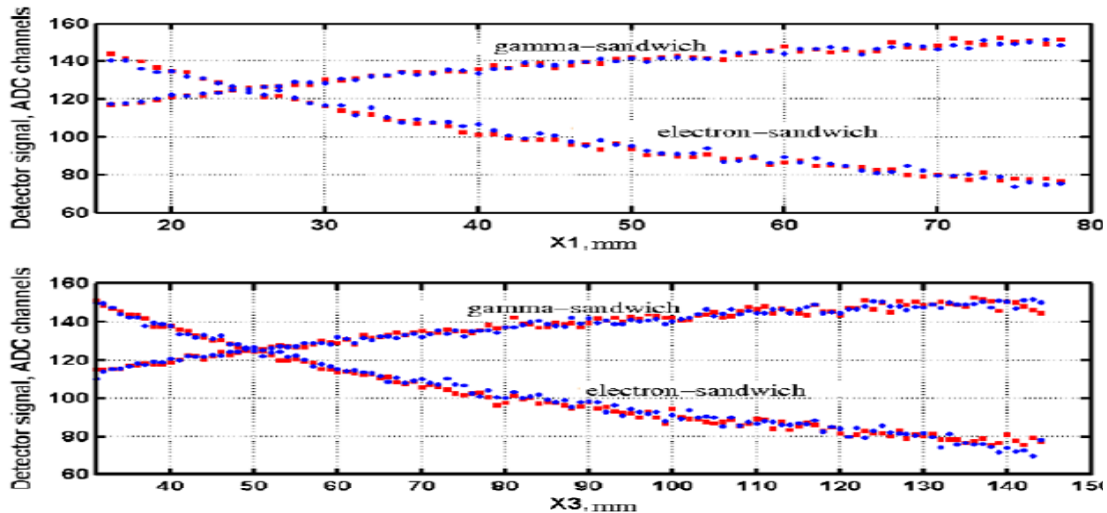
Fig. 2.3. Energy in sandwiches vs. coordinates in GEMs (experimental results and simulations).

3

THEORETICAL PHYSICS

QCD

"Low-X evolution equation for proton green function"
A.V.Grabovsky,
Acta Phys.Polon.Supp. 7 (2014) 3, 493

In the next-to-leading order, we discuss the low-x evolution equation for the baryon Wilson loop operator, which is a natural model for the Green function describing proton scattering in the Regge limit.

"Impact factor for high-energy two and three jets diffractive production"
R. Boussarie, A.V. Grabovsky,
L. Szymanowski, S. Wallon,
JHEP 1409 (2014) 026.

We present the calculation of the impact factor for the $\gamma(*) \to q\bar{g}$ transition within Balitsky's high energy operator expansion. We also rederive the impact factor for the $\gamma(*) \to q\bar{g}$ transition within the same framework. These results provide the necessary building blocks for further phenomenological studies of inclusive diffractive deep inelastic scattering as well as for two and three jets diffractive production which go beyond approximations discussed in the litterature.

"Hard exclusive two photon processes in QCD"
Progress in Particle and Nuclear Physics (online),
V.L. Chernyak, S.I. Eidelman,
http:dx.doi.org/10.1016/j.ppnp.2014.09.002, pp. 1-42,
arXiv,:1409.3348 [hep-ph], pp. 1-58

This is a short review of some hard two-photon processes:
a) $\gamma\gamma \to P_1P_2$, $P_1P_2 = \{\pi^+\pi^-, K^+K^-, K_SK_S, \pi^o\pi^o, \pi^o\eta\}$;
b) $\gamma\gamma \to V_1V_2$, $V_1V_2 = \{\rho^o\rho^o, \phi\phi, \omega\phi, \omega\omega\}$;
c) $\gamma\gamma \to$ барион-антибарион;
d) $\gamma^*\gamma \to P^o$, $P^o = \{\pi^o, \eta, \eta', \eta_c\}$.
The available experimental data are presented. A number of theoretical approaches to calculation of these processes is described, both those based mainly on QCD and more phenomenological (the handbag model, the diquark model, etc). Some theoretical questions tightly connected with this subject are discussed, in particular: the applications of various types of QCD sum rules, the endpoint behavior of the leading twist meson wave functions, etc.

"Gluon Reggeization Proof in Yang-Mills Theories"
V.S. Fadin, M.G. Kozlov, A.V. Reznichenko,
INP-preprint 2014-19

The proof of the gluon Reggeization in Yang-Mills within the framework of next-to-leading logarithmic approximation (NLA) are reviewed. Recently we obtained the results extending the proof of the multi-Regge form

from QCD to the supersymmetric Yang-Mills theories. Explicit expressions for new (in comparison with QCD) effective Reggeon vertices are presented up to one-loop level both in multi-Regge and quasi-multi-Regge kinematics in SYM. Special attention is given to one-loop radiative corrections resulting from the scalar SYM sector. We demonstrate the fulfilment of new elastic and inelastic bootstrap conditions both for multi-Regge and quasi-multi-Regge kinematics in the scalar sector of SYM. It ensures the validity of the multi-Regge form of the amplitude with the gluon exchange in NLA together with our early demonstrations in the gluon and fermion sectors of QCD. Some interesting details of the bootstrap verifications are described for the first time. Remnant problems of the Reggeization proof are stressed for the future consideration.

"Multi-Regge Form of Gluon-Exchange Amplitudes in Supersymmetric Yang-Mills Theories"
V.S. Fadin, M.G. Kozlov, A.V. Reznichenko,
Physics of Atomic Nuclei, 2014,
Vol. 77, No. 2, pp. 251-273

Within supersymmetric Yang-Mills theories, all effective vertices for the interaction of Reggeized gluons with particles were found both in the leading-logarithm approximation and in the next-to-leading order approximation. The contributions of scalars to the eigenfunction of the Balitsky-Fadin-Kuraev-Lipatov (BFKL) kernel for the adjoint representation of the gauge group and to impact factors similar to those in QCD were calculated. The impact factors that arise in supersymmetric Yang-Mills theories, but which are not present in QCD, are also found. Fulfillment of all bootstrap conditions, which guarantees the multi-Regge form of multiparticle amplitudes in supersymmetric Yang-Mills theories in the next-to-leading-order approximation, was proven. A method for testing bootstrap relations without calculating explicit expressions for vertices and impact factors was developed. This method was used to prove fulfillment of bootstrap conditions in theories featuring any number of fermions and scalar particles transformed according to any representations of the color group and involved in interactions with one another via Yukawa coupling.

"Regge vertex for quark production in the central region of rapidity in the next-to-leading order"
M. G. Kozlov, A. V. Reznichenko,
To be published in Yadernaya Fizika, 2015.

We calculate the effective vertex for quark production in the collision of Reggeized quark and Reggeized gluon within the next-to-leading order (NLO). Vertex calculated is the NLO missing element of the multi-Regge amplitude with quark and gluon exchanges in t-channels. Results of our calculation allow one to develop the bootstrap approach to the proof of the quark Reggeization

hypothesis in the next-to-leading logarithmic approximation (NLA).

"Regge amplitudes with quark and gluon exchange"
A.V. Reznichenko, M.G. Kozlov,
Poster report (in English) in XII
conference "Young scientists of Russia"
of the Dynasty Foundation, April 13-16 (2014).

We present the state of art for the quark Reggeization hypothesis within next-to-leading logarithmic approximation in QCD. The NLO quark effective vertex calculations are considered.

"Three Loop Cusp Anomalous Dimension in QCD"
Andrey Grozin, Johannes M. Henn,
Gregory P. Korchemsky, Peter Marquard
arXiv:1409.0023 [hep-th]
Phys.Rev.Lett.114 (2015) 062006 p.5

We present the full analytic result for the three loop angle-dependent cusp anomalous dimension in QCD. With this result, infrared divergences of planar scattering processes with massive particles can be predicted to that order. Moreover, we define a closely related quantity in terms of an effective coupling defined by the lightlike cusp anomalous dimension. We find evidence that this quantity is universal for any gauge theory and use this observation to predict the nonplanar n_f-dependent terms of the four loop cusp anomalous dimension.

"The n_f terms of the three-loop cusp anomalous dimension in QCD"
Andrey Grozin, Johannes M. Henn,
Gregory P. Korchemsky, Peter Marquard
Proceedings of Science LL2014 (2014) 016 (8 p.);
arXiv:1406.7828 [hep-th]

In this talk we present the result for the n_f dependent piece of the three-loop cusp anomalous dimension in QCD. Remarkably, it is parametrized by the same simple functions appearing in analogous anomalous dimensions in N=4 SYM at one and two loops. We also compute all required master integrals using a recently proposed refinement of the differential equation method. The analytic results are expressed in terms of harmonic polylogarithms of uniform weight.

"Reducing differential equations for multiloop master integrals"
R.N. Lee
arXiv: 1411.0911

We present an algorithm of the reduction of the differential equations for master integrals to the Fuchsian form with the right-hand side matrix linearly depending on dimensional regularization parameter ε.

"Effective weak Lagrangians in the Standard Model and B decays"
A.G.Grozin
Proceedings of the Helmholtz International School
"Physics of Heavy Quarks and Hadrons'"
ed. A.Ali, Yu.Bystritskiy, M.Ivanov,
Verlag Deutsches Elektronen-Synchrotron (2014),
p.78-98,
ISBN 978-3-935702-82-9, ISSN 1435-8077

Weak processes (e.g., B decays) with characteristic energies $<< M_W$ can be described by an effective theory which does not contain $W,\ Z$ and other heavy particles (Higgs, t). Its Lagrangian contains four-fermion interaction operators. Essentially it is the theory proposed by Fermi and improved by Feynman, Gell-Mann, Marshak, Sudarshan.

"Introduction to Mathematica for Physicists"
A.G.Grozin
Graduate Texts in Physics, Springer (2014),
219 pages ISBN 978-3-319-00893-6;
ebook ISBN 978-3-319-00894-3

Mathematica is the most widely used system for doing mathematical calculations by computer, including symbolic and numeric calculations and graphics. It is used in physics and other branches of science, in mathematics, education and many other areas. Many important results in physics would never be obtained without a wide use of computer algebra. This book describes ideas of computer algebra and the language of the Mathematica system. It also contains a number of examples, mainly from physics, also from mathematics and chemistry. After reading this book and solving problems in it, the reader will be able to use Mathematica efficiently for solving his/her own problems.

"Isoscalar amplitude dominance in e+e- annihilation to $N\bar{N}$ pair close to the threshold"
V.F. Dmitriev, A.I. Milstein, and S.G. Salnikov
Physics of Atomic Nuclei, 77, 1173-1177 (2014)

We use the Paris nucleon-antinucleon optical potential for explanation of experimental data in the process $e+e-\rightarrow p\bar{p}$ near threshold. It turns out that final-state interaction due to Paris optical potential allows us to reproduce available experimental data. It follows from our consideration that the isoscalar form factor is much larger than the isovector one.

"Impact factors for Reggeon-gluon transition in N=4
SYM with large number of colours"
V.S.Fadin and R.Fiore
Phys. Lett. B 734 (2014) 86-91

Impact factors for Reggeon-gluon transition in supersymmetric Yang-Mills theory with four supercharges at large number of colours are considered. In the next-to-leading order impact factors are not uniquely defined and must accord with BFKL kernels and energy scales. We obtain the impact factor corresponding to the kernel and the energy evolution parameter, which is invariant under Möbius transformation in momentum space, and show that it is also Möbius invariant up to terms taken into account in the BDS ansatz.

"Discontinuities of multi-Regge amplitudes"
V.S.Fadin
arXiv:1412.3253 [hep-th]

In the BFKL approach, discontinuities of multiple production amplitudes in invariant masses of produced particles are discussed. It turns out that they are in evident contradiction with the BDS ansatz for n-gluon amplitudes in the planar $N = 4$ SYM at $n > 5$. An explicit expression for the NLO discontinuity of the two-to-four amplitude in the invariant mass of two produced gluons is is presented.

CHAOS

"Elastic Enhancement Factor: from Mesoscopic Systems
to Macroscopic Analogous Devices"
Valentin.V. Sokolov, Oleg V. Zhirov
Short version: arXiv:1411.6211v2 [nucl-th] 12 Dec 2014

Excess of probabilities of the elastic processes over the inelastic ones is a common feature of the resonance scattering processes that are described with the aid of random matrix theory (RMT). Quantitatively, this phenomenon is characterized by the elastic enhancement factor F that is a typical ratio of elastic and inelastic cross sections. Being measured experimentally, this quantity can supply us with important information about the character of the complicated states formed on the intermediate stage of a resonance reaction. Generally speaking, this factor depends on the number M of scattering channels as well as on the channel's transmission coefficients T. However, when the number of channels is very large, what is typical of the processes such as, for example, the resonance nuclear reactions, the enhancement factor is entirely controlled by the only parameter $\eta = MT$ that changes in very wide bounds (Verbaarschot's regime). We substantiate, in particular, the interpretation of this parameter as a ratio of two characteristic times one of which (the Heisenberg time) defines the internal motion whereas the second one (the

dwell or Weisskopf time) describes influence of the openness. On the contrary, in the macroscopic analogous experiments with 2D irregularly shaped electromagnetic resonators, that are widely used to mimic the chaotic quantum dynamics, the number of channels is very restricted. We show that in this case the enhancement factor depends, contrary to the Verbaarschot's regime, on the number of channels and on transmission coefficients separately. We juxtapose the two specified regimes in detail and demonstrate that complete analytical solution valid for any fixed number M of equivalent channels with transmission coefficients $0 < T < 1$ is possible in the case of the systems without time-reversal symmetry. More than that, in the practically important case of only two scattering channels, $M = 2$, influence of the absorption due to ohmic losses can also be described analytically. Meanwhile, no explicit analytical results can be derived in the case of a T-invariant devices. Therefore we have used numerical methods to be able to demonstrate the similarity as well as distinctions between the two last cases.

"Anderson transition for Google matrix eigenstates"
O. V. Zhirov, and D. L. Shepelyansky,
Annalen der Physik, 2014

We introduce a number of random matrix models describing the Google matrix G of directed networks. The properties of their spectra and eigenstates are analyzed by numerical matrix diagonalization. We show that for certain models it is possible to have an algebraic decay of PageRank vector with the exponent similar to real directed networks. At the same time the spectrum has no spectral gap and a broad distribution of eigenvalues in the complex plain. The eigenstates of G are characterized by the Anderson transition from localized to delocalized states and a mobility edge curve in the complex plane of eigenvalues.

GRAVITY AND COSMOLOGY

"Gravit four-fermion interaction in early Universe"
A.S.Rudenko, I.B.Khriplovich
UFN 184, No. 2, 177-181 (2014)
Phys. Usp. 57, iss. 2, 167-170 (2014)

If torsion exists, it generates gravitational four-fermion interaction (GFFI), essential on the Planck scale. We analyze the influence of this interaction on the Friedmann-Lemaitre-Robertson-Walker cosmology. An explicit analytical solution is derived for the problem where both the energy-momentum tensor generated by GFFI and the common ultrarelativistic energy-momentum tensor are included. We demonstrate that gravitational four-fermion interaction does not result in Big Bounce.

"Shape of the inflaton potential and the efficiency of the universe heating"
A.D. Dolgov, A.V. Popov, and A.S. Rudenko
arXiv:1412.0112 [astro-ph.CO]

It is shown that the efficiency of the universe heating by an inflaton field depends not only on the possible presence of parametric resonance in production of scalar particles but also strongly depends on the shape of the oscillations of the inflaton around its equilibrium point. In particular, when the inflaton oscillations deviate from pure harmonic one towards a succession of step functions, the production probability rises by several orders of magnitude. This in turn leads to a higher temperature of the universe after the inflaton decay. An example of the inflaton potential is presented, which creates a proper modification of the shape of the inflaton oscillations and does not destroy sufficiently long inflation.

QED

"On effective mass of a photon in a strong magnetic field"
V.M. Katkov
arXiv:1403.3983

For the magnetic field in order of the Schwinger critical value or much larger it, the effective mass of a real photon with a preset polarization is investigated in the energy region including two lower thresholds of electron-positron pair creation on Landau levels. In the high-energy range, when the number of thresholds is large, the quasiclassical approach is used.

"Spectral-integral representation of the photon polarization operator in a constant uniform magnetic field"
V.M. Katkov
arXiv:1411.2339

The polarization operator in a constant and homogeneous magnetic field of arbitrary strength is investigated on mass shell. The calculations are carried out at all photon energies higher the pair creation threshold as well as lower this threshold. The general formula for the effective mass of the photon with given polarization has been obtained being useful for an analysis of the problem under consideration as well as at a numerical work. Approximate expressions for strong or weak fields, compared with the critical field, have been found. Depending on the ratio of these fields we consider the pure quantum region of photon energy, where particles are created on lower Landau levels or created not at all. Also the energy region of large level numbers is considered where the quasiclassical approximation is valid.

"Effective mass of a photon in strong field "
V.M. Katkov
Book of abstracts of 6-th International Conference "Channeling 2014", p.36.
October 5-10, 2014, Capri, Italy

There is a series of evidences for the existence of neutron star possessing magnetic fields close and stronger the Schwinger critical field. The effective mass of photon in these fields is investigated. The imaginary part of this mass determines the probability of pair creation. The real part defines the dispersive properties of the space region with magnetic field.

"A new event generator for the elastic scattering of charged leptons on protons"
A.V. Gramolin, V. S. Fadin, A. L. Feldman, R. E. Gerasimov, D. M. Nikolenko,
I. A. Rachek and D. K. Toporkov
J. Phys. G: Nucl. Part. Phys. 41 (2014) 115001 (28pp)

This paper describes a new multipurpose event generator, ESEPP, which has been developed for the Monte Carlo simulation of unpolarized elastic scattering of charged leptons on protons. The generator takes into account the lowest-order QED radiative corrections to the Rosenbluth cross section including first-order bremsstrahlung without using the soft-photon or ultrarelativistic approximations. ESEPP can be useful for several significant ongoing and planned experiments.

"Approximations used in calculations of radiative corrections to electron-proton scattering cross section"
R.E. Gerasimov
Nonlinear Dynamics and Applications: Proceedings of the Twenty first Annual Seminar NPCS'2014,
Vol. 20 (2014) p. 56 – 63

We study the difference between the results of Mo and Tsai and Maximon and Tjon for the radiative corrections to unpolarized electron-proton scattering cross section. Particular attention is paid to the soft-photon approximation, which underlies the both calculations.

"Analysis of Approximations Used in Calculations of Radiative Corrections to Electron-Proton Scattering Cross Section"
R. E. Gerasimov and V. S. Fadin
BINP Preprint 2014-10

An analysis of approximations used in calculations of radiative corrections to electron-proton scattering cross section is presented. We investigate the difference between the relatively recent Maximon and Tjon result and the Mo and Tsai result, which was used in the analysis

of experimental data. We also discuss the proton form factors ratio dependence on the way we take into account radiative corrections.

"Coulomb corrections to electron scattering on the extended source and the proton charge radius"
R.N. Lee and A. I. Milstein
arXiv: 1402.3054

It is shown that the account for the proton charge form factor in the Coulomb corrections to the electron-proton scattering cross section noticeably diminishes the difference between the value of the proton charge radius r_E , extracted from the ep scattering data, and that following from the muonic hydrogen data. For the electron energy much higher than the electron mass but much smaller than $r^{-1}_E \approx 230$ MeV, the relative correction has the universal form $\delta r_E/r_E = -\pi\alpha/2$, where α is the fine structure constant.

"High-energy e^+e^- photoproduction in the field of a heavy atom accompanied by bremsstrahlung"
P.A. Krachkov, R.N. Lee, A. I. Milstein
Phys. Rev. A 90, 062112 (2014)

Helicity amplitudes and differential cross section of high-energy e^+e^- photoproduction accompanied by bremsstrahlung in the electric field of a heavy atom (i.e., the amplitudes of the process $\gamma_{1Z} \to e^+e^- \gamma_{2Z}$) are derived. The results are exact in the nuclear charge number and obtained in the leading quasiclassical approximation. They correspond to the leading high-energy small-angle asymptotics of the amplitude. It is shown that, in general, accounting for the Coulomb corrections essentially modify the differential cross section. When the initial photon is circularly polarized the Coulomb corrections lead to the asymmetry in the distribution over the azimuth angles φ_i of produced particles with respect to the replacement $\varphi_i \to \varphi_i$.

"Ultrarelativistic quasiclassical wave functions in strong laser and atomic fields"
A. Di Piazza and A.I. Milstein
Phys. Rev. A 89, 062114 (2014)

The problem of an ultrarelativistic charge in the presence of an atomic and a plane-wave field is investigated in the quasiclassical regime by including exactly the effects of both background fields. Starting from the quasiclassical Green's function obtained in [Phys. Lett. B **717**, 224 (2012)], the corresponding in- and out-wave functions are derived in the experimentally relevant case of the particle initially counterpropagating with respect to the plane wave. The knowledge of these electron wave functions opens the possibility of investigating a variety of problems in strong-field QED,

where both the atomic field and the laser field are strong enough to be taken into account exactly from the beginning in the calculations.

"Charge asymmetry in high-energy $\mu^+\mu^-$ photoproduction in the electric field of a heavy atom"
E.J. Downie, R.N. Lee, A.I. Milstein, and G. Ron
Physics Letters B 728, 645 (2014)

The charge asymmetry in the differential cross section of high-energy $\mu^+\mu^-$ photoproduction in the electric field of a heavy atom is obtained. This asymmetry arises due to the Coulomb corrections to the amplitude of the process (next-to-leading term with respect to the atomic field). The deviation of the nuclear electric field from the Coulomb field at small distances is crucially important for the charge asymmetry. Though the Coulomb corrections to the total cross section are negligibly small, the charge asymmetry is measurable for selected final states of μ^+ and μ^-. We further discuss the feasibility for experimental observation of this effect.

GRAVITY

"Some minisuperspace model for the Faddeev formulation of gravity"
V. M. Khatsymovsky
Mod. Phys. Lett. A, v.29, p. 1450141, 2014

We consider Faddeev formulation of general relativity in which the metric is composed of ten vector fields or a 4×10 tetrad. This formulation reduces to the usual general relativity upon partial use of the field equations. A distinctive feature of the Faddeev action is its finiteness on the discontinuous fields. This allows to introduce its minisuperspace formulation where the vector fields are constant everywhere on R^4 with exception of a measure zero set (the piecewise constant fields). The fields are parameterized by their constant values *independently* chosen in, e. g., the 4-simplices or, say, parallelepipeds into which R^4 can be decomposed. The form of the action for the vector fields of this type is found. We also consider the piecewise constant vector fields approximating the fixed smooth ones. We check that if the regions in which the vector fields are constant are made arbitrarily small, the minisuperspace action and eqs of motion tend to the continuum Faddeev ones.

"Modern techniques of multiloop calculations"
In Proceedings of the 49th Rencontres de Moriond,
R. N. Lee
ARISF, 2014, p 297

I present a few new and recent ideas of the multiloop calculations.

In the Faddeev formulation of gravity, the metric is regarded as composite field, bilinear of $d = 10$ 4-vector fields. We derive the minisuperspace (discrete) Faddeev action by evaluating the Faddeev action on the spacetime composed of the (flat) 4-simplices with constant 4-vector fields. This is an analog of the Regge action obtained by evaluating the Hilbert-Einstein action on the spacetime composed of the flat 4-simplices. One of the new features of this formulation is that the simplices are not required to coincide on their common faces and can be regarded virtually as independent ones. Also a parity-odd term can be introduced in this formalism vanishing on the field equations and characterized by some parameter, an analog of the Barbero-Immirzi parameter γ in GR responsible for the (discrete) area spectrum in quantum theory.

4

PLASMA PHYSICS AND CONTROLLED THERMONUCLEAR FUSION

4.1. GDL FACILITY

4.1.1. ECR heating of plasma in GDL facility.

In 2014, a series of successful experiments on electron cyclotron resonance (ECR) plasma heating was carried out on the GDL facility. The purpose of the experiment was adjustment of the scenario of combined plasma heating with 5 MW neutral beams and the ECR heating of a power of up to 0.7 MW, study of the physical mechanisms of hydromagnetic instability of plasma in such heating and finding ways to suppress this instability.

The ECR heating system consists of two 54.5 GHz pulsed gyrotrons of a power of 300 and 400 kW as measured at the entry to the plasma. Each gyrotron is powered by specially designed high-voltage power supplies, which form a rectangular high voltage pulse with an amplitude of 70 kV (with a stability not worse than 0.5%), a current of up to 25 A, and a duration of up to 3 ms. Radiation from the gyrotrons is delivered by separate closed quasi-optical lines to the vacuum chamber in the vicinity of the two magnetic plugs as shown in Fig. 4.1.1.
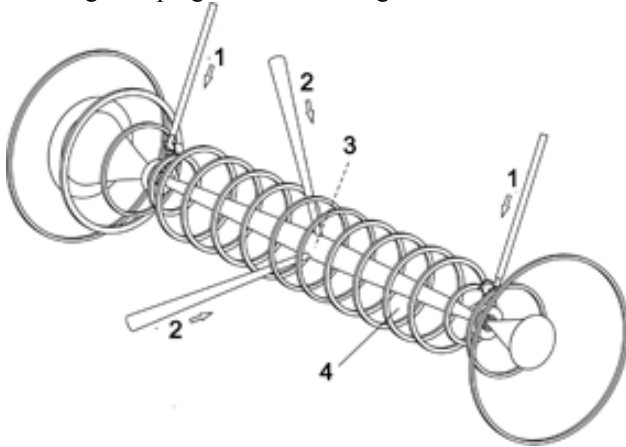
Fig. 4.1.1. Scheme ECR plasma heating in GDL facility. 1 – ECR, 2 – neutral beams, 3 – Tompson scattering, 4 – central solenoid.

To create optimal conditions for the ECR heating it is necessary to increase the magnetic field in separate coils placed around the absorption area. The additional current required for effective absorption on the opposite ends of the trap was attained at the expense of reduction of the magnetic field in the main body of the trap (from 0.35 to 0.27 T in the center of the facility). Such a perturbation of the magnetic configuration resulted in a significant deterioration of plasma confinement. In particular, without the ECR heating the electron temperature decreased from 250 eV to 150 eV.

In such a magnetic configuration, two scenarios of ECR heating were optimized. The first scenario was to improve the lifetime of hot ions arising when the plasma captures the heating neutral beams. This mode is characterized by absorption of the radiation of the gyrotrons almost throughout the cross section of the plasma, which led to

increase in the electron temperature throughout the plasma volume.
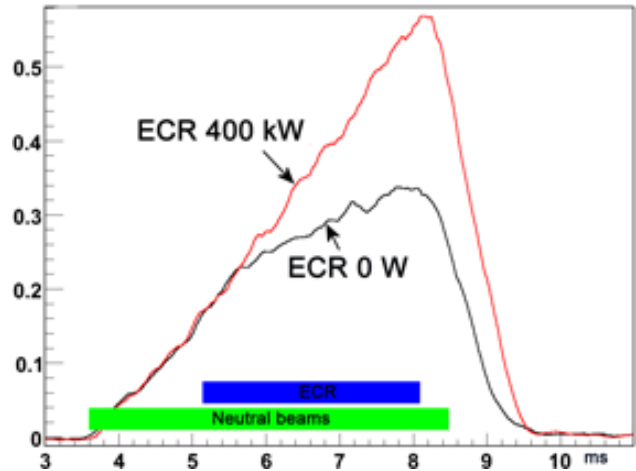
Fig. 4.1.2. Increase in neutron flux in ECR heating of plasma in GDL facility.

Since the lifetime of hot ions is proportional to the electron temperature raised to the power of 3/2, the ECR leads to a significant increase in the plasma energy and in the flux of DD fusion neutrons arising in collisions of hot ions (Fig. 4.1.2.). A stable discharge in this mode was only obtained at an ECR heating power of 400 kW at most. The electron temperature on the axis of the GDL facility was up to 200 eV.
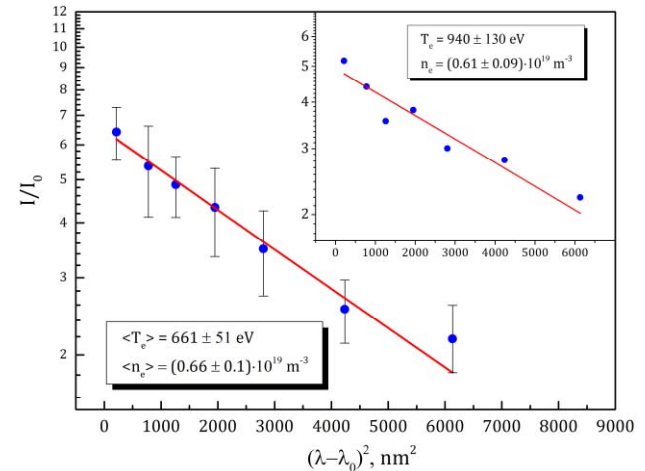
Fig. 4.1.3. Spectrum of Thomson scattering of laser radiation on plasma electrons on axis of GDL facility (averaged over a series of shots). Top right: one of record shots.

The second scenario was optimized for attaining of the maximum electron temperature. In this mode, most of the microwave power captured by the plasma is absorbed in a narrow region near the axis. So, when the gyrotrons were switched on, a discharge with a central temperature of 600 eV to 1 keV was formed in a few hundreds of microseconds (Fig. 4.1.3.). Although the radial temperature profile was heavily peaked, the energy balance showed

that plasma confinement in the axial zone occured in gas-dynamic mode, the radial transport and the classic longitudinal (Spitzer) electron heat conductivity being strongly suppressed. Thomson scattering measurements revealed that the energy was redistributed between thermal electrons, i.e. it was the question of electron temperature, not energy stored in the "tail" of high-energy electrons. These experiments the GDL resulted in open-systems' record temperature in a quasi-steady-state discharge (~ 1 ms), and the plasma parameters for the first time approached values comparable with those for toroidal systems.
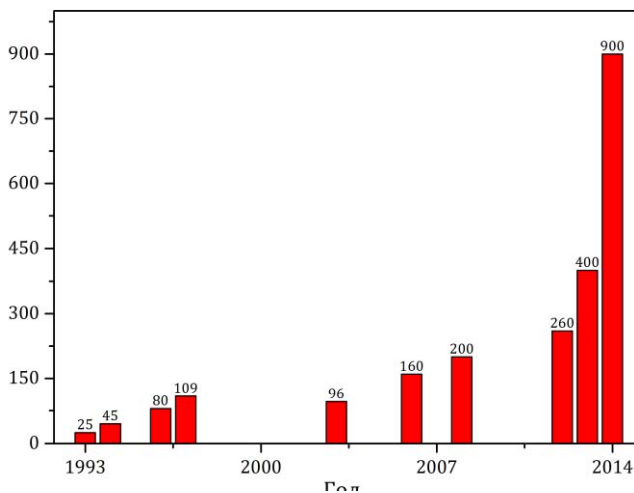
Fig. 4.1.4. Evolution of electron temperature of plasma in experiments on GDL facility (temperature (eV) vs Year).

This fact led us to a conclusion on good prospects for fusion applications based on open traps. For comparison, Fig. 4.1.4. presents a graph showing the progress of electron temperature growth in experiments on the GDL facility for 25 years.

A sudden and significant increase in the electron temperature upon switch-on of the ECR heating leads to the development of MHD instability of flute type plasma. In a standard GDL facility discharge (without the ECR), this instability is suppressed by the method of "vortex confinement", when a constant electric potential is applied to the periphery of the plasma, which makes the plasma rotate in the crossed electric and magnetic fields. For effective suppression of transverse losses in flute instability, the radial potential applied needs to be comparable with the electron temperature. With a large increase in the plasma temperature in the ECR heating, this condition can be violated. To solve this problem, we used the method of stepwise increase in the radial potential with the temperature increase in the ECR heating being monitored. As a result, we managed to realize relatively stable ECR heating of plasma of a power of 700 kW for a time comparable with the total charge duration in the facility.

Namely optimal scenarios of ECR plasma heating with an extraordinary wave at the first harmonic in the main volume of the trap enabled the demonstration of discharge of a record high electron temperature. This result gives a reliable basis for creation of open-trap nuclear fusion reactors with axis-symmetrical configuration of magnetic field simplest in terms of engineering. An immediate application of such reactors can be a powerful source of neutrons produced in fusion of deuterium and tritium nuclei. Such source is necessary in a number of problems of thermo-nuclear materials science, as well as in control of sub-critical nuclear reactors, including radioactive waste disposal facilities.

4.1.2. Studying AIC instability.

Besides that, the development of kinetic Alfven ion-cyclotron (AIC) plasma instability and its impact on losses of hot ions from plasma were studied this year on the GDL facility. Analysis of predictions of the theoretical model describing the interaction of ions with an Alfven wave enabled a conclusion that in the GDL facility conditions only a small portion of hot ions actively interacts with the wave. Those are hot ions in a narrow phase space region near the point corresponding to the angular spread and speed of trapped ions of neutral beams. This gives an open-trap-favorable prediction on the effect of this micro-instability on confinement of hot ions, because the region of active interaction of particles with the wave is rather far from the border of the loss cone in the phase space. It was expected that the Alfven ion cyclotron instability in a GDT and fusion-class systems based on it would not cause a significant increase in the loss of hot ions. A number of experiments were carried out on the GDL facility for experimental verification of these theoretical conclusions. The main diagnostics was done with a five-channel magnetic energy analyzer placed in the expansion tank. The analyzer was used for measurement of the energy spectrum of ions leaving the central cell of the GDL facility along the magnetic field lines; the time dependences of the absolute values of the power carried out to the plug and the average energy of particles leaving the facility were analyzed for a wide energy range.
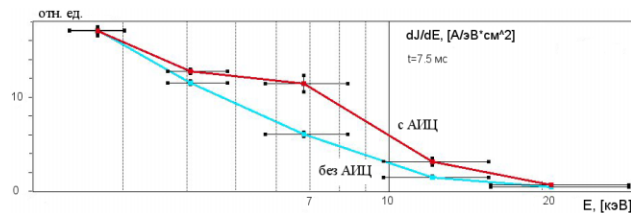
Fig.4.1.5. Distribution function of ions leaving plasma along magnetic field lines.

Fig.4.1.5 shows the ion energy distribution measured during development of AIC and without it in the energy range from 2.5 keV to 25 keV. Analysis of the experimental data revealed widening of the hot ion density peak in the stopping region during the development of AIC (the degree of anisotropy decreases) and increase in the loss of particles along the magnetic field force lines at energies about 7-10 keV, which is significantly less than the energy

of deuterons injected (25 keV). The ratio of the loss power in the non-stability development to the power captured by plasma during heating with an atomic injection of ~ 2 MW is less than 0.5%. This experimental fact confirms the theoretical conclusions on the insignificant influence of AIC development on longitudinal losses of hot ions in the experiment on the GDL facility.

4.1.3. Study of global acoustic modes.

Another important result was obtained in 2014 in the study of global acoustic modes using a system of low-frequency magnetic probes. In a regime with ECR heating, vibrations at a frequency of about 90-100 kHz with the azimuthal mode $m = 0$ were observed in the spectral decomposition of signals from the magnetic sensors (Fig. 4.1.6). From analysis of phase signals from the linear assembly sensors, a longitudinal structure of the vibrations was detected: oscillations with the longitudinal mode $N = 1$ were observed. The azimuthal and longitudinal structure and the frequency of the vibrations repeat the pattern that was observed in a regime without ECR heating.

The oscillations detected in the regime with ECR heating are distinguished by their amplitude. It is 2-3 times as large as the maximum amplitude of respective oscillations without ECR heating at the place where the linear assembly sensors are placed. The amplitude of oscillations of the relative plasma pressure at the point of stop of fast ions is about 1-2 percent of the full pressure value. The nature of the oscillation damping also changed in the regime with ECR heating. Without ECR heating, an abrupt increase in the amplitude to the maximum values is observed at the moments when the AIC instability is excited. The amplitude returns to the previous level in 4-5 periods after its sharp rise. On the other hand, with the ECR heating the amplitude of oscillations stays large until the beginning of the plasma decay stage and even 0.5 ms after the switch-off of the gyrotrons. Despite the development of a global acoustic mode of considerable amplitude, the plasma confinement in the GDL is not deteriorated, at least if judged by the energy content of the plasma and the integrated neutron output.
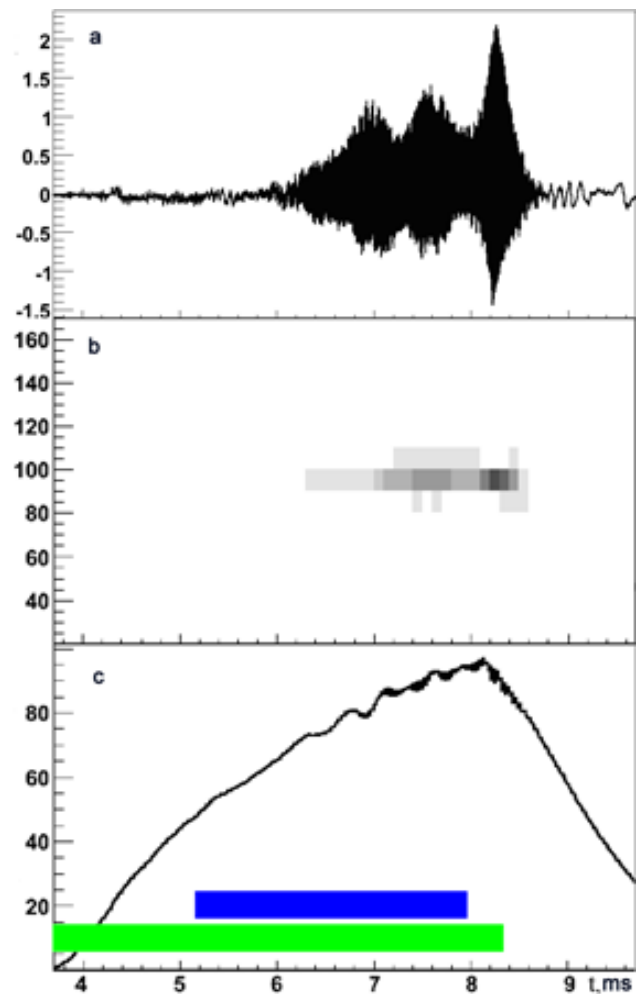
Fig. 4.1.6. Development of global acoustic mode: a) signal from magnetic probe (amplitude, V); b) spectrum of signal from magnetic probe (frequency, kHz); c) energy content of plasma (diamagnetism, kMks)

4.2. GOL-3 FACILITY

4.2.1. GOL-3 facility: reconstruction program.

Investigations into processes occurring in collective relaxation of electron beam in plasma play an important role in plasma physics. These processes define the properties and behavior of plasma in areas of very different parameters, e.g. dynamics of stellar atmospheres or heating of fusion targets in the "fast ignition" scheme. The GOL-3 facility, which has been operated since 1988, is one of the largest plants intended for beam-plasma experiments.

The main scientific objective of the construction of the GOL-3 facility was to determine conditions for fast collective heating of plasma confined in a multiple-mirror trap. The GOL-3 facility has the following parameters: plasma density of 10^{21} m^{-3}, plasma column length of 12 m, plasma diameter of 8 cm, guiding magnetic field of the solenoid of up to 6 T, electron energy of up to 1 MeV; electron beam current of up to 30 kA, beam length of 8 - 12 μs, and total energy content of 100 - 200 kJ. The generator of relativistic beam is the accelerator U-2 with a megavolt strip diode.

The unique technical capabilities of the GOL-3 facility enabled significant expansion of research as compared with the initial plans. The facility has worked in the following fields:

1) physics of beam-plasma interaction;

2) physics of multiple-mirror confinement of plasma;

3) impact of high-power flows of hot electron plasma on materials of the first wall, up to loads corresponding to major disruption in reactor-class tokamaks;

4) generation of subterahertz electromagnetic radiation in a turbulent plasma heated by an electron beam.

Recently at the GOL-3 facility, along with the activity on using a high-current relativistic electron beam, experiments with a subrelativistic electron beam with an energy of 80 - 100 keV, a power of 2 - 8 MW and duration of about 100 μs were conducted at lower plasma parameters. The primary objective of these experiments was to study processes in quasi-stationary conditions, which cannot be realized with a relativistic electron beam.

Multiple-problems research necessitates selection of a particular experimental configuration and plasma parameters in a transition from an actual research topic to next one, whereas some capacities of the facility can be used not in all configurations. For example, the 12-meter length of the solenoid with a magnetic field is required only for experiments on the physics of multiple-mirror confinement of plasma.

Analysis of the development opportunities has led to a decision on extensive reconstruction of the GOL-3 facility, to optimize the configuration of the equipment for more efficient solution of scientific problems and reduce the time for transition from one experimental configuration to another. Two new specialized facilities will be constructed on the site of the multiple-mirror trap GOL-3, see. Fig. 4.2.1. The first stage of the reconstruction will be creation of a facility for research on the physics of beam-plasma interaction and generation of terahertz electromagnetic-magnetic radiation. This facility was named GOL-3T; it is a direct continuation of GOL-3. The second facility, GOL-NB, which will be created at further stages of the reconstruction, will be intended for research on multiple-mirror plasma confinement; the basic method of heating will be injection of neutral beams.

4.2.2. GOL-3T facility.

The technical parameters of the new plasma part of GOL-3T were selected with due account of the experience of work with electron beams with large energy content. Such electron beams have sufficient energy and may irreversibly destroy the vacuum chamber in case of loss of stability during its transportation along the magnetic field. The insufficiently high conductivity of plasma beyond the electron beam cross-section hampers formation of reverse current in this area, which leads to growth of uncompensated total current along the plasma column with the risk of breach of the Kruskal-Shafranov criterion,
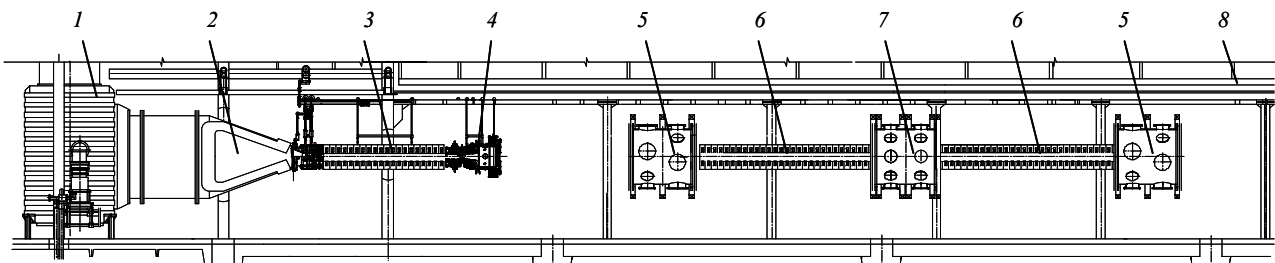
Fig. 4.2.1. Scheme of GOL-3 after reconstruction (side view). In the left is the electron beam generator U-2 with a short plasma section intended for research on the physics of beam-plasma interaction. In the right is a new installation, designed for study of quasi-stationary multiple-mirror confinement of plasma heated with a powerful neutral beam. 1 - diode tank of accelerator U-2, 2 - section for re-shaping and magnetic compression of relativistic electron beam, 3 - solenoid 2.4 m long, 4 - system for production of pre-plasma, 5 - tanks of end expanders, 6 – multiple-mirror solenoids, 7 - central trap with system of neutral injection; 8 - existing suspension structures of GOL-3.

$$q = \frac{2\pi a}{L}\frac{B_z}{B_\theta} = \frac{(2\pi a)^2 B_z}{\mu_0 LI} > 1, \qquad (1)$$

where q is the stability margin; B_z and B_θ are the longitudinal and azimuthal magnetic field components; a and L are the radius and length of current-carrying plasma; μ_0 is the magnetic permeability of the vacuum; I is the total current in the plasma. With the typical parameters of the GOL-3 experiment, if the conditions for formation of compensating reverse current are violated, this may lead to a many-fold excess of the threshold current and loss of the stability of the beam-plasma system.

Therefore, it was decided to reduce several times the length of the magnetic system for the Kruskal-Shafranov criterion to be matched even in most adverse conditions. In the reconstruction, the existing elements of the GOL-3 facility were used to the full: the coils of the magnetic system, the sections of the vacuum chamber, the power supply systems, and the subsidiary systems.

The entire magnetic system of the facility includes the main solenoid, high-field coils, magnetic system of the accelerator U-2, and magnetic coils for production of pre-plasma and of the output expander of magnetic flux. The solenoid consists of 20 standard coils with a spacing of 11 cm. The power supply system enables operation in a regime with a homogeneous magnetic field with an induction of 4.5 T, as well as in regimes with periodic modulation (corrugation) of magnetic field with periods of 22 and 44 cm with the same magnitude of magnetic fields in the maxima of the corrugation.

The vacuum chamber is partitioned, which enables easy adaptation of the facility to requirements of a particular experiment. The inner diameter of the chamber is 10 cm.

An initial low-temperature plasma is produced using a special high-current discharge flowing along a magnetic field throughout the facility. Provisionally, the electrode system of the discharge consists of three high-voltage ring electrodes and two groups of several floating diaphragms located in the area of each exit magnetic mirror. At the opposite end of the solenoid, the discharge current is closed to the wall of vacuum chamber across the magnetic field in the area of final compression of the electron beam prior to its injection into the solenoid. The conductivity is provided by a short cloud of krypton. As expected, the configuration with the shorter solenoid turned out to be best for discharge operation. This enables expansion of the range of operating parameters toward higher plasma concentration.

The electron beam dump is intended for a magnetic field of about 0.1 T, in which the specific heat load on the surface of the dump does not lead to a significant erosion of the graphite surface.

The starter set of diagnostics includes measurement of currents and voltages at different points of the facility, eight diamagnetic loops, three digital cameras with a frame of 7 microseconds the least, equipment for recording of the spectrum and polarization of subterahertz radiation of plasma, a Michelson interferometer with an operating wavelength of 10.6 m, a detector of VUV radiation, and an 8-channel X-ray monitor of electron beam symmetry at the entrance.

Upon the mounting of the plasma part of the GOL-3T facility, a physical start of the facility was performed for demonstration of operation of the main systems and production of an initial low-temperature plasma of a predetermined density range. The experiments were performed in two basic configurations. At the first stage, the magnetic system of the GOL-3T facility operated independently of the magnetic system of the accelerator U-2. The end of the vacuum chamber opposite to the system for production of the initial plasma was closed with a stainless steel flange electrically connected with the housing. In this configuration, the discharge current flew through the end flange and further on the vacuum chamber. Later on, the end flange was removed and the solenoid and the vacuum chamber were connected to the accelerator U-2, and the facility was tested in the project configuration. In this case, the discharge current was closed to the housing of the facility due to the transverse collision conductivity, which was provided by a krypton clot injected in pulses at $z = -22$ cm in front of the entrance magnetic mirror. In these experiments, hydrogen was injected into the chamber via one pulse valve at $z = 150$ cm. In the future, the second pulse valve at $z = 51$ cm will be used for formation of a more accurate profile of the initial concentration of hydrogen along the length of the facility, for optimization of conditions for generation of subterahertz radiation.

Figure 4.2.2 shows typical discharge parameters in a high-density regime in a configuration with the discharge current closed to the metal surface at the far end of the vacuum chamber; the average $n_e > 5 \times 10^{21}$ m^{-3}. The plasma current oscillates for a few periods with decaying amplitude. The current amplitude J_{pl} is as high as 20 - 25 kA with low plasma density and decreases with increasing initial concentration of hydrogen.

In general, experimentation at the stage of physical start of the plasma part confirmed the existing views on the mechanism and the features of work with high-current discharge with ring electrodes, by means of which the initial low-temperature plasma is produced at the facility. A plasma of density in the range of 2×20^{20} to 5×20^{21} m^{-3} was produced. The plasma system and the starter diagnostics set are ready for injection of relativistic electron beam into plasma under the program of research on the plasma mechanisms of generation of high-power terahertz electromagnetic radiation.
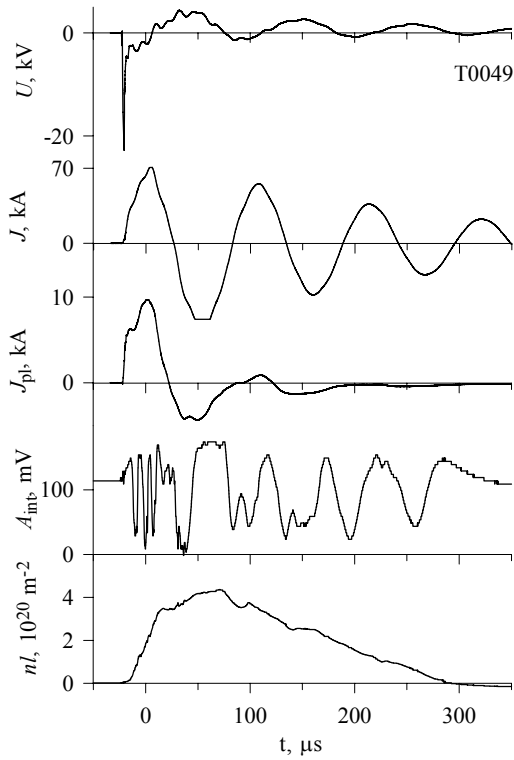
Fig. 4.2.2. Typical dynamics of discharge parameters in high-density regime. From top to bottom: voltage U across high-voltage direct-discharge electrode, total current J in feed circuit of pre-plasma production system, plasma current J_{pl}, unprocessed signal of interferometer A_{in}, and density integral over diameter of plasma nl, calculated from signal of interferometer. $t = 0$ corresponds to the standard beginning of electron beam injection in experiments on beam plasma heating.

4.2.3. Measurement of angular spread of velocities of beam electrons in accelerator U-2.

The spread of the directions of the velocities of electrons relative to the guiding magnetic field at the point where the beam enters the plasma is one of the important parameters that determine the efficiency of the beam-plasma interaction. At the same time, namely the magnetization of the motion of electrons in the beam in the guiding magnetic field hampers the measurement of this parameter. In previous series of experiments at the installations INAR, U-1 and U-2, the angular spread of the velocities of magnetized electrons was measured using a method based on the passage of electrons through a round collimating hole the axis of which coincides with the direction of the magnetic field guiding the electrons. A modification of this method enables calculation of the average value of the angular divergence of electron velocities and determination of characteristic features of the angular distribution of electron velocities. It was applied at the accelerator U-2 in 2014.

The essence of this method is as follows. A flow of magnetized electrons is directed along the magnetic field lines to a sensor, which is a set of graphite ring collectors, placed coaxially and securely isolated one from another (see Fig. 4.2.3). From the electron flow, only a slender jet cut by a thin collimator gets to the working volume of the sensor. In experiments in 2014, the collimator was a tantalum disc with a thickness $L_0 = 0.5$ mm and a hole of a diameter of 0.4 mm. The thickness of tantalum is enough to stop electrons with energy of 1 MeV or less. At the same time, with this thickness of the disc, the cylindrical hole in the collimator is much less than the characteristic longitudinal Larmor radius of the beam electrons in the guiding magnetic field ($\rho_L \gg L_0$). In the experiment, the disc was grounded and the current of electrons absorbed in it was not measured.

The radii of the holes in the graphite collectors of electrons behind the collimator were gradually decreasing with increasing distance from the collimator. The hole radius r_i in each ith collector was chosen such that it was close to the largest Larmor radius of electrons with a given pitch angle θ_i.
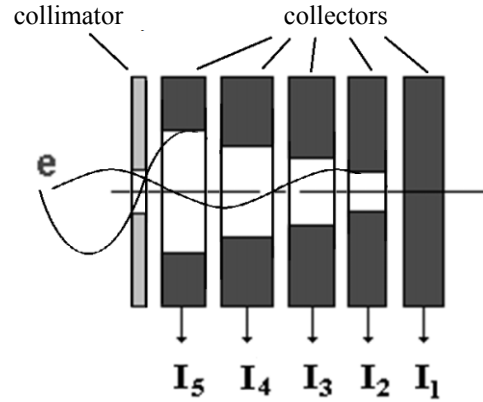
Fig. 4.2.3. Schematic of multiple-collector angular-spread sensor.

Under these conditions, the ith collector is mostly reached by electrons for which the condition $r_i = \rho_L \sin(\theta_i)$ is fulfilled. The thickness of the ring collectors was chosen sufficient for absorption of 1 MeV electrons. For graphite, it must be 5 mm at least. Calculations show that this sensor design provides consecutive selection of electrons from the incoming stream: firstly particles with large pitch angles; then with medium angles, and finally with small angles. Thus, the detection procedure used can separate electrons into detection channels depending on the transverse Larmor radius. With careful selection of the diameter of the inner holes and thicknesses of the ring collectors, the sensitivity function of each channel to different values of pitch angles can be quite narrow. In these circumstances, an overlap in the detection of electrons with a given pitch angle can occur only between two adjacent channels, thus the function of the angular distribution of electrons can be restored with reasonable accuracy. In addition to this advantage, the influence of electron reflection from the wall of a certain ring collector on the currents of signals from other collectors is lower as

56

compared with a sensor in which all collectors are of the same internal diameter.

Using the results of the work [V.D. Aleksin, B.G. Bocharov. Plasma diagnostics. Atomizdat, 1973, p. 345], we calculated the sensitivities S_i of the channels as functions of the pitch angle θ of electrons coming from the collimator. In this case, the sensitivity is the probability that an electron that passed through the collimator with a given value of the pitch angle will arrive at the ith ring collector. Quantitatively, the sensitivity of the ith ring collector is $S_i(\theta) = I_i/I_{in}$, where I_i is the current of electrons absorbed in the ith collector, and I_{in} is the electron current at the input to the collimator.

Since the experiments involved research on electron beams with angular spread of 5° - 10°, the detector was to have a good angular resolution for electron pitch angles of 0° to 10° and thus the specified range of angles was to include the maximums of the sensitivity curves of three to four ring collectors. Fitting of the diameters of the inner holes of the rings and their lengths yielded the sensitivity of the channels in dependence on the electron pitch angle for a guiding magnetic field of 0.6 Tesla. These relations are shown in Fig. 4.2.4. From the nature of these relations, one can see that electrons with the angles θ in the range of 0° to 10° are preferably absorbed in collectors 1, 2, 3, and 4.

For the measurement of the angular spread of electrons of beam formed by the accelerator U-2, an area of quasi-uniform magnetic field was formed at the output of the magnetic compression system of the accelerator region. A sensor was placed in this area. Measurements showed that the field heterogeneity over a length of the sensor of about 8 cm did not exceed 5%. The inlet of the collimator was centered in the cross section of the beam, the axis of the sensor aligned in parallel with the magnetic field line within 0.2°. After a preparatory work, a series of experiments on the measurement of the angular spread of beam electrons at the output of the accelerator U-2 was carried out. Fig. 4.2.5 presents signals from the collectors, as well as a signal of the diode voltage, which were recorded in a typical shot.
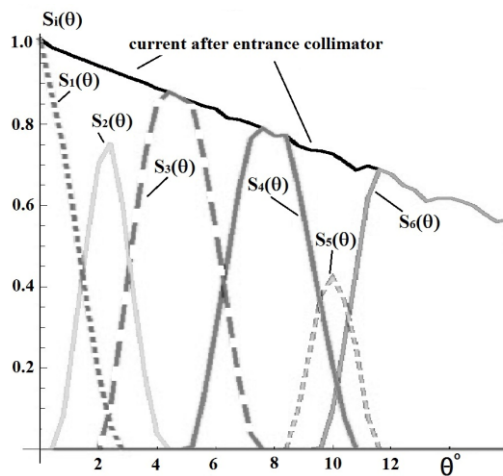
The experimental data were pre-processed; the characteristic angular spread of beam electrons was 0.1 rad in a magnetic field of 0.6 T, which corresponds to a spread of 0.25 rad when the beam enters the plasma in a magnetic field of 4.5 T.

4.2.4. Development of plasma-emitter technology of sources of long-pulse electron beams

A diagnostic system was developed for creation of a quantitative picture of electron beam current density distribution over the cross section in one working pulse. The diagnostics is based on the detection of X-ray beam imprint on a metal target due to the bremsstrahlung and characteristic radiation.

The electron beam source was set in the end vacuum tank of GOL-3 (see Fig. 4.2.6). The electron beam was transported over a distance of 1.3 m in a longitudinal magnetic field created by coil 4 of the end tank of GOL-3 and there arrived at flat molybdenum target 5 under an angle of 45° to the axis of the facility. A typical value of the magnetic field was 9 mT and 16 mT in the area of the electronic-optical system and near the target, respectively.

The X-ray image of the beam imprint on the target was recorded by a pinhole camera, a diagram of which is shown in the inset in Fig 4.2.6. The camera is a box with lead front wall 6 for protection against stray X-rays. In the front wall there is a special inset of copper-tungsten composite with an aperture pinhole of 2 mm in diameter. The X-ray image is projected onto phosphor screen 7, the glow of which is recorded with CCD camera SDU-285 8, equipped with SONY ICX285AL matrix of 1392 × 1032 pixels.

Fig. 4.2.4. Response curves of ring collectors of electrons with pitch angle θ and energy of 0.6 MeV for angle spread sensor placed in uniform magnetic field of 0.6 Tesla.
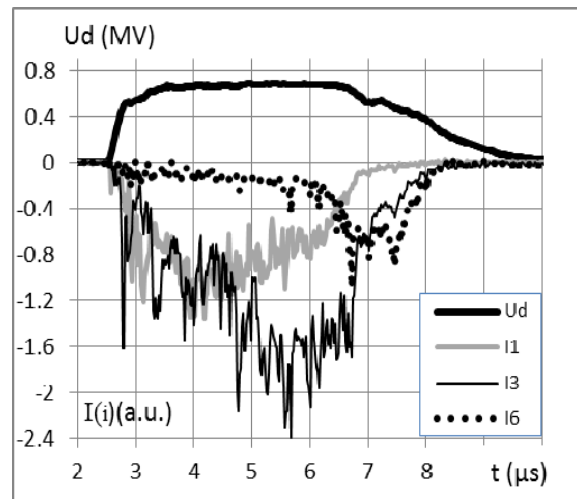
Fig. 4.2.5. Oscillograms of currents from collectors I_1, I_3, and I_6 and voltage U_d across diode of accelerator in typical shots.

In view of the frequency content of the radiation, a medical intensifying screen RENEX on the basis of gadolinium oxysulfide ($Gd_2O_2S:Te$) was taken as a luminescent screen. This screen is a 240×180×0.3 mm sheet of flexible plastic; it emits light mostly in the "green" (~ 540 nm) part of the spectrum. The characteristic luminescence time is ~ 600 μs, while the average beam duration in the experiments was about 200 μs. The use of the screen allows one to get a pulse-integrated beam picture.

Fig. 4.2.7 shows a typical picture of X-ray emission from target because of incident electron beam with an energy of 80 keV, a current of 100 A and a duration of 150 microseconds. The right-hand part of the figure shows the normalized profiles of the output signal ("brightness") of the CCD camera pixels, measured along two perpendicular lines passing through the maximum of the image brightness. As one can see, the shape of the profiles is close to that of Gaussian curve. To reveal a direct relation of the brightness of CCD camera pixel and the current of the beam incident on the corresponding portion of the target, it was necessary to verify the linearity of the charac-

Fig. 4.2.6. Schematic of experiment with X-ray pinhole camera: 1 − high-voltage electrode, 2 - arc plasma generator, 3 - anode of accelerating diode, 4 - coils of end tank of GOL-3, 5 - molybdenum beam dump, 6 - lead sheet, 7 - luminescent screen, 8 - CCD camera.

Fig. 4.2.7. Typical imprint of X-ray beam and normalized profiles of luminescence intensity.

teristic of the "luminophore-camera" system. That was done in a series of special experiments. The beam current strength varied in the range of 15 to 150 A, and the pulse duration was 50 to 200 microseconds. The magnetic field in the beam source and the drift region, the accelerating voltage and camera settings were maintained constant.

The spatial resolution of the diagnostics was evaluated in a special experiment with a stainless steel target and tantalum foil strips 3 mm wide welded to it. The intensity of X-ray emission from the tantalum strips was estimated to about 2.3 times exceed the intensity of luminescence of the steel substrate. In the pinhole pictures, one can clearly see separate strips, which suggests the spatial resolution of diagnostic system be not worse than 3 mm.

Measurements with the X-ray pinhole camera showed the position of the center of gravity of the beam on the target to be quite stable from pulse to pulse. The distribution of the luminescence intensity (i.e. the distribution of beam current density) is close to a two-dimensional Gaussian one. In a beam with a current of 100 A the maximum current density was 6 A/cm². With a 20% geometrical

transparency of the emission electrode, the emission current density per unit aperture was estimated to be 30 A/cm². The effective beam diameter was calculated as the diameter of a circle with an area equal to the area occupied by pixels with non-zero brightness (after subtraction of the parasitical background). For the beam imprint in Fig. 4.2.7, the diameter was 73 mm, which is consistent with the transverse dimension of the multiple-aperture EOS. The effective diameter of the area containing half the beam current was 38 mm, which is close to half the total diameter of the beam, and also shows the similarity of the experimentally obtained distribution to a two-dimensional Gaussian. Note that despite the "multi-jet" nature of the generated beam, the X-ray imprint on the target shows good homogeneity, which is also confirmed by the structure of the burn-off spot on the metal of the target.

4.2.5. Use of long-pulse electron beam for experimental modeling of effects of high-power pulse heat loads on metals.

This work is due to the problem of erosion of divertor plates in the International Thermonuclear Experimental Reactor (ITER) under construction. Excess of the gradient of plasma pressure near the borders at facilities like ITER often leads to plasma instability, the so-called ELMs. ELMs give rise to recurrent release of hot plasma particles on the metal wall in the divertor, a special device for acceptance of particle flows and radiation from the periphery of the plasma column. The density of the energy released on the wall may be enough for melting of the wall material (tungsten) and appearance of molten layer on its surface.

Modeling experiments and calculations show that the tungsten erosion increases sharply in this regime. The products of erosion spread mostly in the form of droplets or micro-particles with characteristic sizes of 10 - 200 microns. The appearance of such microparticles is undesirable, since their entry into the hot plasma can cause its overcooling, loss of stability and drift to the wall. In addition, accumulation of metal dust in the chamber of the reactor will result in significant uptake of radioactive tritium in it, which is strictly limited by the requirements of radiation safety. The mechanism of the spraying of molten layer is still not clear. The possible explanations include the Kelvin-Helmholtz instability, boiling, cavitation etc. The experimental modeling of the spraying of tungsten is hampered by the lack of facilities that can reproduce in full the conditions in the ITER divertor when ELMs occur. Most often plasma guns and lasers are used for pulse heating of wall. Lasers typically generate pulses of duration several orders of magnitude smaller than the characteristic times of ELMs. Besides, the laser radiation is often shielded by plasma arsing in the erosion flame. The same shielding effect is typical to plasma flows generated in plasma guns, due to the fact that the energy of particles in the flow is much lower than that expected in the ITER divertor. An even more important consequence of the low energy of the particles is that the pressure on the molten layer from the particle flow from plasma guns more than one order of magnitude exceeds the similar parameter in the ITER divertor. It is clear that the pressure on the molten layer is a critical parameter, both for occurrence of instabilities and for flashing. A long electron beam of the GOL-3 facility is a convenient tool for experimental simulation of pulsed heating of the wall surface, which accompanies the appearance of ELMs in ITER. Its important difference from the above methods of pulsed heating is the absence of electron flow pressure on the molten layer and of the effect of flux shielding by the erosion flame, which makes the simulation conditions similar to the conditions in ITER. Launched in 2014, experiments on the surface effects of long-pulse electron beam are a logical continuation of the research on the effects of microsecond relativistic electron beams on materials, which

have been conducted for several years at the GOL-3 facility. In the experiments with long-pulse electron beam, new methods of diagnostics of erosion flame and spreading microparticles were also used. Fig. 4.2.8 shows the emission spectrum of the erosion flame formed during exposure on tungsten target to an electron beam of a duration of 150 μs and an energy density of 2.2 MJ/m^2.
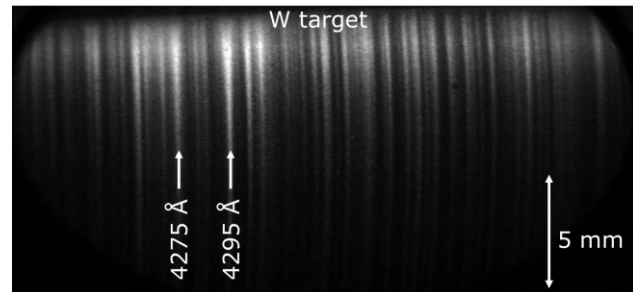
Fig. 4.2.8. Spectrum of erosion flame under action of electron beam with energy density of 2.2 MJ/m^2 and duration of 150 μs 130 μs after beginning of action on tungsten target (on top).
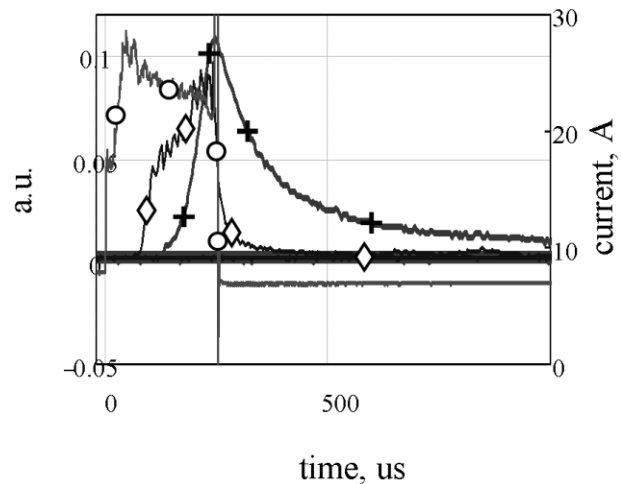
Fig. 4.2.9. Time course of electron beam current (circles), own glow of erosion flame plasma (diamonds) and intensities of scattered laser radiation (crosses), characterizing presence of microparticles in flame. Energy density: 3MJ/m^2, beam duration: 220 μs, target material: stainless steel.

The spatial-resolution spectrum contains lines of neutral and singly ionized tungsten; the target is on the top of the figure. The information contained in this spectrum will allow one to determine the parameters of the erosion flame and evaluate its effect on the molten layer. In addition, a technique of diagnostics of microparticles by small-angle scattering of laser radiation was tested. Fig. 4.2.9 shows oscillograms of the electron beam current, glow of the erosion flame and intensity of scattered radiation, which characterizes the metal microparticles in the plume.

It can be seen that the self-radiation of the flame corresponding to the emergence of the plasma occurs later than the beginning of the influence on the target and stops shortly after the end of the beam. The injection of microparticles from a target starts the latest and lasts for a considerable time after the end of the thermal effect on the target.

4.2.6. Precision spatial-resolution spectral diagnostics.

The GOL-3 facility has an advanced complex of spectral diagnostics. Until now, the complex was used for determination of plasma temperature and density in different experimental conditions. The maximum requirements to the spectral systems were such that it was possible to determine plasma temperature from $T = 5$ eV or higher, which corresponds to a spectral broadening of atomic hydrogen of 0.1 nm and more. Such a moderate resolution was achieved with a double focusing spectrometer DFS-24 with photometric diagnostics based on multi-channel fiber-optic system with photomultiplier tubes (PMTs). This device was used without spatial localization of the plasma parameters. However, new experiments at the GOL-3 facility on the research on plasma stability with high-current electron beams have imposed tougher requirements. As a result, a new spectral instrument with high spectral and spatial resolution was put into operation. Under the GOL-3 experimental conditions, the basic requirements to the spectral diagnostics developed were as follows:

- possibility of resolving the velocity of emitting particle $V < V_0 = 4 \times 10^4$ m/s, where V_0 is the expected linear velocity of the azimuthal rotation of plasma at the edge;
- spatial resolution better than 1 mm with a transverse field of vision of 60 mm;
- temporal resolution of 1 μs or better.

The target spectral lines for the diagnostics were the lines of single-charge carbon ion *CII* (657.8 and 658.29 nm), the concentration of which in the plasma of GOL-3 is high enough for measurements with the required precision. This formulation of the problem implies high spectral resolution. With the DFS-24 spectrometer with an ultimate spectral resolution of 1 cm^{-1} in the green spectral range, which corresponds to a hardware profile with $\Delta\lambda_{1/2} = 3 \times 10^{-2}$ 2 nm, a reliable measurement of spectral line shift requires a large number of points in the hardware circuit of the spectrometer.

After the optimization, the diagnostics complex consists of the modified spectral instrument DFS-24, an electro-optical converter (EOC) operating as brightness intensifier and optical shutter with an exposure time of 1 μs, and a digital camera, recording images in the exit window of the EOC. As a result, the inverse linear dispersion on the digital camera is $D = 6.4 \times 10^{-3}$ nm, and the instrument function width corresponds to $\Delta\lambda_{1/2} = 4.5 \times 10^{-2}$ nm and is close to the rated resolution of the device. With a suffi-
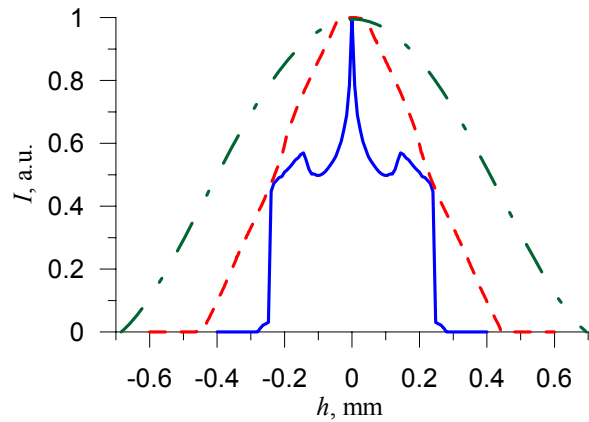
Fig. 4.2.10 Transverse resolution of spectral system. Dash-dot curve: measured resolution. Solid curve: calculated resolution for 6.45×6.45 μm^2 two-dimensional unit cell. Dashed curve: calculated resolution for real photodetector based on EOC with digital camera with entrance slit 100 μm wide. Dash-dot curve: achieved experimental spatial resolution.

ciently large number of significant points in the line profile ($N \geq 8$) and the confidence level $(100\% - \alpha) = 70\%$, the experimental accuracy of the instrument to determine displacement of spectral line due to directional movement of emitting carbon ions is $\delta(\Delta\lambda) = 6.5 \times 10^{-3}$ nm. This precision meets the requirements to the system, because the error in the determination of the speed of emitting particles in the direction of the line of sight is $\Delta V = 3 \times 10^3$ m/s,
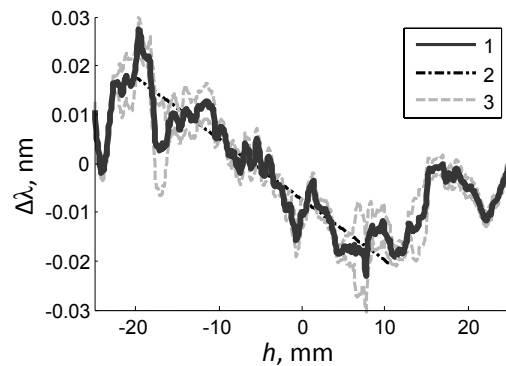
Fig. 4.2.11. Result of measurement of plasma rotation at time $t = 2.6$ μs after beginning of REB. 1 - experimentally measured displacement of spectral lines of *CII* (657.8 nm) in shot PL14370, 2 - straight line with slope corresponding to rotation with frequency $f = -85 \pm 30$ kHz, 3 - error in experimentally measured shift of spectral line .

which is by one order of magnitude less than the expected speed of rotation on the plasma edge in the experiment.

The parameters and positioning of the optical elements of the spectrometer optical circuit were calculated with

the numerical package ZEMAX. The distance from the spectrometer to the plasma must be fixed (1 m), and the coefficient of plasma image transfer to the entrance slit of the spectrometer must be 2:7 with due account of the sagittal focal surface of the collimation lens of the spectrometer. The optimization yielded the rated spatial characteristics of the resolution of the system (see the solid and dotted curves in Fig. 4.2.10) for the transverse direction (across the magnetic field confining the plasma). The dot-dashed curve presents the measured transverse resolution realized in accordance with the calculations of the spectral system.

The measurements of the spectrum of the line of *CII* (657.8 nm) during passage of high-current relativistic electron beam (REB) enable calculation of line shift relative to its initial position depending on the radius of the chord of observation of the spectral line (see Fig. 4.2.11). The dashed curve in the figure indicates the accuracy of the measurement of the line center position in accordance with the experimental variance of the line profile. The radial position of the REP in the experiment corresponds in the figure to area h = [-22; 13] mm. One can see that in the REB area the plasma tends to whole-body rotation with a constant angular velocity. The linear function appropriately inscribed in the radial region occupied by the REB shows that the plasma rotates with the linear frequency f = -85±30 kHz. The negative frequency means that this rotation can be explained by the drift in the crossed electric and magnetic fields, which are determined by the plasma of uniform negative charge.

4.2.7. Examination of impurities in plasma of GOL-3.

One of the important results of the experiments at GOL-3 is the improved confinement of low-density plasma. It was found that the effects of multiple-mirror confinement of plasma appeared at plasma density considerably less than that predicted by the theory, in which only Coulomb collisions are taken into account. The good confinement time in the GOL-3 experiments evidences that the effective frequency of collisions in the plasma more than 30 times exceeds the classical value. This discrepancy can be explained in an assumption that the frequency of collisions increases due to the turbulence caused by the plasma flow through the multiple-mirror structure. This phenomenon may have an alternative interpretation, although, of scattering of ions on multiply charged impurity ions. Therefore, to harmonize the experimental results with the theory, it is necessary to estimate the effective charge of ions in the GOL-3 plasma.

The basic approach to the detection of impurities in plasma and assessment of their concentration is analysis of the plasma emission spectrum and measurement of the intensities of the spectral lines of impurities. To this end, a set of optical spectral diagnostics was installed. Vision-range and vacuum-ultra-violet (VUV) survey spectrome-

ters distinguish principal impurities in plasma and measure the emission power of their spectral lines. High-resolution spectrometers are used for accurate measurement of the wavelengths of the observed spectral lines, analysis of line profiles and measurement of the dynamics of emission from the spectral lines. Besides that, the residual vacuum is analyzed using the industrial mass spectrometer Pfeiffer Prizma QMG 220.

From the measured density of impurities and numerical modeling of the dynamics of their ionization balance, one can estimate the effective charge of ions in the GOL-3 plasma. At the GOL-3 facility, a high-electron-temperature plasma loves for a rather short time, and thus heavy impurities do not have time to achieve a high degree of ionization and the effective charge of the plasma is determined mainly by light impurities. The effective charge of plasma estimated from measurements of the concentration of light impurities (oxygen, nitrogen, and carbon) was Z_{eff} = 1.2 – 1.6. Measurements of the content of heavy impurities (argon, crypton, sodium, and silicon) and calculation of their ionization states in the GOL-3 plasma show the contribution of the heavy impurities into the effective charge of the plasma to be less than 0.2.

The Z_{eff} value influences the frequency of collisions and thereby the total time of plasma confinement. Investigations showed the total contribution of the principal observed impurities to give an effective charge value Z_{eff} = 1.8 at most, and this cannot explain the better confinement of low-density plasma, which was observed in the experiments. This means that scattering of plasma ions on multiply-charged impurity ions has no significant effect on plasma confinement in a multiple-mirror trap, and the plasma confinement is defined mainly by collective effects.

4.2.8. GOL-3 findings.

In 2014, a program of large reconstruction of GOL-3 was started, which will be completed by the creation of two new facilities optimized for research in narrower scientific fields.

The first facility, GOL-3T, is intended for research on the physics of beam-plasma interaction and plasma methods of generation of high-power terahertz electromagnetic radiation. The facility consists of the accelerator U-2, which generates a high-current relativistic electron beam, and the plasma system about 2.5 m long. In 2014, all the preparatory works at this facility were completed; a physical start was performed and a low-temperature pre-plasma was produced. The facility is ready for experiments on injection of high-current relativistic electron beam.

Works on the designing of GOL-NB were begun. This facility is intended for research on quasi-stationary plasma confinement in a trap with multiple-mirror end sections. Relevant systems and technologies are being created and tested.

Some parts of GOL-3 were also involved in basic, methodological and applied research in different areas.

4.3. PLASMA THEORY

4.3.1. Alfvén ion-cyclotron and drift-cyclotron instabilities.

Study of the Alfvén ion-cyclotron (AIC) instability in a mirror trap with skew injection of fast neutral beams is continued. (I.S. Chernoshtanov and Yu.A. Tsidulko, Alfvén ion-cyclotron instability in an axisymmetric trap with oblique injection of fast atoms. Plasma Physics Reports. 2014. V. 40. N. 12. p. 955-964)

Method of searching for plasma parameters at the AIC instability boundary via transverse Pearlstein-Berk correction averaged over WKB-trajectory of longitudinal problem is developed.

Dependence of hot plasma parameters near the stability boundary on injection and target plasma parameters is studied. It is shown that increasing of injection angle width and electron temperature reduces ion distribution angle anisotropy and stabilizes the AIC instability. Increasing of the target plasma density, magnetic field scale length and ratio of charge-exchange time to drag time facilitates the AIC instability development. Reduction of injection angle, plasma radius and longitudinal scale length of trap magnetic field are the most effective methods of stabilizing the AIC instability.

Asymptotes of AIC perturbation amplitude and polarization in the peripheral plasma are studied. It is shown that the perturbed field can rotate in the peripheral area either in the electron-cyclotron direction or in the ion-cyclotron direction, depending on the peripheral plasma parameters. Condition of the rotation direction change is obtained.

Study of the drift-cyclotron instabilities in non-uniform magnetic field was started. Effect of ion gradient drift in non-uniform magnetic field on flute-like kinetic instabilities with frequency close to the ion-cyclotron frequency is studied in the report of Yu.A. Tsidulko, I.S. Chernoshtanov, in proc. of XLII International conf. on plasma physics and CTF, Zvenigorod, (2015).

Taking into account the magnetic field non-uniformity results in the new unstable modes occurrence apart from "traditional" drift-cyclotron instabilities (e.g. DCLC or Double Humped instability). The new modes are driven by gradient drift velocity inverse population near Landau resonances. The estimated anomalous particle transport caused by the new modes would exceed the transport caused by the "traditional" mode.

4.3.2. Efficient regime of electromagnetic emission in a plasma with counterstreaming electron beams

Efficiency of electromagnetic emission produced in a magnetized plasma with counterstreaming electron beams was investigated using both the linear kinetic theory and particle-in-cell simulations. We calculated the growth rate of the beam-plasma instability taking into account both kinetic and relativistic effects and showed that there exists a regime in which transversely propagating electromagnetic waves can be generated by the coupling of the most unstable oblique beam-driven modes. It was confirmed by numerical simulations that such a tune-up of system parameters for a specific nonlinear process can lead to a substantial increase in electromagnetic emission efficiency. It was found that electromagnetic radiation emerging from the plasma in such a regime is generated near the harmonics of the pump frequency that is determined by the typical eigenfrequency of the beam-driven modes. It was also shown that the peak emission power can reach 5% of the maximal power lost by beam electrons.

4.4. BEAM INJECTORS OF HYDROGEN ATOMS AND IONS

4.4.1. Beam Injectors of Hydrogen Atoms.

For the upgraded C-2U plasma open trap (Tri Alpha Energy Company, USA) the system of six atomic injectors was designed, manufactured and supplied to TAE. The total power of the fast hydrogen atoms is 10 MW. At the end of 2014 the injection system was launched in TAE and the design parameters were achieved: particle energy - 15 keV, the beam currents in the extracted ions - 150 A, pulse duration - 8 ms, more than 90% full energy fraction. To extract the 150 A ion beam the plasma source has four arc plasma generators. Plasma jets from four sources are mixed in the expander chamber. For beam formation the multislit 3-electrode accelerating ion-optical system are used with the original geometry forming cells.

Neutral injection system has passed acceptance tests and ready for use in the planned research program at C-2U machine. Involves the use of powerful neutral beam injection to maintain the reversed magnetic field configuration and plasma heating in C-2U device.

4.4.2. Development of powerful continuous injector of beam of fast hydrogen atoms.

Works under the project of powerful continuous injector of beam of fast hydrogen atoms with 500-1000 keV energy on the basis of negative ions are continued. The project is based on separate formation and acceleration of negative ion beam. Basic elements of the injector are manufactured. At experimental stand prototype of hydrogen negative ion source with beam current up to 1,5 A and beam energy up to 120 keV is tested. Now negative ion beam current of 1 A at energy 85 keV was achieved. Large experimental stand for acceleration of hydrogen negative ion beam with ~ 5 A current to energy ~ 800 keV is under preparation.

4.5. THEORY OF PLASMA WAKE-FIELD ACCELERATION

A novel scheme of the wakefield accelerator in a hollow plasma channel is proposed, in which a weakly focusing plasma structure is formed near the beam axis. The structure preserves the emittance of the accelerated beam and produces low radiation losses. Moreover, the structure allows for a considerable decrease of the witness energy spread at the driver depletion stage.

A novel effect of fast heating and charging a finite-radius plasma is discovered in the context of plasma wakefield acceleration. As the plasma wave breaks, most of its energy is transferred to plasma electrons. The electrons gain substantial transverse momentum and escape the plasma radially, which gives rise to a strong charge-separation electric field and azimuthal magnetic field around the plasma. The slowly varying field structure is preserved for hundreds of wakefield periods and contains (together with hot electrons) up to 80% of the initial wakefield energy.

Preparation of the AWAKE experiment at CERN has been continued with the participation of Budker INP. The experiment is aimed to study in detail the important physical processes and to demonstrate the power of proton-driven plasma wakefield acceleration. The underlying physical principles and some technical considerations related to AWAKE were reviewed.

The dependence of wakefield amplitude and phase on beam and plasma parameters is studied in the parameter area of interest for self-modulating proton beam-driven plasma wakefield acceleration. The wakefield phase is shown to be extremely sensitive to small variations of the plasma density, while sensitivity to small variations of other parameters is reasonably low. The study of large parameter variations clarifies the effects that limit the achievable accelerating field in different parts of the parameter space: nonlinear elongation of the wakefield period, insufficient charge of the drive beam, emittance-driven beam divergence, and motion of plasma ions.

A parallel 3D numerical model is created on the basis of Particle-In-Cell method. The model is designed for simulation of relaxation processes of the warm electron beam in plasma. Growth saturation of a separate unstable mode is studied in different regimes. The comparative analysis of methods for diagnostics of the instability is carried out. The results accuracy dependence on model particle number is determined. Minimal model particle number for correct instability increment calculation is defined.

Conditions for efficient trapping of low-energy electron bunches by the plasma wakefield of a self-modulating proton bunch are found in case of initially co-linear propagation of the two beams. The co-linear injection scheme is optimized for high energy gain and low energy spread of electron or positron beams. The effect of smooth plasma density increase at the plasma entrance on the electron trapping is discovered and clarified. Reduction of trapping efficiency with increase of the electron bunch charge is found and described.

4.6. RADIATION SPECTRUM OF TWO-CHANNEL FEM AT STRONG ELECTRODYNAMIC COUPLING BETWEEN CHANNELS

4.6.1. Introduction.

The main result of the experimental research at the ELMI facility in 2012-2014 was the demonstration of the possibility of simultaneous generation in two channels of the planar FEM of quasi-monochromatic high-power mm-wave radiation pulses at one of the eigenfrequencies of the resonator. These experiments had the following principal particularity: the electrodynamic systems were strictly separated one from another throughout the channels, and only at the output, where a collector is installed for acceptance of passed electron beams, some fraction of the radiation fluxes might penetrate from one channel to the other. That provided weak electro-dynamic coupling between the channels of the FEM. The parameters of radiation pulses in these conditions were as follows: the characteristic power of radiation from a single channel was ~ 10-20 MW; the pulse duration was up to 200 ns; the frequency of the electromagnetic wave in the middle of emission line was 74.6 GHz. The spectral line width was close to its natural width and did not exceed 20 MHz. According to the results of the experiments, with a given energy of electrons the optimal for generation values of the longitudinal and transverse components of the static undulator field - are in good agreement with the predictions of the theoretical model. This model describes the FEM operation under conditions when the undulator synchronism is shifted by a detuning value corresponding to the maximum of the electron efficiency. However, in this series of experiments, the single-frequency co-phase generation in the two channels was achieved not in each pulse of operation of the facility. There was a significant fraction of shots in which a frequency was "jumped over" in switching from one oscillation mode to another, either simultaneously in the channels or not. In a series of experiments shots were observed in which the generation of radiation in the two channels occurred at different frequencies throughout the pulse. This fact led us to using strong electro-dynamic coupling between the channels, which should provide co-phase radiation output from the channels in a maximum number of shots at a single-frequency operation mode.

4.6.2. Experimental conditions.

The scheme of experiments on radiation generation in the two-channel planar FEM is shown in Fig. 4.5.1. A detailed description of the scheme and the diagnostics of microwave radiation is given in the BINP report for the year 2012.
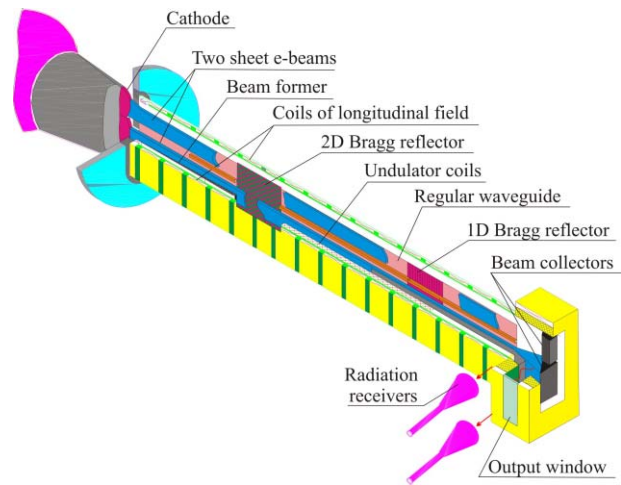
Fig. 4.6.1. Schematic of experiments on generation of mm-wave radiation in two-channel planar FEM at strong electrodynamic coupling between channels.

The electrodynamic system of the two-channel FEM consists of two identical planar resonators formed by the upstream two-dimensional Bragg reflector and the downstream one-dimensional one; the reflectors are connected by a segment of rectangular waveguide. It should be noted that in experiments in 2014, unlike the previous years, the two channels were connected in the area of the two-dimensional Bragg reflector, because the metal baffle separating the channels was removed in this segment. The joining of the two channels in the region of the two-dimensional reflector enabled passage of electromagnetic radiation flow from one channel to the other, which should lead to mutual synchronization of electromagnetic oscillations produced by electron beams. Moreover, due to the exchange of flows, normal to the axis of the channels, the resonators of the channels could be linked into a single electrodynamic system, which was confirmed experimentally in analysis of the eigenmodes spectrum of such joined resonator.

4.6.3. Results of research.

In a series of experiments with the two-channel FEM at strong coupling between the channels, we varied from shot to shot, simultaneously in both channels, the values of the transverse and longitudinal components of the magnetic field of the undulator. From the experimental data we selected for detailed spectral analysis only those shots in which the diode voltage matched the energy of electrons derived from the condition of the undulator synchronism taking into account the previously established regularity for choosing the detuning.

When processing the spectrograms of the mm-wave radiation pulses obtained in this series of experiments, we revealed the following features of the dynamics of the emission spectra.

Firstly, in almost all shots, the generation of the radiation in both channels occurred identically, i.e. in case of single-frequency operation mode the frequency of waves in the channels almost always coincided during the pulse,

and for shots in which a jump from one frequency to another was observed, this process occurred simultaneously in both channels.

Secondly, in the frequency range of 74.5-75.5 GHz, which, in accordance with prior "cold" measurements, included the eigenfrequencies of the resonators of individual channels, high-Q modes with frequencies between them were found. These frequencies correspond to oscillations that are common for the combined two-channel electrodynamic system and are realized in these conditions in the two-channel FEM.

Third, in the series of experiments there was no generation of radiation at the frequencies of the longitudinal modes of the resonator in the range of 77.5-78.5 GHz. These frequencies correspond to the spurious reflectance band of one-dimensional Bragg reflector. Generation at these frequencies was detected in the previous series of experiments at low electrodynamic coupling between the channels of the FEM.

Fourth, it was found that at strong coupling between the channels, even if the magnetic field of the undulator and the diode voltage varied in a fairly wide range, single-mode single-frequency generation of the radiation is realized in both channels simultaneously throughout the radiation pulse. This is a principal difference between this series of experiments and experiments at weak coupling between the channels.

Fig. 4.6.2. presents an example of typical shot with a single-frequency generation in both channels. The shot was done at a longitudinal component of the magnetic field of 1.4 T and an amplitude of the sinusoidal (a spatial period of 4 cm) transverse component of 0.14 T. The spectra of radiation from the two channels of the FEM obtained using heterodyne diagnostics in the same shot are presented in Figure 4.6.3.

As can be seen from the figures, generation in this shot is observed in both channels with a small (about 20 ns) time shift. The pulse has a trapezoidal shape with a duration by the base of about 100 ns. The spectra of radiation from the different channels of the FEM, registered in a shot using heterodyne diagnostics, have the same center frequency of 74.96 GHz and a bandwidth of 20 MHz, which is close to the natural width.

Thus, the use of strong electrodynamic coupling between resonators in the two-channel FEM enabled almost 100% synchronization of the radiation coming out of the channels, both in the oscillation phase and in the spectral line width. This result is extremely important from a practical point of view.
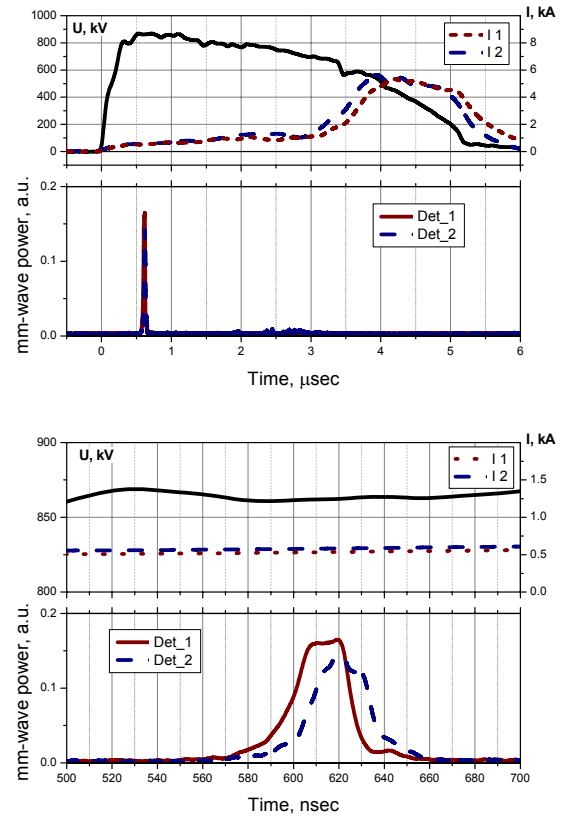
Fig. 4.6.2. Oscillograms of diode voltage - U, sheet beam currents (I1, I2) and power of mm-wave radiation from two channels of FEM in typical shot with single-mode single-frequency 75 GHz generation. The upper and lower figures differ only in the time scale.
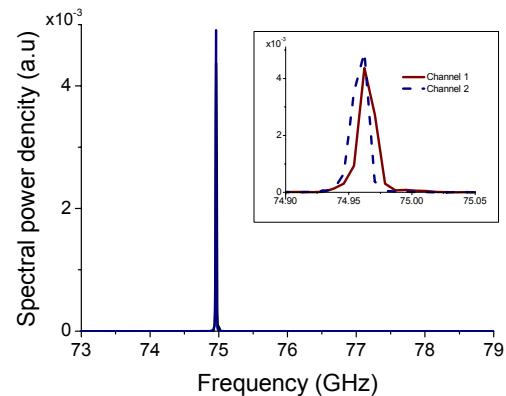
Fig. 4.6.3. Fine structure of mm-wave radiation spectrum in one of the shots with single-frequency generation in time interval of 560-660 ns.

5

ELECTRON – POSITRON COLLIDERS

5.1. MODERNIZATION OF VEPP-2000 COMPLEX

The VEPP-2000 complex is now in upgrade stage for work with beams at energy of 1 GeV. The average luminosity reached to the middle of 2013 is shown in the Fig. 5.1.1. The peak luminosity of 1.2×10^{31} cm^{-2}s^{-1} was obtained at the energy of 500 MeV, this exceeds achievements of VEPP-2M by 4 times.
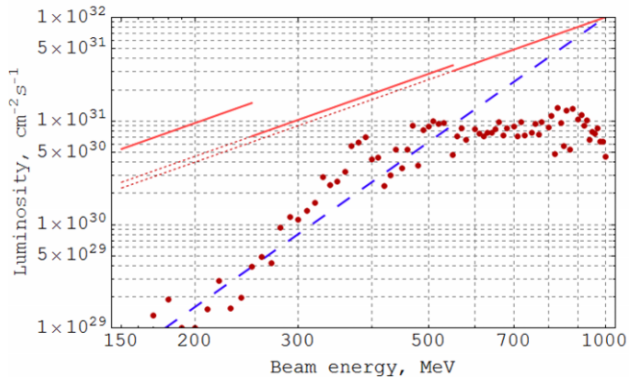
Fig. 5.1.1. VEPP-2000 luminosity.

The luminosity at 900 MeV is 2.5×10^{31} cm^{-2}s^{-1}, but the projected one should be 10^{32} cm^{-2}s^{-1}. From the Figure above, one can see that beginning from 500 MeV there is obvious lack of luminosity. Beam-beam parameter ξ (effectiveness of beams' collisions) defined by various methods is 0.12, this is a world record.

Limitations that do not allow us to obtain projected luminosity at the high energy are:

1. the need of particles' acceleration in the VEPP-2000 ring: "dead" time for injection and lowering/rise energy of beams; losses during accelerating intensive beams; unattainability of ξ threshold at energies higher than injection energy. Losses of luminosity are up to 60%.

2. deficiency of positrons.

Hence the need of VEPP-2000 accelerating complex modernization. First, we need to connect to the intensive source of positrons. Second, we have to inject at the energy of experiment.

Modernization program consists of four steps:

1. Start of K-500 channel from injection complex VEPP-5

2. Booster BEP modernization for work at 1 GeV

3. BEP–VEPP-2000 channel modernization for injection at 1 GeV

4. Small modification of VEPP-2000 ring.

5.1.1. K-500 channel.

Injection channel K-500 is large enough construction; it has the length of 250 m. In 2014 some small works were carried out. Construction of special lodge over lead-in mine was the important stage (Fig. 5.1.2). Because the channel is deep, the strong convection flows arise. This disturbed works with laser tracker to place magnetic elements.

Fig. 5.1.2. Lodge over mine of K-500 channel.

Besides, cable routes were built to feed dipole correctors (Fig. 5.1.3) and get signals from image current monitors. Principle diagram of feeding and controlling the luminophore probes was developed, Faraday cup was designed, and magnets in BEP hall were installed.

Fig. 5.1.3. K-500 unit: dipole corrector, quadrupole, luminophore probe.

5.1.2. BEP reconstruction.

The greatest work is booster BEP modernization, which consists of several steps:

- manufacturing new injection dipole
- new RF cavity
- modification of 12+1 bending magnets
- modification of 24+2 quadrupoles
- modification of aluminum vacuum chamber
- new BUMP magnets
- synchrotron radiation output.
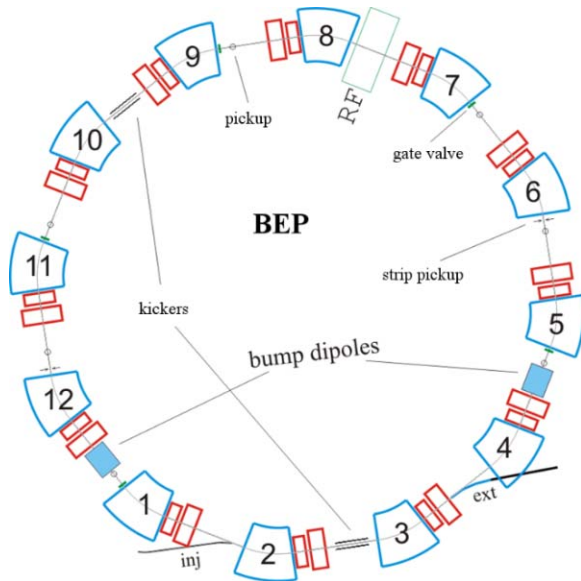
Fig. 5.1.4. BEP ring scheme.

Booster BEP is a simple machine with 12 fold symmetry and doublet focusing (Fig. 5.1.4). Modernization applies to all magnetic elements; modification of vacuum chamber is needed and creation of BUMP magnets. These are pulse magnets for orbit distortion before ejection of a beam. Synchrotron radiation output is made from the ninth bending magnet. Besides, vertical betatron tune will be lowered as compared with that we worked earlier. Tis will allow us not so strongly decrease the aperture of small quadrupoles and make smaller deformations of vacuum chamber.

New RG cavity was installed (frequency is 174.3755 MHz, accelerating voltage is 112 kV) in the ring, it was tested and we got all projected parameters. The new RF cavity is needed because the energy loss is 70 keV at 1 GeV and the old cavity is not able to fill this up.

5.1.3. BEP dipole magnets.

The main goal of dipoles' modernization is to obtain magnetic field of 26 kGs to work at 1 GeV. This task is hard enough because magnets' yoke is strongly saturated at this field level. For that purpose 4 mm plates were installed on the poles (Fig. 5.1.5), the gap becomes 32 mm.

We installed also ending plates of 12 mm to enlarge the magnet. New correcting coils are manufactured. To concentrate magnetic flux and increase the field we narrowed the pole from 120 mm to 90 mm. Bent plates of 50 mm are installed on inner radius of magnet yoke to decrease the saturation. Binding of survey markers of ready dipoles to the poles are made (Fig. 5.1.6).

Fig. 5.1.5. Plates on the BEP magnet' pole.

Fig. 5.1.6. Surveyor binds survey markers.

Magnetic measurements of new dipoles were made in December (Fig. 5.1.7). Though visually measured points are in good agreement with predicted curve, the difference of average measured field from the predicted one is about 1.7×10^{-3} at low field level and 4.3×10^{-3} at high field. It was expected that accuracy will be 10^{-3}. The discrepancy is because the iron saturation curve differs from expected one. Variation between magnets is acceptable and lies in the limits of our corrections.

To work at 1 GeV the feeding current more than 10 kA will be needed, hence we will make small modification of power supply.
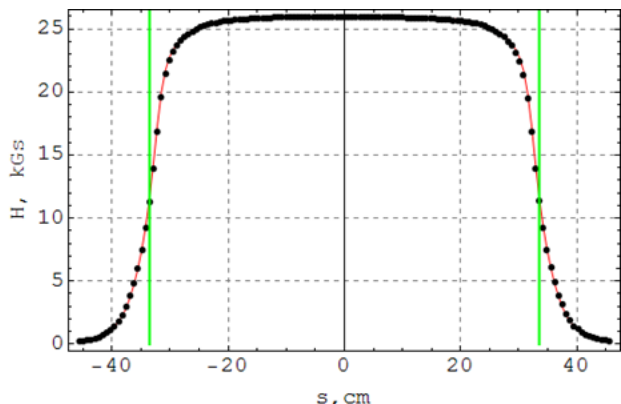
Fig. 5.1.7. Measured field.

5.1.4. BEP quadrupoles.

The hardest work was connected with quadrupoles. The main idea is as follows: to use old yoke, to make new profile with smaller inscribed radius and increase sextupole component (Fig. 5.1.8).
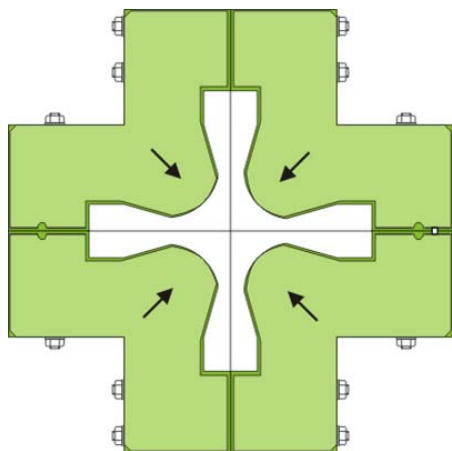
Fig. 5.1.8. New profile of BEP quadrupole.

The problem is that quadrupoles and dipoles are fed from the same power supply. Existing corrections are weak and become weaker with iron saturation. We should hit into the corridor provided by corrections. Saturation curves of sextupole and quadrupole harmonics are very different, sectupole component is hardly saturated at 6 kA current (Fig. 5.1.9).
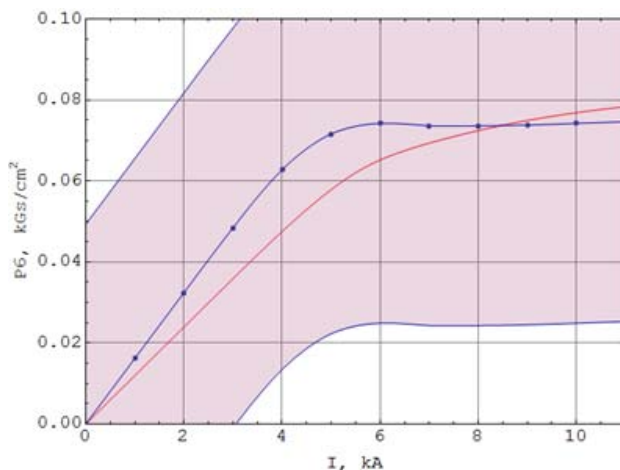
Fig. 5.1.9. Saturation curve of sextupole harmonic as compared with quadrupole one.

Beside, in tight setting of the ring there is strong influence (~3.5%) of neighbor sextupole correctors.

Quadrupole prototype was manufactured and measured a year ago. Since then the work on production of these quadrupoles began. It was necessary to make the new correcting coils as the old ones do not fit into diameter of a quadrupole.

5.1.5. BUMP magnets.

Bump magnets (Fig. 5.1.10) are pulse C-shape layer magnets placed in two straight drifts. They are needed to distort the orbit of a beam before ejection from BEP. At the same place we should provide port of vacuum pumping.
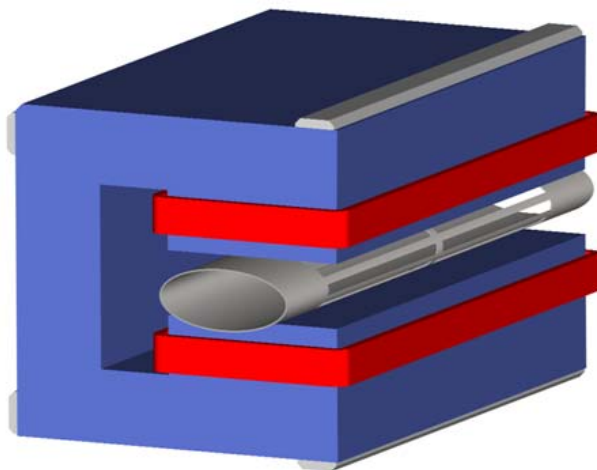
Fig. 5.1.10. Model of BUMPmagnet.

5.1.6. Vacuum chamber of BEP.

Fig. 5.1.11. Modification of vacuum chamber.

It is decided to keep old vacuum chamber. Aluminum vacuum chamber is deformed locally for magnets (decrease the gap), and in locations of quadrupoles special hollows for poles are made (Fig. 5.1.11). In addition, we made cleaning of SR channels, replacing of olives, repairing one chamber.

There was an offer to make SR output for collaborations with CERN (FCCpp experiment). It appeared that SR output could be done conveniently enough between core of dipole and quadrupole, we only need to modify vacuum chamber at this place.
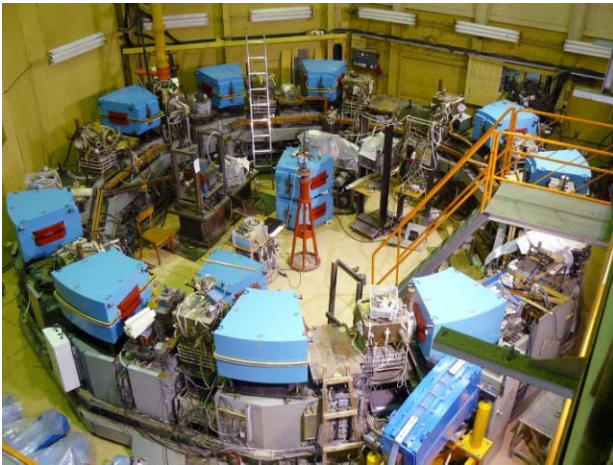
Fig. 5.1.12. BEP current state.

BEP ring as of January 2015 is shown in Fig. 5.1.12. Bending magnets are placed in their positions, a part of dipoles wait installations of correcting coils.

5.1.7. BEP–VEPP-2000 channel.

The main modification is manufacturing new "blue" magnets and new vacuum chambers for these magnets. They are fed in series with dipoles of BEP. Hence, we have the same problems: one should fit saturation curves to work synchronously with BEP ring. First dipole is manufactured (Fig. 5.1.13), measurement of edge field is done (Fig. 5.1.14.).

Fig. 5.1.13. Short 'blue' magnet.
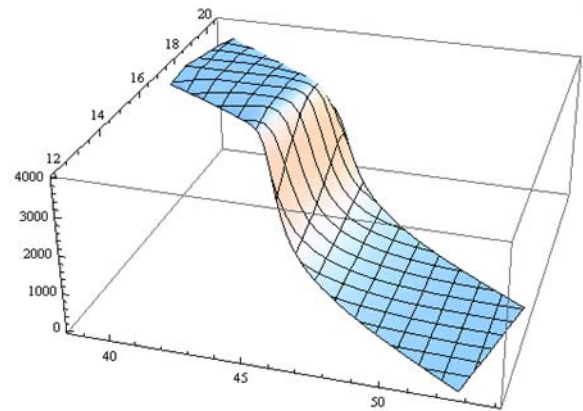
Fig. 5.1.14. Measurements of 'blue' magnet's edge field.

At present all four long and one short magnets are ready, remaining three short dipoles are in production.

5.1.7. Works on VEPP-2000 ring.

A year ago after rolling out of CMD-3 detector repair of solenoids was done (we had leak of guarded vacuum). Now all is restored, solenoids with CMD-3 roll in the ring.

Two new vacuum chambers are manufactured for magnets 2M2 and 3M2, addition inflector paltes are also installed (Fig. 5.1.13). This is required for injecting at 1 GeV because old inflector plates are not sufficient.

Fig. 5.1.13. New vacuum chambers with additional inflector plates.

Earlier one scraper was installed in the ring, which worked for Touschek probes. We placed one more scraper in diametrically opposite point. This should improve background conditions in detectors.

One more hard task was replacement of SR output mirrors for diagnostics. The old mirror construction is cupper indirect cooled prism with pasted plates of mirrors. When warmed by the beam these mirror plates fell. As it is planned to work at 1 GeV and with greater current (up to 200 mA) the new mirrors were produced: prism with located at right angle polished faces with necessary cover (Fig. 5.1.14). All the mirrors in whole ring were replaced.
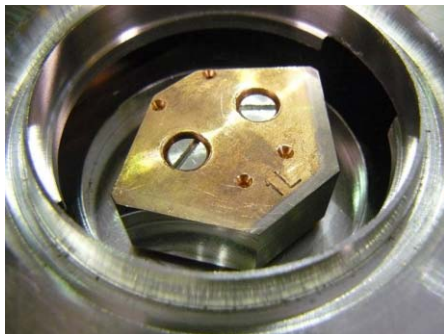
Fig. 5.1.14. New SR output mirror.

After completion of all vacuum tasks it was decided to warm RF cavity. Now the whole ring VEPP-2000 is under vacuum.

VEPP-2000 is completely assembled for now: all the magnet elements, vacuum system, solenoids, cryostats (Fig. 5.1.15). The ring is entirely ready to accept the beams, except the absent channels from BEP.

Fig. 5.1.15. VEPP-2000 ring in January 2015.

One more work was producing new F1 quadrupoles. These are weak slim lenses near solenoids with weak-current coils. It is planned to make coils with water-cooling to reach higher gradient for work in technical regimes: outgassing, polarization at high energy. Increasing diameter and placing survey markers will allow us to make independent precise installation of these quadrupoles.

In addition to listed modernization tasks of VEPP-2000 it is planned to make special support between solenoids and CMD-3 detector. During the work detector strongly pulls by its field the focusing solenoids, so that solenoids have to rest on iron of CMD-3. This very complicates installation of solenoids. Special supports with articulated joint will allow one make free solenoids' installation.

Planes on starting the modernized VEPP-2000 complex are as follows. In February assembling of K-500 channel ascent section will come to the end. In February–March we will have delivery of remaining magnets, measurement of BEP quadrupoles and assembling the channels. In April the BEP ring will be completely assembled and in May will be ready to accept the beams from injection complex.

5.2. ACCELERATOR COMPLEX VEPP-4

The accelerator complex VEPP-4 is a unique facility for experiments with colliding high-energy electron-positron beams. The complex includes the injector "Positron", multitask storage ring VEPP-3, and electron-positron collider VEPP-4M with the universal magnetic detector KEDR. The main purpose of the collider VEPP-4M is experimental investigation into the properties of elementary particles, resonance parameters, and cross sections of electron-positron annihilation.

5.2.1. Runtime distribution.

Fig. 5.2.1 shows the distribution of time for different types of work at the complex VEPP-4 in 2014.
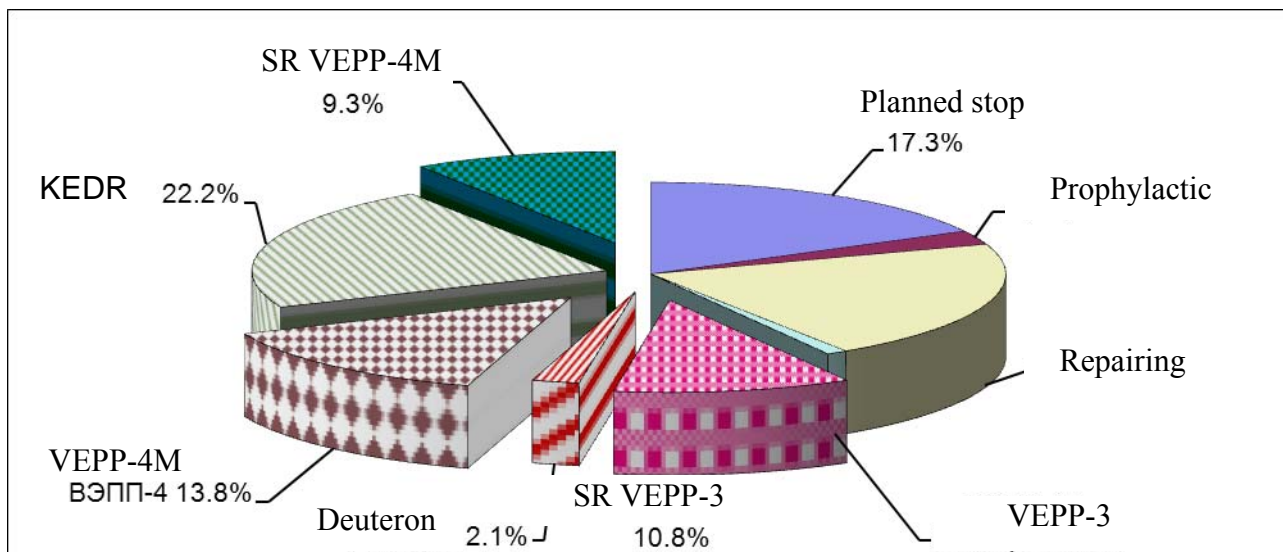
Fig. 5.2.1. Runtime distribution at complex VEPP-4.

As one can see, this year the working time of the complex was distributed primarily among experiments using synchrotron radiation at VEPP-3 and VEPP-4M, as well as collection of statistics at the detector KEDR. Regular maintenance works (2.5%) are performed weekly. Experiments on accelerator physics at VEPP-4M were carried out for increase in the luminosity of the collider and correction of its magnetic structure. Table 5.2.1. presents long-term statistics on runtime distribution at the complex. The increase in the number of emergency shutdowns in the last year was caused by the wear and aging of the equipment of the complex.

Table 5.2.1. Long-term statistics on runtime distribution at complex VEPP-4.

% of total time	2009	2010	2011	2012	2013	2014
VEPP-4 KEDR	14.6	33.2	14.8	0	0	22.2
VEPP-4 SR	4.7	3.7	2.8	1.6	4.4	9.3
VEPP-4 Accelerator	2.8	7.9	6.2	3.4	4.5	13.8
VEPP-3 SR	13.8	15.2	20.7	16.9	24.9	10.8
VEPP-3 Deuteron	18.9	0	17.3	17.4	16.5	2.1
VEPP-3 Positron	1.1	2.5	2.5	1.1	1.5	0.9
Repair	6.1	10.5	6.5	3.4	2.7	21.0
Maintenance	2.0	2.3	2.6	1.8	2.5	2.5
Scheduled shutdowns	36	24.6	26.6	49.9	39.3	17.3

5.2.2. Experiments with detector KEDR.

The acquisition of experimental data for measurement of R (the ratio of the total cross section of production of hadrons to the cross section of production of muon pairs) for energies in the centre-of-mass system (cms) of 1.86 to 3.7 GeV was completed last year; preliminary results were obtained for measurement of R in the range from the J/Ψ meson to Ψ′ meson; the results of measurement of the probability of decay of the J/Ψ meson to $\eta_c\gamma$, done with the world's best precision and proving theoretical predictions, were published. A program of works with the detector KEDR until 2018 was developed. Table 5.2.2 presents the experimental results and the statistics collected in this energy range.

Table 5.2.2. Energy distribution of collected statistics.

No.	E, GeV	Lt, nb^{-1}	No.	E, GeV	Lt, nb^{-1}
1	1538.0	52.89	10	1760.4	154.29
2	1547.9	17.58	11	1809.1	184.38
3	1548.6	173.00	12	1840.5	41.30
4	1549.3	13.41	13	1842.5	52.10
5	1552.0	14.70	14	1843.1	42.20
6	1560.0	129.60	15	1843.6	31.72
7	1611.0	101.90	16	1846.5	44.48
8	1657.3	182.60	17	1859.8	161.37
9	1709.1	169.32			
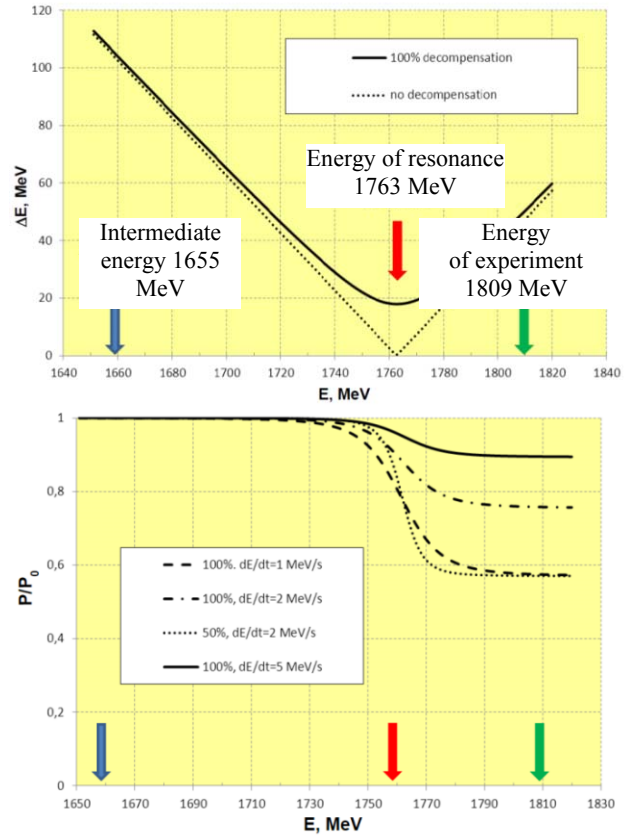
Fig. 5.2.2. Top: the tuning out of integer spin resonance with the anti-solenoids of KEDR switched off does not vanish at the resonance energy. Bottom: degree of polarization conservation depending on final energy with varying degree of decompensation and acceleration rate (with due account of radiation depolarization).

5.2.3. Experiments with polarized beams.

A series of experiments on the measurement of beam energy by the resonance polarization method was done, with crossing of the spin resonance. Fig. 5.2.2 presents the idea of experiments on polarization conservation during beam acceleration in VEPP-4M with crossing of the energy of integer spin resonance.

As a result, it was shown that calibration could be performed by the resonant depolarization method at an energy of 1809 MeV during beam acceleration from an injection energy of 1655 MeV (Fig. 5.2.3).
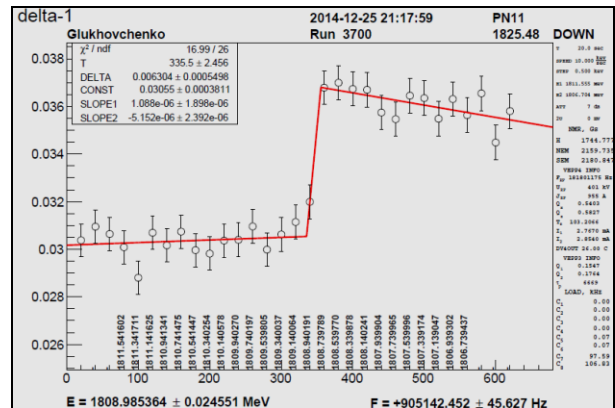
Fig. 5.2.3. Calibration with experiment energy of 1809 MeV and acceleration rate of 2.4 MeV/sec.

75

5.2.4. Correction of optics of VEPP-4M using code SixTrack.

The optics of the collider VEPP-4M was corrected using the code SixTrack. Recording the response matrix would take about 2 hours. The magnetic structure of VEPP-4M was substantially corrected. In particular, a few faulty power supplies were removed; three wrongly-commutated low-current corrections were taken off; the difference in the polarity of skew-quadrupoles and abnormal position of one vertical corrector in the semicircle were eliminated. The magnetic structure of VEPP-4M became closer to the design model, which will enable experiments on improvement of the luminosity of the collider via radial adjustment of the beta-function at the collision point.

5.2.5. System for detection of scattered electrons.

The "positron" part of the system for detection of scattered electrons (SDSE) was put into operation in 2014. It includes an Nd:YLF laser with two wavelengths and an optical system in the experimental hall of VEPP-4M. That enables continuous automated calibration of the electron and positron directions of the SDSE and examination of the energy resolution and stability of parameters. In addition, the scattered laser photons are used on the "extracted beam on VEPP-4M" facility (Fig. 5.2.4).
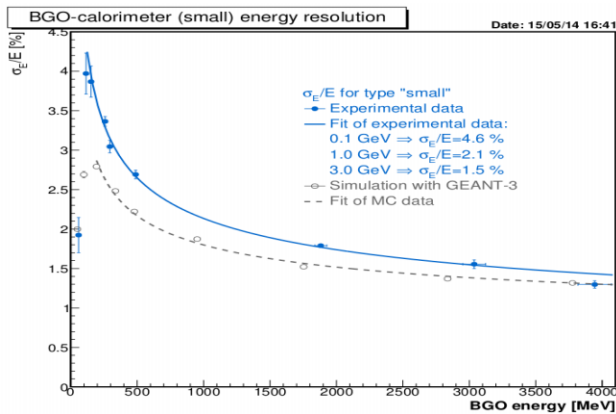
Fig. 5.2.4. Energy of scattered gamma quanta measured with BGO calorimeter.

5.2.6. Cross-feedback system.

The cross-feedback system, which suppresses dipole oscillations of beams and thus enables storage of current of up to 20 mA at an energy 4 GeV in VEPP-4M, is also used in operation at lower energies and currents, which significantly increases the average effectiveness of beam injection from VEPP-3 to VEPP-4M. The window of the control program with data relating to a injection moment is shown in Fig. 5.2.5.
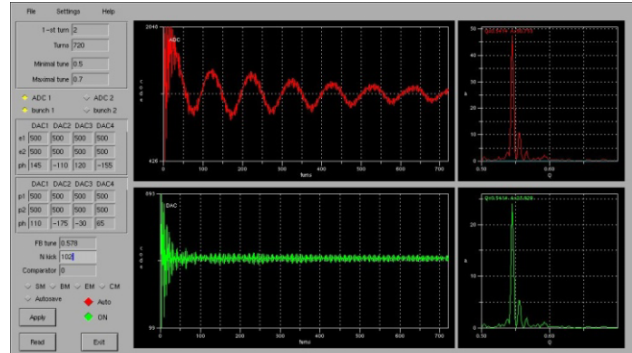
Fig. 5.2.5. Window of control program of cross-feedback system at VEPP-4M.

5.3. INJECTION COMPLEX VEPP - 5

5.3.1. Works in 2014.

Works on the refinement and tuning of the injection complex (IC) were done in 2014, as well as on the improvement of the stability of its systems and organization of interaction with the users. Developments for the planned replacement of obsolete or unsupported electronics of the systems of the complex were underway.

Works for increasing the rate of accumulation of electrons in the cooling storage ring were done. The program "sixdsimulation", which was developed for VEPP-2000 and integrated into the control system of the injection complex, was used for correction of the equilibrium orbit and the magnetic structure of the cooling storage ring for a beam energy of 360 MeV. The dynamic aperture was increased from 1-2 millimeters to 1 centimeter. The threshold current of electron beam in this case was about 160 mA in three bunches. The corrected β functions of the cooling storage ring storage of the IC are shown in Fig. 5.3.1.
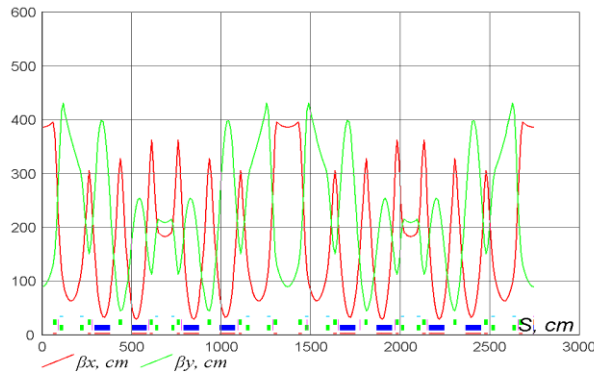
Fig. 5.3.1. Corrected β functions of storage ring of IC.

The waveguide vacuum windows and the microwave loads are key elements of microwave linear accelerators. Vacuum windows enable restriction of the vacuum volume of microwave devices and withdrawal of the microwave power of klystrons in waveguide lines of accelerators. Microwave loads are necessary for absorption of the power of traveling-wave accelerating structures or testing of high-power microwave supplies. Creation of such products is necessary for scientific and industrial accelerators. Fig. 5.3.2 shows the calculation of the amplitude of the electric field in the H and E planes of a traveling-wave can-type vacuum window.

The calculated gain-frequency characteristic is shown in Fig. 5.3.3. One can see that the bandwidth is 2.815-2.995 GHz (VSWR = 1.22).

This vacuum window enables work with powers of over 60 MW, which is interesting not only to industrial accelerators, but also to scientific complexes with high-energy beams. Currently, the development of the design documentation for manufacturing is underway.

The microwave group of the IC developed and manufactured new directional couplers for the waveguide line of the IC (Fig. 5.3.4). The tapping ratios of all the direc-

tional couplers were measured. The calibrated couplers will enable power measurement in the waveguide line of the accelerator within 3%.
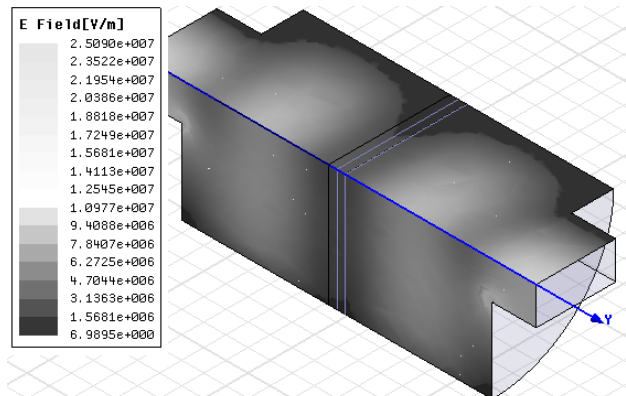
Fig. 5.3.2. Electric field amplitude in H and E planes of traveling-wave can-type vacuum window.
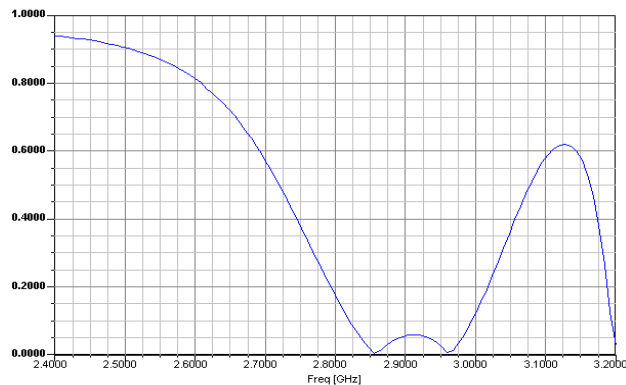
Fig. 5.3.3. Reflection coefficient vs. frequency of traveling-wave can-type vacuum window.

A prototype of the new high-power microwave load for the accelerating sections of the complex was developed and released for implementation. The general view of the microwave load is shown in Fig. 5.3.7. It has a resistive coating developed by BOLID (Novosibirsk), which enables absorption of microwave power of up to 60 MW without the resonance methods. A prototype load is under manufacturing now.

Fig. 5.3.4. Directional waveguide coupler.
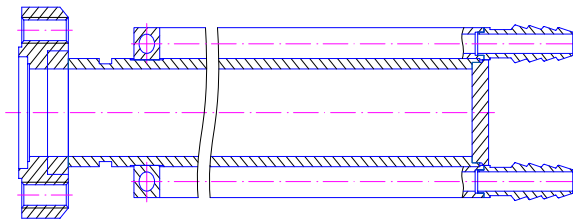
Fig. 5.3.5. General view of microwave load.

A microwave switch was designed and tested. It is a switching device on p-i-n diodes, which is used in microwave technology for formation of pulse signals of controlled duration and amplitude, improvement of parameters of already formed signals, e.g. reduction of their leading edges, and protection of elements of microwave circuits. The microwave switch is intended for the system of control over pulse parameters of microwave signal, e.g. a signal applied to the high voltage electrode of the electron gun with microwave control over injection current in installations for pulse radiolysis on linear accelerators. It can also be used in the microwave system of the IC.
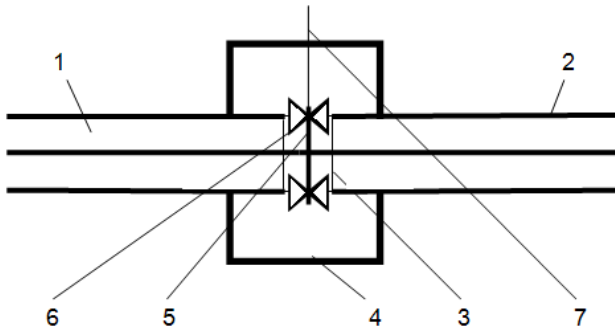
Fig. 5.3.6. Coaxial microwave switch: 1 – input of coaxial line, 2 – output of coaxial line 3 - line break (gap of cavity), 4 – cavity, 5 - conductive ring, 6 – p-i-n diodes, 7 - control electrode.

The device is a piece of coaxial line with a broken external conductor. Control p-i-n diodes are embedded in the break of the conductor - an annular clearance - as shown in Fig. 5.3.6. A toroidal cavity is mounted in alignment with the line, the gap of the cavity aligned with the break of the external conductor of the line. The microwave switch was made in two variants, with working frequencies of 2450 MHz and 2856 MHz and a maximum pulse microwave power of 3 kW (p-i-n diodes KA520), 1 kW (p-i-n diodes KA507), and 0.2 kW (p-i-n diodes KA509). The leading edges of microwave pulses are 200 ns, 50 ns, and 30 ns at most, respectively. The microwave pulse envelope formed with the switch is presented in Fig. 5.3.7. Fig. 5.3.8 shows an example of the switch.

This device is unique, which is confirmed by a patent issued in 2014.

New operating electronics of beam position monitors on linear accelerators were installed and are being prepared for operation.

A new power source for the magnetic system, RF-1000, was tested on the installation. A scheduled replacement of the earliest version of the power supplies V-1000 was being prepared.
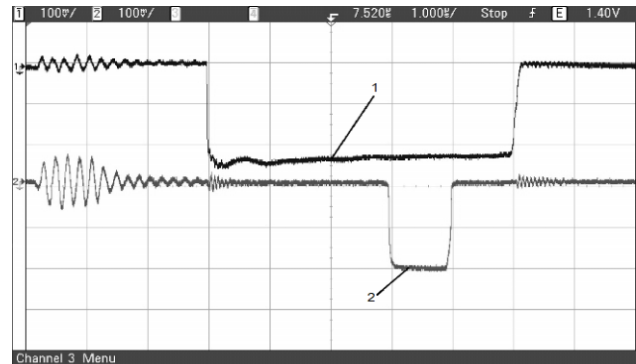
Fig. 5.3.7. Envelopes of initial (1) and resulting microwave pulses (2).

Fig. 5.3.8. Coaxial microwave switch.

New electronics of the pickup station for the cooling storage ring were developed and successfully tested. A scheduled replacement of the entire electronics of the pickup station of the cooling storage ring is being prepared.

The magnetic elements of the extraction line were put into operation; the work of the power supplies of these elements was settled.

Trial extractions of electron beams of different energies from the cooling storage ring were carried out. The maximum energy of the electrons was 480 MeV.

As part of these tests and refinement of interaction with the users, hardware for organization of accumulation-bypass cycle was completed and successfully tested. Test programs for automation of beam storage and extraction were written. Add-ins to the complex control software were designed. They are required for communication with the users. The computer infrastructure of the complex control system was designed. It provides reliable operation of the complex and interaction with the users.

5.3.2. Investigation into wakefield acceleration.

The investigation into wakefield acceleration continued in 2014. Bunches from the cooling storage ring will be used for experiments on plasma wakefield acceleration. Currently, this installation includes an additional transport line for electron and positron beams extracted from the storage ring, a plasma section and a spectrometer (see Fig. 5.3.9). The full version of this installation will include a system for beam compression. At the first stage, a simplified version of the installation will be commissioned, in which beams will be injected in plasma without compression. Significant changes in the energy and angular spread of beam through the development of transverse two-stream instability in the plasma can also be observed in this case.
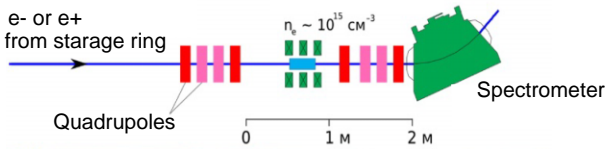
Fig. 5.3.9. General scheme of wakefield acceleration installation.

A conceptual scheme of wakefield acceleration in a hollow plasma channel is shown in Fig. 5.3.10.
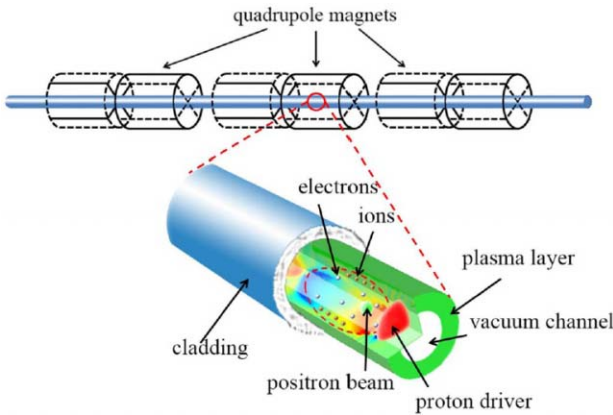
Fig. 5.3.10. Conceptual scheme of wakefield acceleration in hollow plasma channel. Quadrupole magnets are used for focusing of proton driver. Translucent color shows longitudinal electric field.

As part of the wakefield acceleration activity, a kinetic quasi-static code was created. The energy flow in the plasma is conserved with high accuracy and the plasma wakefield acceleration is modelled. The interface of the code is convenient for periodic multiple start of the code by outside wrappers on computers of different architectures and running under different operating systems. The new code was used for analysis of wakefield acceleration

of positrons in a narrow plasma channel with a wave built-up by a short proton bunch.

Due to the high accuracy of the new code, a numerical simulation of long-term dynamics of plasma wake wave with parameters of experiments being prepared was done for the first time. It was found that when a wake wave was broken in a finite-radius plasma, the latter was rapidly heated and an uncompensated positive charge and a longitudinal current appeared in the plasma (Fig. 5.3.11). It was shown that up to 80% of the wake wave energy went into hot electrons and the energy of the slowly changing field around the plasma.
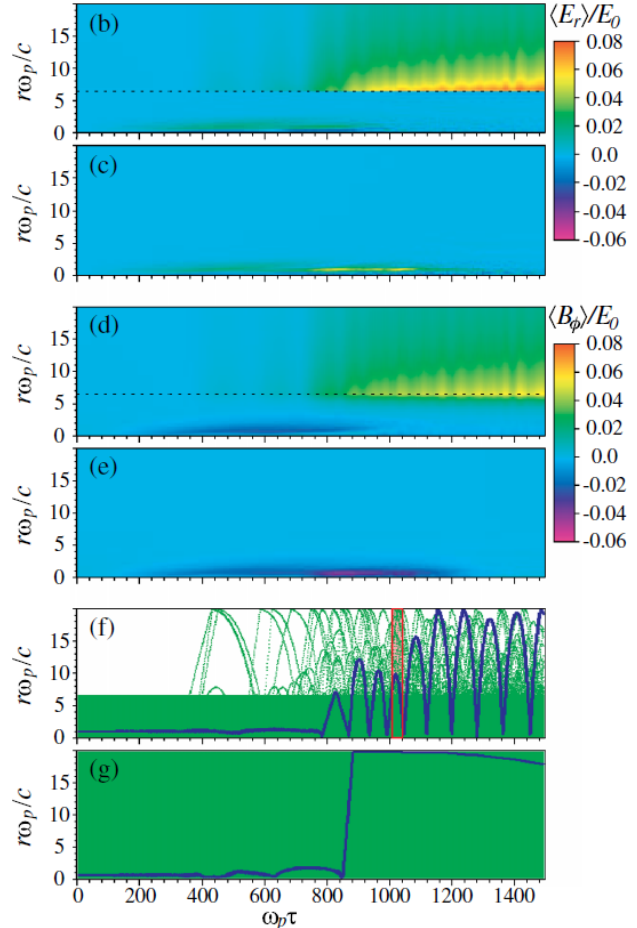
Fig. 5.3.11. Comparison of distributions of electric field, magnetic field and trajectories of individual plasma electrons in restricted (top fragments) and unlimited (lower fragments) plasma.

A vacuum system for extraction of beam from the storage ring to the plasma section was designed and manufactured (Fig. 5.3.12).

The vacuum system will be mounted during the shutdown of the IC of VEPP-5, for the reasons of the radiation safety of the premises in which the plasma section is placed. The analysis and optimization of parameters of the storage ring from which a beam will be extracted are underway now. Fig. 5.3.13 shows a photograph of synchrotron radiation in the ring with a circulating electron beam. The beam parameters are as follows: current of 160

mA, energy of 360 MeV, and accumulation rate of 1.8×10^9 e⁻/s.

Fig. 5.3.12. Elements of vacuum system of plasma section.

Fig. 5.3.13. Photo of synchrotron radiation from cooling storage ring of IC of VEPP-5.

5.4. OPTIMIZATION OF OPERATION OF X-RAY COMPLEX LIU-2

5.4.1. Optimization of start time of each modulator.

To reduce the diameter of electron beam spot on a target, it is necessary to have a minimum energy spread in the electron beam throughout the flat part of pulse.

Individual adjustment of the start time of each modulator allows one to smooth the total pulse of accelerating voltage due to the mutual compensation of ripple on the shelves of pulses across different inductors. The data acquisition system of the accelerator allows one to record the waveforms of all inductor voltage pulses simultaneously. Fig. 5.4.1 presents waveforms of high-voltage pulses across every second inductor (one modulator feeds two inductors in parallel). Using these measurements and taking into account the timing delay in different-length cables that start different oscillographs, one can individu-

ally choose the start time for each modulator to minimize the ripple of the flat part of the total voltage pulse.
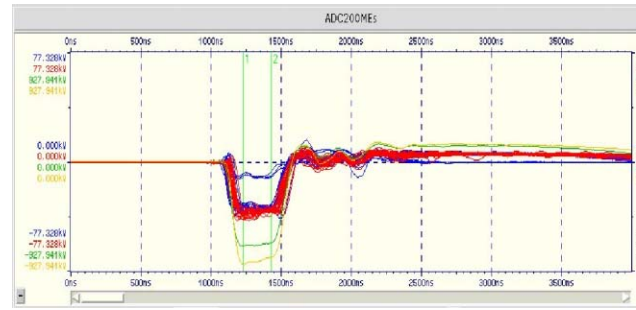
Fig. 5.4.1. Vertical scale: voltage; horizontal scale: time. Blue and red waveforms: high-voltage pulses across inductors supplying diode and second accelerating tube, respectively. Green waveform: total voltage pulse across diode (≈710 kV); yellow waveform: total voltage across second accelerating tube (≈850 kV).

Conclusions. The fall in the flat portion of total-voltage pulse is related with the dependence of the transfer ratio of the measurement equipment (divider and matching circuit of ADC) on the frequency, which leads to a signal fall of about 5% in measurement of voltage across the inductors.

As seen from Fig. 5.4.1, although the initial shape of the voltage pulse in individual modulators varies up to ± 12%, adjusting the start time of each modulator, one can make the fluctuations of the total voltage pulse across the diode less than ± 1%.

5.4.2. Gamma pulse reduction.

The gamma pulse duration can be reduced via application of voltage to the second accelerating tube 150 ns earlier than to the diode. In such conditions, the electron beam leaving the diode has a duration of 230 ns (Fig. 5.4.3), whereas the target unit is achieved by a beam 145 ns long (Fig. 5.4.4). The remaining portion of the non-accelerated electron beam is thrown by lenses to the vacuum chamber walls. This regime is difficult for the modulators feeding the second accelerating tube, because without the electron beam they work for unmatched load for some time (Fig. 5.4.2).
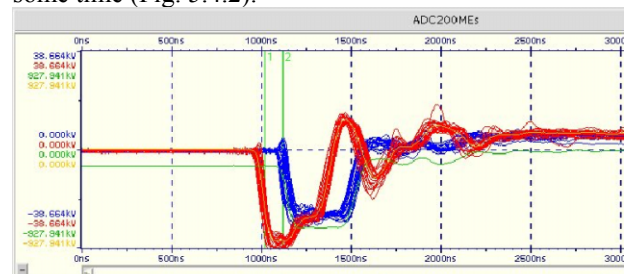
Fig. 5.4.2. Blue waveforms: voltage pulses across inductors that feed diode; red waveforms: voltage pulses across second accelerating tube.
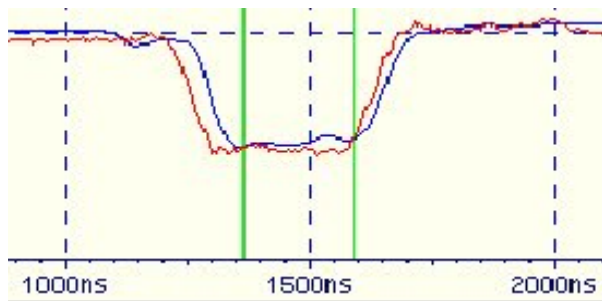
Fig. 5.4.3. Blue waveform: current emitted from diode; duration of 230 ns.
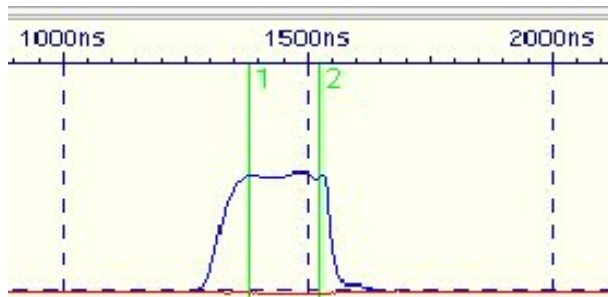
Fig. 5.4.4. Blue waveform: current reaching target unit; duration of 145 ns.

Alternatively, the gamma pulse duration can be reduced via introduction of additional time shift between the starts of each modulator. This leads to a lengthening of the leading edges of the total voltage pulse and a shortening of its flat part. Since the lenses "throw away" the flat leading edges of the electron beam current, one can use this effect to reduce the duration of the gamma pulse by a value of about 40 ns (Fig. 5.4.5).

The duration of the first current pulse as compared with the second current pulse was reduced by 40 ns. The possibility of reducing the second pulse from 230 to 145 ns due to a shift in the start of the modulators feeding the second accelerating tube was shown (see Figs. 5.4.2 - 5.4.4).

5.4.3. Tuning of electron-optical system of LIU-2 for minimum phase volume of beam.

High-quality radiographic images require a point x-ray source with a diameter as small as possible.

In the operation of the accelerator we identified the following factors preventing good focusing of electron beam on the target and stable repetition of this result from shot to shot:

Attempts to compensate inaccuracies in the alignment of the electron-optical system using three two-coordinate correctors resulted in asymmetry of electron beam. When such a beam was focused on the target, the hole was oval, and it was difficult to compress such beam to a diameter less than 1.5 mm (see Fig. 5.4.6).

1. During focusing of beam on the target, fragments of tantalum were absorbed by the graphite placed before the outlet window. That led to considerable degrada-

tion of the vacuum and subsequent breakdowns in the accelerating tubes. To eliminate this effect, we replaced the graphite disc 8 mm thick before the outlet window with an aluminum disc 1 mm thick.

2. The final short-focus lens can be adjusted in three directions. The position of the final lens was adjusted for the best possible overlapping of the focus of the lens with the optical axis of the accelerator.
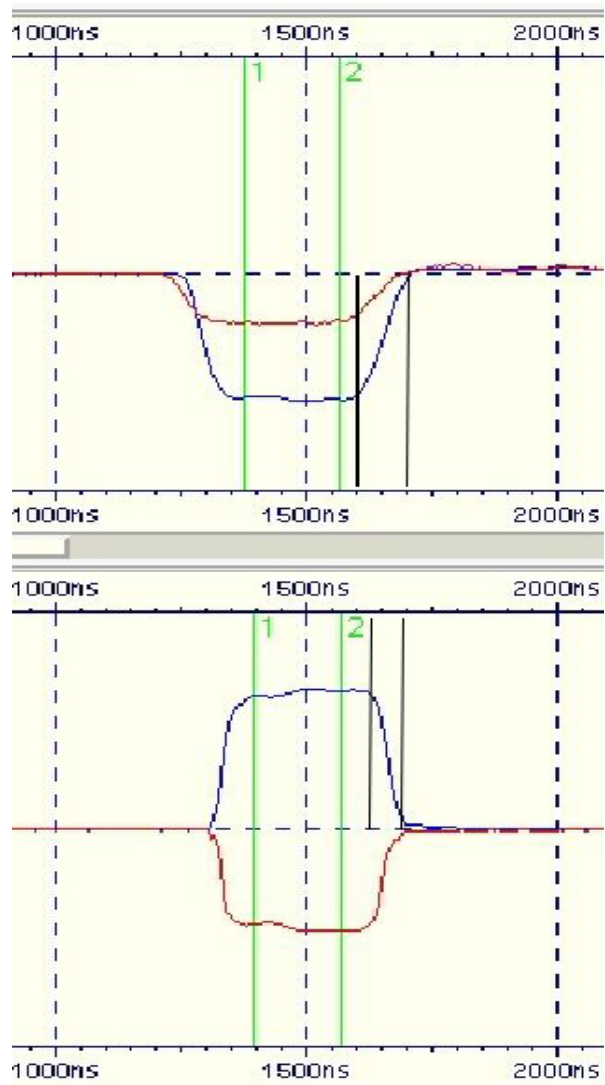
Fig. 5.4.5. Top blue waveform: beam current at output of diode; leading edge length of 100 ns. Bottom blue waveform: beam current after passing through three solenoidal lenses; leading edge length of 60 ns.

Fig. 5.4.7 shows a tantalum target 0.5 mm thick with holes burnt with a constant energy of 1.52 MeV and a beam current of 1.3 kA. The correction system was switched off. Only the magnetic field of the final short-focus lens varied within ± 1%. The almost two-fold difference in the diameters of the holes with a little change in the lens power indicates that the optimal tuning of the optical system is in a very narrow zone.

81
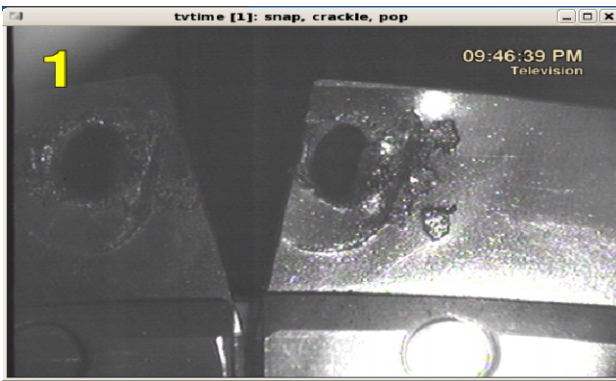
Fig. 5.4.6. Holes burnt by electron beam with use of beam correction system.

Fig. 5.4.7. Holes burnt by electron beam with correction system switched off.

Conclusions. According to calculations, when the alignment of the cathode, the lenses and the transport line is ± 0.1 mm or better, the optical system of the accelerator allows one to compress an electron beam to a diameter less than 1.5 mm without the use of correctors (see Fig.5.4.7).

It would take three days at least to warm the cathode in rate doperation in order to ensure reproducibility of focusing of the beam from shot to shot.

5.4.4. Fine tuning of pulse forming lines of individual modulators.

The parameters of the pulse forming lines (PFLs) were recalculated. The pulse forming lines used in the supply system of the injector are E lines consisting of eight inductance-capacitance cells with wave impedance distributed inhomogeneously along the electric length of line. Computer simulation of discharge of pulse forming line for an equivalent load of the accelerator revealed that the misalignment of the line and the load could be compensated via increase in the capacitance of the first two cells of the line and change in the inductances of the first four cells. Figs. 5.4.8 and 5.4.9 present voltage pulse forms of the modulator of the power system of the injector calculated for the equivalent load, before and after tuning of line.

The lower pulse forming lines were adjusted for correction of the leading edge and the peak of the accelerating voltage of the first pulse. In compliance with the calculations, it was necessary to increase the capacitance of the first cell by about 40% in order to raise the voltage growth rate in the leading edge of the pulse. Such large increase in the capacitance will result in a higher overshoot in the leading edge of individual modulators (Fig. 5.4.10). This overshoot is to compensate the insufficient rate of voltage growth in the leading edge of modulators where non-adjustable PFLs are set (Fig. 5.4.11). As a result, the capacitance of the first cells of the PFLs was increased from 9 to 13 nF.
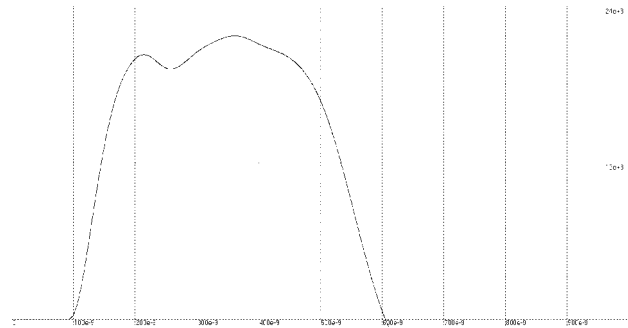
Fig. 5.4.8. Calculated shape of voltage pulse with equivalent load of modulator of pulse system of injector, before adjustment of PFL. Scale: Volts/seconds.
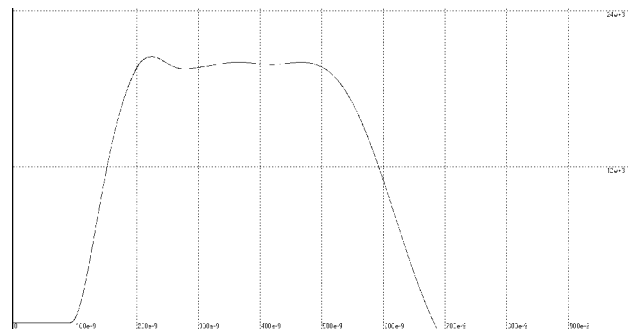
Fig. 5.4.9. Calculated shape of voltage pulse with equivalent load of modulator of pulse system of injector, after adjustment of PFL. Scale: Volts/seconds.
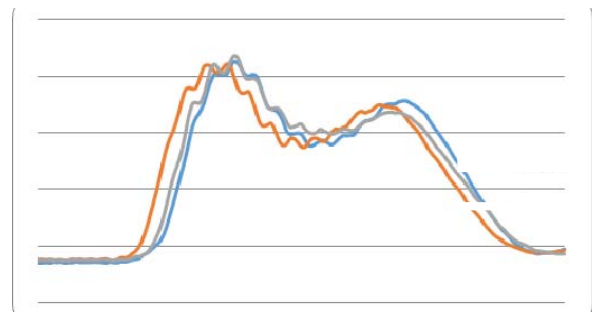
Fig. 5.4.10. Inductor voltage formed by modulators 8A, 8B, and 8C with adjustable pulse forming lines on capacitors K15-10.
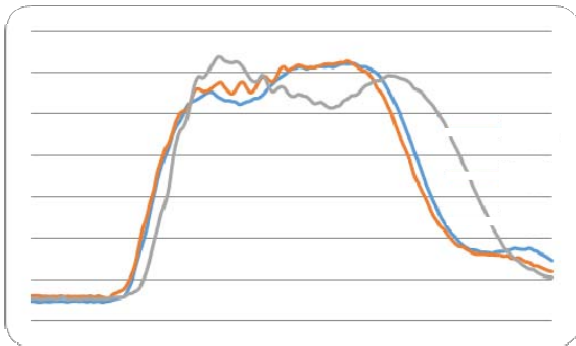
Fig. 5.4.11. Inductor voltage formed by modulators 8D, 8E, and 8F with non-adjustable pulse forming lines.

Conclusions. Calculations were done for optimization of the voltage shape at the output of the modulators of the pulse system. In accordance with the calculations, 24 pulse forming lines on capacitors K15-10 were changed. This is the half of the pulse forming lines used for generation of the first pulse of accelerating voltage.

That allowed reducing the ripple in the peak of the first current pulse at the output of the electron gun to a level of $\pm$ 2.5% (Fig. 5.4.12).

In addition, due to the possibility of non-synchronous start of individual modulators and separation of individual inductor voltage pulses in time, we managed to reduce the ripple in the peak of the second current pulse at the output of the electron gun to a level of $\pm$ 1% (Fig. 5.4.13).
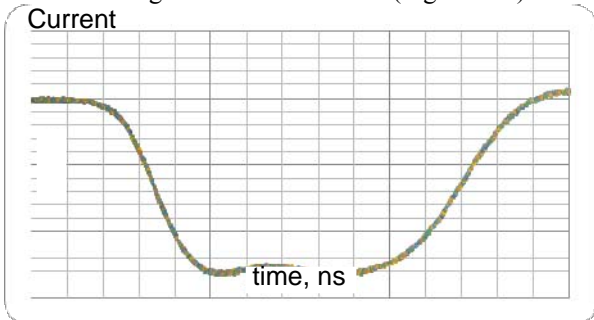
Fig. 5.4.12. Shape of first pulse current at output of electron gun.
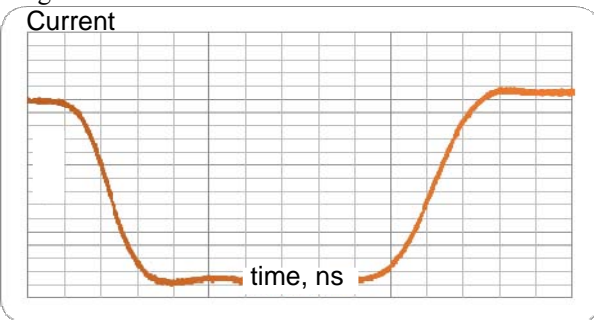
Fig. 5.4.13. Shape of second pulse current at output of electron gun.

Results

• The duration of the first current pulse was reduced by 40 ns as compared with the second current pulse;

• the second pulse duration can be reduced from 230 to 145 ns via shift in the start of the modulators feeding the second accelerating tube;

• according to the calculations, the optical system of the accelerator enables compression of electron beam to a diameter less than 1.5 mm without the use of correctors;

• the likelihood of high-voltage breakdowns after shooting a target was significantly reduced due to replacement of the graphite absorber before the outlet window with an aluminum one;

• if the microperveance of the electron gun is constant, the result of beam focusing on a target can be reproduced from shot to shot;

• the adjustment of the lines enabled reducing the ripple in the peak of the first current pulse at the output of the electron gun to a level of $\pm$ 2.5%;

• the ripple in the peak of the second current pulse at the output of the electron gun was reduced to a level of $\pm$ 1%.

The optimization of the operation regimes and the hardware-software complex of LIU-2 markedly improved its operation in the X-ray regime.

5.5. ELECTRON-BEAM WELDING

The manufacturing of a motion system for an electron-beam welder was completed. The system includes a two-coordinate mechanism for movement in a plane and a mechanism for rotating a part to weld about the longitudinal axis of the welder. The electron-beam welder has been installed, debugged and put into operation. The technology for welding of vacuum chamber of accelerator of charged particles is being tested.

Below are given the main parameters of the motion system for the electron-beam welder:

No.	Parameter of module	Module for longitudinal motion	Module for cross motion
1.	Maximum possible motion, mm	1930	310
2.	Positioning accuracy, mm	+/- 0.05	
3.	Positioning reproducibility, mm	+/- 0.02	

A model of 3D printer of metal products, including those of refractory metals, was designed and manufactured. The source metal is a wire, which is welded on a product with an electron-beam. The electron beam was produced by the power unit of the electron-beam welder. Cylindrical structures of steel and tungsten were made for the testing of the model.

Fig. 5.5.1. Electron-beam welder. Foreground: mechanism for moving part to weld.

A device for rotation of electron beam was manufactured and tested. The device consists of one or several magnetic quadrupoles and a dipole magnet, the magnetic field in which is such that the electron beam trajectory is a loop in the plane of rotation (α magnet). This device enables elimination of the direct visibility between the cathode of the electron beam welder and the place where a part is welded. Due to this, the cathode and the high-voltage region of the electron gun are protected from the vapor and small drops of metal from the workpiece. The electron gun field is screened from the workpiece by the vacuum chamber walls or protective screens.

Fig. 5.5.3. Samples grown from tungsten wire.

5.6. CONNECTION MODULE FOR EUROPEAN XFEL (DESY)

In December 2013, ahead of schedule, BINP fulfilled all obligations under the contract **Connection Modules for XFEL Horizontal MBK.** 27 assemblies of connection modules (CMs) were delivered to DESY.

A connection module is a unit that became a simple solution to the problem of power supply from pulse transformers to horizontal-design klystrons like Toshiba Electron Devices or Thales Electron Devices via a high-voltage cable connection.
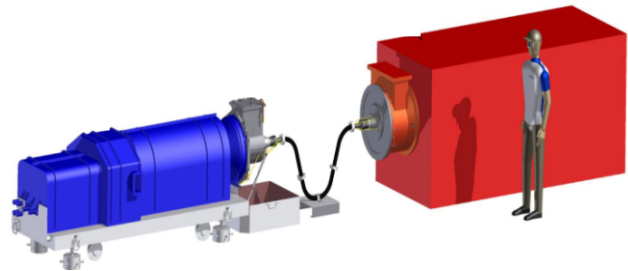
Fig. 5.6.1. Link-up of horizontal-design klystrons via Connection Module and cable connection.

The Connection Module design suggested by BINP enabled the following:
• powering of horizontal-design klystrons from a pulse transformer through a flexible cable connection;
• stable filament power supply of klystrons via an isolation transformer with open magnetic circuit from a specially developed inverter controlled remotely via the Ethernet protocol;
• pulse measurements of voltage and current of the klystrons;
• cooling of the cathode volumes of the klystrons.

The design of the Connection Module is shown in Fig. 5.6.2.
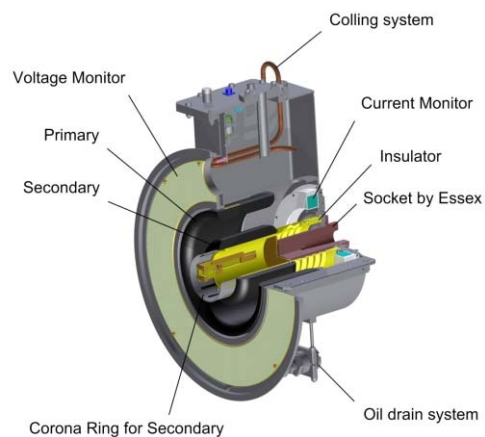
Fig. 5.6.2. Three-dimensional view of Connection Module.

The main parameters of a coaxial isolating transformer with open magnetic core are shown in Table 5.6.1.

Table 5.6.1. Main parameters of isolating transformer.

Parameter	Value
Gap between primary and secondary windings, mm	49
Magnetic coupling ratio	0.62
Resonance frequency, Hz	1600
Ex-casing efficiency of transformer in operation for equivalent of load of Toshiba Electron Devices (E3736H)	0.94
In-casing efficiency of transformer in operation for equivalent of load of Toshiba Electron Devices (E3736H)	0.92

By November 2014, 96% of the Connection Modules delivered were successfully tested on DESY stands; the remaining modules were prepared for testing. The first two Connection Modules tested were put into operation and have been in operation on the injector of XFEL since September 2013.

Another contract for the supply of additional 7 assemblies of the Connection Modules was signed in August of 2014.

Fig. 5.6.3. Storage of tested klystrons with Connection Modules before their installation in tunnel of XFEL.

5.7. LIQUID-METAL POSITRON TARGET

Creation of an intense source of positrons is associated with destruction of the target because of enormous thermomechanical loads. Using a jet of liquid lead as a conversion target is one of the possible solutions to this problem.

A stand for testing of such positron target was created in 2014. A jet of liquid lead at ~ 300° C is the material in which the conversion occurs. The liquid alloy is pumped with a modified gear pump. From anti-oxidation considerations, the tank with the alloy is under vacuum. The rotary motion feedthrough in the vacuum is performed using a magnetic-fluid clutch. The entire system is heated to a temperature of ~300° C.

The housing of the target is made of Kovar. The housing is a channel of rectangular cross section. Along the axis of the primary beam in the casing of the target there are two holes, in which windows made of boron-nitride ceramics are brazed (see Fig. 5.7.2). This ceramics have high mechanical resistance to shock loads that occur in the target.

Fig. 5.7.1. Stand for liquid-metal positron target.

Fig. 5.7.2. Target with ceramic windows.

The brazed connection of Kovar and ceramics is a critical spot of the design. Because of the high chemical activity of liquid lead, the latter dissolves the brazing material rather quickly, which may result in leaks. In future, either another brazing material and technology will be chosen or the design of the brazed unit will be changed, for hampering or preventing access of lead to the brazed junction.

5.8. ELECTRON COOLING INSTALLATION FOR GERMAN SYNCHROTRON COSY

In 2013, after 3 month's work, the 2 MeV electron cooling installation was mounted inside the accelerator ring. The installation was commissioned and first cooling was performed in October 2013. In 2014, works on the installation were continued. This electron cooler provides a unique opportunity to experiment with a detector of elementary particles in suppression of effects associated with scattering on nuclei of target and spread of pulses caused by fluctuations of ionization losses. The high-voltage cooler was designed based on the scientific research results and developments of Budker Institute of Nuclear Physics.

During the operation of the installation, electron cooling was performed at electron energies of 100, 200, 300 and 900 keV. Experiments on combined electron and stochastic cooling were carried out successfully. The maximum current reached 0.9 A.

Figs. 5.8.1-5.8.3 show results of electron cooling at an energy of 909 keV. One can see that the transverse size of proton beam is reduced under the influence of the electron beam (Fig. 5.8.1). From the measurement of the spectral width of the Schottky noise it is evident that the spread in the longitudinal pulse also becomes much less (Fig. 5.8.3).
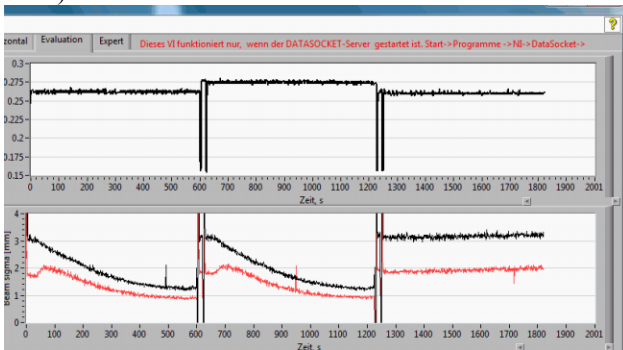
Fig. 5.8.1. Variation in beam transverse profile under electron cooling. Top: variation in number of particles during cycles. Bottom: dynamics of transverse size of proton beam (horizontal and vertical sizes). The cycle time is 600 seconds. The first two cycles are with electron cooling; the last cycle is without electron cooling.
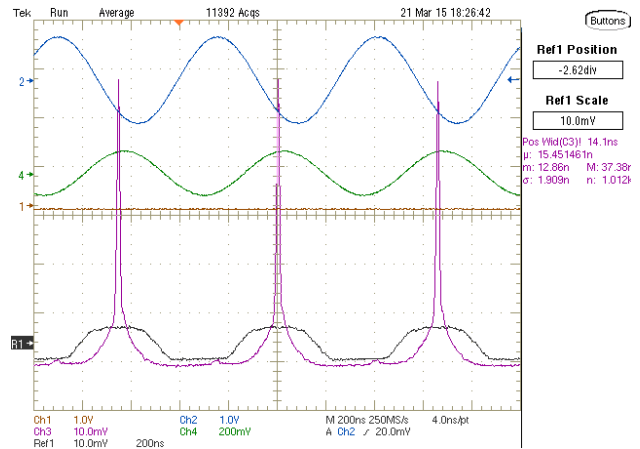
Fig. 5.8.2. Formation of short bunches of proton beam under combined action of RF and electron cooling.
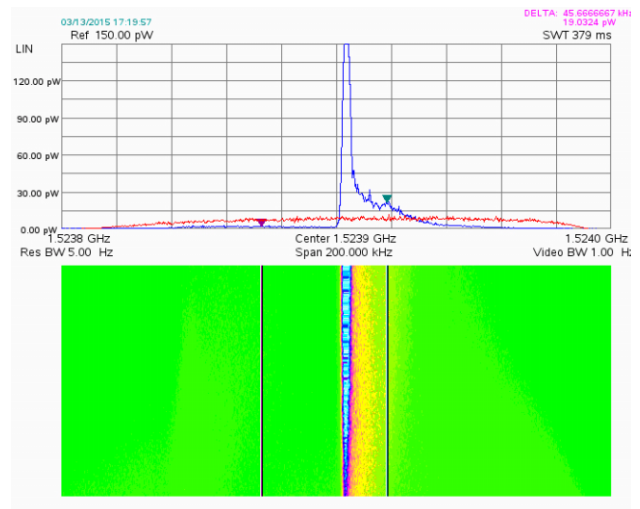
Fig. 5.8.3. Longitudinal cooling of proton beam with electron cooling. Blue line: Schottky noise for initial distribution; yellow line: distribution at the end of cooling cycle. The number of protons in a cycle is 108; the energy of the electron beam is 909 keV; the electron beam current is 400 mA. The cycle duration is 300 seconds.

5.9. ACCELERATOR MASS SPECTROMETER

Traditionally, works on the BINP accelerator mass spectrometer (AMS), which differs from foreign analogues with reliable separation of pure radiocarbon beam, can be divided into two large groups: routine AMS analysis of samples and works associated with further improvement of the BINP AMS.

1. Works on the improvement of BINP AMS and results obtained.

- The optics of the AMS were improved (the regime of "hard" input of ion beam to the electrostatic accelerator was implemented)

- The algorithm for AMS analysis of samples was improved (a 2-fold increase in the frequency of switching between isotopes to analyze at the AMS exit and a 2-fold increase in the time of collection of radiocarbon ions on normalization samples).
- A partial modernization of the optical elements of the AMS and related electronics was per formed.

As a result, the achieved count rate for radiocarbon ions from modern samples is 10Hz, which enables a statistical accuracy of analysis of 1% when 20 user samples (plus 3 control and normalization ones) are measured within 10 hours.

2. Works on AMS analysis of samples.

In 2014, the AMS analysis of samples was performed in the field of archeology, geology, biomedicine, ecology, metallurgy etc., over 700 samples in total. A typical example of AMS analysis is shown in Fig.5.9.1.
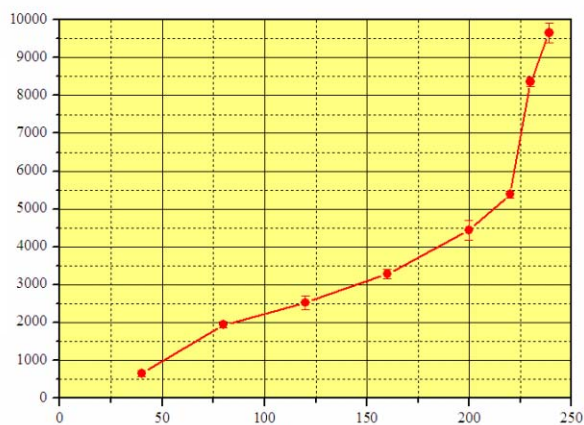
Fig. 5.9.1. Radiocarbon age of bottom sediments of lake Lozhok (Vengerovo district of the Novosibirsk region) vs. depth, sm.

5.10. VACUUM SYSTEMS

5.10.1. Designing, manufacture and delivery of cryogenic vacuum equipment for XFEL.

The fabrication and testing of cryogenic vacuum equipment for the international project of the X-ray free electron laser, XFEL (Gamburg, Germany) were completed in 2014. At the initial stage of the project, only one injector will be installed, but the helium distribution system is designed to integrate the second injector. In addition, the distribution system will allow replacement of accelerating modules of one injector during operation of the main accelerator and the second injector.

The equipment supplied by BINP includes the following (Fig. 5.10.1):

• Equipment for connection of cryomodules of the injector to the cryogenic system for helium admission (Feed Cap) and for closure of helium flows (End Cap). This equipment also covers the vacuum volumes of the injector;

• a Joule-Thomson refrigerator box to provide the accelerating system of the cryomodules of the injector with 2K superfluid helium;

• Feed Box, a junction box of injector 1 (XI1FB);

• Valve Box, a junction box distributing flows for two injectors of the XFEL (XIVB)

• XLVB, a junction box distributing flows for the linear accelerator and injectors of the XFEL;

• cryogenic lines to ensure delivery of 4.5K and 40K helium for two injectors of the XFEL and pumping of the 2K line to 30 mbar;

• heat exchangers of the 2K system, connection lines to collectors of the DESY helium plant, systems for pumping and purification of the helium lines, emergency release lines including 34 cryogenic safety valves;

• dashboards with pressure meters, temperature meters, meters of the level of helium vessels, gauges of flow meters of the system for heating of liquid helium for adjustment of dynamic parameters of the system, and sensors of condition of cryogenic pneumatic valves and control valves.

All the design calculations for heat penetration and mechanical strength were performed at BINP subject to international standards of the maximum category for vessels under high pressure. The calculations were performed for all possible values and drops of pressure and temperatures of the cryogenic equipment, including cooling down/heating regime and emergency cases. The temperature range is 2K-300K; the pressure range is 0 to 4 atm for the 2K line and 0 to 20 atm for the rest limes. An example of calculation is shown in Fig. 5.10.2. The calculations took into account parameters of flexible elements, e.g. bellows and hoses. Since these elements reduce the system reliability, optimization of the number of flexible elements was carried out. A system of supports for the pipelines was developed. The system includes fixed pedestals, slide and spring supports and suspension systems. By the results of the preliminary calculations of the cryogenic lines and optimization of the heat inflows, additional heat intercepts, including control valves, were installed on the 2K line for reduction of the load on the line.

Fig. 5.10.3. presents the trim assembly of the most complex and bulk distribution box XLVB, which controls the flows of cryogenic liquids and gases in the injectors and the linear accelerator (length of 1.7 km) of the XFEL.
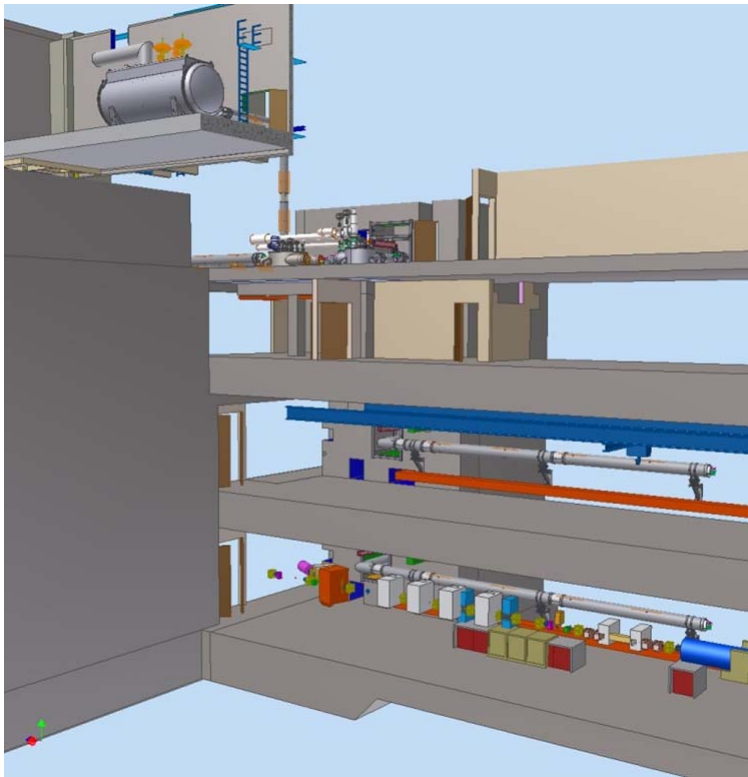
- second level. Distribution box of linac.

- 4th and 5th levels. XIVB and XI1FB distribution boxes and pipelines XLTL, XI1TL, XI2TL.

- 6th level. Second injector pipeline XI2TL.

- 7th level. Equipment of first injector.

Fig. 5.10.1. Cryogenic equipment for linac and injector of XFEL.
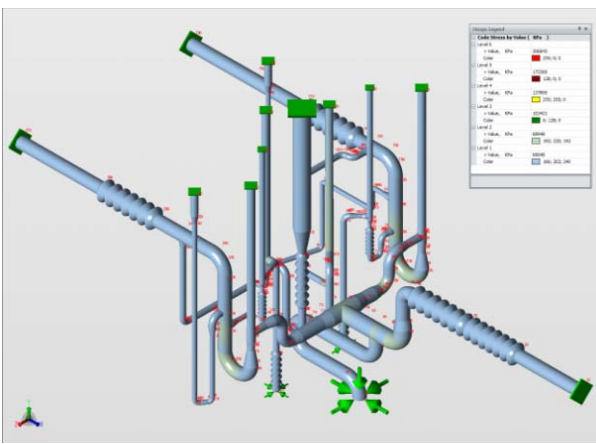
Fig. 5.10.2. Example of calculation of mechanical strength of 5K line of XIVB distribution box of injector.

Fig. 5.10.3 Mounting of cold mass of distribution box XLVB in casing. Casing diameter: 2.5m. Casing length: over 7m. Total weight: about 20 tons.

The equipment has passed acceptance tests at BINP (Fig. 5.10.4). The results of all the tests are in compliance with high requirements to the cryogenic equipment of the XFEL. Results of the tests for leaks, pressures, and leaks in the valve seat seal and the integral test with the design pressure are much better than the specified values.

Fig.5.10.4. Acceptance tests at BINP carried out by DESY experts.

The equipment was delivered to the XFEL site. The mounting started in 2014 (Fig. 5.10.5 and 5.10.6.). The completion of the mounting of the equipment and commissioning are planned on 2015.

Fig. 5.10.5. Mounting of cryogenic equipment in hall of injector 1.

Fig. 5.10.6. Mounting of pipeline in shaft of XFEL building.

6

SYNCHROTRON AND TERAHERZ RADIATION,
FREE ELECTRON LASER

6.1. INTRODUCTION

The shared-equipment Siberian Center for Synchrotron and Terahertz radiation (SCSTR) started its work at Budker Institute of Nuclear Physics almost 40 years ago. Works at the center have two directions: with synchrotron and terahertz radiation.

The "Synchrotron radiation (SR)" direction includes works on the VEPP-3 and VEPP-4 storage rings and development and creation of SR generation systems for Russian and foreign SR centers.

Works with terahertz radiation are conducted at the Novosibirsk free electron laser (FEL).

Besides, the center in engaged in educational and training programs for students and post-graduates.

In 2014, there were allocated 962 hours for work on SR beams from the VEPP-3 storage ring (2075 hours in 2013) and 630 hours on beams from VEPP-4 (348 hours in 2013). The experiments involved 10 stations on 7 SR extraction beamlines on VEPP-3 and 3 SR stations on beamlines from VEPP-4. In 2014, the Novosibirsk FEL worked for users for about 1000 hours, the same as in 2013.

6.2. WORK ON SR BEAMS FROM VEPP-3

6.2.1. Station "Experimental state of matter".

The station is intended for analysis of fast explosive and shock-wave processes. The station is equipped with an explosion chamber and a system with detector DIMEX for detection of passed SR and small-angle X-ray scattering (SAXS) of SR.

Participating organizations:
- Institute of Hydrodynamics SB RAS,
- Russian Federal Nuclear Center "All-Russian Research Institute of Experimental Physics (VNIIEF), Sarov,
- Russian Federal Nuclear Center "All-Russian Research Institute of Technical Physics (VNIITF, Snezhinsk,
- Institute of Solid State Chemistry and Mechanochemistry SB RAS, and
- Budker Institute of Nuclear Physics SB RAS.

In 2014, works at the station were carried out under the research plans of the participating institutions and had financial support from the following projects and contracts:
- RFBR project 14-03-00770, Diffraction measurements in detonation processes (2014-2016);
- Agreement 6/2014 between LIH SB RAS and VNIITF (Snezhinsk) "SR research to clarify equations of state of high explosives and explosion products " (2014).
- Agreement 4/2014 between LIH SB RAS and VNIEF (Sarov) "SR research on properties of high explosives materials " (2014).

Below are given examples of work in 2014.

1. Measurement of distribution of gas-dynamic parameters in detonation of PTO charge (mixture of plasticized TATB with octogene)

For measurement of passed radiation, the detonating charge was probed in two directions: in the beam plane and perpendicular to it. After calibration of the detector, from the measured passed radiation one can obtain data on the dynamics of mass distribution in a line along the charge and in a fixed cross section. In the first case, it is possible to accurately determine the coordinates of the front and the velocity of detonation. In the second case, the measurement results are initial data for tomography tasks on reconstruction of internal flow parameters.

Despite the high intensity of direct SR beam, immediate application of absorption data does not result at once in the desired density of explosion products, because tomography tasks impose strict requirements on the accuracy of experimental data. This problem can be solved via development of specialized density reconstruction techniques based on regularization of the desired solution on density distribution and with intense use of *a priori* information on the structure of flow under study. An original method was developed for reconstruction of gas-dynamic parameters of detonation flows from X-ray experiment data. Although the method was adapted to a specific task, it allows significant improvement in the accuracy of density reconstruction and determination of the other gas-dynamic characteristics, i.e. the mass flowrate and pressure distribution.

Below are presented the measurement results for PTO and BTF charges.
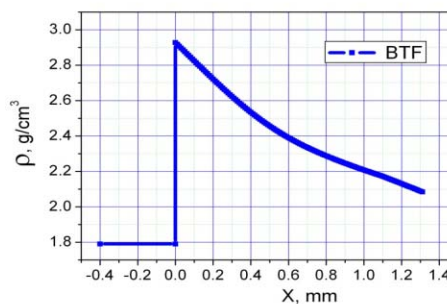
Fig. 6.2.1. Density distribution on BTF detonation front.
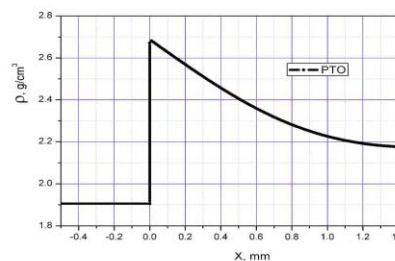
Fig. 6.2.2. Density distribution on PTO detonation front.
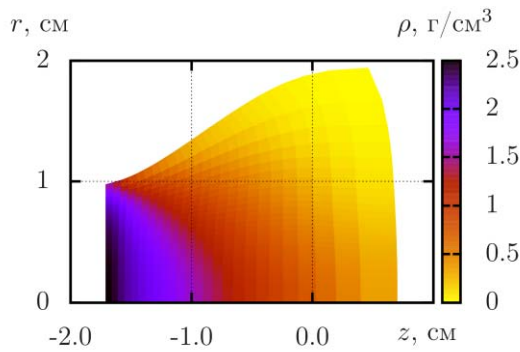
Fig. 6.2.3. Density distribution behind PTO detonation front.
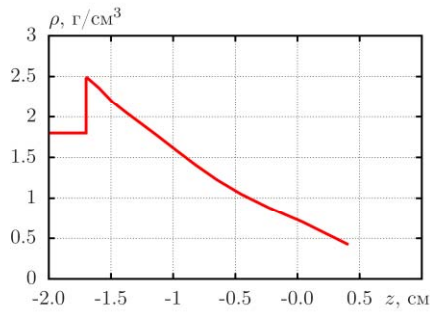
Fig. 6.2.4. Density distribution along detonation axis.
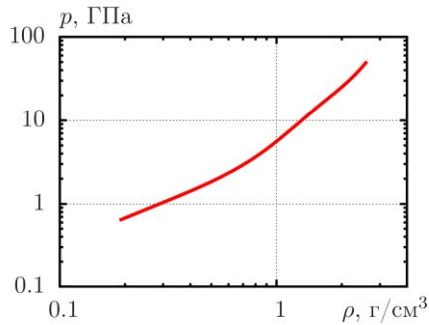
Fig. 6.2.5. Pressure vs. density behind BTF detonation front.
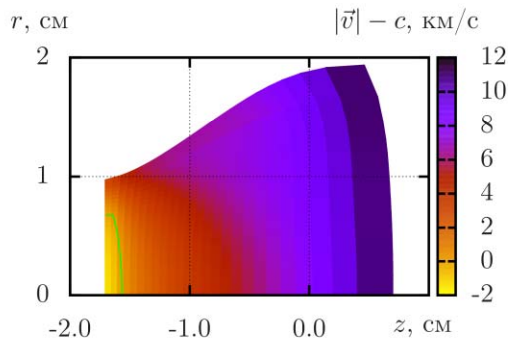
Fig. 6.2.6. Acoustic border in detonation of cylindrical BTF charge 2 microseconds after initiation.
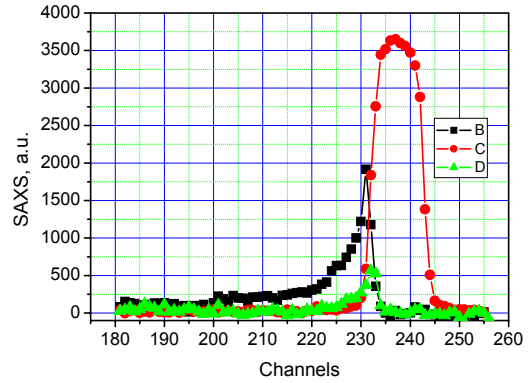
Fig. 6.2.7. Positions of blades before SAXS detection. The X axis shows the height in the detector channels. C: direct beam; B: SAXS signal from hoax; D: SAXS signal subject to absorption in charge of 20 mm in diameter.
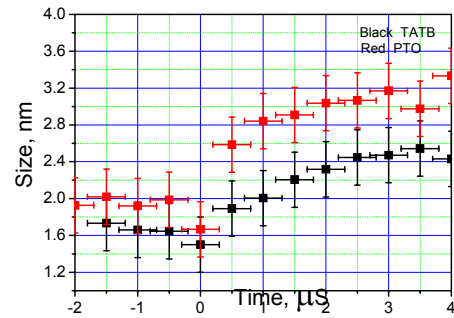
Fig. 6.2.8. Dynamics of average size of condensed carbon nanoparticles in detonation of TATB (dots at the chart bottom) and PTO (dots at the chart top).

The works at the station in 2014 resulted in publication of 2 articles in journals and proceedings of conferences and 22 talks made at international conferences.

6.2.2. Station "LIGA technology and X-ray lithography".

The station is intended for experiments on X-ray lithography in thick resistive layers for fabrication of microstructures, including X-ray masks.

Participating organizations:

● Budker Institute of Nuclear Physics SB RAS, Novosibirsk;

● Institute of Cytology and Genetics SB RAS, Novosibirsk;

● Institute of Solid State Chemistry and Mechano - chemistry SB RAS;

● Institute of Automation and Electrometry SB RAS;

● Vorozhtsov Institute of Organic Chemistry SB RAS;

● Institute for Automation and Control FEB RAS.

In 2014, works at the station were carried out under the research plans of the participating institutions and had financial support of the following projects and contracts:

Below are given examples of work in 2014.

In 2014, the activity at the LIGA station on the VEPP-3 storage ring was aimed mainly at the development of manufacturing of X-ray masks for subsequent production of high-aspect microstructures for applied research (biochips and diffraction gratings). BIn this regard, methods of creating intermediate templates (for X-ray lithography in the soft range) and working patterns for the hard SR spectrum are being refined.

The first stage was devoted to production of thin membranes without X-ray absorbing layer. A sacrificial layer of salt was deposited on a glass substrate by electron beam evaporation, then a titanium layer 1-2 μm thick was deposited by magnetron sputtering. Then a ring was glued to the titanium on the substrate; the salt was dissolved and the ring with the membrane was separated.

It is assumed that an X-ray mask structure will be formed on a substrate with a titanium layer. After formation of a topology of a heavy metal, e.g. gold, the titanium layer with the structure will be separated from the substrate and used for lithographic producing of structures with linear dimensions from 2 micrometers and a height of up to 100 microns.

The earlier designed micro-beam X-ray lithographe (MBXL) was being developed for direct formation of regular structures of blanks of X-ray masks in thick x-ray resist layers. This device directly forms microstructures in deep x-ray resist layers by means of SR micro-beam vector drawing of arbitrarily given topology; no X-ray masks with topological pattern are applied. The rate of the formation of regular micro-structures (arrays of pores or lattices) was significantly increased due to implementation of multibeam parallel SR radiography.
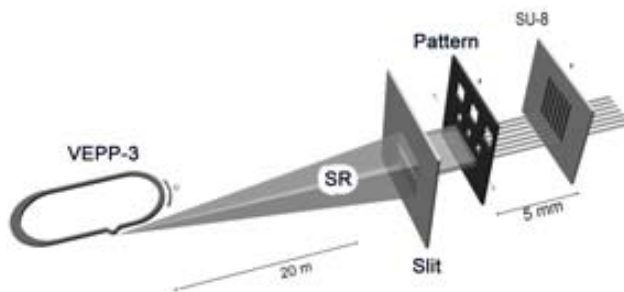
Fig. 6.2.9. Scheme of direct multibeam parallel SR radiography.

The resulting structures of SU-8 resist on carbon-glass substrate are used as blanks for X-ray mask manufacture by means of galvanoplastics of high contrast material. Electroforming processes for Au and Pb were being re-

fined for making X-ray masks for X-ray lithography manufacture of high-aspect regular structures to 1 mm deep.

Within the joint work with ICG SB RAS on the creation and study of microfluidic modules (biochips), an X-ray mask was made for X-ray lithography manufacture of microfluidic modules, and a set of sample modules with calibration channels was created. An impermeable coating was applied on the module surface and then selected calibration channels were filled with fluorescent chelate compounds for comparative calibration of the fluorescent reaction of biochemical reagents in aqueous solutions. UV illumination excites luminescence in the calibration channels. Works on the selection of the concentration of the chelates are going on.
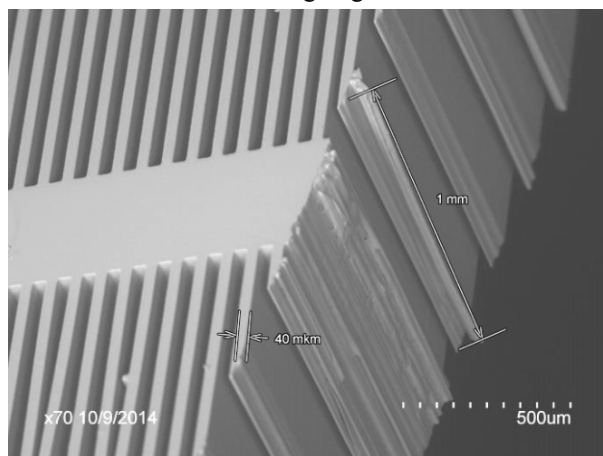
Fig. 6.2.10. Example of deep X-ray lithography with X-ray mask. 40- micron channels in PMMA sheet 1 mm thick.

6.2.3. Station "Anomalous Scattering" and "Precision diffractometry".

Below are listed works that were carried out at the station.

1. Comparative analysis of strontium ferrite samples synthesized by thermal and radiationthermal methods (Institute of Solid State Chemistry and Mechanochemistry SB RAS);
2. Analysis of stability of metal-organic framework (MOF) inclusion complexes Cr-MIL-125 and various halogens (Hal@Cr-MIL-101, Hal=Cl, Br, I) under influence of reactive medium (Institute of Catalysis SB RAS);
3. Investigation of the stability of mesostructured element-silica materials Nb-SBA-3 to the influence of reactive medium;
4. Analysis of phase composition and structure of polymer-carbon and metal-carbon nanocomposites (Institute of Catalysis SB RAS);
5. Research on structure of mixed perovskite-structure oxides (Institute of Chemistry of Solid State Chemistry and Mechanochemistry SB RAS);

6. Research on phase composition of ion-plasma-sputtered hardening coatings of titanium-nitride (Tomsk Polytechnic University);

7. Refinement of methods of structural characterization of samples based of mesostructured silicates in order to create the State Standard Samples (SSSs) of mesoporous materials (Institute of Catalysis SB RAS);

8. Analysis of changes in mayenite structure under high temperature treatment in inert atmosphere (Institute of High-Temperature Electrochemistry UB RAS).

Analysis of stability of metal-organic framework (MOF) inclusion complexes Cr-MIL-125 and various halogens (Hal@Cr-MIL-101, Hal=Cl, Br, I) under influence of reactive medium.

Metal-organic frameworks are promising mesoporous materials of interest, in particular, for catalytic applications. The catalytic activity and selectivity of inclusion compounds based on halides and mesoporous metal-organic framework Cr-MIL-101 (Hal@Cr-MIL-101, Hal = Cl, Br and I) in styrene oxide carboxylation reaction without co-catalyst have been shown earlier. From XFA data, the structure of MIL-101 does not undergo significant changes when impregnated with sodium halides. However, from capillary electrophoresis data, after a catalytic reaction at elevated temperature (50-80° C) the halides are washed out from the solid matrix to the solution, which hampers reuse of the catalysts. Thus, to create stable-in-reaction catalysts it is necessary to develop a method to couple halides to the Cr-MIL-101 matrix with preservation of the structure of the MIL-101 matrix and rise of sufficiently strong connection between the halide and the solid matrix, this connection not destroyed during the catalytic reaction. The preservation of the MIL-101 structure under modification with halides was checked using the XFA method.

Radiographs of samples differing in the way of bromide coupling (with additional ligand, via the amino group of the matrix, etc) were recorded. It was shown that in two of four cases of Br⁻ coupling the MIL-101 structure was partially destroyed (Fig. 6.2.11). In the other cases the destruction was complete.
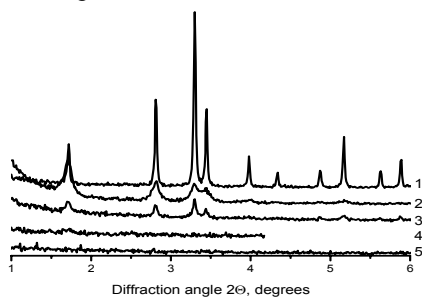
Fig.6.2.11. Radiographs of MIL-101 organometallic framework. Initial sample (1) and samples after Br⁻ coupling in various ways (2-5).

Analysis of changes in mayenite structure under high temperature treatment in inert medium.

The structure of mixed calcium-aluminum oxide $(Ca_{12}Al_{14}O_{32})O$ is shown in Fig. 6.2.11. (a). The compound includes superlattice oxygen, which can provide oxygen transport, which enables use of the material as an oxygen conductor. According to the literature, the material has a cubic structure, whereas radiographs recorded at the station "Anomalous scattering" demonstrate split of the reflections (Fig. 6.2.12. (b)). That can be because the sample has two phases of the same structure, but slightly different lattice parameters. This difference in the two phases may be caused by the different oxygen stoichiometry, appearing at the stage of synthesis of the sample. For determination of the effect of the oxygen content on the lattice parameter of mayenite, the sample was calcined first in an oxidizing medium, and then in an inert environment at a temperature of 800° C.

a

b
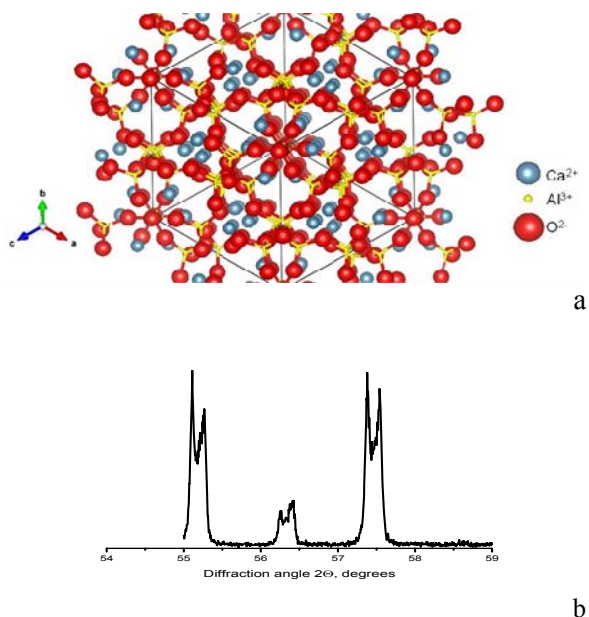
Fig. 6.2.12. Mayenite structure (up) and split reflections in radiographs (down).

Calcination in different media leads to a slight decrease in the intensity and displacement of one reflections in each pair towards larger angles (Fig. 6.2.13), whereas the second reflection changes neither its position nor its intensity. Perhaps this behavior of reflections in the radiographs is caused by a change in the parameters of one of the two phases in the sample, this change being associated with variation of its oxygen stehiometry. Since the synthesis of mayenite occurs at higher temperatures, the link between the changes in the radiographs and oxygen composition of the sample can be clearly determined only under more severe temperature conditions of experiment.
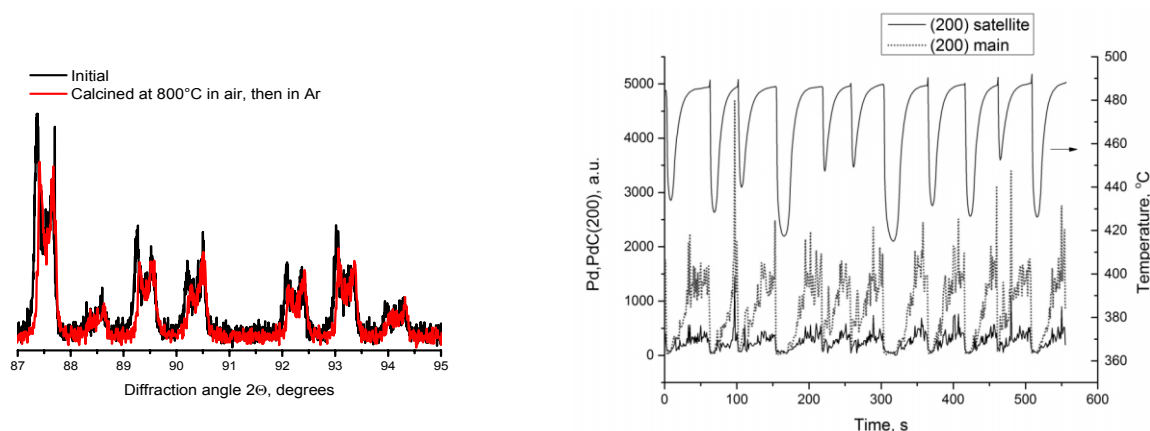
Fig. 6.2.13. Fragments of radiographs of initial mayenit sample and sample after calcination in oxidizing and inert atmosphere.

Below are listed works performed at the station "Precision diffractometry".

1.	Regeneration of catalytic systems "cobalt oxide – nitrogen-containing carbon nanofibers» (Co_3O_4/N-УНВ) in hydrogen stream at temperatures of 25 to 700 °C;

2.	Regeneration of catalytic systems with Ni and Mo oxides applied on SiO_2 in hydrogen stream at temperatures of 25 to 700 °C;

3.	Auto-oscillations in reaction of methane oxidation on palladium in various conditions (partial pressure, temperature, and relative content of reactants);

4.	Investigation into synthesis of catalyst systems (Cu, Ni and Cu, and Ni deposited on SiO_2) in reducing-atmosphere heating of acetate precursors produced by co-precipitation of metal salt solutions with supercritical CO_2;

5.	Comparative analysis of thermal and radiation-thermal method of synthesis of strontium ferrite;

6.	Investigation into structural and phase changes in polymer-carbon nanocomposites near melting point of the polymer;

7.	Investigation into thermal stability of titanium nitride coatings doped with Cu, Al, and Si in heating in air;

8.	Hydrogen-stream reduction of mixed oxides $CuNiMoO_x$, 0, 5, 10% Mo, precursors of catalysts for hydro-refining of pyrolysis of wood products ("bio-oil");

9.	Study of influence of Al^{3+} cations on reduction of metals from mixed Co-Al oxides in model catalyst systems.

***in situ* X-ray diffraction research on self-oscillations in methane oxidation on palladium.** Experiments were carried out on the *in situ* X-ray diffraction study of self-oscillations in oxidation of methane on palladium. During the experiments, the gas mixture composition was checked at the inlet (gas flow regulators Smart-Trak 50 (Sierra)) and output (mass spectrometer SRS UGA-100) of high-temperature X-ray reactor chamber XRK-900 (Anton Paar).

b
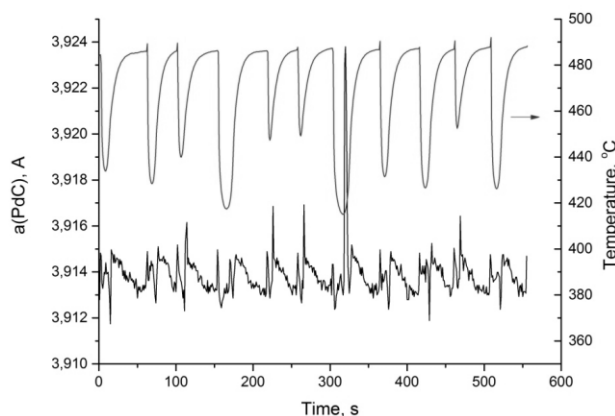
Fig. 6.2.14.. Change in (a) intensity of Pd (200) and PdC (200) reflections; (b) PdC lattice parameter vs time during self-oscillations. Wavelength: 1.72 Å; ratio of CH_4:O_2:Ar reactants: 40:10:50 ml/min; gas mixture temperature: 366 °C. Right scale: palladium foil temperature vs. time.

The *in situ* X-ray diffraction method has shown that the phase content of the palladium foil surface changes periodically in self-oscillations, which is accompanied by a change in the temperature of the catalyst. The radiographs taken during the reaction demonstrate reflections of phases of metallic palladium and palladium oxide PdO, as well as a reflection presumably attributable to palladium carbide PdC. It has been established that in a state of high activity (high temperature of the catalyst and high methane conversion rate) palladium is in the metallic state. Transition to a low activity state is accompanied by sharp fall of the intensity of the palladium reflections (Fig. 6.2.14). It should also be noted that the PdC phase lattice parameter decreases vs. temperature, which is probably because of the carbon escape from the lattice. Analysis of the gas mixture leaving the reactor shows that the main route of the reaction is complete oxidation of methane to CO_2 and H_2O (practically no traces of partial methane oxidation to CO and H_2 were observed). Thus, the study

conducted has shown that self-oscillations in the reaction of catalystic methane oxidation on palladium are defined by periodic oxidation/reduction of palladium.

10. Investigation into synthesis of catalyst systems (Cu, Ni and Cu, and Ni deposited on SiO$_2$) in reducing-atmosphere heating of acetate precursors produced by co-precipitation of metal salt solutions with supercritical CO$_2$.

At present, many researchers investigate the use of supercritical fluids (SCFs) for synthesis of functional materials. So, creation of materials of certain structure, morphology, and set properties includes a rapidly developing direction of using supercritical CO$_2$ (SC CO$_2$) as a supercritical anti-solvent (SAS). The essence of the SAS technique consists in the following: a flow of metal salt solution is inlet through a nozzle in a current of SC CO$_2$. Rapid diffusion of SCF in certain regimes can lead to surge supersaturation of the solution and precipitation of X-ray amorphous disperse sediment.

In this work, Ni$_{88}$Cu$_{12}$ and Ni$_{88}$Cu$_{12}$/SiO$_2$ systems synthesized using the SAS technique were examined.

According to *in situ* X-ray diffraction studies, acetate precursors turned out to be X-ray amorphous phases, which degraded to high-dispersion oxides when reduced in a hydrogen stream and then were reduced to the metals (Fig. 6.2.15). Addition of SiO$_2$ in the system resulted in formation of oxide and then metallic particles smaller than those without the silicate (which was also confirmed by the methods of scanning and transmission electron microscopy), as well as in formation of solid solution of the metals, unlike the Ni$_{88}$Cu$_{12}$ sample.

The research resulted in a method of production of X-ray amorphous precursors of catalytic systems. The *in situ* XFA method has shown that the use of acetate precursors enables synthesis of mixed oxide systems with different degrees of oxidation of metals depending on the atmosphere and the thermal decomposition temperature; varying the SiO$_2$ concentrations, one can regulate the dispersion of both the oxide and metal phases.
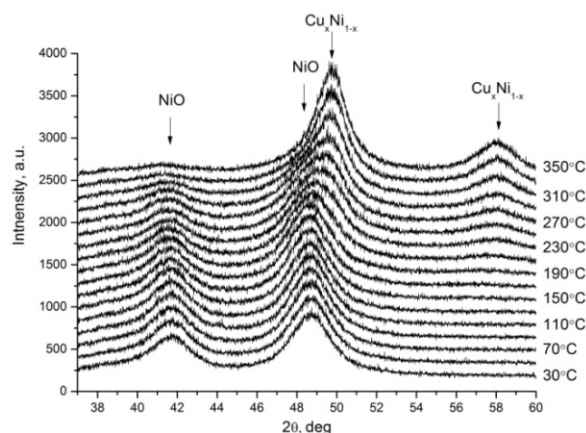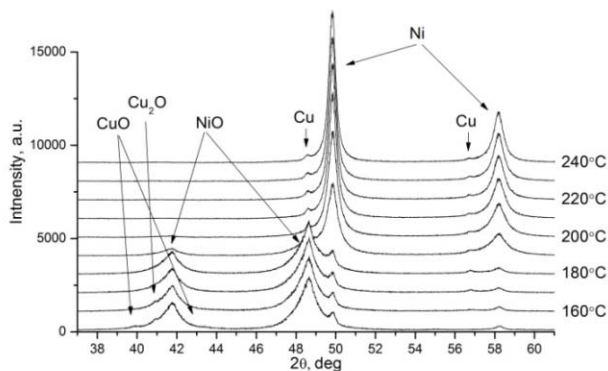
Fig. 6.2.15. *in situ* XFA study of reduction of samples of (a) Ni$_{88}$Cu$_{12}$ and (b) Ni$_{88}$Cu$_{12}$/SiO$_2$ in hydrogen flow produced by SAS method at wavelength of 1.72 Å.

11. Study of influence of Al^{3+} cations on reduction of metals from mixed Co-Al oxides in model catalyst systems.

The Fischer-Tropsch synthesis is a reaction of formation of hydrocarbons from the synthesis gas (a mixture of CO and H2) in the presence of catalysts, particularly cobalt ones. Industrial cobalt catalysts are metal nanoparticles applied on various carriers, e.g. γ-Al$_2$O$_3$. Preparation of catalysts is a lengthy process, comprising the steps of activation of a precursor and reduction in a hydrogen flow at temperatures of ~ 400-600 °C. Reduction of industrial catalysts and model systems (lump samples of Co$_3$O4) proceeds in a different way. Lump Co$_3$O$_4$ is reduced in a single step to metallic hcp Co, whereas the reduction of applied Co$_3$O$_4$/ -Al$_2$O$_3$ samples occurs in two stages, through formation of crystalline CoO to metallic fcc cobalt. One possible factor accounting for this difference is the presence of aluminum ions, which can modify the applied cobalt oxide catalyst at the calcination step and/or during the reduction phase.

A number of samples of Co$_{3-x}$Al$_x$O$_4$ $(0.05 \leq x \leq 1)$ produced by coprecipitation of Co^{2+} and Al^{3+} from solutions of nitrates and subsequent calcination at 500 °C were investigated. The samples were reduced in flow of hydrogen (15 ml/min) with heating with a rate of 10 °C/min. During the reduction, radiographs were recorded *in situ* with an exposure time of 1 min/frame.

Co$_3$O$_4$* and CoO* phases, which differ from the regular Co$_3$O$_4$ and CoO phases, were identified, because the system contains Al and a Co phase with microdomain structure. The phases were consistently appearing in the reduction processes. Radiographs for all samples enabled retrieval of information on the temperature interval of existence of the phases arising during the reduction. With increase in the amount of aluminum, which dopes cobalt oxide, the reduction of the Co$_3$O$_4$ and CoO phases slows down. A slowdown in the appearance of metallic Co is observed when the concentration of aluminum in the system increases. Besides that, for samples with high aluminum content, phase discontinuity is observed, i.e. there is

a temperature range in which the samples contain only CoO, which is consistent with other measurements. Additionally, for samples with high concentration of aluminum, starting from Al:Co = 1:29, the micro-domain structure becomes stabilized – hexagonal Co does not vanish up to temperatures of 745 °C (Fig. 6.2.16).
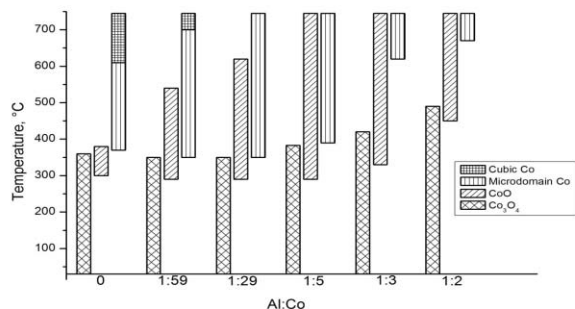
Fig. 6.2.16. Phase composition of model Co-Al systems vs. aluminum content in temperature range of 30 to 735 °C.

6.2.4. Station "X-ray fluorescence analysis".

The station is intended for determination of the elemental composition of samples of different origin –geological rocks, biological tissues, aerosols, etc. – by X-ray fluorescence elemental analysis using synchrotron radiation (SR XFA). The elemental analysis can be implemented both in a local and a scanning mode.

Participating organizations:
- Vinogradov Institute of Geochemistry SB RAS, Irkutsk,
- Budker Institute of Nuclear Physics, SB RAS, Novosibirsk.

In 2014, the works carried out at the stations had financial support of the following projects:
- SB RAS Basic Research Program for 2013 - 2016 Research project V.46.5: "Research on physicochemical processes in formation, distribution, transformation, and migration of dispersed substances in environmental medium",
- RFBR 13-05-90780 mol_rf_nr "Validation of methods of measurement of plant material by X-ray fluorescence analysis with synchrotron radiation."

Below are presented examples of works in 2014.

Changes in natural habitat of lake ecosystems of East Siberia in the Holocene according to X-ray fluorescence analysis using synchrotron radiation

The aim of the project was the reconstruction of the regularities and characteristics of regional ecosystems under the influence of climate changes in the Holocene. The main objectives were to obtain high-resolution sedimentary records from core samples of bottom and peat sediments in small lakes and lake-marsh systems and to perform comprehensive analysis of the data obtained. SR XFA spectra of the samples of bottom and peat sediments

were recorded at the Siberian Center for Synchrotron and Terahertz Radiation (SCSTR). Fig. 6.2.17 presents an example of graphs of Ca, Br and Sr distribution across the depth of core of Lake Arakhley sediments (core BAI 3-B).

It is known that Ca, Br, Sr, as well as some of their ratios, can be geochemical indicators of changes in depositional environment. Changes in the Br content in the bottom sediments of Lake Arakhley may be associated with organic matter and reflect fluctuations in the productivity in the lake basin. The Ca content may be an indicator of a change in the intensity of mineralization in the lake. The Sr distribution and its content in the bottom sediments may be used for assessment of changes in the aridity of the climate.

The revealed changes in the elemental composition of the bottom and lake-marsh sediments will be interpreted in terms of changes in the climatic conditions in the past.
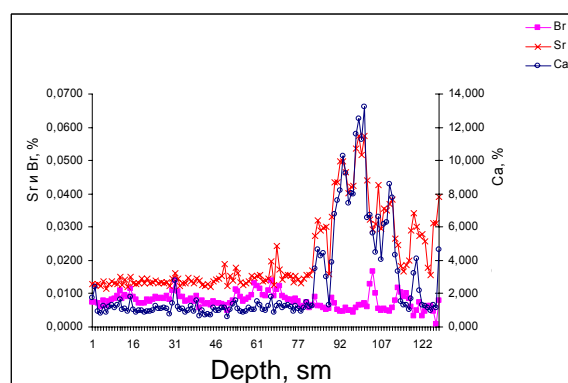
Fig. 6.2.17. Distribution of Ca, Sr, and Br in bottom sediments of Lake Arakhley.

6.2.5. Station "Hard X-ray diffractometry".

The station is intended for diffraction study of polycrystalline materials at high pressures and temperatures in a cell with diamond anvils using hard X-rays.

Participating organizations:
- Institute of Solid State Chemistry and Mechanochemistry SB RAS;
- Institute of Geology and Mineralogy SB RAS;
- Budker Institute of Nuclear Physics SB RAS;
- Institute of Catalysis SB RAS;
- Institute of Metal Physics UB RAS.

In 2014, works on the station were supported by the following projects and contracts:
- RFBR project 12-05-00841-a "Conditions for stability of hydrocarbon compounds at high pressures and temperatures and their implications for deep structure of the Earth and the planets", 2012-2014;
- RFBR project 13-05-00185-a, " Mechanisms of formation and stability of water-containing high-baric silicates of the MgO-SiO2-H2O system under conditions of subduction of the oceanic lithosphere" 2013-2015;

- RFBR project 13-05-00457-a "Microporous aluminosilicates at high pressure: the influence of framework topology and extra-framework subsystem composition on the compressibility and structural transformations" 2013-2015;

- RFBR project 14-05-00616-a «In situ КР исследование взаимодействия силикатов с водной средой при субдукционных Р-Т параметрах», 2014-2016 гг.; In situ Raman study of interaction of silicates with aqueous medium at subduction P-T parameters", 2014-2016.

Below are given examples of works in 2014.

Research on the baric stability of polycyclic hydrocarbon in connection with modeling of depth fluids.

Research on the stability of hydrocarbon co-compounds, such as PAHs, at high pressures was caused by their presence in depth-origin natural objects (inclusions in diamonds) and the necessity of modeling of the composition of reduced C-O-H fluid, which is essential in processes of mantle material melting. Compressibility of coronene $C_{24}H_{12}$ at a pressure of up to 6 GPa has been studied. At 0.9 GPa a high-pressure phase with space group $P2/m$ was detected; parameters of its compressibility to 4 GPa were determined: $K_0 = 6.5(3)$ GPa; $K_0' = 13.4(3)$. The calculated values correlate well with the parameters of compressibility of naphthalene and anthracene and are in poor agreement with earlier data on the compressibility of the coronene. Partial amorphization of the coronene was observed at 5.9 GPa. Upon decompression of the cell to the atmospheric pressure, the high-pressure phase was preserved, which may also be associated with its partial amorphization.
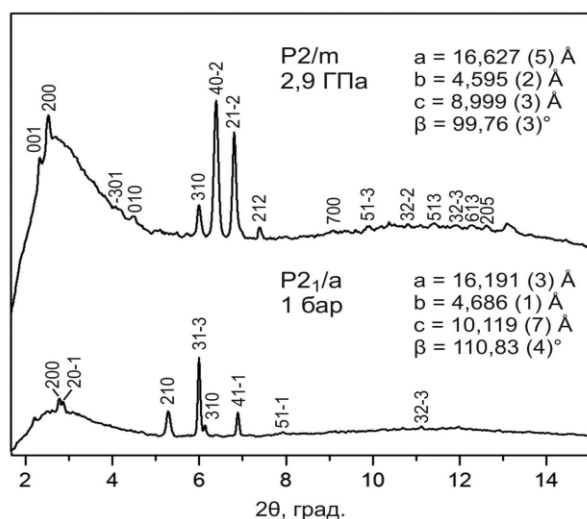
Fig. 6.2.18. Diffraction profiles of coronene at 1 bar and 2.9 GPa (298 K).

Research on formation of high-pressure magnesium silicates (10 Å phase) under P-T conditions simulating "cold" subduction environment (40 kbar, 450 °C) in resistive-heating diamond anvil.

The problem of global recycling of H_2O has caused interest in water-containing magnesium silicates of the $MgO–SiO_2–H_2O$ system as potential carriers of water into the mantle as part of the subducing oceanic lithosphere. For clarification of the structure of the equilibrium 10 Å phase (TAP) of $Mg_3Si_4O_{10} \cdot xH_2O$ and evaluation of water content in it, a diffraction experiment was carried out on hydration of talc at 40 kbar and 450 °C (Fig. 6.2.19).

The reaction products contain 90% of TAP, talc and talc-like aqueous phase. From the clarification of the TAP structure (Fig. 6.2.20.), the water content was estimated to be 1 molecule per formula unit; with the undersaturation of the system with water (the presence of talc), this is the lower limit of the equilibrium water content in TAP. The TAP lattice parameters at 40 kbar and 450 °C are as follows: $a = 5.225(4)$, $b = 9.054(3)$, $c = 10.86(4)$ Å, $\beta = 98.6(1)°$, $V = 508.0(1)$ Å3 (space group $C2/m$). Diffraction and spectroscopic data on quenched sample indicate that a disordered anhydrous phase forms under normal conditions. The observed instability of the TAP phase can confirm the hypothesis about phase stabilization during prolonged synthesis because of formation of defective silanol groups.
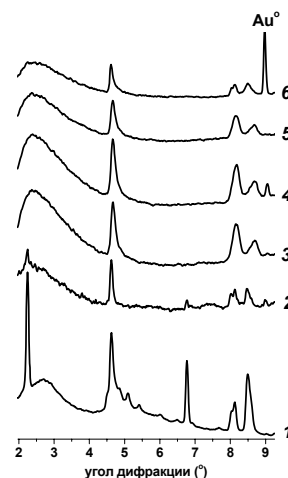
Fig. 6.2.19. Diffractograms of initial talc under normal conditions (1-2), of products of talc hydration 9 hours (3), 14 hours (4) and 19 hours (5) in mode of 40 kb and 450 °C; (6): diffraction pattern of unloaded sample 5 months after synthesis.
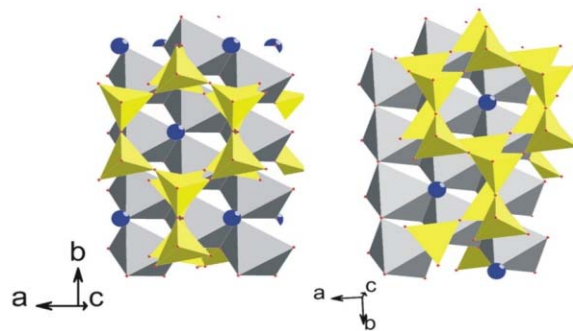
Fig. 6.2.20. Structure of TAP phase (left, according to our data for 40 kbar abd 450 °C) and talc phase with interlayer "defective" positions of H_2O (right, according to Gatta, 2013).

Structural behavior of microporous alumino-silicates (Rb, Cs natrolite and sodalite) under high water pressure: role of mobile interstitial molecular components (H_2O)

The over-hydration effect caused by compression of porous compound in penetrating medium was first found on zeolite natrolite $Na_2[Al_2Si_3O_{10}] \cdot 2H_2O$ [Belitsky 1992]. For clarification of the role of extra-framework cations and in-framework ordering of Si and Al in the structural behavior of natrolite zeolites in over-hydration, the behavior of Rb and Cs natrolite under compression up to 4 GPa in penetrating (water-containing) medium was studied. In room conditions, both forms are anhydrous. Their structures (Fig. 6.2.21) are similar and close to the structure of dehydrated natrolite. The absence of H_2O molecules in the structure of the forms studied determines their substantial compression as compared with hydrated forms.

Behavior of the Cs and Rb forms under compression in water is also similar. Both forms stay anhydrous and demonstrate regular compression throughout the investigated pressure range (Fig.6.2.22). The structural changes come to decrease in the T-O-T angles in the framework and in the lengths of the cation-O-atom bonds. The literature describes hydrated forms of Rb and Cs natrolite stable under normal conditions (Lee et al., 2010). As for the forms we studied, besides the fact that they anhydrous under normal conditions, they remain such even compressed in water. The reasons for such striking differences probably can be found in the differences in the original forms of the natrolite, primarily in the degree of ordering of Si and Al in the framework.
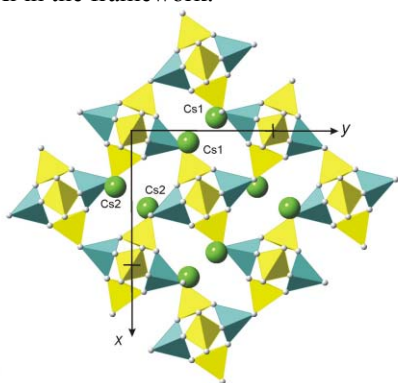
Fig. 6.2.21. Structure of Cs-substituted natrolite under normal conditions in projection along c axis.
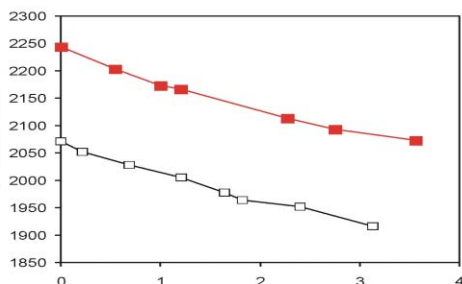
Fig. 6.2.22. Unit cell volume in Rb (□) and Cs (■) forms of natrolite vs. pressure in compression in water.

For research on the features of overhydration in microporous compounds with sodalite framework, the compressibility to 5 GPa of synthetic hydroxy-sodalite $Na_8[AlSiO_4]_6 \cdot (OH)_2 \cdot 4H_2O$ in penetrating (aqueous) and non-penetrating (methanol-ethanol) media was studied. The bulk modulus in compression in spirits is 36(5) GPa. With $P > 0.5$ GPa the compressibility in aqueous medium increases gradually relative to compression in non-penetrating medium; a maximum difference in the unit cell volume of 2% is reached at 2.5 GPa (Fig.6.2.23). Such a difference in the volume was observed for hydroxyl-sodalite and aqueous sodalite with maximum filling of the water tetrahedral sites (8 H_2O molecules per unit cell). Thus, the observed difference between the compressibility curves can be interpreted as additional compression of the sodalite structure under the influence of strong hydrogen bonds between the H_2O molecules and the framework that arise when tetrahedral water sites close to the framework get occupied. Apparently, not only the increase in the population of the Ow sites plays an important role here, but the disappearance of strong bonds with the OH groups in the center of the cages (Oc) also does.
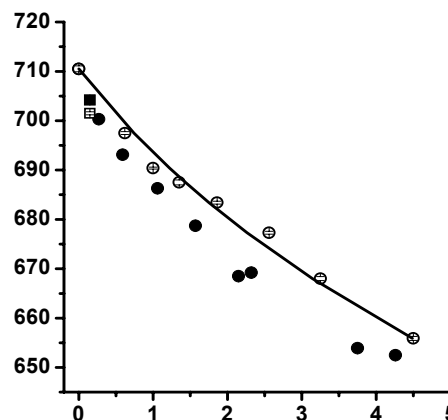
Fig. 6.2.23. Pressure dependence of volume of hydroxyl sodalite cubic cell (*P*-43*n*) in compression up to 5 GPa in aqueous medium and in spirits. Solid line: fit of Birch-Murnaghan equation.

Compressibility and phase transitions of potassium carbonate at pressures of up to 30 kbar.

Geological interest in the high-pressure behavior of potassium carbonate is associated with its participation in the mantle processes of partial melting, metasomatism and diamond genesis. Information about its polymorphic modifications can also be used in determination of the structures of molten alkali carbonates, which may be widely used in power supplies in future. Calculations predict a polymorphic transformation of K_2CO_3 at 8.6 - 27.5 kbar to a phase isostructural with β-Na_2CO_3. For check of this theoretical prediction, the K_2CO_3 diffraction pattern was recorded in a pressure range of 1 to 30 kbar.

At 23.3 to 31 kbar γ-K2CO3 is transformed to a high-pressure phase K_2CO_3-II. The significant rearrangement

of the diffraction pattern (Fig.6.2.24) and amorphization of the sample during decompression allow one to classify this transition as a reconstructive transition of type I. The experimental diffractogram of K_2CO_3-II does not correspond to the theoretically predicted phase (i.e. the phase K_2CO_3-II is not isostructural with β-Na_2CO_3); the closest is the diffraction pattern of Li_2CO_3. More precise determination of the atomic coordinates by the Rietveld method shows structural changes in γ-K2CO3 in the range of 7.6 to 15 kb, presumably related to a distortion polymorphic transition (with a change in the mutual arrangement of the coordination polyhedrons).
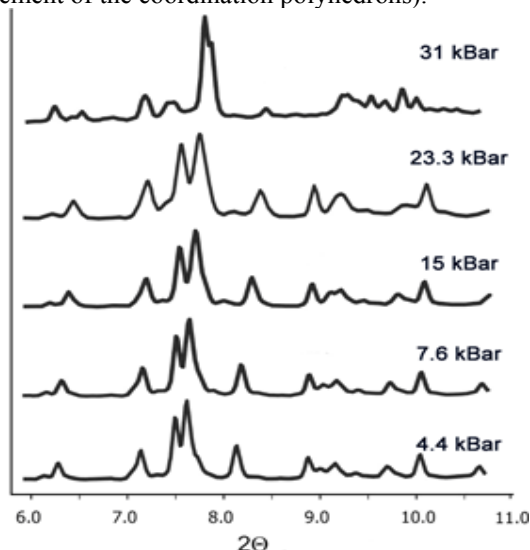
Fig. 6.2.24. Change in diffraction pattern of K_2CO_3 with pressure increasing up to 31 kbar.

***In situ* synchrotron radiation X-ray diffraction study of phase formation staging in cobalt - indium system.**

Chemical interaction between metals in solid and liquid states occurs in a number of important processes: soldering, welding, sintering of powders, etc. There is no predictive theory for processes of such interaction so far. Different processes occur at the interface between the solid and liquid phases: diffusion, dissolution, adhesion etc. The rates of these processes will determine the general course of the processes, and knowledge of their directions will help in the development of theory of interaction between metals in the liquid and solid states.

Interaction in the cobalt-indium system was studied at different temperatures and various heating modes. Diffraction research showed the interaction of indium and cobalt at temperature below the melting point of indium to result in formation of intermetallic compounds $CoIn_3$ and $CoIn2_2$, crystallites of intermetallic phases being extremely small. This indicates a high rate of diffusion of indium in cobalt.

Rapid heating to temperature above the melting point of indium results in the interaction of liquid indium with intermetallic compound $CoIn_3$, formed as a result of diffusion. The intermetallic $CoIn_3$ and cobalt turn into a liquid phase. From the diffraction patterns one can see that

reflections from $CoIn_3$ do not form continuous rings, i.e. $CoIn_3$ crystallite are much larger than $CoIn_2$ crystallites and originated from a liquid phase. Accumulation of experimental data enabled development of an approach to a theory of physicochemical interactions in various systems of solid metal-molten metal.

Chemical interaction of substances in solid and liquid states can occur in two directions. If the rate of diffusion of the solvent in the solid component is greater than the rate of dissolution of the solid-phase component in the solvent, then the reaction go via diffusion of the liquid component into the solid matrix, which results in formation in the interface of a reaction product, through which atoms of the components diffuse in the opposite directions. It is believed that the flux of atoms of the low-melt component exceeds the current of atoms of the high-melt one. The excess in the atoms leads to destruction of the crystallites of the product and lessening of their size or coherent scattering regions. In an X-ray diffraction pattern, diffraction rings from the reaction products should look even and consisting of numerous small reflections. Diffusion of the liquid-phase component in the solid phase leads to a gradient of concentrations. If the system of interacting substances contains different compounds, then, as the concentration of the liquid-phase component decreases with distance from the interface into the solid phase component, there will appear compounds most corresponding to this concentration.

If dissolution processes are faster than the diffusion ones, then compounds will originate in the liquid phase once a certain concentration is reached, at which the size of nuclei exceeds the critical size, either in the area of contact or at some distance from it. The atoms of the solid phase component will be surrounded by mostly atoms of the liquid phase component. And if the system of the interacting compounds has several substances existing at a given temperature, there will arise a compound with maximum concentration of the liquid-phase component. Since the growth of crystallites of the reaction products will occur in the liquid phase, their size can exceed the size of crystallites of the original solid phase by a factor of many times, which will be necessarily reflected in the resulting diffraction pattern. If the solid component is in excess relative to the stoichiometric one, then when the liquid phase component has been spent for the formation of the intermetallic compound with a maximum content of the liquid-phase component, the interaction stops and even a long-duration hold does not lead to formation of an intermetallic compound with a higher content of the solid phase component.

Development of methods for joint analysis of phase and elemental composition of sample.

Hard synchrotron radiation causes fluorescence emission from atoms in a sample. This enables determination of practically all elements except for the lightest (H-Al) ones from the K or L lines. If an energy dispersive detector is placed on one side of the sample (Fig. 6.2.25), it will register the fluorescent emission, while a two-

coordinate detector placed perpendicular to the primary beam will detect the diffracted emission. Thus the phase and elemental composition will be determined simultaneously on the same amount of material. This is particularly useful for study of samples of unknown initial constituent elements or if the distribution of elements in them is non-uniform, as in geological, archaeological, forensic and other samples. Fig. 6.2.26 and Fig. 6.2.27 present a diffraction pattern and spectrum of fluorescence radiation from a fragment of an item from a mound of ancient Huns. From the diffraction and spectral data it can be stated that the fragment consists of the following phases: copper, lead, and intermetallic phase Cu_3Sn. Other elements either do not form phases, included in major phases as impurities, or they form very small crystallites and their peaks merge with others in diffraction patterns.
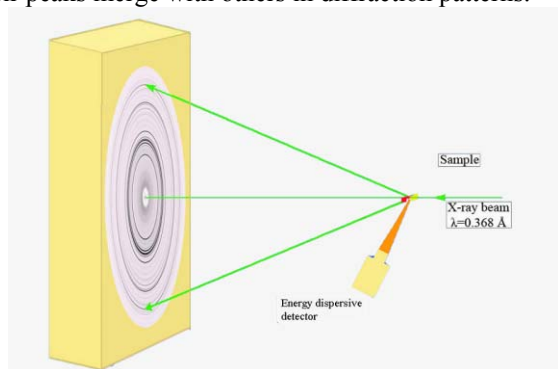
Fig. 6.2.25. Example of analysis of phase and elemental composition of sample.
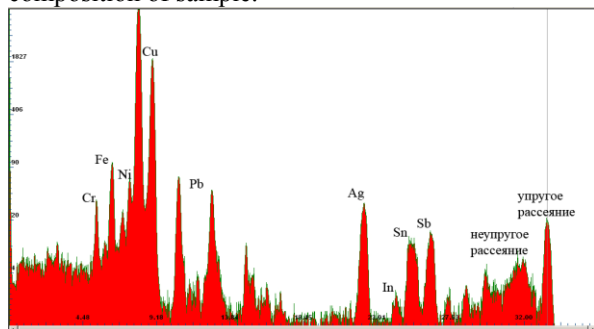
Fig. 6.2.26. Spectrum of fluorescence emission from sample.
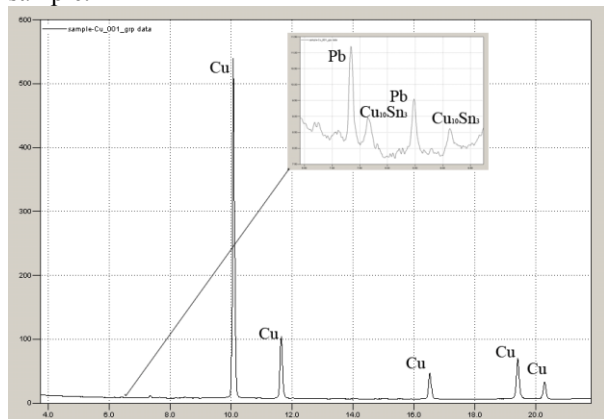
Fig. 6.2.27. Diffractogram from said sample.

6.2.6. Station "Diffraction movies".

The station is intended for time-resolved diffraction experiments, including those at small angles, and general purpose diffractometry.

Participating organizations:
- Institute of Solid State Chemistry and Mechanochemistry SB RAS;
- Budker Institute of Nuclear Physics SB RAS;

Below are presented examples of works in 2014.

Thermal decomposition of some silver carboxylates under certain conditions was found earlier to lead to formation of monodisperse metal nanoparticles of 45-50 nm in diameter and creation from them of a cubic (*Fm3m*) super-crystal with the parameter *a* about 100 A. In this regard, a task of finding similar phenomena for other metals was set. To this end, carboxylates of nickel, cobalt, and lead were synthesized. Next, the samples were heated in an oven with registration of diffractograms at 2θ angles of ~ -4 ÷ 27 degrees at a wavelength λ = 1.516 A. The data obtained showed that after 1-2 phase transitions, these compounds either melted or were degraded with melting without formation of ordered structures. There was an idea to investigate the effect of metal nanoparticles resulting from the decomposition of silver stearate (AgSt) on the decomposition of mixtures with stearates of other metals – Ni, Co, and Cu. In particular, an AgSt:NiSt 3:1 mixture was heated to 245 °C with a rate of 10 C/min. Dynamics of the diffractograms are presented in Fig. 6.2.28.

It can be seen that at a temperature of about 235 °C there forms some ordered structure, which differs from that of pure silver stearate – instead of an intense (111) peak and other peaks rapidly decreasing in intensity, which are typical to a bcc arrangement (Fig. 6.2.29, a), one can see quite a wide area of peaks comparable in intensity (Fig. 6.2.29, b).
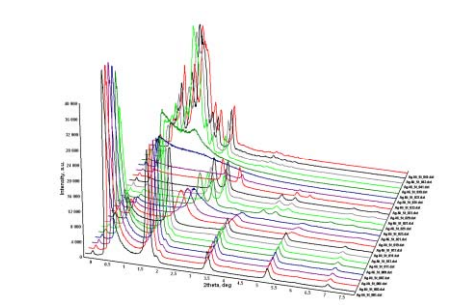
Fig. 6.2.28. Dynamics of diffraction patterns in mixture AgSt + NiSt in heating.

a)

b)
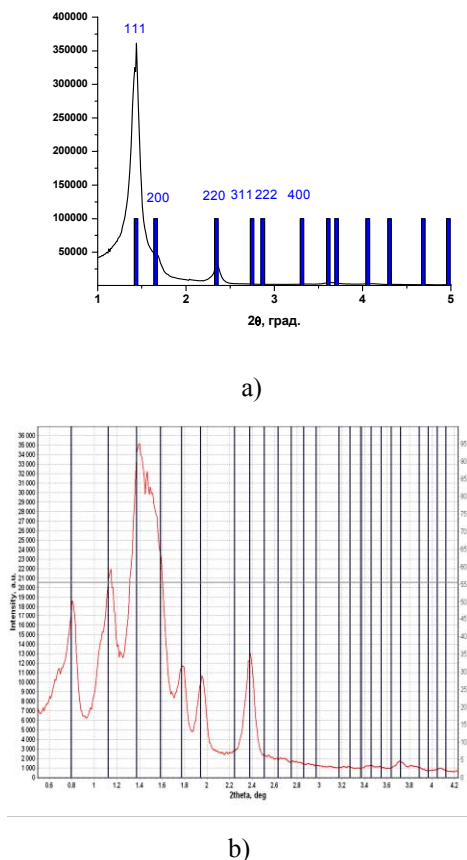
Fig. 6.2.29. Diffractograms of products of decomposition of pure AgSt (a) and mixture AgSt: NiSt (b).

Within the error, the structure can be described as a primitive cubic primitive cell with the parameter **a** ~ 109 Å (Fig. 6.2.30). Determination of the conditions of its formation and existence is underway now, as well as modeling of the calculated diffraction pattern.
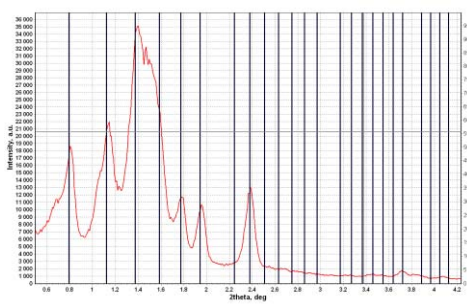
Fig. 6.2.30. Diffractogram of product of decomposition of mixture AgSt-NiSt$_2$ and line diagram of primitive cubic lattice with parameter **a** = 109 Å.

6.2.7. Station "EXAFS spectroscopy".

The station "EXAFS spectroscopy" is intended for recording of X-ray absorption spectra (EXAFS and XANES) of different (usually X-ray amorphous) samples in liquid and solid phase states. The results allow one to determine the electronic structure and parameters of the nearest local environment (coordination number and interatomic distances) of ions of interest, including samples that cannot be investigated by radiographic structural methods.

Participating organizations:

- Institute of Semiconductor Physics SB RAS (ISP);
- Institute of Inorganic Chemistry SB RAS;
- Institute of Solid State Chemistry and Mechanochemistry SB RAS;
- Siberian Federal University, Krasnoyarsk;
- Institute of Chemistry and Chemical Technology SB RAS, Krasnoyarsk;
- Budker Institute of Nuclear Physics SB RAS.

In 2014, works at the station were supported by the following projects and contracts:

- Program No. 24 "Basics of fundamental research on nanotechnology and nanomaterials", project No. 69, "Application of EXAFS and XANES spectroscopy to analysis of microstructure of SiGe quantum rings on Si (100) surface, GaN/AlGaN quantum dots and AlGaN/AlN superlattices with quantum wells", coordinated by S. Erenburg.
- 12-02-00262-a, Analysis of the microstructure and electronic structure of calibrated clusters of gold in cucurbit[n]urils using XAFS spectroscopy", coordinated by S. Erenburg.
- 12-03-00131, Nonequilibrium phase formation in ternary oxide films made by doping of rare-earth elements to HfO2, coordinated by T. Smirnova.
- 12-02-00930-a, Synthesis of AlGaN/AlN structures with quantum dots and analysis of their luminescence and generation properties in excitation with low-voltage electron beams, headed by O. Pchelyakov, ISP SB RAS, Novosibirsk.

Below are presented examples of works in 2014.

SR investigation into structure of complexes of Bi with bioactive ligands in solutions.

It has been long known that execution of some functions in living organism, in particular, of manifestation of pharmaceutical properties, requires certain structural forms of both bioactive ligands and metal complexes with them. Such complexes with bismuth are known to demonstrate a wide range of forms, differing in their structure, chemical properties and, consequently, in functional features in the living organism. Origination and existence of a form is usually associated with particularities of synthesis of the compound, and various forms may exist both in a solid state and in various solutions, differing in the spatial and electronic structure. It should be noted that structural forms can vary in case of different concentrations of complexes in solutions, which can change their functional features in living organisms. This increases the topicality of efforts of coordination and bioinorganic chemistry on synthesis of bioactive metal complexes of a certain struc-

ture and provision of conditions for synthesis, storage and administration of bioactive complexes in the body and presence of required structural forms in it. Medicinal properties of bismuth (III) are largely determined by the formation of complexes, e.g. with O, N, or S donor ligands, which often have a wide range of biological activity.

Structure of complexes of bismuth (III) with thiourea from EXAFS spectroscopy data.

Complexes of bismuth with thiourea $(NH_2)_2C=S$ (tu) occupy a noticeable place in the chemistry of bismuth.

The main structural characteristic of ions of metals in aqueous solutions is the structure of the coordination polyhedron. According to results of quantum chemical calculations in the absence of hydrolysis, stability in highly acidic aqueous solutions is shown by aquacomplexes $Bi(H_2O)_8^{3+}$ and $Bi(H_2O)_9^{3+}$. According to EXAFS (Extended X-ray Absorption Fine Structure) and LAXS (Large-Angle X-ray Scattering) data, particles of $Bi(H_2O)_8^{3+}$ dominate in 1.5M $HClO_4$. In recent years, there were synthesized some different crystal complexes of bismuth (III) with a coordination number (CN) of 7.8 and with ligands containing a dithiocarbamate group CSS coordinated by two S atoms. There are also complexes of Bi the structure of which is based on centrosymmetrical dimers with ligands coordinated by one S atom. In solutions, the steric impediments show up to a less degree than in a solid state; this may lead to stabilization of other spatial shapes in the solution.

The following objects were investigated by the EXAFS and XANES spectroscopy method:

1. a solid complex (powder): $Bi(tu)_6(ClO_4)_3$;
2. a solution: 0.1M $Bi(ClO_4)_3$ + 1.8M (tu) + 1M $HClO_4$;
3. a solution: 0.05M $Bi(ClO_4)_3$ + 1.5M (tu) + 1M $HClO_4$.

It was found that in case of noncrystalline solid sample of the complex $[Bi(tu)_6](ClO_4)_3$ (sample 1), the first coordination sphere of Bi atom contains six sulfur atoms at distances of 2.8 – 2.9 Å. Results obtained from EXAFS measurements of the Bi-S distances are consistent with results of X-ray structure investigations for other complexes of bismuth (III) with thiourea, according to which the Bi-S distances are in the range of 2. 78 – 2.86 Å. From results of modeling of EXAFS spectra of solutions 0.1M $Bi(ClO_4)_3$ + 1.8M(tu) + 1M $HClO_4$ (sample 2) and 0.05M $Bi(ClO_4)_3$ + 1.5M(tu) + 1M $HClO_4$ (sample 3), formation of binuclear complexes of bismuth was supposed, since the possible presence of sulfur atoms at a distance of ~ 3.3 Å from Bi atoms is typical to bridging sulfur in known binuclear complexes of Bi with S-coordinated ligands.
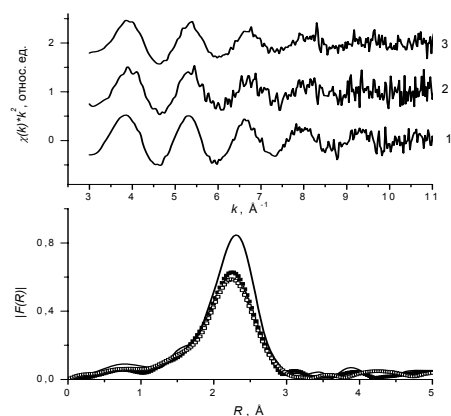
Fig. 6.2.31. BiL_{III} EXAFS spectra of $\chi(k)k^2$ (a) and modules of their Fourier transform for samples 1 - 3.

Structural characteristics of K-Bi-citrate (De Nol) in solid form and aqueous solutions of various concentrations from EXAFS spectra.

In the early 80s of the last century, the peptic ulcer disease was found to be caused, among other factors, by *Helicobacter pilory* contamination of the mucous membrane of the stomach. One of the first antibacterial drugs used for treatment of the *Helicobacter pilory* contamination was De Nol, manufactured by Yamanouchi Europe (the Netherlands). The pharmacologically active part of the drug is bismuthate tripotassium dicitrate (colloidal bismuth subcitrate), $[Bi(cit)]^-$ (cit=$C_6H_4O_7^{4-}$). The drug compares favorably with other bismuth salts because it can dissolve in the gastric mucus and thus penetrate to *Helicobacter pillory* bacteria, which are under the gastric mucus. The solubility of colloidal bismuth subcitrate is 20-100 times higher as compared with other bismuth-containing drugs.

It is known that the main structural element in crystalline compounds of bismuth citrate is the stable dimer fragment (cit^{4-})BiBi(cit^{4-}). With growth of crystals, water molecules join the structure forming process and combine the structural elements in three-dimensional frameworks by means of hydrogen bonds. Therefore, even small changes in the hydration composition may lead to significant changes in the structure of the compounds. Bismuth citrate crystals are unstable in air, probably due to loss of water, so the structure of the solid crystalline complex may differ significantly from amorphous or dried complexes and, moreover, from the corresponding structures in solutions. Investigation into the structure of the complex in aqueous solutions is particularly important as the pharmaceutical action of the drug since occurs namely in solution and optimization of its therapeutic properties via changes in the structural characteristics of the complex in solution may become very important.

The method of EXAFS spectroscopy was used for determination of microstructure parameters (the interatomic distances, coordination numbers, and Debye-Waller factors) for aqueous solutions of colloidal bismuth of different concentrations: 1) with a maximum bismuth concen-

tration of ~ 370 g/l; concentrated solution diluted 2) 3-fold; 3) 5-fold; 4) 10-fold; 5) solid complexes of dried colloidal bismuth subcitrate: a) synthesis carried out at ISSCM SB RAS; 6) synthesis carried out by Yamanouchi Europe (the Netherlands).

The coordination sphere of bismuth atom in aqueous solutions was found to include nine oxygen atoms with unequal Bi-O distances. The minimum distance of 2.13 Å may correspond to the coordination of water molecules (N1 = 2); a distance of ~ 2.42 – 2.53 Å, to the coordination of OH hydroxyl group; of 2.64 – 2.71 Å, to the coordination to the Bi atom of C-O groups with a single bond; of 2.86 – 2.92 Å, to the coordination to the central atom of C=O groups with double bond. Upon dilution of the solution 5- to 10-fold some Bi-O interatomic distances decrease slightly (by $\leq$ 0.1 Å).

The structure of solid CBS forms radically differs from the corresponding structures in solutions. The bismuth atom is surrounded by three oxygen atoms at different distances (2.1 – 2.9 Å).
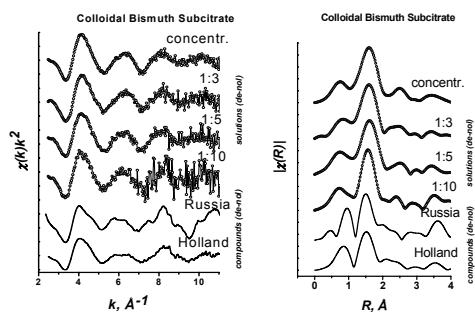
Fig. 6.2.32. BiL_{III} EXAFS spectra of $\chi(k)k^2$ (a) and modules of their Fourier transform (b) for samples.

6.3. WORKS ON SR BEAMS FROM VEPP-4

6.3.1. Station "Detonation".

The commissioning of the station "Detonation" on the new SR beam line on VEPP-4 has enabled work with real samples of special products by VNIITF of 40 mm in diameter and a capacity of 200 grams of TNT. 25 experiments were carried out.
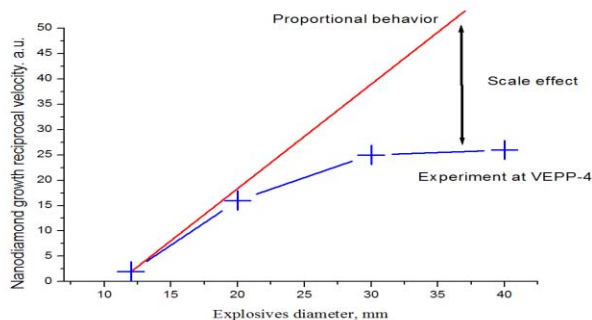
Fig. 6.3.1. Size effect of growth of nanodiamonds in TNT/RDX high-explosive charges of different diameters.

The kinetics of formation of nano-diamonds in the reaction zone was found to vary with the diameter of the charge. This fact could be explained by changes in the geometry of the system, i.e. changes in the diameter, detonation wave area, and reaction volume. The kinetics of formation of nanodiamonds was expected to vary in proportion to one of the geometric parameters. The rate of formation of diamonds however turned out to be in no proportion to the geometric parameters (Fig.6.3.1.). Thus a size effect was observed in the formation of diamonds. The data obtained made it possible to improve the parameters of the special-purpose products under development.

6.3.2. Station "Phase contrast tomography and XFA".

A new station "Phase contrast tomography and XFA" was commissioned at the SCSTR in 2014. The station consists of the 7-pole snake of VEPP-4M. The station is intended for experiments in the photon energy range from 30 to 100 keV. The station was created with partial financial support of RFBR grant 12_02_12071_ofi_m. The high intensity of the source in the hard range (50 keV), as compared with the VEPP-3 spectrum, enables examination of samples of higher X-ray absorption and conduction of experiments on X-ray fluorescence of rare and heavy elements ($Z > 56$) based on K-series lines. The station provided output of monochromatic beam of large horizontal aperture (up to 100 mm), which allows examination of large samples. The station is equipped with a two-crystal monochromator operating in a parallel (non-dispersive) optical scheme (n, -n). Silicon crystals with "111" crystallographic plane are used as energy dispersion elements. The monochromator allows one to select a required energy of X-ray photons from 30 to 100 keV. The full power of SR from VEPP-4M at an electron current of 10 mA that is delivered to the location of the monochromator is 90 watts. To prevent distortions caused by overheating of x-ray optical elements, they at the station use a cooled aluminum filter absorber 2 mm thick. The filter absorbs up to 85% of the incident radiation power of the long-wavelength SR spectrum part which is not used in the experiments. The experimental volume, which is located at a distance of 32 meters from the point of radiation, is a radiation-protected box – absolutely no leakage of ionizing radiation. The internal dimensions of the experimental volume are $2\times1\times1$ m^3, and thus all X-ray optics and equipment required for experiments can be placed inside it. The geometry of the station is shown in Fig. 6.3.2. Table 6.3.1 presents the performance capabilities of the station.

First experiments on SR XFA in the hard X-ray range were conducted at the station in 2014. Preliminary results were obtained for the minimum detection limits for heavy and rare-earth elements ($Z = 55-66$) from lines of K-series

of characteristic radiation excited by photons with energy of 56 and 70 keV. The experiment results lie within the range of 0.5 to 2 ppm.

Besides that, an X-ray Talbot interferometer was designed and developed in 2014. The interferometer is intended for high-resolution recording of phase-contrast images. The experimental setup allows recording of X-ray images and conduction of tomography survey of samples of up to 80 mm in diameter in a short-wavelength range of 0.15 to 0.4 Å (80 - 30 keV) with a contrast of at least 0.1%. With the help of the Talbot X-ray interferometer, first results on the phase-contrast images were obtained in 2014. Besides that, three-dimensional structures of large samples were reconstructed by means of tomography with a spatial resolution of 100 μm.
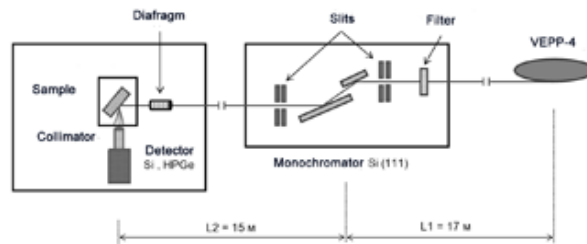
Fig. 6.3.2 SR XFA experimental set-up at station "Phase contrast tomography and XFA" on VEPP-4M.

Table 6.3.1. Station characteristics.

Energy range	30 keV – 100 keV
Energy resolution $\Delta E/E$	$2 * 10^{-3}$ or white beam
Source	Wiggler, B=1.2 T (7 poles), $E_{кр} = 12.8$ keV ($E_{эл} = 4$ GeV)
Optics	Double-crystal monochromator in parallel Bragg non-dispersion scheme (+, -): Si crystals (111), 2d=6.271 A
Beam size on sample	Maximum: 100x2 mm; minimum: 1x1 mm.
Detectors	• Si (SDD) Amptek, S = 25 mm^2 (area of crystal), resolution of 125 eV for 5.9 KeV • HpGe Canberra, S=10 mm^2 (area of crystal); resolution of 125 eV for 5.9 KeV; resolution of 460 eV for 122 KeV • Teledyne DALSA CCD; resolution of 8160 x 256 pixels (vertical x horizontal); pixel size: 27 μm.
Experimental volume	Environment: air; dimensions (LxWxH mm): 2000x1000x1000; wall: 3 mm of lead; windows: 10 mm of lead glass TF-5 (a lead equivalent of 2,5 mm)

6.4. WORK WITH TERAHERTZ RADIA-TION BEAMS

6.4.1. Novosibirsk terahertz free electron laser.

The Novosibirsk free electron laser (FEL) is still the most powerful source of terahertz radiation in the world. The maximum average output power at a pulse repetition of 11.2 MHz is 500 W. In 2014, the time of the Novosibirsk FEL operation for users was about 1000 hours. Works with terahertz radiation was performed by 20 groups from 12 scientific organizations of Novosibirsk, Moscow and South Korea.

In standard operation for users at a repetition rate of 5.6 MHz, the average radiation power at the stations de-pended on the radiation wavelength and tuning of the acceleration system and was about 100 W. The FEL radiation is linearly polarized and fully spatially coherent; the wavelength is tunable in the range of 40 - 240 microns; the relative spectral width (FWHM) is less than 1 %; the pulse duration (FWHM) is about 100 ps.

The scheme of the energy recovery linac (ERL) with three FELS mounted on the first, second and fourth (third stage FEL) tracks is shown in Fig. 6.4.1.

One of the two main objectives in 2014 was the organization of regular works at the six user stations. The second task was to prepare the third stage of the Novosibirsk FEL for commissioning.
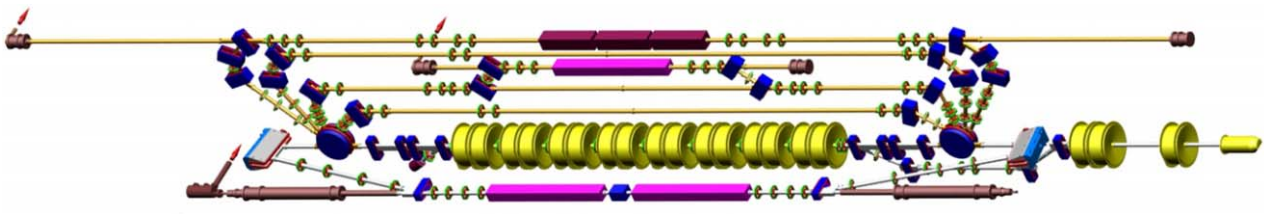
Fig. 6.4.1. General view of ERL with FELs installed on first, second, and fourth tracks.

6.4.2. Upgrade of the FEL and ERL.

The magnetic system of the ERL was upgraded for improvement of the energy acceptance. To this end, sextupole correction magnets were installed in the quadrupole magnets of the achromatic bends (see Fig. 6.4.2). The chosen strength of the correction sextupoles makes the bends second-order achromatic as for energy deviation.

A new high-voltage rectifier for electrostatic electron gun was assembled (see Fig. 6.4.3) and is under tests now. Its application will significantly lower the pulsations of energy of electrons leaving the electron gun. The old rectifier will be replaced in 2015.

Works on the improvement of the high-current electron gun for the ERL are going on (see Fig. 6.4.4).

Fig. 6.4.3. New high-voltage rectifier for electrostatic electron gun.

Fig. 6.4.2. Quadrupole lenses in achromatic bend.
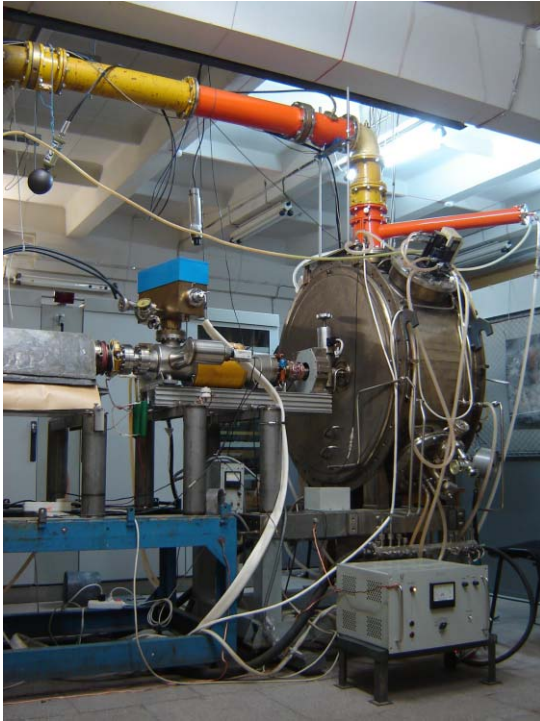
Fig. 6.4.4. High-voltage electron gun with diagnostic beam line.

Fig. 6.4.5. Radiation extraction to the second floor. Vessels comprising mirrors are connected by pipes and have adjustment units.

6.4.3. Creating new user stations.

An extension of the radiation distribution system was designed, manufactured and assembled for construction of new user stations. Radiation emitted from the end of the old beam line is directed to the second floor (see Fig. 6.4.5).

The distribution system for the new stations was mounted on the second floor (see Fig. 6.4.6).

The improvement in the existing experimental stations and operation at them with radiation of the FELs of first and second stages goes on.

Fig. 6.4.6. Horizontal distribution beam line in hall intended for new user stations.

6.4.4. Development of nanodiagnostics methods at the Novosibirsk FEL.

A method was developed for investigation into the characteristics of surface plasmon polaritons (SPPs) in the THZ range by detection of free electron-electromagnetic wave arising in the diffraction of SPPs on the edge of sample, as well as by registration of radiation losses in movement of SPPs over a cylindrical surface. SPPs were shown to be able to "jump" to surfaces up to 100 mm apart (Fig. 6.4.7), which is important for creation of opto-electronic integrated circuits in the terahertz range.

111
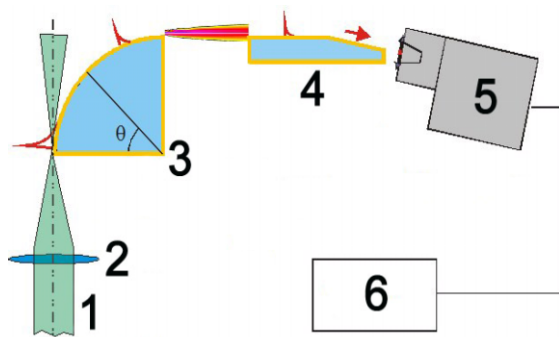
Fig. 6.4.7. Schematic of experiment with "jump" of surface wave across gap between conductors. 1 - Free-electron laser beam, 2 - Polyethylene cylindrical lens, 3 - Element for generation of surface plasmon (gold + 1.5 microns of ZnS), 4 - Receiving element (gold + ZnS), 5 - Optoacoustic Golay detector, 6 - Lock-in amplifier.

Self-reproduction of wave front that passed through periodic lattices with hole size about the wavelength was reported for the first time. The experiments were carried out on two-dimensional lattices at a wavelength of 130 microns. The self-reproduction was observed even with a copper foil thickness of about 0.75 of the wavelength and the same hole diameter; its position corresponded exactly to the scalar diffraction theory calculations.

A system was created for registration of weak THz pulses. It is based on cryogenic detector on hot electrons with application of a synchronous detector specially developed for near-field microscopy on free electron laser. The characteristics of this system have been investigated. In measurements of terahertz radiation intensity at a wavelength of 130 microns, the dynamic range was 80 at least, which enables conduction of experiments on the near-field microscope.

The performance of a prototype spectrally selective polarimeter/ellipsometer was investigated (Fig. 6.4.8) with application of terahertz FEL radiation. The prototype ellipsometer was equipped with an attenuated total reflection unit, which enables investigation of the polarization characteristic of strongly absorbing substances. In the THz range, all water-based solutions, including biological solutions of enantiomers, are strongly absorbing substances. The ellipsometric parameters of the unit were investigated and turned out to be in good agreement with the theoretical calculations; the unit is ready for study, at the first phase, of test biological samples.
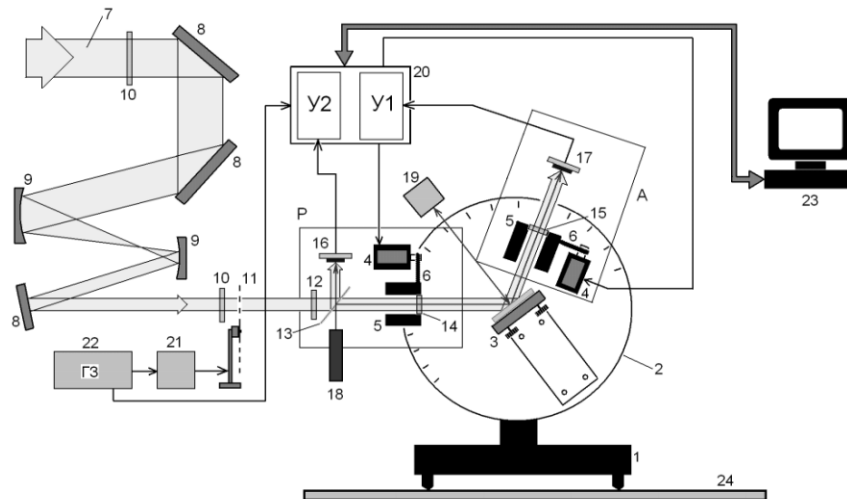
Fig. 6.4.8. Prototype spectrally selective polarimeter/ellipsometer.

6.4.5. Complex study of terahertz optical discharge.

Under an RFBR project, standards measurements were conducted in 2014 in relation to conditions of ignition and maintenance of quasi-continuous optical discharge, as well as study of its dynamics. This discharge was shown to be described well in terms of the classical theory of microwave gas breakdown. A constitutive breakdown parameter is the product of intensity by pulse duration. With maximum focusing of radiation with a wavelength of 130 microns and a pulse duration of 70 ps, the breakdown intensities of the main atmospheric gases are in the range of 1.1-1.4 GW/cm^2. Dynamics of discharge varies heavily with the radiation power increasing from practically independent individual pulses at a frequency of 5.6 MHz near the breakdown to a quasi-continuous plasma discharge with gas-dynamic oscillation frequencies of 100-200 kHz.
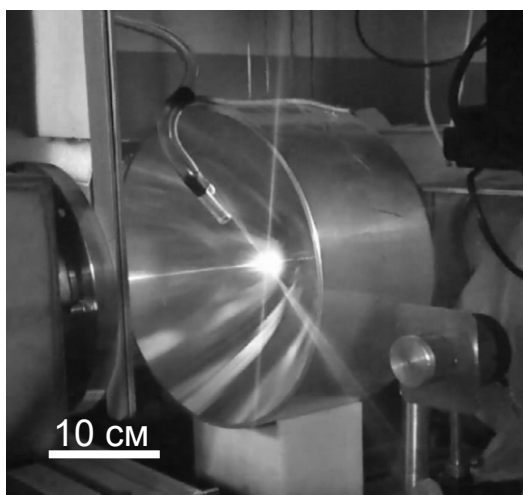
Fig. 6.4.9. High-intensity plasma optical discharge in argon at metrology station.

Practical applications of this phenomenon will be studied in future, including generation of the 2nd radiation harmonic, synthesis of nanomaterials, creation of a specific source of UV radiation and others.

6.4.6. Development of methods of ultrafast THz molecule spectroscopy.

Research on the development of various methods of ultrafast molecule spectroscopy was continued. In 2014, most effort was devoted to refinement of methods of simple analytical spectroscopy by the signal of coherent radiation of free induction of molecules after their excitation with a short laser pulse. These signals, like spectra, are an individual characteristic of molecules in the time domain and allow very fast execution of their quantitative diagnostics.
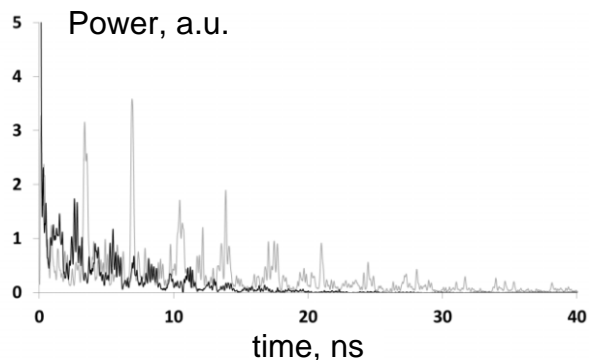
Fig. 6.4.10. Free induction decay signals of close rotational lines of NO_2 (gray) and CH_3OH (black) molecules with different hyperfine structure of tens of lines. The spectrum overlap integral is 0.011.

6.5. DEVELOPMENT AND CREATION OF INTENDED SYNCHROTRON RADIATION GENERATORS

6.5.1. Superconducting wigglers.

In 2014, under contracts with different accelerator centers, works were carried out for production of new superconducting cryogenic magnet systems and upgrade of already existing generators of synchrotron radiation (SR).

In July 2014 a 40-pole wiggler CATACT with a magnetic field of 2.5 T and a period of 48 mm was put into operation on the ANKA storage ring (Karlsruhe, Germany). Zero consumption of liquid helium was demonstrated, as well as negative pressure in the helium vessel with the temperature helium decreasing to 3.5 K. That enables generation of a higher magnetic field due to a temperature shift in the loading characteristics of the superconductive wire used. This wiggler is intended for use on the spectroscopy beam line. Fig. 6.5.1 presents the wiggler CATACT, mounted on the ANKA storage ring.

Fig. 6.5.1. 40-pole wiggler with field of 2.5 T and a period of 48 mm installed on ANKA storage ring (Karlsruhe, Germany) for research in spectroscopy.

Many of the wigglers produced earlier by BINP and working now on different storage rings need upgrading. Due to the updated design, cryostats developed at BINP in recent years can be served as rarely as once every few years, because no liquid helium is consumed. However, operation at reduced pressure has necessitated improvements to already existing cryostats for the purpose of avoidance of ice formation and in-leakage of the outer atmosphere. In November 2014, such a modernization was carried out to the cryostat of 27-pole 4 T wiggler, which operated since 2008 on the BioMedical Imaging and Therapy (BMIT) beam line on the CLS storage ring (Canada). The magnetic system was not changed. Fig. 6.5.2 shows the process of installing the wiggler on the storage ring after the upgrade.

Fig. 6.5.2. Installation of upgraded 27-pole 4 T wiggler BMIT on CLS storage ring (Canada).

The design of the wiggler CLIC with a field of 3 T, period of 51 mm and magnetic gap of 18 mm, which is being fabricated for the ANKA storage ring (Karlsruhe, Germany), is radically different from all previous wigglers. In this wiggler, cooling to low temperatures is performed not with liquid helium, but with refrigerating machines through mechanical thermal contacts and heat pipes. The magnetic system itself is in vacuum. A full-size 72-pole dry wiggler was tested in 2014 in its own cryostat and cooled to a temperature of ~ 3 K. Initially, the attained level of stable magnetic field was ~ 2.8 T instead of the required 3 T. At the moment, the prototype is still being tested in different operation modes. The purpose is to obtain the required level of magnetic field. Commissioning of the full-sized magnet with indirect cooling on the ANKA storage ring is planned for June 2015.

7
RADIOPHYSICS AND ELECTRONICS

7.1. DEVELOPMENT OF EQUIPMENT AND SYSTEMS FOR AUTOMATION OF PHYSICAL RESEARCH

7.1.1. Controller of accelerating RF stations of NICA booster.

A contract with the Joint Institute for Nuclear Research (Dubna) for the manufacture and commissioning of two accelerating RF stations of the NICA booster was successfully completed in late 2014.

The controller of the RF stations is one of the main elements of the equipment delivered. The most important function of the controller is high-precision measurement of magnetic field in booster magnets and generation of master sinusoidal signal, which is in link with the measured field value. The error of keeping the field/frequency ratio should be better than $5 \cdot 10^{-5}$, which implies that the error of field measurement and dynamic errors of the master oscillator should be not worse than $2 \cdot 10^{-5}$.

In addition to the above task, the controller adjusts the amplitude of the voltages of the cavities by a given law in accordance with the booster operation phase, controls the modes of the high-power stages of the stations and monitors their operation. The controller also measures about twenty signals that characterize the behavior of elements of the stations during an acceleration cycle.

A photo of the controller PCB is shown in Fig.7.1.1.

Fig. 7.1.1. Photo of PCB of controller of NICA booster RF stations.

The device is based on a single-board computer with 536 MHz microcontroller ARM Cortex-A5 Atmel SAMA5D31. The peripherals are controlled via SPI and I^{2}C buses with clock frequencies of 50 MHz and 400 kHz, respectively.

Since the booster of the NICA complex is under construction, a specialized unit, a tester of RF stations, was fabricated for tests of the operation of the RF stations. The tester simulated the entire set of signals to come from the booster systems, including the signal from the induction magnetic field sensor, which was generated with high accuracy.
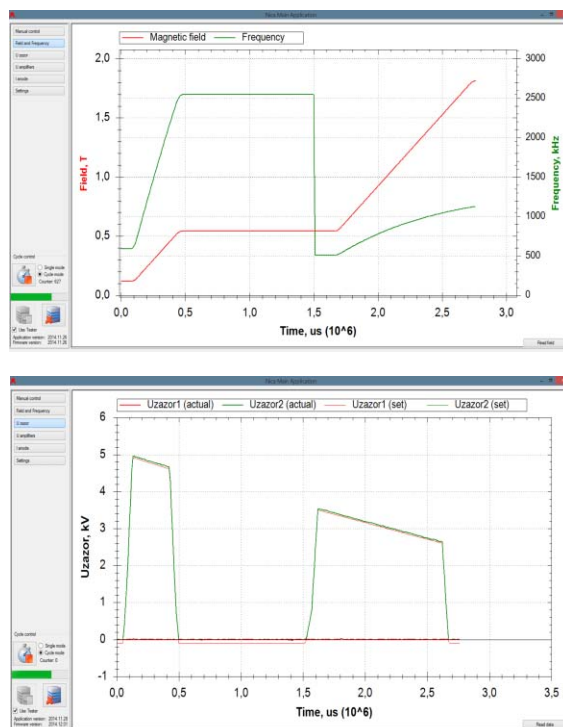
Fig.7.1.2. Windows of engineering program for tuning and testing of stations.

An engineering program was written for testing of the equipment of the stations and testing of their functioning in a simulated "acceleration" cycle. Fig.7.1.2 shows windows of the program with "field-frequency" and "voltage across cavities" graphs during an acceleration cycle.

7.1.2. LIA-20 project.

Year 2014 was associated with intense works on a project of LIA-20, a 20 MeV linear induction accelerator. At this stage, the laboratory was to develop the structure of control system for this installation, which is rather unusual for BINP, as well as to design a wide range of hardware and software. Due to the experience gained in previous years, in development of the LIA-2 installation, the following control system features were stated clearly and the basic requirements to the new accelerator control system were defined:

- structure of the control system should be based on standardized local controllers distributed over the installation;
- it is necessary to ensure work with a large number of individually-adjustable high-voltage elements operating in the nanosecond range (the linear part alone comprises 480 modulators);
- it is necessary to ensure work with a large number of pulse elements working in the micro- and millisecond ranges (the linear part comprises 30 demagnetization generators, 72 pulse lenses and 28 chargers);
- it is necessary to perform oscillographic testing of all pulse processes in order to obtain detailed informa-

117

tion about the operation of the accelerator and prediction and prevention of possible malfunctions;

- the control system should use standard protocols, system buses, and constructs;
- it is necessary to ensure gradual development of the control system: the linear part with the transport beam line, the three-pulse mode, and multi-angle radiography.

A local controller is placed in an Euromechanics rack and performs all necessary operations to control two nearest accelerating elements (short accelerating modules) that ensure growth of the beam energy at 0.67 MeV.

The intellectual center of local controller is a VME64 rack. In addition to the VME64 specifications, the bottom line of the crate comprises a number of installation-specific buses. To this end, the reserve buses of the 64-bit bottom line are used, which is not prohibited by the standard. Fig.7.1.4. shows the rack structure.

First of all, the additional options enable a common time for all local controllers and thus for all measurement and control modules placed in the local controllers. The common time is important for a pulse installation with element spaced by about 200 m, in which synchronization in the nanosecond range is necessary. The common time will have a delay spread of ± 2 ns and a noise of a few tens of picoseconds.
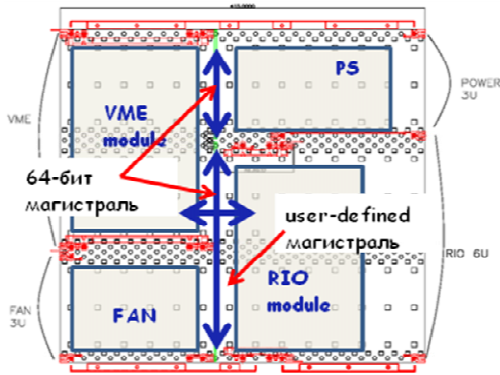
Fig.7.1.4. Cross section of BINP VME64 crate.

Further, the additional buses will ensure distribution of trigger signals to all devices in the crate and relieve the face plates of the modules.

The crate will be made with a VME controller MVME 31006 made by Emerson. It is the only purchased unit. Table 7.1.1 lists the BINP-developed modules installed in the crate.

Table 7.1.1.

Module type	Function, parameters, and quantity in crate
System Timer	Synchro-pulse resolution: 4ns; inter-module synchronization accuracy: ± 2 ns; VME 10 bus synchro-frequency: 10 MHz; 8 channels for TTL triggers; 1 module per crate.

ADC 4x250	"Fast" oscillographic monitoring; 4 synchronous channels; 4 ns/point; 100 MHz; 0.5, 1, 2, and 4V; 700 kwords/channel; 6 modules per crate.
VME↔CAN	2 master channels; rate of exchange: 125 kbit/s to 1 Mbit/s; CAN Specifications 2.0.
ADC 132	"Slow" oscillographic monitoring; 32 multiplexed channels; 1 μs/channel; 100 kHz; 0.5, 1, 2, 4, and 80 kwords/channel; 2 modules per crate.
Timer VME DL250	16 channels; tuning resolution: 4 ns; tuning range: 300 μs; output pulse duration: 0.5 μs; 4 modules per crate.
RIO module VME F16	16 channels; output current: 200 mA; 10 V@50 Ohms; front: 5 ns; short circuit protection; 4 modules per crate.

7.1.3. Smart electronics for coolers.

Works on the electronics for the coolers were performed in two directions. The first was associated with the following upgrade and various improvements to the electronics of the cooler delivered earlier to COSY.

1. Replacement of the "ground"/ HV-terminal communication system with one of higher noise immunity. The new communication has two significant benefits: multi-beam radio signal (MIMO technology) and remote diagnostics of signal level. In addition, the frequency of the radio signal carrier in the new devices is in a less "noisy" band of 5 GHz. The works on the replacement of the communication system and mounting of the new equipment were successfully completed in February 2014.

2. Development and commissioning of the Data-Logger electronic device at COSY in November 2014. This device enables real-time 10 ms/count collection of analogous and logical data that are available in the HV terminal and their digitization and storage in a compressed format to a standard USB flash drive. In addition, it has an option of recording of current CAN traffic collected in every 10ms and a built-in microphone with option of recording of surround sound. The internal rechargeable battery ensures operation for up to 20 minutes with no external power supply. The internal clock enables switching on the logging at a given time.

The second area of the works in 2014 is the designing of the control system and fabrication of various measurement/control devices for the cooler of the NICA complex.

The designing resulted in an overall structure of the control system, circuit diagram for the elements of the system, and detailed scheme for the high-voltage terminal cabinet. Based on the overall structure, small-signal control and measurement electronics were planned, fabricated and prepared for operation.

Unlike previous electron cooling systems, voltages on the control electrodes in the cooler for the NICA complex shall be tuned depending on the current stage of booster acceleration cycle. Such tuning necessitated designing of

electronic components capable of high-accuracy (0.1%) and rather fast (a transition time of less than 10 ms) tuning of output high voltages in a bipolar mode with a swing of up to 6 kV with a 20-meter cabling load.

The timing chart was organized using the table mode of control of CAN modules for formation of respective voltages. It was confirmed experimentally that a common broadcast command to all modules could initiate synchronous operation by tables. This option will be applied to the cooler control for the first time.

Stabilization of 60 kV voltage turned out to be quite a challenge. Proper functioning of the cooler requires the stability of this voltage to be about 10^{-5}. This can be achieved with a set of special measures only: a proper design of the high-voltage divider, its thermostabilization, and appropriate circuit solutions in the electronics.

Fig.7.1.5. Equipment of 60 kV precision regulation system.

Fig.7.1.5. presents a photo of the equipment of the stabilization system. The high-voltage divider placed between rings under a potential is immersed in an oil tank the temperature of which is stabilized with an accuracy of ± 1 C°. All the electronics are mounted on the flat walls of the tank and are heat-insulated, whereby the boards with the components also have a constant temperature. The integration of the stabilization devices in the structure of the high-voltage 60 kV power supply will begin in the second half of 2015.

7.1.4. New systems for magnetic measurements.

The Radiophysics Laboratory is traditionally aimed at provision of hardware and software for magnetic measurements. A new work performed in this direction in 2014 is magnetic measurements of spiral permanent-magnet undulators created by BINP for the Brookhaven Laboratory (Fig.7.1.6). For the first time, the magnetic measurements were performed using a three-coordinate Hall sensor. To this end, the standard electronics for Hall measurements were upgraded and the software was modified. Accurate coordinate measurement was provided by a laser interferometer, a VME adapter for which was designed at the Laboratory.

The new equipment and programs made it possible to attain a first integral measurement error of ± 10 G·cm, which is a very good result for Hall measurements.
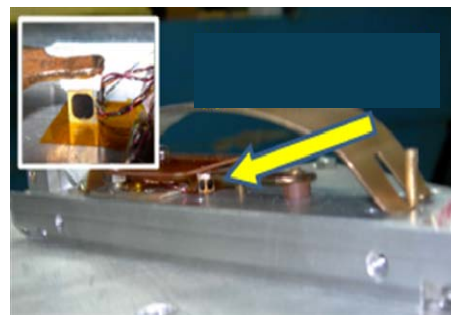
Fig.7.1.6. Top: spiral undulator on measurement stand; below: three-coordinate sensor on carriage.

The contract on the fabrication and delivery of pulse dipole magnets (TPD) for Flash III (DESY, Germany) was executed using a stand for pulsed magnetic measurements based on integrators VsDC2. The field in the magnets reaches 1.2 T; the first field integral in an area of ± 10 mm vertically and ± 5 mm horizontally must be close to the nominal value within ± 10^{-3}.
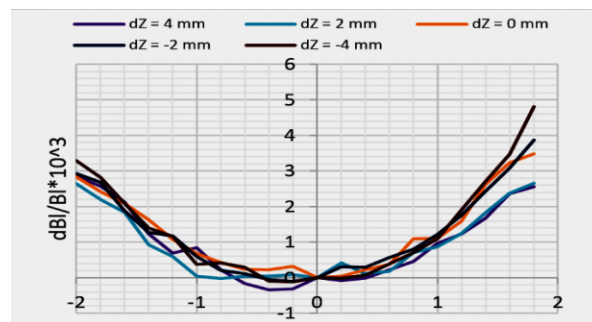
Fig. 7.1.7. Graphs of transverse distribution of field integrals for TPD magnet at different heights.

The results of the measurements of the transverse distribution of the first field integral for different heights are presented in Fig.7.1.7.

The graphs show that the error of the measurement of pulsed magnetic fields is not worse than $5 \cdot 10^{-4}$.

119

7.1.5. Production of power supply controllers for correction magnets for European XFEL.

A controller for the power supplies of the corrective magnets for the European Free Electron Laser (European XFEL) realizes all the functions of control of the power source units. It contains an 18-bit DAC, which sets the output current, a multi-channel 24-bit analog-to-digital converter, which provides measurement of a number of voltages, I/O registers, and a CAN bus interface to the control system of the installation. The prototype power sources, including the controller, successfully passed tests for compliance with the European standards at ÜV NORD CERT GmbH, Abteilung EMV Services, EMC-Laboratory in April 2014. After that, BINP was entitled to mark its electronics with the CE conformity sign, and the production of the power sources was authorized.

Control of the source using the DESY software was successfully put in operation in August 2014. The production of the first batch of the sources was started in late 2014. Fig.7.1.8 shows part of the first batch of the controllers manufactured by NEC in Novosibirsk.

Fig.7.1.8. First serial controllers.

Large-batch production of sophisticated electronics is impossible without proper stands and appropriate test software. A stand that allows simultaneous testing of 7 MPS-10 or MPS-5 sources was fabricated in late 2014. A photo of the stand is presented in Fig.7.1.9.

Each channel in the unit has two sockets: one for connection of a source under test and the other for a load. The load current is measured using a stable no-contact shunt calibrated in operation temperature range. All the data obtained are transferred via a CAN line to a computer for analysis and preparation of the data sheet of the source.

7.1.6. Research on broadband stabilization of VEPP-4M guiding field.

Works on the creation of broadband stabilization of the guiding field in the VEPP-4 ring were continued in 2014. The success of CPT experiments to be performed at the VEPP-4M complex depends on the long-term stability and the level of ripples of the guiding field in a band of up to few tens of hertz.

Fig. 7.1.9. Stand for testing of MPS-10 and MPS-5 sources.

A broad band (up to 50 Hz) stabilization system is under creation. Its structure is shown in Fig. 7.1.10.
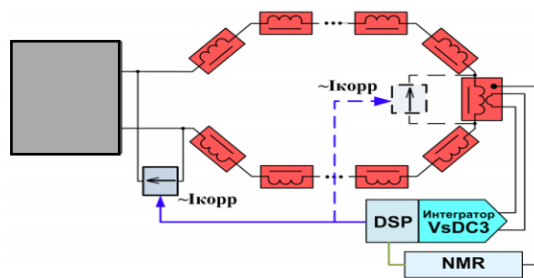
Fig. 7.1.10. Structure of system for broadband stabilization of guiding field in VEPP-4M.

An induction sensor is placed in a gauge magnet; the signal from the sensor is processed by a digital integrator VsDC3, which computes the code of the DAC of the correction current generator, which is connected in parallel with the main field current sources. Slow correction based on NMR indications is implemented in the same structure. The operation mode and feedback parameters are set from the computer in the VEPP-4 control room. Fig. 7.1.11 shows a result of operation of the broadband stabilization system. Two types of graphs are shown: spectra of pulsations and integrated ripples vs. band without and with the correction.
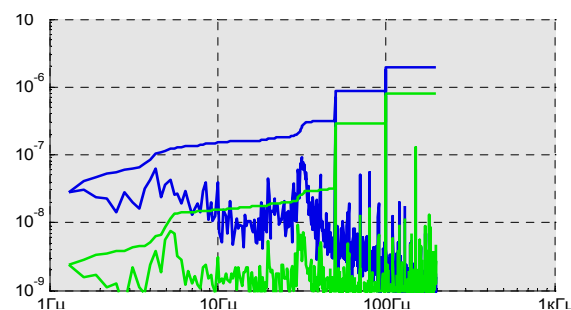
Fig. 7.1.11. Field ripples vs. frequency before (upper curves) and after (lower curves) switch-on stabilization.

The effectiveness of the broadband stabilization system will be checked in high-energy physics experiments in 2015.

7.2. RADIO FREQUENCY SYSTEM FOR THE BEP STORAGE RING

The creation of the new radio frequency (RF) system of the BEP storage ring at BINP, which is the injector of the accelerator complex VEPP-2000, is close to completion. The new RF system will increase the particle energy in the BEP from 0.9 to 1 GeV. The RF system operates at a frequency of 174 MHz (the 13th harmonic of the BEP revolution frequency) and consists of an accelerating cavity, RF power generator and control system.

The coaxial accelerating cavity is designed for a maximum voltage of 120 kV. The RF generator for a maximum power of 20 kW has an output stage on GU-92A tetrode and transistor pre-stages. The power from the generator is transferred to the cavity through a copper coaxial feeder with a characteristic impedance of 75 ohms.

The cavity was installed to the ring in 2014 (Fig. 7.2.1); the installation of RF generators and the feeder line was also completed; the length of the feeder line was selected to be equivalent to half the wavelength (the electric length is 5.5 wavelengths), which is optimal both for the output stage of the generator and for beam resistance to synchrotron oscillations; control system units were fabricated (a frequency multiplier-by-thirteen, a heterodyne, an adjustable RF amplifier and a 100-watt pre-amplifier); the control rack was re-arranged.
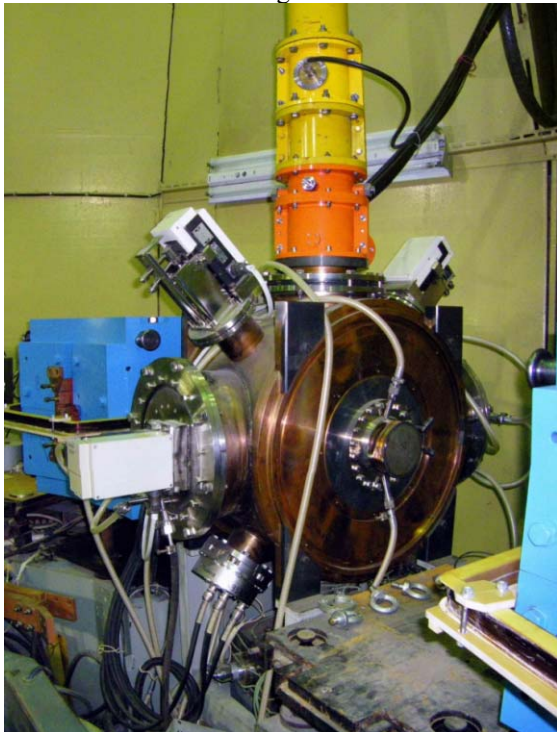
Fig. 7.2.1. Cavity in the BEP ring

The cavity was tested without beam as part of the RF system of the BEP. Pre-burning of a multipactor discharge in the AGC voltage mode resulted in a voltage of 110 kV on the cavity, the power of the generator being 3.2 kW.

7.3. RF SYSTEMS OF PLASMA SOURCES FOR HIGH-POWER CONTINUOUS INJECTORS OF BEAMS OF FAST HYDROGEN ATOMS

In 2014 BINP continued works on the creation of benches for research of the prototype of fast hydrogen atom source based on negative ions. One bench is intended for generation of negative hydrogen ion beam with an energy of 120 keV and a current of up to 9 A. The second bench is to accelerate a beam of negative hydrogen ions with a current of 1.5 A up to energies of 500 - 1000 keV.

Experiments at the first bench will be performed in two stages: with a beam current of 1.5 A (the first stage, which was commissioned last year) and of 9 A (the second stage, which will start working after modification of the equipment).

The plasma source is an RF discharge at a frequency of about 4 MHz. Operation with a beam current of 1.5 A is performed with one channel of the RF system (40 kW); four independent channels (4 × 40 kW) will be used for a current of 9 A.

Each channel of the RF system is based on multistage amplification. The master oscillator generates the 4 MHz low-power signal. The self-tuning systems tunes the master oscillator frequency within ± 3.5% by the resonant frequency of the oscillating circuit formed by the inductor and ceramic capacitors placed on the screen of the RF emitter. The resonant frequency of this circuit depends on the plasma parameters and changes during charge combustion. An adjustable amplifier (AA) amplifies the signal from the master oscillator and thus provides control of the output power level and maintenance of stable amplitude. From the AA output, the signal is sent to the transistor pre-amplification stage. The output stage is based on cermet tetrode 4CW50000E made by Eimac (USA) on a common-cathode circuit. The preamp stage and the output stage are placed in a 800 × 800 × 2000 mm cabinet.

The high voltage anode supply (10 kV) and the screen voltage supply (1.5 kV) is common for the four channels of the system; it is placed in four 800 × 2700 × 2000 mm cabinets. The anode supply is made by a three-phase power transformer circuit with thyristor regulation at the input of the transformer. The rectifier is based on the Larionov scheme. The source is equipped with a high-speed protection system for de-energizing within 30 microseconds at a breakdown.

The RF power is supplied through the insulating transformer to the plasma emitter inductor, which is under a potential of 120 kW (Fig. 7.3.1). The transformer is single-turn and coaxial; the core is stacked of 56 magnetic ferrite rings M200VNP K180x110x20 grouped into four columns. Each ring is mounted on a radiator. The transformer is placed in a container with insulating gas. The operating overpressure is up to 2 atm. After assembly, the transformer is subjected to high-voltage training in the air with feeding from the power source, the breakdown power constrained.

Fig. 7.3.1. Insulating transformer in vessel. View from window for power output.

Fig. 7.3.2. RF system of second bench on 880 kV platform.

During the pre-burning of the first transformer in air at atmospheric pressure, the breakdown voltage increased from 30 kV to 60 kV. The transformer was tested filled with insulating gas under an overpressure of 0.2 atm. At a voltage of 120 kV no breakdowns were observed. Uneven heating of the ferrite rings was revealed during the RF tests. The ferrites were rearranged so that each cross section of the columns contained rings with the same pre-measured parameters. As a result, the heating became uniform, and the overheating did not exceed 20 degrees.

The RF system of the first stage was commissioned in 2013; in 2014 it was used in experiments with beam.

Experiments on the second bench will be carried out using one channel similar to the above (Fig. 7.3.2). The RF system of the second bench is arranged so that all the equipment is placed on a platform under a potential of 880 kV relative to the ground potential.

The anode source for the second stage of the bench was modified in 2014 (9 A). A 400 kW transformer was installed; some elements of the output filter were replaced. The mechanical installation of tube stages was completed. Parameters of ferrites for all the insulating RF transformers were measured. The transformers were assembled and pre-burnt at high voltage. The RF system of the second bench was installed on the platform. The mechanical installation and wiring of the system were completed.

7.4. ACCELERATING STRUCTURES CCDTL FOR LINAC4, CERN

As part of the upgrade of the LHC complex, Linac4 is being created at CERN – a new linear 160 MeV accelerator of H$^-$ ions. Linac4 consists of accelerating structures of various types, optimized for the respective energy range of accelerated particles. BINP together with VNIITF developed, manufactured and delivered to CERN 7 CCDTL (*Coupled Cavity Drift Tube Linac, a linear accelerator with drift tubes and coupled cells*) accelerating modules for acceleration of particles in the energy range from 50 to 104 MeV. The total length of Linac4 CCDTL section is ~ 25 m.

A CCDTL accelerating module is a π/2 structure consisting of three accelerating tanks (with two transit tubes in each) and two coupled side cells between them. The operating frequency is 352.2 MHz.

Four of the seven CCDTL accelerating modules were tuned and tested at a CERN bench in 2014 (see. Fig. 7.4.1) in regimes corresponding to those of Linac4 operation: a peak power of over 700 kW (corresponding to a voltage of 3.6 MV per tank and a maximum surface field strength of 34 MV/m), a pulse duration of 0.8 ms, a pulse repetition frequency of 2 Hz (the repetition frequency, i.e. the average power, of the test regimes is 2 times greater than the working frequency).

Four CCDTL modules were installed in the tunnel (see Fig. 7.4.2) and were tuned for work in Linac4; one module was tested as part of the RF system of the accelerator.

Tests of all the modules will be completed in the first half of 2015. A beam will be passed through the CCDTL structure in October 2015 - January 2016. Operation of Linac4 as part of the LHC injection complex will begin after the LS2 (Long Shutdown, 2018).

Fig. 7.4.1. Preparation of CCDTL module for tests in shielded hatch, CERN.

Fig. 7.7.2. CCDTL modules in Linac4 tunnel.

7.5. RF SYSTEM OF BOOSTER OF ACCELERATION COMPLEX NICA

Works on the creation of two RF stations were successfully completed in 2014. The stations will be used in the accelerator complex NICA under construction at the Joint Institute for Nuclear Research (JINR), Dubna. The RF stations were dispatched to the customer and successfully passed acceptance tests in November 2014 (Fig. 7.5.1).

The stations will be installed in the booster (an ion accelerator in the injection network of the complex). They will enable acceleration of $^{197}Au^{32}$ ions in the energy range of 6.2 MeV/nucleon up to 600 MeV/nucleon.

Each RF station provides an accelerating voltage of 5 kV across the gap in the frequency range of 0.5 - 5.5 MHz.

The cavity of the station is mounted on 4 supports. The RF power amplifier is placed in an individual compartment under the cavity. A radio rack with small-signal control electronics is placed in a radiation-proof room.

Fig. 7.5.1. Tests of acceleration station on bench at the HEP Laboratory (photo from JINR weekly *Dubna: Science, Cooperation, Progress* No.49 (4239), 19.12.2014)

7.5.1. Acceleration cavity

The acceleration cavity is formed by two segments of short-circuited coaxial lines with the accelerating gap in between (Fig. 7.5.2). A vacuum-tight ceramic insulator is installed in the gap. The diameter of the vacuum chamber is 160 mm. The vacuum chamber and the insulator are under vacuum; the rest of the cavity is with air. The main parameters of cavity are given in Table 7.5.1.

The shunt resistance was increased via filling of the air space between the conductors of the coaxial with rings of amorphous iron 5B-M. The $\varnothing 500 \times \varnothing 250 \times 15$ mm rings were ordered at the Asha metallurgical plant, Russia. The relative magnetic permeability modulus of the material of the rings is 2000 the least at 1 MHz and 500 the least at 5 MHz.

In the cavity, the rings are glued in pairs and fixed in cages attached to the outer cylindrical wall of the cavity. Adjacent pairs of rings are separated by a 10 mm gap for the cooling air to flow. Cooling is performed by part of the air flux that cools the generator tubes. The heated air is released into the environment. When in normal mode, the average power dissipation in the rings of the cavity is about 3 kW.
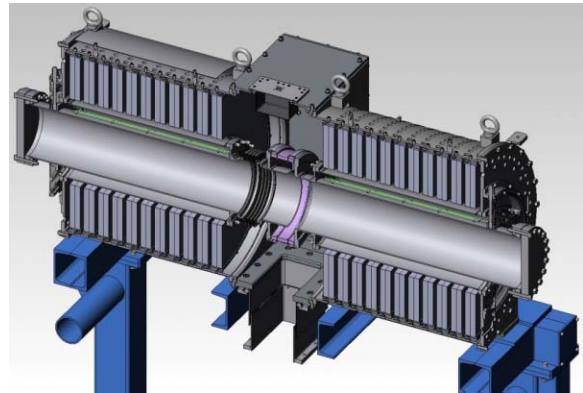
Fig.7.5.2. Section of acceleration cavity.

Table 7.5.1. Main parameters of cavity of acceleration station.

Frequency range, MHz	$0.5 - 5.5$
Voltage across the gap, kV	5
Vacuum chamber diameter, mm	160
Vacuum, no worse than, Torr	$5 \cdot 10^{-11}$
Outer diameter of station, m	1.2
Installation length, m	1.4
Admittance real part reduced to cavity gap, kOhm	1.1

The required vacuum was attained via warm-up of the vacuum chamber at a temperature of 300°C. The resulting vacuum was $3 \cdot 10^{-11}$ Torr.

7.5.2. RF power amplifier.

The output stage of the amplifier contains two tetrodes GU-36B-1 manufactured by JSC "S.E.D.-Petersburg", St. Petersburg, Russia. The tubes operate with antiphase excitation on a common-cathode circuit. The tubes are cooled with air.

The anodes of the tubes are connected through block capacitors directly to the acceleration gap of the cavity. The anode supply, Va = +4.5 kV, is connected to the anodes via throttle Др. The type of the winding allows suppression of even harmonics of the accelerating voltage in the gap.

The tubes are excited by a semiconductor preamplifier with a maximum power output of 500 watts. The maximum power at the input of the preamplifier is 1 watt. In the tests of the stations, the output power of the preamplifier-cardinality did not exceed 200 watts.

For the purpose of reduction of nonlinear distortions of the accelerating voltage, during acceleration of ions the tubes operate in a regime close to class A. For the purpose of reduction of the average power dissipated on the anode, during a pause the tubes shall be locked.

For the same purpose, during acceleration the constant component of the anode current is regulated by a predefined program using a feedback circuit. At frequencies with less load resistance, the constant component is increased. The reference voltage for this circuit is generated by a DAC in the control system.

The maximum DC component of the anode current does not exceed 8 A at a frequency of 3.3 MHz; at the frequency range edges, the current is 5 A at most. The average power dissipated on each anode of tube is 4.9 kW, the allowable value being 15 kW.

The imaginary component of the relative permeability of the ring material significantly exceeds the real-value component, so the load on the tubes that is created by the package of rings itself is almost purely active and is approximately 1 ohm. However, this load is strongly shunted by the capacitance of the insulator and the distributed capacitance of the line filled with the pack of the rings. As a result, the load impedance modulus at the edge of the frequency range (5.5 MHz) decreases almost twofold. The problem can be rectified to some extent via correction of the impedance frequency response by including inductors Lc ~ 10 µH in series with the block capacitors.

7.5.3. Control system.

The small-signal equipment for control of both stations is placed in a SCHROFF rack 2000 mm high. Using feedback loops, it controls the accelerating voltage amplitude, the DC component of the current of the anodes of the tubes, and protects the high-power elements of the station and the staff in case of emergencies.

The feedback loop adjusts the accelerating voltage amplitude by the detected voltage from the accelerating voltage sensor of the cavity. The reference voltage comes from a DAC. The time constant of the feedback loop is 150 microseconds.

The feedback loops for adjustment of the anodic currents of the tubes are separated. Meters based on Hall elements measure the anode current of the sensors. The reference voltage from the DAC is common for both the feedback loops. The loop-time constant is ~ 1 ms.

This rack also comprises a computer control crate, which includes a controller connected with the accelerator control center through the network ETHERNET. The controller manages the following electronic components:
- the master oscillator for the operating frequency of the station (using the DDS technology); the frequency is changed according to the timing signals and the growth of the magnetic guide field of the accelerator; the frequency is also corrected according to signals from pickup electrodes in the vacuum chamber of the accelerator;
- a DAC to set the accelerating voltage and the DC component of the anode current;
- an ADC for measuring the operation regimes of the station;
- control and input registers for setting and control of the operation regimes of the station.

7.6. UPGRADE OF THE RF SYSTEM OF THE MICROTRON RECUPERATOR

The RF system of the microtron recuperator of the Novosibirsk free electron laser includes two 180 MHz RF generators with a maximum power output of 600 kW each. The generators operate in continuous mode. The output stages of the generators are on tubes and consist of four modules (Fig. 7.6.1).

For the purpose of higher output power and better durability and reliability of the generators, domestic tetrodes GU-101A in the output stages were replaced with tubes TH-781 made by THALES. In 2013, the refinement of all the 8 modules of the output stages of the two generators was completed, as well as the installation of the tetrodes TH-781 in them.

In 2014, the output power of the generators was increased at the expense of raise in the anode voltage of the tubes due to a voltage boost device (Fig. 7.6.2); the low-voltage power sources of the control grids of the tubes were refined (Fig. 7.6.3); suppressors of self-excitations at non-working frequencies were designed and installed in the output stages.

As a result, each generator operates steadily at a continuous output power of 620 kW. This, in turn, enabled a 10% increase in the voltage across the accelerating cavities and, consequently, in the energy acquired by the electrons.

Fig. 7.6.1. 4-module output stage of the generator with self-excitation suppressors installed.

Fig. 7.6.2. Transformer and diode bridge (right) of anode voltage boost.

7.7. RADIO FREQUENCY ELECTRON INJECTOR FOR VNIIEF ACCELERATOR

In 2014 BINP completed the fabrication of RF electron injector for the accelerator at VNIIEF. The RF injector includes the following:

• a tube power amplifier on the tetrode GU-92A (the output power up to 16 kW in continuous mode) with a transistor preamplifier;

• a radio rack with low- and high-voltage power supplies for the tube power amplifier;

• a 100 MHz RF cavity with a cathode-grid unit, focusing solenoid, and ion pump;

• a coaxial feeder path for transmission of power from the amplifier into the cavity;

• a control unit for the cathode-grid unit (modulator);

• a radio rack with control electronics.

Fig. 7.6.3. Cabinet for low-voltage power supplies with rectifier of bias voltage boost (bottom).

Table 7.7.1 presents the main characteristics of the RF injector.

Table 7.7.1. Main characteristics of the RF injector.

Average current, mA	>40
Electron energy, keV	50÷100
Emittance, mm·mrad	10
Duration of gate pulse of modulator of cathode-grid unit, ns	1.2
Duration of bunch at maximum compression point (~ 2 m from cathode) with 100 kV across cavity, ns	0.2
Maximum repetition frequency, MHz	100
RF generator power, kW	<16
Permissible operating vacuum, Torr	$<10^{-6}$

The injector was successfully tested on a BINP stand (Fig. 7.7.1). A design average current of 40 mA was generated in the energy range of 50 to 100 keV.

The tests confirmed the assumption that the absence of cathode bombardment by reverse ions in the RF gun enabled increasing the beam average current and the lifetime of the cathodes. Indeed, for a long time, the tests were carried out at a vacuum of $5 \cdot 10^{-7}$ Torr, which was limited by outgassing from the walls of the vacuum chamber of the diagnostics bench. No cathode degradation was observed.
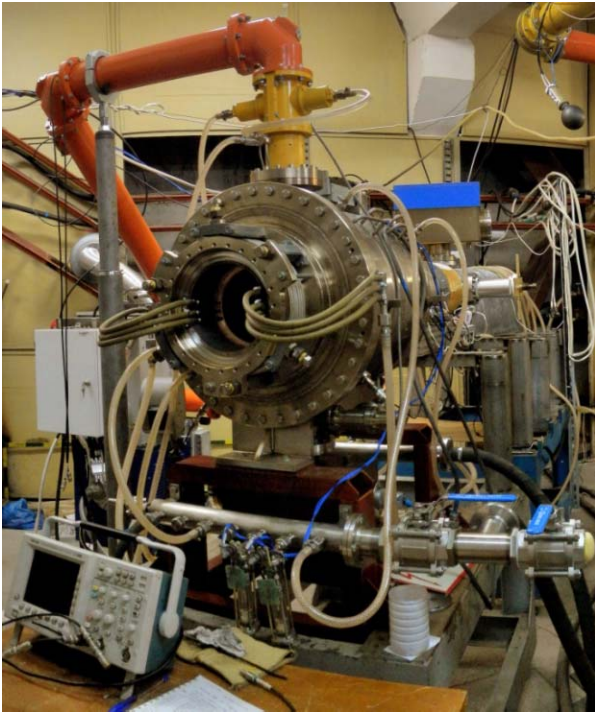
Fig. 7.7.1. RF injector during tests on BINP bench.

7.8. 100 MHz GENERATOR WITH OUTPUT POWER OF 540 kW IN CW REGIME

In 2014, BINP continued the implementation of the agreement with VNIIEF on the creation of a 100 MHz RF generator with an output power of 540 kW in CW regime.

The required power is attained via summation of the powers of three generating modules on domestic tubes GU-101A. Each module provides an output power of 180 kW at least. The powers are summed via connection of the three generation modules to the output two-wire line with a step equal to half the wavelength. Each module is controlled separately. A module comprises a semiconductor pre-amplifier with an output power of 500 W, an intermediate amplification stage on tetrode GU-92A for a power of up to 10 kW, and an output stage on tetrode GU-101A. Each module has its own high and low voltage power supplies.

The first generating unit (RF-1) was manufactured and tested. In 2010, it was delivered and put into operation at VNIIEF. The second module (RF-2) was manufactured in 2013, and the third module (RF-3) in 2014. In 2014, a test bench was constructed in a shielded room at BINP (see Fig 7.8.1), for tuning and tests of individual generator modules, as well as for tests of the power summation system. The bench comprises a power summation line, a water-cooled RF load for a continuous power of 200 kW, two generator modules, high and low voltage power supplies for the modules, and a rack with control electronics.

The generator modules RF-2 and RF-3 were tuned and tested on the bench. Each module was being tested for 12 hours at an output power of over 180 kW.

In 2015 the power summation line will be connected and the summation of the powers of the two modules with a total output power of 200 kW will be tested.

Fig. 7.8.1 Bench for tests of generator modules for VNIIEF.

7.9. UPGRADE OF RF GENERATORS OF SIBIR-2 COMPLEX

In 2013, BINP fabricated and delivered to Kurchatov Center, Moscow, elements for upgrade of the output stages of the RF generators of the complex Sibir-2. Two generators operating in continuous wave mode excite the three accelerating cavities of the complex. The powers of two tube modules are summed in the output stage of each generator. In January - February 2014, BINP members replaced all the 4 domestic tetrodes GU-101A with tetrodes TH-781 made by THALES (Fig. 7.9.1). This upgrade is supposed to increase the tube life and improve the reliability of the generators. Besides that, the pre-amplification

126

stages on tetrodes GU-92A were tuned; a system for protection of the stages against self-excitation at non-working frequencies was put into operation and the generators and the feeder system were tuned for the operating mode with beam in the storage ring Sibir-2.

Fig. 7.9.1 Panorama of generator hall of complex Sibir-2 during replacement of tubes.

8

POWERFUL ELECTRON ACCELERATORS AND BEAM TECHNOLOGIES

8.1. ILU ACCELERATOR DISTRIBUTION

Since 1983 the ILU accelerators are supplied abroad where they are used for researches and are working in the industrial lines. Some of these machines are working round the clock for years. The reliability and technical level of these machines is confirmed by the new supplies.

The ILU-8 machine along with the steel local shield and underbeam cable rewinding device was manufactured and tested in the BINP according the contract with public corporation OKB KP, Mytischi, Moscow region. This equipment is purposed for radiation treatment of cables. The equipment mounting in Mytischi is planned for 2015.

The ILU-10M machine was commissioned in the Bhabha Atomic Research Center (BARC), Mumbai, India.

The joint BINP and Novosibirsk State University research and educational laboratory on radiation technologies started its work. The electron accelerator ILU-10 (Fig. 8.1.1) is the BINP input, the conveyor transportation system (Figure 8.1.2) is the input of the Novosibirsk State University. The treatment of the medical products from Novosibirsk and adjacent regions started.

The ILU-14 electron accelerator with the removable X-ray converter was commissioned in the Burnazyan Federal Medical Biophysical Center, Moscow. The maximum electron energy is 10 MeV, beam power is up to 100 kW, the X-ray converter can is designed for beam power up to 100 kW.

The contract for ILU-10M accelerator modernization was signed, the works started. The accelerator's beam power will be increased from 12 to 50 kW. The machine will be installed in the Institute of Nuclear Physics, Alma-Ata, Kazakhstan.
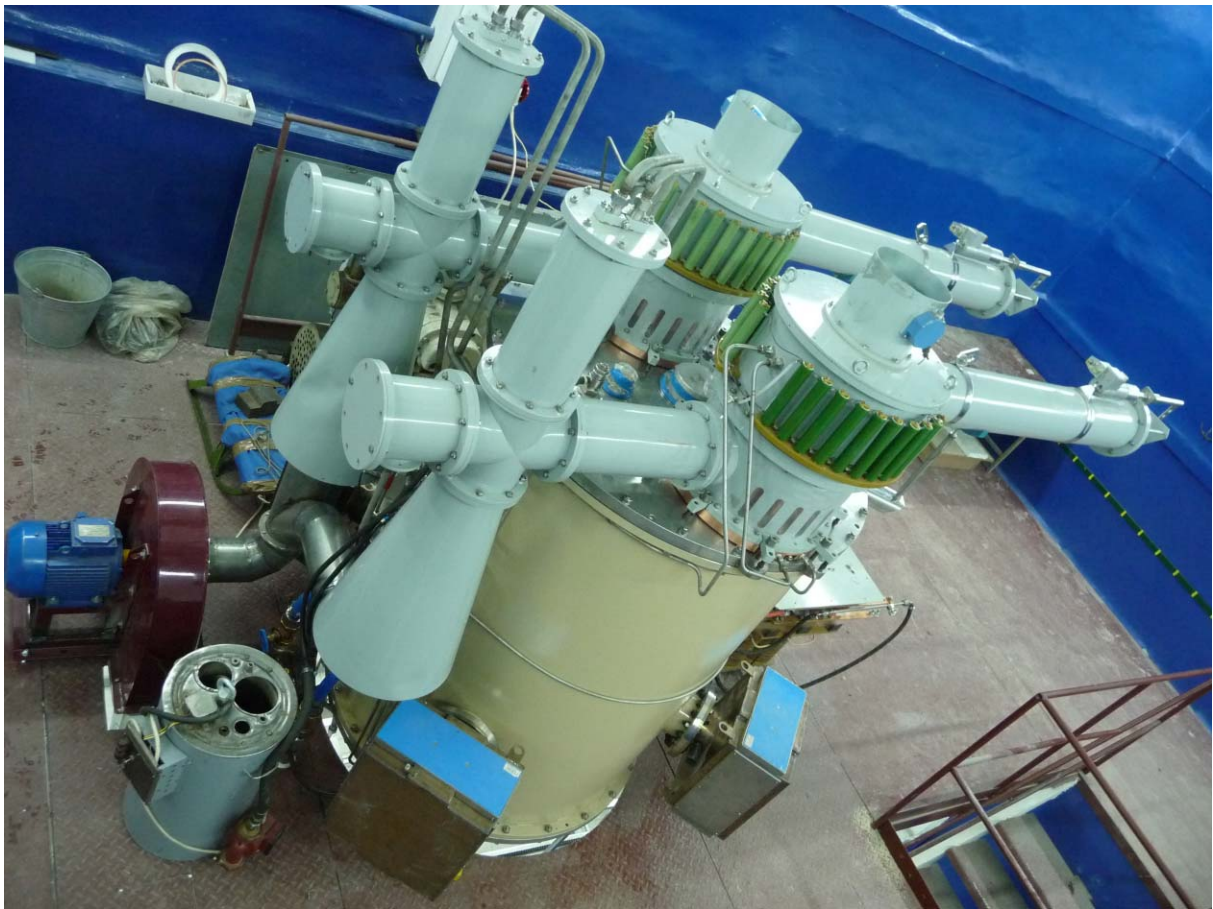
Fig. 8.1.1. ILU-10 accelerator in the joint Budker Institute of Nuclear Physics and Novosibirsk State University laboratory.

Fig. 8.1.2. Boxes with the medical products on the conveyor in the joint Budker Institute of Nuclear Physics and Novosibirsk State University laboratory.

8.2. NEW ACCELERATOR CONTROL SYSTEM DEVELOPMENT

The new accelerator control system design was worked out to replace the old one. The modern intellectual control systems based on various programmable logic controllers (PLC) were considered (Simatic Siemens, Omron lines SJ and CS, Mitsubishi line Melsec, etc.). The PLC line CompactRio produced by National Instruments was chosen.

The new accelerator control system design was developed based on the CompacRio modules. To fully replace the old control system the set of modules ought to have not less than 110 various inputs/outputs. The required set of modules was specified.

8.3. NEW RADIATION TECHNOLOGIES DEVELOPMENT

The beneficated ores radiation treatment studies were carried out in collaboration with the Institute of Mining, Siberian Branch of RAS. The radiation treatment resulted in the energy consumption decrease in the following ore reduction and increase in the output of the useful minerals containing the nonferrous metals.

The iron ore radiation-thermal treatment resulted in the phase transitions and occurrence of the magnetic properties – the magnetite formation was observed. It permits to use this process for following ore benefication.

The mixed feed electron beam treatment was carried out in collaboration with the Institute of Experimental Veterinary for Siberia and Far East, Siberian Branch of Russian Agricultural Academy, to prolong the keeping time for the products delivered to the Northern Territories of Russia.

The irradiation influence on samples made of various polymers (polyethylene, fluorocarbon polymer, polymethylmethacrylate, etc.) was carried out to study the changes in strength properties (plasto-elastic deformations). The work was performed in collaboration with the Institute of Hydrodynamics, Siberian Branch of Russian Academy of Science, to set the data for deformation analysis models.

The irradiation influence on samples made of specially prepared nylon films with various impregnations was continuing to study aiming to create the blood vessels prothetics. This work was carried out in collaboration with the Institute of Chemical Biology and Fundamental Medicine, Siberian Branch of Russian Academy of Science. The prothetics were successfully implanted in mice. The final goal – the growth of the body's own tissues on these prothetics.

The samples preparation conditions and irradiation conditions influence on the implants properties was studied.

The possibilities of electron beam treatment for the heavy hydrocarbon compounds (including tar oil and pitch) were studied in collaboration with the Institute of Solid State Chemistry and Mechanochemistry, Siberian Branch of Russian Academy of Science.

The electron beam treatment influence on the various matters was studied in collaboration with the Institute of Solid State Chemistry and Mechanochemistry, Siberian Branch of Russian Academy of Science. The work was carried out using the synchrotron radiation sources of a Siberian Center of Synchrotron and Terahertz Radiaiton.

8.4. APPLICATIONS OF INDUSTRIAL ELV ACCELERATORS IN SCIENCE AND TECHNOLOGIES

Deliveries of ELV accelerators. In 2014, four ELV accelerators were supplied to the customers. To be noticed is that there is a tendency to modernize the industrial ELV accelerators, which were supplied earlier in Russia and to CIS countries. This modernization is the reason of deterioration of general economic situation and with economic slowdown leading to the use of cost-effective existing models with the power of the electron beam up to 50 kW. In addition, the age of the accelerators being in operation, in some cases, reaches 20-25 years and in order to provide stable and uninterrupted operation of the equipment the service providers should modernize outdated production control and power systems of ELV accelerators onto modern base.

For powerful industrial electron accelerators of ELV series the new system of exchange processes rejection in the accelerating tube has been developed and successfully applied. Exchange processes in the accelerating tube have the further described mechanism. The ion, accelerated up to total voltage, strikes the top electrode of the accelerat-

ing tube and, as a result, generates several tens of secondary electrons. These electrons accelerates and, getting on metal surfaces at the outlet of the accelerating tube, can produce some ions, which are accelerated, move in the direction of the upper electrode. Thus, when appropriate multiplication factor (ion-electron and electron-ion emission) the positive feedback leading to breakdown realizes. Using the "locking" electrode with the potential reduced relatively to the upper electrode (Fig. 8.4.1), i.e. electrode, onto which the ions fall, prevents the acceleration of secondary electrons. Thus, exchange processes that lead to high-voltage breakdowns are suppressed.
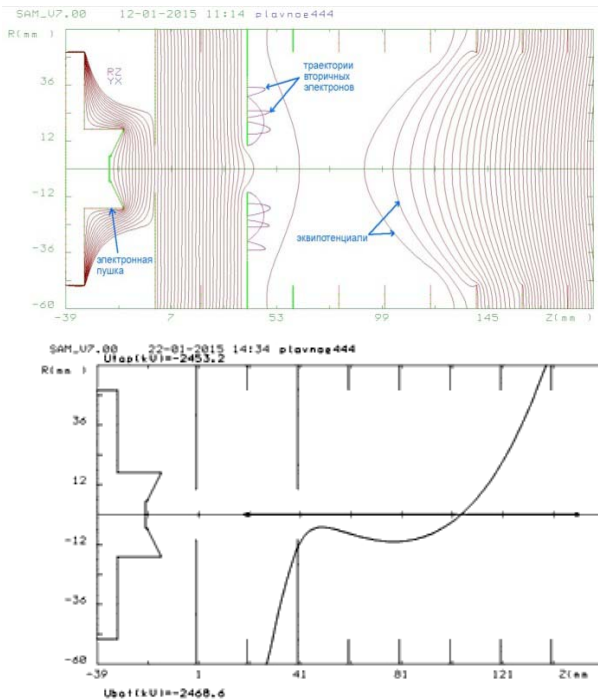
Fig 8.4.1. Electrode system and potential distribution in accelerator tube.

The result of this work was the improvement of operation parameters of industrial accelerators due to the following:

- Reduction of accelerator launch to maximum parameters by an order of time at the primary assembling and at the routine maintenance operations connected with vacuum losses in accelerator tube, such as the change of extraction window foil and exchange of electron injector.
- Increase of current stability and electron beam energy.
- Accelerator operation reliability improvement.
- Competitive recovery at the world market.

The experiments on energy pulsation and beam current decrease of ELV accelerators for industrial tomography applications were hold. As long as accelerating voltage and beam current pulsations leads to undesirable fluctua-

tion of beam location and size and to X-ray radiation intensity this decreases resolution capacity and makes it impossible to find out low-contrast objects such as plastic ingredients and spaces. Our customers formulated the requirements to those parameters as follows:

- energy pulsation on level E=1,0 MeV ≤±5%;
- current pulsations on level 100 mA ≤±2%.

To solve these problems and to satisfy the specific requirements to design the accelerator for quick tomography (see Fig. 8.4.2) based on ELV accelerator was developed and recently it is in commissioning. The specific feature of this accelerator is that accelerator tube may operate at up to 30-degree deflection to the vertical.
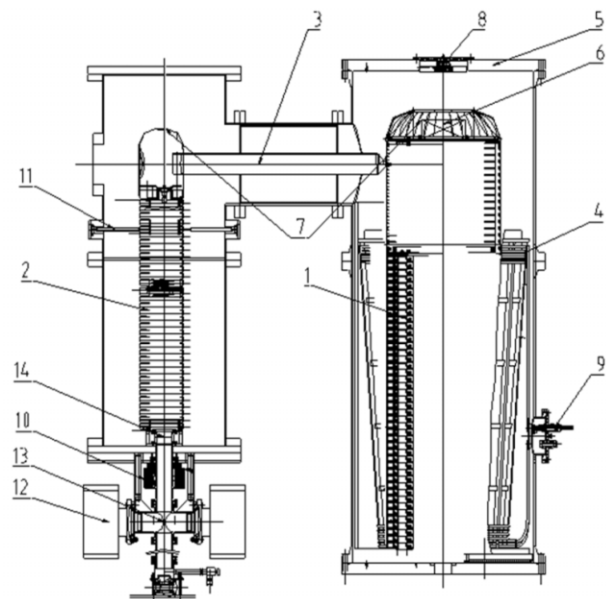
Fig. 8.4.2. 1 – rectifying sections column; 2 – accelerator tube; 3 – gas feeder; 4 – primary winding; 5 – high-pressure vessel; 6 –injector control unit; 7 high-voltage electrodes; 8 – optic elements of beam current control system; 9– primary windings outlets; 10 – lens; 11 – supports for tube holdup; 12 – vacuum system ion pump; 13 – vacuum system assembly joint; 14 – sylphon for accelerator tube fixation.

Analysis of spectrum decomposition of energy signal (Fig. 8.4.3) enabled to localize the sources of pulsation appearance and their contribution into common pulsations:

Fig. 8.4.4. 300 Hz pulsations component at different Сф in dependence on beam current.

Fig. 8.4.3. Oscillograph of energy pulsations at **E=1MeV**, **I_пучка=80 mA** (top) and spectrum performance of energy signal (lower).

300 Hz frequency peak is due to voltage ripples of inverter mains rectifier.

At the inverter input the six-phase rectifier with filter capacity C_ϕ.is installed. Voltage ripples of this rectifier of 300 Hz frequency would contribute into accelerating voltage ripples. The extension of filter capacity at frequency converter input allowed increasing of this energy pulsation component up to 5 kW, equal to ±0.5 % at a current beam of 100 мА, at an energy of 1 MeV (Fig. 8.4.4).

840 Hz frequency peak (basic) is due to double-wave made of high-voltage rectifier. Use of electric circuit with series parallel connection of rectifying sections, shown in Fig. 8.4.5, enabled to limit the pulsations at 6% level.

Third peak has 420 Hz feed voltage frequency. It appears because the capacitors of rectifying sections are feeding from different windings during different half wave. Voltage distribution across secondary windings is not completely uniform. it lightly increases from the center of the column to its upper end. that is why during that half wave, when the capacitors are charged from the upper winding, they get the less charge and, vice versa, when they are charged from the lower winding, they get higher charge, i.e. the pulsation with feeding voltage frequency appears.

Fig. 8.4.5 Accelerator rectifying section wire diagram: W-secondary windings, C=10 000 pF – filter capacitors, R=200 MOhm – resistors providing uniform distribution of voltage between series-connected capacitors.

During beam current pulsation tests the Schottky effect was found out. Schottky effect is that. Cathode saturation current depends on electric field value at its surface. The cathodes in ELV accelerators operate in the total current take-off mode, i.e. in saturation mode. Thus, if electric field will have AC component, than the beam current will pulse with the same frequency. Fig.6 shows the appearance of AC component of electric field near the cathode in accelerator. AC component in the first brake of accelerator tube (cathode brake) arises because of nonuniform distribution of accelerating voltage pulsation voltage by capacitance potential device formed by accelerator tube capacities.

134
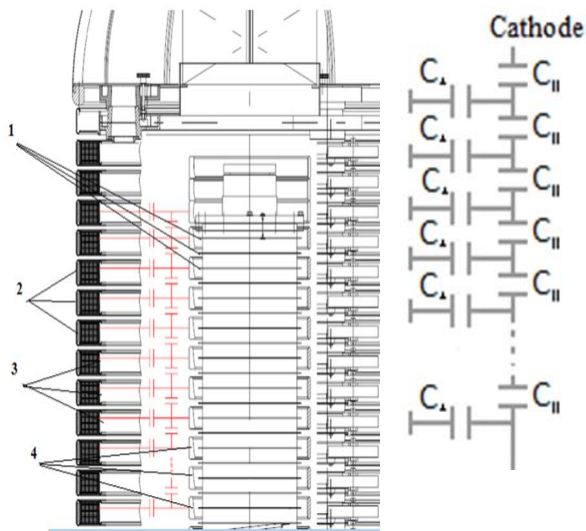
Fig. 8.4.6. Upper part of ELV-4 accelerator.
1 – Electrodes on tube; 2 – secondary windings external shields; 3 – secondary windings internal shields; 4 – Shielding rings.

Decrease of beam current pulsation was achieved due to the placement of accelerator tube out of high-voltage column and the use of additional capacitance potential device at the upper electrodes of accelerator tube (Fig.8.4.7).
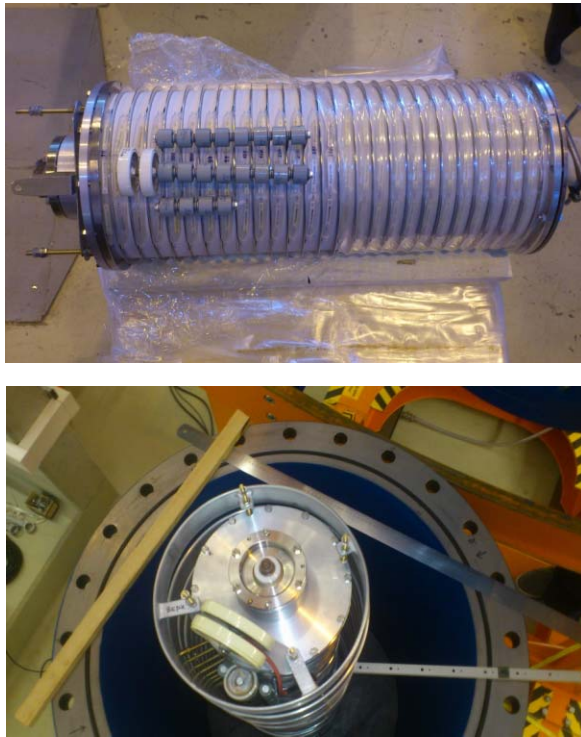
Fig.8.4.7. Additional capacitances at the accelerator tube.

Table 8.4.1 shows the results of current pulsation measurements with different capacitances connected to the tube electrodes, where 30 pF is standard capacitance between electrodes without additional connections.

Table 8.4.1. Results of current pulsation measurements.

Capacitance between electrodes	30 pF	310 pF	590 pF	3400 pF
Beam current pulsations	± 6%	± 1.3%	± 0.8%	± 0.25%
Electric field pulsation near cathode	± 21%	± 1.2%	± 0.7%	± 0.14%

Recently, the ELV accelerator meant for tomography is installed at the customers' site (Fig. 8.4.8).

At the test bench, on the basis of electron accelerator ELV-6, two experiments with the extraction of focused electron beam into air have been carried out:
   − surfacing of powder materials onto metals;
   − production of nanopowders by the method of materials evaporation from parent condensed phase.
   Surfacing onto metals. The tests on surfacing of Ti-Ta-Nb and Ti-Ta-Zr powder systems onto titanium base of BT1-0 grade for the purpose of forming corrosion-resistant surfacing within Federal special purpose programme "Experiments and development of thematic priorities of the development of scientific-technological complex of Russia for 2014-2020" had been hold (Agreement on grant-in-aid from 21th of October 2014 № 14.604.21.0135).
   Fig. 8.4.9 shows the results of experiments by means of weight method of several samples with variation of coatings chemical compounds. The 1x10x10 mm samples were cut from the coatings and put into boiling nitric acid with 68% concentration. The comparison was made with the samples of pure Ti, Nb and Ta of the same size.
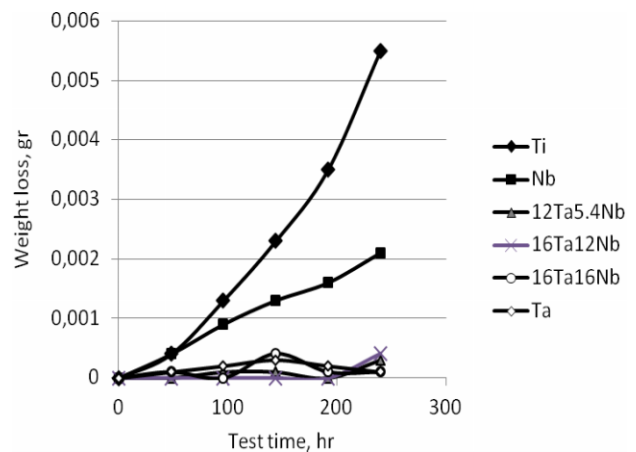
Fig. 8.4.9. Tests on corrosion-resistant coatings of Ti-Ta-Nb system in boiling nitric acid. At the right, the percentage of chemical compound of the samples is shown.

Fig.8.4.8. Accelerator for tomography ready-assembled.

Concentration of alloying components in the coatings may vary over a wide range. When forming the coatings of Ti-Ta-Zr system the triple surfacing resulted in total

alloying concentration of 60%. The same concentration of Zr achieved in a double system Ti-Zr.

Besides corrosion-resistant coatings the coatings on the titanium basis and steel substrate, distinguishing by high hardness and wear resistance, had been formed. Thus, when alloying the boron carbide powder onto BT1-0 titanium alloy plates the precipitate particles TiC and TiB of different morphology distributed in martensite titanium matrix are forming. Average value of micro-hardness of alloyed layers is 5,5 hPa, that is 3 times more than the harness of basic metal. Herewith, titanium matrix in a coating has an average hardness 4,5 hPa, titanium carbide – 7,5 hPa. Average hardness of titanium boride crystals achieves 32 hPa.

Fig. 8.4.10. Installation for anticorrosion alloying surfacing of Ta based on the titanium alloy.

In 2014 the works on nanopowder materials production with the use of electron beam extracted into air were continued.

To organize uninterrupted cycle of nanopowders production with the use of ELV-6 accelerator the installations providing the output of nanopowder collection channel outside the radiation zone in order to provide the possibility of continuous installation work without accelerator turn off had been developed and produced. To place the installations outside radiation zone a special room adjacent to the building, in which accelerator is placed, was designed and constructed.

To improve the efficiency of nanopowder production the separation system was modified. In particular, new chamber of nanopowder separation with extended filtering area and expanded delivery tubes section was produced.

The experiments of copper nanopowders production by means of electron beam evaporation at air pressure in inert-gas blanket had been hold. The works on production of carbon infrastructure were carried out.

136

9
PHYSICS FOR MEDICINE

9. VITA CURRENT STATUS

9.1. Introduction.

Nowadays boron neutron capture therapy is regarded as a promising method for the treatment of malignant tumors. Clinical trials at the reactors showed that BNCT can treat glioblastoma and brain metastases of melanoma. These types of malignant tumors are impossible to treat with any other methods. Progress of the boron neutron capture therapy in clinical trials at the reactors and the potential relevance of techniques have led to intense discussions on the development and creation of a neutron source based on a compact and low-cost accelerator.

At BINP it was proposed an original epithermal neutron source based on vacuum insulation tandem accelerator (VITA). To the present moment the study of parameters of generated neutrons was conducted, namely: energy distribution, neutron flux density and spatial distribution of neutron dose. *In vitro* studies clearly demonstrating the effect of BNCT were carried out. The effects limiting the proton beam current to the level of tens of milliamps were investigated, ways to overcome these effects were suggested.

General scheme of the accelerator is shown in Fig. 9.1. Negative hydrogen ions are generated by H^- ion source and accelerated to 1 MeV. After that they lose two electrons in charge-exchange target and accelerated again to total energy of 2 MeV. Pumping is carried out by cryogenic and turbomolecular pumps through the blinds system. High voltage is applied to the electrodes from a high voltage source through the insulator having a resistive divider.

The created accelerator is characterized by a large area of electrodes (41 m^2). Due to the absence of data on the high-voltage strength of similar systems, at first the electric intensity at the single gap (45 mm) prototype with a high-voltage electrode area of 0.7 m^2 was determined and it was 60 kV/cm. This result served as a basis for selecting the electric field intensity in inter-electrode gaps of the created accelerator (25 kV/cm). In addition to vacuum gaps, the bushing insulator also determines the high-voltage strength of the accelerator: the high-voltage strength over the surface of insulators in the form of rings, operated in the SF^6 under a pressure of over 3 atm, is over 100 kV/cm. It is also known from practice that the first surface vacuum breakdowns of insulators with a height of several centimeters occur at an intensity of ~10kV/cm. As a result, in the gas part of the designed bushing insulator (9 in Fig. 9.1), the intensity of the electric field over the surface of ceramic rings was 15 kV/cm and in the vacuum part of the insulator (8) it was 12 kV/cm over the surface of glass rings. One can see that the experimental data did not completely confirm the selection of the electric intensity in the interelectrode gaps and over the outer surface of the glass rings of the vacuum part of the bushing insulator.
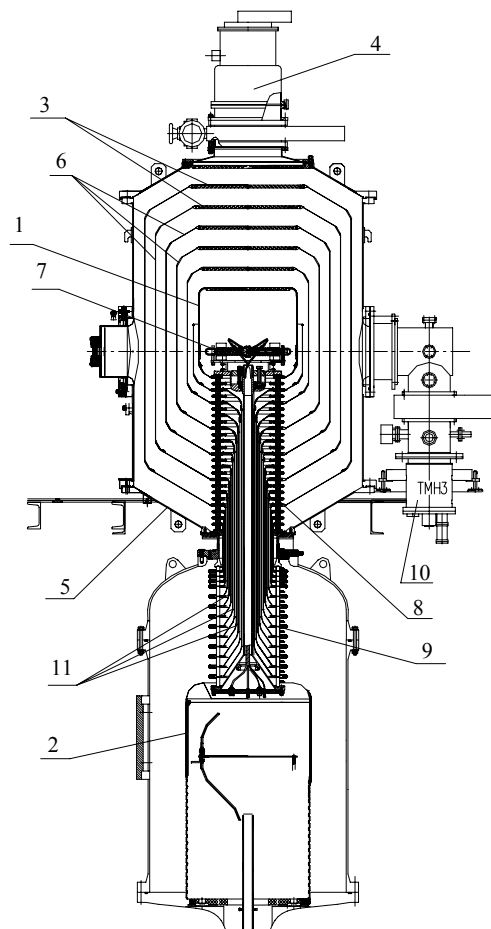
Fig. 9.1. General appearance of the six-gap tandem accelerator with the vacuum insulation: (1) high-voltage electrode of the tandem accelerator; (2) high-voltage electrode of the voltage source; (3) jalousie of the electrodes–screens; (4) cryogenic pump; (5) vacuum tank of the accelerator; (6) intermediate electrodes–screens; (7) gas stripping target; (8) vacuum part of the bushing insulator; (9) gas part of the bushing insulator; (10) turbomolecular pump; and (11) internal coaxial cylinders.

9.2. Rising of the voltage on the high-voltage vacuum gaps of the tandem accelerator with vacuum insulation.

The designed electric strength in the inter-electrode gaps and over the surface of the insulator can be achieved by the high-voltage breakdown aging. It was studied the effect of breakdowns on the electric strength of the high-voltage components of the accelerator for obtaining the required voltage at the accelerator. Due to the novelty of the design of the tandem accelerator, i.e., large area of electrodes and complex design of the bushing insulator, it was proposed to perform the breakdown aging in two stages. At first, the voltage was raised at separate gaps, and then the gaps were connected in series and the complete voltage buildup was carried out. Before the voltage

was raised, the vacuum tank of the accelerator was heated up to a temperature of 110°C by heaters located on the outer surface of the tank.

For testing both separate and serially connected gaps, a special work tool in the form of two bars moving throughout the height was designed and manufactured. The bars were attached to the insulator between the high-voltage electrode and the wall of the tank of the high-voltage rectifier. Each vacuum accelerating gap (together with corresponding gas gaps, glass and ceramic insulators) was tested for a voltage of up to 200 kV.

Figure 9.2 shows the voltage buildup at one of accelerating gaps owing to the gap-by-gap aging. One can see that the first breakdown occurred at 140 kV, corresponding to an electric intensity over the glass insulator surface of ~10kV/cm.
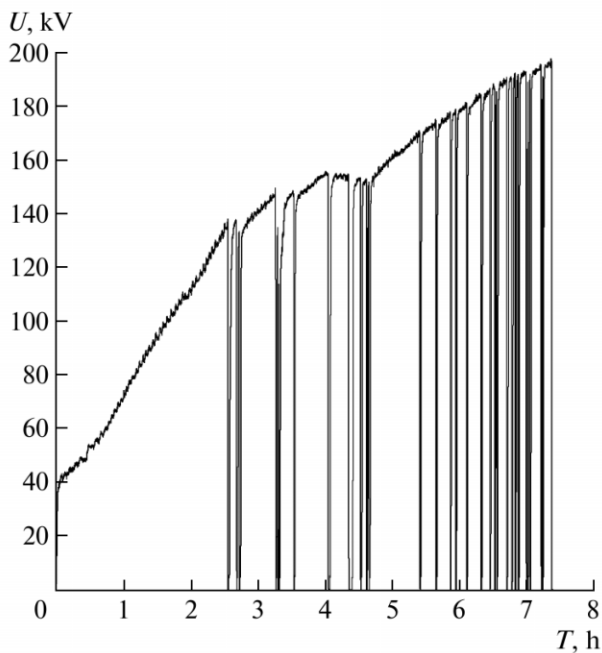
Fig. 9.2. Voltage buildup at the single gap.

The tests with gaps, which were connected in series, were performed under a 6 atm pressure of SF^6 gas inside the tank of the high-voltage rectifier, and the pressure inside the bushing insulator was 3 atm. Fig. 9.3 shows the dependences of the breakdown voltage on the number of breakdowns for one, two, three, four, and five serially connected gaps. One can see from the graphs that, as the number of gaps goes up, the breakdown voltage of the accelerator increases, and a 1 MV voltage was reached at five gaps. Intensities of ~30kV/cm (Fig. 9.4), which were reached for a short time in the experiments, are 20% higher than the working intensity (designated by the dotted curve in the graph).
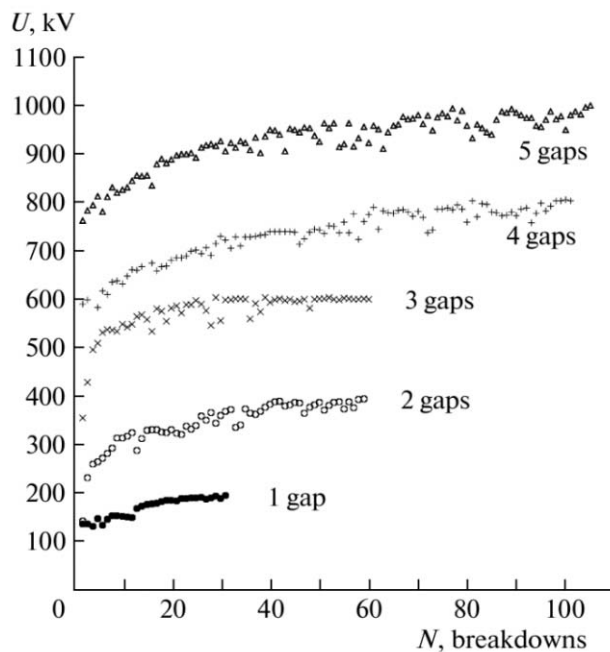
Fig. 9.3. Dependence of the breakdown voltage on the number of breakdowns.
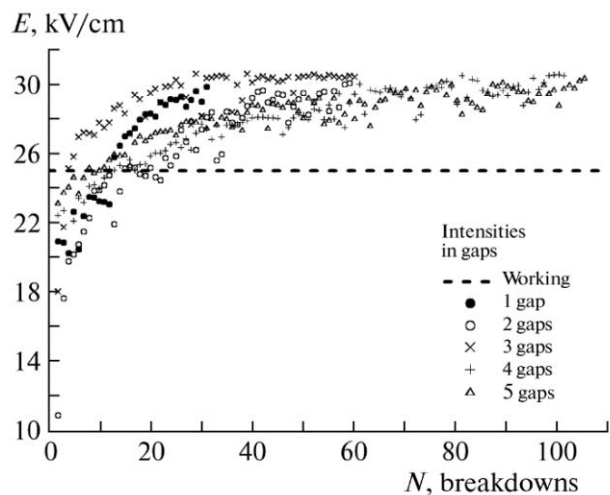
Fig. 9.4. Dependence of the intensity in the gaps on the number of breakdowns.

After high-voltage strength tests of all components of separate accelerating gaps, the full voltage was applied to the accelerator, and the aging curve of one of the first experiments is shown in Fig. 9.5(a). The first breakdown occurred at a voltage of 770 kV, corresponding to a 20 kV/cm electric intensity in the gaps. The voltage buildup and breakdowns were accompanied by changing the residual pressure in the vacuum tank. A 1 MV voltage was obtained at the accelerator, and the dynamics of reaching the operation without breakdowns is shown in Fig. 9.5. The maximal time of the voltage withstanding without breakdowns was over 2 h.

140
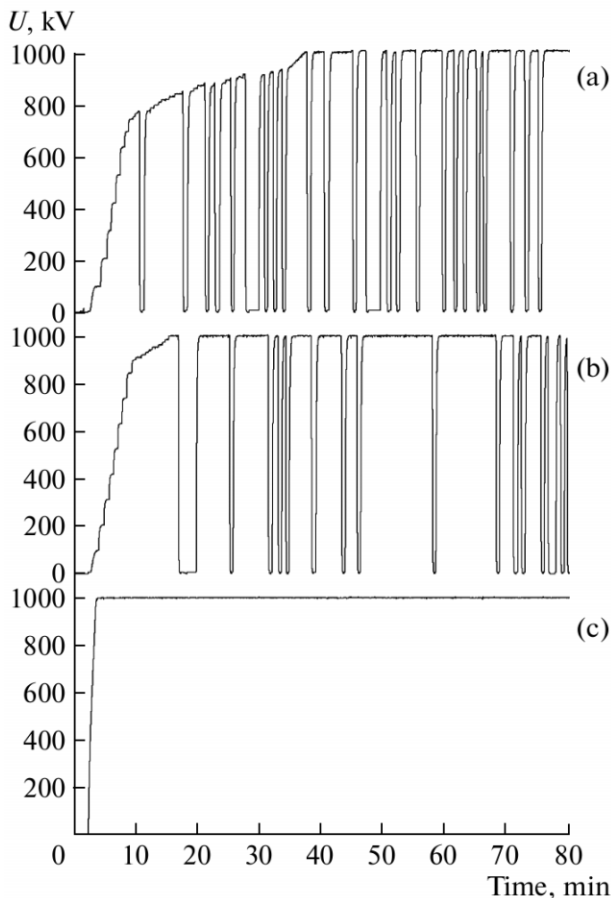
Fig. 9.5. Dynamics of reaching the operating voltage of the mode without breakdowns: (a) beginning, (b) middle, and (c) end of aging.

9.3. The concept of orthogonal neutron beam.

Now the proton beam incidents on the neutron producing target vertically. We propose to change the configuration and use the horizontal proton beam for neutron generation. The vertical positioning of the target allows to reduce significantly the size of the facility and to locate the whole facility on the same floor. It is very important advantage when planning the practical use of the source in medical clinics.

To form the therapeutic beam of epithermal neutrons the beam shaping assembly (BSA) is usually used. The BSA involves moderator, reflector, absorber, and a filter in some cases. The BSA was accurately optimized by different scientific teams for ^{7}Li(p,n)^{7}Be reaction at 2.3 – 3 MeV protons. With the characteristic proton beam current of 10 mA it provides a dose rate in tumor ~1 RBE Gy per minute, advantage depth of 9 cm, and therapeutic ratio up to 6.

In all these cases therapeutic neutron beam is coaxial with a proton beam. The next suggestion is that for the therapy we should use the orthogonal neutron beam. According to calculations performed such a beam geometry

can assure the similar quality as a beam of straight geometry. Moreover, as the energy of neutrons emitted to the side is smaller than the energy of neutrons emitted to the front, it is more suitable for obtaining a better therapeutic beam. But the suggestion is not just to use the orthogonal beam. It is very important that such orthogonal beam can be used to easily direct the beam to the patient at any angle as it is shown in Fig. 9.6.

This solution is "à la gantry" for proton therapy. The change of direction of therapeutic neutron beam is ensured by the rotation of the whole BSA or its part containing moderator around the proton beam axis.
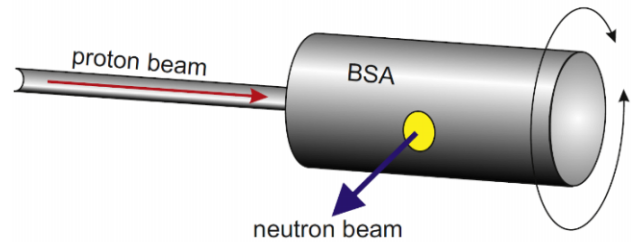
Fig. 9.6. The concept of orthogonal rotating neutron beam.

9.4. Results and prospects.

At the tandem accelerator with the vacuum insulation of electrodes it was studied the influence of breakdowns on the electric strength of high-voltage vacuum accelerating gaps. The gap-by-gap aging of all the gaps was performed. It is confirmed that the vacuum breakdowns do not reduce the high-voltage strength of the tandem accelerator. As a result of the performed experiments, the required voltage (1 MV) was reached and the stable operation of the accelerator without breakdowns was ensured within several hours.

It is proposed a new concept of the orthogonal therapeutic neutron beam, allowing us to obtain a number of advantages over traditional schemes. In particular, it is possible to apply the neutron beam to the patient at horizontal and vertical directions.

The results of the work were presented at the 52 International Student Conference at NSU; at the Scientific Student Conference "Intellectual potential of Siberia" in Novosibirsk; at Workshop on Accelerator based Neutron Production, Padova, Italy; at 16 International Congress on Neutron Capture Therapy, Helsinki, Finland; at the RUPAC-2014, Obninsk, Russia and at the Scientific and Practical Conference "Radiation technology: achievements and prospects. Nuclear Medicine", Yalta, Russia.

The results of the work are published, and also received several patents.

BIBLIOGRAPHY

List of publications 2014

[1] Grozin A. Introduction to Mathematica for physicists.. // Cham., Heidelberg, New York: Springer, 2014. - 219 p. - (Graduate Texts in Physics).

[2] M.N. Achasov, R.R. Akhmetshin, A.V. Anisenkov, V.M. Aulchenko, V.S. Banzarov, L.M. Barkov, A.Yu. Barnyakov, N.S. Bashtovoy, K.I. Beloborodov, A.V. Berdyugin, D.E. Berkaev, A.G. Bogdanchikov, A.E. Bondar, A.A. Botov, A.V. Bragin, T.V. Dimova, V.P. Druzhinin, S.I. Eidelman, D.A. Epifanov, L.B. Epshteyn, A.L. Erofeev, G.V. Fedotovich, S.E. Gayazov, V.B. Golubev, A.A. Grebenuk, K.A. Grevtsov, D.N. Grigoriev, E.M. Gromov, F.V. Ignatov, L.V. Kardapoltsev, S.V. Karpov, V.F. Kazanin, A.G. Kharlamov, B.I. Khazin, A.N. Kirpotin, I.A. Koop, A.A. Korol, S.V. Koshuba, O.A. Kovalenko, D.P. Kovrizhin, A.N. Kozyrev, E.A. Kozyrev, P.P. Krokovny, A.S. Kupich, A.E. Kuzmenko, A.S. Kuzmin, I.B. Logashenko, P.A. Lukin, A.P. Lysenko, K.A. Martin, K.Yu. Mikhailov, A.E. Obrazovsky, V.S. Okhapkin, E.V. Pakhtusova, E.A. Perevedentsev, Yu.N. Pestov, A.S. Popov, Yu.S. Popov, G.P. Razuvaev, Yu.A. Rogovsky, A.L. Romanov, A.A. Ruban, N.M. Ryskulov, A.E. Ryzhenenkov, S.I. Serednyakov, P.Yu. Shatunov, Yu.M. Shatunov, V.E. Shebalin, D.N. Shemyakin, D.A. Shtol, B.A. Shwartz, A.L. Sibidanov, Z.K. Silagadze, E.P. Solodov, I.K. Surin, A.A. Talyshev, V.M. Titov, A.V. Vasiljev, A.I. Vorobiov, Yu.V. Yudin, I.M. Zemlyansky and Yu.M. Zharinov. Results and perspectives on nucleon form factors from SND and CMD-3. // Int. J. Mod. Phys. Conf. - 2014. - Ser. 35. - 1460424.

[3] Levichev E.B., Skrinsky A.N., Tikhonov Yu.A., Todyshev K.Yu. High precision particle mass measurements using the KEDR detector at the VEPP-4M collider. // Physics Uspekhi. - 2014. - Vol. 57. - P. 66-79. [2014. - Vol 184, № 1. - P. 75-88].

[4] Mikhailichenko M.A., Ancharova U.V., Shtarklev E.A., Vlasov A.Yu., Korobeinikov M.V., Kozlov A.S., Petrov A.K., Tolochko B.P., Lyakhov N.Z. Study of the mechanically activated metal oxides reactivity in the radiation-thermal Ni-Zn ferrite synthesis. // Chemistry in behalf of sustainable development . - 2014. - Vol. 22, № 1. - P. 49-53.

[5] Zaytsev K.V., Anikeev A.V., Bagryansky P.A., Donin A.S., Korobeinikova O.A., Korzhavina M.S., Kovalenko Yu.V., Lizunov A.A., Maximov V.V., Pinzhenin E.I., Prikhodko V.V., Soldatkina E.I., Solomakhin A.L., Savkin V.Ya., Yakovlev D.V. Kinetic instability observations in the Gas Dynamic Trap. // (PLASMA-2013: Intern. Conf. on Research and Applications of Plasmas, 2-6 Sept. 2013, Warsaw, Poland). - Physica Scripta. - 2014. - Vol.: T161. - P. 014004.

[6] Kulipanov G.N., Skrinsky A.N., Serednyakov S.I., Onuchin A.P., Tumaikin G.M., Petrov V.V. The first Colliders of BINP. // The 50th anniversary of the beginning of the experiments in elementary particle physics. - Novosibirsk: INP SB RAS, 2014. - 76 p.

[7] Darin F., Kalugin I., Darin A., Rakshun Ya. The study internal structure of the annual layers in lake sediments using synchrotron radiation with X-ray focusing optics. // Acta Geologica Sinica (English edition). - 2014. - Vol. 88, SupP. 1. - P. 5-6.

[8] Darin A., Kalugin I., Maksimova N., Markovich T., Rakshun Ya., Sorokoletov D., Darin F., Ragozin D. Lake Shira level changes in late holocene. // Acta Geologica Sinica (English edition). - 2014. - Vol. 88, SupP.1. - P. 3-4.

[9] Zevakov S.A., Gauzshtein V.V., Golovin R.A., Gramolin A.V., Dmitriev V.F., Dusaev R.R., Lazarenko B.A., Mishnev S.I., Nikolenko D.M., Rachek I.A., Sadykov R.Sh., Stibunov V.N., Toporkov D.K., Shestakov Yu.V. Coherent photoproduction of neutral pion on tensor-polarized deuteron at the VEPP-3 storage ring. // Bulletin of the Russian Academy of Scinces. Physics. - 2014. - Vol. 78, № 7. - P. 826-831.

[10] Vinokurov N.A. Derivation of the equations of analytical mechanics and field theory from energy conservation law. // Uspekhi Fizicheskikh Nauk. - 2014. - Vol. 184, № 6. - P. 641-644.

[11] Dmitrieva V.D., Dubov D.Yu., Kazyritskaya O.N., Kurilko S.S., Meshkov O.I., Spitsin R.I. Spectroscopic measurement of the proton spin. // Bulletin of the Novosibirsk State University: Physics. - 2014. - Vol. 9, № 1. - P. 95-104.

[12] Ivanov A.A. Calculation of self inductance and mutual inductance of coils with rectangular cross section. // Bulletin of the Novosibirsk State University: Physics. - 2014. - Vol. 9, № 1. - P. 10-14.

[13] Gentselev A.N. Zelinsky A.G., Kondratiev V.I. Patterns for deep X-ray lithography. // Bulletin of the NSTU Sciences. - 2014. - № 1(54). - P. 78-87.

[14] Burdakov A.V., Koidan V.S., Mekler K.I., Polosatkin S.V., Postupaev V.V. Creation of a long magnetized plasma column in a metal chamber. // Plasma Physics Reports. - 2014. - Vol. 40, No. 3. - P. 161-177. [Plasma Physics Reports. - 2014. - Т. 40, № 3. - С. 223-240], ISSN 1063_780X, Pleiades Publishing, Ltd., 2014, DOI: 101134/ S1063780X14030039.

[15] Dimov G.I., Emelev I.S. Experiments to study the confinement of a target plasma in a magnetic trap with inverse plugs and circular multipole walls. // Zhurnal Tekhnicheskoi Fiziki. - 2014. - Vol. 84, № 2. - P. 27-34.

[16] Astrelin V.T., Kandaurov I.V., Trunev Yu.A. Generation of a submillisecond electron beam with a high density current in a plasma emitter diode under the conditions of open plasma boundary emission. // Technical Physics. - 2014. - Vol. 59, № 2. - P. 258-263 [Technical Physics. - 2014. - Vol. 84, № 2. – P. 106-111].

[17] Rudenko A.S., Khriplovich I.B. Gravitational four-fermion interaction in the early universe. // PHYSICS-USPEKHI - 2014. - Vol. 57, Is. 2. - P. 167-170 [PHYSICS-USPEKHI. - 2014. - Vol. 184, № 2. - P. 177-181. - ISSN 1063-7869, DOI 10.3367/UFNe.0184.201402f.0177].

[18] Korobeischikov N.G., Kalyada V.V., Shmakov A.A., Shulzhenko G.I. Experimental study of accelerated argon ion-cluster beams. // JTP Letters - 2014. - Vol. 40, № 1. - P. 50-57.

[19] V.S. Fadin, M.G. Kozlov, A.V. Reznichenko. Multi-Regge form of gluon-exchange amplitudes in supersymmetric Yang-Mills theories. // PHYSICS OF ATOMIC NUCLEI. - 2014. - Vol. 77, Is. 2. - P. 251-273. [Yadernaya Fizika. - 2014. - Vol. 77, № 2. - P. 273-294]. ISSN 1063-7788, DOI 10.1134/S1063778814020112.

[20] Shestakov Yu.V., Barkov L.M., Dmitriev V.F., Golovin R.A., Kudryavtsev V.N., Lazarenko B.A., Mishnev S.I., Nikolenko D.M., Rachek I.A., Sadykov R.Sh., Stibunov V.N., Toporkov D.K., Shekhtman L.I., Zevakov S.A. Tagging system for almost-real photons at VEPP-3 storage ring. // Physics of Particles and Nuclei Letters. - 2014. - Vol. 45, № 1. - P. 539-543.

[21] Zelenski A., Atoian G., Ritter J., Steski D., Podolyako F., Sorokin I., Vizgalov I., Klenov V., Zubets V., Davydenko V., Ivanov A., Kolmogorov A. The RHIC polarized source upgrade. // Physics of Particles and Nuclei Letters. - 2014. - Vol. 45, № 1. - P. 486-491. [Physics of Particle and Nuclei. - 2014. - Vol. 45, Is. 1. - P. 308-311]. - ISSN 1063-7796, DOI 10.1134/S1063779614011140.

[22] Koop I.A., Otboyev A.V., Shatunov P.Yu., Shatunov Yu.M. Two examples of in-flight spin flippers. // Phys. Part. Nucl. - 2014. - T. 45, №1. - P. 436-442.

[23] Obrazovsky, A.E. Serednyakov S.I. Energy dependence of $e^+e^- \to 6\pi$ and $e^+e^- \to N$ anti-N cross sections near the N anti N threshold. // Physics of Particles and Nuclei Letters. - 2014. - Vol. 99, № 5-6. - P. 363-364. [JETP LETTERS. - 2014. - Vol. 99, Is. 6. - P. 315-316].

[24] Blinov V.E. Space accelerator (in Russian). // Science first hand. - 2014. - № 1(65). - P. 25-29.

[25] Skuridin G.M., Chankina O.V., Legkodymov A.A., Baginskaya N.V., Kutsenogii K.P. Element composition and intensity of accumulation of chemical elements in the leaves of sea buckthorn (Hippiophae rhamnoides L. // Chemistry for Sustainable Development . - 2014. - Vol. 22, № 3. - P. 301-305.

[26] V.F. Dmitriev, A.I. Milstein, and S.G. Salnikov. Isoscalar amplitude dominance in e^+e^- annihilation to N $\bar{N}$ pair close to the threshold. // Physics of Atomic Nuclei. - 2014. - Vol. 77, Is. 9. - P. 1173-1177. [Yadernaya Fizika. - 2014. - Vol. 77, № 9. - P. 1234-1238. ISSN 1063-7788, DOI 10.1134/S1063778814080043.

[27] Boris Valerianovich Chirikov - the legislator of chaos (in Russian). // Novosibirsk SO RAN: - 282 p. + 16 p. - (Nauka in Siberia (in person).

[28] Aleynik V., Bashkirtsev A., Kanygin V., Kasatov D., Kuznetsov A., Makarov A., Schudlo I., Sorokin I., Taskaev S., Tiunov M. Current progress and future prospects of the VITA based neutron source. // Applied Radiation and Isotopes. - 2014. - Vol. 88, № SI (Special Issue). - P. 177-179.

[29] Scuridin G.M., Chankina O.V., Legkodymov A.A., Kreimer V.K., Baginskaya N.V. Trace element composition of Seabuckthorn (Hippophae rhamnoides L.) parts [Ксерокопия]. // Seabuckthorn. Research for a promising crop: Selected articles from ISA 2013 Congress Proc. (October 2013, Potsdam, Germany / ed.: J.-Th. Morsel, Yu. Zubarev, D. Eagl. - Norderstedt: Books on Demand, 2014. - P. 67-68.

[30] Demidov E.A., Starostin K.V., Popik V.M., Peltek S.E. Use of MALDI time-of-flight mass spectrometry for microorganism identification. // Russian Journal of Genetics: Applied Research. - 2014. - Vol. 4, № 4. - P. 254-258.

[31] A.V. Dostovalov, A.V. Dostovalov, V.P. Korolkov, S.K. Golubtsov, V.I. Kondrat'ev. Specific features of formation of self-induced gratings on metal foils during scanning by a tightly focused femtosecond laser beam. // QUANTUM ELECTRON. - 2014. - Vol. 44 (4), P. 330-334. DOI: 10.1070/QE2014v044n04ABEH015376.

[32] Alexander F. Brodnikov, Victor Ya. Cherepanov. Use of calibrators of temperature for reproduction reference of points in tiny ampoules. // JOURNAL PRIBORY. - 2014. - № 9 (171). - P. 28-33.

[33] Gauzshtein V.V., Gramolin A.V., Zevakov S.A., Loginov A.Yu., Nikolenko D.M., Rachek I.A., Sidorov A.A., Toporkov D.K. Measurement of the analyzing power of the reaction of photoproductin of negative pions in the $\Delta(1232)$-resonance region. // Russ. Phys. J.-2015,-Vol. 57, - P. 1189-1194]. [Izvestiya Vuzov. Physics - 2014. - Vol. 57, № 9. - P. 36-40].

[34] Arzhannikov A.V., Ginzburg N.S., Denisov G.G., Kalinin P.V., Peskov N.Yu, Sergeev A.S., Sinitsky S.L. A travelling-wave ring resonator with Bragg deflectors in a two-stage terahertz free-electron laser. // Technical Physics Letters. - 2014. - Vol. 40, №9. - P. 730-734. [Technical Physics Letters. - 2014. - Vol. 40, №17. - C. 11-21 (in Russian)].

[35] Aleinik V.I., Kasatov D.A., Makarov A.N., Taskaev S.Yu. Measuring the Neutron Spectrum of the Accelerator-Based Source Using the Time-of-Flight Method. // Instruments and Experimental Techniques. – 2014. - Vol. 57, No. 4. - P. 381–385.

[36] Sorokin I.N., Taskaev S.Yu. A voltage buildup at high-voltage vacuum gaps of a Tandem Accelerator with Vacuum Insulation // Instruments and Experimental Techniques. - 2014. - № 4. - P. 5-8.

[37] Kuznetsov G.I., Batazova M.A. Optics of Electron Induction Accelerator LIA-2. // Physics of Particles and Nuclei Letters. - 2014. - Vol. 11, № 5 (189). - P. 945-949.

[38] Kuksanov N.K., Fadeev S.N., Salimov R.A., Golubenko Yu.I., Kogut D.A., Korchagin A.I., Lavrukhin A.V., Nemytov P.I., Domarov E.V., Semenov A.V. Technical Means of Improving the Quality of Material Irradiation ELV by Accelerators // Particles and Nuclei Letters. - 2014. - Vol. 11, №5 (189). - P. 950-957.

[39] Blinov V.E., Bobrovnikov V.S., Zolotarev K.V., Kiselev V.A., Kononov S.A., Kurkin G.Ya., Levichev E.B., Meshkov O.I., Muchnoi N.Yu., Nikitin S.A., Nikolenko D.M., Sukhanov D.P., Tikhonov Yu.A., Tolochko B.P., Tumaikin G.M., Shamov A.G., Shatilov D.N. Status of Accelerator complex VEPP-4. // Physics of Particles and Nuclei Letters. - 2014. - Vol. 11, № 5 (189). - P. 966-980. [Physics of Particles and Nuclei Letters, 2014. - Vol. 11, № 5. - P. 620-631].

[40] Rastigeev S.A., Goncharov A.D., Klyuev V.F., Konstantinov E.S., Kutnyakova L.A., Parkhomchuk V.V., Petrozhitskii A.V., Frolov A.R. BINP AMS Adaptation for Biomedical Applications // Physics of Particles and Nuclei Letters. - 2014. - Vol. 11, № 5 (189). - P. 994-999.

[41] Rogovsky Yu.A., Berkaev D.E., Zemlyansky I.M., Zharinov Yu.M., Kasaev A.S., Koop I.A., Kyrpotin A.N., Lysenko A.P., Perevedentsev E.A., Prosvetov V.P., Romanov A.L., Senchenko A.I., Skrinsky A.N., Shatunov P.Yu., Shatunov Yu.M., Shwartz D.B. Status and Perspectives of Electron-Positron Collider VEPP-2000. // Physics of Particles and Nuclei Letters. - 2014. - Vol. 11, № 5 (189). - P. 1007-1015.

[42] D.A. Starostenko, P.V. Logachev, A.V. Akimov, A.A. Korepanov, P.A. Bak, A.N. Panov, A.A. Pachkov, A.A. Eliseev, A.V. Ottmar, Ya.V. Kulenko, D.Yu. Bolkhovityanov, G.A. Fatkin, O.A. Pavlov, G.I. Kuznetsov, I.V. Nikolaev, M.A. Batazova, A.M. Batrakov, Yu.M. Boimelshtein, and A.V. Pavlenko. The Performance Results of the LIA-2 in Radiographic Mode // Physics of Particles and Nuclei Letters. - 2014. - Vol. 11, № 5 (189). – P. 660-664. [Physics of Particles and Nuclei Letters. - 2014. - Vol. 11, №. 5. - P. 1022-1028].

[43] A. Boettcher Ju., Golubkov E.A., Egorov V.A., Zaytseva Yu.K., Zamriy V.N., Kayukov A.S., Kobets V.V., Korokin A.Zh., Minashkin V.F., Pyataev V.G., Repkin A.N., Skrypnik A.V., Sumbaev A.P., Udovichenko K.V., Shabratov V.G., Schvets V.A., Shvetsov V.N., Pavlov V.M. LUE-200 Accelerator of IREN Facility: Current Status and Development. // Physics of Particles and Nuclei Letters. - 2014. - Vol. 11, № 5 (189). - P. 1029-1039.

[44] Khriplovich I.B. Electromagnetic production of electron and positron in collisions of heavy nuclei. // JETP Letters. - 2014. - T. 100, № 8. - C. 552-554.

[45] KovalenkoYu.V. Yakovlrv D.V. An electron cyclotron resonance heating (ECRH) control and data acquisition system on the gas dynamic trap. // Instruments and Experimental Techniques. - September 2014, Volume 57, Issue 5. –P. 601-606 [2014. - № 5. - P. 93-98].

[46] Lukin P.A. Monte-Karlo methods for physicists (tutorial). - Novosibirsk: BINP SB RAS. - 2014. - 20 p.

[47] Barsukov V.P., Verhoglad A.G., Gerasimov V.V., Glebus I.S., Zavjalova M.A., Knyazev B.A., Makarov S.N., Stupak M.F., Ovchar V.K., Rodionov D.G., Choporova Yu.Yu., Shtatnov V.Yu. A terahertz scanning near-field optical microscope with an attenuated total internal reflection module. // Instruments and Experimental Techniques. - September 2014, Vol. 57, Issue 5. - P. 579-586 [2014. - № 5. - P. 68-76]

[48] Dolgov A.D., Bondar A.E. On the dark side of the Universe. // Science first hand. - 2014. - № 5 (59). - P. 24-39.

[49] Agafonov A.N., Volodkin B.O., Kaveev A.K., Knyazev B.A., Kropotov G.I., Paveliev V.S., Tukmakov K.N., Choporova Yu.Yu. Control of transverse modal spectrum of terahertz laser irradiation by binary silicon optical elements. // Computer Optics. - 2014. - Vol. 38, № 4. - P. 763-767.

[50] D.V. Yurov, V.V. Prikhod'ko. Hybrid systems for transuranic waste transmulation in nuclear power reactors: state-of-the-art and future prospects. // Uspehi-Physicheskih-Nauk. - 2014. - Vol. 184, № 11. - P. 1237-1248.

[51] Dzuba A.V. Arzhannikov A.VB. Superconducting resonators: decrease of Q-factorat high accelerating field // Bulletin of Novosibirsk State University. Series: Physics. - 2014. - Vol. 9, № 2. - P. 22-35.

[52] Tiunov M.A. The full calculation of three-dimentional quasi-stationary electromagnetic fields in approach of the strong skin effect by the method of the boundary integral equations. // Bulletin of Novosibirsk State University. Series: Physics. - 2014. - Vol. 9, № 2. - P. 36-54.

[53] Yu. A. Tsidulko, I. S. Chernoshtanov. Alfvén ion-cyclotron instability in an axisymmetric trap with oblique injection of fast atoms. // PLASMA PHYSICS REPORTS. - 2014. - Vol. 40, Is. 12. - P. 955-964. [Fizika Plazmy. - 2014. - T. 40, № 12. - P. 1074-1083]. - ISSN 1063-780X, DOI 10.1134/S1063780X1412006X].

[54] Goldenberg B.G., Lemzyakov A.G., Zelinsky A.G., Pindyurin V.F. On the direct X-ray lithographic formation of deep microstructures. // Journal of Surface Investigation. X-ray, Synchrotron and Neutron Techniques. - November 2014. - Volume 8, Issue 6. - P. 1201-1204. [Surface Investigation. X-ray, Synchrotron and Neutron Techniques. - 2014. - № 12. - P. 11-15 (in Russian).

[55] A.L. Solomakhin, P.A. Bagryansky, Yu.V. Kovalenko, V.Ya. Savkin, D. V. Yakovlev. Electron cyclotron resonance heating of plasma in the gas dynamic trap // Bulletin of Novosibirsk State University. Physics, Novosibirsk. - 2014. - Vol. 9, № 2. - P. 13-21.

[56] A.V. Bogomyagkov, V.L. Dorokhov, O.I. Meshkov, A.S. Polygalov, A.L. Shcheglov. Young's experiment on slits with an angle between them. // Bulletin of Novosibirsk State University. Physics, Novosibirsk. - 2014. - Vol. 9, № 2. - P. 173-179.

[57] Shwartz D.B., Berkaev D.E., Koop I.A., Perevedentsev E.A., Rogovsky Yu.A., Shatunov Yu.M., Levichev E.B., Romanov A.L., Shatilov D.N., Shatunov P.Yu. Recent beam-beam effects at VEPP-2000 and VEPP-4M. // ICFA Mini-Workshop on Beam-Beam Effects in Hadron Colliders, BB 2013; CERN, Geneva; Switzerland; 18-22 March 2013: Proc.. - 2014. - P. 43-49. - DOI 10.5170/CERN-2014-004.43.

[58] Eidelman S. Measurement of $e^+e^- \rightarrow$ hadrons in Novosibirsk. // Intern. Symposium Lepton and Hadron Physics at Meson-Factories, LHPMF 2013; Messina; Italy; 13-15 October 2013. - EPJ Web of Conferences: 2014. - Vol. 72. - P. 00007. - DOI10.1051/epjconf/ 20147200007.

[59] Cortese P., ALICE Collab., Budnikov D., Bugaiev K., Cheshkov C., Dobrin A., Dobrowolski T., Feofilov G., Finogeev D., Gorbunov S., Grigoriev V., Ippolitov M., Ivan C., Ivanov V., Ivanov A., Ivanov M., Ivanytskyi O., Kaplin V., Karavichev O., Karavicheva T., Karpechev E., Kazantsev A., Kisel I., Kiselev S., Kisiel A., Kondratiev V., Kondratyeva N., Konevskikh A., Korneev A., Krivda M., Kryshen E., Kucheriaev Y., Kurashvili P., Kurepin A., Kurepin A.B., Kuryakin A., Kushpil V., Kushpil S., Kvaerno H., Lakomov I., Loginov V., Malinina L., Mamonov A., Marin A., Martashvili I., Naumov N.P., Nazarenko S., Nazarov G., Nedosekin A., Nikolaev S., Nikulin V., Nikulin S., Nomokonov P., Novitzky N., Ostrowski P., Peskov V., Pestov Yu., Petrov P., Rak J., Reshetin A., Sadovsky S., Samsonov V., Senyukov S., Sukhorukov M., Vasiliev A., Vodopyanov A., Voloshin S., Voloshin K., Vrlakova J., Zinovjev G., Zynovyev M. Neutron emission from electromagnetic dissociation of Pb nuclei at v s NN = 2.76 TeV measured with the ALICE ZDC. // 1st Intern. Conf. on New Frontiers in Physics, ICFP 2012; Kolymbari, Crete; Greece; 10 June - 16 June 2012. - EPJ Web of Conferences: 2014. - Vol. 70. - P. 00073. - DOI 10.1051/epjconf/20147000073.

[60] Achasov M.N., Akhmetshin R.R., Anisenkov A.V., Aulchenko V.M., Banzarov V.S., Barkov L.M., Barnyakov A.Y., Bashtovoy N.S., Beloborodov K.I., Berdyugin A.V., Berkaev D.E., Bogdanchikov A.G., Bondar A.E., Botov A.A., Bragin A.V., Dimova A.V., Druzhinin V.P., Eidelman S.I., Epifanov D.A., Epshteyn L.B., Erofeev A.L., Fedotovich G.V., Gayazov S.E., Golubev V.B., Grebenuk A.A., Grevtsov K.A., Grigoriev D.N., Gromov E.M., Ignatov F.V., Kardapoltsev L.V., Karpov S.V., Kazanin V.F., Kharlamov A.G., Khazin B.I., Kirpotin A.N., Koop I.A., Korol A.A., Koshuba S.V., Kovalenko O.A., Kovrizhin D.P., Kozyrev A.N., Kozyrev E.A., Krokovny P.P., Kupich A.S., Kuzmenko A.E., Kuzmin A.S., Logashenko I.B., Lukin P.A., Lysenko A.P., Martin K.A., Mikhailov K.Yu., Obrazovsky A.E., Okhapkin V.S., Otboev A.V., Pakhtusova E.V., Perevedentsev E.A., Pestov Yu.N., Popov A.S., Popov Yu.S., Razuvaev G.P., Rogovsky Yu.A., Romanov A.L., Ruban A.A., Ryskulov N.M., Ryzhenenkov A.E., Serednyakov S.I., Shatunov P.Yu., Shatunov Yu.M., Shebalin V.E., Shemyakin D.N., Shtol D.A., Shwartz B.A., Shwartz D.B., Sibidanov A.L., Silagadze Z.K., Solodov E.P., Surin I.K., Talyshev A.A., Titov V.M., Vasiljev A.V., Vorobiov A.I., Yudin Yu.V., Zemlyansky I.M., Zharinov Yu.M. Precise measurements of the hadronic cross sections with the CMD-3 and SND detectors at the VEPP-2000 e^+e^- Collider. // 2nd Intern. Conf. on New Frontiers in Physics, ICNFP 2013; Kolymbari, Crete; Greece; 28 August - 5 September 2013: EPJ Web of Conferences. - 2014. - Vol. 71. - P. 00121.

[61] Huber A., Arakcheev A., Sergienko G., Steudel I., Wirtz M., Burdakov A.V., Coenen J.W., Kreter A., Linke J., Mertens P., Philipps V., Pintsuk G., Reinhart M., Samm U., Shoshin A., Schweer B., Unterberg B., Zlobinski M. Investigation of the impact of transient heat loads applied by laser irradiation on ITER-grade tungsten. // 14th Intern. Conf. on Plasma-Facing Materials and Components for Fusion Applications, PFMC 2013; Julich; Germany; 13 May - 17 May 2013. - Physica Scripta: 2014. - Vol. T159:P. 014005. - DOI 10.1088/0031-8949/2014/T159/014005.

[62] Lee R.N. LiteRed 1.4: a powerful tool for reduction of multiloop integrals. // 15TH INTERN. WORKSHOP ON ADVANCED COMPUTING AND ANALYSIS. - 2014. - Vol. 523: 15th Intern. Workshop on Advanced Computing and Analysis (MAY 16-21, 2013, Chinese Acad Sci, Inst High Energy Phys, Beijing, PEOPLES R CHINA). - P. 012059. - (Journal of Physics Conference Series). - ISSN 1742-6588, DOI 10.1088/1742-6596/523/1/012059.

[63] Anisenkov A., ATLAS Collab. Di Girolamo A., Klimentov A., Oleynik D., Petrosyan A. (AGIS: The ATLAS Grid Information System). // 20TH INTERN. CONF. ON COMPUTING IN HIGH ENERGY AND NUCLEAR. - 2014. - Vol. 513: 20th Intern. Conf. on Computing in High Energy and Nuclear (OCT 14-18, 2013, Amsterdam, NETHERLANDS). - P. 032001. - (Journal of Physics Conference Series). - ISBN 1742-6588, DOI 10.1088/1742-6596/513/3/032001.

[64] Chesnokov E.N. Kubarev V.V., Koshlyakov P.V. Rotation commensurate echo of asymmetric molecules-Molecularfingerprints in the time domain. // APPLIED PHYSICS LETTERS. - 2014. - Vol. 105, Is. 26. - P. 261107. - ISSN 0003-6951, DOI 10.1063/1.4905205.

[65] Bataev I.A., Golkovskii M.G., Losinskaya A.A., Bataev A.A., Popelyukh A.I., Hassel T., Golovin D.D. Non-vacuum electron-beam carburizing and surface hardening of mild steel. // APPLIED SURFACE SCIENCE. - 2014. - Vol. 322. - P. 6-14. - ISSN 0169-4332, DOI 10.1016/j.apsusc.2014.09.137.

[66] Silagadze Z.K. Relativistic mass and modern physics. // CANADIAN JOURNAL OF PHYSICS. - 2014. - Vol. 92, Is. 12. - P. 1643-1651. - ISSN 0008-4204, DOI 10.1139/cjp-2014-0257.

[67] Olive K.A., Particle Data Grp., Eidelman S. REVIEW OF PARTICLE PHYSICS. // CHINESE PHYSICS C. - 2014. - Vol. 38, Is. 9. - P. 090001. - ISSN 1674-1137, DOI 10.1088/1674-1137/38/9/090001.

[68] Druzhinin V.P., Kardapoltsev L.V., Tayursky V.A. // GGRESRC: A Monte Carlo generator for the two-photon process e(+)e(-) → e(+)e(-)R (J(PC)=0(-+)) in the single-tag mode. // COMPUTER PHYSICS COMMUNICATIONS. - 2014. - Vol. 185, Is. 1. - P. 236-243. - ISSN 0010-4655, DOI 10.1016/j.cpc.2013.07.017.

[69] Bondar A., Buzulutskov A., Dolgov A., Grishnyaev E., Polosatkin S., Shekhtman L., Shemyakina E., Sokolov A. Measurement of the ionization yield of nuclear recoils in liquid argon at 80 and 233 keV. // EPL. - 2014. - Vol. 108, Is. 1. - P. 12001. - ISSN 0295-5075, DOI 10.1209/0295-5075/108/12001.

[70] Aad G., ATLAS Collab., Anisenkov A.V., Bobrovnikov V.S., Bogdanchikov A.G., Kazanin V.F., Koenig A.C., Korol A.A., Malyshev V. M., Maslennikov A. L., Maximov D.A., Peleganchuk S. V., Rezanova O. L., Skovpen K.Yu., Soukharev A.M., Talyshev A.A., Tikhonov Yu A. Search for contact interactions and large extra dimensions in the dilepton channel using proton-proton collisions at root s=8 TeV with the ATLAS detector. // EUROPEAN PHYSICAL JOURNAL C. - 2014. - Vol. 74, Is. 12. - P. 3134. - ISSN 1434-6044, DOI 10.1140/epjc/s10052-014-3134-6.

[71] Aad G., ATLAS Collab., Anisenkov A.V., Bobrovnikov V.S., Bogdanchikov A.G., Kazanin V.F., Korol A.A., Malyshev V. M., Maslennikov A. L., Maximov D.A., Peleganchuk S. V., Rezanova O. L., Skovpen K.Yu., Soukharev A.M., Talyshev A.A., Tikhonov Yu A. Measurement of distributions sensitive to the underlying event in inclusive Z-boson production in pp collisions at root s=7 TeV with the ATLAS detector. // EUROPEAN PHYSICAL JOURNAL C. - 2014. - Vol. 74, Is. 12. - P. 3195. - ISSN 1434-6044, DOI 10.1140/epjc/s10052-014-3195-6.

[72] Aad G., ATLAS Collab., Anisenkov A.V., Bogdanchikov A.G., Kazanin V.F., Korol A.A., Malyshev V. M., Maximov D.A., Peleganchuk S. V., Rezanova O. L., Skovpen K.Yu., Soukharev A.M., Talyshev A.A., Tikhonov Yu. A. A measurement of the ratio of the production cross sections for W and Z bosons in association with jets with the ATLAS detector. // EUROPEAN PHYSICAL JOURNAL C. - 2014. - Vol. 74, Is. 12. - P. 3168. - ISSN 1434-6044, DOI 10.1140/epjc/s10052-014-3168-9.

[73] Aad G., ATLAS Collab., Anisenkov A.V., Bobrovnikov V.S., Bogdanchikov A.G., Kazanin V.F., Korol A.A., Malyshev V. M., Maslennikov A. L., Maximov D.A., Peleganchuk S. V., Rezanova O. L., Skovpen K.Yu., Soukharev A.M., Talyshev A.A., Tikhonov Yu. A. Measurement of the muon reconstruction performance of the ATLAS detector using 2011 and 2012 LHC proton-proton collision data. // EUROPEAN PHYSICAL JOURNAL C. - 2014. - Vol. 74, Is. 11. - P. 3130. - ISSN 1434-6044, DOI 10.1140/epjc/s10052-014-3130-x.

[74] Bevan A.J., Druzhinin V.P., Eidelman S., Poluektov A., Kuzmin A., Shwartz B., Solodov E.P., Todyshev K. Yu., Vinokurova A., Akhmetshin R., Arinstein K., Aulchenko V., Bedny I., Beiline D., Blinov V.E., Bondar A., Botov A.A., Bukin A.D., Buzykaev A.R., Dneprovsky L., Gabyshev N., Garmash A., Golubev V.B., Ivanchenko V.N., Korol A.A., Kravchenko E. A., Krokovny P., Lukin P., Matvienko D., Onuchin A.P., Romanov A.L., Root N., Serednyakov S.I., Shebalin V., Sidorov A., Sidorov V., Skovpen Yu. I., Telnov V. I., Usov Y., Vorobyev V., Yushkov A. N., Zhilich V., Zhulanov V., Zyukova O. The Physics of the B Factories. // EUROPEAN PHYSICAL JOURNAL C. - 2014. - Vol. 74, Is. 11. - P. I-898. - (In the list of authors mistakenly indicated Romanov L.). - ISSN 1434-6044, DOI 10.1140/epjc/s10052-014-3026-9.

[75] Aad G., ATLAS Collab., Anisenkov A.V., Bobrovnikov V.S., Bogdanchikov A.G., Kazanin V.F., Korol A.A., Malyshev V. M., Maslennikov A. L., Maximov D.A., Peleganchuk S. V., Rezanova O. L., Skovpen K.Yu., Soukharev A.M., Talyshev A.A., Tikhonov Yu. A. Measurements of jet vetoes and azimuthal decorrelations in dijet events produced in pp collisions at root s=7 TeV using the ATLAS detector. // EUROPEAN PHYSICAL JOURNAL C. - 2014. - Vol. 74, Is. 11. - P. 3117. - ISSN 1434-6044, DOI 10.1140/epjc/s10052-014-3117-7.

[76] Aad G., ATLAS Collab., Anisenkov A.V., Bobrovnikov V.S., Bogdanchikov A.G., Kazanin V.F., Korol A.A., Malyshev V. M., Maslennikov A.L., Maximov D.A., Peleganchuk S. V., Rezanova O.L., Skovpen K.Yu., Soukharev A.M., Talyshev A.A., Tikhonov Yu.A. Measurement of the t(t)over-bar production cross-section using e mu events with b-tagged jets in pp collisions at root s=7 and 8 TeV with the ATLAS detector. // EUROPEAN PHYSICAL JOURNAL C. - 2014. - Vol. 74, Is. 10. - P. 3109. - ISSN 1434-6044, DOI 10.1140/epjc/s10052-014-3109-7.

[77] Brambilla, N. Eidelman S., et al. QCD and strongly coupled gauge theories: challenges and perspectives. // EUROPEAN PHYSICAL JOURNAL C. - 2014. - Vol. 74, Is. 10. - P. 2981. - ISSN 1434-6044, DOI 10.1140/epjc/s10052-014-2981-5.

[78] Abelev B. ALICE Collab., Pestov Y. Neutral pion production at midrapidity in pp and Pb-Pb collisions at root(NN)-N-S=2.76 TeV. // EUROPEAN PHYSICAL JOURNAL C. - 2014. - Vol. 74, Is. 10. - P. 3108. - ISSN 1434-6044, DOI 10.1140/epjc/s10052-014-3108-8.

[79] Abelev B. ALICE Collab., Pestov Y. Event-by-event mean p(T) fluctuations in pp and Pb-Pb collisions at the LHC. // EUROPEAN PHYSICAL JOURNAL C. - 2014. - Vol. 74, Is. 10. - P. 3077. - ISSN 1434-6044, DOI 10.1140/epjc/s10052-014-3077-y.

[80] Aaij R., LHCb Collab., Bondar A., Eidelman S., Krokovny P., Kudryavtsev V., Poluektov A., Shekhtman L., Vorobyev V. Study of χ(b) meson production in pp collisions at root s=7 and 8 TeV and observation of the decay χ_b (3P) → γ(3S) γ. // EUROPEAN PHYSICAL JOURNAL C. - 2014. - Vol. 74, Is. 10. - P. 3092. - ISSN 1434-6044, DOI 10.1140/epjc/s10052-014-3092-z.

[81] Aad G., ATLAS Collab., Anisenkov A.V., Bobrovnikov V.S., Bogdanchikov A.G., Kazanin V.F., Korol A.A., Malyshev V.M., Maslennikov A.L., Maximov D.A., Peleganchuk S.V., Rezanova O.L., Skovpen K.Yu., Soukharev A.M., Talyshev A.A., Tikhonov Yu. A. Electron and photon energy calibration with the ATLAS detector using LHCRun 1 data. // EUROPEAN PHYSICAL JOURNAL C. - 2014. - Vol. 74, Is. 10. - P. 3071. - ISSN 1434-6044, DOI 10.1140/epjc/s10052-014-3071-4.

[82] Aad G., ATLAS Collab., Anisenkov A.V., Bobrovnikov V.S., Bogdanchikov A.G., Kazanin V.F., Korol A.A., Malyshev V.M., Maslennikov A.L., Maximov D.A., Peleganchuk S.V., Rezanova O.L., Skovpen K.Yu., Soukharev A.M., Talyshev A.A., Tikhonov Yu. A. Light-quark and gluon jet discrimination in collisions at root s=7 TeVwith the ATLAS detector. // EUROPEAN PHYSICAL JOURNAL C. - 2014. - Vol. 74, Is. 8. - P. 3023. - ISSN 1434-6044, DOI 10.1140/epjc/s10052-014-3023-z.

[83] Aad G., ATLAS Collab., Anisenkov A.V., Bobrovnikov V.S., Bogdanchikov A.G., Kazanin V.F., Korol A.A., Malyshev V.M., Maslennikov A.L., Maximov D.A., Peleganchuk S.V., Rezanova O.L., Skovpen K.Yu., Soukharev A.M., Talyshev A.A., Tikhonov Yu. A. Measurement of the centrality and pseudorapidity dependence of the integrated elliptic flow in lead-lead collisions at root S-NN=2.76 TeV with the ATLAS detector. // EUROPEAN PHYSICAL JOURNAL C. - 2014. - Vol. 74, Is. 8. - P. 2982. - ISSN 1434-6044, DOI 10.1140/epjc/s10052-014-2982-4.

[84] Abelev, B. ALICE Collab., Pestov Y. Measurement of quarkonium production at forward rapidity in collisions at TeV. // EUROPEAN PHYSICAL JOURNAL C. - 2014. - Vol. 74, Is. 8. - P. 2974. - ISSN 1434-6044, DOI 10.1140/epjc/s10052-014-2974-4.

[85] Aad G., ATLAS Collab., Anisenkov A.V., Bobrovnikov V.S., Bogdanchikov A.G., Kazanin V.F., Korol A.A., Malyshev V. M., Maslennikov A.L., Maximov D.A., Peleganchuk S. V., Rezanova O.L., Skovpen K.Yu., Soukharev A.M., Talyshev A.A., Tikhonov Yu.A. Measurement of the underlying event in jet events from 7 proton-proton collisions with the ATLAS detector. // EUROPEAN PHYSICAL JOURNAL C. - 2014. - Vol. 74, Is. 8. - P. 2965. - ISSN 1434-6044, DOI 10.1140/epjc/s10052-014-2965-5.

[86] Aad G., ATLAS Collab., Anisenkov A.V., Bobrovnikov V.S., Bogdanchikov A.G., Kazanin V.F., Korol A.A., Malyshev V.M., Maslennikov A.L., Maximov D.A., Peleganchuk S.V., Rezanova O.L., Skovpen K.Yu., Soukharev A.M., Talyshev A.A., Tikhonov Yu.A. Electron reconstruction and identification efficiency measurements with the ATLAS detector using the 2011 LHC proton-proton collision data. // EUROPEAN PHYSICAL JOURNAL C. - 2014. - Vol. 74, Is. 7. - P. 2941. - ISSN 1434-6044, DOI 10.1140/epjc/s10052-014-2941-0.

[87] Aad G., ATLAS Collab., Anisenkov A.V., Beloborodova O.L., Bobrovnikov V.S., Bogdanchikov A.G., Kazanin V.F., Korol A.A., Maslennikov A. L., Maximov D.A., Orlov I., Peleganchuk S. V., Schamov A.G., Skovpen K.Yu., Soukharev A.M., Talyshev A.A., Tikhonov Yu.A. The differential production cross section of the φ(1020) meson in roots=7 TeV pp collisions measured with the ATLAS detector. // EUROPEAN PHYSICAL JOURNAL C. - 2014. - Vol. 74, Is. 7. - P. 2895. - ISSN 1434-6044, DOI 10.1140/epjc/s10052-014-2895-2.

[88] Aad G., ATLAS Collab., Anisenkov A.V., Beloborodova O.L., Bobrovnikov V.S., Bogdanchikov A.G., Kazanin V.F., Korol A.A., Malyshev V.M., Maslennikov A.L., Maximov D.A., Peleganchuk S.V., Skovpen K.Yu., Soukharev A.M., Talyshev A.A., Tikhonov Yu.A. Search for direct top squark pair production in events with a boson-jets and missing transverse momentum in TeV collisions with the ATLAS detector. // EUROPEAN PHYSICAL JOURNAL C. - 2014. - Vol. 74, Is. 6. - P. 2883. - ISSN 1434-6044, DOI 10.1140/epjc/s10052-014-2883-6.

[89] Aaij R., LHCb Collab., Bondar A., Eidelman S., Krokovny P., Kudryavtsev V., Poluektov A., Shekhtman L., Vorobyev V. Measurement of charged particle multiplicities and densities in pp collisions root s=7 TeV in the forward region. // EUROPEAN PHYSICAL JOURNAL C. - 2014. - Vol. 74, Is. 5. - P. 2888. - ISSN 1434-6044, DOI 10.1140/epjc/s10052-014-2888-1.

[90] Aaij R., LHCb Collab., Bondar A., Eidelman S., Krokovny P., Kudryavtsev V., Poluektov A., Shekhtman L., Vorobyev V. Measurement of ψ(2S) polarisation in pp collisions at root s=7 TeV. // EUROPEAN PHYSICAL JOURNAL C. - 2014. - Vol. 74, Is. 5. - P. 2872. - ISSN 1434-6044, DOI 10.1140/epjc/s10052-014-2872-9.

[91] Aaij R., LHCb Collab., Bondar A., Eidelman S., Krokovny P., Kudryavtsev V., Poluektov A., Shekhtman L., Vorobyev V. Measurement of the B-c(+) meson lifetime using B-c(+) → J/ψ μ+ν X - μ decays. // EUROPEAN PHYSICAL JOURNAL C. - 2014. - Vol. 74, Is. 5. - P. 2839. - ISSN 1434-6044, DOI 10.1140/epjc/s10052-014-2839-x.

[92] Aaij R., LHCb Collab., Bondar A., Eidelman S., Krokovny P., Kudryavtsev V., Poluektov A., Shekhtman L., Vorobyev V. Measurement of Upsilon production in collisions at root s=2.76 TeV. // EUROPEAN PHYSICAL JOURNAL C. - 2014. - Vol. 74, Is. 4. - P. 2835. - ISSN 1434-6044, DOI 10.1140/epjc/s10052-014-2835-1.

[93] Korneev V.N., Lanina N.F., Zabelin A.V., Tolochko B.P., Vazina A.A. Instrumental and methodical approaches to the study of thetrans formation of nanostructural parameters in biological objects. // GLASS PHYSICS AND CHEMISTRY. - 2014. - Vol. 40, Is. 4. - P. 457-466. - ISSN 1087-6596, DOI 10.1134/ S108765961404004X.

[94] Grigoriev D.N., Akhmetshin R.R., Babichev E.A., Borovlev YuA., Chistokhin I.B., Ivannikova N.V., Kazanin V.F., Kuznetsov G.N., Postupaeva A.G., Shlegel

V.N., Vasiliev Ya.V. The Radiation hard BGO crystals for astrophysics applications. // IEEE TRANSACTIONS ON NUCLEAR SCIENCE. - 2014. - Vol. 61, Is. 4. - P. 2392-2396. - ISSN 0018-9499, DOI 10.1109/TNS.2014.2327996.

[95] Khriplovich I.B. Rudenko A.S. Gravitational four-fermion interaction in the early Universe. // II RUSSIAN-SPANISH CONGRESS ON PARTICLE AND NUCLEAR PHYSICS AT ALL. - 2014. - Vol. 1606: 2nd Russian-Spanish Congress on Particle and Nuclear Physics at all (OCT 01-04, 2013, St Petersburg, RUSSIA): AIP Conference Proc.. - P. 121-127. - ISSN 0094-243X, DOI 10.1063/1.4891123.

[96] Barsukov V.P., Verhoglad A.G., Gerasimov V.V., Glebus I.S., Zavyalova M.A., Knyazev B.A., Makarov S.N., Stupak M.F., Ovchar V.K., Rodionov D.G., Choporova Yu.Yu., Shtatnov V.Yu. A terahertz scanning near-field optical microscope with an attenuated total internal reflection module. // INSTRUMENTS AND EXPERIMENTAL TECHNIQUES. - 2014. - Vol. 57, Is. 5. - P. 579-586. - ISSN 0020-4412, DOI 10.1134/S0020441214040125.

[97] Kovalenko Yu.V. Yakovlev D.V. An ECRH control and data acquisition system on the gas dynamic trap. // INSTRUMENTS AND EXPERIMENTAL TECHNIQUES. - 2014. - Vol. 57, Is. 5. - P. 601-606. - ISSN 0020-4412, DOI 10.1134/S0020441214050078.

[98] Aleinik V.I., Kasatov D.A., Makarov A.N., Taskaev S.Yu. Measuring the neutron spectrum of the accelerator-based source using the time-of-flight method. // INSTRUMENTS AND EXPERIMENTAL TECHNIQUES. - 2014. - Vol. 57, Is. 4. - P. 381-385. - ISSN 0020-4412, DOI 10.1134/S0020441214030026.

[99] Sorokin I.N. Taskaev S.Yu. A voltage buildup at high-voltage vacuum gaps of a tandem accelerator with vacuum insulation. // INSTRUMENTS AND EXPERIMENTAL TECHNIQUES. - 2014. - Vol. 57, Is. 4. - P. 377-380. - ISSN 0020-4412, DOI 10.1134/S0020441214030099.

[100] Abelev, B. ALICE Collab., Pestov Y. Performance of the ALICE experiment at the CERN LHC. // INTERN. JOURNAL OF MODERN PHYSICS A. - 2014. - Vol. 29, Is. 24. - P. 1430044. - ISSN 0217-751X, DOI 10.1142/S0217751X14300440.

[101] Khriplovich I.B. Electromagnetic Production of an electron-positron pair in collisions of heavy nuclei. // JETP LETTERS. - 2014. - Vol. 100, Is. 8. - P. 494-496. - ISSN 0021-3640, DOI 10.1134/S0021364014200077.

[102] Dimov, G.I. Helium-3 from the moon for the low radioactive nuclear energetics. // JOURNAL OF FUSION ENERGY. - 2014. - Vol. 33, Is. 5. - P. 453-455. - ISSN 0164-0313, DOI 10.1007/s10894-014-9711-8.

[103] Aad G., ATLAS Collab., Anisenkov A.V., Bobrovnikov V.S., Bogdanchikov A.G., Kazanin V.F., Korol A.A., Malyshev V.M., Maslennikov A.L., Maximov D.A., Peleganchuk S.V., Rezanova O.L., Skovpen K.Yu., Soukharev A.M., Tikhonov Yu.A. Search for pair and single production of new heavy quarks that decay toa Z boson and a third-generation quark in pp collisions at root s=8 TeVwith the ATLAS detector. // JOURNAL OF HIGH ENERGY PHYSICS. - 2014. - Is. 11. - P. 104. - ISSN 1029-8479, DOI 10.1007/JHEP11(2014)104.

[104] Aad G., ATLAS Collab., Anisenkov A., Bobrovnikov V.S., Bogdanchikov A.G., Kazanin V.F., Korol A.A., Malyshev V. M., Maslennikov A. L., Maximov D.A., Peleganchuk S. V., Rezanova O. L., Skovpen K.Yu., Soukharev A.M., Talyshev A.A., Tikhonov Yu. A. Search for long-lived neutral particles decaying into lepton jets inproton-proton collisions at root s=8 Tev with the ATLAS detector. // JOURNAL OF HIGH ENERGY PHYSICS. - 2014. - Is. 11. - P. 088. - ISSN 1029-8479, DOI 10.1007/JHEP11(2014)088.

[105] Aaij R., LHCB Collab. Bondar A., Eidelman S, Krokovny P., Poluektov A., Shekhtman L., Vorobyev V. Measurement of CP asymmetry in B-s(0) - D-s(-/+) K--/+ decays. // JOURNAL OF HIGH ENERGY PHYSICS. - 2014. - Is. 11. - P. UNSP 060. - ISSN 1029-8479, DOI 10.1007/JHEP11(2014)060.

[106] Aad G., ATLAS Collab., Anisenkov A.V., Bobrovnikov V.S., Bogdanchikov A.G., Kazanin V.F., Korol A.A., Malyshev V.M., Maslennikov A.L., Maxiimov D.A., Peleganchuk S.V., Rezanova O.L., Skovpen K.Yu., Soukharev A.M., Talyshev A.A., Tikhonov Yu.A. Search for neutral Higgs bosons of the minimal supersymmetric standard model in pp collisions at root s=8 TeV with the ATLAS detector. // JOURNAL OF HIGH ENERGY PHYSICS. - 2014. - Is. 11. - P. 056. - ISSN 1029-8479, DOI 10.1007/JHEP11(2014)056.

[107] Santelj L., BELLE Collab. Aulchenko V., Bondar A., Eidelman S., Gabyshev N., Garmash A., Krokovny P., Kuzmin A., Matvienko D., Shebalin V., Vorobyev V, Zhilich V., Zhulanov V. Measurement of time-dependent CP violation in $B^0 \to \eta'K^0$ decays. // JOURNAL OF HIGH ENERGY PHYSICS. - 2014. - Is. 10. - P. UNSP 165. - ISSN 1029-8479, DOI 10.1007/JHEP10(2014)165.

[108] Aad G., ATLAS Collab., Anisenkov A.V., Bobrovnikov V.S., Bogdanchikov A.G., Kazanin V.F., Korol A.A., Malyshev V.M., Maslennikov A.L., Maxiimov D.A., Peleganchuk S.V., Rezanova O.L., Skovpen K.Yu., Soukharev A.M., Talyshev A.A., Tikhonov Yu.A. Measurement of differential production cross-sections for a Z boson inassociation with b-jets in 7 TeV proton-proton collisions with the ATLAS detector. // JOURNAL OF HIGH ENERGY PHYSICS. - 2014. - Is. 10. - P. 141. - ISSN 1029-8479, DOI 10.1007/JHEP10(2014)141.

[109] Aad G., ATLAS Collab., Anisenkov A.V., Bobrovnikov V.S., Bogdanchikov A.G., Kazanin V.F., Korol A.A., Malyshev V.M., Maslennikov A.L., Maxiimov D.A., Peleganchuk S.V., Rezanova O.L.,

Skovpen K.Yu., Soukharev A.M., Talyshev A.A., Tikhonov Yu.A. Search for the direct production of charginos, neutralinos and staus infinal states with at least two hadronically decaying tau s and missing transverse momentum in pp collisions at root s=8 TeV with the ATLAS detector. // JOURNAL OF HIGH ENERGY PHYSICS. - 2014. - Is. 10. - P. 096. - ISSN 1029-8479, DOI 10.1007/JHEP10(2014)096.

[110] Aaij R., LHCb Collab., Bondar A., Eidelman S, Krokovny P., Poluektov A., Shekhtman L., Vorobyev V. Measurement of the CKM angle γ using B $\rightarrow$ DK with D $\rightarrow$ KS$\pi^+\pi^-$, KSK$^+$K$^-$, decays. // JOURNAL OF HIGH ENERGY PHYSICS. - 2014. - Is. 10. - P. 097. - P. 1-52. [arXiv:1408.2748 [hep-ex]].

[111] Aaij R., LHCb Collab., Bondar A., Eidelman S, Krokovny P., Poluektov A., Shekhtman L., Vorobyev V. Measurement of the chi(b) (3 P) mass and of the relative rate of chi(b1)(1 P) and chi(b2) (1 P) production. // JOURNAL OF HIGH ENERGY PHYSICS. - 2014. - Is. 10. - P. 088. - ISSN 1029-8479, DOI 10.1007/ JHEP10(2014)088.

[112] Aad G., Anisenkov A.V., Bobrovnikov V.S., Bogdanchikov A.G., Kazanin V.F., Korol A.A., Malyshev V.M., Maslennikov A.L., Maximov D.A., Peleganchuk S.V., Rezanova O.L., Skovpen K.Yu., Soukharev A.M., Talyshev A.A., Tikhonov Yu.A. Search for strong production of supersymmetric particles in final states with missing transverse momentum and at least three b-jets at root s=8TeV proton-proton collisions with the ATLAS detector. // JOURNAL OF HIGH ENERGY PHYSICS. - 2014. - Is. 10. - P. UNSP 024. - ISSN 1029-8479, DOI 10.1007/JHEP10(2014)024.

[113] Aaij R., LHCb Collab., Bondar A., Eidelman S, Krokovny P., Poluektov A., Shekhtman L., Vorobyev V. Search for CP violation in D (+/-) - (KSK +/-)-K-0 and D-s(+/-) -K-S(0)pi(+/-) decays. // JOURNAL OF HIGH ENERGY PHYSICS. - 2014. - Is. 10. - P. 025. - ISSN 1029-8479, DOI 10.1007/JHEP10(2014)025.

[114] Aaij R., LHCb Collab. Bondar A., Eidelman S, Krokovny P., Poluektov A., Shekhtman L., Vorobyev V., Search for CP violation using T-odd correlations in D-0 -K+K-pi(+)pi(-) decays. // JOURNAL OF HIGH ENERGY PHYSICS. - 2014. - Is. 10. - P. 005. - ISSN 1029-8479, DOI 10.1007/JHEP10(2014)005.

[115] Aad G., ATLAS Collab., Anisenkov A.V., Bobrovnikov V.S., Bogdanchikov A.G., Kazanin V.F., Korol A.A., Malyshev V.M., Maslennikov A.L., Maxiimov D.A., Peleganchuk S.V., Rezanova O.L., Skovpen K.Yu., Soukharev A.M., Talyshev A.A., Tikhonov Yu.A. Search for squarks and gluinos with the ATLAS detector in final states with jets and missing transverse momentum using root s=8 TeV proton-proton collision data. // JOURNAL OF HIGH ENERGY PHYSICS. - 2014. - Is. 9. - P. 176. - ISSN 1029-8479, DOI 10.1007/JHEP09(2014)176.

[116] Aaij R., LHCb Collab., Bondar A., Eidelman S, Krokovny P., Poluektov A., Shekhtman L., Vorobyev V. Measurement of CP asymmetries in the decays B^0 $\rightarrow$ K$^-_0$ $\mu^+\mu^-$ and B$^+$ $\rightarrow$ K$^+$ $\mu^+\mu^-$. // JOURNAL OF HIGH ENERGY PHYSICS. - 2014. - Is. 9. - P. 177. - ISSN 1029-8479, DOI 10.1007/JHEP09(2014)177.

[117] Aad G., ATLAS Collab., Anisenkov A.V., Bobrovnikov V.S., Bogdanchikov A.G., Kazanin V.F., Korol A.A., Malyshev V.M., Maslennikov A.L., Maxiimov D.A., Peleganchuk S.V., Rezanova O.L., Skovpen K.Yu., Soukharev A.M., Talyshev A.A., Tikhonov Yu.A. Measurement of the Z/gamma* boson transverse momentum distribution in pp collisions at root s=7 TeV with the ATLAS detector. // JOURNAL OF HIGH ENERGY PHYSICS. - 2014. - Is. 9. - P. 145. - ISSN 1029-8479, DOI 10.1007/JHEP09(2014)145.

[118] Aad G., ATLAS Collab., Anisenkov A.V., Bobrovnikov V.S., Bogdanchikov A.G., Kazanin V.F., Korol A.A., Malyshev V.M., Maslennikov A.L., Maxiimov D.A., Peleganchuk S.V., Rezanova O.L., Skovpen K.Yu., Soukharev A.M., Talyshev A.A., Tikhonov Yu.A. Measurements of fiducial and differential cross sections for Higgs boson production in the diphoton decay channel at TeV with ATLAS. // JOURNAL OF HIGH ENERGY PHYSICS. - 2014. - Is. 9. - P. 1-61. - ISSN 1029-8479, DOI 10.1007/ JHEP09(2014)112.

[119] Aad G., ATLAS Collab., Anisenkov A.V., Bobrovnikov V.S., Bogdanchikov A.G., Kazanin V.F., Korol A.A., Malyshev V.M., Maslennikov A.L., Maxiimov D.A., Peleganchuk S.V., Rezanova O.L., Skovpen K.Yu., Soukharev A.M., Talyshev A.A., Tikhonov Yu.A. Search for supersymmetry in events with large missing transverse momentum, jets, and at least one tau lepton in 20 fb(-1) of root s=8 TeV proton-proton collision data with the ATLAS detector. // JOURNAL OF HIGH ENERGY PHYSICS. - 2014. - Is. 9. - P. 103. - ISSN 1029-8479, DOI 10.1007 /JHEP09(2014)103.

[120] Aad G., ATLAS Collab., Anisenkov A.V., Bobrovnikov V.S., Bogdanchikov A.G., Kazanin V.F., Korol A.A., Malyshev V.M., Maslennikov A.L., Maxiimov D.A., Peleganchuk S.V., Rezanova O.L., Skovpen K.Yu., Soukharev A.M., Talyshev A.A., Tikhonov Yu.A. Measurement of the production cross-section of ψ(2S) $\rightarrow$ J/ψ $\mu^+\mu^-$ $\pi^+\pi^-$ in pp collisions at root s=7 TeV at ATLAS. // JOURNAL OF HIGH ENERGY PHYSICS. - 2014. - Is. 9. - P. 1-49. - ISSN 1029-8479, DOI 10.1007/JHEP09(2014)079.

[121] Aad G., ATLAS Collab., Anisenkov A.V., Bobrovnikov V.S., Bogdanchikov A.G., Kazanin V.F., Korol A.A., Malyshev V.M., Maslennikov A.L., Maxiimov D.A., Peleganchuk S.V., Rezanova O.L., Skovpen K.Yu., Soukharev A.M., Talyshev A.A., Tikhonov Yu.A. Search for new particles in events with one lepton and missing transverse momentum in pp collisions at root s=8 TeV with the ATLASdetector. //

JOURNAL OF HIGH ENERGY PHYSICS. - 2014. - Is. 9. - P. UNSP 037. - ISSN 1029-8479, DOI 10.1007/ JHEP09(2014)037.

[122] Aaij R., LHCb Collab., Bondar A., Eidelman S, Krokovny P., Poluektov A., Shekhtman L., Vorobyev V. Observation of Z production in proton-lead collisions at LHCb. // JOURNAL OF HIGH ENERGY PHYSICS. - 2014. - Is. 9. - P. 030. - ISSN 1029-8479, DOI 10.1007/ JHEP09(2014)030.

[123] Boussarie R., Grabovsky A. V., Szymanowski L., Wallon S. Impact factor for high-energy two and three jets diffractive production. // JOURNAL OF HIGH ENERGY PHYSICS. - 2014. - Is. 9. - P. 026. - ISSN 1029-8479, DOI 10.1007/JHEP09(2014)026.

[124] Aad G., ATLAS Collab., Anisenkov A.V., Bobrovnikov V.S., Bogdanchikov A.G., Kazanin V.F., Korol A.A., Malyshev V.M., Maslennikov A.L., Maxiimov D.A., Peleganchuk S.V., Rezanova O.L., Skovpen K.Yu., Soukharev A.M., Talyshev A.A., Tikhonov Yu.A. Search for direct pair production of the top squark in all-hadronic final states in proton-proton collisions at=8 TeV with the ATLAS detector. // JOURNAL OF HIGH ENERGY PHYSICS. - 2014. - Is. 9. - P. 015. - ISSN 1029-8479, DOI 10.1007/ JHEP09(2014)015.

[125] Aaij R., LHCb Collab., Bondar A., Eidelman S, Krokovny P., Poluektov A., Shekhtman L., Vorobyev V. Study of the kinematic dependences of Lambda(0)(b) production in pp collisions and a measurement of the Lambda(0)(b) - Lambda(+)(c)pi(-)branching fraction. // JOURNAL OF HIGH ENERGY PHYSICS. - 2014. - Is. 8. - P. 143. - ISSN 1029-8479, DOI 10.1007/ JHEP08(2014)143.

[126] Feldman A., Pomeransky A. General triple charged black ring solution in supergravity. // JOURNAL OF HIGH ENERGY PHYSICS. - 2014. - Is. 8. - P. 059. - ISSN 1029-8479, DOI 10.1007/JHEP08(2014)059.

[127] Aad G., ATLAS Collab., Anisenkov A.V., Bobrovnikov V.S., Bogdanchikov A.G., Kazanin V.F., Korol A.A., Malyshev V.M., Maslennikov A.L., Maxiimov D.A., Peleganchuk S.V., Rezanova O.L., Skovpen K.Yu., Soukharev A.M., Talyshev A.A., Tikhonov Yu.A. Measurement of chi(c1) and chi(c2) production with root s=7 TeV pp collisions at ATLAS. // JOURNAL OF HIGH ENERGY PHYSICS. - 2014. - Is. 7. - P. 154. - ISSN 1029-8479, DOI 10.1007/ JHEP07(2014)154.

[128] Aaij R., LHCb Collab. Bondar A., Eidelman S, Krokovny P., Poluektov A., Shekhtman L., Vorobyev V. Observation of the B-s(0) - J/psi (KsK +/-)-K-0 pi(-/+) decay. // JOURNAL OF HIGH ENERGY PHYSICS. - 2014. - Is. 7. - P. 140. - ISSN 1029-8479, DOI 10.1007/ JHEP07(2014)140.

[129] Aaij R., LHCb Collab., Bondar A., Eidelman S, Krokovny P., Poluektov A., Shekhtman L., Vorobyev V.

Observation of the Lambda(0)(b) - J/psi p pi(-) decay. // JOURNAL OF HIGH ENERGY PHYSICS. - 2014. - Is. 7. - P. 103. - ISSN 1029-8479, DOI 10.1007/ JHEP07(2014)103.

[130] Aaij R., LHCb Collab. Bondar A., Eidelman S, Krokovny P., Poluektov A., Shekhtman L., Vorobyev V. Study of production and cold nuclear matter effects in pPb collision sat=5 TeV. // JOURNAL OF HIGH ENERGY PHYSICS. - 2014. - Is. 7. - P. 094. - ISSN 1029-8479, DOI 10.1007/JHEP07(2014)094.

[131] Aaij R., LHCb Collab., Bondar A., Eidelman S, Krokovny P., Kudryavtsev V., Poluektov A., Shekhtman L., Vorobyev V. Measurement of CP asymmetry in D-0 - K- K+ and D-0 - pi(-) pi(+)decays. // JOURNAL OF HIGH ENERGY PHYSICS. - 2014. - Is. 7. - P. 041. - ISSN 1029-8479, DOI 10.1007/ JHEP07(2014)041.

[132] Aaij R., LHCb Collab., Bondar A., Eidelman S, Krokovny P., Poluektov A., Shekhtman L., Vorobyev V. Differential branching fractions and isospin asymmetries of B - K ((*))mu (+) mu (-) decays. // JOURNAL OF HIGH ENERGY PHYSICS. - 2014. - Is. 6. - P. 133. - ISSN 1029-8479, DOI 10.1007/JHEP06(2014)133.

[133] Aad G., ATLAS Collab., Anisenkov A.V., Bobrovnikov V.S., Bogdanchikov A.G., Kazanin V.F., Korol A.A., Malyshev V.M., Maslennikov A.L., Maxiimov D.A., Peleganchuk S.V., Rezanova O.L., Skovpen K.Yu., Soukharev A.M., Talyshev A.A., Tikhonov Yu.A. Search for direct top-squark pair production in final states with two leptons in pp collisions at root s=8 TeV with the ATLAS detector. // JOURNAL OF HIGH ENERGY PHYSICS. - 2014. - Is. 6. - P. 124. - ISSN 1029-8479, DOI 10.1007/JHEP06(2014)124.

[134] Aad G., ATLAS Collab., Anisenkov A.V., Bobrovnikov V.S., Bogdanchikov A.G., Kazanin V.F., Korol A.A., Malyshev V.M., Maslennikov A.L., Maxiimov D.A., Peleganchuk S.V., Rezanova O.L., Skovpen K.Yu., Soukharev A.M., Talyshev A.A., Tikhonov Yu.A. Search for supersymmetry at root 8=8 TeV in final states with jets and two same-sign leptons or three leptons with the ATLAS detector. // JOURNAL OF HIGH ENERGY PHYSICS. - 2014. - Is. 6. - P. 035. - ISSN 1029-8479, DOI 10.1007/JHEP06(2014)035.

[135] Aad G., ATLAS Collab., Anisenkov A.V., Bobrovnikov V.S., Bogdanchikov A.G., Kazanin V.F., Korol A.A., Malyshev V.M., Maslennikov A.L., Maxiimov D.A., Peleganchuk S.V., Rezanova O.L., Skovpen K.Yu., Soukharev A.M., Talyshev A.A., Tikhonov Yu.A. Search for top quark decays t - q H with H - gamma gamma using the ATLAS detector. // JOURNAL OF HIGH ENERGY PHYSICS. - 2014. - Is. 6. - P. 008. - ISSN 1029-8479, DOI 10.1007/JHEP06(2014)008.

[136] Aaij R., LHCb Collab., Bondar A., Eidelman S, Krokovny P., Poluektov A., Shekhtman L., Vorobyev V. Evidence for the decay B-c(+) - J/psi 3 pi(+)2 pi(-). //

JOURNAL OF HIGH ENERGY PHYSICS. - 2014. - Is. 5. - ISSN 1029-8479, DOI 10.1007/JHEP05(2014)148.

[137] Aaij R., LHCb Collab., Bondar A., Eidelman S, Krokovny P., Poluektov A., Shekhtman L., Vorobyev V. Angular analysis of charged and neutral $B \to K\ \mu^+\mu^-$ decays. // JOURNAL OF HIGH ENERGY PHYSICS. - 2014. - Is. 5. - P. 082. - ISSN 1029-8479, DOI 10.1007/JHEP05(2014)082.

[138] Aad G., ATLAS Collab., Anisenkov A.V., Bobrovnikov V.S., Bogdanchikov A.G., Kazanin V.F., Korol A.A., Malyshev V.M., Maslennikov A.L., Maxiimov D.A., Peleganchuk S.V., Rezanova O.L., Skovpen K.Yu., Soukharev A.M., Talyshev A.A., Tikhonov Yu.A. Search for direct production of charginos, neutralinos and sleptons infinal states with two leptons and missing transverse momentum in pp collisions at root s=8 TeV with the ATLAS detector. // JOURNAL OF HIGH ENERGY PHYSICS. - 2014. - Is. 5. - P. 071. - P. 1-52. - ISSN 1029-8479, DOI 10.1007/ JHEP05(2014)071.

[139] Aad G., ATLAS Collab., Anisenkov A.V., Bobrovnikov V.S., Bogdanchikov A.G., Kazanin V.F., Korol A.A., Malyshev V.M., Maslennikov A.L., Maxiimov D.A., Peleganchuk S.V., Rezanova O.L., Skovpen K.Yu., Soukharev A.M., Talyshev A.A., Tikhonov Yu.A. Measurement of the production of a W boson in association with a charm quark in pp collisions at root s=7 TeV with the ATLAS detector. // JOURNAL OF HIGH ENERGY PHYSICS. - 2014. - Is. 5. - P. 1-67. - ISSN 1029-8479, DOI 10.1007/JHEP05(2014)068.

[140] Aaij R., LHCb Collab., Bondar A., Eidelman S, Krokovny P., Poluektov A., Shekhtman L., Vorobyev V. Measurement of polarization amplitudes and CP asymmetries in B-0 $\to$ phiK*(892)(0). // JOURNAL OF HIGH ENERGY PHYSICS. - 2014. - Is. 5. - P. 069. - ISSN 1029-8479, DOI 10.1007/JHEP05(2014)069.

[141] Aad G., ATLAS Collab., Anisenkov A.V., Bobrovnikov V.S., Bogdanchikov A.G., Kazanin V.F., Korol A.A., Malyshev V.M., Maslennikov A.L., Maxiimov D.A., Peleganchuk S.V., Rezanova O.L., Skovpen K.Yu., Soukharev A.M., Talyshev A.A., Tikhonov Yu.A. Measurement of dijet cross-sections in pp collisions at 7 TeV centre-of-mass energy using the ATLAS detector. // JOURNAL OF HIGH ENERGY PHYSICS. - 2014. - Is. 5. - P. 059. - ISSN 1029-8479, DOI 10.1007/JHEP05(2014)059.

[142] Aad G., ATLAS Collab., Anisenkov A.V., Bobrovnikov V.S., Bogdanchikov A.G., Kazanin V.F., Korol A.A., Malyshev V.M., Maslennikov A.L., Maxiimov D.A., Peleganchuk S.V., Rezanova O.L., Skovpen K.Yu., Soukharev A.M., Talyshev A.A., Tikhonov Yu.A. Search for direct production of charginos and neutralinos in events with three leptons and missing transverse momentum in root s=8 TeV pp collisions with the ATLAS detector. // JOURNAL OF HIGH ENERGY PHYSICS. - 2014. - Is. 4. - P. 169. - ISSN 1029-8479, DOI 10.1007/JHEP04(2014)169.

[143] Aad G., ATLAS Collab., Anisenkov A.V., Bobrovnikov V.S., Bogdanchikov A.G., Kazanin V.F., Korol A.A., Malyshev V.M., Maslennikov A.L., Maxiimov D.A., Peleganchuk S.V., Rezanova O.L., Skovpen K.Yu., Soukharev A.M., Talyshev A.A., Tikhonov Yu.A. Measurement of the production cross section of prompt j/psi mesons inassociation with a W (+/-) boson in pp collisions root s=7 TeV with the ATLAS detector. // JOURNAL OF HIGH ENERGY PHYSICS. - 2014. - Is. 4. - P. 172. - ISSN 1029-8479, DOI 10.1007/JHEP04(2014)172.

[144] Aaij R., LHCb Collab. Bondar A., Eidelman S, Krokovny P., Poluektov A., Shekhtman L., Vorobyev V. Measurements of the B+, B-0, B-s(0) meson and Lambda(0)(b) baryon lifetimes. // JOURNAL OF HIGH ENERGY PHYSICS. - 2014. - Is. 4. - P. 114. - ISSN 1029-8479, DOI 10.1007/JHEP04(2014)114.

[145] Aaij R., LHCb Collab., Bondar A., Eidelman S, Krokovny P., Poluektov A., Shekhtman L., Vorobyev V. Observation of associated production of a Z boson with a D meson in the forward region. // JOURNAL OF HIGH ENERGY PHYSICS. - 2014. - Is. 4. - P. 91. - ISSN 1029-8479, DOI 10.1007/ JHEP04(2014)091.

[146] Aaij R., LHCb Collab., Bondar A., Eidelman S, Krokovny P., Poluektov A., Shekhtman L., Vorobyev V. Searches for and decays to and final states with first observation ofthe decay. // JOURNAL OF HIGH ENERGY PHYSICS. - 2014. - Is. 4. - P. 087. - ISSN 1029-8479, DOI 10.1007/JHEP04(2014)087.

[147] Aad G., ATLAS Collab., Anisenkov A.V., Bobrovnikov V.S., Bogdanchikov A.G., Kazanin V.F., Korol A.A., Malyshev V.M., Maslennikov A.L., Maxiimov D.A., Peleganchuk S.V., Rezanova O.L., Skovpen K.Yu., Soukharev A.M., Talyshev A.A., Tikhonov Yu.A. Measurement of the electroweak production of dijets in association witha Z-boson and distributions sensitive to vector boson fusion in proton-proton collisions at=8 TeV using the ATLAS detector. // JOURNAL OF HIGH ENERGY PHYSICS. - 2014. - Is. 4. - P. 031. - ISSN 1029-8479, DOI 10.1007/JHEP04 (2014)031.

[148] Aaij R., LHCb Collab., Bondar A., Eidelman S, Krokovny P., Poluektov A., Shekhtman L., Vorobyev V. Addendum: Observation of double charm production involving open charm inpp collisions at p root s=7 TeV. // JOURNAL OF HIGH ENERGY PHYSICS. - 2014. - Is. 3. - P. 108. - ISSN 1029-8479, DOI 10.1007/JHEP03(2014)108.

[149] Abelev B., ALICE Collab., Pestov Y. Measurement of charged jet suppression in Pb-Pb collisions at roots(NN)=2.76 TeV. // JOURNAL OF HIGH ENERGY PHYSICS. - 2014. - Is. 3. - P. 013. - ISSN 1029-8479, DOI 10.1007/JHEP03(2014)013.

[150] Aad G., Atlas Collab., Anisenkov A.V., Bobrovnikov V.S., Bogdanchikov A.G., Kazanin V.F., Korol A.A., Malyshev V.M., Maslennikov A.L.,

Maxiimov D.A., Peleganchuk S.V., Rezanova O.L., Skovpen K.Yu., Soukharev A.M., Talyshev A.A., Tikhonov Yu.A. Measurement of the top quark pair production charge asymmetry inproton-proton collisions at root s=7 TeV using the ATLAS detector. // JOURNAL OF HIGH ENERGY PHYSICS. - 2014. - Is. 2. - P. 107. - ISSN 1029-8479, DOI 10.1007/JHEP02(2014)107.

[151] Aaij R., LHCb Collab., Bondar A., Eidelman S, Krokovny P., Poluektov A., Shekhtman L., Vorobyev V. Study of J/ψ production and cold nuclear matter effects in pPb collisions at root S-NN=5 TeV. // JOURNAL OF HIGH ENERGY PHYSICS. - 2014. - Is. 2. - P. 072. - ISSN 1029-8479, DOI 10.1007/ JHEP02(2014)072.

[152] Abelev B., ALICE Collab., Pestov Y. J/psi production and nuclear effects in p-Pb collisions at=5.02 TeV. // JOURNAL OF HIGH ENERGY PHYSICS. - 2014. - Is. 2. - P. 073. - ISSN 1029-8479, DOI 10.1007/JHEP02(2014)073.

[153] Bicer M. (Design Study Working Grp), Gramolin A., Telnov V. First look at the physics case of TLEP. // JOURNAL OF HIGH ENERGY PHYSICS. - 2014. - Is. 1. - P. 164. - ISSN 1029-8479, DOI 10.1007/ JHEP01(2014)164. [arXiv:1308.6176 [hep-ex]].

[154] Aad G., ATLAS Collab., Anisenkov A.V., Bobrovnikov V.S., Bogdanchikov A.G., Kazanin V.F., Korol A.A., Malyshev V.M., Maslennikov A.L., Maxiimov D.A., Peleganchuk S.V., Rezanova O.L., Skovpen K.Yu., Soukharev A.M., Talyshev A.A., Tikhonov Yu.A. Search for new phenomena in final states with large jet multiplicities and missing transverse momentum at root s = 8 TeV proton-proton collisions using the ATLAS experiment (vol 10, pg 130, 2013). // JOURNAL OF HIGH ENERGY PHYSICS. - 2014. - Is. 1. - P. 109. - ISSN 1029-8479, DOI 10.1007/JHEP01 (2014)109.

[155] Aaij R., LHCb Collab., Bondar A., Eidelman S, Krokovny P., Poluektov A., Shekhtman L., Vorobyev V. Study of forward Z plus jet production in pp collisions at root s=7 TeV. // JOURNAL OF HIGH ENERGY PHYSICS. - 2014. - Is. 1. - P. 033. - ISSN 1029-8479, DOI 10.1007/JHEP01(2014)033.

[156] Thumm M.K.A., Arzhannikov A.V., Astrelin V.T., Burdakov A.V., Ivanov I.A., Kalinin P.V., Kandaurov I.V., Kurkuchekov V.V., Kuznetsov S.A., Makarov M.A., Mekler K.I., Polosatkin S.V., Popov S.A., Postupaev V.V., Rovenskikh A.F., Sinitsky S.L., Sklyarov V.F., Stepanov V.D., Trunev Yu.A., Timofeev I.V., Vyacheslavov L.N. Generation of high-power sub-THz waves in magnetized turbulent electron beam plasmas. // JOURNAL OF INFRARED MILLIMETER AND TERAHERTZ WAVES. - 2014. - Vol. 35, Is. 1. - P. 81-90. - ISSN 1866-6892, DOI 10.1007/s10762-013-9969-3.

[157] Aaij R., LHCb Collab., Bondar A., Eidelman S, Krokovny P., Poluektov A., Shekhtman L., Vorobyev V. Precision luminosity measurements at LHCb. // JOURNAL OF INSTRUMENTATION. - 2014. - Vol. 9.

- P. P12005. - ISSN 1748-0221, DOI 10.1088/1748-0221/9/12/P12005.

[158] Abelev B., Alice Collab., Pestov Y. Measurement of visible cross sections in proton-lead collisions at roots(NN)=5.02 TeV in van der Meer scans with the ALICE detector. // JOURNAL OF INSTRUMENTATION. - 2014. - Vol. 9. - P. P11003. - ISSN 1748-0221, DOI 10.1088/1748-0221/9/11/P11003.

[159] Akhmetshin R. R., Grigoriev D. N., Kazanin V. F., Kuzmenko A. E., Yudin Yu. V. Performance of the BGO endcap calorimeter of the CMD-3 detector. // Intern. Conf. on Instrumentation for Colliding Beam Physics (FEB 24-MAR 01, 2014, Budker Inst. Nucl. Phys, Novosibirsk, RUSSIA): JOURNAL OF INSTRUMENTATION. - 2014. - Vol. 9. - P. C10002. - ISSN 1748-0221, DOI 10.1088/1748-0221/9/10/C10002.

[160] Basok I.Yu., Blinov V.E., Bykov A.V., Kharlamova T.A., Prisekin V.G., Rodyakin V.A., Savinov G.A., Shamov A.G., Todyshev K.Yu. New drift chamber for the KEDR detector. // Intern. Conf. on Instrumentation for Colliding Beam Physics, Feb 24 - Mar 01, 2014, Budker Inst Nucl Phys, Novosibirsk, RUSSIA: JOURNAL OF INSTRUMENTATION. - 2014. - Vol. 9 - P. C10004. - ISSN 1748-0221, DOI 10.1088/1748-0221/9/10/C10004.

[161] Bobrovnikov V.S., Grigoriev D.N., Kaminskiy V.V., Kudryavtsev V.N., Muchnoi N.Yu., Rezanova O.L., Shekhtman L.I., Zhilich V.N. The energy calibration system of the KEDR tagger. // Intern. Conf. on Instrumentation for Colliding Beam Physics, Feb 24 - Mar 01, 2014, Budker Inst Nucl Phys, Novosibirsk, RUSSIA: JOURNAL OF INSTRUMENTATION. - 2014. - Vol. 9. - P. C10017. - ISSN 1748-0221, DOI 10.1088/1748-0221/9/10/C10017.

[162] Kozyrev A.N., Aulchenko V.M., Epshteyn L.B., Epifanov D.A., Popov A.S., Ruban A.A., Selivanov A.N., Talyshev A.A., Titov V.M., Yudin Y.V. The CMD-3 TOMA DAQ infrastructure. // Intern. Conf. on Instrumentation for Colliding Beam Physics (FEB 24-MAR 01, 2014, Budker Inst Nucl Phys, Novosibirsk, RUSSIA): JOURNAL OF INSTRUMENTATION. - 2014. - Vol. 9. - P. C10016. - ISSN 1748-0221, DOI 10.1088/1748-0221/9/10/C10016.

[163] Polosatkin S., Grishnyaev E., Dolgov A. On calibration of the response of liquid argon detectors to nuclearrecoils using in elastic neutron scattering on Ar-40. // JOURNAL OF INSTRUMENTATION. - 2014. - Vol. 9. - P. P10017. - ISSN 1748-0221, DOI 10.1088/1748-0221/9/10/P10017.

[164] Shebalin V.E., Anisenkov A.V., Bashtovoy N.S., Epifanov D.A., Erofeev A.L., Grebenuk A.A., Karpov S.V., Khazin B.I., Kovalenko O.A., Kozyrev A.N., Kuzmin A.S., Mikhailov K.Yu., Razuvaev G.P., Ruban A.A., Shwartz B.A., Titov V.M., Talyshev A.A., Yudin Yu.V. Combined Liquid Xenon and crystal CsI calorimeter of the CMD-3 detector. // Intern. Conf. on

Instrumentation for Colliding Beam Physics (FEB 24-MAR 01, 2014, Budker Inst Nucl Phys, Novosibirsk, RUSSIA): JOURNAL OF INSTRUMENTATION. - 2014. - Vol. 9. - P. C10013. - ISSN 1748-0221, DOI 10.1088/1748-0221/9/10/C10013.

[165] Aad G., ATLAS Collab., Anisenkov A.V., Bobrovnikov V.S., Bogdanchikov A.G., Kazanin V.F., Korol A.A., Malyshev V.M., Maslennikov A.L., Maxiimov D.A., Peleganchuk S.V., Rezanova O.L., Skovpen K.Yu., Soukharev A.M., Talyshev A.A., Tikhonov Yu.A. A neural network clustering algorithm for the ATLAS silicon pixel detector. // JOURNAL OF INSTRUMENTATION. - 2014. - Vol. 9. - P. P09009. - ISSN 1748-0221, DOI 10.1088/1748-0221/9/09/P09009.

[166] Akhmetshin R.R., Anisenkov A.V., Aulchenko V.M., Banzarov V.S., Bashtovoy N.S., Berkaev D.E., Bragin A.V., Eidelman S.I., Epifanov D.A., Epshteyn L.B., Erofeev A.L., Fedotovich G.V., Gayazov S.E., Grebenuk A.A., Grigoriev D.N., Gromov E.M., Ignatov F.V., Karpov S.V., Ivanov V.L., Kazanin V.F., Khazin B.I., Kirpotin A.N., Koop I.A., Kovalenko O.A., Kozyrev A.N., Kozyrev E.A., Krokovny P.P., Kuzmenko A.E., Kuzmin A.S., Logashenko I.B., Lukin P.A., Lysenko A.P., Mikhailov K.Yu., Okhapkin V.S., Pestov Yu.N., Perevedentsev E.A., Popov A.S., Popov Yu.S., Razuvaev G.P., Rogovsky Yu.A., Romanov A.L., Ruban A.A., Ryskulov N.M., Ryzhenenkov A.E., Shebalin V.E., Shemyakin D.N., Shwartz B.A., Shwartz D.B., Sibidanov A.L., Shatunov P.Yu., Shatunov Yu.M., Solodov E.P., Titov V.M., Talyshev A.A., Vorobiov A.I., Yudin Yu.V., Zharinov Yu.M. Current status of luminosity measurement with the CMD-3 detector at the VEPP-2000 e^+e^- collider. // Intern. Conf. on Instrumentation for Colliding Beam Physics (FEB 24-MAR 01, 2014, Budker Inst Nucl Phys, Novosibirsk, RUSSIA): JOURNAL OF INSTRUMEN-TATION. - 2014. - Vol. 9. - P. C09003. - ISSN 1748-0221, DOI 10.1088/1748-0221/9/09/C09003.

[167] Aulchenko V., Cheon B. G., Kuzmin A., Matvienko D., Miyabayashi K., Nakamura I., Shebalin V., Usov Y., Zhulanov V. Upgrade of trigger and DAQ for CsI at Belle II. // Intern. Conf. on Instrumentation for Colliding Beam Physics (FEB 24-MAR 01, 2014, Budker Inst Nucl Phys, Novosibirsk, RUSSIA): JOURNAL OF INSTRUMENTATION. - 2014. - Vol. 9. - P. C09014. - ISSN 1748-0221, DOI 10.1088/1748-0221/9/09/C09014.

[168] Barnyakov A.Yu., Barnyakov M.Yu., Bobrovnikov V.S., Buzykaev A.R., Gulevich V.V., Danilyuk A.F., Katcin A.A., Kononov S.A., Kravchenko E.A., Kuyanov I..A., Onuchin A.P., Ovtin I.V., Rodyakin V.A. Threshold aerogel Cherenkov counters of the KEDR detector. // Intern. Conf. on Instrumentation for Colliding Beam Physics, Feb 24 - Mar 01, 2014, Budker Inst Nucl Phys, Novosibirsk, RUSSIA: JOURNAL OF INSTRUMENTATION. - 2014. - Vol. 9. - P. C09005. - ISSN 1748-0221, DOI 10.1088/1748-0221/9/09/C09005.

[169] Barnyakov A.Yu., Barnyakov M.Yu., Beloborodov K.I., Bobrovnikov V.S., Buzykaev A.R., Danilyuk A.F., Golubev V.B., Gulevich V.V., Kononov S.A., Kravchenko E.A., Onuchin A.P., Martin K.A., Serednyakov S.I., Vesenev V.M. Particle identification system based on dense aerogel for SND detector at VEPP-2000 collider. // Intern. Conf. on Instrumentation for Colliding Beam Physics (FEB 24-MAR 01, 2014, Budker Inst Nucl Phys, Novosibirsk, RUSSIA): JOURNAL OF INSTRUMENTATION. - 2014. - Vol. 9. - P. C09023. - ISSN 1748-0221, DOI 10.1088/1748-0221/9/09/C09023.

[170] Blinov V.E., Kaminsky V.V., Kudryavtsev V.N., Muchnoi N.Yu., Nikitin S.A., Nikolaev I.B., Shekhtman L.I. The project of laser polarimeter for beam energy measurement of VEPP-4M collider by resonance depolarization method. // Intern. Conf. on Instrumentation for Colliding Beam Physics, Feb 24 - Mar 01, 2014, Budker Inst Nucl Phys, Novosibirsk, RUSSIA: JOURNAL OF INSTRUMENTATION. - 2014. - Vol. 9. - P. C09010. - ISSN 1748-0221, DOI 10.1088/1748-0221/9/09/C09010.

[171] Epshteyn, L.B. Yudin Yu.V. Processing of the Liquid Xenon calorimeter's signals for timing measurements. // Intern. Conf. on Instrumentation for Colliding Beam Physics (FEB 24-MAR 01, 2014, Budker Inst Nucl Phys, Novosibirsk, RUSSIA): JOURNAL OF INSTRUMENTATION. - 2014. - Vol. 9. - P. C09019. - ISSN 1748-0221, DOI 10.1088/1748-0221/9/09/C09019.

[172] Fedotovich G. V., Kozyrev A. N., Kulidzhoglyan V. A., Ruban A. A., Ryskulov N. M., Ryzhenenkov A. E., Shemyakin D. N., Tolmachev S. S. Upgrade of the CMD-3 TOF system. // Intern. Conf. on Instrumentation for Colliding Beam Physics (FEB 24-MAR 01, 2014, Budker Inst Nucl Phys, Novosibirsk, RUSSIA): JOURNAL OF INSTRUMENTATION. - 2014. - Vol. 9. - P. C09022. - ISSN 1748-0221, DOI 10.1088/1748-0221/9/09/C09022.

[173] Grigoriev D. N., Danevich F. A., Shlegel V. N., Vasiliev Ya. V. Development of crystal scintillators for calorimetry in high energy and astroparticle physics. // Intern. Conf. on Instrumentation for Colliding Beam Physics (FEB 24-MAR 01, 2014, Budker Inst Nucl Phys, Novosibirsk, RUSSIA): JOURNAL OF INSTRU-MENTATION. - 2014. - Vol. 9. - P. C09004. - ISSN 1748-0221, DOI 10.1088/1748-0221/9/09/C09004.

[174] Kudryavtsev V.N., Shekhtman L.I., Bobrovnikov V.S., Maltsev T.V., Nikolenko D.N., Rachek I.A. The development of high resolution coordinate detectors for the DEUTERON facility. // Intern. Conf. on Instrumentation for Colliding Beam Physics (Feb.24-Mar.1 2014, Budker Inst Nucl Phys, Novosibirsk, RUSSIA): JOURNAL OF INSTRUMENTATION. - 2014. - Vol. 9: - P. C09024. - ISSN 1748-0221, DOI 10.1088/1748-0221/9/09/C09024.

[175] Miyabayashi K., (Belle II Electromagnetic Calorimet), Aulchenko V., Kuzmin A., Matvienko D., Shebalin V., Shwartz B., Usov Y., Vinokurova A., Zhulanov V. Upgrade of the Belle II electromagnetic

154

calorimeter. // JOURNAL OF INSTRUMENTATION. - 2014. - Vol. 9. - P. P09011.

[176] Shekhtman, L.I. Telnov V.I. A concept of the photon collider beam dump. // Intern. Conf. on Instrumentation for Colliding Beam Physics (FEB 24-MAR 01, 2014, Budker Inst Nucl Phys, Novosibirsk, RUSSIA): JOURNAL OF INSTRUMENTATION. - 2014. - Vol. 9. - P. C09031. - ISSN 1748-0221, DOI 10.1088/1748-0221/9/09/C09031.

[177] Surin I. K., Achasov M. N., Golubev V. B., Serednyakov S. I., Bogdanchikov A. G., Druzhinin V. P., Koshuba S. V., Kovrizhin D. P., Tekut'ev A. I., Usov Yu. V. New electronics with high time and energy resolution for SND detector calorimeter. // Intern. Conf. on Instrumentation for Colliding Beam Physics (FEB 24-MAR 01, 2014, Budker Inst Nucl Phys, Novosibirsk, RUSSIA): JOURNAL OF INSTRUMENTATION. - 2014. - Vol. 9. - P. C09025. - ISSN 1748-0221, DOI 10.1088/1748-0221/9/09/C09025.

[178] Telnov, V.I. Photon collider Higgs factories. // Intern. Conf. on Instrumentation for Colliding Beam Physics (FEB 24-MAR 01, 2014, Budker Inst Nucl Phys, Novosibirsk, RUSSIA): JOURNAL OF INSTRUMENTATION. - 2014. - Vol. 9. - P. C09020. - ISSN 1748-0221, DOI 10.1088/1748-0221/9/09/C09020.

[179] Telnov V.I. Energy calibration at high-energy photon colliders. // Intern. Conf. on Instrumentation for Colliding Beam Physics (FEB 24-MAR 01, 2014, Budker Inst Nucl Phys, Novosibirsk, RUSSIA): JOURNAL OF INSTRUMEN-TATION. - 2014. - Vol. 9. - P. C09029. - ISSN 1748-0221, DOI 10.1088/1748-0221/9/09/C09029.

[180] Aad G., ATLAS Collboration, Anisenkov A.V., Bobrovnikov V.S., Bogdanchikov A.G., Kazanin V.F., Korol A.A., Malyshev V.M., Maslennikov A.L., Maxiimov D.A., Peleganchuk S.V., Rezanova O.L., Skovpen K.Yu., Soukharev A.M., Talyshev A.A., Tikhonov Yu.A. Operation and performance of the ATLAS semiconductor tracker. // JOURNAL OF INSTRUMENTATION. - 2014. - Vol. 9. - P. UNSP P08009. - ISSN 1748-0221, DOI 10.1088/1748-0221/9/08/P08009.

[181] Abramov G.N., Ahmetshin R.R., Barnyakov A.Yu., Barnyakov M.Yu., BasokYu., Blinov V.E., Bobrovnikov V.S., Borodenko A.A., Buzykaev A.R., Grigoriev D.N., Gulevich V.V., Kazanine V.F., Kravchenko E.A., Kononov S.A., Kudryavtsev V.N., Kuyanov I.A., Muchnoy N.Yu., Ovtin I.V., Shekhtman L.I., Onuchin A.P., Prisekin V.G., Rodiakin V.A., Yudin Yu.V., Zhilich V.N. Extracted electron and gamma beams in BINP. // Intern. Conf. on Instrumentation for Colliding Beam Physics (FEB 24-MAR 01, 2014, Budker Inst Nucl Phys, Novosibirsk, RUSSIA): JOURNAL OF INSTRUMENTATION. - 2014. - Vol 9: - P. C08022. - ISSN 1748-0221, DOI 10.1088/1748-0221/9/08/C08022.

[182] Barnyakov A.Yu., Barnyakov M.Yu., Beloborodov K.I., Bobrovnikov V.S., Buzykaev A.R., Golubev V.B., Kononov S.A., Koshuba S.V., Kravchenko E.A., Martin K.A., Onuchin A.P., Serednyakov S.I., Vesenev V.M. Test results of the threshold aerogel Cherenkov counter system with n=1.05 using electrons and muons at p 500 MeV/c. // Intern. Conf. on Instrumentation for Colliding Beam Physics (FEB 24-MAR 01, 2014, Budker Inst Nucl Phys, Novosibirsk, RUSSIA): JOURNAL OF INSTRUMENTATION. - 2014. - Vol. 9. - P. UNSP C08010. - ISSN 1748-0221, DOI 10.1088/1748-0221/9/08/C08010.

[183] Bondar A., Buzulutskov A., Dolgov A., Shekhtman L., Shemyakina E., Sokolov A., Breskin A., Thers D. Performance degradation of Geiger-mode APDs at cryogenic temperatures. // JOURNAL OF INSTRUMENTATION. - 2014. - Vol. 9. - P. P08006. - ISSN 1748-0221, DOI 10.1088/1748-0221/9/08/P08006.

[184] Bondar A., Buzulutskov A., Dolgov A., Grishnyaev E., Polosatkin S., Shemyakina E., Sokolov A. Nuclear recoil detection in liquid argon using a two-phase CRAD and DD neutron generator. // Intern. Conf. on Instrumentation for Colliding Beam Physics (FEB 24 - MAR 01, 2014, Budker Inst Nucl Phys, Novosibirsk, RUSSIA): JOURNAL OF INSTRUMENTATION. - 2014. - Vol. 9. - P. C08020. - ISSN 1748-0221, DOI 10.1088/1748-0221/9/08/C08020.

[185] Fedotovich G.V., Shekhtman L.I., Ruban A.A., Kozyrev A.N. Proposal for the upgrade of the tracking and trigger systems of the CMD-3 detector. // Intern. Conf. on Instrumentation for Colliding Beam Physics (FEB 24-MAR 01, 2014, Budker Inst Nucl Phys, Novosibirsk, RUSSIA): JOURNAL OF INSTRUMENTATION. - 2014. - Vol. 9. - P. C08008. - ISSN 1748-0221, DOI 10.1088/1748-0221/9/08/C08008.

[186] Gaiazov S.E., Banzarov V.S., Ignatov F.V., Logashenko I.B., Pirogov S.A., Sukharev A.M., Zaytsev A.S. Distributed data analysis system for CMD-3 detector. // Intern. Conf. on Instrumentation for Colliding Beam Physics (FEB 24-MAR 01, 2014, Budker Inst Nucl Phys, Novosibirsk, RUSSIA): JOURNAL OF INSTRUMENTATION. - 2014. - Vol. 9. - P. C08011. - ISSN 1748-0221, DOI 10.1088/1748-0221/9/08/C08011.

[187] Golubev V.B., Dimova T.V., Koshuba S.V., Oleinikov V.P., Rogozina E.V., Shtol D.A. Muon system of SND detector. // Intern. Conf. on Instrumentation for Colliding Beam Physics (FEB 24 - MAR 01, 2014, Budker Inst Nucl. Phys, Novosibirsk, RUSSIA): JOURNAL OF INSTRUMENTATION. - 2014. - Vol. 9. - Art. nr C08006: .

[188] Kaminskiy V.V. Muchnoi N.Yu., Zhilich V.N. Compton backscattering for the calibration of KEDR tagging system. // Intern. Conf. on Instrumentation for Colliding Beam Physics, Feb 24 -Mar 01, 2014, Budker Inst Nucl Phys, Novosibirsk, RUSSIA: JOURNAL OF INSTRUMENTATION. - 2014. - Vol. 9. - P. C08021. - ISSN 1748-0221, DOI 10.1088/1748-0221/9/08/C08021.

[189] Shekhtman L.I., Aulchenko V.M., Bobrovnikov V.S., Bondar A.E., Fedotovich G.V., Kudryavtsev V.N., Maltsev T.V., Nikolaev I.B., Nikolenko D.M., Rachek I.A., Zhilich V.N., Zhulanov V.V. Development of high resolution tracking detectors with Gas Electron Multipliers. // Intern. Conf. on Instrumentation for Colliding Beam Physics (FEB 24-MAR 01, 2014, Budker Inst Nucl Phys, Novosibirsk, RUSSIA): JOURNAL OF INSTRUMENTATION. - 2014. - Vol. 9. - P. C08017. - ISSN 1748-0221, DOI 10.1088/1748-0221/9/08/C08017.

[190] Sukharev A.M., KEDR Collab., Anashin V.V., Aulchenko V.M., Baldin E.M., Barladyan A.K., Barnyakov A.Yu., Barnyakov M.Yu., Baru S.E., Basok I.Yu., Bedny I.V., Beloborodova O.L., Blinov A.E., Blinov V.E., Bobrov A.V., Bobrovnikov V.S., Bogomyagkov A.V., Bondar A.E., Buzykaev A.R., Eidelman S.I., Glukhovchenko Yu.M., Gulevich V.V., Gusev D.V., Karnaev S.E., Karpov G.V., Karpov S.V., Kharlamova T.A., Kiselev V.A., Kononov S.A., Kotov K.Yu., Kravchenko E.A., Kulikov V.F., Kuper E.A., Kurkin G.Ya., Levichev E.B., Maksimov D.A., Malyshev V.M., Maslennikov A.L., Medvedko A.S., Meshkov O.I., Mishnev S.I., Morozov I.I., Muchnoi N.Yu., Neufeld V.V., Nikitin S.A., Nikolaev I.B., Okunev I.N., Onuchin A.P., Oreshkin S.B., Orlov I.O., Osipov A.A., Peleganchuk S.V., Petrov V.V., Piminov P.A., Pivovarov S.G., Poluektov A.O., Pospelov G.E., Prisekin V.G., Ruban A.A., Sandyrev V.K., Savinov G.A., Shamov A.G., Shatilov D.N., Shwartz B.A., Simonov E.A., Sinyatkin S.V., Skovpen Yu.I., Skrinsky A.N., Smaluk V.V., Sokolov A.V., Starostina E.V., Talyshev A.A., Tayursky V.A., Telnov V.I., Tikhonov Yu.A., Todyshev K.Yu., Tumaikin G.M., Usov Yu.V., Vorobiov A.I., Yushkov A.N., Zhilich V.N., Zhulanov V.V., Zhuravlev A.N. Muon system of the KEDR detector. // Intern. Conf. on Instrumentation for Colliding Beam Physics, (Feb 24 - Mar 01, 2014, Budker Inst Nucl Phys, Novosibirsk, RUSSIA: JOURNAL OF INSTRUMENTATION. - 2014. - Vol. 9: - P. C08026. - ISSN 1748-0221, DOI 10.1088/1748-0221/9/08/C08026.

[191] Vorobyev V., Kuzmin A., Matvienko D., Vinokurova A. Test bench of shaper-digitizer modules for Belle II calorimeter. // Intern. Conf. on Instrumentation for Colliding Beam Physics (FEB 24-MAR 01, 2014, Budker Inst Nucl Phys, Novosibirsk, RUSSIA): JOURNAL OF INSTRUMEN-TATION. - 2014. - Vol. 9. - P. C08016. - ISSN 1748-0221, DOI 10.1088/1748-0221/9/08/C08016.

[192] Aad G., ATLAS Collab., Anisenkov A.V., Bobrovnikov V.S., Bogdanchikov A.G., Kazanin V.F., Korol A.A., Malyshev V.M., Maslennikov A.L., Maxiimov D.A., Peleganchuk S.V., Rezanova O.L., Skovpen K.Yu., Soukharev A.M., Talyshev A.A., Tikhonov Yu.A. Monitoring and data quality assessment of the ATLAS liquid argon calorimeter. // JOURNAL OF INSTRUMENTATION. - 2014. - Vol. 9. - P. P07024. - ISSN 1748-0221, DOI 10.1088/1748-0221/9/07/P07024.

[193] Berger N., Buniatyan A., Eckert P., Foerster F., Gredig R., Kovalenko O., Kiehn M., Philipp R., Schoening A., Wiedner D. Multiple Coulomb scattering in thin silicon. // JOURNAL OF INSTRUMENTATION. - 2014. - Vol. 9. - P. P07007. - ISSN 1748-0221, DOI 10.1088/1748-0221/9/07/P07007.

[194] Achasov, M.N. Muchnoi N.Yu. Beam energy determination in experiments at electron-positron colliders. // Intern. Conf. on Instrumentation for Colliding Beam Physics (FEB 24-MAR 01, 2014, Novosibirsk, RUSSIA): JOURNAL OF INSTRUMENTATION. - 2014. - Vol. 9. - P. C06011. - ISSN 1748-0221, DOI 10.1088/1748-0221/9/06/C06011.

[195] Kaminskiy V.V., Gramolin A.V., Mishnev S.I., Muchnoi N.Yu, Neufeld V.V., Nikolenko D.M., Rachek I.A., Toporkov D.K., Zhilich V.N. Beam energy measurements for an experiment on elastic $e^{\pm}$ p scattering at the VEPP-3 storage ring. // JOURNAL OF INSTRUMEN-TATION. - 2014. - Vol. 9. - P. T06006. - ISSN 1748-0221, DOI 10.1088/1748-0221/9/06/T06006.

[196] Aad G., ATLAS Collab., Anisenkov A.V., Bobrovnikov V.S., Bogdanchikov A.G., Kazanin V.F., Korol A.A., Malyshev V.M., Maslennikov A.L., Maxiimov D.A., Peleganchuk S.V., Rezanova O.L., Skovpen K.Yu., Soukharev A.M., Talyshev A.A., Tikhonov Yu.A. Standalone vertex finding in the ATLAS muon spectrometer. // JOURNAL OF INSTRUMEN-TATION. - 2014. - Vol. 9. - P. P02001. - ISSN 1748-0221, DOI 10.1088/1748-0221/9/02/P02001.

[197] Aaij R., LHCb Collab., Bondar A., Eidelman S, Krokovny P., Poluektov A., Shekhtman L., Vorobyev V. Observation of charmonium pairs produced exclusively in pp collisions. // JOURNAL OF PHYSICS G-NUCLEAR AND PARTICLE PHYSICS. - 2014. - Vol. 41, Is. 11. - P. UNSP 115002. - ISSN 0954-3899, DOI 10.1088/0954-3899/41/11/115002.

[198] Gramolin A.V., Fadin V.S., Feldman A.L., Gerasimov R.E., Nikolenko D.M., Rachek I.A., Toporkov D.K. A new event generator for the elastic scattering of charged leptons on protons. // JOURNAL OF PHYSICS G-NUCLEAR AND PARTICLE PHYSICS. - 2014. - Vol. 41, Is. 11. - P. 115001. - ISSN 0954-3899, DOI 10.1088/0954-3899/41/11/115001.

[199] Abelev B., ALICE Collab., Pestov Y. Upgrade of the ALICE experiment letter of intent. // JOURNAL OF PHYSICS G-NUCLEAR AND PARTICLE PHYSICS. - 2014. - Vol. 41, Is. 8. - P. 087001. - ISSN 0954-3899.

[200] Abelev B., ALICE Collab., Pestov Y. Technical Design Report for the Upgrade of the ALICE Inner Tracking System. // JOURNAL OF PHYSICS G-NUCLEAR AND PARTICLE PHYSICS. - 2014. - Vol. 41, Is. 8. - P. 087002. - ISSN 0954-3899.

[201] Aaij R., LHCb Collab., Bondar A., Eidelman S, Krokovny P., Kudryavtsev V., Poluektov A., Shekhtman L., Vorobyev V. Updated measurements of exclusive J/ψ and ψ(2S) production cross-sections in pp collisions at

root s=7 TeV. // JOURNAL OF PHYSICS G-NUCLEAR AND PARTICLE PHYSICS. - 2014. - Vol. 41, Is. 5. - P. 055002. - ISSN 0954-3899, DOI 10.1088/0954-3899/41/5/055002.

[202] Goryainov S.V., Likhacheva A.Y., Rashchenko S.V., Shubin A.S., Afanas'ev V.P., Pokhilenko N.P., Raman identification of lonsdaleite in Popigai impactites. // JOURNAL OF RAMAN SPECTROSCOPY. - 2014. - Vol. 45, Is. 4. - P. 305-313. - ISSN 0377-0486, DOI 10.1002/jrs.4457.

[203] Vereschagin K.A., Vorob'ev N.S., Gornostaev P.B., Zinin E.I., Ivanova S.R., Kulichenkova T.P., Levina G.P., Lozovoi V.I., Makushina V.A., Meshkov O.I., Mikhal'kov Yu.M., Semichastnova Z.M., Smirnov A.V., Shashkov E.V., Schelev M.Ya. Laser Diagnostics of picosecond streak tubes supplied with fast-response phosphor screens. // JOURNAL OF RUSSIAN LASER RESEARCH. - 2014. - Vol. 35, Is.6. - P. 617 -622. - ISSN 1071-2836, DOI 10.1007/s10946-014-9469-5.

[204] Khatsymovsky V.M. Some minisuperspace model for the Faddeev formulation of gravity. // MODERN PHYSICS LETTERS A. - 2014. – Vol. 29, Is. 27. - P. 1450141. [arXiv:1408.6375].

[205] Aaij R., LHCb Collab., Bondar A., Eidelman S, Krokovny P., Poluektov A., Shekhtman L., Vorobyev V. Observation of B-s(0) - K* (+/-) K -/+ and evidence for B-s(0) - K*(-)pi(+) decays. // NEW JOURNAL OF PHYSICS. - 2014. - Vol. 16. - ISSN 1367-2630, DOI 10.1088/1367-2630/16/12/123001.

[206] Aad G., ATLAS Collab., Anisenkov A.V., Bobrovnikov V.S., Bogdanchikov A.G., Kazanin V.F., Korol A.A., Malyshev V.M., Maslennikov A.L., Maxiimov D.A., Peleganchuk S.V., Rezanova O.L., Skovpen K.Yu., Soukharev A.M., Talyshev A.A., Tikhonov Yu.A. Measurement of the cross-section of high transverse momentum vector bosons reconstructed as single jets and studies of jet substructure in pp collisions at root s=7TeV with the ATLAS detector. // NEW JOURNAL OF PHYSICS. - 2014. - Vol. 16. - P. 113013. - ISSN 1367-2630, DOI 10.1088/1367-2630/16/11/113013.

[207] Reusch, J. A. Anderson J. K., Tsidulko Y. Full particle orbit tracing with the RIO code in the presence of broad-spectrum MHD activity in a reversed-field pinch. // NUCLEAR FUSION. - 2014. - Vol. 54: 13th IAEA Technical Meeting on Energetic Particles in Magnetic (SEP 17-20, 2013, Peking Univ, Fus Simulat Ctr, Beijing, PEOPLES R CHINA), Is. 10. - P. 104007. - ISSN 0029-5515, DOI 10.1088/0029-5515/54/10/104007.

[208] Bagryansky P.A., Kovalenko Yu.V., Savkin V.Ya., Solomakhin A.L., Yakovlev D.V. First results of an auxiliary electron cyclotron resonance heating experiment in the GDT magnetic mirror. // NUCLEAR FUSION. - 2014. - Vol. 54, Is. 8. - P. 082001. - ISSN 0029-5515, DOI 10.1088/0029-5515/54/8/082001.

[209] Barnyakov A.Yu., Barnyakov M.Yu., Basok I.Yu., Blinov V.E., Bobrovnikov V.S., Borodenko A.A., Buzykaev A.R., Danilyuk A.F., Degenhardt C., Dorscheid R., Finogeev D.A., Frach T., Gulevich V.V., Karavicheva T.L., Kasyanenko P.V., Kononov S.A., Korda D.V., Kravchenko E.A., Kudryavtsev V.N., Kurepin A.B., Kuyanov I.A., Muelhens O., Onuchin A.P., Ovtin I.V., Podgornov N.A., Predein A.Yu., Prisekin V.G., Protsenko R.S., Razin V.I., Reshetin A.I., Schulze R., Shekhtman L.I., Talyshev A.A., Usenko E.A., Zwaans B. Tests of FARICH prototype with precise photon position detection. // 8th Intern. Workshop on Ring Imaging Cherenkov Detectors (RICH) (DEC 02-06, 2013, Nagoya Univ, JAPAN): NUCLEAR INSTRUMENTS & METHODS IN PHYSICS RESEARCH SECTION A-ACCELERATORS. - 2014. - Vol. 766. - P. 88-91. - ISSN 0168-9002, DOI 10.1016/j.nima.2014.04.086.

[210] Barnyakov A.Yu., Barnyakov M.Yu., Bobrovnikov V.S., Buzykaev A.R., Gulevich V.V., Danilyuk A.F., Kononov S.A., Kravchenko E.A., Kuyanov I.A., Lopatin S.A., Onuchin A.P., Ovtin I.V., Podgornov N.A., Porosev V.V., Predein A.Yu., Protsenko R.S. Aerogel for FARICH detector. // 8th Intern. Workshop on Ring Imaging Cherenkov Detectors (RICH) (DEC 02-06, 2013, Nagoya Univ, JAPAN): NUCLEAR INSTRUMENTS & METHODS IN PHYSICS RESEARCH SECTION A. ACCELERATORS. - 2014. - Vol. 766. - P. 235-236. - ISSN 0168-9002, DOI 10.1016/j.nima.2014.05.023.

[211] Acosta G., Andre T., Bermudez J., Blinov M. F., Jamet C., Logatchev P. V., Semenov Y. I., Starostenko A. A., Tecchio L. B., Tsyganov A. S., Udup E., Vasquez J. Measurement of the response time of the delay window for the neutron converter of the SPIRAL2 project. // NUCLEAR INSTRUMENTS & METHODS IN PHYSICS RESEARCH SECTION A-ACCELERATORS. - 2014. - Vol. 758. - P. 83-90. - ISSN 0168-9002, DOI 10.1016/j.nima.2014.05.018.

[212] Pestrikov D.V. Landau damping and the head-tail instability of the coupled synchro-betatron coherent oscillations (vol 743, pg 51, 2014). // NUCLEAR INSTRUMENTS & METHODS IN PHYSICS RESEARCH SECTION A-ACCELERATORS. - 2014. - Vol. 758. - P. 97-97. - ISSN 0168-9002, DOI 10.1016/j.nima.2014.03.036.

[213] Abakumova E.V., Achasov M.N., Berkaev D.E., Kaminsky V.V., Koop I.A., Korol A.A., Koshuba S.V., Krasnov A.A., Muchnoi N.Yu., Perevedentsev E.A., Pyata E.E., Shatunov P.Yu., Shatunov Yu.M., Shwartz D.B. A system of beam energy measurement based on the Compton back scattered laser photons for the VEPP-2000 electron-positron collider. // NUCLEAR INSTRU-MENTS & METHODS IN PHYSICS RESEARCH: SECTION A-ACCELERATORS. - 2014. - Vol. 744. - P. 35-40. - ISSN 0168-9002, DOI 10.1016/j.nima.2014.01.020.

[214] Pestrikov D.V. Landau damping and the head-tail instability of the coupled synchro-betatron coherent oscillations. // NUCLEAR INSTRUMENTS & METHODS IN PHYSICS RESEARCH SECTION A-ACCELERATORS. - 2014. - Vol. 743. - P. 51-55. - ISSN 0168-9002, DOI 10.1016/j.nima.2014.01.019.

[215] Pestrikov D.V. Effect of the lattice octupole fields on the synchro-betatron mode coupling instability. // NUCLEAR INSTRUMENTS & METHODS IN PHYSICS RESEARCH SECTION A-ACCELE-RATORS. - 2014. - Vol. 738. - P. 34-40. - ISSN 0168-9002, DOI 10.1016/j.nima.2013.12.004.

[216] Aad G., ATLAS Collab., Anisenkov A.V., Bobrovnikov V.S., Bogdanchikov A.G., Kazanin V.F., Korol A.A., Malyshev V.M., Maslennikov A.L., Maxiimov D.A., Peleganchuk S.V., Rezanova O.L., Skovpen K.Yu., Soukharev A.M., Talyshev A.A., Tikhonov Yu.A. Measurement of the total cross section from elastic scattering in pp collisions at root s=7 TeV with the ATLAS detector. // NUCLEAR PHYSICS B. - 2014. - Vol. 889. - P. 486-548. - ISSN 0550-3213, DOI 10.1016/j.nuclphysb.2014.10.019.

[217] Aaij R., LHCb Collab., Bondar A., Eidelman S, Krokovny P., Poluektov A., Shekhtman L., Vorobyev V. Measurement of CP violation and constraints on the CKM angle gamma in B-+/- - DK +/- with D - K-s(0)pi(+)pi(-) decays. // NUCLEAR PHYSICS B. - 2014. - Vol. 888. - P. 169-193. - ISSN 0550-3213, DOI 10.1016/j.nuclphysb.2014.09.015.

[218] Aaij R., ATLAS Collab., Bondar A., Eidelman S, Krokovny P., Kudryavtsev V., Poluektov A., Shekhtman L., Vorobyev V. Evidence for the decay X(3872) → ψ(2S) γ. // NUCLEAR PHYSICS B. - 2014. - Vol. 886. - P. 665-680. - ISSN 0550-3213, DOI 10.1016/j.nuclphysb.2014.06.011.

[219] Huber A., Arakcheev A., Sergienko G., Steudel I., Wirtz M., Burdakov A. V., Coenen J. W., Kreter A., Linke J., Mertens P.h., Philipps V., Pintsuk G., Reinhart M., Samm U., Shoshin A., Schweer B., Unterberg B., Zlobinski M. Investigation of the impact of transient heat loads applied by laser irradiation on ITER-grade tungsten. // PHYSICA SCRIPTA. - 2014. - Vol. T159. - P. 014005. - ISSN 0031-8949, DOI 10.1088/0031-8949/2014/T159/014005.

[220] Krachkov P.A. Lee R.N., Milstein A.I. High-energy e^+e^- photo production in the field of a heavy atom accompanied by bremsstrahlung. // PHYSICAL REVIEW A. - 2014. - Vol. 90, Is. 6. - P. 062112. - ISSN 1050-2947, DOI 10.1103/PhysRevA.90.062112.

[221] Di Piazza A. Milstein A.I. Ultrarelativistic quasiclassical wave functions in strong laser andatomic fields. // PHYSICAL REVIEW A. - 2014. - Vol. 89, Is. 6. - P. 062114. - ISSN 1050-2947, DOI 10.1103/PhysRevA.89.062114.

[222] Abelev B., ALICE Collab., Pestov Y. Multiparticle azimuthal correlations in p-Pb and Pb-Pb

collisions at the CERN Large Hadron Collider. // PHYSICAL REVIEW C. - 2014. - Vol. 90, Is. 5. - P. UNSP 054901. - ISSN 0556-2813, DOI 10.1103/PhysRevC.90.054901.

[223] Adlarson P., WASA-At-COSY Collab., Bondar A., Kuzmin A., Shwartz B. Measurement of the eta - pi(+)pi(-)pi(0) Dalitz plot distribution. // PHYSICAL REVIEW C. - 2014. - Vol. 90, Is. 4. - P. 045207. - ISSN 0556-2813, DOI 10.1103/Phys RevC.90.045207.

[224] Aad G., ATLAS Collab., Anisenkov A.V., Bobrovnikov V.S., Bogdanchikov A.G., Kazanin V.F., Korol A.A., Malyshev V.M., Maslennikov A.L., Maxiimov D.A., Peleganchuk S.V., Rezanova O.L., Skovpen K.Yu., Soukharev A.M., Talyshev A.A., Tikhonov Yu.A. Measurement of long-range pseudo-rapidity correlations and azimuthal harmonics in root s(NN)=5.02 TeV proton-lead collisions with the ATLAS detector. // PHYSICAL REVIEW C. - 2014. - Vol. 90, Is. 4. - P. 044906. - ISSN 0556-2813, DOI 10.1103/PhysRevC.90.044906.

[225] Aad G., ATLAS Collab., Anisenkov A.V., Bobrovnikov V.S., Bogdanchikov A.G., Kazanin V.F., Korol A.A., Malyshev V.M., Maslennikov A.L., Maxiimov D.A., Peleganchuk S.V., Rezanova O.L., Skovpen K.Yu., Soukharev A.M., Talyshev A.A., Tikhonov Yu.A. Measurement of event-plane correla-tions in root s(NN)=2.76 TeV lead-lead collisions with the ATLAS detector. // PHYSICAL REVIEW C. - 2014. - Vol. 90, Is. 2. - P. 024905. - ISSN 0556-2813, DOI 10.1103/PhysRevC.90.024905.

[226] Abelev B., ALICE Collab., Pestov Y. Two- and three-pion quantum statistics correlations in Pb-Pb collisions at root S-NN=2.76 TeV at the CERN Large Hadron Collider. // PHYSICAL REVIEW C. - 2014. - Vol. 89, Is. 2. - P. 024911. - ISSN 0556-2813, DOI 10.1103/PhysRevC.89.024911.

[227] Ablikim M., BESIII Collab., Achasov M.N., Muchnoi N.Yu., Nikolaev I.B. Search for the weak decays J/psi - D-s(()*()-) e(+)nu(e) + c.c. // PHYSICAL REVIEW D. - 2014. - Vol. 90, Is. 11. - P. 112014. - ISSN 1550-7998, DOI 10.1103/PhysRevD.90.112014.

[228] Lees J.P., BABAR Collab., Blinov V.E., Buzykaev A.R., Druzhinin V.P., Golubev V.B., Kravchenko E.A., Onuchin A.P., Serednyakov S.I., Skovpen Yu.I., Solodov E.P., Todyshev K.Yu. Search for new pi(0)-like particles produced in association with a tau-lepton pair. // PHYSICAL REVIEW D. - 2014. - Vol. 90, Is. 11. - P. UNSP 112011. - ISSN 1550-7998, DOI 10.1103/PhysRevD.90.112011.

[229] Achasov M.N., Barnyakov A.Yu., Beloborodov K.I., Berdyugin A.V., Berkaev D.E., Bogdanchikov A.G., Botov A.A., Dimova T.V., Druzhinin V.P., Golubev V.B., Kardapoltsev L.V., Kasaev A.S., Kharlamov A.G., Kirpotin A.N., Koop I.A., Korol A.A., Koshuba S.V., Kovrizhin D.P., Kupich A.S., Martin K.A., Obrazovsky A.E., Pakhtusova E.V., Rogovsky Yu.A., Senchenko A.I.,

Serednyakov S.I., Silagadze Z.K., Shatunov Yu.M., Shtol D.A., Shwartz D.B., Skrinsky A.N., Surin I.K., Tikhonov Yu.A., Usov Yu.V., Vasiljev A.V. Study of the process $e^+e^- \to$ n anti-n at the VEPP-2000 e^+e^- collider with the SND detector. // PHYSICAL REVIEW D. - 2014. - Vol. 90, Is. 11. - Art. nr 112007.

[230] Aad G., ATLAS Collab., Anisenkov A.V., Bobrovnikov V.S., Bogdanchikov A.G., Kazanin V.F., Korol A.A., Malyshev V.M., Maslennikov A.L., Maxiimov D.A., Peleganchuk S.V., Rezanova O.L., Skovpen K.Yu., Soukharev A.M., Talyshev A.A., Tikhonov Yu.A. Comprehensive measurements of t-channel single top-quark production cross sections at root S=7 TeV with the ATLAS detector. // PHYSICAL REVIEW D. - 2014. - Vol. 90, Is. 11. - P. 112006. - ISSN 1550-7998, DOI 10.1103/PhysRevD.90.112006.

[231] Aaij R., LHCb Collab., Bondar A., Eidelman S, Krokovny P., Poluektov A., Shekhtman L., Vorobyev V. Measurements of CP violation in the three-body phase space of charmless B-+/- decays. // PHYSICAL REVIEW D. - 2014. - Vol. 90, Is. 11. - P. 112004. - ISSN 1550-7998, DOI 10.1103/PhysRev D.90.112004.

[232] Aad G., ATLAS Collab., Anisenkov A.V., Bobrovnikov V.S., Bogdanchikov A.G., Kazanin V.F., Korol A.A., Malyshev V.M., Maslennikov A.L., Maxiimov D.A., Peleganchuk S.V., Rezanova O.L., Skovpen K.Yu., Soukharev A.M., Talyshev A.A., Tikhonov Yu.A. Search for nonpointing and delayed photons in the diphoton and missing transverse momentum final state in 8 TeV pp collisions at the LHC using the ATLAS detector. // PHYSICAL REVIEW D. - 2014. - Vol. 90, Is. 11. - P. UNSP 112005. - ISSN 1550-7998, DOI 10.1103/PhysRevD.90.112005.

[233] Aaij R., LHCB Collab. Bondar A., Eidelman S, Krokovny P., Poluektov A., Shekhtman L., Vorobyev V. Measurement of CP violation parameters in B-0 - DK*(0) decays. // PHYSICAL REVIEW D. - 2014. - Vol. 90, Is. 11. - P. 112002. - ISSN 1550-7998, DOI 10.1103/PhysRevD.90.112002.

[234] Lees J.P., BaBar Collab., Blinov V.E., Buzykaev A.R., Druzhinin V.P., Golubev V.B., Kravchenko E.A., Onuchin A.P., Serednyakov S.I., Skovpen Yu.I., Solodov E.P., Todyshev K.Yu., Yushkov A.N. Measurements of direct CP asymmetries in B - X-s gamma decays using sumof exclusive decays. // PHYSICAL REVIEW D. - 2014. - Vol. 90, Is. 9. - P. 092001. - ISSN 1550-7998, DOI 10.1103/PhysRevD.90.092001.

[235] Ablikim M., BESIII Collab., Achasov M.N., Muchnoi N.Yu., Nikolaev I.B. Search for C-parity violation in J/$\psi \to \gamma\gamma$ and $\gamma\varphi$. // PHYSICAL REVIEW D. - 2014. - Vol. 90, Is. 9. - P.092002. - ISSN 1550-7998, DOI 10.1103/PhysRev D.90.092002.

[236] Aad G., ATLAS Collab., Anisenkov A.V., Bobrovnikov V.S., Bogdanchikov A.G., Kazanin V.F., Korol A.A., Malyshev V.M., Maslennikov A.L., Maxiimov D.A., Peleganchuk S.V., Rezanova O.L.,

Skovpen K.Yu., Soukharev A.M., Talyshev A.A., Tikhonov Yu.A. Search for the lepton flavor violating decay Z - e mu in pp collisions at root s=8 TeV with the ATLAS detector. // PHYSICAL REVIEW D. - 2014. - Vol. 90, Is. 7. - P. 072010. - ISSN 1550-7998, DOI 10.1103/PhysRevD.90.072010.

[237] Sato S., Belle Collab., Aulchenko V., Bondar A., Eidelman S., Gabyshev N., Garmash A., Krokovny P., Kuzmin A., Matvienko D., Shebalin V., Vorobyev V, Zhilich V., Zhulanov V. Observation of the decay $B^0 \to \eta'K^*(892)^0$. // PHYSICAL REVIEW D. - 2014. - Vol. 90, Is. 7. - P. UNSP 072009. - ISSN 1550-7998, DOI 10.1103/PhysRevD.90.072009.

[238] Aaij R., LHCb Collab. Bondar A., Eidelman S, Krokovny P., Poluektov A., Shekhtman L., Vorobyev V., Dalitz plot analysis of $B_s^0 \to \overline{D}{}^0 K^- \pi^+$ decays. // PHYSICAL REVIEW D. - 2014. - Vol. 90, Is. 7. - P. 072003. [arXiv:1407.7712 [hep-ex]].

[239] Aad G., ATLAS Collab., Anisenkov A.V., Bobrovnikov V.S., Bogdanchikov A.G., Kazanin V.F., Korol A.A., Malyshev V.M., Maslennikov A.L., Maxiimov D.A., Peleganchuk S.V., Rezanova O.L., Skovpen K.Yu., Soukharev A.M., Talyshev A.A., Tikhonov Yu.A. Measurements of normalized differential cross sections for t(t)over-bar production in pp collisions at root(s)=7 TeV using the ATLAS detector. // PHYSICAL REVIEW D. - 2014. - Vol. 90, Is. 7. - P.072004. - ISSN 1550-7998, DOI 10.1103/PhysRev D.90.072004.

[240] Aaij R., LHCb Collab., Bondar A., Eidelman S, Krokovny P., Poluektov A., Shekhtman L., Vorobyev V. Measurement of CP violation in B-s(0) -Phi Phi decays. // PHYSICAL REVIEW D. - 2014. - Vol. 90, Is. 5. - P. 052011. - ISSN 1550-7998, DOI 10.1103/ PhysRevD.90.052011.

[241] Ablikim M., BESII Collab., Achasov M.N., Muchnoi N.Yu., Nikolaev I.B. Observation of J/psi - p(p) over-bar a(0)(980) at BESIII. // PHYSICAL REVIEW D. - 2014. - Vol. 90, Is. 5. - P. 052009. - ISSN 1550-7998, DOI 10.1103/PhysRevD.90.052009.

[242] Aad G., ATLAS Collab., Anisenkov A.V., Bobrovnikov V.S., Bogdanchikov A.G., Kazanin V.F., Korol A.A., Malyshev V.M., Maslennikov A.L., Maxiimov D.A., Peleganchuk S.V., Rezanova O.L., Skovpen K.Yu., Soukharev A.M., Talyshev A.A., Tikhonov Yu.A. Search for pair-produced third-generation squarks decaying via charm quarks or in compressed supersymmetric scenarios in pp collisions atroot s = 8 TeV with the ATLAS detector. // PHYSICAL REVIEW D. - 2014. - Vol. 90, Is. 5. - ISSN 1550-7998, DOI 10.1103/PhysRevD.90.052008.

[243] Aad G., ATLAS Collab., Anisenkov A.V., Bobrovnikov V.S., Bogdanchikov A.G., Kazanin V.F., Korol A.A., Malyshev V.M., Maslennikov A.L., Maxiimov D.A., Peleganchuk S.V., Rezanova O.L., Skovpen K.Yu., Soukharev A.M., Talyshev A.A.,

Tikhonov Yu.A. Flavor tagged time-dependent angular analysis of the B-s(0) - J/psi phi decay and extraction of Delta Gamma(s) and the weak phase phi(s) in ATLAS. // PHYSICAL REVIEW D. - 2014. - Vol. 90, Is. 5. - P. 052007. - ISSN 1550-7998, DOI 10.1103/PhysRev D.90.052007.

[244] Aad G., ATLAS Collab., Anisenkov A.V., Bobrovnikov V.S., Bogdanchikov A.G., Kazanin V.F., Korol A.A., Malyshev V.M., Maslennikov A.L., Maxiimov D.A., Peleganchuk S.V., Rezanova O.L., Skovpen K.Yu., Soukharev A.M., Talyshev A.A., Tikhonov Yu.A. Search for high-mass dilepton resonances in pp collisions at root s = 8TeV with the ATLAS detector. // PHYSICAL REVIEW D. - 2014. - Vol. 90, Is. 5. - P. 052005. - ISSN 1550-7998, DOI 10.1103/ PhysRevD.90.052005.

[245] Aad G., ATLAS Collab., Anisenkov A.V., Bobrovnikov V.S., Bogdanchikov A.G., Kazanin V.F., Korol A.A., Malyshev V.M., Maslennikov A.L., Maxiimov D.A., Peleganchuk S.V., Rezanova O.L., Skovpen K.Yu., Soukharev A.M., Talyshev A.A., Tikhonov Yu.A. Measurement of the Higgs boson mass from the H - gamma gamma and H -ZZ* - 4l channels in pp collisions at center-of-mass energies of 7 and 8 TeV with the ATLAS detector. // PHYSICAL REVIEW D. - 2014. - Vol. 90, Is. 5. - P. 052004. - ISSN 1550-7998, DOI 10.1103/PhysRevD.90.052004.

[246] Lees J.P., BaBar Collab. Blinov V.E., Buzykaev A.R., Druzhinin V.P., Golubev V.B., Kravchenko E.A., Onuchin A.P., Serednyakov S.I., Skovpen Yu.I., Solodov E.P., Todyshev K.Yu., Measurement of Collins asymmetries in inclusive production of charged pion pairs in e^+e^- annihilation at BABAR. // PHYSICAL REVIEW D. - 2014. - Vol. 90, Is. 5. - P. 052003. - ISSN 1550-7998, DOI 10.1103/ PhysRevD.90.052003.

[247] Aad G., ATLAS Collab., Anisenkov A.V., Bobrovnikov V.S., Bogdanchikov A.G., Kazanin V.F., Korol A.A., Malyshev V.M., Maslennikov A.L., Maxiimov D.A., Peleganchuk S.V., Rezanova O.L., Skovpen K.Yu., Soukharev A.M., Talyshev A.A., Tikhonov Yu.A. Search for supersymmetry in events with four or more leptons in root s=8TeV pp collisions with the ATLAS detector. // PHYSICAL REVIEW D. - 2014. - Vol. 90, Is. 5. - P. 052001. - ISSN 1550-7998, DOI 10.1103/PhysRevD.90.052001.

[248] Aaij R., LHCb Collab., Bondar A., Eidelman S, Krokovny P., Poluektov A., Shekhtman L., Vorobyev V. Measurement of the ratio of B-c(+) branching fractions to J/ψ π^+ and J/ψ $\mu^+\nu\mu$ final states. // PHYSICAL REVIEW D. - 2014. - Vol. 90, Is. 3. - P. 032009. - ISSN 1550-7998, DOI 10.1103/ PhysRevD.90.032009.

[249] Ablikim M., BESIII Collab., Achasov M.N., Muchnoi N.Yu., Nikolaev I.B. Study of $e^+e^- \rightarrow p\ \bar{p}\ \pi^0$ in the vicinity of the ψ(3770). // PHYSICAL REVIEW D. - 2014. - Vol. 90, Is. 3. - P. 032007. - ISSN 1550-7998, DOI 10.1103/PhysRev D.90.032007.

[250] Achasov M.N., Aulchenko V.M., Barnyakov A.Yu., Beloborodov K.I., Berdyugin A.V., Bogdanchikov A.G., Botov A.A., Dimova T.V., Druzhinin V.P., Golubev V.B., Grevtsov K.A., Kardapoltsev L.V., Kharlamov A.G., Kovrizhin D.P., Koop I.A., Korol A.A., Koshuba S.V., Lysenko A.P., Martin K.A., Obrazovsky A.E., Pakhtusova E.V., Perevedentsev E.A., Romanov A.L., Serednyakov S.I., Silagadze Z.K., Skrinsky A.N., Surin I.K., Tikhonov Yu.A., Vasiljev A.V., Shatunov P.Yu., Shatunov Yu.M., Shtol D.A. Study of the process $e^+e^- \rightarrow \eta\ \gamma$ in the center-of-mass energy range 1.07-2.00 GeV. // PHYSICAL REVIEW D. - 2014. - Vol. 90, Is. 3. - Art. nr 032002.

[251] Aad G., ATLAS Collab., Anisenkov A.V., Bobrovnikov V.S., Bogdanchikov A.G., Kazanin V.F., Korol A.A., Malyshev V.M., Maslennikov A.L., Maxiimov D.A., Peleganchuk S.V., Rezanova O.L., Skovpen K.Yu., Soukharev A.M., Talyshev A.A., Tikhonov Yu.A. Search for dark matter in events with a Z boson and missing transverse momentum in pp collisions at root s=8 TeV with the ATLAS detector. // PHYSICAL REVIEW D. - 2014. - Vol. 90, Is. 1. - P. 012004. - ISSN 1550-7998, DOI 10.1103/PhysRev D.90.012004.

[252] Aaij R., LHCb Collab. Bondar A., Eidelman S, Krokovny P., Poluektov A., Shekhtman L., Vorobyev V., Measurement of the resonant and CP components in $\bar{B}^0 \rightarrow$ J/ψ $\pi^+\pi^-$ decays. // PHYSICAL REVIEW D. - 2014. - Vol. 90, Is. 1. - P. 012003. - ISSN 1550-7998, DOI 10.1103/PhysRev D.90.012003.

[253] Chobanova V., Belle Collab., Aulchenko V., Bondar A., Eidelman S., Gabyshev N., Garmash A., Krokovny P., Kuzmin A., Matvienko D., Shebalin V., Vorobyev V, Zhilich V., Zhulanov V. Measurement of branching fractions and CP violation parameters in $B \rightarrow \omega K$ decays with first evidence of CP violation in $B0 \rightarrow \omega K_s^0$. // PHYSICAL REVIEW D. - 2014. - Vol. 90, Is. 1. - P. 012002. - ISSN 1550-7998, DOI 10.1103/ PhysRevD.90.012002.

[254] Ablikim M., BESIII Collab., Achasov M.N., Muchnoi N.Yu., Nikolaev I.B. Precision measurement of the mass of the tau lepton. // PHYSICAL REVIEW D. - 2014. - Vol. 90, Is. 1. - ISSN 1550-7998, DOI 10.1103/ PhysRevD.90.012001.

[255] Lees J.P., BABAR Collab., Blinov V.E., Buzykaev A.R., Druzhinin V.P., Golubev V.B., Kravchenko E.A., Onuchin A.P., Serednyakov S.I., Skovpen Yu.I., Solodov E.P., Todyshev K.Yu. Study of the reaction $e^+e^- \rightarrow$ ψ(2S) $\pi^+\pi^-$ via initial-state radiation at BABAR. // PHYSICAL REVIEW D. - 2014. - Vol. 89, Is. 11. - P. 111103. - ISSN 1550-7998, DOI 10.1103/ PhysRevD.89.111103.

[256] Ablikim M., BESIII Collab., Achasov M.N., Muchnoi N.Yu., Nikolaev I.B. Measurement of the branching fraction for ψ(3686) $\rightarrow \omega K^+K^-$. // PHYSICAL

REVIEW D. - 2014. - Vol. 89, Is. 11. - P. 112006. - ISSN 1550-7998, DOI 10.1103/PhysRev D.89.112006.

[257] Lees J.P., BABAR Collab., Blinov V.E., Buzykaev A.R., Druzhinin V.P., Golubev V.B., Kravchenko E.A., Onuchin A.P., Serednyakov S.I., Skovpen Yu.I., Solodov E.P., Todyshev K.Yu. Antideuteron production in Upsilon(nS) decays and in e(+)e(-) - q(q)over bar at root s approximate to 10.58 GeV. // PHYSICAL REVIEW D. - 2014. - Vol. 89, Is. 11. - P. 111102. - ISSN 1550-7998, DOI 10.1103/ PhysRevD.89.111102.

[258] Ablikim M., BESIII Collab., Achasov M.N., Muchnoi N.Yu., Nikolaev I.B. Search for the radiative transitions $\psi(3770) \to \gamma\eta_c$ and $\gamma\eta_c$ (2S). // PHYSICAL REVIEW D. - 2014. - Vol. 89, Is. 11. - P. 112005. - ISSN 1550-7998, DOI 10.1103/PhysRevD.89.112005.

[259] Vanhoefer P., Belle Collab., Aulchenko V., Bondar A., Eidelman S., Gabyshev N., Garmash A., Krokovny P., Kuzmin A., Matvienko D., Shebalin V., Vorobyev V, Zhilich V., Zhulanov V. Study of $B^0 \to \rho^0 \rho^0$ decays, implications for the CKM angle $\varphi(2)$ and search for other B^0 decay modes with a four-pion final state (vol 89, 072008, 2014). // PHYSICAL REVIEW D. - 2014. - Vol. 89, Is. 11. - P. 119903. - ISSN 1550-7998, DOI 10.1103/PhysRev D.89.119903.

[260] Lees J.P., BABAR Collab., Blinov V.E., Buzykaev A.R., Druzhinin V.P., Golubev V.B., Kravchenko E.A., Onuchin A.P., Serednyakov S.I., Skovpen Yu.I., Solodov E.P., Todyshev K.Yu. Dalitz plot analysis of eta(c) - K+K-eta and eta(c) - K+K-pi(0) in two-photon interactions. // PHYSICAL REVIEW D. - 2014. - Vol. 89, Is. 11. - P. 112004. - ISSN 1550-7998, DOI 10.1103/PhysRevD.89.112004.

[261] Lees J.P., BaBar Collab., Blinov V.E., Buzykaev A.R., Druzhinin V.P., Golubev V.B., Kravchenko E.A., Onuchin A.P., Serednyakov S.I., Skovpen Yu.I., Solodov E.P., Todyshev K.Yu. Evidence for the baryonic decay (B)over-bar(0) $\to$ D-0 Lambda (Lambda)over-bar. // PHYSICAL REVIEW D. - 2014. - Vol. 89, Is. 11. - P. UNSP 112002. - ISSN 1550-7998, DOI 10.1103/PhysRevD.89.112002.

[262] Peng T., Belle Collab., Aulchenko V., Bondar A., Eidelman S., Gabyshev N., Garmash A., Krokovny P., Kuzmin A., Matvienko D., Shebalin V., Vorobyev V, Zhilich V., Zhulanov V. Measurement of $D^0 - \bar{D}^0$ mixing and search for indirect CP violation using $D^0 - K_S^0 \pi^+\pi^-$ decays. // PHYSICAL REVIEW D. - 2014. - Vol. 89, Is. 9. - P. 091103.

[263] Aad G., ATLAS Collab., Anisenkov A.V., Bobrovnikov V.S., Bogdanchikov A.G., Kazanin V.F., Korol A.A., Malyshev V.M., Maslennikov A.L., Maxiimov D.A., Peleganchuk S.V., Rezanova O.L., Skovpen K.Yu., Soukharev A.M., Talyshev A.A., Tikhonov Yu.A. Measurement of the parity-violating asymmetry parameter ab and the helicity amplitudes for the decay Lambda(0)(b) - J/psi Lambda(0) with the ATLAS detector. // PHYSICAL REVIEW D. - 2014. - Vol. 89, Is. 9. - P. 092009. - ISSN 1550-7998, DOI 10.1103/PhysRevD.89.092009.

[264] Lee S. -H., Belle Collab., Aulchenko V., Bondar A., Eidelman S., Gabyshev N., Garmash A., Krokovny P., Kuzmin A., Matvienko D., Shebalin V., Vorobyev V, Zhilich V., Zhulanov V. Measurements of the masses and widths of the (2455) and (2520) baryons. // PHYSICAL REVIEW D. - 2014. - Vol. 89, Is. 9. - ISSN 1550-7998, DOI 10.1103/PhysRevD.89.091102.

[265] Ablikim M., BESIII Collab., Achasov M.N., Muchnoi N.Yu., Nikolaev I.B. Observation of electromagnetic Dalitz decays $J/\psi \to P\ e^+e^-$. // PHYSICAL REVIEW D. - 2014. - Vol. 89, Is. 9. - P. 092008. - ISSN 1550-7998, DOI 10.1103/PhysRev D.89.092008.

[266] Aaij R., LHCb Collab., Bondar A., Eidelman S, Krokovny P., Poluektov A., Shekhtman L., Vorobyev V. Measurement of resonant and CP components in (B)over-bar(s)(0) - J/psi pi(+) pi(-) decays. // PHYSICAL REVIEW D. - 2014. - Vol. 89, Is. 9. - P. 092006. - ISSN 1550-7998, DOI 10.1103/PhysRev D.89.092006.

[267] Lees J.P., BaBar Collab., Blinov V.E., Buzykaev A.R., Druzhinin V.P., Golubev V.B., Kravchenko E.A., Onuchin A.P., Serednyakov S.I., Skovpen Yu.I., Solodov E.P., Todyshev K.Yu. Cross sections for the reactions e_e-. K0 SK0 L, K0 SK0 Lp_p-, K0 SK0Sp_p-, and K0 SK0 SK_K- from events with initial-state radiation. // PHYSICAL REVIEW D. - 2014. - Vol. 89, Is. 9. - P. 092002. - ISSN 1550-7998, DOI 10.1103/ PhysRevD.89.092002.

[268] Lees J.P., BaBar Collab., Blinov V.E., Buzykaev A.R., Druzhinin V.P., Golubev V.B., Kravchenko E.A., Onuchin A.P., Serednyakov S.I., Skovpen Yu.I., Solodov E.P., Todyshev K.Yu. Search for the decay (B)over-bar(0) $\to$ Lambda(+)(c)(p)over-bar p(p)over-bar. // PHYSICAL REVIEW D. - 2014. - Vol. 89, Is. 7. - P. 071102(R). - ISSN 1550-7998, DOI 10.1103/PhysRevD.89.071102.

[269] Shen C. P., Belle Collab., Aulchenko V., Bondar A., Eidelman S., Gabyshev N., Garmash A., Krokovny P., Kuzmin A., Matvienko D., Shebalin V., Vorobyev V, Zhilich V., Zhulanov V. Updated cross section measurement of $e^+e^- \to K^+K^-J/\psi$ and $K_S^0 K_S^0 J/\psi$ via initial state radiation at Belle. // PHYSICAL REVIEW D. - 2014. - Vol. 89, Is. 7. - P. 072015. - ISSN 1550-7998, DOI 10.1103/PhysRevD.89.072015.

[270] Aad G., ATLAS Collab., Anisenkov A.V., Bobrovnikov V.S., Bogdanchikov A.G., Kazanin V.F., Korol A.A., Malyshev V.M., Maslennikov A.L., Maxiimov D.A., Peleganchuk S.V., Rezanova O.L., Skovpen K.Yu., Soukharev A.M., Talyshev A.A., Tikhonov Yu.A. Study of heavy-flavor quarks produced in association with top-quark pairs at root s=7 TeV using

the ATLAS detector. // PHYSICAL REVIEW D. - 2014. - Vol. 89, Is. 7. - P. 072012. - ISSN 1550-7998, DOI 10.1103/PhysRevD.89.072012.

[271] Ablikim M., BESIII Collab., Achasov M.N., Muchnoi N.Yu., Nikolaev I.B. Measurement of χ_{cJ} decaying into η' K^+K^-. // PHYSICAL REVIEW D. - 2014. - Vol. 89, Is. 7. - P. 074030. - ISSN 1550-7998, DOI 10.1103/PhysRevD.89.074030.

[272] Ablikim M., BESIII Collab., Achasov M.N., Muchnoi N.Yu., Nikolaev I.B. Search for the rare decays $J/\psi \to D_{s-} \rho^+$ and $J/\psi \to \bar{D}^0 \bar{K}^0$. // PHYSICAL REVIEW D. - 2014. - Vol. 89, Is. 7. - P. 071101. - ISSN 1550-7998, DOI 10.1103/PhysRevD.89.071101.

[273] Ryu S., Belle Collab., Aulchenko V., Bondar A., Eidelman S., Gabyshev N., Garmash A., Krokovny P., Kuzmin A., Matvienko D., Shebalin V., Vorobyev V, Zhilich V., Zhulanov V. Measurements of branching fractions of τ lepton decays with one or more K_S^0. // PHYSICAL REVIEW D. - 2014. - Vol. 89, Is. 7. - P. 072009. - ISSN 1550-7998, DOI 10.1103/PhysRevD.89.072009.

[274] Vanhoefer P., Belle Collab., Aulchenko V., Bondar A., Eidelman S., Gabyshev N., Garmash A., Krokovny P., Kuzmin A., Matvienko D., Shebalin V., Vorobyev V, Zhilich V., Zhulanov V. Study of B-0 → rho(0)rho(0) decays, implications for the CKM angle phi(2) and search for other B-0 decay modes with a four-pion final state. // PHYSICAL REVIEW D. - 2014. - Vol. 89, Is. 7. - P. 072008. - ISSN 1550-7998, DOI 10.1103/PhysRevD.89.072008.

[275] Ablikim M., BESIII Collab., Achasov M.N., Muchnoi N.Yu., Nikolaev I.B. Precision measurements of B(D+ - mu(+)nu(mu)), the pseudoscalar decayconstant fD+, and the quark mixing matrix element vertical bar V-cdvertical bar. // PHYSICAL REVIEW D. - 2014. - Vol. 89, Is. 5. - P. 051104. - ISSN 1550-7998, DOI 10.1103/PhysRevD.89.051104.

[276] Aad G., ATLAS Collab., Anisenkov A.V., Bobrovnikov V.S., Bogdanchikov A.G., Kazanin V.F., Korol A.A., Malyshev V.M., Maslennikov A.L., Maxiimov D.A., Peleganchuk S.V., Rezanova O.L., Skovpen K.Yu., Soukharev A.M., Talyshev A.A., Tikhonov Yu.A. Measurement of the inclusive isolated prompt photons cross section in pp collisions at root s=7 TeV with the ATLAS detector using 4.6 fb(-1). // PHYSICAL REVIEW D. - 2014. - Vol. 89, Is. 5. - P. 052004. - ISSN 1550-7998, DOI 10.1103/PhysRevD.89.052004.

[277] Kato Y., Belle Collab., Aulchenko V., Bondar A., Eidelman S., Gabyshev N., Garmash A., Krokovny P., Kuzmin A., Matvienko D., Shebalin V., Vorobyev V, Zhilich V., Zhulanov V. Search for doubly charmed baryons and study of charmed strange baryons at Belle. // PHYSICAL REVIEW D. - 2014. - Vol. 89, Is. 5. - P. 052003. - ISSN 1550-7998, DOI 10.1103/PhysRevD.89.052003.

[278] Ablikim M., BESIII Collab., Achasov M.N., Muchnoi N.Yu., Nikolaev I.B. Amplitude analysis of the $D^+ \to KS^0_S \pi^+ \pi^0$ Dalitz plot. // PHYSICAL REVIEW D. - 2014. - Vol. 89, Is. 5. - P. 052001. - ISSN 1550-7998, DOI 10.1103/PhysRevD.89.052001.

[279] Lai Y-T, Belle Collab., Aulchenko V., Bondar A., Eidelman S., Gabyshev N., Garmash A., Krokovny P., Kuzmin A., Matvienko D., Shebalin V., Vorobyev V, Zhilich V., Zhulanov V. Search for $B^0 \to p \bar{\Lambda}\pi^-\gamma$ at Belle. // PHYSICAL REVIEW D. - 2014. - Vol. 89, Is. 5. - P. 051103. - ISSN 1550-7998, DOI 10.1103/PhysRevD.89.051103.

[280] Lees J.P., BABAR Collab., Blinov V.E., Buzykaev A.R., Druzhinin V.P., Golubev V.B., Kravchenko E.A., Onuchin A.P., Serednyakov S.I., Skovpen Yu.I., Solodov E.P., Todyshev K.Yu. Evidence for the decay B-0 - omega omega and search for B-0 – omega phi. // PHYSICAL REVIEW D. - 2014. - Vol. 89, Is. 5. - P. 051101. - ISSN 1550-7998, DOI 10.1103/PhysRevD.89.051101.

[281] He X. H., Belle Collab., Aulchenko V., Bondar A., Eidelman S., Gabyshev N., Garmash A., Krokovny P., Kuzmin A., Matvienko D., Shebalin V., Vorobyev V, Zhilich V., Zhulanov V. Search for the process $e^+e^- \to J/\psi$ X(1835) at $\sqrt{s}$ approximate to 10.6 GeV. // PHYSICAL REVIEW D. - 2014. - Vol. 89, Is. 3. - P. 032003. - ISSN 1550-7998, DOI 10.1103/PhysRevD.89.032003.

[282] Aad G., ATLAS Collab., Anisenkov A.V., Bobrovnikov V.S., Bogdanchikov A.G., Kazanin V.F., Korol A.A., Malyshev V.M., Maslennikov A.L., Maxiimov D.A., Peleganchuk S.V., Rezanova O.L., Skovpen K.Yu., Soukharev A.M., Talyshev A.A., Tikhonov Yu.A. Search for a multi-Higgs-boson cascade in W(+)W(- b(b)over-bar events with the ATLAS detector in pp collisions at root s=8 TeV. // PHYSICAL REVIEW D. - 2014. - Vol. 89, Is. 3. - P. 032002. - ISSN 1550-7998, DOI 10.1103/PhysRevD.89.032002.

[283] Aaij R., LHCb Collab., Bondar A., Eidelman S, Krokovny P., Poluektov A., Shekhtman L., Vorobyev V. Studies of beauty baryon decays to D0 ph(-) and Λc+ h- final states. // PHYSICAL REVIEW D. - 2014. - Vol. 89, Is. 3. - P. 032001. [arXiv:1311.4823 [hep-ex]].

[284] Lees J.P., BaBar Collab., Blinov V.E., Buzykaev A.R., Druzhinin V.P., Golubev V.B., Kravchenko E.A., Onuchin A.P., Serednyakov S.I., Skovpen Yu.I., Solodov E.P., Todyshev K.Yu. Search for lepton-number violating B+ → X(-)l(+)l '(+) decays. // PHYSICAL REVIEW D. - 2014. - Vol. 89, Is. 1. - P. 011102. - ISSN 1550-7998, DOI 10.1103/PhysRevD.89.011102.

[285] Tien K. -J., Belle Collab., Aulchenko V., Bondar A., Eidelman S., Gabyshev N., Garmash A., Krokovny P., Kuzmin A., Matvienko D., Shebalin V., Vorobyev V, Zhilich V., Zhulanov V. Evidence for semileptonic B- - p(p)over-bar l(-)(nu)over-bar(l) decays. // PHYSICAL

REVIEW D. - 2014. - Vol. 89, Is. 1. - P. 011101. - ISSN 1550-7998, DOI 10.1103/PhysRev D.89.011101.

[286] Aaij R., LHCb Collab., Bondar A., Eidelman S, Krokovny P., Poluektov A., Shekhtman L., Vorobyev V. Precision measurement of the mass and lifetime of the Xi(-)(b) Baryon. // PHYSICAL REVIEW LETTERS. - 2014. - Vol. 113, Is. 24. - P. 242002. - ISSN 0031-9007, DOI 10.1103/PhysRevLett.113.242002.

[287] Abelev B., ALICE Collab., Pestov Y. Exclusive J/psi Photoproduction of protons in ultraperipheral p-Pb collisions at root s(NN)=5.02 TeV. // PHYSICAL REVIEW LETTERS. - 2014. - Vol. 113, Is. 23. - P. 232504. - ISSN 0031-9007, DOI 10.1103/ PhysRevLett.113.232504.

[288] Abelev B., ALICE Collab., Pestov Y. Measurement of Prompt D-Meson Production in p-Pb collisions at roots(NN)=5.02 TeV. // PHYSICAL REVIEW LETTERS. - 2014. - Vol. 113, Is. 23. - P. 232301. - ISSN 0031-9007, DOI 10.1103/PhysRev Lett.113.232301.

[289] Terekhov I.S. Vergeles S.S., Turitsyn S.K. Conditional Probability Calculations for the Nonlinear Schrodinger equation with additive noise. // PHYSICAL REVIEW LETTERS. - 2014. - Vol. 113, Is. 23. - P. 230602. - ISSN 0031-9007, DOI 10.1103/ PhysRevLett.113.230602.

[290] Aad G., ATLAS Collab., Anisenkov A.V., Bobrovnikov V.S., Bogdanchikov A.G., Kazanin V.F., Korol A.A., Malyshev V.M., Maslennikov A.L., Maxiimov D.A., Peleganchuk S.V., Rezanova O.L., Skovpen K.Yu., Soukharev A.M., Talyshev A.A., Tikhonov Yu.A. Observation of an excited B-c(+/-) meson state with the ATLAS detector. // PHYSICAL REVIEW LETTERS. - 2014. - Vol. 113, Is. 21. - P. 212004. - ISSN 0031-9007, DOI 10.1103/PhysRev Lett.113.212004.

[291] Aaij R., LHCb Collab., Bondar A., Eidelman S, Krokovny P., Poluektov A., Shekhtman L., Vorobyev V. Measurement of the CP-violating phase phi(s) in (B)over-bar(s)(0) $\to$ Ds+Ds- decays. // PHYSICAL REVIEW LETTERS. - 2014. - Vol. 113, Is. 21. - P. 211801. - ISSN 0031-9007, DOI 10.1103/PhysRevLett.113.211801.

[292] Ablikim M., BESIII Collab., Achasov M.N., Muchnoi N.Yu., Nikolaev I.B. Observation of $e^+e^- \to \pi^0\pi^0 h_c$ and a neutral charmonium like structure $Z_c(4020)^0$. // PHYSICAL REVIEW LETTERS. - 2014. - Vol. 113, Is. 21. - P. 212002. - ISSN 0031-9007, DOI 10.1103/PhysRev Lett.113.212002.

[293] Lees J.P., BABAR Collab., Blinov V.E., Buzykaev A.R., Druzhinin V.P., Golubev V.B., Kravchenko E.A., Onuchin A.P., Serednyakov S.I., Skovpen Yu.I., Solodov E.P., Todyshev K.Yu. Search for a dark photon in e^+e^- collisions at BABAR. // PHYSICAL REVIEW LETTERS. - 2014. - Vol. 113, Is. 20. - P. 201801. - ISSN 0031-9007, DOI 10.1103/ PhysRevLett.113.201801.

[294] Aaij R., LHCb Collab., Bondar A., Eidelman S, Krokovny P., Poluektov A., Shekhtman L., Vorobyev V. Measurement of the (B)over-bar(s)(0) meson lifetime in D-s(+) pi(-) Decays. // PHYSICAL REVIEW LETTERS. - 2014. - Vol. 113, Is. 17. - P. 172001. - ISSN 0031-9007, DOI 10.1103/PhysRev Lett.113.172001.

[295] Aad G., ATLAS Collab., Anisenkov A.V., Bobrovnikov V.S., Bogdanchikov A.G., Kazanin V.F., Korol A.A., Malyshev V.M., Maslennikov A.L., Maxiimov D.A., Peleganchuk S.V., Rezanova O.L., Skovpen K.Yu., Soukharev A.M., Talyshev A.A., Tikhonov Yu.A. Search for scalar diphoton resonances in the mass range 65-600 GeV with the ATLAS detector in pp collision data at root s=8 TeV. // PHYSICAL REVIEW LETTERS. - 2014. - Vol. 113, Is. 17. - P. UNSP 171801. - ISSN 0031-9007, DOI 10.1103/PhysRevLett.113.171801.

[296] Aaij R., LHCb Collab., Bondar A., Eidelman S, Krokovny P., Poluektov A., Shekhtman L., Vorobyev V. Observation of overlapping Spin-1 and Spin-3 $\bar{D}^0K^-$ resonances at mass 2.86 GeV/c(2). // PHYSICAL REVIEW LETTERS. - 2014. - Vol. 113, Is. 16. - P. 162001. [arXiv:1407.7574 [hep-ex]].

[297] Aaij R., LHCb Collab., Bondar A., Eidelman S, Krokovny P., Poluektov A., Shekhtman L., Vorobyev V. First Observation of a baryonic B-c(+) decay. // PHYSICAL REVIEW LETTERS. - 2014. - Vol. 113, Is. 15. - P. 152003. - ISSN 0031-9007, DOI 10.1103/PhysRevLett.113.152003.

[298] Aaij R., LHCb Collab., Bondar A., Eidelman S, Krokovny P., Poluektov A., Shekhtman L., Vorobyev V. Test of Lepton universality using B+ - K(+)l(+)l(-) decays. // PHYSICAL REVIEW LETTERS. - 2014. - Vol. 113, Is. 15. - P. 151601. - ISSN 0031-9007, DOI 10.1103/PhysRevLett.113.151601.

[299] Aad G., ATLAS Collab., Anisenkov A.V., Bobrovnikov V.S., Bogdanchikov A.G., Kazanin V.F., Korol A.A., Malyshev V.M., Maslennikov A.L., Maxiimov D.A., Peleganchuk S.V., Rezanova O.L., Skovpen K.Yu., Soukharev A.M., Talyshev A.A., Tikhonov Yu.A. Evidence for electroweak production of W(+/-)W(+/-)jj in pp collisions at root s=8 TeV with the ATLAS detector. // PHYSICAL REVIEW LETTERS. - 2014. - Vol. 113, Is. 14. - P. 141803. - ISSN 0031-9007, DOI 10.1103/PhysRevLett.113.141803.

[300] He X. H., Belle Collab., Aulchenko V., Bondar A., Eidelman S., Gabyshev N., Garmash A., Krokovny P., Kuzmin A., Matvienko D., Shebalin V., Vorobyev V, Zhilich V., Zhulanov V. Observation of $e^+e^- \to \pi^+\pi^-\pi^0\chi_{bJ}$ and search for $X_b \to \omega Y(1S)$ at $\sqrt{s} = 10.867$ GeV. // PHYSICAL REVIEW LETTERS. - 2014. - Vol. 113, Is. 14. - Art. nr 142001.

[301] Aaij R., LHCb Collab., Bondar A., Eidelman S, Krokovny P., Poluektov A., Shekhtman L., Vorobyev V. Evidence for CP violation in B+ → p(p)over-bar K(+) decays. // PHYSICAL REVIEW LETTERS. - 2014. - Vol. 113, Is. 14. - P. 141801. - ISSN 0031-9007, DOI 10.1103/PhysRevLett.113.141801.

[302] Aaij R., LHCb Collab., Bondar A., Eidelman S, Krokovny P., Poluektov A., Shekhtman L., Vorobyev V. First Measurement of the charge asymmetry in beauty-quark pair production. // PHYSICAL REVIEW LETTERS. - 2014. - Vol. 113, Is. 8. - P. 082003. - ISSN 0031-9007, DOI 10.1103/PhysRevLett.113.082003.

[303] Zupanc A., Belle Collab., Aulchenko V., Bondar A., Eidelman S., Gabyshev N., Garmash A., Krokovny P., Kuzmin A., Matvienko D., Shebalin V., Vorobyev V, Zhilich V., Zhulanov V. Measurement of the branching fraction $B(\Lambda^+_c \to pK^-\pi^+)$. // PHYSICAL REVIEW LETTERS. - 2014. - Vol. 113, Is. 4. - P. 042002. - ISSN 0031-9007, DOI 10.1103/PhysRev Lett.113.042002.

[304] Aaij R., LHCb Collab., Bondar A., Eidelman S, Krokovny P., Poluektov A., Shekhtman L., Vorobyev V. Precision measurement of the mass and lifetime of the Xi(0)(b) Baryon. // PHYSICAL REVIEW LETTERS. - 2014. - Vol. 113, Is. 3. - P. 032001. - ISSN 0031-9007, DOI 10.1103/PhysRevLett.113.032001.

[305] Ablikim M., BESIII Collab., Achasov M.N., Muchnoi N.Yu., Nikolaev I.B. Observation of $\eta' \to \pi^+\pi^- \pi^+\pi^-$ and $\eta' \to \pi^+\pi^- \pi^0\pi^0$. // PHYSICAL REVIEW LETTERS. - 2014. - Vol. 112, Is. 25. - P. 251801. - ISSN 0031-9007, DOI 10.1103/PhysRevLett.112.251801.

[306] Aad G., ATLAS Collab., Anisenkov A.V., Bobrovnikov V.S., Bogdanchikov A.G., Kazanin V.F., Korol A.A., Malyshev V.M., Maslennikov A.L., Maxiimov D.A., Peleganchuk S.V., Rezanova O.L., Skovpen K.Yu., Soukharev A.M., Talyshev A.A., Tikhonov Yu.A. Measurements of four-lepton production at the Z resonance in pp collisions at root s=7 and 8 TeV with ATLAS. // PHYSICAL REVIEW LETTERS. - 2014. - Vol. 112, Is. 23. - P. 231806. - ISSN 0031-9007, DOI 10.1103/PhysRevLett.112.231806.

[307] Aaij R., LHCb Collab., Bondar A., Eidelman S, Krokovny P., Poluektov A., Shekhtman L., Vorobyev V. Observation of the resonant character of the Z(4430)(-) state. // PHYSICAL REVIEW LETTERS. - 2014. - Vol. 112, Is. 22. - P. 222002. - ISSN 0031-9007, DOI 10.1103/PhysRevLett.112.222002.

[308] Lees J.P., BABAR Collab., Blinov V.E., Buzykaev A.R., Druzhinin V.P., Golubev V.B., Kravchenko E.A., Onuchin A.P., Serednyakov S.I., Skovpen Yu.I., Solodov E.P., Todyshev K.Yu. Measurement of the B → X(s)l(+)l(-) branching fraction and search for direct CP violation from a sum of exclusive final states. // PHYSICAL REVIEW LETTERS. - 2014. - Vol. 112, Is. 21. - P. 211802. - ISSN 0031-9007, DOI 10.1103/PhysRevLett.112.211802.

[309] Nisar N. K., Belle Collab., Aulchenko V., Bondar A., Eidelman S., Gabyshev N., Garmash A., Krokovny P., Kuzmin A., Matvienko D., Shebalin V., Vorobyev V, Zhilich V., Zhulanov V. Search for CP violation in $D^0 \to \pi^0\pi^0$ decays. // PHYSICAL REVIEW LETTERS. - 2014. - Vol. 112, Is. 21. - P. 211601. - ISSN 0031-9007, DOI 10.1103/PhysRevLett.112.211601.

[310] Aaij R., LHCb Collab., Bondar A., Eidelman S, Krokovny P., Poluektov A., Shekhtman L., Vorobyev V. Study of beauty hadron decays into pairs of charm hadrons. // PHYSICAL REVIEW LETTERS. - 2014. - Vol. 112, Is. 20. - P. 202001. - ISSN 0031-9007, DOI 10.1103/PhysRevLett.112.202001.

[311] Aad G., ATLAS Collab., Anisenkov A.V., Bobrovnikov V.S., Bogdanchikov A.G., Kazanin V.F., Korol A.A., Malyshev V.M., Maslennikov A.L., Maxiimov D.A., Peleganchuk S.V., Rezanova O.L., Skovpen K.Yu., Soukharev A.M., Talyshev A.A., Tikhonov Yu.A. Search for invisible decays of a Higgs boson produced in association with a Z boson in ATLAS. // PHYSICAL REVIEW LETTERS. - 2014. - Vol. 112, Is. 20. - P. 201802. - ISSN 0031-9007, DOI 10.1103/PhysRevLett.112.201802.

[312] Lotov K.V. Sosedkin A.P., Petrenko A.V. Long-term evolution of broken wakefields in finite-radius plasmas. // PHYSICAL REVIEW LETTERS. - 2014. - Vol. 112, Is. 19. - P. 194801.

[313] Aaij R., LHCb Collab., Bondar A., Eidelman S, Krokovny P., Poluektov A., Shekhtman L., Vorobyev V. Observation of photon polarization in the b - s gamma transition. // PHYSICAL REVIEW LETTERS. - 2014. - Vol. 112, Is. 16. - P. 161801. - ISSN 0031-9007, DOI 10.1103/PhysRevLett.112.161801.

[314] Aaij R., LHCb Collab., Bondar A., Eidelman S, Krokovny P., Poluektov A., Shekhtman L., Vorobyev V. Search for Majorana neutrinos in $B^- \to \pi^+\mu^-\mu^-$ decays. // PHYSICAL REVIEW LETTERS. - 2014. - Vol. 112, Is. 13. - P. 131802. - ISSN 0031-9007, DOI 10.1103/PhysRevLett.112.131802.

[315] Ablikim M., BESIII Collab., Achasov M.N., Muchnoi N.Yu., Nikolaev I.B. Observation of a charged charmonium like structure in $e^+e^- \to$ (D*(D)over-bar*)(+/-)pi(-/+) at root s=4.26 GeV. // PHYSICAL REVIEW LETTERS. - 2014. - Vol. 112, Is. 13. - P. 132001. - ISSN 0031-9007, DOI 10.1103/Phys RevLett.112.132001.

[316] Aaij R., LHcb Collab., Bondar A., Eidelman S, Krokovny P., Poluektov A., Shekhtman L., Vorobyev V. Measurement of the B-s(o) → Ds-Ds+ and B-s(o) → Ds-Ds+ EffectiveLifetimes. // PHYSICAL REVIEW LETTERS. - 2014. - Vol. 112, Is. 11. - P. 111802. - ISSN 0031-9007, DOI 10.1103/PhysRev Lett.112.111802.

[317] Ko B.R., Belle Collab., Aulchenko V., Bondar A., Eidelman S., Gabyshev N., Garmash A., Krokovny P., Kuzmin A., Matvienko D., Shebalin V., Vorobyev V, Zhilich V., Zhulanov V. Observation of $D^0 \to \bar{D}^0$

164

Mixing in e⁺e⁻ collisions. // PHYSICAL REVIEW LETTERS. - 2014. - Vol. 112, Is. 11. - P. 111801. - ISSN 0031-9007, DOI 10.1103/PhysRev Lett.112.111801.

[318] Aad G., ATLAS Collab., Anisenkov A.V., Bobrovnikov V.S., Bogdanchikov A.G., Kazanin V.F., Korol A.A., Malyshev V.M., Maslennikov A.L., Maxiimov D.A., Peleganchuk S.V., Rezanova O.L., Skovpen K.Yu., Soukharev A.M., Talyshev A.A., Tikhonov Yu.A. Search for Quantum Black Hole production in high-invariant-mass lepton plus jet final states using pp collisions at root s=8 TeV and the ATLAS detector. // PHYSICAL REVIEW LETTERS. - 2014. - Vol. 112, Is. 9. - P. 091804. - ISSN 0031-9007, DOI 10.1103/PhysRevLett.112.091804.

[319] Aaij R., LHCb Collaborat ion, Bondar A., Eidelman S, Krokovny P., Poluektov A., Shekhtman L., Vorobyev V. Observation of (B)over bar((s))(0)- J/psi f(1)(1285) Decays and Measurement of the f(1)(1285) mixing angle. // PHYSICAL REVIEW LETTERS. - 2014. - Vol. 112, Is. 9. - P. 091802. - ISSN 0031-9007, DOI 10.1103/PhysRevLett.112.091802.

[320] Ablikim M., Achasov M.N., Muchnoi N.Yu., Nikolaev I. B. Observation of e⁺e− → γ X(3872) at BESIII. // PHYSICAL REVIEW LETTERS. - 2014. - Vol. 112, Is. 9. - P. 092001. - ISSN 0031-9007, DOI 10.1103/PhysRevLett.112.092001.

[321] Kabantsev, A.A. Tsidulko Yu.A., Driscoll C.F. Chaotic neoclassical separatrix dissipation in parametric drift-wave decay. // PHYSICAL REVIEW LETTERS. - 2014. - Vol. 112, Is. 5. - P. 055003. - ISSN 0031-9007, DOI 10.1103/PhysRevLett.112.055003.

[322] Aaij R., LHCb Collab. Bondar A., Eidelman S, Krokovny P., Poluektov A., Shekhtman L., Vorobyev V., Measurements of indirect CP asymmetries in D-0 - K-K+ and D-0 -pi(-)pi(+) decays. // PHYSICAL REVIEW LETTERS. - 2014. - Vol. 112, Is. 4. - P. 041801. - ISSN 0031-9007, DOI 10.1103/Phys RevLett.112.041801.

[323] Aad G., ATLAS Collab., Anisenkov A.V., Bobrovnikov V.S., Bogdanchikov A.G., Kazanin V.F., Korol A.A., Malyshev V.M., Maslennikov A.L., Maxiimov D.A., Peleganchuk S.V., Rezanova O.L., Skovpen K.Yu., Soukharev A.M., Talyshev A.A., Tikhonov Yu.A. Search for dark matter in events with a hadronically decaying W or Z boson and missing transverse momentum in pp collisions at root s=8 TeV with the ATLAS detector. // PHYSICAL REVIEW LETTERS. - 2014. - Vol. 112, Is. 4. - P. 041802. - ISSN 0031-9007, DOI 10.1103/PhysRevLett.112.041802.

[324] Belous K., Belle Collab., Aulchenko V., Bondar A., Eidelman S., Gabyshev N., Garmash A., Krokovny P., Kuzmin A., Matvienko D., Shebalin V., Vorobyev V, Zhilich V., Zhulanov V. Measurement of the tau-lepton lifetime at Belle. // PHYSICAL REVIEW LETTERS. - 2014. - Vol. 112, Is. 3. - P. 031801. - ISSN 0031-9007, DOI 10.1103/PhysRevLett.112.031801.

[325] Ablikim M., BESIII Collab., Achasov M.N., Muchnoi N.Yu., Nikolaev I.B. Observation of a charged (D(D)over-bar*)(+/-) mass peak in e(+)e(-) → pi D(D)over-bar* at root s=4.26 GeV. // PHYSICAL REVIEW LETTERS. - 2014. - Vol. 112, Is. 2. - P. 022001. - ISSN 0031-9007, DOI 10.1103/PhysRev Lett.112.022001.

[326] Aaij R., LHCb Collab., Bondar A., Eidelman S, Krokovny P., Poluektov A., Shekhtman L., Vorobyev V. Measurement of CP Violation in the phase space of B-+/- - K+K-pi(+/-)and B-+/- → pi(+)pi(-)pi(+/-) decays. // PHYSICAL REVIEW LETTERS. - 2014. - Vol. 112, Is. 1. - P. 011801. - ISSN 0031-9007, DOI 10.1103/ PhysRevLett.112.011801.

[327] Mun Jungho, Jeong Young Uk, Vinokurov Nikolay A., Lee Kitae, Jang Kyu-Ha, Park Seong Hee, Jeon Min Yong, Shin Sang-In. Variable-period permanent-magnet helical undulator. // PHYSICAL REVIEW SPECIAL TOPICS-ACCELERATORS AND BEAMS. - 2014. - Vol. 17, Is. 8. - P. 080701. - ISSN 1098-4402, DOI 10.1103/PhysRevSTAB.17.080701.

[328] Strelnikov N.O. Vasserman I.B. Earth's field effect on magnetic performance of horizontally andvertically polarizing undulators. // PHYSICAL REVIEW SPECIAL TOPICS-ACCELERATORS AND BEAMS. - 2014. - Vol. 17, Is. 6. - P. 062401. - ISSN 1098-4402, DOI 10.1103/PhysRevSTAB.17.062401.

[329] Bogomyagkov A., Levichev E., Shatilov D. Beam-beam effects investigation and parameters optimization for acircular e⁺e⁻ collider at very high energies. // PHYSICAL REVIEW SPECIAL TOPICS-ACCELERATORS AND BEAMS. - 2014. - Vol. 17, Is. 4. - P. 041004. - ISSN 1098-4402, DOI 10.1103/ PhysRevSTAB.17.041004.

[330] Aad G., ATLAS Collab., Anisenkov A.V., Bobrovnikov Bogdanchikov Kazanin Korol A.A., Malyshev V.M., Maslennikov A.L., Maximov D.A., Peleganchuk S.V., Rezanova O.L., Skovpen K.Yu., Soukharev A.M., Talyshev A.A., Tikhonov Yu.A. Measurement of inclusive jet charged-particle fragmentation functions in Pb plus Pb collisions at root S-NN=2.76 TeV with the ATLAS detector. // PHYSICS LETTERS B. - 2014. - Vol. 739. - P. 320-342. - ISSN 0370-2693, DOI 10.1016/j.physletb.2014.10.065.

[331] Aaij R., LHCb Collab., Bondar A., Eidelman S, Krokovny P., Poluektov A., Shekhtman L., Vorobyev V. Measurement of the (B)over-bar(0)-B-0 and (B)over-bars(0)-B-s(0) production asymmetries in pp collisions at root s=7 TeV. // PHYSICS LETTERS B. - 2014. - Vol. 739. - P. 218-228. - ISSN 0370-2693, DOI 10.1016/j.physletb.2014.10.005.

[332] Abelev B., ALICE Collab., Pestov Y. Freeze-out radii extracted from three-pion cumulants in pp, p-Pb and Pb-Pb collisions at the LHC. // PHYSICS LETTERS B. - 2014. - Vol. 739. - P. 139-151. - ISSN 0370-2693, DOI 10.1016/j.physletb.2014.10.034.

[333] Adlarson P., Augustyniak W., Bardan W., Bashkanov M., Bergmann F. S., Berlowski M., Bhatt H., Bondar A., Buescher M., Calen H., Ciepal I., Clement H., Coderre D., Czerwinski E., Demmich K., Doroshkevich E., Engels R., Erven A., Erven W., Eyrich W., Fedorets P., Foehl K., Fransson K., Goldenbaum F., Goslawski P., Goswami A., Grigoryev K., Gullstrom C. -O., Hanhart C., Hauenstein F., Heijkenskjold L., Hejny V., Hoistad B., Huesken N., Jarczyk L., Johansson T., Kamys B., Kemmerling G., Khan F. A., Khoukaz A., Kirillov D. A., Kistryn S., Kleines H., Klos B., Krzemien W., Kulessa P., Kupsc A., Kuzmin A., Lalwani K., Lersch D., Lorentz B., Magiera A., Maier R., Marciniewski P., Marianski B., Mikirtychiants M., Morsch H. -P., Moskal P., Ohm H., Ozerianska I., del Rio E. Perez, Piskunov N. M., Podkopal P., Prasuhn D., Pricking A., Pszczel D., Pyszw K., Pyszniak A., Redmer C. F., Ritman J., Roy A., Rudy Z., Sawant S., Schadmand S., Sefzick T., Serdyuk V., Shwartz B., Siudak R., Skorodko T., Skurzok M., Smyrski J., Sopov V., Stassen R., Stepaniak J., Stephan E., Sterzenbach G., Stockhorst H., Stroher H., Szczurek A., Taschner A., Trzcinski A., Varma R., Wolke M., Wronska A., Wustner P., Wurm P., Yamamoto A., Yurev L., Zabierowski J., Zielinski M. J., Zink A., Zlomanczuk J., Zupranski P., Zurek M. Charge symmetry breaking in dd - He-4 pi(0) with WASA-at-COSY. // PHYSICS LETTERS B. - 2014. - Vol. 739. - P. 44-49. - ISSN 0370-2693, DOI 10.1016/j.physletb.2014.10.029.

[334] Aad G., ATLAS Collab. Anisenkov A.V., Bobrovnikov V.S., Bogdanchikov A.G., Kazanin V.F., Korol A.A., Malyshev V.M., Maslennikov A.L., Maximov D.A., Peleganchuk S.V., Rezanova O.L., Skovpen K.Yu., Soukharev A.M., Talyshev A.A., Tikhonov Yu.A. Measurement of the cross section of high transverse momentum Z -b(b)over-bar production in proton-proton collisions at root s=8 TeV with the ATLAS detector. // PHYSICS LETTERS B. - 2014. - Vol. 738. - P. 25-43. - ISSN 0370-2693, DOI 10.1016/j.physletb. 2014.09.020.

[335] Aad G., ATLAS Collab., Anisenkov A.V., Bobrovnikov V.S., Bogdanchikov A.G., Kazanin V.F., Korol A.A., Malyshev V.M., Maslennikov A.L., Maximov D.A., Peleganchuk S.V., Rezanova O.L., Skovpen K.Yu., Soukharev A.M., Talyshev A.A., Tikhonov Yu.A. Search for the Standard model Higgs boson decay to mu(+)mu(-) with the ATLAS detector. // PHYSICS LETTERS B. - 2014. - Vol. 738. - P. 68-86. - ISSN 0370-2693, DOI 10.1016/j.physletb.2014.09.008.

[336] Aad G., ATLAS Collab., Anisenkov A.V., Bobrovnikov V.S., Bogdanchikov A.G., Kazanin V.F., Korol A.A., Malyshev V.M., Maslennikov A.L., Maximov D.A., Peleganchuk S.V., Rezanova O.L., Skovpen K.Yu., Soukharev A.M., Talyshev A.A., Tikhonov Yu.A. Fiducial and differential cross sections of Higgs boson production measured in the four-lepton decay channel in pp collisions at root s=8TeV with the ATLAS detector. // PHYSICS LETTERS B. - 2014. -

Vol. 738. - P. 234-253. - ISSN 0370-2693, DOI 10.1016/j.physletb.2014.09.054.

[337] Aad G., ATLAS Collab., Anisenkov A.V., Bobrovnikov V.S., Bogdanchikov A.G., Kazanin V.F., Korol A.A., Malyshev V.M., Maslennikov A.L., Maximov D.A., Peleganchuk S.V., Rezanova O.L., Skovpen K.Yu., Soukharev A.M., Talyshev A.A., Tikhonov Yu.A. Search for new resonances in W gamma and Z gamma final states in pp collisions at root s=8 TeV with the ATLAS detector. // PHYSICS LETTERS B. - 2014. - Vol. 738. - P. 428-447. - ISSN 0370-2693, DOI 10.1016/j.physletb.2014.10.002.

[338] Abelev B., ALICE Collab., Pestov Y. Beauty production in pp collisions at root s=2.76 TeV measured via semi-electronic decays. // PHYSICS LETTERS B. - 2014. - Vol. 738. - P. 97-108. - ISSN 0370-2693, DOI 10.1016/j.physletb.2014.09.026.

[339] Abelev B., ALICE Collab., Pestov Y. Suppression of Upsilon(1S) at forward rapidity in Pb-Pb collisions at root s(NN)=2.76 TeV. // PHYSICS LETTERS B. - 2014. - Vol. 738. - P. 361-372. - ISSN 0370-2693, DOI 10.1016/j.physletb.2014.10.001.

[340] Anashin V.V., Aulchenko V.M., Baldin E.M., Barladyan A.K., Barnyakov A.Yu., Barnyakov M.Yu., Baru S.E., Basok I.Yu., Bedny I.V., Blinov A.E., Blinov V.E., Bobrov A.V., Bobrovnikov V.S., Bogomyagkov A.V., Bondar A.E., Buzykaev A.R., Eidelman S.I., Glukhovchenko Yu.M., Gulevich V.V., Gusev D.V., Karnaev S.E., Karpov G.V., Karpov S.V., Kharlamova T.A., Kiselev V.A., Kononov S.A., Kotov K.Yu., Kravchenko E.A., Kulikov V.F., Kurkin G.Ya., Kuper E.A., Levichev E.B., Maksimov D.A., Malyshev V.M., Maslennikov A.L., Medvedko A.S., Meshkov O.I., Mishnev S.I., Morozov I.I., Muchnoi N.Yu., Neufeld V.V., Nikitin S.A., Nikolaev I.B., Okunev I.N., Onuchin A.P., Oreshkin S.B., Orlov I.O., Osipov A.A., Peleganchuk S.V., Pivovarov S.G., Piminov P.A., Petrov V.V., Poluektov A.O., Pospelov G.E., Prisekin V.G., Rezanova O.L., Ruban A.A., Sandyrev V.K., Savinov G.A., Shamov A.G., Shatilov D.N., Shwartz B.A., Simonov E.A., Sinyatkin S.V., Skrinsky A.N., Smaluk V.V., Sokolov A.V., Sukharev A.M., Starostina E.V., Talyshev A.A., Tayursky V.A., Telnov V.I., Tikhonov Yu.A., Todyshev K.Yu., Tumaikin G.M., Usov Yu.V., Vorobiov A.I., Yushkov A.N., Zhilich V.N., Zhulanov V.V., Zhuravlev A.N. Measurement of $J/\psi \to \gamma\eta_c$ decay rate and η_c parameters at KEDR. // PHYSICS LETTERS B. - 2014. - Vol. 738. - P. 391-396. - ISSN 0370-2693, DOI 10.1016/j.physletb.2014.09.064.

[341] Aad G., ATLAS Collab., Anisenkov A.V., Bobrovnikov V.S., Bogdanchikov A.G., Kazanin V.F., Korol A.A., Malyshev V.M., Maslennikov A.L., Maximov D.A., Peleganchuk S.V., Rezanova O.L., Skovpen K.Yu., Soukharev A.M., Talyshev A.A., Tikhonov Yu.A. Search for WZ resonances in the fully leptonic channel using pp collisions at root s=8 TeV with the ATLAS detector. // PHYSICS LETTERS B. - 2014. -

Vol. 737. - P. 223-243. - ISSN 0370-2693, DOI 10.1016/j.physletb.2014.08.039.

[342] Aaij R., LHCb Collab. Bondar A., Eidelman S, Krokovny P., Poluektov A., Shekhtman L., Vorobyev V. Measurement of the Xi(-)(b) and Omega(-)(b) baryon lifetimes. // PHYSICS LETTERS B. - 2014. - Vol. 736. - P. 154-162. - ISSN 0370-2693, DOI 10.1016/j.physletb.2014.06.064.

[343] Aaij R., LHCb Collab., Bondar A., Eidelman S, Krokovny P., Poluektov A., Shekhtman L., Vorobyev V. Measurement of the CP-violating phase phi(s) in (B)over-bar(s)(0) - J /psi pi(+)pi(-) decays. // PHYSICS LETTERS B. - 2014. - Vol. 736. - P. 186-195. - ISSN 0370-2693, DOI 10.1016/j.physletb.2014.06.079.

[344] Aaij R., LHCb Collab., Bondar A., Eidelman S, Krokovny P., Kudryavtsev V., Poluektov A., Shekhtman L., Vorobyev V. Effective lifetime measurements in the B-s(0) - K+K-, B-0 - K+pi(-) and B-s(0) - pi K-+(-) decays. // PHYSICS LETTERS B. - 2014. - Vol. 736. - P. 446-454. - ISSN 0370-2693, DOI 10.1016/j.physletb.2014.07.051.

[345] Abelev B., ALICE Collab., Pestov Y. Production of charged pions, kaons and protons at large transverse momenta in pp and Pb-Pb collisions at root s(NN)=2.76 TeV. // PHYSICS LETTERS B. - 2014. - Vol. 736. - P. 196-207. - ISSN 0370-2693, DOI 10.1016/j.physletb.2014.07.011.

[346] Ablikim M., BESIII Collab.,Achasov M.N., Muchnoi N.Yu., Nikolaev I.B. Study of $e^+e^-. \to p\ \bar{p}$ in the vicinity of $\psi(3770)$. // PHYSICS LETTERS B. - 2014. - Vol. 735. - P. 101-107. - ISSN 0370-2693, DOI 10.1016/j.physletb.2014.06.013.

[347] Aaij R., LHCb Collab., Bondar A., Eidelman S, Krokovny P., Poluektov A., Shekhtman L., Vorobyev V. Precision measurement of the ratio of the Lambda(0)(b) to (B)over-bar(0) lifetimes. // PHYSICS LETTERS B. - 2014. - Vol. 734. - P. 122-130. - ISSN 0370-2693, DOI 10.1016/j.physletb.2014.05.021.

[348] Abelev B., ALICE Collab., Pestov Y. Centrality, rapidity and transverse momentum dependence of J/Psi suppression in Pb-Pb collisions at root(NN)-N-S=2.76TeV. // PHYSICS LETTERS B. - 2014. - Vol. 734. - P. 314-327. - ISSN 0370-2693, DOI 10.1016/j.physletb.2014.05.064.

[349] Fadin, V.S. Fiore R. Impact factors for Reggeon-gluon transition in N=4 SYM with large number of colours. // PHYSICS LETTERS B. - 2014. - Vol. 734. - P. 86-91. [arXiv:1402.5260 [hep-th]].

[350] Aaij R., LHCb Collab. Bondar A., Eidelman S, Krokovny P., Poluektov A., Shekhtman L., Vorobyev V. A study of CP violation in B → DK and B → Dπ decays with D → KSKπ final states. // PHYSICS LETTERS B. - 2014. - Vol. 733. - P. 36-45. - ISSN 0370-2693, DOI 10.1016/j.physletb.2014.03.051.

[351] Aad G., ATLAS Collab., Anisenkov A.V., Bobrovnikov V.S., Bogdanchikov A.G., Kazanin V.F., Korol A.A., Malyshev V.M., Maslennikov A.L., Maximov D.A., Peleganchuk S.V., Rezanova O.L., Skovpen K.Yu., Soukharev A.M., Talyshev A.A., Tikhonov Yu.A. Search for Higgs boson decays to a photon and a Z boson in pp collisions at root s=7 and 8 TeV with the ATLAS detector. // PHYSICS LETTERS B. - 2014. - Vol. 732. - P. 8-27. - ISSN 0370-2693, DOI 10.1016/j.physletb.2014.03.015.

[352] Aulchenko V.M., Baldin E.M., Barladyan A.K., Barnyakov A.Yu., Barnyakov M.Yu., Baru S.E., Basok I.Yu., Batrakov A.M., Blinov A.E., Blinov V.E., Bobrov A.V., Bobrovnikov V.S., Bogomyagkov A.V., Bondar A.E., Buzykaev A.R., Eidelman S.I., Grigoriev D.N., Groshev V.R., Glukhovchenko Yu.M., Gulevich V.V., Gusev D.V., Karnaev S.E., Karpov G.V., Karpov S.V., Kharlamova T.A., Kiselev V.A., Kolmogorov V.V., Kononov S.A., Kotov K.Yu., Kravchenko E.A., Kudryavtsev V.N., Kulikov V.F., Kurkin G.Ya., Kuper E.A., Kuyanov I.A., Levichev E.B., Maksimov D.A., Malyshev V.M., Maslennikov A.L., Meshkov O.I., Mishnev S.I., Morozov I.I., Muchnoi N.Yu., Neufeld V.V., Nikitin S.A., Nikolaev I.B., Okunev I.N., Onuchin A.P., Oreshkin S.B., Orlov I.O., Osipov A.A., Ovtin I.V., Peleganchuk S.V., Pivovarov S.G., Piminov P.A., Petrov V.V., Poluektov A.O., Prisekin V.G., Rezanova O.L., Ruban A.A., Sandyrev V.K., Savinov G.A., Shamov A.G., Shatilov D.N., Shwartz B.A., Simonov E.A., Sinyatkin S.V., Skrinsky A.N., Sokolov A.V., Sukharev A.M., Starostina E.V., Talyshev A.A., Tayursky V.A., Telnov V.I., Tikhonov Yu.A., Todyshev K.Yu., Tumaikin G.M., Usov Yu.V., Vorobiov A.I., Zhilich V.N., Zhulanov V.V., Zhuravlev A.N. Measurement of the ratio of the lepton widths $\Gamma_{ee}/\Gamma_{\mu\mu}$ for the J/ψ meson. // PHYSICS LETTERS B. - 2014. - Vol. 731. - P. 227-231. - ISSN 0370-2693, DOI 10.1016/j.physletb.2014.02.046.

[353] Aad G., ATLAS Collab., Anisenkov A.V., Bobrovnikov V.S., Bogdanchikov A.G., Kazanin V.F., Korol A.A., Malyshev V.M., Maslennikov A.L., Maximov D.A., Peleganchuk S.V., Rezanova O.L., Skovpen K.Yu., Soukharev A.M., Talyshev A.A., Tikhonov Yu.A. Measurement of the mass difference between top and anti-top quarks in pp collisions at root s=7 TeV using the ATLAS detector. // PHYSICS LETTERS B. - 2014. - Vol. 728. - P. 363-379. - ISSN 0370-2693, DOI 10.1016/j.physletb.2013.12.010.

[354] Aad G., ATLAS Collab., Anisenkov A.V., Bobrovnikov V.S., Bogdanchikov A.G., Kazanin V.F., Korol A.A., Malyshev V.M., Maslennikov A.L., Maximov D.A., Peleganchuk S.V., Rezanova O.L., Skovpen K.Yu., Soukharev A.M., Talyshev A.A., Tikhonov Yu.A. Search for new phenomena in photon plus jet events collected inproton-proton collisions at root s=8 TeV with the ATLAS detector. // PHYSICS LETTERS B. - 2014. - Vol. 728. - P. 562-578. - ISSN 0370-2693, DOI 10.1016/j.physletb.2013.12.029.

[355] Aaij R., LHCB Collab., Bondar A., Eidelman S, Krokovny P., Poluektov A., Shekhtman L., Vorobyev V. Measurement of the charge asymmetry in B-+/- - phi K +/- and search forB-+/- - phi pi(+/-) decays. // PHYSICS LETTERS B. - 2014. - Vol. 728. - P. 85-94. - ISSN 0370-2693, DOI 10.1016/j.physletb.2013.11.036.

[356] Aaij R., LHCb Collab., Bondar A., Eidelman S, Krokovny P., Poluektov A., Shekhtman L., Vorobyev V. Search for the decay D-0 - pi(+) pi(-) mu(+) mu(-). // PHYSICS LETTERS B. - 2014. - Vol. 728. - P. 234-243. - ISSN 0370-2693, DOI 10.1016/ j.physletb.2013.11.053.

[357] Aaij R., LHCb Collab., Bondar A., Eidelman S, Krokovny P., Poluektov A., Shekhtman L., Vorobyev V. Search for CP violation in the decay D+ $\rightarrow$ pi(-)pi(+)pi(+). // PHYSICS LETTERS B. - 2014. - Vol. 728. - P. 585-595. - ISSN 0370-2693, DOI 10.1016/ j.physletb.2013.12.035.

[358] Aaij R., LHCb Collab., Bondar A., Eidelman S, Krokovny P., Poluektov A., Shekhtman L., Vorobyev V. Measurement of the flavour-specific CP-violating asymmetry a(sl)(s) in B-s(0) decays. // PHYSICS LETTERS B. - 2014. - Vol. 728. - P. 607-615. - ISSN 0370-2693, DOI 10.1016/j.physletb.2013.12.030.

[359] Abelev B., ALICE Collab., Pestov Y. Multiplicity dependence of pion, kaon, proton and lambda production in p-Pb collisions at root s(NN)=5.02 TeV. // PHYSICS LETTERS B. - 2014. - Vol. 728. - P. 25-38. - ISSN 0370-2693, DOI 10.1016/j.physletb. 2013.11.020.

[360] Abelev B., ALICE Collab., Pestov Y. Multi-strange baryon production at mid-rapidity in Pb-Pb collisions atroot s(NN)=2.76 TeV. // PHYSICS LETTERS B. - 2014. - Vol. 728. - P. 216-227. - ISSN 0370-2693, DOI 10.1016/j.physletb.2013.11.048.

[361] Downie E.J., Lee R.N., Milstein A.I., Ron G. Charge asymmetry in high-energy $\mu^+\mu^-$ photoproduction in the electric field of a heavy atom. // PHYSICS LETTERS B. - 2014. - Vol. 728. - P. 645-649. - ISSN 0370-2693, DOI 10.1016/j.physletb.2013.12.049.

[362] Shestakov Yu.V., Barkov L.M., Dmitriev V.F., Golovin R.A., Kudryavtsev V.N., Lazarenko B.A., Mishnev S.I., Nikolenko D.M., Rachek I.A., Sadykov R.Sh, Stibunov V.N., Toporkov D.K., Shekhtman L.I., Zevakov S.A. Tagging system for almost-real photons at VEPP-3 storage ring. // PHYSICS OF PARTICLES AND NUCLEI. - 2014. - Vol. 45, Is. 1. - P. 338-340. - ISSN 1063-7796, DOI 10.1134/S1063779614010924.

[363] Kotelnikov I.A. On the density limit in the helicon plasma sources. // PHYSICS OF PLASMAS. - 2014. - Vol. 21, Is. 12. - P. 122101. - ISSN 1070-664X, DOI 10.1063/1.4903329.

[364] Lotov K.V., Sosedkin A.P., Petrenko A.V., Amorim L.D., Vieira J., Fonseca R.A., Silva L.O., Gschwendtner E., Muggli P. Electron trapping and acceleration by the plasma wake field of aself-modulating proton beam. // PHYSICS OF PLASMAS. - 2014. - Vol. 21, Is. 12. - P. 123116.

[365] Arzhannikov A.V., Burdakov A.V., Burmasov V.S., Gavrilenko D.E., Ivanov I.A., Kasatov A.A., Kuznetsov S.A., Mekler K.I., Polosatkin S.V., Postupaev V.V., Rovenskikh A.F., Sinitsky S.L., Sklyarov V.F., Vyacheslavov L.N. Observation of spectral composition and polarization of sub-terahertze mission from dense plasma during relativistic electron beam-plasma interaction. // PHYSICS OF PLASMAS. - 2014. - Vol. 21, Is. 8. - P. 082106. - ISSN 1070-664X, DOI 10.1063/ 1.4891884.

[366] Lotov K.V. Minakov V.A., Sosedkin A.P. Parameter sensitivity of plasma wakefields driven by self-modulating proton beams. // PHYSICS OF PLASMAS. - 2014. - Vol. 21, Is. 8. - P. 083107.

[367] Timofeev I.V. Annenkov V.V. Efficient regime of electromagnetic emission in a plasma with counter streaming electron beams. // PHYSICS OF PLASMAS. - 2014. - Vol. 21, Is. 8. - P. 083109. - ISSN 1070-664X, DOI 10.1063/1.4892965.

[368] Burdakov A.V. Postupaev V.V., Sudnikov A.V. Magnetohydrodynamically stable plasma with supercritical current density at the axis. // PHYSICS OF PLASMAS. - 2014. - Vol. 21, Is. 5. - P. 052507. - ISSN 1070-664X, DOI 10.1063/1.4876745.

[369] Kim Kyung Nam, Lee Kitae, Park Seong Hee, Lee Ji Young, Jeong Young Uk, Vinokurov Nikolay, Kim Yong Gi. Generation of a quasi-monoenergetic high energy proton beam from a vacuum-sand wiched double layer target irradiated by an ultraintense laser pulse. // PHYSICS OF PLASMAS. - 2014. - Vol. 21, Is. 4. - P. 043110. - ISSN 1070-664X, DOI 10.1063/1.4871862.

[370] Levichev E.B., Skrinsky A.N., Tikhonov Yu.A., Todyshev K.Yu. High-precision particle mass measurements using the KEDR detector at theVEPP-4M collider. // PHYSICS-USPEKHI. - 2014. - Vol. 57, Is. 1. - P. 66-79. - ISSN 1063-7869, DOI 10.3367/UFNr.0184. 201401c.0075.

[371] Assmann R., Bingham R., Bohl T., Bracco C., Buttenschoen B., Butterworth A., Caldwell A., Chattopadhyay S., Cipiccia S., Feldbaumer E., Fonseca R. A., Goddard B., Gross M., Grulke O., Gschwendtner E., Holloway J., Huang C., Jaroszynski D., Jolly S., Kempkes P., Lopes N., Lotov K., Machacek J., Mandry S. R., McKenzie J. W., Meddahi M., Militsyn B. L., Moschuering N., Muggli P., Najmudin Z., Noakes T. C. Q., Norreys P. A., Oez E., Pardons A., Petrenko A., Pukhov A., Rieger K., Reimann O., Ruhl H., Shaposhnikova E., Silva L. O., Sosedkin A., Tarkeshian R., Trines R. M. G. N., Tueckmantel T., Vieira J., Vincke H., Wing M., Xia G. (AWAKE Collab.). Proton-driven plasma wakefield acceleration: a path to the future of high-energy particle physics. // PLASMA PHYSICS AND CONTROLLED FUSION. - 2014. - Vol. 56, Is. 8. - P. 084013. [arXiv:1401.4823 [physics.acc-ph].

[372] Burdakov A.V., Koidan V.S., Mekler K.I., Polosatkin S.V., Postupaev V.V. Creation of a long

magnetized plasma column in a metal chamber. // PLASMA PHYSICS REPORTS. - 2014. - Vol. 40, Is. 3. - P. 161-177. - ISSN 1063-780X, DOI 10.1134/ S1063780X14030039.

[373] Iwashita T., Belle Collab., Aulchenko V., Bondar A., Eidelman S., Gabyshev N., Garmash A., Krokovny P., Kuzmin A., Matvienko D., Shebalin V., Vorobyev V, Zhilich V., Zhulanov V. Measurement of branching fractions for B→ J/ψηK decays and search for a narrow resonance in the J/ψη final state. // PROGRESS OF THEORETICAL AND EXPERIMENTAL PHYSICS. - 2014. - Is. 4. - P. 043C01. - ISSN 2050-3911, DOI 10.1093/ptep/ptu043.

[374] Dostovalov A.V., Korolkov V.P., Golubtsov S.K., Kondrat'ev V.I. Specific features of formation of self-induced gratings on metal foils during scanning by a tightly focused femtosecond laser beam. // QUANTUM ELECTRONICS. - 2014. - Vol. 44, Is. 4. - P. 330-334. - ISSN 1063-7818, DOI 10.1070/QE2014v044n04 ABEH015376.

[375] Lizunov A. Anikeev A. First measurements of D-alpha spectrum produced by anisotropic fast ions in the gas dynamic trap. // REVIEW OF SCIENTIFIC INSTRUMENTS. - 2014. - Vol. 85, Is. 11. - P. 113110. - ISSN 0034-6748, DOI 10.1063/1.4902181.

[376] Magee R. M., Clary R., Korepanov S., Smirnov A., Garate E., Knapp K., Tkachev A. Fusion proton diagnostic for the C-2 field reversed configuration. // REVIEW OF SCIENTIFIC INSTRUMENTS. - 2014. - Vol. 85, Is. 11. - P. 11D851. - ISSN 0034-6748, DOI 10.1063/1.4892861.

[377] Strelnikov N., Trakhtenberg E., Vasserman I., Xu J., Gluskin E. Vertically polarizing undulator with the dynamic compensation of magnetic forces for the next generation of light sources. // REVIEW OF SCIENTIFIC INSTRUMENTS. - 2014. - Vol. 85, Is. 11. - P. 113303. - ISSN 0034-6748, DOI 10.1063/1.4900544.

[378] Belchenko Yu., Gorbovsky A., Sanin A., Savkin V. The 25 mA continuous-wave surface-plasma source of H- ions. // REVIEW OF SCIENTIFIC INSTRUMENTS. - 2014. - Vol. 85, Is. 2. - P. 02B108. - ISSN 0034-6748, DOI 10.1063/1.4828373.

[379] Belchenko Y. Sanin A., Sotnikov O. Comparative analysis of continuous-wave surface-plasma negative ion sources with various discharge geometry. // REVIEW OF SCIENTIFIC INSTRUMENTS. - 2014. - Vol. 85, Is. 2. - P. 02B116. - ISSN 0034-6748, DOI 10.1063/ 1.4833929.

[380] Ivanov A.A., Abdrashitov G.F., Anashin V.V., Belchenko Yu.I., Burdakov A.V., Davydenko V.I., Deichuli P.P., Dimov G.I., Dranichnikov A.N., Kapitonov V.A., Kolmogorov V.V., Kondakov A.A., Sanin A.L., Shikhovtsev I.V., Stupishin N.V., Sorokin A.V., Popov S.S., Tiunov M.A., Belov V.P., Gorbovsky A.I., Kobets V.V., Binderbauer M., Putvinski S., Smirnov A., Sevier L. Development of a negative ion-based neutral beam injector in Novosibirsk. // REVIEW OF SCIENTIFIC INSTRUMENTS. - 2014. - Vol. 85, Is. 2. - P. 02B102. - ISSN 0034-6748, DOI 10.1063/1.4826326.

[381] Ivanov A.A., Belchenko Yu.I., Davydenko V.I., Ivanov I.A., Kolmogorov V.V., Listopad A.A., Mishagin V.V., Putvinsky S.V., Shulzhenko G.I., Smirnov A. Arc plasma generator of atomic driver for steady-state negative ionsource. // REVIEW OF SCIENTIFIC INSTRUMENTS. - 2014. - Vol. 85, Is. 2. - P. 02B129. - ISSN 0034-6748, DOI 10.1063/1.4835415.

[382] Kolmogorov A., Atoian G., Davydenko V., Ivanov A., Ritter J., Stupishin N., Zelenski A. Production, formation, and transport of high-brightness atomic hydrogen beam studies for the relativistic heavy ion collider polarized source upgrade. // REVIEW OF SCIENTIFIC INSTRUMENTS. - 2014. - Vol. 85, Is. 2. - P. 02A734. - ISSN 0034-6748, DOI 10.1063/1.4857195.

[383] Polosatkin S.V., Ivanov A.A., Listopad A.A., Shikhovtsev I.V. Study of sublevel population mixing effects in hydrogen neutral beams. // REVIEW OF SCIENTIFIC INSTRUMENTS. - 2014. - Vol. 85, Is. 2. - P. 02A707. - ISSN 0034-6748, DOI 10.1063/1.4826339.

[384] Yi Longqing, Shen Baifei, Ji Liangliang, Lotov Konstantin, Sosedkin Alexander, Zhang Xiaomei, Wang Wenpeng, Xu Jiancai, Shi Yin, Zhang Lingang, Xu Zhizhanю Positron acceleration in a hollow plasma channel up to TeV regime. // SCIENTIFIC REPORTS. - 2014. - Vol. 4. - P. 4171.

[385] Bataev I. A., Golkovskii M. G., Bataev A. A., Losinskaya A. A., Dostovalov R. A., Popelyukh A. I., Drobyaz E. A. Surface hardening of steels with carbon by non-vacuum electron-beam processing. // SURFACE & COATINGS TECHNOLOGY. - 2014. - Vol. 242. - P. 164-169. - ISSN 0257-8972, DOI 10.1016/ j.surfcoat.2014.01.038.

[386] Astrelin, V.T. Kandaurov I.V., Trunev Yu.A. Generation of a submillisecond electron beam with a high-density current in a plasma-emitter diode under the conditions of open plasma boundary emission. // TECHNICAL PHYSICS. - 2014. - Vol. 59, Is. 2. - P. 258-263. - ISSN 1063-7842, DOI 10.1134/ S1063784214020042.

[387] Dimov G.I. Emelev I.S. Experiments to study the confinement of a target plasma in a magnetic trap with inverse plugs and circular multipole walls. // TECHNICAL PHYSICS. - 2014. - Vol. 59, Is. 2. - P. 181-189. - ISSN 1063-7842, DOI 10.1134/S1063784214020078.

[388] Korobeishchikov N.G., Kalyada V.V., Shmakov A.A., Shul'zhenko G.I. Experimental study of accelerated argon ion-cluster beams. // TECHNICAL PHYSICS LETTERS. - 2014. - Vol. 40, Is. 1. - P. 25-28. - ISSN 1063-7850, DOI 10.1134/S1063785014010076.

[389] Aad G., ATLAS Collab., Anisenkov A.V., Bobrovnikov V.S., Bogdanchikov A.G., Kazanin V.F., Korol A.A., Malyshev V.M., Maslennikov A.L., Maxiimov D.A., Peleganchuk S.V., Rezanova O.L., Skovpen K.Yu., Soukharev A.M., Talyshev A.A., Tikhonov Yu.A. Measurement of Higgs boson production in the diphoton decay channel in pp collisions at center-of-mass energies of 7 and 8 TeV with the ATLAS detector. // PHYSICAL REVIEW D. - 2014. - Vol. 90, № 11. - P. 112015.

[390] Aad G., ATLAS Collab., Anisenkov A.V., Bobrovnikov V.S., Bogdanchikov A.G., Kazanin V.F., Korol A.A., Malyshev V.M., Maslennikov A.L., Maxiimov D.A., Peleganchuk S.V., Rezanova O.L., Skovpen K.Yu., Soukharev A.M., Talyshev A.A., Tikhonov Yu.A. Measurements of spin correlation in top-antitop quark events from proton-proton collisions at root s=7 TeV using the ATLAS detector. // PHYSICAL REVIEW D. - 2014. - Vol. 90, № 11. - P. 112016.

[391] Ablikim M., BESIII Collab., Achasov M.N., Muchnoi N.Yu., Nikolaev I.B. Search for the weak decays J/psi - D-s(()*()-) e(+)nu(e) + c.c. // PHYSICAL REVIEW D. - 2014. - Vol. 90, № 11. - P. 112014.

[392] Chilikin K., BELLE Collab., Arinstein K., Aulchenko V., Bondar A., Eidelman S., Gabyshev N., Garmash A., Krokovny P., Kuzmin A., Lukin P., Shebalin V., Shwartz B., Vinokurova A., Zhilich V., Zhulanov V. Observation of a new charged charmonium like state in B-0 - J/psi K- pi(+) decays. // PHYSICAL REVIEW D. - 2014. - Vol. 90, № 11. - P. 112009.

[393] Yang S.D., BELLE Collab., Arinstein K., Aulchenko V., Bobrov A., Eidelman S., Gabyshev N., Garmash A., Krokovny P., Kuzmin A., Lukin P., Shebalin V., Shwartz B., Usov Y., Vinokurova A., Vorobyev V., Zhilich V., Zhulanov V. Evidence of gamma(1S) - J/Psi +chi(c1) and search for double-charmonium production in γ(1S) and γ(2S) decays. // PHYSICAL REVIEW D. - 2014. - Vol. 90, № 11. - P. 112008.

[394] Aad G., ATLAS Collab., Anisenkov A.V., Bobrovnikov V.S., Bogdanchikov A.G., Kazanin V.F., Korol A.A., Malyshev V.M., Maslennikov A.L., Maxiimov D.A., Peleganchuk S.V., Rezanova O.L., Skovpen K.Yu., Soukharev A.M., Talyshev A.A., Tikhonov Yu.A. Measurement of flow harmonics with multi-particle cumulants in Pb plus Pb collisions at root(NN)-N-S=2.76 TeV with the ATLAS detector. // EUROPEAN PHYSICAL JOURNAL C. - 2014. - Vol. 74, № 11. - P. 3157.

[395] Aad G., ATLAS Collab., Anisenkov A.V., Bobrovnikov V.S., Bogdanchikov A.G., Kazanin V.F., Korol A.A., Malyshev V.M., Maslennikov A.L., Maxiimov D.A., Peleganchuk S.V., Rezanova O.L., Skovpen K.Yu., Soukharev A.M., Talyshev A.A., Tikhonov Yu.A. Search for top squark pair production in final states with one isolated lepton, jets, and missing transverse momentum in root s=8 TeV pp collisions with the ATLAS detector. // JOURNAL OF HIGH ENERGY PHYSICS. - 2014. - № 11. - P. UNSP 118.

[396] Yurov D.V. Prikhodko V.V. Hybrid systems for transuranic waste transmutation in nuclear power reactors: state of the art and future prospects. // PHYSICS-USPEKHI. - 2014. - Vol. 57, № 11. - P. 1118-1129.

[397] M.N. Achasov, V.M. Aulchenko, A.Yu. Barnyakov, K.I. Beloborodov, A.V. Berdyugin, D.E. Berkaev, A.G. Bogdanchikov, A.A. Botov, T.V. Dimova, V.P. Druzhinin, V.B. Golubev, L.V. Kardapoltsev, A.S. Kasaev, A.G. Kharlamov, A.N. Kirpotin, I.A. Koop, A.A. Korol, S.V. Koshuba, D.P. Kovrizhin, E.A. Kravchenko, A.S. Kupich, K.A. Martin, A.E. Obrazovsky, E.V. Pakhtusova, Yu.A. Rogovsky, A.I. Senchenko, S.I. Serednyakov, Yu.M. Shatunov, D.A. Shtol, D.B. Shwartz, Z.K. Silagadze, A.N. Skrinsky, I.K. Surin, Yu.A. Tikhonov, Yu.V. Usov and I.M. Zemlyansky, Hadronic Cross Section Measurements at SND. // Int. J. Mod. Phys. Conf. Ser. 35 (2014) 1460388.

[398] M.N. Achasov, V.M. Aulchenko, A.Yu. Barnyakov, K.I. Beloborodov, A.V. Berdyugin, D.E. Berkaev, A.G. Bogdanchikov, A.A. Botov, T.V. Dimova, V.P. Druzhinin, V.B. Golubev, L.V. Kardapoltsev, A.S. Kasaev, A.G. Kharlamov, A.N. Kirpotin, I.A. Koop, A.A. Korol, S.V. Koshuba, D.P. Kovrizhin, E.A. Kravchenko, A.S. Kupich, K.A. Martin, A.E. Obrazovsky, E.V. Pakhtusova, Yu.A. Rogovsky, A.I. Senchenko, S.I. Serednyakov, Yu.M. Shatunov, D.A. Shtol, D.B. Shwartz, Z.K. Silagadze, A.N. Skrinsky, I.K. Surin, Yu.A. Tikhonov, Yu.V. Usov and I.M. Zemlyansky, Hadronic cross section measurements at CMD-3. // Int. J. Mod. Phys. Conf. Ser. 35 (2014) 1460387.

[399] A.G. Bogdanchikov, V.P. Druzhinin, A.A. Korol, S.V. Koshuba, A.I. Tekutiev and Yu.V. Usov. SND data acquisition system upgrade, JINST 9 (2014), C06013.

[400] K. Martin, A.Yu. Barnyakov, M.Yu. Barnyakov, K.I. Beloborodov, V.S. Bobrovnikov, A.R. Buzykaev, V.B. Golubev, S.A. Kononov, S.V. Koshuba, E.A. Kravchenko, A.P. Onuchin, S.I. Serednyakov. Aerogel Cherenkov counters for experiments at VEPP-2000 e$^+$e$^-$ collider with SND detector, Proc. of Science (2014), PoS(TIPP2014)076.

[401] P.A. Bak, A.V. Ottmar, D.A. Starostenko. Alternative technique of inverter power source synchronization. // Bulletin of Novosibirsk State University. Physics, Novosibirsk. - 2014. - Vol. 9, Ser. 3. - P. 20-24.

[402] K.V. Lotov, E.A. Mesyats, A.V. Snytnikov. Particle in cell simulation of kinetic instability of an electron beam in plasma. // Mathematical Modelling - 2014. - Vol. 26, №11. - P. 45-50.

[403] V.T. Astrelin, V.I. Davydenko, A.V. Kolmogorov. Numerical simulation of the secondary plasma surface in the ion beam formation. // Bulletin of Higher Educational Institutions. Physics. Publishing

House of Scientific and Technical Literature. Tomsk. - 2014. – Vol. 57, Is. 11/3. - P. 128-132.

[404] V.V. Kurkuchekov, I.A. Ivanov, I.V. Kandaurov, Yu.A. Trunev. Diagnostics for Measuring of the Electron Beam Current Distribution on a Metal Target. // Bulletin of Higher Educational Institutions. Physics. Publishing House of Scientific and Technical Literature. Tomsk. - 2014. – Vol. 57, Is. 11/3. - P. - 302-307.

[405] Yu.A. Rogovsky, D.E. Berkaev, I.M. Zemlyansky, Yu.M. Zharinov, A.S. Kasaev, I.A. Koop, A.N. Kirpotin, A.P. Lysenko, E.A. Perevedentsev, V.P. Prosvetov A.L. Romanov, A.I. Senchenko, P.Yu. Shatunov, Yu.M. Shatunov, D.B. Shwartz et al. Status and prospects of VEPP-2000 electron-positron collider. // Phys. Part. Nucl. Lett. - 2014. - Vol. 11. - P. 651-655.

[406] D.E. Berkaev, A.N. Kirpotin, I.A. Koop, A.P. Lysenko, E.A. Perevedentsev, Yu.A. Rogovsky, A.L. Romanov, D.B. Shwartz, P.Yu. Shatunov, Yu.M. Shatunov, Yu.M. Zharinov et al. Measurement of the $e^+e^- \to p\,\bar{p}$ cross section with the CMD-3 detector at VEPP-2000. // Int. J. Mod. Phys. Conf. Ser. - 2014. - Ser. 35. - P. 1460457.

[407] D.E. Berkaev, A.N. Kirpotin, I.A. Koop, A.P. Lysenko, E.A. Perevedentsev, Yu.A. Rogovsky, A.L. Romanov, D.B. Shwartz, P.Yu. Shatunov, Yu.M. Shatunov, Yu.M. Zharinov et al. Study of the process $e^+e^- \to K^+K^-\pi^+\pi^-$ with the CMD-3 detector at the VEPP-2000 e+e− collider. // Int. J. Mod. Phys. Conf. – 2014. - Ser. 35. - 1460450.

[408] I.A. Koop, et al. Overview prospects at BINP. // Int. J. Mod. Phys. Conf. Ser. - 2014. - Ser. 35. - 1460448.

[409] A.A. Ruktuev, V.V. Samoylenko, M.G. Golkovski. Structure and corrosion resistance of ti-ta-nb coatings obtained by electron beam cladding in the air-atmosphere. // Applied Mechanics and Materials. – 2014. - Vol. 682. - P. 100-103. // Trans Tech Publications, Switzerland. doi:10.4028/www.scientific.net/ AMM. 682.100.

[410] P.I. Nemytov. Power and control systems of industrial electron accelerators. // PALMARIUM Academic Publishing is a trademark of: OmniScriptum GmbH & Co. - 14 July 2014. - P. 248. ISBN 978-3-639-79906-4.

[411] D. Kasatov, A. Kuznetsov, A. Makarov, I. Shchudlo, I. Sorokin, S. Taskaev. Proton beam of 2 MeV 1.6 mA on a tandem accelerator with vacuum insulation. // Journal of Instrumentation. - 1914. – Vol. 9. - P12016.

[412] A.V. Grabovsky. Low-X evolution equation for proton green function. // Acta Phys.Polon.Supp. - 2014. - Vol. 7, №3. - P. 493.

[413] V.L. Chernyak, S.I. Eidelman. Hard exclusive two photon processes in QCD. // Progress in Particle and Nuclear Physics (online). [http://dx.doi.org/10.1016/j.ppnp.2014.09.002. - P. 1-42. arXiv:1409.3348 [hep-ph]. - P. 1-58.

[414] A.G. Grozin. Introduction to Mathematica for Physicists. Graduate Texts in Physics. - Springer (2014), 219 pages. ISBN 978-3-319-00893-6; ebook ISBN 978-3-319-00894.

[415] O.V. Zhirov, and D.L. Shepelyansky. Anderson transition for Google matrix eigenstates. // Annalen der Physik, 2014.

[416] V. M. Khatsymovsky. Faddeev gravity action on the piecewise constant fundamental vector fields. // TSPU Bulletin - 2014. - Is. 12(153). - P. 131-134. [arXiv:1412.7403].

[417] S.A. Rastigeev, A.R. Frolov, A.D. Goncharov, V.F. Klyuev, E.S. Konstantinov, L.A. Kutnykova, V.V. Parkhomchuk, A.V. Petrozhitskii. Acceleration mass spectrometer of the BINP for biomedical applications. // Physics of Particles and Nuclei Letters. - 2014. - 11 (5). - P. 642-646.

[418] A.P. Zavjalov, K.V. Zobov, I.K. Chakin, V.V. Syzrantsev, S.P. Bardakhanov. Synthesis of copper nanopowders by electron beam evaporation of inert gas under atmospheric pressure // Russian Nanotechnology. - 2014. - Vol. 9, №11-12. - P. 64-68.

[419] KEDR Collab., Aulchenko V.M., Baldin E.M., Barladyan A.K., Barnyakov A.Yu., Barnyakov M.Yu., Baru S.E., Basok I.Yu., Batrakov A.M., Blinov A.E., Blinov V.E., Bobrov A.V., Bobrovnikov V.S., Bogomyagkov A.V., Bondar A.E., Buzykaev A.R., Eidelman S.I., Grigiriev D.N., Groshev V.R., Glukhovchenko Yu.M., Gulevich V.V., Gusev D.V., Karnaev S.E., Karpov G.V., Karpov S.V., Kharlamova T.A., Kiselev V.A., Kolmogorov V.V., Kononov S.A., Kotov K.Yu., Kravchenko E.A., Kudryavtsev V.N., Kulikov V.F., Kurkin G.Ya., Kuper E.A., Kuyanov I.A., Levichev E.B., Maksimov D.A., Malyshev V.M., Maslennikov A.L., Meshkov O.I., Mishnev S.I., Morozov I.I., Muchnoi N.Yu., Neufeld V.V., Nikitin S.A., Nikolaev I.B., Okunev I.N., Onuchin A.P., Oreshkin S.B., Orlov I.O., Osipov A.A., Ovtin I.V., Peleganchuk S.V., Petrov V.V., Piminov P.A., Pivovarov S.G., Poluektov A.O., Prisekin V.G., O.L. Rezanova., Ruban A.A., Sandyrev V.K., Savinov G.A., Shamov A.G., Shatilov D.N., Shwartz B.A., Simonov E.A., Sinyatkin S.V., Skrinsky A.N., Sokolov A.V., Starostina E.V., Sukharev A.M., Talyshev A.A., Tayursky V.A., Telnov V.I., Tikhonov Yu.A., Todyshev K.Yu., Tumaikin G.M., Usov Yu.V., Vorobiov A.I., Zhilich V.N., Zhulanov V.V., Zhuravlev A.N. Study of $\psi(2S) \to \mu^+\mu^-$ decay with KEDR detector. // Int. J. Mod. Phys. Conf. Ser. - 2014. - 2014. - Vol. 35. - P. 1460462.

[420] V.E. Blinov, E.A. Bekhtenev, A.P. Chabanov, O.P. Gordeev, V.A. Kiselev, S.A. Krutikhin, G.Ya. Kurkin, E.B. Levichev, O.I. Meshkov, A.I. Mikaiylov, V.V. Neifeld, S.A. Nikitin, I.B Nikolaev, D.N. Shatilov, G.M. Tumaikin and A.I. Zhmaka. RF system for electron and positron orbit separation at VEPP-4M. // JINST. – 2014. – Vol. 9. - P12011.

[421] KEDR Collab., Anashin V.V., Aulchenko V.M., Baldin E.M., Barladyan A.K., Barnyakov A.Yu., Barnyakov M.Yu., Baru S.E., Basok I.Yu., Bedny I.V., Beloborodova O.L., Blinov A.E., Blinov V.E., Bobrov A.V., Bobrovnikov V.S., Bogomyagkov A.V., Bondar A.E., Buzykaev A.R., Eidelman S.I., Glukhovchenko Yu.M., Gulevich V.V., Gusev D.V., Karnaev S.E., Karpov G.V., Karpov S.V., Kharlamova T.A., Kiselev V.A., Kononov S.A., Kotov K.Yu., Kravchenko E.A., Kulikov V.F., Kuper E.A., Kurkin G.Ya., Levichev E.B., Maksimov D.A., Malyshev V.M., Maslennikov A.L., Medvedko A.S., Meshkov O.I., Mishnev S.I., Morozov I.I., Muchnoi N.Yu., Neufeld V.V., Nikitin S.A., Nikolaev I.B., Okunev I.N., Onuchin A.P., Oreshkin S.B., Orlov I.O., Osipov A.A., Peleganchuk S.V., Petrov V.V., Piminov P.A., Pivovarov S.G., Poluektov A.O., Pospelov G.E., Prisekin V.G., Ruban A.A., Sandyrev V.K., Savinov G.A., Shamov A.G., Shatilov D.N., Shwartz B.A., Simonov E.A., Sinyatkin S.V., Skovpen Yu.I., Skrinsky A.N., Smaluk V.V., Sokolov A.V., Starostina E.V., Sukharev A.M., Talyshev A.A., Tayursky V.A., Telnov V.I., Tikhonov Yu.A., Todyshev K.Yu., Tumaikin G.M., Usov Yu.V., Vorobiov A.I., Yushkov A.N., Zhilich V.N., Zhulanov V.V., Zhuravlev A.N. Parameters of charmonium states from KEDR. // Int. J. Mod. Phys.Conf. Ser. - 2014. - Vol. 35, P. 1460429. doi:10.1142/S2010194514604293.

[422] M. Ablikim (BESIII Collab.) M.N. Achasov, I.N. Nikolaev, N.Yu. Muchnoi. Measurement of the $D \to K^- \pi^+$ strong phase difference in $\psi(3770) \to D^0 \bar{D}^0$. // Phys. Lett. - 2014. - B734. - P. 227-233. arXiv:1404.4691 [hep-ex]. 10.1016/j.physletb.2014.05.071.

[423] Buzulutskov A.F, Bondar A.E., Dolgov A.D., Sokolov A.V, Shekhtman L.I.. Two-phase cryogenic avalanche detector. // Patent for the invention: RF № 2517777. Priority of invention: 20.08.2012. Date of registration: 03.04.2014. Date of publication: 27.05.2014, № 15.

[424] Bondar A.E., Buzulutskov A.F, Dolgov A.D., Porosev V.V. Device for monitoring the ion beam parameters. // Patent for the invention: RF № 2520940. Priority of invention: 05.10.2012. Date of registration: 03.04.2014. Date of publication: 27.06.2014, № 18.

[425] Chernousov YuD., Ivannikov V.I., Shebolaev I.V., Levichev A.E, Barnyakov A.M. Coaxial high-frequency switch. Patent for the invention: № RU2532852C1, Priority of invention: 10.11.2014, №31.

[426] Alaykrinsky O.N., Baru S.E., Dikansky N.S., Kocheev A.A., Leonov V.V., Porosev V.V. Multichannel ionization chamber. Patent for the invention: №2530903. Bulletin of invention: N29-2014, 20.10.2014.

[427] Logachev P.V., Semenov Yu.I., Stelvaga A.A., Danilov V.V. A method of electron beam welding of nonmagnetic metals and alloys. Application: №2014100704. State: Review.

[428] Polosatkin S.V., Grishnyaev E.S. Invention Patent No.Ru 2531550. Method of calibrating liquid argon based cryogenic particle detector and apparatus therefore. Application: 2013123249/28, 21.05.2013. Date for property rights: 21.05.2013. Date of publication 20.10.14. Bull. No 29. http://www.findpatent.ru/patent/253/2531550.html.

[429] S.Yu. Taskaev. Method to produce beam of monoenergetic neutrons, device for production of beam of monoenergetic neutrons and method to calibrate detector of dark matter with using of beam of monoenergetic neutrons. Patent RF № 2515523 от 14.03.2014.

[430] Sorokin I.N., Taskaev S.Yu. Vacuum insulation tandem-accelerator. The patent application. Registration number 2014139866 from 01.10.2014 (priority date).

[431] Taskaev S.Yu., Kanygin V.V., Muhamadiyarov R.A., Kichigin A.I. Method of delivery of boron drags for boron neutron capture therapy. The patent application. Registration number 2014148670 from 02.12.2014 (priority date).

[432] Vobly P.D., Makarov A.N., Ostreinov Yu.M., Taskaev S.Yu. Gas stripping target. The patent application. Registration number 2014152394 from 23.12.2014 (priority date).

[433] Kanygin V.V., Taskaev S.Yu. Neutron beam shaping assembly. Patent RF № 2540124 from 16.12.2014.

[434] Varand A.V., Tolochko B.P., Gadetsky A.Yu., Bryazgin A.A., Korobeinikov M.V., Mikhailenko M.A., Lyakhov N.Z., Belokrinitsky S.A. A method and apparatus for recycling of hydrocarbon waste. Patent for the invention: №2543378. The patent application: №2013123227. Priority date: 21 May, 2013. Registration number: RF 28 January, 2015.

Reports of the conferences 2014

[435] A.V. Sudnikov, A.V. Burdakov, V.S. Burmasov, L.N. Vyacheslavov, D.E. Gavrilenko, I.A. Ivanov, A.A. Kasatov, K.I. Mekler, S.V. Polosatkin, S.S. Popov, V.V. Postupaev, A.F. Rovenskikh, S.L. Sinitsky, V.D. Stepanov. Stabilization of the kink instability of conducting plasma with supercritical current density in GOL–3 device. // XLI Intern. Zvenigorod Conference on Plasma Physics and Controlled Fusion, 10-14 February 2014, Zvenigorod: Abstracts. - M: PLASMAIOFAN, 2014. - P. 66.

[436] Bagryansky P.A., Zaitsev K.V., Korzhavina M.S., Lizunov A.A., Prikhodko V.V. Study of the kinetic instabilities at the GDT facility. // XLI Intern. Zvenigorod Conference on Plasma Physics and Controlled Fusion, 10-14 February 2014, Zvenigorod: Abstracts. - M: PLASMAIOFAN, 2014. - P. 67.

[437] Kolesnikov E.Yu. Murakhtin S.V., Sorokin A.V. Modernization project of the atomic injection system for the GDT facility. // XLI Intern. Zvenigorod Conference on Plasma Physics and Controlled Fusion, 10-14 February

2014, Zvenigorod: Abstracts. - M: PLASMAIOFAN, 2014. - P. 68.

[438] Stupishin N.V., Belov V.P., Davydenko V.I., Deichuli P.P., Dranichnikov A.N., Ivanov A.A., Mishagin V.V., Sorokin A.V., Tkachev. The project of 60 kV, 2 A, 1 sec diagnostic neutral beam for the upgraded T-15 tokamak. // XLI Intern. Zvenigorod Conference on Plasma Physics and Controlled Fusion, 10-14 February 2014, Zvenigorod: Abstracts. - M: PLASMAIOFAN, 2014. - P. 81.

[439] Stupishin N.V., Deichuli P.P. Plasma emitter forming by adding four jets for 2 MW neutral beam. // XLI Intern. Zvenigorod Conference on Plasma Physics and Controlled Fusion, 10-14 February 2014, Zvenigorod: Abstracts. - M: PLASMAIOFAN, 2014. - P. 87.

[440] Solomakhin A.L., Bagryansky P.A., Kovalenko Yu.V., Savkin V.Ya., Yakovlev D.V. Electron cyclotron resonance heating of plasma in the gas dynamic trap. // XLI Intern. Zvenigorod Conference on Plasma Physics and Controlled Fusion, 10-14 February 2014, Zvenigorod: Abstracts. - M: PLASMAIOFAN, 2014. - P. 89.

[441] Belov V.P., Davydenko V.I., Ivanov A.A., Kapitonov V.A., Mishagin V.V., Sorokin A.V. The ion optical system of heating injector for TCV Tokamak. // XLI Intern. Zvenigorod Conference on Plasma Physics and Controlled Fusion, 10-14 February 2014, Zvenigorod: Abstracts. - M: PLASMAIOFAN, 2014. - P. 100.

[442] Deichuli P.P., Amirov V.Kh., Belov V.P., Vilkin A.I., Voskoboinikov R.V., Gorbovsky A.I., Davydenko V.I., Donin A.S., Dranichnikov A.N., Ivanov A.A., Kapitonov V.A, Kolmogorov V.V., Abdrashitov A.G., Abdrashitov G.F., Mishagin V.V., Pirogov K.A., Sorokin A.V., Stupishin N.V., Tkachev A.A., Usov P.V. The powerful 2 MW unit of neutral beam injection system for plasma heating in magnetic confinement devices. // XLI Intern. Zvenigorod Conference on Plasma Physics and Controlled Fusion, 10-14 February 2014, Zvenigorod: Abstracts. - M: PLASMAIOFAN, 2014. - P. 101.

[443] Deichuli P.P., Khrestolyubov V.S. Dump-calorimeter of atomic beams megawatt range. // XLI Intern. Zvenigorod Conference on Plasma Physics and Controlled Fusion, 10-14 February 2014, Zvenigorod: Abstracts. - M: PLASMAIOFAN, 2014. - P. 102.

[444] Skovorodin D.I., Beklemishev A.D. Influence of electron scattering on plasma density in expander. // XLI Intern. Zvenigorod Conference on Plasma Physics and Controlled Fusion, 10-14 February 2014, Zvenigorod: Abstracts. - M: PLASMAIOFAN, 2014. - P. 103.

[445] Vyacheslavov L.N., Ivantsivsky M.V., Kasatov A.A., Popov S.S., Puryga E.A., Rovenskikh A.F., Khilchenko A.D. Application of Thomson scattering techniques to study the interaction of the plasma with an electron beam in the experiments on generation of microwave radiationю // XLI Intern. Zvenigorod Conference on Plasma Physics and Controlled Fusion, 10-

14 February 2014, Zvenigorod: Abstracts. - M: PLASMAIOFAN, 2014. - P. 106.

[446] Yu.A. Trunev, V.T. Astrelin, I.V. Kandaurov, V.V. Kurkuchekov. Analysis of three-electrode electron optical system for high power electron beam source with plasma cathode. // XLI Intern. Zvenigorod Conference on Plasma Physics and Controlled Fusion, 10-14 February 2014, Zvenigorod: Abstracts. - M: PLASMAIOFAN, 2014. - P. 275.

[447] M.V. Ivantsivskiy, E.V. Alexandrov, A.V. Burdakov, T.V. Berbasova, N.A. Zolotukhina, Yu.S. Sulyaev, A.A. Shoshin. The development status of port-plags in BINP. // XLI Intern. Zvenigorod Conference on Plasma Physics and Controlled Fusion, 10-14 February 2014, Zvenigorod: Abstracts. - M: PLASMAIOFAN, 2014. - P. 331.

[448] M.V. Ivantsivskiy, V.N. Amosov, A.V. Burdakov, G.E. Nemtcev, K.V. Pishchinskiy, P.V. Usov. The design proposal of diagnostic module and neutron shielding for vertical neutron camera of ITER // XLI Intern. Zvenigorod Conference on Plasma Physics and Controlled Fusion, 10-14 February 2014, Zvenigorod: Abstracts. - M: PLASMAIOFAN, 2014. - P. 332.

[449] Akhmetshin R. Performance of the BGO endcap calorimeter with phototriode readout for the CMD-2 detector. // Instrumentation for Colliding Beam Physics, 24 February - 1 March 2014, Novosibirsk, Russia: book of abstracts. - Novosibirsk: BINP, 2014. - P. 4.

[450] Shebalin V. The combined liquid xenon - crystal CsI calorimeter of CMD-3 detector. // Instrumentation for Colliding Beam Physics, 24 February - 1 March 2014, Novosibirsk, Russia: book of abstracts. - Novosibirsk: BINP, 2014. - P. 7.

[451] Achasov M. Beam energy determination in collider experiments using backscattering of laser light. // Instrumentation for Colliding Beam Physics, 24 February - 1 March 2014, Novosibirsk, Russia: book of abstracts. - Novosibirsk: BINP, 2014. - P. 9.

[452] Telnov V. Photon collider Higgs factories. // Instrumentation for Colliding Beam Physics, 24 February - 1 March 2014, Novosibirsk, Russia: book of abstracts. - Novosibirsk: BINP, 2014. - P. 10.

[453] Buzulutskov A. Two-phase detectors. // Instrumentation for Colliding Beam Physics, 24 February - 1 March 2014, Novosibirsk, Russia: book of abstracts. - Novosibirsk: BINP, 2014. - P. 13.

[454] Shekhtman L. Development of high resolution tracking detectors with Gas Electron Multipliers. // Instrumentation for Colliding Beam Physics, 24 February - 1 March 2014, Novosibirsk, Russia: book of abstracts. - Novosibirsk: BINP, 2014. - P. 19.

[455] Kononov S. Study of focusing aerogels with electron beam. // Instrumentation for Colliding Beam Physics, 24 February - 1 March 2014, Novosibirsk,

Russia: book of abstracts. - Novosibirsk: BINP, 2014. - P. 19.

[456] Barnyakov A. Threshold aerogel Cherenkov counters of the KEDR detector. // Instrumentation for Colliding Beam Physics, 24 February - 1 March 2014, Novosibirsk, Russia: book of abstracts. - Novosibirsk: BINP, 2014. - P. 19.

[457] Barnyakov M. MCP PMT in colliding beam experiments. // Instrumentation for Colliding Beam Physics, 24 Feb - 1 March 2014, Novosibirsk, Russia: book of abstracts. - Novosibirsk: BINP, 2014. - P. 20.

[458] Fedotovich G. Upgrade of the TOF system CMD-3 detector. // Instrumentation for Colliding Beam Physics, 24 Feb - 1 March 2014, Novosibirsk, Russia: book of abstracts. - Novosibirsk: BINP, 2014. - P. 22.

[459] Gayazov S. Distributed data analysis system for CMD-3 detector. // Instrumentation for Colliding Beam Physics, 24 February - 1 March 2014, Novosibirsk, Russia: book of abstracts. - Novosibirsk: BINP, 2014. - P. 23.

[460] Matvienko D. Testbench of shaper-digitizer modules for Belle II calorimeter. // Instrumentation for Colliding Beam Physics, 24 February - 1 March 2014, Novosibirsk, Russia: book of abstracts. - Novosibirsk: BINP, 2014. - P. 24.

[461] Kaminskiy V. Compton backscattering for the calibration of KEDR Tagging System. // Instrumentation for Colliding Beam Physics, 24 February - 1 March 2014, Novosibirsk, Russia: book of abstracts. - Novosibirsk: BINP, 2014. - P. 25.

[462] Beloborodov K. Particle identification system based on dense aerogel for SND detector at VEPP-2000 collider. // Instrumentation for Colliding Beam Physics, 24 February - 1 March 2014, Novosibirsk, Russia: book of abstracts. - Novosibirsk: BINP, 2014. - P. 25.

[463] Bobrovnikov V. Extracted e- and gamma beams in BINP SB RAS. // Instrumentation for Colliding Beam Physics, 24 February - 1 March 2014, Novosibirsk, Russia: book of abstr. - Novosibirsk: BINP, 2014. - P. 25.

[464] Epshteyn L. Processing of the Liquid Xenon Calorimeter's signals for timing measurements. // Instrumentation for Colliding Beam Physics, 24 February - 1 March 2014, Novosibirsk, Russia: book of abstracts. - Novosibirsk: BINP. - P. 26.

[465] Martin K. Test results of the aerogel Cherenkov counters with n=1.05 using electrons and muons at p 500 MeV/c. // Instrumentation for Colliding Beam Physics, 24 February - 1 March 2014, Novosibirsk, Russia: book of abstracts. - Novosibirsk: BINP, 2014. - P. 27.

[466] Mikhailov, K. Liquid xenon calorimeter of the CMD-3 detector. // Instrumentation for Colliding Beam Physics, 24 February - 1 March 2014, Novosibirsk, Russia: book of abst.. - Novosibirsk: BINP, 2014. - P. 27.

[467] Fedotovich G. Luminosity measurement with CMD-3 detector at the VEPP-2000 e+e- collider. // Instrumentation for Colliding Beam Physics, 24 February - March 2014, Novosibirsk, Russia: book of abstracts. - Novosibirsk: BINP, 2014. - P. 28.

[468] Nikolaev I. The project of laser polarimeter for beam energy measurement of VEPP-4M collider by resonance depolarization method. // Instrumentation for Colliding Beam Physics, 24 February - 1 March 2014, Novosibirsk, Russia: book of abstracts. - Novosibirsk: BINP, 2014. - P. 29.

[469] Telnov V. Calibration of energies at photon colliders. // Instrumentation for Colliding Beam Physics, 24 February - 1 March 2014, Novosibirsk, Russia: book of abstracts. - Novosibirsk: BINP, 2014. - P. 29.

[470] Telnov V. Shekhtman L. A conception of the photon collider beam dump. // Instrumentation for Colliding Beam Physics, 24 February - 1 March 2014, Novosibirsk, Russia: book of abstracts. - Novosibirsk: BINP, 2014. - P. 30.

[471] Kudryavtsev V. The development of high resolution coordinate detectors for the DEUTRON facility. // Instrumentation for Colliding Beam Physics, 24 February - 1 March 2014, Novosibirsk, Russia: book of abstracts. - Novosibirsk: BINP, 2014. - P. 31.

[472] Korol A. SND data acquisition system upgrade. // Instrumentation for Colliding Beam Physics, 24 February - 1 March 2014, Novosibirsk, Russia: book of abstracts. - Novosibirsk: BINP, 2014. - P. 31.

[473] Shtol D. Muon system of SND detector. // Instrumentation for Colliding Beam Physics, 24 February - 1 March 2014, Novosibirsk, Russia: book of abstracts. - Novosibirsk: BINP, 2014. - P. 32.

[474] Shekhtman L. Fedotovich G. Proposal for the upgrade of the tracking and trigger system of the CMD-3 detector. // Instrumentation for Colliding Beam Physics, 24 February - 1 March 2014, Novosibirsk, Russia: book of abstracts. - Novosibirsk: BINP, 2014. - P. 32.

[475] Surin I. New measuring electronics channel for the SND detector electromagnetic calorimeter. // Instrumentation for Colliding Beam Physics, 24 February - 1 March 2014, Novosibirsk, Russia: book of abstracts. - Novosibirsk: BINP, 2014. - P. 32.

[476] Sukharev A. Muon system of the KEDR detector. // Instrumentation for Colliding Beam Physics, 24 February - 1 March 2014, Novosibirsk, Russia: book of abstracts. - Novosibirsk: BINP, 2014. - P. 33.

[477] Korol A. ATLAS TDAQ application gateway upgrade during LS1. // Instrumentation for Colliding Beam Physics, 24 February - 1 March 2014, Novosibirsk, Russia: book of abstracts. - Novosibirsk: BINP, 2014. - P. 33.

[478] Zhulanov V. Upgrade of trigger and DAQ for CsI at BelleII. // Instrumentation for Colliding Beam Physics, 24 February - 1 March 2014, Novosibirsk, Russia: book of abstr. - Novosibirsk: BINP, 2014. - P. 41.

[479] Ruban A. CMD-3 detector DAQ upgrade. // Instrumentation for Colliding Beam Physics, 24 February - 1 March 2014, Novosibirsk, Russia: book of abstracts. - Novosibirsk: BINP, 2014. - P. 43.

[480] Ancharova U.V. Nazmov V.P. Project of increase in SR intensity for diffraction experiments at high pressure using X-ray refractive lenses. // XX National Conference on Synchrotron Radiation "SR-2014", 7-10 July 2014, Novosibirsk: Book of abstracts. - Novosibirsk: BINP SB RAS, 2014. - P. 9.

[481] Gentselev A.N., Goldenberg B.G., Kondratjev V.I., Lemzyakov A.G. Fabrication of X-ray masks using contact photolithography. The X-ray masks making by using contact photolithography. // XX National Conference on Synchrotron Radiation "SR-2014", 7-10 July 2014, Novosibirsk: Book of abstracts. - Novosibirsk: BINP SB RAS, 2014. - P. 10.

[482] Gentselev A.N., Zelinsky A.G., Kondratjev V.I., Lemzyakov A.G. Titanium X-ray masks. // XX National Conference on Synchrotron Radiation "SR-2014", 7-10 July 2014, Novosibirsk: Book of abstracts. - Novosibirsk: BINP SB RAS, 2014. - P. 11.

[483] Tolochko B.P., Kosov A.V., Ten K.A., Pruuel E.R., Aulchenko V.M., Shekhtman L.I., Evdokov O.V., Zhogin I.L., Sharafutdinov M.R., Nazmov V.P., Zolotarev K.V., Mezentsev N.A., Sheromov M.A., Panchenko V.E. Experimental Station "Detonation" on SR beam from 7-pole snake of VEPP-4. // XX National Conference on Synchrotron Radiation "SR-2014", 7-10 July 2014, Novosibirsk: Book of abstracts. - Novosibirsk: BINP SB RAS, 2014. - P. 11.

[484] Zabluda V.N., Knyazev B.A., Kulipanov G.N., Sokolov A.E., Ovchinnikov S.G., Tugarinov V.I. The concept of magneto-optical modulator of X-rays at terahertz frequencies. // XX National Conference on Synchrotron Radiation "SR-2014", 7-10 July 2014, Novosibirsk: Book of abstracts. - Novosibirsk: BINP SB RAS, 2014. - P. 12.

[485] Korneev V.N., Shlektarev V.A., Zabelin A.V., Lanina N.F., Aulchenko V.M., Tolochko B.P., Vazina A.A. Results of equipping with SR apparatus in problems of structural biology of tissues. // XX National Conference on Synchrotron Radiation "SR-2014", 7-10 July 2014, Novosibirsk: Book of abstracts. - Novosibirsk: BINP SB RAS, 2014. - P. 12.

[486] Nazmov V., Volker A., Fischbock T., Rothe J., Huttel E. Mass defect in SU-8 polymer exposed to X-rays. // XX National Conference on Synchrotron Radiation "SR-2014", 7-10 July 2014, Novosibirsk: Book of abstracts. - Novosibirsk: BINP SB RAS, 2014. - P. 13.

[487] Aleshaev A.N., Mishnev S.I., Pischenyuk S.M., Rovenskihh A.F., Selivanov A.N., Selivanov P.A., Fedotov M.G. Development of system for 2D stabilization of SR beams in VEPP-3 storage ring. // XX National Conference on Synchrotron Radiation "SR-

2014", 7-10 July 2014, Novosibirsk: Book of abstracts. - Novosibirsk: BINP SB RAS, 2014. - P. 14-15.

[488] Shekhtman L.I., Aulchenko V.M., Zhulanov V.V., Pruuel E.R., Tolochko B.P., Ten K.A. Development of high-speed solid-state X-ray detector for fast processes. // XX National Conference on Synchrotron Radiation "SR-2014", 7-10 July 2014, Novosibirsk: Book of abstracts. - Novosibirsk: BINP SB RAS, 2014. - P. 15-16.

[489] Kubarev V.V. Ultra-fast single-pulse time-domain spectroscopy as method of diagnostics of modulation instability in free-electron laser. // XX National Conference on Synchrotron Radiation "SR-2014", 7-10 July 2014, Novosibirsk: Book of abstracts. - Novosibirsk: BINP SB RAS, 2014. - P. 16.

[490] Miginsky S.V. Mode HE11 in waveguide THz FEL. // XX National Conference on Synchrotron Radiation "SR-2014", 7-10 July 2014, Novosibirsk: Book of abstracts. - Novosibirsk: BINP SB RAS, 2014. - P. 16.

[491] Serednyakov S.S. Kubarev V.V. The measurement and monitoring of spectrum and wavelength of coherent radiation at Novosibirsk free electron laser. // XX National Conference on Synchrotron Radiation "SR-2014", 7-10 July 2014, Novosibirsk: Book of abst.. - Novosibirsk: BINP SB RAS, 2014. - P. 16-17.

[492] Salikova T.V., Vinokurov N.A., Deichuli O.I., Repkov A.B., Shevchenko O.A., Scheglov M.A. Radiation-sensor system for localization of beam losses in FEL microtron vacuum chamber. // XX National Conference on Synchrotron Radiation "SR-2014", 7-10 July 2014, Novosibirsk: Book of abstracts. - Novosibirsk: BINP SB RAS, 2014. - P. 17.

[493] Ancharova U.V., Mikhailenko M.A., Tolochko B.P., Korobeinikov M.V., Vinokurov Z.S. Structural analysis of ferrite ceramicd produced by radiation-thermal method. // XX National Conference on Synchrotron Radiation "SR-2014", 7-10 July 2014, Novosibirsk: Book of abstracts. - Novosibirsk: BINP SB RAS, 2014. - P. 20.

[494] Vazina A.A., Lanina N.F., Korneev V.N., Zabelin A.V., Kulipanov G.N. The role of exogenous and endogenous effects on structure of cytoskeleton and the extracellular matrix of biological tissue by example of hair tissue. // XX National Conference on Synchrotron Radiation "SR-2014", 7-10 July 2014, Novosibirsk: Book of abstracts. - Novosibirsk: BINP SB RAS, 2014. - P. 25.

[495] Smirnov E.B., Muzyrya A.K., Kostitsyn O.V., Badretdinova L.Kh., Ten K.A., Pruuel E.R., Tolochko B.P., Sharafutdinov M.R., Shmakov A.N., Kuper K.E. Analysis of micro-, meso- and macrostructure of condensed heterogeneous high-explosives using synchrotron radiation. // XX National Conference on Synchrotron Radiation "SR-2014", 7-10 July 2014, Novosibirsk: Book of abstracts. - Novosibirsk: BINP SB RAS, 2014. - P. 29.

[496] Vobly P.D. Kolokolnikov Yu.M. The design of permanent magnet vacuum undulator with pole gap

following envelope of electron beam. // XX National Conference on Synchrotron Radiation "SR-2014", 7-10 July 2014, Novosibirsk: Book of abstracts. - Novosibirsk: BINP SB RAS, 2014. - P. 33.

[497] Batrakov A.M., Vobly P.D., Gurov D.S., Zuev V.V., Iljin I.V., Klimenko A.S., Kolokolnikov Yu.M., Ogurtsov A.B., Utkin A.V., Khavin Kh.G. Permanent magnet undulator with variable gap for a free electron laser. // XX National Conference on Synchrotron Radiation "SR-2014", 7-10 July 2014, Novosibirsk: Book of abstracts. - Novosibirsk: BINP SB RAS, 2014. - P. 33.

[498] Zorin A.V., Mezentsev N.A., Tsukanov V.M., et al. Systems for magnetic measurement of superconducting wigglers with stretched wire under current. // XX National Conference on Synchrotron Radiation "SR-2014", 7-10 July 2014, Novosibirsk: Book of abstracts. - Novosibirsk: BINP SB RAS, 2014. - P. 33.

[499] Zorin A.V., Mezentsev N.A., Volkov A.A., Shkaruba V.A., Khruschev S.V., Tsukanov V.M. 4.2 T superconducting multipole wiggler for Australian Synchrotron. // XX National Conference on Synchrotron Radiation "SR-2014", 7-10 July 2014, Novosibirsk: Book of abstracts. - Novosibirsk: BINP SB RAS, 2014. - P. 34.

[500] Batrakov A.M., Vobly P.D., Gurov D.S., Zuev V.V., Kobets V.V., Ogurtsov A.B., Pavlenko A.V., Utkin A.V., Filipchenko A.V. Multipole electrical magnets for BNL booster (USA) and MAX IV Lab linac (Sweden). // XX National Conference on Synchrotron Radiation "SR-2014", 7-10 July 2014, Novosibirsk: Book of abstracts. - Novosibirsk: BINP SB RAS, 2014. - P. 34.

[501] Batrakov A.M., Vobly P.D., Gurov D.S., Zuev V.V., Iljin I.V., Klimenko A.S., Kolokolnikov Yu.M., Ogurtsov A.B., Utkin A.V., Khavin N.G. Helical undulators for Relativistic Heavy Ion Collider (RHIC) at Brookhaven National Laboratory. // XX National Conference on Synchrotron Radiation "SR-2014", 7-10 July 2014, Novosibirsk: Book of abstracts. - Novosibirsk: BINP SB RAS, 2014. - P. 34.

[502] Khruschev S.V., A.A., Shkaruba V.A., Tsukanov V.M., Mezentsev N.A., Lev V.Kh. Particularities of vanishing integrals of magnetic field in wigglers and undulators with even number of poles. // XX National Conference on Synchrotron Radiation "SR-2014", 7-10 July 2014, Novosibirsk: Book of abstracts. - Novosibirsk: BINP SB RAS, 2014. - P. 34-35.

[503] Volkov A.A., Zorin A.V., Lev V.Kh., Mezentsev N.A., Syrovatin V.M., Tarasenko O.A., Khruschev S.V., Tsukanov V.M., Shkaruba V.A. Superconducting 15-pole wiggler with field 7.5 Tesla for LSU-CAMD. // XX National Conference on Synchrotron Radiation "SR-2014", 7-10 July 2014, Novosibirsk: Book of abstracts. - Novosibirsk: BINP SB RAS, 2014. - P. 35.

[504] Ivanov V.Yu., Zinin E.I., Pustovarov V.A. Photoluminescence and X-ray fluorescence of complex oxides in selective photon excitation. // X XX National Conference on Synchrotron Radiation "SR-2014", 7-10 July 2014, Novosibirsk: Book of abstracts. - Novosibirsk: BINP SB RAS, 2014. - P. 38-39.

[505] Erenburg S.B., Trubina S.V., Kovalenko E.A., Gerasko O.A., Zaikovsky V.I., Pindyurin V.F., Kvashnina K.O. The structure and size of small clusters of gold in samples containing molecules of cucurbit[n]uril (n=6, 7, 8). // XX National Conference on Synchrotron Radiation "SR-2014", 7-10 July 2014, Novosibirsk: Book of abstracts. - Novosibirsk: BINP SB RAS, 2014. - P. 53-54.

[506] Nazmov V. Reznikova E. Unmatched potential of deep X-ray lithography: microstructure 7 mm and more high. // XX National Conference on Synchrotron Radiation "SR-2014", 7-10 July 2014, Novosibirsk: Book of abstracts. - Novosibirsk: BINP SB RAS, 2014. - P. 55.

[507] Fedotov M.G. Potential of promising SR source at BINP in shadow radiography of detonation processes. // XX National Conference on Synchrotron Radiation "SR-2014", 7-10 July 2014, Novosibirsk: Book of abstracts. - Novosibirsk: BINP SB RAS, 2014. - P. 56.

[508] Knyazev B.A. New results at workstation SPIN of Novosibirsk terahertz FEL. // XX National Conference on Synchrotron Radiation "SR-2014", 7-10 July 2014, Novosibirsk: Book of abstracts. - Novosibirsk: BINP SB RAS, 2014. - P. 57. - (в тексте автор указан Knyazev B.A.).

[509] Vasiljev A.A., Palchikov E.I., Kubarev V.V., Chesnokov E.N., Koshlyakov P.V., Dolgikh A.V., Krasnikov I.Yu. Analysis of unsteady combustion waves and detonation waves of hydrogen-oxygen mixture in optical and terahertz ranges. // XX National Conference on Synchrotron Radiation "SR-2014", 7-10 July 2014, Novosibirsk: Book of abstracts. - Novosibirsk: BINP SB RAS, 2014. - P. 57-58.

[510] Gerasimov V.V., Gorovoj V.O., Knyazev B.A., Nikitin A.K., Zhizhin M.G., Vlasenko I.A., Kotelnikov I.A. Distribution of terahertz surface plasmon polaritons over straight and curved metal-dielectric surfaces with air gaps. // XX National Conference on Synchrotron Radiation "SR-2014", 7-10 July 2014, Novosibirsk: Book of abstracts. - Novosibirsk: BINP SB RAS, 2014. - P. 58.

[511] Barsukov V.P., Verkhoglyad A.G., Gerasimov V.V., Glebus I.S., Zavjalova M.A., Knyazev B.A., Makarov S.N., Stupak M.F., Ovchar V.K., Rodionova D.G., Choporova Yu.Yu., Shtatnov V.Yu. Development and fabrication of near-field terahertz scanning optical microscope with unit of frustrated total internal reflection. // XX National Conference on Synchrotron Radiation "SR-2014", 7-10 July 2014, Novosibirsk: Book of abstracts. - Novosibirsk: BINP SB RAS, 2014. - P. 58-59.

[512] Mitkov M.S., Choporova Yu.Yu., Knyazev B.A. Phase modulated terahertz polarimeter on the Novosibirsk Free Electron Laser. // XX National Conference on Synchrotron Radiation "SR-2014", 7-10 July 2014, Novosibirsk: Book of abstracts. - Novosibirsk: BINP SB RAS, 2014. - P. 59.

[513] Pavel'ev V.S., Agafonov A.N., Volodkin B.O., Kaveev A.K., Kachalov D.G., Knyazev B.A., Kropotov G.I., Tukmakov K.N., Tsygankova E.V. Tsypishka D.I., Choporova Yu.Yu. Silicon diffractive optics to control laser radiation in submillimeter range. // XX National Conference on Synchrotron Radiation "SR-2014", 7-10 July 2014, Novosibirsk: Book of abstracts. - Novosibirsk: BINP SB RAS, 2014. - P. 62-63.

[514] Demidova E.V., Demidov E.A., Popik V.M., Mescheryakova I.A., Semenov A.I., Goryachkovskaya T.N., Kolchanov N.A., Kulipanov G.N., Peltek S.E. Proteomic response of E. Coli cells to effectt of terahertz radiation. // XX National Conference on Synchrotron Radiation "SR-2014", 7-10 July 2014, Novosibirsk: Book of abstracts. - Novosibirsk: BINP SB RAS, 2014. - P. 63-64.

[515] Goryachkovskaya T.N., Kuibida L.V., Peltek S.E., Popik V.M., Semenov A.I., Timofeeva M.S., Scheglov M.A. A new method for accurate measurement of mass of nanoparticles using terahertz radiation.// XX National Conference on Synchrotron Radiation "SR-2014", 7-10 July 2014, Novosibirsk: Book of abstracts. - Novosibirsk: BINP SB RAS, 2014. - P. 64.

[516] Choporova Yu.Yu., Mitkov M.S., Cherkassky V.S., Knyazev B.A., Vlasenko M.S. Holographic imaging in an attenuated total reflection system. // XX National Conference on Synchrotron Radiation "SR-2014", 7-10 July 2014, Novosibirsk: Book of abstracts. - Novosibirsk: BINP SB RAS, 2014. - P. 67.

[517] Azarov I.A., Choporova Yu.Yu., Mitkov M.S., Knyazev B.A., Shvets V.A. Ellipsometric studies at Novosibirsk free electron laser. // XX National Conference on Synchrotron Radiation "SR-2014", 7-10 July 2014, Novosibirsk: Book of abstracts. - Novosibirsk: BINP SB RAS, 2014. - P. 68.

[518] Darin A.V., Kalugin I.A., Tretiakov G.A., Maximov M.A., Rogozin D.Yu., Zykov V.V., Rakshun Ya.V., Darin F.A., Sorokoletov D.A. Reconstruction of changes in lake Shira level in Late Holocene on annual time scale. // XX National Conf. on Synchrotron Radiation "SR-2014", 7-10 July 2014, Novosibirsk: Book of abstracts. - Novosibirsk: BINP SB RAS, 2014. - P. 73-75.

[519] Darin A.V. Kalugin I.A. Maximova N.V., Markovich T.I., Alexandrin M.Yu., Solomina O.N., Rakshun Ya.V., Darin F.A., Sorokoletov D.A. Analysis of seasonal geochemical signal in annual layers of bottom. // XX National Conference on Synchrotron Radiation "SR-2014", 7-10 July 2014, Novosibirsk: Book of abstracts. - Novosibirsk: BINP SB RAS, 2014. - P. 75.

[520] Darin A.V., Kalugin I.A., Rakshun Yu.V. Techniques of high- resolution analytical micro-stratigraphy using synchrotron radiation in limnological and paleoclimatic studies. // XX National Conference on Synchrotron Radiation "SR-2014", 7-10 July 2014, Novosibirsk: Book of abstracts. - Novosibirsk: BINP SB RAS, 2014. - P. 78.

[521] Darin A.V., Rakshun Ya.V., Sorokoletov D.S. Polycapillary optics adjustment system at station "SR XFA". // XX National Conference on Synchrotron Radiation "SR-2014", 7-10 July 2014, Novosibirsk: Book of abstracts. - Novosibirsk: BINP SB RAS, 2014. - P. 80.

[522] Markova Yu.N., Kerber E.V., Anchutina E.A., Zolotarev K.V. Analysis of bottom and lake-boggy sediments in Baikal region by SR XFA. // XX National Conference on Synchrotron Radiation "SR-2014", 7-10 July 2014, Novosibirsk: Book of abstracts. - Novosibirsk: BINP SB RAS, 2014. - P. 86.

[523] Sidorina A.V., Trunova V.A., Zolotarev K.V., Kriventsov V.V. Ways to improve metrological characteristics of X-ray fluorescence analysis. // XX National Conference on Synchrotron Radiation "SR-2014", 7-10 July 2014, Novosibirsk: Book of abstracts. - Novosibirsk: BINP SB RAS, 2014. - P. 88.

[524] Skuridin G.M., Chankina O.V., Kutsenogii K.P., Baginskaya N.V., Rakshun Ya.V., Sorokaletov D.S. Trace Element Composition of Sea-buckthorn Pollen (Hippophae rhamnoides L.). // XX National Conference on Synchrotro Radiation "SR-2014", 7-10 July 2014, Novosibirsk: Book of abstracts. - Novosibirsk: BINP SB RAS, 2014. - P. 90.

[525] Khramova E.P., Chankina O.V., Andysheva E.V., Rakshun Ya.V., Sorokaletova D.S. The element composition of plants Pentaphylloides (Rosaceae) of Far East of Russia. // XX National Conference on Synchrotron Radiation "SR-2014", 7-10 July 2014, Novosibirsk: Book of abstracts. - Novosibirsk: BINP SB RAS, 2014. - P. 92.

[526] Vlasenko M.G., Knyazev B.A., Nikitin A.A., Cherkassky V.S. Absolute meter of radiation power density distribution based on heat-sensitive Fizeau interferometer. // XX National Conference on Synchrotron Radiation "SR-2014", 7-10 July 2014, Novosibirsk: Book of abstracts. - Novosibirsk: BINP SB RAS, 2014. - P. 96.

[527] Semenov A.M., Anashin V.V., Gurov S.M., Krasnov A.A., Hseuh N.S., Shaftan T. Status of vacuum system of NSLS-II booster. // XX National Conference on Synchrotron Radiation "SR-2014", 7-10 July 2014, Novosibirsk: Book of abstracts. - Novosibirsk: BINP SB RAS, 2014. - P. 97.

[528] Brodnikov A.F. Cherepanov V.Ya. Optimization of a thermal mode at reproduction of reference points a temperature scale. // X Intern. Scientific Congress and Show "Interexpo Geo-Siberia-2014". Intern. Scientific Conference SibOptica-2014: Book of abst.. - Novosibirsk: Siberian State Academy of Geodesy, 2014. - P. 65-70.

[529] Zatrimailov K.V. Study of characteristics of cryogenic PMT for two-phase cryogenic avalanche detectors. // Proc of. 52-nd Intern. Students Scientific Conference "ISSC-2014". Quantum physics, 11-18 April, 2014, Novosibirsk: NSU, 2014. - P. 47.

[530] Kovalenko O.A. Study of the process $e^+e^- \to \pi^+\pi^-\pi^0$ in the range of 2 ГэВ with the CMD-3 detector. // Proc of. 52-nd Intern. Students Scientific Conference "ISSC-2014". Quantum physics, 11-18 April, 2014, Novosibirsk: NSU, 2014. - P. 48.

[531] Kozyrev E.A. Study of electron-positron annihilation into kaon-antikaon pair near phi(1020) resonance. // Proc of. 52-nd Intern. Students Scientific Conference "ISSC-2014". Quantum physics, 11-18 April, 2014, Novosibirsk: NSU, 2014. - P. 49.

[532] Korobov A.A. Monte-Carlo generator for multiple hadron production at VEPP-2000. // Proc of. 52-nd Intern. Students Scientific Conference "ISSC-2014". Quantum physics, 11-18 April, 2014, Novosibirsk: NSU, 2014. - P. 50.

[533] Maltsev T.V. Study of characteristics of detectors based on gas electron multipliers. // Proc of. 52-nd Intern. Students Scientific Conference "ISSC-2014". Quantum physics, 11-18 April, 2014, Novosibirsk: NSU, 2014. - P. 51.

[534] Oleynikov V.P. Measurement of the detector parameters for X-ray densitometry. // Proc of. 52-nd Intern. Students Scientific Conference "ISSC-2014". Quantum physics, 11-18 April, 2014, Novosibirsk: NSU, 2014. - P. 52.

[535] Rabusov A.V. Study of characteristics of electromagnetic calorimeter detector for a Super c-tau-Factory. // Proc of. 52-nd Intern. Students Scientific Conference "ISSC-2014". Quantum physics, 11-18 April, 2014, Novosibirsk: NSU, 2014. - P. 54.

[536] Razuvaev G.P. Study of the processes $e^+e^- \to \eta\gamma$, $\pi^\circ\gamma \to 3\gamma$ with the CMD-3 detector at the VEPP-2000 Collider. // Proc of. 52-nd Intern. Students Scientific Conference "ISSC-2014". Quantum physics, 11-18 April, 2014, Novosibirsk: NSU, 2014. - P. 55.

[537] Savrovsky P.A. Separation of isobaric ions in TOF detector at output of accelerator mass spectrometer. // Proc of. 52-nd Intern. Students Scientific Conference "ISSC-2014". Quantum physics, 11-18 April, 2014, Novosibirsk: NSU, 2014. - P. 56.

[538] V.O. Gorovoi. Research on propagation of tera-hertz surface plasmons over metal-dielectric surfaces of various configurations. // Proc of. 52-nd Intern. Students Scientific Conference "ISSC-2014". Quantum physics, 11-18 April, 2014, Novosibirsk: NSU, 2014. - P. 65.

[539] Goldenberg B.G., Lemzyakov A.G., Gentselev A.N., Zelinsky A.G., Kondratiev V.I., Nazmov V.P., Pindyurin V.F. Development of LIGA techniques for fabrication of deep microstructures at Siberian Centre for Synchrotron and Terahertz Radiation // Meeting and Youth Conference on the Use of Neutron Scattering and Synchrotron Radiation in Condensed Matter: RNSI-KS 2014, October 27-31, 2014 St. Petersburg: book of abst-racts. - Gatchina: NRC Kurchatov Institute, 2014. - P. 57.

[540] Darin F.A., Rakshun Ya.V., Sorokaletov D.S, Dar'in A.V. Analysis of internal structure of annual layers in lake sediments using synchrotron radiation with X-ray focusing optics. // Meeting and Youth Conference on the Use of Neutron Scattering and Synchrotron Radiation in Condensed Matter: RNSI-KS 2014, October 27-31, 2014 St. Petersburg: book of abst-racts. - Gatchina: NRC Kurchatov Institute, 2014. - P. 189.

[541] Darin A., Kalugin I., Maksimova N., Markovich T., Aleksandrin M., Solomina O., Rakshun Ya., Darin F., Sorokoletov D. Model of formation seasonal geochemical signal in lake Donguz-orun (Caucasus) annually laminated sediments according to micro scanning XRFA using focuses X-ray optics. // Paleolimnology of northern Eurasia: Proc. of the Intern. Conf., Petrozavodsk, 21-25 September 2014. - Petrozavodsk: Karelian Research Centre, 2014. - P. 70-71.

[542] Kozlovsky Yu.M., Stankus S.V., Yatsuk O.S., Zhmurikov E.I. Thermal expansion of constructional materials in wide temperature range // Thermodynamics and Materials: The 9th Seminar of SB RAS –UB RAS dedicated to the memory of academician F.A.Kuznetsov, Novosibirsk, 30 June - 4 July 2014: abstracts. - Novosibirsk: Nikolaev IIC SB RAS, 2014. - P. 183.

[543] Bogomyagkov A., Karyukina K., Levichev E. Damping wiggler with tapered period [Electronic resource]. // IPAC2014: Proc. of the 5th Intern. Particle Accelerator Conference, June 15-20 2014, Dresden, Germany. - Dresden, 2014. - P. 2038-2040.

[544] Alinovsky N., Bedareva T., Bekhtenev E., Belikov O., Bocharov V., Borodich V., Bryzgunov M., Bubley A., Chekavinskiy V., Cheskidov V., Dovzhenko B., Erokhin A., Fedotov M., Goncharov A., Gorchakov K., Gosteev V., Gusev I., Karpov G., Koisin Y., Kondaurov M., Kozak V., Kruchkov A., Lisitsyn A., Lopatkin I., Mamkin V., Medvedko A., Panasyuk V., Parkhomchuk V., Poletaev I., Polukhin V., Protopopov A., Pureskin D., Putmakov A., Reva V., Selivanov P., Semenov E., Senkov D., Skorobogatov D., Zapiatkin N., Bechstedt U., Esser F., Felden O., Gebel R., Halama A., Kamerdzhiev V., Klehr F., Langenberg G., Lehrach A., Lorentz B., Maier R., Prasuhn D., Reimers K., Retzlaff M., Richert A., Simon M., Stassen R., Stockhorst H., Tölle R., Mao L., Katayama T., Dietrich J. 2 MeV electron cooler for COSY and HESR - first results [Electronic resource]. // IPAC2014: Proc. of the 5th Intern. Particle Accelerator Conference, June 15-20 2014, Dresden, Germany: MOPRI070. - P. 765-767, ISBN 978-3-95450-132-8.

[545] Reva V.B., Alinovsky N.I., Bedareva T.V., Bekhtenev E.A., Belikov O.V., Bocharov V.N., Borodich V.V., Bryzgunov M.I., Bubley A.V., Chekavinskiy V.A., Cheskidov V.G., Dovzhenko B.A., Erokhin A.I., Fedotov M.G., Goncharov A.D., Gorchakov K.M., Gosteev V.K., Gusev I.A., Ivanov A.V., Karpov G.V., Koisin Yu.I., Kondaurov M.N., Kozak V.R., Lisitsyn A.D., Lopatkin I.A., Mamkin V.R., Medvedko A.S., Panasyuk V.M.,

178

Parkhomchuk V.V., Poletaev I.V., Polukhin V.A., Protopopov A.Yu., Pureskin D.N., Putmakov A.A., Selivanov P.A., Semenov E.P., Senkov D.V., Skorobogatov D.N., Zapiatkin N.P., Kamerdzhiev V., Mao L., Dietrich J. COSY 2 MeV cooler: design, diagnostic and commissioning [Electronic resource]. // IPAC2014: Proc. of the 5th Intern. Particle Accelerator Conference, June 15-20 2014, Dresden, Germany: MOPRI075, p. 777-779, ISBN 978-3-95450-132-8.

[546] Shwartz D., Berkaev D., Bochek D., Koop I., Krasnov A., Shatunov Yu., Korenev I., Sedlyarov I., Shatunov P., Zemlyansky I. Booster of electrons and positrons (BEP) upgrade to 1 GeV [Electronic resource]. // IPAC2014: Proc. of the 5th Intern. Particle Accelerator Conference, June 15-20 2014, Dresden, Germany. - Dresden, 2014. - P. 102-104.

[547] Shwartz D., Berkaev D., Koop I., Perevedentsev E., Rogovsky Yu., Shatunov Yu., Kasaev A., Kyrpotin A., Lysenko A., Prosvetov V., Romanov A., Senchenko A., Shatunov P., Zemlyansky I., Zharinov Yu. Recent beam-beam effects and luminosity at VEPP-2000 [Electronic resource]. // IPAC2014: Proc. of the 5th Intern. Particle Accelerator Conference, June 15-20 2014, Dresden, Germany. - Dresden, 2014. - P. 924-927.

[548] Gorda O., Dolinskii A., Litvinov S., Berkaev D., Koop I., Shatunov P., Shwartz D. Status of ion-optical design of the collector ring [Electronic resource]. // IPAC2014: Proc. of the 5th Intern. Particle Accelerator Conference, June 15-20 2014, Dresden, Germany. - Dresden, 2014. - P. 1114-1116.

[549] Bogomyagkov, A. Levichev E., Piminov P. Low emittance lattice cell with large dynamic aperture // IPAC2014: Proc. of the 5th Intern. Particle Accelerator Conference, June 15-20 2014, Dresden, Germany. - Dresden, 2014. - P. 99-101. [http://arxiv.org/abs/1405.7501].

[550] Bogomyagkov, A. Levichev E., Piminov P. Interaction region lattice for FCC-ee (TLEP) [Electronic resource]. // IPAC2014: Proc. of the 5th Intern. Particle Accelerator Conference, June 15-20 2014, Dresden, Germany. - Dresden, 2014. - P. 3779-3781.

[551] Hofmann A., Aulenbacher K., Bruker M.-W., Dietrich J., Weilbach W., Bryzgunov M.I., Denisov A.P., Panasyuk V.M., Parkhomchuk V.V., Reva V.B. Turbo generators for powering the HV-solenoids at the HESR electron cooler [Electronic resource]. // IPAC2014: Proc. of the 5th Intern. Particle Accelerator Conference, June 15-20 2014, Dresden, Germany. - Dresden, 2014: MOPME051. - P. 492-494, ISBN 978-3-95450-132-8.

[552] Bryzgunov M., Denisov A., Panasyuk V., Parkhomchuk V., Reva V., Kamerdjiev C.S., Aulenbacher K., Dietrich J. Conceptual project relativistic electron cooler for FAIR/HESR [Electronic resource]. // IPAC2014: Proc. of the 5th Intern. Particle Accelerator Conference, June 15-20 2014, Dresden, Germany: MOPRI074. - P. 774-776, ISBN 978-3-95450-132-8.

[553] Stirin A., Kovachev G., Korchuganov V., Odintsov D., Tarasov Yu., Zabelin A., Dorohov V., Khilchenko A., Scheglov A., Schegolev L., Zinin E., Zhuravlev A., Meshkov O. New station for optical observation of electron beam parameters at electron storage ring SIBERIA-2 [Electronic resource]. // IPAC2014: Proc. of the 5th Intern. Particle Accelerator Conference, June 15-20 2014, Dresden, Germany. - Dresden, 2014. - P. 3611-3613.

[554] Kotelnikov A.I., Khilchenko A.D., Dorohov V.L., Korchuganov V.N., Meshkov O.I., Stirin A., Zubarev P.V., Kvashnin A.N., Ivanova A.A., Puryga E.A., Ivanenko S.V. The new optical device for turn-to-turn beam profile measurement [Electronic resource]. // IPAC2014: Proc. of the 5th Intern. Particle Accelerator Conference, June 15-20 2014, Dresden, Germany. - Dresden, 2014. - P. 3617-3619.

[555] Eliseev A., Korepanov A., Panov A., Starostenko A. Pulse power supplies for the dipole kickers of MAX-IV and Solaris storage rings [Electronic resource]. // IPAC2014: Proc. of the 5th Intern. Particle Accelerator Conference, June 15-20 2014, Dresden, Germany. - Dresden, 2014. - P. 535-537.

[556] Akimov A.V., Bak P.A., Barnyakov A.M., Blinov M.F., Boimelshtein Yu.M., Emanov F.A., Frolov A.R., Gusev E.A., Dikansky N.S., Kazantseva E.S., Klyushchev S.N., Kot N.Kh., Korepanov A.A., Lapik R.M., Lebedev N.N., Logachev P.V., Martyshkin P.V., Nikiforov D.A., Pavlov V.M., Petrenko A.V., Pivovarov I.L., Samoilov S.L., Rybitskaya T.V., Skarbo B.A., Starostenko A.A., Shiyankov S.V., Tsyganov A.S. Status of injection complex VEPP-5: machine commissioning and first experience of positron storage [Electronic resource]]. // IPAC2014: Proc. of the 5th Intern. Particle Accelerator Conference, June 15-20 2014, Dresden, Germany. - Dresden, 2014. - P. 538-540.

[557] Glukhov S.A, Levichev E.B, Nikitin S.A, Piminov P.A, Shatilov D.N, Sinyatkin S.V. IBS simulations with Compute Unified Device Architecture (CUDA) technology [Electronic resource]. // IPAC2014: Proc of the 5th Intern. Particle Accelerator Conference, June 15-20 2014, Dresden, Germany. - Dresden, 2014. - P. 436-438.

[558] Gurov S., Karnaev S., Kiselev V., Levichev E., Smaluk V., Sinyatkin S., Zhuravlev A. Commissioning of NSLS-II booster [Electronic resource]. // IPAC2014: Proc. of the 5th Intern. Particle Accelerator Conference, June 15-20 2014, Dresden, Germany. - Dresden, 2014. - P. 295-297.

[559] Gurov S.M., Meshkov O.I., Smalyuk V.V., Yang X. Application of the optical diagnostics during the commissioning of the booster of NSLS-II [Electronic resource]. // IPAC2014: Proc. of the 5th Intern. Particle Accelerator Conference, June 15-20 2014, Dresden, Germany. - Dresden, 2014. - P. 3614-3616.

[560] Litvinenko V.N., Altinbas F.Z., Belomestnykh S.A., Ben-Zvi I., Beavis D., Brown K.A., Brutus C., Curcio A.J., DeSanto L., Elizarov A., Folz C.M., Gassner D.M., Hahn H., Hao Y., Ho C., Huang Y., Hulsart R., Ilardo M., Jamilkowski J., Jing Y., Karl F.X., Kayran D., Kellermann R., Lambiase R., Laloudakis N.D., Mahler G., Mapes M., Meng W., Michnoff R., Miller T.A., Minty M., Orfin P., Pendzik A., Pinayev I., Randazzo F., Rao T., Reich J., Roser T., Sandberg J., Seda T., Sheehy B., Skaritka J., Smart L.A., Smith K., Snydstrup L., Steszyn A., Than R., Theisen C., Todd R.J., Tuozzolo J., Wang E., Wang G., Weiss D., Willinski M., Xin T., Xu W., Zaltsman A., Kholopov M.A., Vobly P., Bell G.I., Cary J.R., Paul K., Pogorelov I.V., Schwartz B.T., Sobol A., Webb S.D., Boulware C., Grimm T., Jecks R., Miller N., McIntosh P., Wheelhouse A. Present status of coherent electron cooling proof-of-principle experiment [Electronic resource]. // IPAC2014: Proc. of the 5th Intern. Particle Accelerator Conference, June 15-20 2014, Dresden, Germany. - Dresden, 2014. - P. 87-90.

[561] Zangrando D., Bracco R., Castronovo D., Cautero M., Karantzoulis E., Krecic C., Loda G., Millo D., Pivetta L., Scalamera G., Visintini R., Khrushchev S., Mezentsev N., Shkaruba V., Syrovatin V., Tarasenko O., Tsukanov V., Volkov A. The Elettra 3.5 T superconducting wiggler refurbishment [Electronic resource]. // IPAC2014: Proc. of the 5th Intern. Particle Accelerator Conference, June 15-20 2014, Dresden, Germany. - Dresden, 2014. - P. 2687-2689.

[562] Romanov A., Koop I., Perevedentsev E., Shwartz D. Beam phase space reconstruction for monitoring the luminosity in the VEPP-2000 collider [Electronic resource]. // IPAC2014 – Proc. of the 5th Intern. Particle Accelerator Conference, June 15-20 2014, Dresden, Germany. - Dresden, 2014. - P. 3623-3625.

[563] Papash A., Mueller A.-S., Levichev E., Piminov P., Sinyatkin S., Zolotarev K. An ultra-low emittance model for the ANKA synchrotron radiation source including non-linear effects [Electronic resource]. // IPAC2014: Proc. of the 5th Intern. Particle Accelerator Conference, June 15-20 2014, Dresden, Germany. - Dresden, 2014. - P. 228-230.

[564] Levichev E.B., Meshkov O.I., Piminov P.A., Zhuravlev A.N. Turn-by-turn beam profile study at VEPP-4M [Electronic resource]. // IPAC2014: Proc. of the 5th Intern. Particle Accelerator Conference, June 15-20 2014, Dresden, Germany. - Dresden, 2014. - P. 3620-3622.

[565] Petrenko A., Bracco C., Gschwendtner E., Lotov K., Muggli P. Electron injection studies for the AWAKE experiment at CERN [Electronic resource]. // IPAC2014: Proc. of the 5th Intern. Particle Accelerator Conference, June 15-20 2014, Dresden, Germany. - Dresden, 2014. - P. 1537-1539.

[566] Romanov A., Kafka G., Nagaitsev S., Valishev A. Lattice correction modeling for Fermilab IOTA ring [Electronic resource]. // IPAC2014: Proc. of the 5th Intern. Particle Accelerator Conference, June 15-20 2014, Dresden, Germany. - Dresden, 2014. - P. 1165-1167.

[567] Milardi C., Alesini D., Biagini M.E., Boscolo M., Buonomo B., Guiducci S., Cantarella S., De Santis A., Di Pirro G., Delle Monache G., Drago A., Foggetta L., Frasciello O., Gallo A., Ghigo A., Guatieri F., Iungo F., Ligi C., Mazzitelli G., Pellegrino L., Ricci R., Rotundo U., Sanelli C., Sensolini G., Serio M., Stella A., Stecchi A., Zobov M., Gargana R., Michelotti A., Shatilov D., Valishev A., Tobyiama M. DAΦNE operation with the upgraded KLOE-2 detector [Electronic resource]. // IPAC2014: Proc. of the 5th Intern. Particle Accelerator Conference, June 15-20 2014, Dresden, Germany. - Dresden, 2014. - P. 1883-1885.

[568] Ohmi K., Zhou D., Shatilov D., Zhang Y. Beam-beam simulation study for CEPC [Electronic resource]. // IPAC2014: Proc. of the 5th Intern. Particle Accelerator Conference, June 15-20 2014, Dresden, Germany. - Dresden, 2014. - P. 3763-3765.

[569] Litvinenko V.N., Wang G., Bell G.I., Bruhwiler D.L., Elizarov A., Hao Y., Jing Y., Kayran D., Pogorelov I.V., Ratner D., Schwartz B.T., Shevchenko O., Sobol A., Webb S.D. Advances in coherent electron cooling [Electronic resource]. // IPAC2014: Proc. of the 5th Intern. Particle Accelerator Conference, June 15-20 2014, Dresden, Germany. - Dresden, 2014. - P. 91-94.

[570] Volkov V., Getmanov Ya., Shevchenko O., Vinokurov N., Matveenko A. Energy recovering for linac RF injectors [Electronic resource]. // IPAC2014: Proc. of the 5th Intern. Particle Accelerator Conference, June 15-20 2014, Dresden, Germany. - Dresden, 2014. - P. 356-358.

[571] Gambaryan V. Starostenko A. Fast kicker [Electronic resource]. // IPAC2014: Proc. of the 5th Intern. Particle Accelerator Conference, June 15-20 2014, Dresden, Germany. - Dresden, 2014. - P. 1280-1282.

[572] Zvereva V.V., Trunova V.A., Polosmak N.V., Sorokoletov D.S. Analysis of finds of organic origin from mounds of Hun elite (Noin-Ula, Mongolia) by methods of SR XFA, micro SR XFA and X-ray absorption spectroscopy. // VIII All-Russian Conference on X-ray analysis, Irkutsk, 22-26 September 2014: abstr. - Irkutsk Institute of the Earth's Crust SB RAS, 2014. - P. 53.

[573] Sidorina A.V., Trunova V.A., Zolotarev K.V. Effect of absorbing properties of different matrices on results of X-ray analysis.// VIII All-Russian Conference on X-ray analysis, Irkutsk, 22-26 September 2014: abstracts. - Irkutsk Institute of the Earth's Crust SB RAS, 2014. - P. 116.

[574] Pinayev I., Altinbas F.Z., Beavis D.R., Belomestnykh S., Ben-Zvi I., Brown K.A., Brutus J.C., Curcio A.L., DeSanto L., Elizarov A., Folz C.M., Gassner D.M., Hahn H., Hao Y., Ho C., Huang Y., Hulsart R., Ilardo M., Jamilkowski J., Jing Y., Karl F.X., Kayran D., Kellermann R., Laloudakis N.D., Lambiase R., Litvinenko V.N., Mahler G., Mapes M., Meng W.,

Michnoff R., Miller M.A., Minty M., Orfin P., Pendzik A., Randazzo F., Rao T., Reich J., Roser T., Sandberg J., Sheehy B., Skaritka J., Smith K., Snydstrup L., Steszyn A., Than R., Theisen C., Todd R.J., Tuozzolo J., Wang E., Wang G., Weiss D., Wilinski M., Xin T., Xu W., Zaltsman A., Kholopov M.A., Vobly P., Bell G.I., Cary J.R., Paul K., Pogorelov I.V., Schwartz B.T., Sobol A., Webb S.D., Boulware C., Grimm T., Jecks R., Miller N., McIntosh P., Wheelhouse A. Present status of coherent electron cooling proof-of-principle experiment. // Proc. of the 36th Intern. Free Electron Laser Conference: FEL2014, Congress Center Basel, Switzerland 25-29 August 2014. - Villigen: Paul Scherrer Institut, 2014. - P. 524-527.

[575] Kim H.W., Bae S., Gudkov B., Jang K.H., Jeong Y.U., Kim Y., Lee K., Mun J., Park S.H., Park S.J., Vinokurov N., Miginsky S.V. Analysis of beam stability in the KAERI ultrashort pulse accelerator. // Proc. of the 36th Intern. Free Electron Laser Conference: FEL2014, Congress Center Basel, Switzerland 25-29 August 2014. - Villigen: Paul Scherrer Insitut, 2014. - P. 697-698.

[576] Shevchenko O.A., Tcheskidov V.G., Vinokurov N.A., Davidyuk I. Modeling and design of the variable period and pole number undulator for the second stage of the Novosibirsk FEL. // Proc. of the 36th Intern. Free Electron Laser Conference: FEL2014, Congress Center Basel, Switzerland 25-29 August 2014. - Villigen: Paul Scherrer Insitut, 2014. - P. 96-99.

[577] Shevchenko O.A., Vinokurov N.A. Characterization of the undulator magnetic field quality by the angle averaged radiation spectrum. // Proc. of the 36th Intern. Free Electron Laser Conference: FEL2014, Congress Center Basel, Switzerland 25-29 August 2014. - Villigen: Paul Scherrer Insitut, 2014. - P. 100-102.

[578] Sokolov N. A. Vinokurov N. Estimating effect of undulator field errors using the radiation hodograph methodh. // Proc. of the 36th Intern. Free Electron Laser Conference: FEL2014, Congress Center Basel, Switzerland 25-29 August 2014. - Villigen: Paul Scherrer Insitut, 2014. - P. 93-95.

[579] Mun J., Jeong Y.U., Vinokurov N., Lee K., Park S.H., Jang K.H., Jeon M.Y. Performance analysis of variable-period helical undulator with permanent magnet for a KAERI THz FEL. // Proc. of the 36th Intern. Free Electron Laser Conference: FEL2014, Congress Center Basel, Switzerland 25-29 August 2014. - Villigen: Paul Scherrer Insitut, 2014. - P. 84-86.

[580] Nikolenko D.M., Arrington J., Barkov L.M., Dmitriev V.F., Gauzshtein V.V., Golovin R.A., Gramolin A.V., Holt R.J., Kaminsky V.V., Lazarenko B.A., Mishnev S.I., Muchnoi N.Yu., Neufeld V.V., Rachek I.A., Sadykov R.Sh., Shestakov Yu.V., Stibunov V.N., Toporkov D.K., De Vries H., Zevakov S.A., Zhilich V.N. Two-photon exchange contribution in elastic electron-proton scattering, experiment at the VEPP-3 storage ring. // 2013 Intern. Nuclear Physics Conference, INPC 2013;

Firenze; Italy; 2 -7 June 2013: EPJ Web of Conferences. - 2014. - Vol. 66. - P. 06002. - DOI10.1051/epjconf/20146606002.

[581] Litvinov S., Dolinskii A., Gorda O., Koop I. Nonlinear corrections in the CR storage ring at FAIR. // 20th Intern. Workshop on Beam Dynamics and Optimization, BDO 2014; St. Petersburg; Russian Federation; 30 June - 4 July 2014. - 2014. - P. 6890051. - DOI 10.1109/BDO.2014.6890051.

[582] Kubarev V.V. Dynamics of the THz optical discharge. // 39th Intern. Conf. on Infrared, Millimeter and Terahertz Waves, IRMMW-THz 2014, The University of Arizona, Tucson, United States, 14-19 September 2014. - P. 6956280. - DOI 10.1109/IRMMW-THz.2014.6956280.

[583] Shemyakin D.N., Akmetshin R.R., Anisenkov A.V., Aulchenko V.M., Banzarov V.S., Bashtovoy N.S., Berkaev D.E., Bondar A.E., Bragin A.V., Eidelman S.I., Epifanov D.A., Epshteyn L.B., Erofeev A.L., Fedotovich G.V., Gayazov S.E., Grebenuk A.A., Grigoriev D.N., Gromov E.M., Ignatov F.V., Karpov S.V., Kazanin V.F., Khazin B.I., Koop I.A., Kovalenko O.A., Kozyrev A.N., Kozyrev E.A., Krokovny P.P., Kuzmenko A.E., Kuzmin A.S., Logashenko I.B., Lukin P.A., Mikhailov K.Y., Muchnoi N.Y., Okhapkin V.S., Pestov Y.N., Perevedentsev E.A., Popov A.S., Razuvaev G.P., Rogovsky Y.A., Romanov A.L., Ruban A.A., Ryskulov N.M., Ryzhenenkov A.E., Shebalin V.E., Shemyakin D.N., Shwartz B.A., Shwartz D.B., Sibidanov A.L., Shatunov P.Y., Shatunov Y.M., Solodov E.P., Titov V.M., Talyshev A.A., Vorobiov A.I., Yudin Y.V. Study of the processes $e^+e^- \rightarrow K^+K^- \pi^+\pi^-$, $e^+e^- \rightarrow K^+K^- \varphi\eta$ with the CMD-3 detector at the e^+e^- Collider VEPP-2000. // EPJ Web of Conferences: 13th Intern. Workshop on Meson Production, Properties and Interaction, MESON 2014; Cracow; Poland; 29 May - 3 June 2014: EPJ Web of Conferences. - Vol. 81. - P. 02019. - DOI 10.1051/epjconf/ 20148102019.

[584] Lukin P.A., Akmetshin R.R., Anisenkov A.V., Aulchenko V.M., Banzarov V.S., Bashtovoy N.S., Berkaev D.E., Bondar A.E., Bragin A.V., Eidelman S.I., Epifanov D.A., Epshteyn L.B., Erofeev A.L., Fedotovich G.V., Gayazov S.E., Grebenuk A.A., Grigoriev D.N., Gromov E.M., Ignatov F.V., Karpov S.V., Kazanin V.F., Khazin B.I., Koop I.A., Kovalenko O.A., Kozyrev A.N., Kozyrev E.A., Krokovny P.P., Kuzmenko A.E., Kuzmin A.S., Logashenko I.B., Mikhailov K.Y., Muchnoi N.Y., Okhapkin V.S., Pestov Y.N., Perevedentsev E.A., Popov A.S., Razuvaev G.P., Rogovsky Y.A., Romanov A.L., Ruban A.A., Ryskulov N.M., Ryzhenenkov A.E., Shebalin V.E., Shemyakin D.N., Shwartz B.A., Shwartz D.B., Sibidanov A.L., Shatunov P.Y., Shatunov Y.M., Solodov E.P., Titov V.M., Talyshev A.A., Vorobiov A.I., Yudin Y.V. Study of the process $e^+e^- \rightarrow 2(\pi^+\pi^-\pi^0)$ with the CMD-3 detector at VEPP-2000 collider. // EPJ Web of Conferences: 13th Intern. Workshop on Meson Production, Properties and Interaction, MESON 2014,

Cracow, Poland, 29 May - 3 June 2014: EPJ Web of Conferences. - Vol. 81. - P. 02010. - DOI 10.1051/epjconf/20148102010.

[585] Achasov M.N., Barnyakov A.Y., Barnyakov M.Y., Beloborodov K.I., Berdyugin A.V., Berkaev D.E., Blinov V.E., Bobrovnikov V.S., Bogdanchikov A.G., Botov A.A., Buzykaev A.R., Dimova T.V., Druzhinin V.P., Golubev V.B., Kardapoltsev L.V., Kharlamov A.G., Kirpotin A.N., Kononov S.A., Koop I.A., Korol A.A., Koshuba S.V., Kovrizhin D.P., Kravchenko D.P., Kupich A.S., Lysenko A.P., Martin K.A., Obrazovsky A.E., Onuchin A.P., Pakhtusova E.V., Serednyakov S.I., Romanov A.L., Senchenko A.I., Shatunov P.Y., Shatunov Y.M., Shtol D.A., Shwartz D.B., Silagadze Z.K., Skrinsky A.N., Surin I.K., Tikhonov Y.A., Usov Y.V., Vasiljev A.V., Zemlyansky I.M. Light hadron production in experiments with the SND detector at the e^+e^- Collider VEPP-2000. // 13th Intern. Workshop on Meson Production, Properties and Interaction, MESON 2014; Cracow; Poland; 29 May - 3 June 2014: EPJ Web of Conferences, 2014. - Vol. 81. - P. 02018.

[586] Mezentsev, N. Shkaruba V., Syrovatin V. Superconducting multipole wigglers: Magnetic and cryogenic systems. // Refrigeration Science and Technology. - 2014. - 13th Intern. Institute of Refrigeration Conference on Cryogenics, CRYOGENICS 2014; Prague; Czech Republic; 7-11 April 2014. - P. 81-87.

[587] Epov V.S., Klimov A.E., Kubarev V.V., Paschin N.S., Shumsky V.N. Effect of magnetic field on the sensitivity of PbSnTe:In films to THz radiation. // 2014 IEEE 15th Intern. Conf. of Young Specialists on Micro/Nanotechnologies and Electron Devices, EDM 2014; Altai; Russian Federation; 30 June - 4 July 2014. - P. 81-84. - DOI 10.1109/EDM.2014.6882482.

[588] Knyazev B.A., Gerasimov V.V., Gorovoy V.O., Cherkassky V.S., Kulipanov G.N., Kotelnikov I.A., Nikitin A.K., Zhizhin G.N. A thorough study of terahertz surface waves travelling along metal-dielectric surfaces of different curvature and jumping through air gaps. // 39th Intern. Conf. on Infrared, Millimeter and Terahertz Waves, IRMMW-THz 2014; The University of Arizona, Tucson; United States; 14-19 September 2014. - 2014. - P. 6956462. - DOI 10.1109/IRMMW-THz.2014. 6956462.

[589] Stirin A., Kovachev G., Korchuganov V., Odintsov D., Tarasov Y., Zabelin A., Meshkov O., Dorohov V., Khilchenko A., Scheglov A., Schegolev L., Zinin E., Zhuravlev A. New station for optical observation of electron beam parameters at electron storage ring Siberia-2. // 2014 20th Intern. Workshop on Beam Dynamics and Optimization, BDO 2014; St. Petersburg; Russian Federation; 30 June-4 July 2014. - 2014. - P. 6890083. - ISSN 9781-4799, DOI 10.1109/BDO.2014.6890083.

[590] Kubarev V.V. Chesnokov E.N., Koshlyakov P.V. Pulse effects of terahertz radiation in molecular gas mediums. // 39th Intern. Conf. on Infrared, Millimeter and Terahertz Waves, IRMMW-THz 2014; The University of Arizona, Tucson; United States; 14-19 September 2014. - 2014. - P. 6956469. - DOI 10.1109/IRMMW-THz.2014. 6956469.

[591] Logashenko I.B., Akhmetshin R.R., Anisenkov A.V., Aulchenko V.M., Banzarov V.S., Bashtovoy N.S., Berkaev D.E., Bragin A.V., Eidelman S.I., Epifanov D.A., Epshteyn L.B., Erofeev A.L., Fedotovich G.V., Gayazov S.E., Grebenuk A.A., Grigoriev D.N., Gromov E.M., Ignatov F.V., Karpov S.V., Kazanin V.F., Khazin B.I., Kirpotin A.N., Koop I.A., Kovalenko O.A., Kozyrev A.N., Kozyrev E.A., Krokovny P.P., Kuzmenko A.E., Kuzmin A.S., Lukin P.A., Lysenko A.P., Mikhailov K.Y., Okhapkin V.S., Pestov Y.N., Perevedentsev E.A., Popov A.S., Razuvaev G.P., Rogovsky Y.A., Romanov A.L., Ruban A.A., Ryskulov N.M., Ryzhenenkov A.E., Shebalin V.E., Shemyakin D.N., Shwartz B.A., Shwartz D.B., Sibidanov A.L., Shatunov P.Y., Shatunov Y.M., Solodov E.P., Titov V.M., Talyshev A.A., Vorobiov A.I., Yudin Y.V., Zharinov Y.M. Measurement of $e^+e^- \to \pi^+\pi^-$ cross section at CMD-3. // Intern. Symposium Lepton and Hadron Physics at Meson-Factories, LHPMF 2013; Messina; Italy; 13-15 October 2013.- EPJ Web of Conferences: 2014. - Vol. 72. - P. 00013. - DOI 10.1051/epjconf/20147200013.

[592] Choporova Y.Y., Azarov I.A., Mitkov M.S., Kruchinina M.V., Kruchinin V.N., Shvets V.A., Knyazev B.A. Polarimetry at Novosibirsk terahertz free electron laser facility. // 39th Intern. Conf. on Infrared, Millimeter and Terahertz Waves, IRMMW-THz 2014; The University of Arizona, Tucson; United States; 14-19 September 2014. - 2014. - P. 6956293. - DOI 10.1109/IRMMW-THz.2014.6956293.

[593] Kotelnikov I.A. Stupakov G.V. Paraxial equation for the surface wave on a conducting cylinder. // 39th Intern. Conf. on Infrared, Millimeter and Terahertz Waves, IRMMW-THz 2014; The University of Arizona, Tucson; US; 14-19 Sept. 2014. - 2014. - P. 6956398. - DOI 10.1109/IRMMW-THz.2014. 6956398.

[594] Ruktuev A., Golkovsky M., Samoylenko V., Komarov P., Bataev I., Bataev A. Corrosion resistance of multilayer Ti-Ta coatings obtained by electron beam cladding in the atmosphere. // Advanced Materials Research. - 2014. - Vol. 1040: Intern. Conf. for Young Scientists "High Technology: Research and Applications 2014", HTRA 2014; Tomsk; Russian Federation; 26-28 March 2014. - P. 759-763. - DOI 10.4028/www.scientific.net/ AMR.1040.759.

[595] Mezentsev N., Shkaruba V., Syrovatin V. Superconducting Multipole Wigglers: Magnetic and Cryogenic Systems, 2014. // 13th Cryogenics IIR Intern. Conf. (Apr 07-11, 2014, Prague, Czech Republic): 13th Cryogenics 2014 IIR Intern. Conf. - 2014. - Is. 1. - P. 81-87. - (Refrigeration Science and Technology). - ISSN 0151-1637.

[596] LHCB Collab., Bondar A., Eidelman S, Krokovny P., Poluektov A., Shekhtman L., Vorobyev V.,

et al. // Improved constraints on γ: CKM2014 update. // LHCb-CONF-2014-004: 8th Intern. Workshop on the CKM Unitarity Triangle, Univ. Tech., Vienna, Austria, 08 - 12 September 2014.

[597] A. Poluektov. Rare B(s) and CPV in B(s) physics at LHCb. // KEK Flavour Factory Workshop, 13-15 February 2014, KEK, Tsukuba, Japan.

[598] A. Poluektov. Rare decays and CP violation with Bu and Bd mesons at LHCb. // KEK Flavour Factory Workshop / Belle II Theory Interface Platform Meeting, 28-31 October 2014, KEK, Tsukuba, Japan.

[599] A. Poluektov. Model-independent γ measurement with B → DK, D → Kshh at LHCb. // KEK Flavour Factory Workshop / Belle II Theory Interface Platform Meeting, 28-31 October 2014, KEK, Tsukuba, Japan.

[600] A.V. Arzhannikov, N.S. Ginzburg, V.Y. Zaslavsky, P.V. Kalinin, N.Y. Peskov, A.S. Sergeev, S.L. Sinitsky, V.D. Stepanov, M.K. A. Thumm. Spectral Dynamics of mm-wave Radiation from Two-Channel Planar FEM with Two Dimensional Distributed Feedback. // Proc. of 41st IEEE Intern. Conf. on Plasma Science and the 20th Intern. Conf. on High-Power Particle Beams, May 25 - 29, 2014, Washington DC.

[601] A.A. Shoshin, A.S. Arakcheev, A.V. Arzhannikov, V.A. Bataev, A.V. Burdakov, A. Huber, I.A. Ivanov, K.N. Kuklin, S.V. Polosatkin, V.V. Postupaev, S.L. Sinitsky and A.A. Vasilyev. Tungsten surface modification after irradiation at the GOL-3. // 21st Intern. Conf. on Plasma Surface Interactions in Controlled Fusion Devices, 26-30 May 2014, Kanazawa, Japan. [http://psi2014.nifs.ac.jp/Files/Files/Abstracts/ P3-035_Shoshin_PSI2014.pdf].

[602] A. Arakcheev, A. Huber, M. Wirtz, G. Sergienko, I. Steudel, A. Burdakov, J. W. Coenen, A. Kreter, J. Linke, Ph. Mertens, V. Philipps, G. Pintsuk, M. Reinhart, U. Samm, A. Shoshin, B. Schweer, B. Unterberg, A. Vasilyev. Theoretical investigation of cracks formation in tungsten after heat loads. // 21st Intern. Conf. on Plasma Surface Interactions in Controlled Fusion Devices, 26-30 May 2014, Kanazawa, Japan. [http://psi2014.nifs.ac.jp/Files/Files/Abstracts/ P2-089_Arakcheev_PSI2014.pdf].

[603] A.V. Arzhannikov, N.S. Ginzburg, V.Y. Zaslavsky, P.V. Kalinin, N.Y. Peskov, A.S. Sergeev, S.L. Sinitsky, V.D. Stepanov, M.K.A. Thumm. Spectral dynamics of mm-wave radiation from two-channel planar FEM with two dimensional distributed feedback. // Proc. of 41st IEEE Intern. Conference on Plasma Science and the 20th Intern. Conference on High-Power Particle Beams, Washington DC, May 25-29, 2014.

[604] A.A. Shoshin, A.S. Arakcheev, A.V. Arzhannikov, V.A. Bataev, A.V. Burdakov, A. Huber, I.A. Ivanov, K.N. Kuklin, S.V. Polosatkin, V.V. Postupaev, S.L. Sinitsky and A.A. Vasilyev Tungsten surface modification after irradiation at the GOL-3. // 21st

Intern. Conf. on Plasma Surface Interactions in Controlled Fusion Devices, 26-30 May 2014, Kanazawa, JAPAN. [http://psi2014.nifs.ac.jp/Files/Files/Abstracts/ P3-035_Shoshin_PSI2014.pdf].

[605] A. Arakcheev, A. Huber, M. Wirtz, G. Sergienko, I. Steudel, A. Burdakov, J. W. Coenen, A. Kreter, J. Linke, Ph. Mertens, V. Philipps, G. Pintsuk, M. Reinhart, U. Samm, A. Shoshin, B. Schweer, B. Unterberg, A. Vasilyev. Theoretical investigation of cracks formation in tungsten after heat loads. // 21st Intern. Conf. on Plasma Surface Interactions in Controlled Fusion Devices, 26-30 May 2014, Kanazawa. JAPAN. [http://psi2014.nifs.ac.jp/Files/Files/Abstracts/ P2-089_Arakcheev_PSI2014.pdf].

[606] Astrelin V., Kandaurov I., Sveshnikov V. Calculation of the limiting current of electron beam injected into multi-mirror trap GOL-3 // Intern. Conference on Advanced Mathematics, Computations and Applications (AMCA'14). June 8-11, 2014, Akademgorodok, Novosibirsk, Russia. [http://conf.nsc.ru/ amca14/en/reportlist].

[607] A.V. Arzhannikov, M.V. Astafjev, A.V. Burdakov, V.S. Burmasov, D.E. Gavrilenko, I.A. Ivanov, A.A. Kasatov, S.A. Kuznetsov, K.I Mekler, S.V. Polosatkin, V.V. Postupaev, A.F. Rovenskikh, S.L. Sinitsky, V.F. Sklyarov, and L.N. Vyacheslavov. Observation of the spectral and polarization dynamics of sub-THz emission from E-beam - plasma interaction area. // 41st EPS Conference on Plasma Physics, 23-27 June 2014, Berlin, Germany, P2.150. [http://ocs.ciemat.es/ EPS2014PAP/pdf/P2.150.pdf].

[608] V.V. Postupaev, A.V. Burdakov, A.V. Sudnikov. MHD stability of plasma with supercritical current density at the axis. // 41st EPS Conference on Plasma Physics, 23-27 June 2014, Berlin. - P4.040. [http://ocs.ciemat.es/EPS2014PAP/ pdf/ P4.040.pdf].

[609] A.V. Arzhannikov, A.V. Burdakov, V.S. Burmasov, D.E. Gavrilenko, I.A. Ivanov, A.A. Kasatov, I.V. Kandaurov, V.V. Kurkuchekov, S.A. Kuznetsov, K.I. Mekler, S.S. Popov, V.V. Postupaev, A.F. Rovenskikh, V.F. Sklyarov, A.V. Sudnikov, Yu.A. Trunev and L.N. Vyacheslavov. Microwave generation in experiments on sub-relativistic electron beam relaxation in magnetized plasmas. // 41st EPS Conference on Plasma Physics, 23-27 June 2014, Berlin, Germany, P5.091. http://ocs.ciemat.es/EPS2014PAP/pdf/P5.091.pdf

[610] Burdakov A.V. Multimirror linear trap for fusion plasma confinement: status and future. // 26th Symposium on Plasma Physics and Technology, June 16-19, 2014, Prague. [http://www.plasmaconference.cz/invited_ lectures.php].

[611] S.A. Kuznetsov, S.N. Makarov, V.N. Koshelenko, M.A. Astafev and A.V. Arzhannikov. 140 GHZ Active imaging system based on FMCW radar. // Proc. of the 9th Intern. Workshop "Strong Microwaves and Terahertz Waves: Sources and Applications", IAP

RAS, July 24-30, 2014, Nizhny Novgorod, Russia. - P. 75-76.

[612] A.V. Arzhannikov, N.S. Ginzburg, P.V. Kalinin, N.Yu. Peskov, A.S. Sergeev, S.L. Sinitsky, V.D. Stepanov, M. Thumm, and V.Yu. Zaslavsky. MM-wave generation in two-channel planar FEM on eigen modes of resonator at various detuning of undulator synchronism. // Proc. of the 9th Intern. Workshop "Strong Microwaves and Terahertz Waves: Sources and Applications", IAP RAS, July 24 - 30, 2014, Nizhny Novgorod, Russia. - P. 170-171.

[613] A.V. Arzhannikov, A.V. Burdakov, I.A. Ivanov, I.V. Kandaurov, A.A. Kasatov, V.V. Kurkuchekov, S.A. Kuznetsov, M.A. Makarov, K.I. Mekler, S.V. Polosatkin, V.V. Postupaev, A.F. Rovenskikh, S.L. Sinitsky, V.F. Sklyarov, M.K.A. Thumm, Yu.A. Trunev, L.N. Vyacheslavov. Spectrum and polarization of plasma emission at high current beam relaxation (invited talk). // Proc. of the 9th Intern. Workshop "Strong Microwaves and Terahertz Waves: Sources and Applications", IAP RAS, July 24 - 30, 2014, Nizhny Novgorod, Russia. - P. 197-198.

[614] S.A. Kuznetsov, M.A. Astafjev, E.A. Lonshakov and A.V. Arzhannikov. Submillimeter-wave planar focusing devices based on holographic reflectarrays. // Proc. of the 9th Intern. Workshop "Strong Microwaves and Terahertz Waves: Sources and Applications", IAP RAS, July 24 - 30, 2014, Nizhny Novgorod, Russia. - P. 207-208.

[615] N.Yu. Peskov, N.S. Ginzburg, G.G. Denisov, A.S. Sergeev, A.V. Arzhannikov, P.V. Kalinin, S.L. Sinitsky and M. Thumm. Project of two-stage planar THz-band FEL based on four-mirror Bragg ring cavity and parallel intense sheet electron beams. // Proc. of the 9th Intern. Workshop "Strong Microwaves and Terahertz Waves: Sources and Applications", IAP RAS, July 24 - 30, 2014, Nizhny Novgorod, Russia. - P. 229-230.

[616] Astrelin V., Kandaurov I., Sveshnikov V. Numerical simulation of transport of electron beam with limiting current and initial angles at injection into multiple mirror trap GOL-3. // X Intern. Asian School-Seminar "Optimization Problems of Complex Systems", July 25 - August 5, Kyrgyz Republic, 2014. Part 1, P.73. [http://conf.ict. nsc.ru/opcs2014/ru/reportlist].

[617] A.V. Burdakov, A.P. Avrorov, A.V. Arzhannikov, V.T. Astrelin, V.I. Batkin, V.S. Burmasov, A.V. Bykov, D.E. Gavrilenko, I.A. Ivanov, I.V. Kandaurov, A.A. Kasatov, V.V. Kurkuchekov, K.N. Kuklin, K.I. Mekler, S.V. Polosatkin, S.S. Popov, V.V. Postupaev, A.F. Rovenskikh, A.A. Shoshin, S.L. Sinitsky, V.F. Sklyarov, N.V. Sorokina, V.D. Stepanov, A.V. Sudnikov, Yu.S. Sulyaev, Yu.A. Trunev and L.N. Vyacheslavov. Recent experiments in GOL-3 Multiple Mirror Trap. // The 10th Intern. Conf. on Open Magnetic Systems for Plasma Confinement, August 26-29, 2014, Daejeon, Korea: Abstract Book of OS2014. - P. 23 (invited talk OS1-04). http://www.os2014. org/sub0202

[618] S. Polosatkin, A. Anikeev, V. Astrelin, A. Beklemishev, A. Burdakov, A. Ivanov, I. Ivanov, V. Postupaev, S. Sinitsky, N. Sorokina. Impurities and Particle Balance in GDMT Facility. // The 10th Intern. Conf. on Open Magnetic Systems for Plasma Confinement, August 26-29, 2014, Daejeon, Korea: Abstract Book of OS2014. - P. 66 (poster OS4-29). http://www.os2014.org/sub0202.

[619] A. Anikeev, V. Astrelin, A. Beklemishev, A. Bragin, A. Burdakov, D. Gavrilenko, A. Ivanov, I. Ivanov, M. Ivantsivsky, E. Kolesnikov, S. Polosatkin, V. Postupaev, S. Sinitsky, V. Yarovoy. Superconducting Magnetic System of GDMT Facility. // The 10th Intern. Conf. on Open Magnetic Systems for Plasma Confinement, August 26-29, 2014, Daejeon, Korea: Abstract Book of OS2014. P. 67 (poster OS4-30). http://www.os2014.org/sub0202.

[620] A.V. Sudnikov, A.V. Burdakov, D.E. Gavrilenko, I.A. Ivanov, I.V. Kandaurov, V.V. Kurkuchekov, V.V. Postupaev, S.V. Polosatkin, Yu.A. Trunev. Charge Injection by Multiple-Pulse Electron Beam in GOL-3. // The 10th Intern. Conf. on Open Magnetic Systems for Plasma Confinement, August 26-29, 2014, Daejeon, Korea: Abstract Book of OS2014. P. 69 (poster OS4-32). [http://www.os2014.org/sub0202].

[621] A.V. Arzhannikov, A.V. Burdakov, V.S. Burmasov, D.E. Gavrilenko, I.A. Ivanov, I.V. Kandaurov, V.V. Kurkuchekov, S.A. Kuznetsov, K.I. Mekler, S.S. Popov, V.V.Postupaev, A.F. Rovenskikh, V.F. Sklyarov, Yu.A. Trunev and L.N. Vyacheslavov. Microwave generation from magnetized plasmas during sub-relativistic electron beam relaxation. // The 10th Intern. Conf. on Open Magnetic Systems for Plasma Confinement, August 26-29, 2014, Daejeon, Korea: Abstract Book of OS2014ю - P. 70 (poster OS4-33). http://www.os2014.org/sub0202.

[622] V.V. Kurkuchekov, V.T. Astrelin, A.P. Avrorov, A.V. Burdakov, A.V. Bykov, V.I. Davydenko, G.E. Derevyankin, A.A. Ivanov, I.A. Ivanov, I.V. Kandaurov, S.V. Polosatkin, A.F. Rovenskikh, Yu.A. Trunev, V.A. Yarovoy. Twenty Megawatt Electron Injector for GOL-3 Multiple Mirror trap. // The 10th Intern. Conf. on Open Magnetic Systems for Plasma Confinement, August 26-29, 2014, Daejeon, Korea: Abst. Book of OS2014. - P. 73 (poster OS4-36). [http://www.os2014.org/ sub0202].

[623] L.N. Vyacheslavov, A.A. Kasatov, A.S. Arakcheev, I.A. Ivanov, A.A. Shoshin, A.V. Burdakov, I.V. Kandaurov, V.V. Kurkuchekov, K.I. Mekler, A.F. Rovenskikh, and Yu.A. Trunev. Observation of Metal Erosion under Transient Heat Load Produced by Long Pulse Electron Beam. // The 10th Intern. Conf. on Open Magnetic Systems for Plasma Confinement, August 26-29, 2014, Daejeon, Korea: Abstract Book of OS2014. - P. 76 (poster OS4-39). [http://www.os2014.org/sub0202].

[624] A.A. Shoshin, A.S. Arakcheev, A.V. Arzhannikov, V.A. Bataev, A.V. Burdakov, I.A. Ivanov, K.N. Kuklin, S.V. Polosatkin, V.V. Postupaev, S.L.

Sinitsky, A.A. Vasilyev. Preheated tungsten surface modification after irradiation at the GOL-3. // The 10th Intern. Conf. on Open Magnetic Systems for Plasma Confinement, August 26-29, 2014, Daejeon, Korea: Abstract Book of OS2014. - P .77 (poster OS4-40). [http://www.os2014.org/sub0202].

[625] A.D. Beklemishev, P.A. Bagryansky, A.V. Burdakov, V.I. Davydenko, A.I. Gorbovsky, A.A. Ivanov, I.A. Ivanov, S.V. Polosatkin, V.V. Postupaev, and S.L. Sinitsky. Development of the GDMT project in BINP: status and perspectives. // The 10th Intern. Conf. on Open Magnetic Systems for Plasma Confinement, August 26-29, 2014, Daejeon, Korea: Abstract Book of OS2014. - P. 82 (invited talk OS5-01). [http://www.os2014.org/sub0202].

[626] A.V. Arzhannikov, A.V. Anikeev, A.D. Beklemishev, A.V. Burdakov, W. Hortond, A.A. Ivanov. Gas-dynamic trap with Q ~ 0.1 as a driver for hybrid thorium reactor. // The 10th Intern. Conf. on Open Magnetic Systems for Plasma Confinement, August 26-29, 2014, Daejeon, Korea: Abstract Book of OS2014. - P. 85 (OS5-04). [http://www.os2014.org/sub0202].

[627] A.A. Ivanov, A.V. Burdakov and P.A. Bagryansky. Recent progress in studies of plasma heating and stabilization in axisymmetric magnetic mirrors in Novosibirsk. // The 10th Intern. Conf. on Open Magnetic Systems for Plasma Confinement, August 26-29, 2014, Daejeon, Korea: Abstract Book of OS2014. - P. 86 (invited talk OS6-01). [http://www.os2014. org/sub0202].

[628] V.V. Postupaev, A.V. Burdakov, and A.A. Ivanov. Outlook for new experimental program on multiple-mirror confinement in GOL-3 with NBI-heated plasma. // The 10th Intern. Conf. on Open Magnetic Systems for Plasma Confinement, August 26-29, 2014, Daejeon, Korea: Abstract Book of OS2014. - P. 91 (OS6-06). [http://www.os2014.org/sub0202].

[629] A.V. Burdakov, A.P. Avrorov, A.V. Arzhannikov, V.T. Astrelin, V.I. Batkin, V.S. Burmasov, A.V. Bykov, D.E. Gavrilenko, I.A. Ivanov, M.V. Ivantsivsky, I.V. Kandaurov, A.A. Kasatov, K.N. Kuklin, V.V. Kurkuchekov, S.A. Kuznetsov, K.I. Mekler, S.V. Polosatkin, S.S. Popov, V.V. Postupaev, A.F. Rovenskikh, A.A. Shoshin, S.L. Sinitsky, V.F. Sklyarov, N.V. Sorokina, V.D. Stepanov, A.V. Sudnikov, Yu.S. Sulyaev, Yu.A. Trunev, and L.N. Vyacheslavov. Status of GOL-3 multiple mirror trap experiments. // 25th Fusion Energy Conference (IAEA FEC 2014), St. Petersburg, 13-18 October 2014, EX-P4-23. [http://www-pub.iaea.org/MTCD/Meetings/PDFplus/2014/cn221/cn221ProvisionalProgramme.pdf].

[630] Alexander Huber, Marius Wirtz, Gennady Sergienko, Isabel Steudel, Aleksey Arakcheev, Aleksander Burdakov, Guenter Esser, Michaele Freisinger, Arkadi Kreter, Jochen Linke, Christian Linsmeier, Philippe Mertens, Soren Moller, Volker Philipps, Gerald Pintsuk, Michael Reinhart, Bernd Schweer, Andrey Shoshin, Alexis Terra, Bernhard Unterberg, Impact on Tungsten of Transient Heat Loads on top of steady state Plasma Exposure. // Book of Abstracts 28th Symposium on Fusion Technology (SOFT 2014). - P. 338, San Sebastian, Spain, 2014. [http://www.soft2014.eu/book_of_abstracts.pdf, P2.089].

[631] V.T. Astrelin, V.I. Davydenko, A.V. Kolmogorov. Numerical Simulation of the Secondary Plasma Surface in the Ion Beam Formation. // Intern. Congress on Energy Fluxes and Radiation Effects: Book of Abstracts, Tomsk, September 21-26, 2014. - P. 17.

[632] V.V. Kurkuchekov, I.A. Ivanov, I.V. Kandaurov, Yu.A. Trunev. Quantitative X-Ray Diagnostics for Measuring of the Electron Beam Current Density Distribution on a Metal Target. // Intern. Congress on Energy Fluxes and Radiation Effects, Book of Abstracts, Tomsk, Russia, September 21-26, 2014. - P. 18.

[633] I.V. Kandaurov, V.T. Astrelin, Yu.A. Trunev, V.V. Kurkuchekov. Development and experimental characterization of an electron beam source based on a plasma emitter and multiple aperture electron optical system. // Intern. Congress on Energy Fluxes and Radiation Effects, Book of Abstracts, Tomsk, Russia, September 21-26, 2014. - P. 241.

[634] I.M. Zemlyansky, D.E. Berkaev, I.A. Koop, A.V. Otboev et al. Electron and positron beams transportation channels to BINP Colliders. // Proc. of XXIV Russian Conference on Charged Particle Accelerators (RuPAC14), 6-10 October 2014, Obninsk, Russia.

[635] V.V. Samoylenko, I.A. Polyakov, M.G. Golkovski, I.A. Bataev, A.A. Ruktuev. Surface alloying of titanium with tantalum and zirconium by the method of vacuum-free electron beam fused deposition of powder materials. Proc. of a XXIV Intern. Conference "Radiation Physics of Solids", Sevastopol, 7-14 Jule, 2014. - P. 345-351. ISBN 978-5-89671-018-9, Moscow-2014.

[636] I.A. Bataev, M.G. Golkovskii, N.K. Kuksanov, A.A. Ruktuev, V.V. Samoilenko, I.A. Polyakov, and A.A. Bataev. Surface alloying of titanium alloys with refractory elements by non-vacuum electron-beam processing. // XXI Intern. Conference on Electron Beam Technology, 8-10 June, Varna, Bulgaria, 2014.

[637] I.A. Bataev, M.G. Golkovskii, V.V. Samoilenko, A.A. Ruktuev, A.A. Polyakov, A.A. Bataev. Non-vacuum electron beam multilayer cladding of Ta on Ti plates. // Interfinish-Seria 2014: book abstr., Intern. Conf. on Surface Engineering for Research and Industrial Applications, 30 June - 4 July 2014, Novosibirsk: NSTU Publ., 2014. - P. 32. ISBN 978-5-7782-2475-9.

[638] D.O. Mul, D.S. Krivezhenko, M.G. Golkovski, I.A. Bataev, O.G. Lenivtseva, P.N. Komarov. Structure and properties of coatings obtained by electron-beam alloying at air atmosphere. // Interfinish-Seria 2014: book abstr., Intern. Conf. on Surface Engineering for Research and Industrial Applications, 30 June - 4 July 2014,

185

Novosibirsk: NSTU Publ., 2014, - P. 53. ISBN 978-5-7782-2475-9.

[639] N.K. Kuksanov, A.I. Rojkh, M.N. Stepanov. Experience of 30 Years Operation of EB treatment installations at "PODOLSKKABEL" plant. // Proc. of Eleventh Intern. Conf. on Electron Beam Technologies (EBT 2014), 8 June - 12 June 2014, Bulgaria, Varna.

[640] N.K. Kuksanov, Yu.I. Golubenko, P.I. Nemytov, R.A. Salimov, S.N. Fadeev, A.I. Korchagin, D.A. Kogut, E.V. Domarov, A.V. Lavruchin, V.G. Cherepkov, A.V. Semenov. Extended scope of aplication of industrial ELV accelerator. // XXIV Всероссийская конференция по ускорителям заряженных частиц (RUPAC 2014), 6-10 октября 2014, Обнинск (уст. доклад).

[641] N.K. Kuksanov, R.A. Salimov, P.I. Nemytov, S.N. Fadeev, E.V. Domarov, K.A. Bryazgin, D.A. Kogut. The utilization of standard DC accelerator ELV for the tomography. // XXIV Russian Particle Accelerator Conference (RUPAC 2014), 6-10 October, 2014, Obninsk.

[642] D. Kasatov, A. Koshkarev, A. Kuznetsov, A. Makarov, Yu. Ostreinov, I. Sorokin, I. Shchudlo, S. Taskaev. Problems and prospects of the tandem accelerator with vacuum insulation. // Proc. of RUPAC 2014, Obninsk, Russia, 6-10 October 2014. - P 465-466.

[643] D. Kasatov, A. Makarov, I. Shchudlo, S. Taskaev. Studying of the accompanying charged particles in the tandem accelerator with vacuum insulation. // Proc. of RUPAC 2014, Obninsk, Russia, 6-10 October 2014. - P. 189-190.

[644] A. Kuznetsov, A. Ivanov, A. Koshkarev, D. Kasatov, M. Tiunov. Development of the injector for vacuum insulation tandem acceleratior. // Proc. of RUPAC 2014, Obninsk, Russia, 6-10 October 2014. - P. 191-193.

[645] A. Koshkarev, P. Zubarev, A. Sanin, U. Belchenko, A. Kvashnin. Development of automation system of the ion source. // Proc. of RUPAC 2014, Obninsk, Russia, 6-10 October 2014. - P. 380-382.

[646] D. Kasatov, A. Makarov, I. Shchudlo, S. Taskaev. Measurement of the dose rate and the radiation spectrum of the interaction of 2 MeV proton beam with a variety of structural materials. // Proc. of RUPAC 2014, Obninsk, Russia, 6-10 October 2014. - P. 113-115.

[647] I. Shchudlo, D. Kasatov, A. Makarov, S. Taskaev. Measurement of the spatial distribution of gamma radiation at tandem accelerator with vacuum insulation. // Proc. of RUPAC 2014, Obninsk, Russia, 06-10 October 2014. - P. 116-117.

[648] A. Makarov, S. Taskaev, P. Vobly, Yu. Ostreinov. Modification of the argon stripping target of the tandem accelerator. // Proc. of RUPAC 2014, Obninsk, Russia, 06-10 October 2014. - P. 194-196.

[649] Alexander N. Karpushov, Stefano Alberti, René Chavan, Vladimir I. Davydenko, Basil P. Duval, Alexander A. Ivanov, Damien Fasel, Ambrogio Fasoli, Aleksander I. Gorbovsky, Timothy Goodman, Vyacheslav V. Kolmogorov, Yves Martin, Olivier Sauter, Aleksey V. Sorokin, Matthieu Toussaint. Upgrade of the TCV Tokamak, first phase: neutral beam heating system. // 28th Symposium on Fusion Technology SOFT 2014, Sept .29 - Oct .3 2014, San Sebastian, Spain: Book of abstr. - P. 278.

[650] Matthieu Toussaint, Vladislav H. Amirov, Robert Bertizzolo, Edoardo Busato, René Chavan, Pascal Conti, Paolo Dallona, Vladimir I. Davydenko, Frédéric Dolizy, Basil Duval, Ambrogio Fasoli, Carlo Fusa, Aleksander I. Gorbovsky, Gavin Henstock, Christoph Hollenstein, Alexander N. Karpushov, Claude Raggi, Diego Ruaro, Aleksey V. Sorokin, Roberto Venezia. In-situ upgrade of the TCV vacuum vessel with tangential ports for the neutral beam plasma heating system. // 28th Symp. on Fusion Technology SOFT 2014, Sept 29 - Oct 3 2014, San Sebastian, Spain: Book of abstracts. - P. 282.

[651] P.A. Bagryansky, A.A. Ivanov, A.A. Lizunov, Yu.V. Kovalenko, V.V. Maximov, S.V. Murakhtin, V.V. Prikhodko, V.Ya. Savkin, E.I. Soldatkina, A.L. Solomakhin, D.V. Yakovlev, K.V. Zaytsev. Record electron temperature in the quasistationary open magnetic trap at auxiliary microwave heating mode. // Intern. Scientific Conference "Science of the Future", 17-20 Sept 2014, St-Petersburg. [http://www.p220conf.ru/abstracts/download/15-y-phys/462-e-soldatkina].

[652] P.A. Bagryansky, A.A. Ivanov, A.A. Lizunov, Yu.V. Kovalenko, V.V. Maximov, S.V. Murakhtin, V.V. Prikhodko, V.Ya. Savkin, E.I. Soldatkina, A.L. Solomakhin, D.V. Yakovlev, K.V. Zaytsev. Recent Achievements in the Experiments with ECR Heating in the Gas Dynamic Trap. // 25th Fusion Energy Conference (FEC 2014), Saint Petersburg, 13-18 October 2014 Conference ID: 46091 (CN-221). - Book of Abstracts. - P. 253. [http://www-pub.iaea.org/iaeameetings/46091/25thFEC-2014].

[653] A.V. Anikeev, P.A. Bagryansky, A.D. Beklemishev, A.A. Ivanov, O.A. Korobeinikova, Yu.V. Kovalenko, A.A. Lizunov, V.V. Maximov, S.V. Murakhtin, E.I. Pinzhenin, V.V. Prikhodko, V.Ya. Savkin, E.I. Soldatkina, A.L. Solomakhin, D.V.Yakovlev, K.V. Zaytsev. The GDT Experiment: Status and recent progress in plasma parameters. // The 10th Intern. Conf. on Open Magnetic Systems for Plasma Confinement, August 26-29, 2014, Daejeon, Korea: Abstract Book of OS2014. - P. 1. [http://internetdisk. nfri.re.kr:8081/api.link/3d_baLoIErze TOcL_w~~.pdf].

[654] A.V. Anikeev, P.A. Bagryansky, A.D. Beklemishev, O.A.Korobeinikova, A.A. Lizunov, V.V. Maximov, S.V. Murakhtin, V.V. Prikhodko, V.Ya. Savkin, E.I. Soldatkina, A.L. Solomakhin, D.V. Yakovlev, K.V. Zaytsev. Plans and methodic of experiments to study axial losses and transverse transport in the Gas Dynamic Trap. // The 10th Intern. Conf. on Open Magnetic Systems for Plasma Confinement, August 26-29, 2014, Daejeon, Korea: Abstract Book of OS2014. - P. 7.

[655] P.A. Bagryansky, E.D. Gospodchikov, Yu.V. Kovalenko, A.A. Lizunov, V.V. Maximov, S.V. Murakhtin, E.I. Pinzhenin, V.V. Prikhodko, V.Ya. Savkin, A.G. Shalashov, E.I. Soldatkina, A.L. Solomakhin, D.V. Yakovlev. ECR Heating Experiment in the GST Magnetic Mirror: Recent Experiments and Future Plans. // The 10th Intern. Conf. on Open Magnetic Systems for Plasma Confinement, August 26-29, 2014, Daejeon, Korea: Abstract Book of OS2014. - P. 154.

[656] A.V. Anikeev, V.V. Prikhodko, D.V. Yurov. Parameters of a fusion neutron source based on the last GDT experimental data and possible applications. // The 10th Intern. Conf. on Open Magnetic Systems for Plasma Confinement, August 26-29, 2014, Daejeon, Korea: Abstract Book of OS2014. - P. 19.

[657] A.V. Anikeev, V.V. Kuzenov, S.V. Ryzhkov, V.V. Shumaev, Thermophysical Properties of Plasma in Open Systems in Ultrahigh Magnetic Fields. // The 10th Intern. Conf. on Open Magnetic Systems for Plasma Confinement, August 26-29, 2014, Daejeon, Korea: Abstract Book of OS2014. - P. 49.

[658] Fadin V.S. Impact factors for Reggeon-gluon transition in the next-to-leading order. // Intern. Workshop "Scattering Amplitudes and the Multi-Regge Limit 2014", February 10-14, 2014, Madrid, Spain.

[659] V.S. Fadin. Impact Factors for Reggeon-Gluon Transitions. // The Intern. Workshop on Low x Physics, June 17-21, 2014, Kioto, Japan.

[660] V.S. Fadin. Discontinuities of multi-Regge amplitudes in the next-to-leading order. // Intern. Workshop on Diffraction in High-Energy Physics "DIFFRACTION 2014", September 10-16, 2014, Primosten, Croatia.

[661] A.V. Reznichenko, M.G. Kozlov. Regge amplitudes with quark and gluon exchange. // Poster report in XII Conference "Young Scientists of Russia" of the Dynasty Foundation, April 13-16, 2014, Moscow.

[662] Andrey Grozin, Johannes M. Henn, Gregory P. Korchemsky, Peter Marquard. The n_f terms of the three-loop cusp anomalous dimension in QCD. // Proc. of Science LL2014 (2014) 016 (8 p.). [arXiv:1406.7828 [hep-th].

[663] A.G. Grozin. Effective weak Lagrangians in the Standard Model and B decays. // Proc. of the Helmholtz Intern. School ``Physics of Heavy Quarks and Hadrons'', \ed. A. Ali, Yu. Bystritskiy, M. Ivanov. - Verlag Deutsches Elektronen-Synchrotron, - 2014. - P. 78-98. [ISBN 978-3-935702-82-9, ISSN 1435-8077].

[664] V.V. Sokolov. Invited talk: Elastic Enhancement Factor as an Indicator of Peculiarities of the Internal Dynamics of Open Chaotic quantum Systems. // ISF Research Workshop on Non-Hermitean Random Matrices: 50 Years after Ginibre". 20-27 October 2014, Israel.

[665] R.E. Gerasimov. Approximations used in calculations of radiative corrections to electron-proton scattering cross section. // Nonlinear Dynamics and Applications: Proc. of the Twenty first Annual Seminar NPCS'2014, Minsk, 2014. - Vol. 20. - P. 56 - 63.

[666] R.N. Lee. Modern techniques of multiloop calculations. // Proc. of the 49th Rencontres de Moriond, ed. E. Auge, J. Dumarchez, and J.Tran Thanh Van: ARISF, 2014. - P. 297.

[667] V.S. Fadin. Impact factors for reggeon-gluon transitions in the next-to-leading order. // Intern. Workshop "Scattering Amplitudes and the Multi-Regge Limit", February 10-14, 2014, Madrid, Spain.

[668] V.M. Katkov. Effective mass of a photon in strong field. // 6th Intern. Conf. "Channeling 2014", October 5-10, 2014, Capri, Italy: Book of abstr. - P. 36.

[669] V.S. Fadin. Introduction to the BFKL equation. // "New Trends in High-Energy Physics and QCD", the School and the Workshop, October 21 - November 06, 2014, Natal, Brasilia.

[670] V.S. Fadin. Discontinuities of multiparticle amplitudes in the multi-Regge kinematics and the BDS ansatz. // Intern. Session-Conference of SNF NSD RAS "Physics of Fundamental Interactions", November 17-21, 2014, Moscow, Russia.

[671] A. Bryazgin, V. Bezuglov, K. Chernov, B. Faktorovich, V. Gorbunov, E. Kokin, M. Korobeynikov, A. Lukin, I. Makarov, S. Maximov, A. Panfilov, V. Radchenko, E. Shtarklev, A. Sidorov, V. Tarnetsky, M. Tiunov, V. Tkachenko, A. Vlasov, L. Voronin. New modular ILU RF accelerators for E-beam and X-ray. // Conference "Development of New Applications of Machine Generated Food Irradiation Technologies", 27-28 May 2014, Vienna, Austria.

[672] V. Bezuglov, A. Bryazgin, K. Chernov, B. Faktorovich V. Gorbunov, E. Kokin, M. Korobeynikov, A. Lukin, I. Makarov, S. Maximov, A. Panfilov, V. Radchenko, E. Shtarklev, A. Sidorov, V. Tarnetsky, M. Tiunov, V. Tkachenko, A. Vlasov, L. Voronin. // High-power industrial accelerator ILU-14 for E-beam and X-ray processing. // Conference: XXVII Intern. Linear Accelerator Conference (LINAC14), Switzerland, 31 August - 5 September, 2014, Geneva.

[673] V.V. Bezuglov, A.A. Bryzgin, A.Yu. Vlasov, L.A. Voronin, V.A. Gorbunov, E.N. Kokin, M.V. Korobeinikov, A.N. Lukin, I.G. Makarov, V.E. Nekhaev, S.A. Maximov, A.D. Panfilov, V.M. Radchenko, E.A. Shtarklev, A.V. Sidorov, V.V. Tarnetsky, V.O. Tkachenko, B.L. Faktorovich, K.N. Chernov. Industrial accelerators type ILU in the modern radiation-technological complexes. // Conference: Radiation Technologies: Achievements and Trends, October 21-23, 2014, Krym, Yalta.

[674] A.A. Bryazgin, M.V. Korobeinikov. Industrial RF accelerators of INP SB RAS and technologies of their

187

application. // Belarus days in Siberia: Practical Conference on Scientific, Technical and Innovation Collaboration Agreements of the Republic of Belarus and SB RAS, 22 October 2014, Novosibirsk.

[675] M.I. Bryzgunov, A.V. Bubley, V. K. Gosteev, V.M. Panasyuk, V.V. Parkhomchuk, V. B. Reva, (BINP, Novosibirsk, Russia) V. Kamerdzhiev, J. Dietrich (FZJ, COSY, Juelich, Germany). Coolers with Magnetized beam for different energies: experience and future possibilities. // Proc. of the Intern. Workshop on Accelerator Science and Technology for Electron-Ion Collider (EIC2014), Thomas Jefferson National Accelerator Facility (Newport News, USA), March 17 - 21, 2014.

[676] S.A. Rastigeev, A.R. Frolov, A.D. Goncharov, V. F. Klyuev, E.S. Konstantinov, L. A. Kutnykova, V.V. Parkhomchuk, A.V. Petrozhitskii. Operation and development of the BINP AMS facility. // Proc. of 24th All-Russian Conference on Charged Particle Accelerators (RuPAC14), 6-10 October 2014, Obninsk, Russia. - P. 134-136.

[677] S.A. Zevakov, V.F. Dmitriev, R.R. Dusaev, V.V. Gauzshteyn, R.A. Golovin, A.V. Gramolin, B.A. Lazarenko, D.M. Nikolenko, S.I. Mishnev, I.A. Rachek, R.Sh. Sadykov, V.N. Stibunov, Yu.V. Shestakov, D.K. Toporkov. Measurements of the tensor analyzing power component T20 of coherent photoproduction of neutral pion on tensor-polarized deuteron at the VEPP-3 storage ring. // 64 Intern. Conference "NUCLEUS 2014". Fundamental Problems of Nuclear Physics and Atomic Power Engineering, Minsk, Belarus, July 1-4 2014: Book of Abstracts, 2014. - P.103.

[678] I.A. Rachek, J. Arrington, V.F. Dmitriev, V.V. Gauzshtein, R.J. Holt, A.V. Gramolin, V.V. Kaminsky, B.A. Lazarenko, S.I. Mishnev, N.Yu. Muchnoi, V.V. Neufeld, D.M. Nikolenko, R.Sh. Sadykov, Yu.V. Shestakov, V.N. Stibunov, D.K. Toporkov, H. De Vries, S.A. Zevakov and V.N. Zhilich. Two-photon exchange contribution in elastic electron-proton scattering: measurements at VEPP-3 storage ring. // 9th Intern. Conference on Nuclear Physics at Storage Rings, September 28 - October 3, 2014, Sankt Goar, Germany: Book of Abstracts, 2014. - P. 73.

[679] V.V. Bezuglov, A.A. Bryazgin, A.Yu. Vlasov, L.A. Voronin, V.A. Gorbunov, E.N. Kokin, M.V. Korobeynikov, A.N. Lukin, V.E. Nekhaev, S.A. Maximov, A.D. Panfilov, V.M. Radchenko, E.A. Shtarklev, A.V. Sidorov, V.O. Tkachenko, B.L. Faktorovich. Radiation treatment development in Budker INP – new trends. // X Intern. Conf. "Radiation-Thermal Effects and Processes in the Inorganic Materials" RTEP-2014, 21-23 November 2014, Phuket, Thailand.

[680] M.V. Korobeinikov, A.A. Bryazgin, V.V. Bezuglov, E.A. Shtarklev, A.Yu. Vlasov, S.A. Kondratyev and V.I. Rostovtsev. Radiation-thermal treatment in ore dressing. // X Intern. Conference "Radiation-Thermal Effects and Processes in the

Inorganic Materials" RTEP-2014, 21-23 November 2014, Phuket, Thailand.

[681] U.V. Ancharova, M.A. Mikhailenko, B.P. Tolochko, N.Z. Lyakhov, Z.S. Vinokurov, M.V. Korobeinikov, A.A. Bryazgin, V.V. Bezuglov, E.A. Shtarklev, A.Yu. Vlasov. Synthesis and staging of the phase formation for strontium ferrites in thermal and radiation-thermal reactions // X Intern. Conference "Radiation-Thermal Effects and Processes in the Inorganic Materials" RTEP-2014, November 21-23 2014, Phuket, Thailand.

[682] M.A. Mikhailenko, U.V. Ancharova, B.P. Tolochko, M.V. Korobeinikov, A.A. Bryazgin, V.V. Bezuglov, E.A. Shtarklev, A.Yu. Vlasov, L.M. Pokrovsky and K.G. Korolev. Radiation-thermal paraffin cracking. // X Intern. Conference "Radiation-Thermal Effects and Processes in the Inorganic Materials" RTEP-2014, 21-23 November 2014, Phuket, Thailand.

[683] A.G. Shamov, V.V. Anashin, V.M. Aulchenko, E.M. Baldin, A.K. Barladyan, A.Yu. Barnyakov, M.Yu. Barnyakov, S.E. Baru, I.Yu. Basok, A.E. Blinov, V.E. Blinov, A.V. Bobrov, V.S. Bobrovnikov, A.V. Bogomyagkov, A.E. Bondar, A.R. Buzykaev, S.I. Eidelman, D.N. Grigoriev, Yu.M. Glukhovchenko, V.V. Gulevich, D.V. Gusev, S.E. Karnaev, G.V. Karpov, S.V. Karpov, T.A. Kharlamova, V.A. Kiselev, V.V. Kolmogorov, S.A. Kononov, K.Yu. Kotov, E.A. Kravchenko, V.F. Kulikov, G.Ya.Kurkin, E.A. Kuper, I.A. Kuyanov, E.B. Levichev, D.A. Maksimov, V.M. Malyshev, A.L. Maslennikov, A.S. Medvedko, O.I. Meshkov, S.I. Mishnev, I.I. Morozov, N.Yu. Muchnoi, V.V. Neufeld, S.A. Nikitin, I. B. Nikolaev, I V. Ovtin, I.N. Okunev, A.P. Onuchin, S.B. Oreshkin, I.O. Orlov, A.A. Osipov, S.V. Peleganchuk, S.G. Pivovarov, P.A. Piminov, V.V. Petrov, A.O. Poluektov, V.G. Prisekin, O.L. Rezanova, A.A. Ruban, V.K. Sandyrev, G.A. Savinov, D.N. Shatilov, B.A. Shwartz, E.A. Simonov, S.V. Sinyatkin, A.N. Skrinsky, V.V. Smaluk, A.V. Sokolov, E.V. Starostina, A.M. Sukharev, A.A. Talyshev, V.A. Tayursky, V.I. Telnov, Yu.A. Tikhonov, K.Yu. Todyshev, G.M. Tumaikin, Yu.V. Usov, A.I. Vorobiov, A.N. Yushkov, V.N. Zhilich, V.V. Zhulanov, A.N. Zhuravlev. Main results in the charmonium region from KEDR. // Intern. Workshop on Heavy Quarkonium 2014, CERN, November 10-14 2014.

[684] A.G. Shamov, V.V. Anashin, V.M. Aulchenko, E.M. Baldin, A.K. Barladyan, A.Yu. Barnyakov, M.Yu. Barnyakov, S.E. Baru, I.Yu. Basok, A.E. Blinov, V.E. Blinov, A.V. Bobrov, V.S. Bobrovnikov, A.V. Bogomyagkov, A.E. Bondar, A.R. Buzykaev, S.I. Eidelman, D.N. Grigoriev, Yu.M. Glukhovchenko, V.V. Gulevich, D.V. Gusev, S.E. Karnaev, G.V. Karpov, S.V. Karpov, T.A. Kharlamova, V.A. Kiselev, V.V. Kolmogorov, S.A. Kononov, K.Yu. Kotov, E.A. Kravchenko, V.F. Kulikov, G.Ya. Kurkin, E.A. Kuper, I.A. Kuyanov, E.B. Levichev, D.A. Maksimov, V.M. Malyshev, A.L. Maslennikov, A.S. Medvedko, O.I. Meshkov, S.I. Mishnev, I.I. Morozov, N.Yu. Muchnoi,

V.V. Neufeld, S.A. Nikitin, I.B. Nikolaev, I.V. Ovtin, I.N. Okunev, A.P. Onuchin, S.B. Oreshkin, I.O. Orlov, A.A. Osipov, S.V. Peleganchuk, S.G. Pivovarov, P.A. Piminov, V.V. Petrov, A.O. Poluektov, V.G. Prisekin, O.L. Rezanova, A.A. Ruban, V.K. Sandyrev, G.A. Savinov, D.N. Shatilov, B.A. Shwartz, E.A. Simonov, S.V. Sinyatkin, A.N. Skrinsky, V.V. Smaluk, A.V. Sokolov, E.V. Starostina, A.M. Sukharev, A.A. Talyshev, V.A. Tayursky, V.I. Telnov, Yu.A. Tikhonov, K.Yu. Todyshev, G.M. Tumaikin, Yu.V. Usov, A.I. Vorobiov, A.N. Yushkov, V.N. Zhilich, V.V. Zhulanov, A.N. Zhuravlev. The main results of the KEDR in the charmonium physics. // Report at the Int. Session Conference of the DPS RAS MEPhI (Moscow Engineering Physics Institute) Nuclear Physics Section, 17-21 November, 2014, Moscow.

[685] I.V. Ovtin, V.V. Anashin, V.M. Aulchenko, E.M. Baldin, A.K. Barladyan, A.Yu. Barnyakov, M.Yu. Barnyakov, S.E. Baru, I.Yu. Basok, A.E. Blinov, V.E. Blinov, A.V. Bobrov, V.S. Bobrovnikov, A.V. Bogomyagkov, A.E. Bondar, A.R. Buzykaev, S.I. Eidelman, D.N. Grigoriev, Yu.M. Glukhovchenko, V.V. Gulevich, D.V. Gusev, S.E. Karnaev, G.V. Karpov, S.V. Karpov, T.A. Kharlamova, V.A. Kiselev, V.V. Kolmogorov, S.A. Kononov, K.Yu. Kotov, E.A. Kravchenko, V.N. Kudryavtsev, V.F. Kulikov, G.Ya. Kurkin, E.A. Kuper, I.A. Kuyanov, E.B. Levichev, D.A. Maksimov, V.M. Malyshev, A.L. Maslennikov, A.S. Medvedko, O.I. Meshkov, S.I. Mishnev, I.I. Morozov, N.Yu. Muchnoi, V.V. Neufeld, S.A. Nikitin, I.B. Nikolaev, I.N. Okunev, A.P. Onuchin, S.B. OreshkOrlov, A.A. Osipov, S.V. Peleganchuk, S.G. Pivovarov, P.A. Piminov, V.V. Petrov, A.O. Poluektov, V.G. Prisekin, O.L. Rezanova, A.A. Ruban, V.K. Sandyrev, G.A. Savinov, A.G. Shamov, D.N. Shatilov, B.A. Shwartz, E.A. Simonov, S.V. Sinyatkin, A.N. Skrinsky, V.V. Smaluk, A.V. Sokolov, E.V. Starostina, A.M. Sukharev, A.A. Talyshev, V.A. Tayursky, V.I. Telnov, Yu.A. Tikhonov, K.Yu. Todyshev, G.M. Tumaikin, Yu.V. Usov, A.I. Vorobiov, A.N. Yushkov, V.N. Zhilich, V.V. Zhulanov, A.N. Zhuravlev. Status of the AShIF system of the KEDR detector. // Report at the Session Conference of the DPS RAS MEPhI (Moscow Engineering Physics Institute) Nuclear Physics Section, 17-21 November, 2014.

[686] V.I. Telnov. Prospects of high energy photon colliders. // 37 Intern. Conf. on High Energy Physics (ICHEP), 2-9 July 2014, Valencia, Spain.

[687] V.I. Telnov. Effects in high energy linear colliders due to particle fields. // Intern. Conf. of Linear Colliders (LCWS2014), 6-10 October 2014, Belgrad. http://agenda.linearcollider.org/event/6389/session/10/contribution/103/material/slides/0.pdf.

[688] V.I. Telnov. Future of circular high energy proton and e^+e^- colliders. // Intern. Session Conference of the DPS RAS Nuclear Physics Section. Physics of Fundamental Interactions, November 17-21, 2014, Moscow. http: //www.icssnp.mephi.ru/content/file/2014/plenar/0_22_ Telnov-sessia-2014.pdf.

[689] F.V. Ignatov. Hadronic cross-sections measurement on the VEPP-2000. // QCD14, 30 June - 4 July 2014, Montpellier, France.

[690] T.V. Dimova. The last results of the cross sections measurement of $e^+e^- \to$ hadrons with the SND and CMD-3 detectors at VEPP-2000. // 37th Intern. Conference on High Energy Physics (ICHEP2014), 2 - 9 July 2014, Valencia, Spain.

[691] P.A. Lukin. The last results from the CND-3 detector at VEPP-2000. // Quark Confinement 2014, 7-12 September, 2014, St-Petersburg, Russia.

[692] I.B. Logashenko, R.R. Akmetshin, A.V. Anisenkov, V.M. Aulchenko, V.Sh. Banzarov, N.S. Bashtovoy, D.E. Berkaev, A.E. Bondar, A.V. Bragin, S.I. Eidelman, D.A. Epifanov, L.B. Epshteyn, A.L. Erofeev, G.V. Fedotovich, S.E. Gayazov, A.A. Grebenuk, D.N. Grigoriev, E.M. Gromov, F.V. Ignatov, S.V. Karpov, V.F. Kazanin, B.I. Khazin, I.A. Koop, O.A. Kovalenko, A.N. Kozyrev, E.A. Kozyrev, P.P. Krokovny, A.E. Kuzmenko, A.S. Kuzmin, P.A. Lukin, K.Yu. Mikhailov, N.Yu. Muchnoi, V.S. Okhapkin, Yu.N. Pestov, E.A. Perevedentsev, A.S. Popov, G.P. Razuvaev, Yu.A. Rogovsky, A.L. Romanov, A.A. Ruban, N.M. Ryskulov, A.E. Ryzhenenkov, V.E. Shebalin, D.N. Shemyakin, B.A. Shwartz, D.B. Shwartz, A.L. Sibidanov, P.Yu. Shatunov, Yu.M. Shatunov, E.P. Solodov, V.M. Titov, A.A. Talyshev, A.I. Vorobiov, Yu.V. Yudin. Measurement of hadronic cross sections in Novosibirsk. // Dark Matter, Hadron Physics, Fusion Physics, 24-26 September 2014, Messina, Italy.

[693] R.R. Akhmetshin, A.V. Anisenkov, V.M. Aulchenko, V.S. Banzarov, N.S. Bashtovoy, D.E. Berkaev, A.V. Bragin, S.I. Eidelman, D.A. Epifanov, L.B.Epshteyn, A.L. Erofeev, G.V. Fedotovich, S.E. Gayazov, A.A. Grebenuk, D.N. Grigoriev, E.M. Gromov, F.V. Ignatov, S.V. Karpov, V.L. Ivanov, V.F. Kazanin, B.I. Khazin, A.N. Kirpotin, I.A. Koop, O.A. Kovalenko, A.N. Kozyrev, E.A. Kozyrev, P.P. Krokovny, A.E. Kuzmenko, A.S. Kuzmin, I.B. Logashenko, P.A. Lukin, A.P. Lysenko, K.Yu. Mikhailov, V.S. Okhapkin, Yu.N. Pestov, E.A. Perevedentsev, A.S. Popov, Yu.S. Popov, G.P. Razuvaev, Yu.A. Rogovsky, A.L. Romanov, A.A. Ruban, N.M. Ryskulov, A.E. Ryzhenenkov, V.E. Shebalin, D.N. Shemyakin, B.A. Shwartz, D.B. Shwartz, A.L. Sibidanov, P.Yu. Shatunov, Yu.M. Shatunov, E.P. Solodov, V.M. Titov, A.A. Talyshev, A.I. Vorobiov, Yu.V. Yudin, Yu.M. Zharinov. Luminosity measurement in experiments with the CMD-3 detector at the VEPP-2000 collider. // Intern. Session Conference of the DPS RAS Nuclear Physics Section. Physics of Fundamental Interactions, November 17-21, 2014, Moscow.

[694] A. Tribendis, Y. Biryuchevsky, E. Kenzhebulatov, Y. Kruchkov, E. Rotov, A. Zhukov (BINP, Novosibirsk), M. Naumenko (RFNC-VNIITF, Snezhinsk), Y. Cuvet, A. Dallocchio, J.F. Fuchs, F.

189

Gerigk, J.M. Giguet, T. Muranaka, J. Hansen, E. Page, B. Riffaud, N. Thaus, M. Tortrat, M. Vretenar, R. Wegner (CERN, Geneva, Switzerland). CONSTRUCTION AND RF CONDITIONING OF THE CELL-COUPLED DRIFT TUBE LINAC (CCDTL) FOR LINAC4 AT CERN. // Proc. of the 27th Linear Accelerator Conference LINAC2014, 31 August – 05 September, 2014, Geneva, Switzerland. - P. 746-750.

[695] V.N. Volkov, V.S. Arbuzov, K.N. Chernov, E.I. Kolobanov, S.A. Krutikhin, G.Ya. Kurkin, E.A. Kuper, I.V. Kuptsov, S.V. Motygin, V.N. Osipov, V.K. Ovchar, V.V. Repkov, V.M. Petrov, I.K. Sedlyarov, G.V. Serdobintzev, S.S. Serednjakov, M.A. Scheglov, S.V. Tararyshkin, A.G. Tribendis, I.A. Zapryagaev (BINP SB RAS, Novosibirsk), I.V. Shorikov, A.V. Telnov, N.V. Zavyalov (RFNC-VNIIEF, Sarov). CW 100 keV ELECTRON RF INJECT OR FOR 40 mA AVERAGE BEAM CURRENT. // Proc. of th 24th Russian Particle Accelerator Conference RuPAC2014, 6 - 10 October, 2014, Obninsk, Kaluga Region, Russia. - P. 309-311.

[696] R.R. Akhmetshin, A.V. Anisenkov, V.M. Aulchenko, V.S. Banzarov, N.S. Bashtovoy, D.E. Berkaev, A.V. Bragin, S.I. Eidelman, D.A. Epifanov, L.B. Epshteyn, A.L. Erofeev, G.V. Fedotovich, S.E. Gayazov, A.A. Grebenuk, D.N. Grigoriev, E.M. Gromov, F.V. Ignatov, S.V. Karpov, V.L. Ivanov, V.F. Kazanin, B.I. Khazin, A.N. Kirpotin, I.A. Koop, O.A. Kovalenko, A.N. Kozyrev, E.A. Kozyrev, P.P. Krokovny, A.E. Kuzmenko, A.S. Kuzmin, I.B. Logashenko, P.A. Lukin, A.P. Lysenko, K.Yu. Mikhailov, V.S. Okhapkin, Yu.N. Pestov, E.A. Perevedentsev, A.S. Popov, Yu.S. Popov, G.P. Razuvaev, Yu.A. Rogovsky, A.L. Romanov, A.A. Ruban, N.M. Ryskulov, A.E. Ryzhenenkov, V.E. Shebalin, D.N. Shemyakin, B.A. Shwartz, D.B. Shwartz, A.L. Sibidanov, P.Yu. Shatunov, Yu.M. Shatunov, E.P. Solodov, V.M. Titov, A.A. Talyshev, A.I. Vorobiov, Yu.V. Yudin, Yu.M. Zharinov. Preliminary results of the process cross section measurement of $e^+e^- \to K^+K^- \eta$. // Intern. Session Conference of the DPS RAS Nuclear Physics Section. Physics of Fundamental Interactions, November 17-21, 2014, Moscow.

[697] V.E. Shebalin, A.V. Anisenkov, N.S. Bashtovoy, D.A. Epifanov, A.L. Erofeev, A.A. Grebenuk, S.V. Karpov, B.I. Khazin, O.A. Kovalenko, A.N. Kozyrev, A.S. Kuzmin, K.Yu. Mikhailov, G.P. Razuvaev, A.A. Ruban, B.A. Shwartz, V.M. Titov, Yu.V. Yudin. Barrel calorimeter of the CMD-3 detector. // Intern. Session Conference of the DPS RAS Nuclear Physics Section. Physics of Fundamental Interactions, November 17-21, 2014, Moscow.

[698] R.R. Akhmetshin, A.V. Anisenkov, V.M. Aulchenko, V.S. Banzarov, N.S. Bashtovoy, D.E. Berkaev, A.V. Bragin, S.I. Eidelman, D.A. Epifanov, L.B. Epshteyn, A.L. Erofeev, G.V. Fedotovich, S.E. Gayazov, A.A. Grebenuk, D.N. Grigoriev, E.M. Gromov, F.V. Ignatov, S.V. Karpov, V.L. Ivanov, V.F. Kazanin, B.I. Khazin, A.N. Kirpotin, I.A. Koop, O.A. Kovalenko, A.N. Kozyrev, E.A. Kozyrev, P.P. Krokovny, A.E. Kuzmenko, A.S. Kuzmin, I.B. Logashenko, P.A. Lukin, A.P. Lysenko, K.Yu Mikhailov, V.S. Okhapkin, Yu N. Pestov, E.A. Perevedentsev, A.S. Popov, Yu S. Popov, G.P. Razuvaev, Yu A. Rogovsky, A.L. Romanov, A.A. Ruban, N.M. Ryskulov, A.E. Ryzhenenkov, V.E. Shebalin, D.N. Shemyakin, B.A. Shwartz, D.B. Shwartz, A.L. Sibidanov, P.Yu Shatunov, Yu M. Shatunov, E.P. Solodov, V.M. Titov, A.A. Talyshev, A.I. Vorobiov, Yu.V. Yudin, Yu.M. Zharinov. Preliminary measurements of hadronic cross sections with the CMD-3 detector at the VEPP-2000 collider. // Workshop on Precision Physics and Fundamental Physical Constants (FPC2014), 1-5 December, 2014, Dubna, Russia.

[699] V. Kiselev (VEPP-4 team BINP), A. Aleshaev, V. Anashin, O. Anchugov, A. Batrakov, E. Behtenev, V. Blinov, A Bogomyagkov, D. Burenkov, S. Vasichev, S. Glukhov, Yu. Glukhovchenko, O. Gordeev, V. Erokhov, K. Zolotarev, V. Zhilich, A. Zhmaka, A. Zhuravlev, V. Kaminsky, S. Karnaev, G. Karpov, G. Kulipanov, E. Kuper, K. Kuper, G. Kurkin, O. Meshkov, S. Mishnev, I. Morozov, N. Muchnoi, V. Neifeld, I. Nikolaev, D. Nikolenko, I. Okunev, A. Onuchin, A. Pavlenko, V. Petrov, P. Piminov, O. Plotnikova, A. Poyansky, Yu. Pupkov, V. Sandyrev, V .Svistchev, I. Sedliarov, E. Simonov, S. Sinyatkin, A. Skrinsky, E. Starostina, Yu. Tikhonov, D. Toporkov, K. Todyshev, G. Tumaikin, A. Shamov, D. Shatilov, D. Shvedov (Novosibirsk State Technical University). Particle and accelerator physics at the VEPP-4M collider. // Proc. of RuPAC2014, Obninsk, Kaluga Region, Russia.

[700] V. Kiselev (VEPP-4 team BINP), A. Akimov, O. Anchugov, A. Batrakov, O. Belikov E. Bekhtenev, P. Cheblakov, A. Chernyakin A. Derbenev, A. Erokhin, S . Gurov, S. Karnaev, G. Karpov, R. Kadyrov, V. Kobets, V. Konstantinov, V. Kolmogorov, A. Korepanov, E. Kuper, V. Kuzminykh, E. Levichev, V. Neyfeld, I. Okunev, V. Petrov, M. Petrichenkov, A. Polyansky, D. Pureskin, A.Rakhimov, S. Ruvinskiy, T. Rybitskaya, L. Schegolev, A. Semenov, D. Senkov, S. Seredniakov, S. Shiyankov, D. Shvedov, S.Sinyatkin, A. Sukhanov, A. Zhuravlev, BNL New York, USA team: G. Bassi, A. Blednykh, E. Blum, W.Cheng, J. Choi, J. de Long, R. Fliller, F. Gao, W. Guo, Y .Hidaka, S. Kramer, S. Krinsky, Y. Li, M. Maggipinto, D. Padrazo, B. Podobedov, J. Rose, S. Seletskiy, O. Singh, V. Smaluk, T. Shaftan, W. Wahl, G. Wang, F. Willeke, L.Yang, X. Yang, L.Yu, E. Zitvogel, P. Zuhoski. The NSLS-II Booster development and commissioning. // Proc. of RuPAC2014, Obninsk, Kaluga Region, Russia.

[701] A. Bogomyagkov, E. Levichev, P. Piminov, S. Sinyatkin. Ultimate synchrotron radiation source with horizontal field wigglers. // Low Emittance Rings 2014 Workshop, 17-19 Sept 2014, INFN-LNF, Frascati, Italy.

[702] P. Piminov, A. Bogomyagkov, E. Levichev, S. Sinyatkin, K. Zolotarev. Low emittance cell with large dynamic aperture. // Low Emittance Rings 2014 Workshop, 17-19 Sept 2014, INFN-LNF, Frascati, Italy.

[703] D. Shatilov. Beam-beam effects for FCC-ee at different energies: crab waist vs. head-on. // FCC-ee/TLEP Physics Workshop (TLEP7), CERN, 19-21 June 2014.

[704] D. Shatilov. Beam-beam effects in High-energy colliders: crab waist vs. head-on. // HF2014 ICFA Workshop, Beijing, 9-12 October 2014.

[705] Aleshaev A., Belov S., Kozak V., Piskunov G., Tararyshkin S. Using Microcomputer "Odrenok" in Basic Research Projects of Institute of Nuclear Physics of Siberian Branch of Soviet Academy of Science and Budker Institute of Nuclear Physics of Siberian Branch of Russian Academy of Science in the 80-th of the Last Century and up to the Present Times. // Proc. of III Intern. Conference on "COMPUTER TECHNOLOGY IN RUSSIA AND IN THE FORMER SOVIET UNION (SORUCOM-2014)": Kazan, October 13-17, 2014, p. 30 (in Russian). http:// www.sorucom.ru/files/news/ sorucom2014_ru.pdfю

[706] K.Yu. Todyshev, V.V. Anashin, V.M. Aulchenko, E.M. Baldin, A.K. Barladyan, A.Yu. Barnyakov, M.Yu. Barnyakov, S.E. Baru, I.Yu. Basok, A.E. Blinov, V.E. Blinov, A.V. Bobrov, V.S. Bobrovnikov, A.V. Bogomyagkov, A.E. Bondar, A.R. Buzykaev, S.I. Eidelman, D.N. Grigoriev, Yu.M. Glukhovchenko, V.V. Gulevich, D.V. Gusev, S.E. Karnaev, G.V. Karpov, S.V. Karpov, T.A. Kharlamova, V.A. Kiselev, V.V. Kolmogorov, S.A. Kononov, K.Yu. Kotov, E.A. Kravchenko, V.N. Kudryavtsev, V.F. Kulikov, G.Ya. Kurkin, E.A. Kuper, I.A. Kuyanov, E.B. Levichev, D.A. Maksimov, V.M. Malyshev, A.L. Maslennikov, A.S. Medvedko, O.I. Meshkov, S.I. Mishnev, I.I. Morozov, N.Yu. Muchnoi, V.V. Neufeld, S.A. Nikitin, I.B. Nikolaev, I.V. Ovtin, I.N. Okunev, A.P. Onuchin, S.B. Oreshkin, I.O. Orlov, A.A. Osipov, S.V. Peleganchuk, S.G. Pivovarov, P.A. Piminov, V.V. Petrov, A.O. Poluektov, V.G. Prisekin, O.L. Rezanova, A.A. Ruban, V.K. Sandyrev, G.A. Savinov, A.G. Shamov, D.N. Shatilov, B.A. Shwartz, E.A. Simonov, S.V. Sinyatkin, A.N. Skrinsky, V.V. Smaluk, A.V. Sokolov, E.V. Starostina, A.M. Sukharev, A.A. Talyshev, V.A. Tayursky, V.I. Telnov, Yu.A. Tikhonov, G.M. Tumaikin, Yu.V. Usov, A.I. Vorobiov, A.N. Yushkov, V.N. Zhilich, V.V. Zhulanov, A.N. Zhuravlev. R-scan (KEDR). // The 13th Intern. Workshop on Tau Lepton Physics, 15-19 September, 2014, Aachen, Germany.

[707] G.A. Fatkin, M.Yu. Vasilyev, A.M. Batrakov, I.V. Ilyin, A.M. Pilan, G.Ya. Kurkin (BINP and NSU, Novosibirsk). CONTROLLER FOR RF STATIONS FOR BOOSTER OF NICA PROJECT. // Proc. of the 24th Russian Particle Accelerator Conference RuPAC2014, 6 - 10 October, 2014, Obninsk, Kaluga Region, Russia. - P. 383-385.

[708] G.Ya. Kurkin, A.M. Batrakov, S.A. Krutikhin, Ya.G. Kruchkov, S.V. Motygin, A.M. Pilan, G.A. Fatkin (BINP and NSU, Novosibirsk). RF system of the booster of NICA facility. // Proc. of the 24th Russian Particle Accelerator Conference (RuPAC2014), 6 - 10 October, 2014, Obninsk, Kaluga Region, Russia. - P. 26-28.

[709] Dmitry Skorobogatov, Maxim Bryzgunov, Anatoly Goncharov, Igor Gusev, Mikhail Kondaurov, Vladimir Reva, Dmitry Senkov, Viktor Kozak, Anatoly Medvedko, Vasily Parkhomchuk, Dmitry Pureskin, Aleksandr Putmakov. The precision high voltage power supply system for the accelerating column of the 2 MeV electron cooler for COSY. // 2014 IEEE Power Modulator and High Voltage Conference (2014 IPMHVC), June 1 - 5, 2014, Santa Fe, CA.

[710] E.A. Bekhtenev, G.V. Karpov. Upgrade of BPM system at VEPP-4M collider. // Proc. of RuPAC2014, Obninsk, Russia, 2014, THPSC23. - P.368-370.

[711] V. Smaluk, O. Meshkov, G. Karpov, E. Bekhtenev, S. Karnaev (BINP, Novosibirsk), O. Singh, D. Padrazo, K. Vetter, G. Wang (BNL, Upton, NY, USA). Status of beam diagnostics for NSLS-II booster. // Proc.of IBIC2013, Oxford, UK, 2014, MOPC02. - P.41-44.

[712] A. Pavlenko A. Batrakov, G. Karpov, I. Nikolaev, V. Svishchev. Method of broadband stabilization of the VEPP-4 main field. // Proc. of RuPAC2014, Obninsk, Russia, 2014, TUPSA29. - P.100-102.

Preprints 2014

1. V.S. Fadin, R. Fiore. Impact factors for Reggeon-gluon–transition in N = 4 SYM with large number of colours. // Budker INP 2014-2, 17p, 2014.

2. E.V. Bykov, V.P. Kozak, S.V. Tararyshkin. Delayed pulse generator. // Preprint INP 2014-5, 18p, Novosibirsk, 2014 (in Russian).

3. O.M. Valov, V.M. Konstantinov, I.N. Okunev, V.V. Petrov. Steering magnets for the booster of the SR source NSLS-II. // Preprint INP 2014-7, 39p, Novosibirsk, 2014 (in Russian).

4. R.E. Gerasimov, V.S. Fadin. Analysis of approximations used in calculations of radiative corrections to electron-proton scattering cross section. // Preprint INP 2014-10, 47p, Novosibirsk, 2014 (in Russian).

5. M.A. Scheglov. Geeration of oscillating ions towards the reactions of synthesis; proposal, estimations, problems. // Preprint INP 2014-11, 30p, Novosibirsk, 2014 (in Russian).

6. A.A. Bryazgin, V.T. Nekhaev, A.D. Panfilov, V.M. Radchenko, B.L, Faktorovich, E.A. Shtarklev. The method of the nonmonochromatic beams bending by magnetic mirrors with the falling field. // Preprint INP 2014-15, 27p, Novosibirsk, 2014 (in Russian).

***

7. R. Assmann, R. Bingham, T. Bohl, C. Bracco, B. Buttenschon, A. Butterworth, A. Caldwell, S. Chattopadhyay, S. Cipiccia, E. Feldbaumer, R.A. Fonseca, B. Goddard, M. Gross, O. Grulke, E. Gschwendtner, J. Holloway, C. Huang, D. Jaroszynski, S.

Jolly, P. Kempkes, N. Lopes, K. Lotov, J. Machacek, S.R. Mandry, J.W. McKenzie, M. Meddahi, B.L. Militsyn, N. Moschuering, P. Muggli, Z. Najmudin, T.C.Q. Noakes, P.A. Norreys, E. Oz, A. Pardons, A. Petrenko, A. Pukhov, K. Rieger, O. Reimann, H. Ruhl, E. Shaposhnikova, L.O. Silva, A. Sosedkin, R. Tarkeshian, R.M.G.N. Trines, T. Tuckmantel, J. Vieira, H. Vincke, M. Wing, G. Xia. Proton-driven plasma wakefield acceleration: a path to the future of high-energy particle physics (AWAKE Collab.). // arXiv:1401.4823 [physics.acc-ph].

8. Lotov K.V. Sosedkin A.P., Petrenko A.V. Long-Term Evolution of Broken Wakefields in Finite-Radius Plasmas. // E-print: arXiv:1402.1261 [physics.plasm-ph].

9. K.V. Lotov, V.A. Minakov, A.P. Sosedkin. Parameter sensitivity of plasma wakefields driven by self-modulating proton beams. // E-print: arXiv:1405.1825 [physics.plasm-ph].

10. K.V. Lotov and I.V. Timofeev. Transition regime of the one-dimensional two-stream instability. // E-print: arXiv:1408.2349 [physics.plasm-ph].

11. K.V. Lotov, A.P. Sosedkin, A.V. Petrenko, L.D. Amorim, J. Vieira, R.A. Fonseca, L.O. Silva, E. Gschwendtner, P. Muggli. Electron trapping and acceleration by the plasma wakefield of a self-modulating proton beam. // E-print: arXiv:1408.4448 [physics.plasm-ph].

12. R. Assmann, R. Bingham, T. Bohl, C. Bracco, B. Buttenschon, A. Butterworth, A. Caldwell, S. Chattopadhyay, S. Cipiccia, E. Feldbaumer, R.A. Fonseca, B. Goddard, M. Gross, O. Grulke, E. Gschwendtner, J. Holloway, C. Huang, D. Jaroszynski, S. Jolly, P. Kempkes, N. Lopes0, K. Lotov, J. Machacek, S.R. Mandry, J.W. McKenzie, M. Meddahi, B.L. Militsyn, N. Moschuering, P. Muggli, Z. Najmudin, T.C.Q. Noakes, P.A. Norreys, E. Oz, A. Pardons, A. Petrenko, A. Pukhov, K. Rieger, O. Reimann, H. Ruhl, E. Shaposhnikova, L.O. Silva, A. Sosedkin, R. Tarkeshian, R.M.G.N. Trines, T. Tuckmantel, J. Vieira, H. Vincke, M. Wing, G. Xia. Proton-driven plasma wakefield acceleration: a path to the future of high-energy particle physics (AWAKE Collab.). AWAKE status report. // E-print: CERN-SPSC-2014-026 / SPSC-SR-143 (2014).

13. K.V. Lotov, I.V. Timofeev, E.A. Mesyats, A.V. Snytnikov, V.A. Vshivkov. Note on quantitatively correct simulations of the kinetic beam-plasma instability. // E-print: arXiv:1410.5617 [physics.plasm-ph].

14. M.G. Kozlov, A.V. Reznichenko. Regge vertex for quark production in the central region of rapidity in the next-to-leading order. - [http://www.icssnp.m mephi.ru/content/file/2014/section7/7_03_kozlovmg-snp-2014.pdf].

15. Andrey Grozin, Johannes M. Henn, Gregory P. Korchemsky, Peter Marquard. Three loop Cusp anomalous dimension in QCD. // arXiv:1409.0023 [hep-th].

16. Valentin.V. Sokolov, Oleg V. Zhirov. Elastic Enhancement Factor: from Mesoscopic Systems to Macroscopic Analogous Devices, Short version. // arXiv:1411.6211v2 [nucl-th] 12 Dec 2014.

17. R.N. Lee and A. I. Milstein. Coulomb corrections to electron scattering on the extended source and the proton charge radius. // arXiv: 1402.3054.

18. R.N. Lee. Reducing differential equations for multiloop master integrals. // arXiv: 1411.0911.

19. V.S. Fadin. Discontinuities of multi-Regge amplitudes. // arXiv:1412.3253 [hep-th].

20. V.M. Katkov. On effective mass of a photon in a strong magnetic field. // arXiv:1403.3983.

21. V.M. Katkov. Spectral-integral representation of the photon polarization operator in a constant uniform magnetic field. // arXiv:1411.2339.

22. I.S. Terekhov, A.V. Reznichenko, S.K. Turitsyn. Mutual information in nonlinear communication channel: Analytical results in large SNR limit. // arXiv 1411.7477v1. - P. 1-11.

23. I.A. Rachek, J. Arrington, V.F. Dmitriev, V.V. Gauzshtein, R.E. Gerasimov, A.V. Gramolin, R.J. Holt, V.V. Kaminskiy, B.A. Lazarenko, S.I. Mishnev, N.Yu. Muchnoi, V.V. Neufeld, D.M. Nikolenko, R.Sh. Sadykov, Yu.V. Shestakov, V.N. Stibunov, D.K. Toporkov, H. de Vries, S.A. Zevakov, and V.N. Zhilich. Measurement of the two-photon exchange contribution to the elastic e± p scattering cross sections at the VEPP–3 storage ring. // 2014, arXiv:1411.7372v1 [nucl-ex].

24. A.D. Dolgov, A.V. Popov, and A.S. Rudenko. Shape of the inflaton potential and the efficiency of the universe heating. // arXiv:1412.0112 [astro-ph.CO].

25. M. Ablikim (BESIII Collab.), M.N. Achasov, I.B. Nikolaev, N.Yu. Muchnoi, et al. Observation of the electromagnetic doubly OZI-sup-pressed decay $J/\psi \rightarrow \varphi\pi^0$. // arXiv: 1504.03194 [hep-ex].

26. M. Ablikim (BESIII Collab.), M.N. Achasov, I.B. Nikolaev, N.Yu. Muchnoi, et al. Measurement of the proton form factor by studying $e^+e^- \rightarrow p\ \bar{p}$. // arXiv:1504.02680 [hep-ex].

27. M. Ablikim (BESIII Collab.), M.N. Achasov, I.B. Nikolaev, N.Yu. Muchnoi, et al. Measurements of $\psi(3686) \rightarrow K^- \Lambda\ \bar{\Xi}^+ + $ c.c. and $\psi(3686) \rightarrow \gamma\ K^- \Lambda\ \bar{\Xi}^+ + $ c.c. // arXiv:1504.02025 [hep-ex].

28. M.N. Achasov, V.M. Aulchenko, A.Yu. Barnyakov, K.I. Beloborodov., A.V. Berdyugin, D.E. Berkaev, A.G. Bogdanchikov, A.A. Botov, T.V. Dimova, V.P Druzhinin, V.B. Golubev, L.V. Kardapoltsev, A.S. Kasaev, A.G. Kharlamov, A.N. Kirpotin, D.P. Kovrizhin, I.A. Koop, A.A. Korol, S.V. Koshuba, A.S. Kupich, K.A. Martin, N.Yu. Muchnoi, A.E. Obrazovsky, A.V. Otboev, E.V. Pakhtusova, A.I. Senchenko, S.I. Serednyakov, P.Yu. Shatunov, Yu.M. Shatunov, D.A. Shtol, D.B. Shwartz, Z.K. Silagadze, I.K. Surin, Yu.A. Tikhonov, Yu.V. Usov, A.V. Vasiljev (SND Collab.). Search for the $\eta' \rightarrow e^+e^-$ decay with the SND detector. // arXiv:1504.01245 [hep-ex].

29. E.V. Abakumova, M.N. Achasov, A.A. Krasnov, N.Yu. Muchnoi, E.E. Pyata, et al. The system for delivery of IR laser radiaton into high vacuum. // arXiv:1504.00130 [physics.acc-ph].

30. M. Ablikim (BESIII Collab.), M.N. Achasov, I.B. Nikolaev, N.Yu. Muchnoi. Observation of the $\psi(1^{3}D_{2})$ state in $e^{+}e^{-} \to \pi+\pi- \gamma \chi_{c1}$ at BESIII. // arXiv:1503.08203 [hep-ex].

31. M. Ablikim (BESIII Collab.), M.N. Achasov, I.B. Nikolaev, N.Yu. Muchnoi. Measurement of the $e^{+}e^{-} \to \eta J/\psi$ cross section and search for $e^{+}e^{-} \to \pi^{0} J/\psi$ at center-of-mass energies between 3.810 and 4.600 GeV. // arXiv:1503.06644 [hep-ex].

32. M. Ablikim (BESIII Collab.), M.N. Achasov, I.B. Nikolaev, N.Yu. Muchnoi. Study of χ_{c1} decaying into φ K*(892) $\bar{\text{K}}$. // arXiv:1503.04699 [hep-ex].

33. M. Ablikim (BESIII Collab.), M.N. Achasov, I.B. Nikolaev, N.Yu. Muchnoi. Precision measurement of the integrated luminosity of the data taken by BESIII at center of mass energies between 3.810 GeV and 4.600 GeV. // arXiv:1 503.03408 [hep-ex].

34. M. Ablikim (BESIII Collab.), M.N. Achasov, I.B. Nikolaev, N.Yu. Muchnoi. Searches for isospin-violating transitions $\chi_{c0,2} \to \pi^{0} \eta_{c}$. // arXiv:1502.02641 [hep-ex].

35. M. Ablikim (BESIII Collab.), M.N. Achasov, I.B. Nikolaev, N.Yu. Muchnoi. Evidence for $e^{+}e^{-} \to \gamma \chi_{c1,2}$ at center-of-mass energies from 4.009 to 4.360 GeV. // arXiv:1411.6336.

36. V.V. Smaluk, E.A. Bekhtenev, S.E. Karnaev, G.V. Karpov, O.I. Meshkov (BINP SB RAS, Novosibirsk, Russia), D. Padrazo, O. Singh, V.V. Smaluk, K. Vetter, G.M. Wang (BNL, Upton, Long Island, New York, USA). For the NSLS II third generation light source, a fullenergy Booster ring has been designed and produced by BINP. // Date: 17/02/2014 Size: 1MB. http://accelconf.web.cern.ch/AccelConf/IBIC2013/papers/mopc02.pdf.

37. G. Baranov, E. Levichev, S. Sinyatkin. Simple expression for minimum emittance with linearly varied bending radius in dipole magnets. // arXiv:1504.01038.

Authorial papers 2014

1. TASKAEV S.Yu. Accelerator based epithermal neutron source. // 01.04.01 - instruments and methods of experimental physics, Author. papers of thesis for the degree of doctor of phys.-math. science: Novosibirsk, 2014, BINP, SB RAS.

2. SOROKIN I.N. High-voltage strength of the tandem accelerator with vacuum insulation. // 01.04.01 - instruments and methods of experimental physics, Author. papers of thesis for the degree of candidate of technical science: Novosibirsk, 2014, BINP, SB RAS.

3. TITOV V.M. Fast one-coordinate gamma-quantum detector. // 01.04.01 - instruments and methods of experimental physics, Author. papers of thesis for the degree of candidate of technical science: Novosibirsk, 2014, BINP, SB RAS.

4. SKOVORODIN D.I. Influence of self-consistent fields on axial confinement in a Mirror Trap. 01.04.08 - physics of plasma. 01.04.08 - physics of plasma, Author. papers of thesis for the degree of candidate of phys.-math. science: Novosibirsk, 2014, BINP, SB RAS.

Participation in conferences 2014

1. XLI International Zvenigorod Conference on Plasma Physics and Controlled Fusion, 10 - 14 February 2014, Zvenigorod, Russia.

2. International Workshop "Scattering Amplitudes and the Multi-Regge Limit", Feb 10 - 14, 2014, Madrid, Spain.

3. International Conference on Instrumentation for Colliding Beam Physics "INST2014", February 24 - March 1, 2014, BINP, Novosibirsk, Russia.

4. International Workshop on Accelerator Science and Technology for Electron-Ion Collider (EIC2014), March 17 - 21, 2014, Thomas Jefferson National Accelerator Facility (Newport News, USA).

5. 13th International Institute of Refrigeration Conference on Cryogenics CRYOGENICS 2014, 7 - 11 April 2014, Prague, Czech Republic.

6. 52nd International Students Scientific Conference "ISSC-2014", 11-18 April, 2014, NSU, Novosibirsk, Russia.

7. XII Conference "Young Scientists of Russia" of the Dynasty Foundation, April 13-16, 2014, Moscow.

8. 41st IEEE International Conference on Plasma Science and the 20th International Conference on High-Power Particle Beams, May 25 - 29, 2014, Washington DC.

9. 21st International Conferenceon Plasma Surface Interactions in Controlled Fusion Devices, 26 - 30 May 2014, Kanazawa, Japan.

10. Conference "Development of New Applications of Machine Generated Food Irradiation Technologies", 27 - 28 May 2014, Vienna, Austria.

11. 13th International Workshop on Meson Production, Properties and Interaction "MESON 2014", 29 May - 3 June 2014, Cracow, Poland.

12. International Conference on Advanced Mathematics, Computations and Applications (AMCA'14). June 8 - 11, 2014, Akademgorodok, Novosibirsk, Russia.

13. 11th International Conference on Electron Beam Technology, 8 - 10 June 2014, Varna, Bulgaria.

14. 5th International Particle Accelerator Conference "IPAC-2014", June 15 - 20 2014, Dresden, Germany.

15. 26th Symposium on Plasma Physics and Technology, June 16-19, 2014, Prague.

16. FCC-ee/TLEP Physics Workshop (TLEP7), CERN, 19-21 June 2014.

17. 41st EPS Conference on Plasma Physics, 23 - 27 June 2014, Berlin.

18. QCD14, 30 June - 4 July 2014, Montpellier, France.

19. 20th International Workshop on Beam Dynamics and Optimization "BDO 2014", 30 June - 4 July 2014, St. Petersburg.

20. International Conference on Surface Engineering for Research and Industrial Applications, 30 June - 4 July 2014, NSTU, Novosibirsk.

21. 15th International Conference of Young Specialists on Micro/Nanotechnologies and Electron Devices "EDM 2014", 30 June - 4 July 2014, Altai, Russian Federation.

22. 9th Seminar of SB RAS – UB RAS Dedicated to the Memory of Academician F.A. Kuznetsov, 30 June - 4 July, 2014, Novosibirsk, Russia.

23. 64 International Conference on Nuclear Physics "Nucleus 2014", July 1 - 4, 2014, Minsk, Belarus.

24. 37th International Conference on High Energy Physics (ICHEP), 2 - 9 July 2014, Valencia, Spain.

25. XX National Conference on Synchrotron Radiation "SR-2014", 7 - 10 July 2014, BINP, Novosibirsk, Russia.

26. XXIV International Conference "Radiation physics of solids", 7 - 14 July, 2014, Sevastopol.

27. 9th International Workshop "Strong Microwaves and Terahertz Waves: Sources and Applications", IAP RAS, July 24 - 30, 2014, Nizhny Novgorod, Russia.

28. X International Asian School-Seminar "Optimization Problems of Complex Systems", July 25 - August 5, Kyrgyz Republic.

29. 36th International Free Electron Laser Conference "FEL2014", Congress Center Basel, 25 - 29 August 2014, Switzerland.

30. 10th International Conference on Open Magnetic Systems for Plasma Confinement, August 26 - 29, 2014, Daejeon, Korea.

31. XXVII International Linear Accelerator Conference (LINAC14), 31 August - 5 September 2014, Switzerland, Geneva.

32. International Workshop on Diffraction in High-Energy Physics "DIFFRACTION 2014", September 10 - 16, 2014, Primosten, Croatia.

33. 39th International Conference on Infrared, Millimeter and Terahertz Waves "IRMMW-THz 2014", 14 - 19 September 2014, The University of Arizona, Tucson; United States.

34. 13th International Workshop on Tau Lepton Physics, 15 - 19 September, 2014, Aachen, Germany.

35. International Scientific Conference "Science of the Future", 17 - 20 September 2014, St-Petersburg.

36. Low Emittance Rings 2014 Workshop, 17 - 19 September 2014, INFN-LNF, Frascati, Italy.

37. Paleolimnology of northern Eurasia: International Conf., 21 - 25 September 2014, Petrozavodsk.

38. International Congress on Energy Fluxes and Radiation Effects, 21 - 26 September 2014, Tomsk, Russia.

39. VIII All-Russian Conference on X-ray Analysis, 22 - 26 September, 2014, Irkutsk, Russia.

40. Dark Matter, Hadron Physics, Fusion Physics, 24-26 September 2014, Messina, Italy.

41. 9th International Conference on Nuclear Physics at Storage Rings, September 28 - October 3, 2014, Sankt Goar, Germany.

42. 28th Symposium on Fusion Technology SOFT 2014, September 29 - October 3 2014, San Sebastian, Spain.

43. 6th International Conference "Channeling 2014", October 5 - 10, 2014, Capri, Italy.

44. XXIV Russian Particle Accelerator Conference "RUPAC 2014", 6 - 10 October, 2014, Obninsk.

45. International Conference of Linear Colliders (LCWS2014), 6 - 10 October 2014, Belgrad.

46. HF2014 ICFA Workshop, 9 - 12 October 2014, Beijing.

47. III International Conference on "COMPUTER Technology in Russia and in the former Soviet Union (SORUCOM-2014)", October 13 - 17, 2014, Kazan, RF.

48. 25th Fusion Energy Conference (FEC2014), 13 - 18 October 2014, St. Petersburg.

49. ISF Research Workshop on Non-Hermitean Random Matrices: 50 Years after Ginibre", 20 - 27 October 2014, Israel.

50. Conference: Radiation Technologies: Achievements and Trends, October 21-23, 2014, Krym, Yalta.

51. Belarus days in Siberia: Practical Conference on Scientific, Technical and Innovation Collaboration Agreements of the Republic of Belarus and SB RAS, 22 October 2014, Novosibirsk.

52. KEK Flavour Factory Workshop; Belle II Theory Interface Platform Meeting, 28 - 31 October 2014, KEK, Tsukuba, Japan.

53. The School and the Workshop "New Trends in High-Energy Physics and QCD", October 21 - November 06, 2014, Natal, Brasilia.

54. Meeting and Youth Conference on the Use of Neutron Scattering and Synchrotron Radiation in Condensed Matter: RNSI-KS 2014, October 27-31, 2014 St. Petersburg, Russia.

55. The 21st International Symposium on Spin Physics (Spin2014), October 20 - 24, 2014, Beijing, China.

56. International Workshop on Heavy Quarkonium 2014, November 10 - 14, 2014, CERN.

57. International Session Conference of SNF NSD RAS (Moscow Engineering Physics Institute) Nuclear Physics Section, 17-21 November, 2014, Moscow, Russia.

58. X International Conference "Radiation-Thermal Effects and Processes in the Inorganic Materials" (RTEP-2014), 21 - 23 November 2014, Phuket, Thailand.

59. Helmholtz International School "Physics of Heavy Quarks and Hadrons", Germany.

60. Workshop on Precision Physics and Fundamental Physical Constants (FPC2014), 1-5 December, 2014, Dubna, Russia.

61. X International Scientific Congress and Show "Interexpo Geo-Siberia-2014", 16-18 April, 2014, International Scientific Conference "SibOptica-2014", Novosibirsk, Russia.

62. 21st Annual Seminar "NPCS'2014", Minsk, 2014.

List of Collaboration Agreements
between the Budker INP and Foreign Laboratories

№	Name of Laboratory	Title or Field of Collaboration	Dates	Principal Investigators
	1	*2*	*3*	*4*
1	*Daresbury (England)*	Generation and utilization of SR.	1977	*G. Kulipanov (INP); I. Munro (Daresbury)*
2	*BESSY (Germany)*	Development of the wigglers for BESSY-2.	1993	*A. Skrinsky, N. Mezentsev (INP); E. Jaeschke (BESSY)*
3	*Research Centre Rossendorf (Germany)*	Physical foundations of a plasma neutron source.	1994	*E. Kruglyakov, A. Ivanov (INP); K. Noack (Germany)*
4	*Nuclear Centre "Karlsruhe" (Germany)*	1. Development of conceptual project and data base for neutron source on the basis of GDT device. 2. Simulation of processes in diverter of ITER device.	1994	*E. Kruglyakov, A. Ivanov, A. Burdakov (INP); G. Kessler (Germany)*
5	*GSI (Germany)*	Collaboration in the field of accelerator physics: electron cooling; electron-ion colliders.	1995	*Yu. Shatunov, V. Parkhomchuk (INP); H. Eickhoff (GSI)*
6	*DESY (Germany)*	Elementary-particle physics, synchrotron radiation, accelerator physics and technology, electronics and experimental equipment.	1995	*A. Skrinsky, G. Kulipanov (INP); A. Vagner, K. Scherff (DESY)*
7	*CIEMAT (Spain)*	Accelerator technology and plasma physics.	2007	*E. Levichev (INP), J. Rubio (CIEMAT)*
8	*CELLS (Spain)*	Collaboration in the field of application of new equipment for SR sources.	2008	*E. Levichev (INP); Joan Bordas and Orpinell (CELLS)*
9	*INFN (Italy)*	Development of intense source for radioactive ion beams for experiments in nuclear physics	1984	*P. Logachev (INP); L. Techio (INFN)*
10	*University of Milan (Italy)*	Theoretical and numerical studies of dynamic chaos in classic and quantum mechanics.	1991	*A. Skrinsky, V. Sokolov (INP); T. Montegazza, J. Kasati (Italy)*
11	*INFN-LNF (Italy)*	Development of collider project DAFNE-II	2004	*E. Levichev (INP); S. Biscari (INFN-LNF)*
12	*University of Padua (Italy)*	Development of cryogenic detectors for experiments in neutrino physicist.	2008	*Yu. Tikhonov, A. Bondar (INP); A. Gudlielmi (Italy)*

№	1	2	3	4
13	*National Nuclear Center. Park of Nuclear Technology (Kazakhstan)*	Development and application of industrial accelerators, generation and utilization of neutron beams, development of SR sources, RF-generators.	2007	*G. Kulipanov (INP); K. Kadyrzhanov, A. Kusainov (Kazakhstan)*
14	*National Nuclear Center. Al-Farabi National University (Kazakhstan)*	Creation and development of a multi-purpose research complex of radiation technology and terahertz radiation.	2009	*G. Kulipanov (INP); K. Kadyrzhanov, B. Zhumagulov (Kazakhstan)*
15	*Institute of Morden Physics and Techniques, Lanchzou (China)*	Collaboration in the field of accelerator physics: electron cooling. .	2000	*V. Parkhomchuk (INP); S. Yang (PRC)*
16	*WOER Company, Shenzhen, (China))*	Using of electron accelerator ILU-10, exchanging of personal, information and experimental equipment.	2005	*A. Bryazgin (INP); Leo Li (WOER)*
17	*SINAP Shanghai, (China)*	Researching in field of industrial electron accelerators.	2006	*A. Bryazgin (INP); Hu Hounku (SINAP)*
18	*IHEP (China)*	Work of Chinese scientists on BINP installations, work of BINP scientists on IHEP installations.	2007	*A. Skrinsky (INP); H. Chen (IHEP)*
19	*Industrial and Technological Center of Cooperation with Russia and Belorussia of Heilongjiang Province (P.R.C) (China)*	Exchange of information about BINP-developed devices and the technology and product demand of the Chinese factories.	2009	*D. Grigoriev (INP); Zhan Hun-Vei (PRC)*
20	*POSTECH (Korea)*	Creation of beam accelerators, add-on devices, SR experiments.	1992	*A. Skrinsky, N. Mezentsev (INP); H. Kim (POSTECH)*
21	*KAERI (Korea)*	Development of FEL and accelerator-recuperator.	1999	*N. Vinokurov (INP); B.Ch. Lee (KAERI)*
22	*BNL, Brookhaven (USA)*	1. Measurement of the magnetic muon anomaly. 2. Joint research of RHIC spin.	1991 1993	*L. Barkov (INP); J. Bunse (BNL) Yu. Shatunov (INP); S. Ozaki (BNL)*
23	*ANL, Argonn (USA)*	1. Experiments with polarized gas jet target at VEPP-3. 2. SR instrumentation.	1988 1993	*L. Barkov (INP); R. Holt (ANL) G. Kulipanov, A. Skrinsky (INP); G. Shenoy (USA)*

№	1	2	3	4
24	*University of Pittsburgh (USA)*	Experiments on VEPP-2M and φ-factory.	1989	*S. Eidelman, E. Solodov (INP); V. Savinov (USA)*
25	*University of Duke (USA)*	Free electron lasers.	1992	*N. Vinokurov (INP); J. Wu (Duke)*
26	*BNL, Brookhaven (USA)*	Collaboration on electron-ion colliders.	1993	*V. Parkhomchuk (INP); I. Benzvi (USA)*
27	*FERMILAB (USA)*	Collaboration in the field of accelerator physics: electron cooling; conversion system.	1995	*V. Parkhomchuk (INP); O. Finli (FERMILAB)*
28	*FERMILAB (USA)*	Exchange of scientists and engineers for scientific research.	2005	*A. Skrinsky (INP); P. Oddone (FERMILAB)*
29	*SLAC, Stanford (USA)*	Obtainment of submicron beams and intensive positron beams, development of B-factory elements, detectors, RF-generators based on magnicons.	1994	*A. Skrinsky (INP); Persis Drel (SLAC)*
30	*Institute of Plasma Physics ASCR (Czech Republic)*	Collaboration in the field of plasma physics and plasma diagnostics research.	2008	*A. Ivanov (INP); P. Hruška (Czech Republic)*
31	*CERN (Switzerland)*	1. Research and development of the detectors for LHC. 2. Development of the LHC elements.	1992 1996	*A. Bondar, Yu. Tikhonov (INP); T. Nakada, P. Yenni (CERN) V. Anashin (INP); L. Evans (CERN)*
32	*Paul Scherrer Institute (Switzerland)*	Collaboration in the field of particle physics.	2009	*D. Grigoriev (INP); D. Mecom (Paul Scherrer Institute)*
33	*CERN (Switzerland)*	Research and development of micro-pattern detector technology..	2009	*Yu. Tikhonov (INP); S. Bertolucci (CERN)*
34	*CERN (Switzerland)*	Collaboration in the development of the electron-positron colliders with super-high luminosity.	2009	*E. Levichev (INP); S. Myers (CERN)*
35	*RIKEN Spring-8 (Japan)*	Collaboration in the field of accelerator physics and synchrotron radiation	1996	*G. Kulipanov (INP); H. Kamitsubo (Japan)*
36	*KEK (Japan)*	Research in accelerator physics and allied fields, development of elementary particle detectors.	1995	*A. Skrinsky (INP); A. Suzuki (KEK)*
37	*Center of Plasma Research, Tsukuba (Japan)*	Collaboration on Open traps.	2007	*A. Ivanov (INP); T. Imai (Japan)*

Research Personnel

Members of Russian Academy of Science

Academicians:

Dikansky Nikolai Sergeevich
Kulipanov Gennady Nikolaevich
Skrinsky Alexandr Nikolaevich

Corresponding members:

Bondar Alexandr Evgenievich
Vinokurov Nikolai Alexandrovich
Dimov Gennady Ivanovich
Logachev Pavel Vladimirovich
Parkhomchuk Vasily Vasilievich
Khriplovich Iosif Bentsionovich
Shatunov Yury Michailovich

Director Board

Director:

Skrinsky Alexandr Nikolaevich

RAS Advisor:

Kulipanov Gennady Nikolaevich

Scientific Secretary:

Vasiljev Alexei Vladimirovich

Deputy Directors (scientific):

Bondar Alexandr Evgenievich
Burdakov Alexandr Vladimirovich
Ivanov Alexandr Alexandrovich
Levichev Evgeny Borisovich
Logachev Pavel Vladimirovich
Mezentsev Nikolai Alexandrovich
Tikhonov Yury Anatoljevich

Scientific Council

1. Academician, Chairman	Skrinsky A.N.
2. Corr. member RAS, Co-Chairman	Bondar A.E.
3. Corr. member RAS, Co-Chairman	Burdakov A.V.
4. Doctor of phys.-math. Science, Co-Chairman	Ivanov A.A.
5. Doctor of phys.-math. Science, Co-Chairman	Levichev E.B.
6. Corr. member RAS, Co-Chairman	Logachev P.V.
7. Doctor of phys.-math. science, Co-Chairman	Mezentsev N.A.
8. Doctor of phys.-math. science, Professor	Tikhonov Yu.A.
9. Candidate of phys.-math. science, Sci. Secretary	Vasiljev A.V.
10. Doctor of phys.-math. science	Bagryansky P.A.
11. Doctor of techn. science	Batrakov A.M
12. Candidate of phys.-math. science	Beklemishev A.D.
13. Doctor of phys.-math. science	Blinov V.E.
14. Candidate of techn. science	Bryazgin A.A.
15. Corr. member RAS	Vinokurov N.A.
16. Academician	Dikansky N.S.

17. Corr. member RAS	Dimov G.I.
18. Doctor of phys.-math. science	Druzhinin V.P.
19. Candidate of phys.-math. science	Zolotarev K.V.
20. Candidate of phys.-math. science	Kardapoltsev L.V. – Chairman of Council of Young scientists
21. Doctor of techn. science	Kolmogorov V.V.
22. Doctor of phys.-math. science	Koop I.A.
23. Candidate of phys.-math. science	Krasnov A.A.
24. Doctor of techn. science	Kuksanov N.K.
25. Academician	Kulipanov G.N.
26. Doctor of phys.-math. science	Lotov K.V.
27. Doctor of phys.-math. science	Meshkov O.I.
28. Doctor of phys.-math. science, Professor	Milstein A.I.
29. Corr. Member RAS	Parkhomchuk V.V.
30. Candidate of phys.-math. science	Rakshun Ya.V. – Chairman of Council of Trade union
31. Doctor of phys.-math. science, Professor	Serednyakov S.I.
32. Candidate of phys.-math. science	Starostenko A.A.
33. Doctor of phys.-math. science, Professor	Fadin V.S.
34. Doctor of phys.-math. science	Khazin B.I.
35. Corr. Member RAS	Khriplovich I.B.
36. Corr. Member RAS	Shatunov Yu.M.
37. Candidate of techn. science	Shiyankov S.V.
38. Doctor of phys.-math. science	Eidelman S.I.

Specialized Sections of Scientific Council

Accelerators for Applied Purposes

Kulipanov G.N. (Chrmn.)
Gorbunov V.A. (Secr.)
Anashin V.V.
Antokhin E.I.
Batrakov A.M.
Bondar A.E.
Bryazgin A.A.
Chernyakin A.D.
Churkin I.N.
Dikansky N.S.
Erokhin A.I.
Fadeev S.N.
Goldenberg B.G.
Gurov D.S.
Ivanov A.A.
Karpov G.V.

Knyazev B.A.
Kolmogorov V.V.
Korchagin A.I.
Kuksanov N.K.
Kuper E.A.
Kuper K.E.
Kurkin G.Ya.
Levichev E.B.
Logachev P.V.
Medvedko A.S.
Mezentsev N.A.
Mishnev S.I.
Nemytov P.I.
Nikolenko A.D.
Onuchin A.P.
Parkhomchuk V.V.

Petrichenkov M.V.
Petrov V.M.
Pindyurin V.F.
Pyata E.E.
Rakshun Ya.V.
Salimov R.A.
Shatunov Yu.M.
Shevchenko O.A.
Shkaruba V.A.
Skrinsky A.N.
Tribendis A.G.
Tumaikin G.M.
Vinokurov N.A.
Vostrikov V.A.
Zolotarev K.V.

Plasma Physics and Controlled Fusion Problems

Ivanov A.A. (Chrmn)
Kandaurov I.V. (Secr.)
Anikeev A.V.
Arakcheev A.S.
Arzhannikov A.V.
Astrelin V.T.
Bagryansky P.A.
Beklemishev A.D.
Belchenko Yu.I.
Burdakov A.V.
Burmasov V.S.
Dimov G.I.
Davydenko V.I.
Gorbovsky A.I.
Ivanov I.A.

Ivantsivsky M.V.
Kapitonov V.A.
Khilchenko A.D.
Konstantinov S.G.
Kotelnikov I.A.
Kulipanov G.N.
Lizunov A.A.
Lotov K.V.
Mekler K.I.
Polosatkin S.V.
Popov S.S.
Postupaev V.V.
Prikhodko V.V.
Sanin A.L.

Sinitsky S.L.
Skrinsky A.N.
Skovorodin D.I.
Soldatkina E.I.
Sorokin A.V.
Sudnikov A.V.
Sulyaev Yu.S.
Taskaev S.Yu.
Timofeev I.V.
Shikhovtsev A.V.
Shiyankov S.V.
Shoshin A.A.
Vasiljev A.V.
Vyacheslavov L.N.

Colliding Beams

Parkhomchuk V.V. (Chrmn)
Petrov V.V. (Secr.)
Anashin V.V.
Batrakov A.M.
Berkaev D.E.
Blinov V.E.
Bondar A.E.
Bryazgin A.A.
Dikansky N.S.
Erokhin A.I.
Gorbunov V.A.
Gurov S.M.
Khazin B.I.
Kiselev V.A.
Kolmogorov V.V.
Koop I.A.
Krasnov A.A.

Kulipanov G.N.
Kuksanov N.K.
Kuper E.A.
Kurkin G.Ya.
Levichev E.B.
Logachev P.V.
Medvedko A.S.
Meshkov O.I.
Mezentsev N.A.
Mishnev S.I.
Nikitin S.A.
Onuchin A.P.
Perevedentsev E.A.
Pestrikov D.V.
Petrov V.M.
Reva V.B.
Salimov R.A.

Shatilov D.N.
Shatunov P.Yu.
Shatunov Yu.M.
Shevchenko O.A.
Shiyankov S.V.
Simonov E.A.
Skrinsky A.N.
Solodov E.P.
Starostenko A.A.
Shwartz D.B.
Tikhonov Yu.A.
Tumaikin G.M.
Vasiljev A.V.
Vinokurov N.A.
Vobly P.D.
Zolotarev K.V.

Physics of Elementary Particles

Bondar A.E. (Chrmn.)
Tayursky V.A. (Secr.)
Achasov M.N.
Aulchenko V.M.
Baru S.E.
Berkaev D.E.
Blinov A.E.
Blinov V.E.
Buzulutskov A.F
Chernyak V.L.
Dimova T.V.
Dmitriev V.F.
Druzhinin V.P.
Eidelman S.I.
Fadin V.S.
Fedotovich G.V.
Garmash A.Yu.
Golubev V.B.
Grebenyuk A.A.
Grigoriev D.N.
Groshev V.R.
Grozin A.G.
Ignatov F.V.
Katkov V.M.
Kharlamov A.G.

Khazin B.I.
Khriplovich I.B.
Kononov S.A.
Koop I.A.
Kravchenko E.A.
Krokovny P.P.
Kuzmin A.S.
Lee R.N.
Levichev E.B.
Logachev P.V.
Logashenko I.B.
Lukin P.A.
Malyshev V.M.
Maslennikov A.L.
Milshtein A.I.
Muchnoi N.Yu.
Nikolaev I.B.
Nikolenko D.M.
Obrazovsky A.E.
Onuchin A.P.
Pakhtusova E.V.
Peleganchuk S.V.
Parkhomchuk V.V.
Pestov Yu.N.
Pivovarov S.G.

Pomeransky A.A.
Popov A.S.
Rachek I.A.
Redin S.I.
Ryskulov N.M.
Serednyakov S.I.
Shamov A.G.
Shatunov Yu.M.
Shekhtman L.I.
Shwartz B.A.
Shwartz D.B.
Silagadze Z.K.
Skovpen Yu.I.
Skrinsky A.N.
Sokolov A.V.
Sokolov V.V.
Solodov E.P.
Telnov V.I.
Terekhov I.S.
Todyshev K.Yu.
Tikhonov Yu.A.
Toporkov D.K.
Vasiljev A.V.
Vorob'ev A.I.
Zhilich V.N.

Automation

Tikhonov Yu.A. (Chrmn)
Kuper E.A. (Co-Chrmn)
Baldin E.M. (Secr.)
Dubrov S.V. (Secr.)
Aleshaev A.N.
Amosov S.A.
Aulchenko V.M.
Banzarov V.Sh.
Batrakov A.M.
Belov S.D.
Berkaev D.E.
Bolkhovityanov D.Yu.
Buzykaev A.R.

Faktorovich B.P.
Grozin A.G.
Karnaev S.E.
Kaplin V.I.
Khilchenko A.D.
Kolmogorov V.V.
Koop I.A.
Korol A.A.
Kovalenko Yu.V.
Kupchik V.I.
Kurilin O.Yu.
Kuzin M.V.
Kvashnin A.N.

Levichev E.B.
Logashenko I.B.
Maximova S.V.
Medvedko A.S.
Nekhanevich E.L.
Shatunov Yu.M.
Shuvalov B.N.
Solodov E.P.
Sukharev A.M.
Tararyshkin S.V.
Tsukanov V.M.
Vasiljev A.V.

216, 224, 225, 230, 232, 236, 239, 242, 243, 244, 245, 247, 251, 263, 270, 276, 282, 290, 295, 299, 306, 311, 318, 323, 330, 334, 335, 336, 337, 340, 341, 351, 352, 353, 354, 389, 390, 394, 395, 419, 421, 683, 684, 685, 706

Belov S.D.   705

Belov V.P.   380, 438, 441, 442

Berbasova T.V.   447

Berdyugin A.V.   2, 60, 229, 250, 397, 398, 585, 28p

Berkaev D.E.   2, 41, 57, 60, 166, 213, 229, 397, 398, 405, 406, 407, 546, 547, 548, 583, 584, 585, 591, 634, 692, 693, 696, 698, 28p

Bezuglov V.V.   671, 672, 673, 679, 680, 681, 682

Biryuchevsky Yu.A.   694

Blinov A.E.   190, 340, 352, 419, 421, 683, 684, 685, 706

Blinov M.F.   211, 556

Blinov V.E.   24, 39, 74, 160, 170, 181, 190, 209, 228, 234, 246, 255, 257, 260, 261, 267, 268, 280, 284, 293, 308, 340, 352, 419, 420, 421, 585, 683, 684, 685, 699, 706

Bobrov A.V.   190, 340, 352, 419, 421, 683, 684, 685, 706

Bobrovnikov V.S.   39, 70, 71, 73, 75, 76, 81, 82, 83, 85, 86, 87, 88, 103, 104, 106, 108, 109, 112, 115, 117, 118, 119, 120, 121, 124, 127, 133, 134, 135, 138, 139, 141, 142, 143, 147, 150, 154, 161, 165, 168, 169, 174, 180, 181, 182, 189, 190, 192, 196, 206, 209, 210, 216, 224, 225, 230, 232, 236, 239, 242, 243, 244, 245, 247, 251, 263, 270, 276, 282, 290, 295, 299, 306, 311, 318, 323, 330, 334, 335, 336, 337, 340, 341, 351, 352, 353, 354, 389, 390, 394, 395, 400, 419, 421, 463, 585, 683, 684, 685, 706

Bochek D.V.   546

Bogdanchikov A.G.   2, 60, 70, 71, 72, 73, 75, 76, 81, 82, 83, 85, 86, 87, 88, 103, 104, 106, 108, 109, 112, 115, 117, 118, 119, 120, 121, 124, 127, 133, 134, 135, 138, 139, 141, 142, 143, 147, 150, 154, 165, 177, 180, 192, 196, 206, 216,

224, 225, 229, 230, 232, 236, 239, 242, 243, 244, 245, 247, 250, 251, 263, 270, 276, 282, 290, 295, 299, 306, 311, 318, 323, 330, 334, 335, 336, 337, 341, 351, 353, 354, 389, 390, 394, 395, 397, 398, 399, 585, 28p

Bogomyagkov A.V.   56, 190, 329, 340, 352, 419, 421, 543, 549, 550, 683, 684, 685, 699, 701, 702, 706

Boimelstein Yu.M.   42, 556

Bolhovitjanov D.Yu.   42

Bondar A.E.   2, 48, 60, 69, 74, 80, 89, 90, 91, 92, 105, 107, 110, 111, 113, 114, 116, 122, 125, 128, 129, 130, 131, 132, 136, 137, 140, 144, 145, 146, 148, 151, 155, 157, 183, 184, 189, 190, 197, 201, 205, 217, 218, 223, 231, 233, 237, 238, 240, 248, 252, 253, 259, 262, 264, 266, 269, 273, 274, 277, 279, 281, 283, 285, 286, 291, 294, 296, 297, 298, 300, 301, 302, 303, 304, 307, 309, 310, 313, 314, 316, 317, 319, 322, 324, 326, 331, 333, 340, 342, 343, 344, 347, 350, 352, 355, 356, 357, 358, 373, 392, 424, 419, 421, 423, 583, 584, 596, 683, 684, 685, 692, 706

Borodenko A.A.   181, 209

Borodich V.V.   544, 545

Botov A.A.   2, 60, 74, 229, 250, 397, 398, 585, 28p

Bragin A.V.   2, 60, 166, 583, 584, 591, 619, 692, 693, 696, 698

Brodnikov A.F.   32, 528

Bryazgin A.A.   434, 671, 672, 673, 674, 679, 680, 681, 682, 6p

Bryazgin K.A.   641

Bryzgunov M.I.   709

Bryzgunov M.I.   544, 545, 551, 552

Bubley A.V.   544, 545

Burdakov A.V.   14, 61, 156, 219, 365, 368, 372, 380, 435, 447, 448, 601, 602, 604, 605, 607, 608, 609, 610, 613, 617, 618, 619, 620, 621, 622, 623, 624, 625, 626, 627, 628, 629, 630

Burenkov D.B.   699

Burmasov V.S.   365, 435, 607, 609, 617, 621, 629

Buzulutskov A.F.   69, 183, 184, 423, 424, 453

206

207

	398, 400, 465, 585, 28p	Morozov I.I.	190, 340, 352, 419, 421, 683, 684, 685, 699, 706
Martyshkin P.V.	556		
Maslennikov A.L.	70, 71, 73, 75, 76, 81, 82, 83, 85, 86, 87, 88, 103, 104, 106, 108, 109, 112, 115, 117, 118, 119, 120, 121, 124, 127, 133, 134, 135, 138, 139, 141, 142, 143, 147, 150, 154, 165, 180, 192, 196, 206, 216, 224, 225, 230, 232, 236, 239, 242, 243, 244, 245, 247, 251, 263, 270, 276, 282, 290, 295, 299, 306, 311, 318, 323, 330, 334, 335, 336, 337, 340, 341, 351, 352, 353, 354, 389, 390, 394, 395, 419, 421, 683, 684, 685, 706	Motygin S.V.	695, 708
		Muchnoi N.Yu.	39, 161, 170, 181, 188, 190, 194, 195, 213, 227, 235, 241, 249, 254, 256, 258, 265, 271, 272, 275, 278, 292, 305, 315, 320, 325, 340, 346, 352, 391, 419, 421, 422, 580, 583, 584, 683, 684, 685, 692, 699, 706, 23p, 25p, 26p, 27p, 28p, 29p, 30p, 31p, 32p, 33p, 34p, 35p
		Murakhtin S.V.	437, 651, 652, 653, 654, 655
		Nazmov V.P.	480, 483, 486, 506, 539
		Nekhaev V.E.	673, 679, 6p
Matvienko D.V.	74, 107, 167, 175, 191, 237, 253, 259, 262, 264, 269, 273, 274, 277, 279, 281, 285, 300, 303, 309, 317, 324, 373, 460	Nemytov P.I.	38, 410, 640, 641
		Neyfeld V.V.	190, 195, 340, 352, 419, 420, 421, 580, 683, 684, 685, 699, 700, 706, 23p
Maximov D.A.	70, 71, 72, 73, 75, 76, 81, 82, 83, 85, 86, 87, 88, 103, 104, 106, 108, 109, 112, 115, 117, 118, 119, 120, 121, 124, 127, 133, 134, 135, 138, 139, 141, 142, 143, 147, 150, 154, 165, 180, 190, 192, 196, 206, 216, 224, 225, 230, 232, 236, 239, 242, 243, 244, 245, 247, 251, 263, 270, 276, 282, 290, 295, 299, 306, 311, 318, 323, 330, 334, 335, 336, 337, 340, 341, 351, 352, 353, 354, 389, 390, 394, 395, 419, 421, 683, 684, 685, 706	Nikiforov D.A.	556
		Nikitin S.A.	39, 170, 190, 340, 352, 419, 421, 420, 557, 683, 684, 685, 706
		Nikolaev I.B.	42, 170, 189, 190, 227, 235, 241, 249, 254, 256, 258, 265, 271, 272, 275, 278, 292, 305, 315, 320, 325, 340, 346, 352, 391, 419, 420, 421, 468, 683, 684, 685, 699, 706, 712, 25p, 26p, 27p, 30p, 31p, 32p, 33p, 34p, 35p
		Nikolenko D.M.	9, 20, 33, 39, 174, 189, 195, 198, 362, 580, 699, 23p
Maximov S.A.	671, 672, 673, 679	Obrazovsky A.E.	2, 23, 60, 229, 250, 397, 398, 585, 28p
Maximov V.V.	5, 651, 652, 653, 654, 655		
Medvedko A.S.	190, 340, 544, 545, 683, 684, 685, 706, 709	Ogurtsov A.B.	497, 500, 501
Mekler K.I.	14, 156, 365, 372, 435, 607, 609, 613, 617, 621, 623, 629	Okhapkin V.S.	2, 60, 166, 583, 584, 591, 692, 693, 696, 698
Meshkov O.I.	11, 39, 56, 190, 203, 340, 352, 419, 421, 420, 553, 554, 559, 564, 589, 683, 684, 685, 699, 706, 711, 36p	Okunev I.N.	190, 340, 352, 419, 421, 683, 684, 685, 699, 700, 706, 3p
		Oleinikov V.P.	187, 534
		Onuchin A.P.	6, 74, 168, 169, 181, 182, 190, 209, 210, 228, 234, 246, 255, 257, 260, 261, 267, 268, 280, 284, 293, 308, 340, 352, 400, 419, 421, 585, 683, 684, 685, 699, 706
Mezetsev N.A.	483, 498, 499, 502, 503, 561, 586, 595		
Miginsky S.V.	490, 575		
Mikaiylov A.I.	420		
Mikhailov K.Yu.	2, 60, 164, 166, 466, 583, 584, 591, 692, 693, 696, 697, 698	Oreshkin S.B.	190, 340, 352, 419, 421, 683, 684, 685, 706
Milstein A.I.	26, 220, 221, 361, 17p	Orlov I.O.	683, 684, 685, 706
Minakov V.A.	9p	Osipov A.A.	190, 340, 352, 419, 421, 683, 684, 685, 706
Mishagin V.V.	381, 438, 441, 442		
Misnev S.I.	9, 20, 190, 195, 340, 352, 362, 419, 421, 487, 580, 683, 684,	Osipov V.N.	695
		Ostreinov Yu.M.	642, 648

Stupishin N.V.	380, 382, 438, 439, 442
Sudnikov A.V.	368, 435, 608, 609, 617, 620, 629
Sukhanov A.V.	700
Sukhanov D.P.	39
Sukharev A.M.	70, 71, 72, 73, 75, 76, 81, 82, 83, 85, 86, 87, 88, 103, 104, 106, 108, 109, 112, 115, 117, 118, 119, 120, 121, 124, 127, 133, 134, 135, 138, 139, 141, 142, 143, 147, 150, 154, 165, 180, 186, 190, 192, 196, 206, 216, 224, 225, 230, 232, 236, 239, 242, 243, 244, 245, 247, 251, 263, 270, 276, 282, 290, 295, 299, 306, 311, 318, 323, 330, 334, 335, 336, 337, 340, 341, 351, 352, 353, 354, 389, 390, 394, 395, 419, 421, 476, 683, 684, 685, 706
Sulyaev Yu.S.	447, 617, 629
Surin I.K.	2, 60, 177, 229, 250, 397, 398, 475, 585, 28p
Svischev V.V.	699, 712
Syrovatin V.M.	503, 561, 586, 595
Talyshev A.A.	2, 60, 70, 71, 72, 73, 75, 76, 81, 82, 83, 85, 86, 97, 88, 104, 106, 108, 109, 112, 115, 117, 118, 119, 120, 121, 124, 127, 133, 134, 135, 138, 139, 141, 142, 143, 147, 150, 154, 162, 164, 165, 166, 180, 190, 192, 196, 206, 209, 216, 224, 225, 230, 232, 236, 239, 242, 243, 244, 245, 247, 251, 263, 270, 276, 282, 290, 295, 299, 306, 311, 318, 323, 330, 334, 335, 336, 337, 340, 341, 351, 352, 353, 354, 389, 390, 394, 395, 419, 421, 583, 584, 591, 683, 684, 685, 692, 693, 696, 698, 706
Tararyshkin S.V.	695, 705, 2p
Tarasenko O.A.	503, 561
Tarnetsky V.V.	671, 672, 673
Taskaev S.Yu.	28, 35, 36, 98, 99, 411, 429, 430, 431, 432, 433, 642, 643, 646, 647, 648, 1A
Tayursky V.A.	68, 190, 340, 352, 419, 421, 683, 684, 685, 706
Tekutiev A.I.	177, 399
Telnov V.I.	74, 153, 176, 178, 179, 190, 340, 352, 419, 421, 452, 469, 470, 683, 684, 685, 686, 687, 688, 706
Terekhov I.S.	289, 22p
Tikhonov Yu.A.	3, 39, 70, 71, 72, 73, 75, 76, 81, 82, 83, 85, 86, 87, 88, 103, 104, 106, 108, 109, 112, 115, 117, 118, 119, 120, 121, 124, 127, 133, 134, 135, 138, 139, 141, 142, 143, 147, 150, 154, 165, 180, 190, 192, 196, 206, 216, 224, 225, 229, 230, 232, 236, 239, 242, 243, 244, 245, 247, 250, 251, 263, 270, 276, 282, 290, 295, 299, 306, 311, 318, 323, 330, 334, 335, 336, 337, 340, 341, 351, 352, 353, 354, 370, 389, 390, 394, 395, 397, 398, 419, 421, 585, 683, 684, 685, 699, 706, 28p
Timofeev I.V.	156, 367, 10p, 13p
Titov V.M.	2, 60, 162, 164, 166, 583, 584, 591, 692, 693, 696, 697, 698, 3A
Tiunov M.A.	28, 52, 380, 644, 671, 672
Tkachenko V.O.	671, 672, 673, 679
Tkachev A.A.	376, 438, 442
Todyshev K.Yu.	3, 74, 160, 190, 228, 234, 246, 255, 257, 260, 261, 267, 268, 280, 284, 293, 308, 340, 352, 419, 421, 683, 684, 685, 699, 706
Tolmachev S.S.	172
Tolochko B.P.	4, 39, 93, 434, 483, 485, 488, 493, 495, 681, 682
Toporkov D.K.	9, 20, 33, 195, 198, 362, 580, 699, 23p
Tribendis A.G.	694, 695
Trunev Yu.A.	16, 156, 386, 404, 446, 609, 613, 617, 620, 621, 622, 623, 629, 632, 633
Tsukanov V.M.	498, 499, 502, 503, 561
Tsydulko Yu.A.	53, 207, 321
Tsyganov A.S.	556
Tumaikin G.M.	6, 39, 190, 340, 352, 419, 420, 421, 683, 684, 685, 699, 706
Usov P.V.	448
Usov Yu.V.	74, 167, 175, 177, 190, 229, 340, 352, 393, 397, 398, 399, 419, 421, 442, 585, 683, 684, 685, 706, 28p
Utkin A.V.	497, 500, 501
Valov O.M.	3p
Vasichev S.P.	699
Vasiljev A.A.	509, 601, 602, 604, 605, 624
Vasiljev A.V.	2, 60, 229, 250, 585, 28p
Vasilyev M.Yu.	707
Vilkin A.I.	442
Vinokurov N.A.	10, 327, 369, 492, 570, 575, 576, 577, 578, 579

SIBERIAN BRANCH OF RUSSIAN ACADEMY OF SCIENCES
BUDKER INSTITUTE OF NUCLEAR PHYSICS

ANNUAL REPORT
2014

Cover E.D. Bender